Tubular Glass Columns

Design and Engineering of Structural, Robust, Fireproof Tubular Glass Columns.

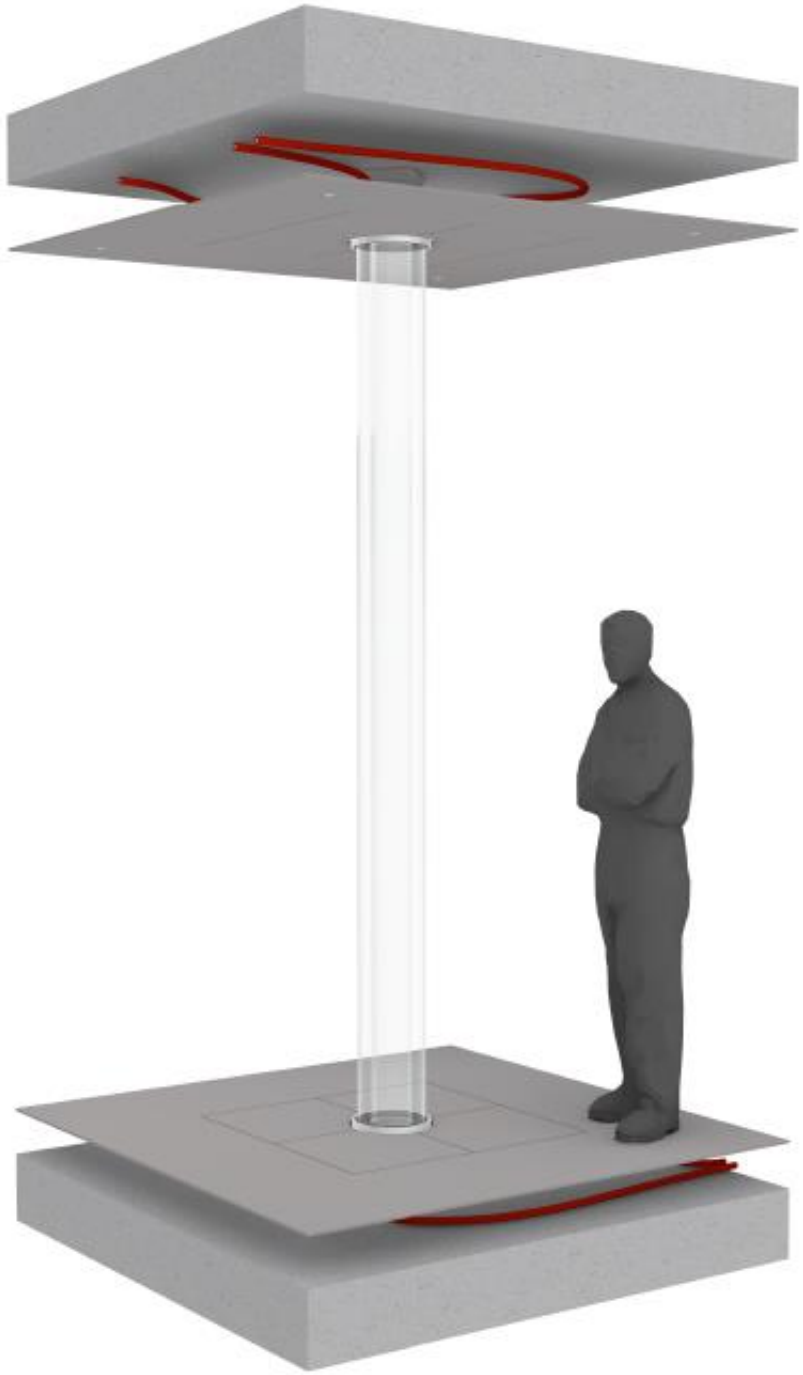

Rozemarijn Veenstra

MSc Civil Engineering – Structural Design

Tubular Glass Columns

Design and Engineering of Structural, Robust, Fireproof Tubular Glass Columns.

Author:

ing. C.R.A. Veenstra
Master student - Delft University of Technology - Civil Engineering - Building Engineering - Structural Design
T: 06-34189923
E: C.r.a.veenstra@student.tudelft.nl

Graduation committee:

prof.dr. M. Overend
Chairman - Delft University of Technology - Architectural Engineering and Technology
T: 015-2784094
E: M.Overend@tudelft.nl

dr. F. Oikonomopoulou
Supervisor - Delft University of Technology - Architectural Engineering and Technology
T: 015-2785835
E: F.Oikonomopoulou@tudelft.nl

ir. C. Noteboom
Supervisor - Delft University of Technology - Civil Engineering
T: 015-2783332
E: C.Noteboom@tudelft.nl

Publication date:
August 2021

Delft University of Technology
Faculty of Civil Engineering and Geosciences

Preface

In 2019, I went to Cuba. To my surprise, they did not use glass in the windows. Instead, wood panels are used to keep the insects out that were rather less effective than glass at doing the job. That was the first time I was really missing glass. It got me thinking about how I appreciate glass.

Besides insects, glass can protect us from weather conditions, due to the fact that it is a waterproof material. Glass is already an old material, which has been used in some iconic buildings like the Crystal Palace and the Glass House at Chatsworth, designed by the engineer Joseph Paxton. Nevertheless, glass is still in development and due to new technologies, amazing structures can be made with glass. For example, the Water Balcony (figure 1). This is a guesthouse of hotel Atami in Japan, designed by architect Kengo Kuma. The floor, fins, beams, and even the furniture is made of glass. Nevertheless, how cool would it be if we are able to replace the concrete columns by tubular glass columns? Then really nothing is blocking the view anymore. There is still a lot unknown about glass and about ways to use glass for structural purposes, especially glass columns. That is why I would like to contribute to the development of glass columns. Furthermore, glass is an amazing and unusual material, which got my attention. Glass is brittle, but strong at the same time. This makes it interesting to find a good way to use the material so that it can make use of its strong properties.

Figure 1 The Water balcony (©ERIETA ATTALI PHOTOGRAPHIC ARCHIVE. 2016).

Rozemarijn Veenstra

Delft, The Netherlands

Acknowledgement

The last approximate ten months, I have been doing research with great joy. During this research, I became more and more interested and enthusiastic in the subject glass, and especially tubular glass columns.

First of all, I want to thank my supervisors for all the knowledge they have given. I would not have reached this level without this knowledge. The meetings had we have had over the time were always a source for new inspiration and knowledge. Mauro Overend, Chris Noteboom, and Faidra Oikonomopoulou thank you for your support.

Next to that, I want to speak out a word of thanks to SCHOTT, H.B.Fuller Kömmerling, Octatube, Hilti, Techniparts and to the laboratory staff of the Stevinlab 2 from the TU Delft. Without their sponsoring and their help to develop all the components, I would never have been able to carry out tests. A special mention goes to Klaas Roelfsma, Folker Steden, Kerstin Kohl and Katrin Djuric from SCHOTT, Chris Davis, Wolfgang Wittwer, Christian Scherer and Jens Wolthaus from H.B.Fuller Kömmerling, Peter van de Rotten and Willem Poot from Octatube, Thomas Goedegebuure from Hilti, Frank Muntz from Techniparts, Roel Schipper, Peter de Vries, Louis den Breejen, Fred Schilperoort, Fred Veer and Telesilla Bristogianni from TU Delft. The designs of the tubular glass column have been enriched, due to all the meetings I have had with so many different areas of expertise.

I cannot close off without expressing my thanks to family and friends, especially my boyfriend Niels Lok. They have given me the spirit to go on each day. So, thanks to all who have been part of this journey.

Summary

Glass has become ever more popular in the building industry. Glass is already used in facades, staircases, fins, floors, and beams. Nevertheless, free-standing load-bearing glass columns are rarely used. Columns are primary structural elements. It needs to be robust, which means that it needs to give a warning before failure so that people can evacuate. Glass is a brittle material and has a sudden failure, which means that it is not directly logical to use solid glass as a load-bearing structural column. However, glass has a large compressive strength, which can reach 1000 N/mm^2. Rather despite the high compressive strength, due to complications with manufacturing, spontaneous failure, and lack of satisfactory of fireproof performance, more research needs to be done on the manufacturing, the fire safety, and the robustness of glass columns. In the literature study, the layered tubular glass column was found to be most promising for further investigating, due to its transparency and its good buckling and torsional buckling resistance.

Objective

The aim of this research is to design and engineer a transparent tubular glass column as a structural element, which is robust and fireproof. The research was performed by means of a literature study followed by the design phase, and by numerical and experiments investigations. The research is concluded with a discussion, a conclusion and recommendations.

Literature study

In the literature study a few aspects emerged, which may have an influence on the design. These aspects need to be taken into account while designing:

- The tubular shape of the column reduces the internal stresses, because there are no corners or angles. The circle-shaped cross-section contributes to a resistance to buckling and torsional buckling of the column.
- It is not possible to clean the column on the inside. So, the column needs to be sealed to avoid the column from becoming dirty. This has an influence on the design of end connections. It becomes a closed cavity whereby air cannot flow in or out of the column. The closed air inside the cavity will be exposed to isochoric pressures due to climatic loading. Hereby the risk of condensation increases. Due to condensation, water will be on the inside of the column for a certain time, which results in the growth of mould for example, and this cannot be cleaned anymore. This means that condensation needs to be avoided.
- Next to that, differences in air pressures will result in stresses in the glass. Borosilicate glass has a higher resistance for the occurring stresses by temperature changes than soda-lime glass, due to a lower coefficient of thermal expansion.
- Furthermore, end connections are of great influence. The column needs to be designed with a hinged connection, so that it will only take up normal forces. Moreover, a soft material, with a lower Young's modulus (like POM), needs to be put in between the glass and the steel. Not only the column, but also its end connections must be fireproof. Lastly the forces need to be introduced uniformly in the column. This can be done with a Hilti mortar.
- Geometric tolerances in the glass tubes need to be taken into account as well, because, as a result, also the thickness of the interlayer will vary. The thicker the interlayer, the more stresses occur. The thinner the interlayer, the less the tubes will bond.
- The free-standing load-bearing column is a primary structural element. This means that it needs to be robust. It needs to give a warning before complete failure.

Design

With these aspects in mind, three designs were engineered in this thesis, the MLA (Multi Layered with Air) (2x) and the SLW (Single Layered with water) (1x) which fulfil the defined design criteria and main concerns. The designs were engineered for a case study: Bouwdeel D in Delft, but the designs can also be applied to other buildings. Bouwdeel D is a four-storey office building. The restrictions from the case study were that the column needs to be:

- fire resistant for 60 minutes
- demountable
- 3.2 meters long
- to be able to carry loads of:
    - N_{ed}=300 kN (N_{ed}=500 kN including a safety factor of 1.5)
    - N_{ek}=280 kN (N_{ek}=420 kN including a safety factor of 1.5)

To be able to carry the abovementioned loads, the following dimensions were determined for this column: an outer tube with an outer diameter of 180 mm and a wall thickness of 7 mm, and an inner tube with an outer diameter of 160 mm and a wall thickness of 7 mm. Then the corresponding compression stresses are between 39-69 N/mm^2 and the tensile stresses are between 7.8-13.8 N/mm^2. These values should be acceptable, because they are below the allowable tensile stress of 15.5-36.6 N/mm^2, and below the allowable compression stress of 260-350 N/mm^2. Furthermore, a risk analysis is performed for this case study. One layer of glass is needed as a protective layer. So, in case this layer breaks, the other layer(s) are still able to take over the loads. In case of the MLA, there is an extra outer tube, which is not load-bearing. The SLW does not have an extra outer layer. Even though, if the outer layer is broken, it is still able to carry some load. That is because the glass tubes will be bonded together. Besides, the column has been engineered on the guideline of disassembly and reuse, by the use of dry connections. In this way, almost all the components can be dissembled and reused. Only the Hilti mortar cannot be reused and delamination of the glass tubes is not possible. Moreover, a way to assemble the column has been designed.

Manufacturing of the samples

Six small samples with a length of 300 mm were produced to test the lamination process with regard to bubble formation and possible breakage of the glass by internal stresses.

Three laminated DURAN (annealed) samples and three laminated DURATAN (heat-strengthened) samples were tested. The glass tubes were manufactured by extruding. DURAN and DURATAN borosilicate glass tubes were made by SCHOTT.

H.B.Fuller Kömmerling carried out the lamination process. There were two options for the interlayer material: a 2 PU-component (Ködistruct LG) material which cured slowly by room-temperature, or a UV-light cured material (Acrylate UV). The UV-light cured material had a lower Young's modulus, but a higher shrinkage value. For the 2 PU-component material this was vice versa. According to GSA models which were made in this project, more stresses occurred when the interlayer material was stiffer. Nevertheless, H.B.Fuller Kömmerling proposed to use an interlayer material which cures in room-temperature for two reasons. The first reason was to reduce the impact of chemical induced reaction shrinkage, by shifting from van-der-Waals interactions to chemical bonds during curing. The second reason was to keep the curing temperature as low as possible to avoid additional thermal shrinkage in the post-gelling phase. Some samples had a few air bubbles, especially sample 4. With polarised light, stresses were visible around the bubbles.

Furthermore, the connection components (steel and POM) were produced and arranged by Octatube, the steel hinges were arranged by Techniparts, and the Hilti mortar was arranged by Hilti.

Numerical and experimental Investigations

Afterwards, these samples were tested on compression strength, to investigate the behaviour of the interlayer material, the post-failure behaviour of the designs, the differences between annealed and heat-strengthened glass samples, the behaviour of the connections under pressure, and the capacity of the glass tubes and the connections. The tests were performed at the Stevin lab II at the Technical University in Delft. Some numerical models on the thermal stresses and buckling behaviour of the columns were made. Due to the fact that the tested samples in this project were low slenderness, buckling did not occur. The tests were verified by hand calculations.

During experiments, cracks started appearing in the glass close to the top and the bottom connection, which means that it is probably caused by transversal elongation, which resulted in tensile stresses. The cracks due to the compression forces were propagating parallel to the length of the glass tubes. Cracks propagated slowly at the annealed glass samples and fast at the heat-strengthened samples. A good cooperation was present between the annealed glass tubes, since cracks appeared in the inner and the outer tubes. For the heat-strengthened samples, cracks appeared first in the outer tube and when the force was taken off, the inner tube broke into small pieces. The first crack appeared earlier than expected. Reasons could be:

- Large hinges were used which could affected the functioning of the hinge as a hinged connection.
- The glass tubes had defects.
- Tolerances in the glass affected the sample. The tolerances in the glass can result in different thicknesses of the interlayer whereby extra stresses can occur.
- A few air bubbles were located in the cavity. Stresses were localised around these air bubbles.

The first cracks appeared between 95 and 160 kN. The hand calculations were based on 250 kN, whereby the tensile stress is 15.6 N/mm^2 and the compression stress is 78 N/mm^2. The allowable calculated tensile stress for annealed glass is 15.5 N/mm^2 (short-term loading). For heat-strengthened glass, the allowable tensile stress is higher, 36.3 N/mm^2 (short-term loading). The allowable tensile stress is normative, since the compression stress is around 260-350 N/mm^2 (for borosilicate glass), which is higher. The corresponding compression stress for 95 kN is 29.5 N/mm^2 with a tensile stress of 5.9 N/mm^2. The corresponding compression stress for 160 kN is 49.7 N/mm^2 with a tensile stress of 9.9 N/mm^2. The tensile stresses 5.9 and 9.9 N/mm^2 are lower than the theoretical allowable tensile stress of 15.5 N/mm^2.

The samples seemed to be really robust, because the samples had a large load-bearing capacity even after the first cracks occurred. As said before, the first crack appeared between 95-160 kN in the DURAN samples, and after that the samples were still able to carry a load of 700-750 kN. So, after the first crack, the specimens were able to have around 4-5 times more load. The heat-strengthened samples first cracked at 120-160 kN. The maximum force of these samples was 390-490 kN. This means that after the first crack, the specimens were able to have around 3 times more load.

The results were compared to the project from Van Nieuwenhuijzen. Van Nieuwenhuijzen tested three DURAN (annealed) samples and in this project three DURAN (annealed) and

three DURATAN (heat-strengthened) samples were tested. The samples of Van Nieuwenhuijzen had almost the same diameter and wall thickness. The length of the samples was: 1.2 m (1x) and 1.5 m (2x), which is longer than the samples that have been tested in this project. Nevertheless, the samples only failed on compression and not on buckling. The samples from this thesis project failed on compression forces as well. For the 1.2 and 1.5 m samples of Van Nieuwenhuijzen, the failure load was between 137-196 kN and the first crack appeared at 40-73 kN. After the first crack the specimens were able to have around 2-3 times more load. This is less than the results obtained in this research. Moreover, in this thesis, higher stresses were arrived compared to the values of Van Nieuwenhuijzen:

- Van Nieuwenhuijzen: lowest failure stress was 12 N/mm^2 and the highest was 29 N/mm^2.
- Veenstra: lowest failure stress was 30 N/mm^2 and the highest was 50 N/mm^2.
- Van Nieuwenhuijzen: lowest maximum stress was 41 N/mm^2 and the highest was 58 N/mm^2.
- Veenstra: lowest maximum stress was 121 N/mm^2 and the highest was 233 N/mm^2.

Perhaps the improvements achieved in this project can be attributed to better detailing. Van Nieuwenhuijzen used PMMA sheets to create a hinged connection between the support and the glass column, because of the lower Young's modulus of PMMA compared to glass, and in this thesis, steel hinges and Hilti mortar were used for a better introduction and distribution of the forces into the glass tubes.

Table of Contents

List of Symbols

°C	Degree Celsius
K	Kelvin
N	Newton
GPa	Gigapascal
J	Joule
kN	kilonewton
kg	kilogram
MJ	Megajoule
MPa	Mega Pascal
mm	millimetre
mm^2	squared millimetre
mm^3	cubic millimetre
m	metres
m^2	squared metre
m^3	cubic metre
µm	micrometre
W	Watt

Introduction

1. Introduction

1.1. Problem Definition

Glass is one of the oldest manmade materials. The exact date of discovery is unknown, but it was discovered before the time of Christ (BC). Glass has a large compressive strength, which can reach 1000 N/mm^2 (Saint-Gobain 2016). Glass is often used as parts of façades, but as a result of the large compressive strength, it is possible to use glass even for structural elements as fins, floors, beams, staircases, and columns. In figure 2, The Apple Store in New York is shown. In this building, there is been made use of glass elements as the façade, fins, beams and the staircase. Nevertheless, glass columns are rarely applied. Reasons could be (figure 3): lack of data, complications with manufacturing, costs, poor fire resistance, uncertain variables, low tensile strength, high safety factors and the material is brittle. However, glass can be a viable material for a column. As said, glass has a large compressive strength. Furthermore, glass is recyclable, durable and transparent (figure 3).

''Glass is the most striking feature in modern building designs.'' (Achintha, M. 2016).

Figure 2 The Apple Store at Fifth Avenue New York (iDesignArch. 2010-2021).

Is there a demand for glass columns? High compressive strength together with transparency allows us to make almost dematerializes compressive member such as columns which in turn allows us for light and space continuity. On the other hand, these columns are still in an infant stage of development due to spontaneous failure and lack of satisfactory of fireproof performance. Some research is done about tubular glass columns in 1999. One of the conclusions was:

''When fully developed, this column can be used for loadbearing structures, combining the transparency of glass with the safety and strength of steel.'' (Veer, F.A., et al 1999).

So, if the tubular glass column is designed and engineered safely, this transparent material can be the solution for a structural, load-bearing, strong, safe, and transparent glass column.

''Light, comfort, well-being, style, safety, security and sustainability are among the benefits that can be achieved from the appropriate use of modern glass products in buildings.'' (Achintha, M. 2016).

In an interview with Joost Heijnis, building engineer at cepezed, he mentioned that it would be nice to have a new element, like glass columns, in the toolkit of architects. It is good that new possibilities are still being researched and developed. Thinking of glass columns,

according to him it will fit in luxury buildings, like the entrance of a court, or buildings with a modern appearance. If the choice is to work with glass columns, it must have a prominent place. Cepezed keeps structural elements in sight as much as possible. ‘’If it is designed properly and efficient, why hide it?’’ he said. Making the column out of glass can contribute to the aesthetics of the design. In appendix 1.3. the complete interview is included.

Figure 3 Negative and positive features of glass.

There are five types of glass columns: profiled, layered tubular, stacked, bundled and cast (see figure 4). So far, the only free-standing structural glass columns, applied two times in buildings, are the glass profiled columns with a cruciform cross-section. In figure 5, the cruciform cross-section columns are shown in Danfoss Headquarter in Denmark (more on this in chapter 2.2.5. and appendix A.2.8.). However, the tubular shape is the most efficient shape for a column. This is confirmed by other articles, see the two citations below.

‘’Material efficiency of the cross section led to open profiles which were extremely good for bending. Tubes are better in compression, but tubes also have an aesthetic appearance which lifts them above open profiles. They are not angular, but more fluent.’’ (Eekhout, M. 2019).

‘’Research shows that because of buckling, torsion and commercial availability a tube is the best shape for this transparent column.’’ (Van Nieuwenhuijzen, E.J., et al. 2005).

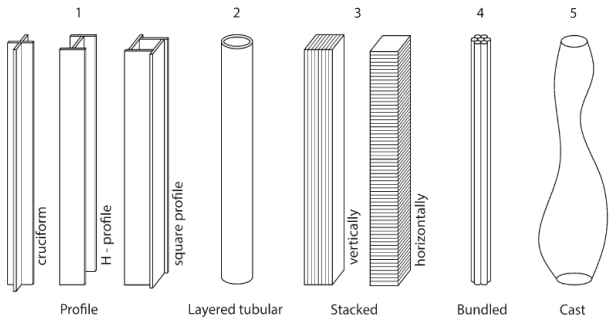

Figure 4 Five types of glass columns (Nijsse, R., et al 2014).

Figure 5 Cruciform cross-section glass columns in Danfoss Headquarter (Schmidt Hammer Lassen Architects. n.d.).

Why are tubular glass columns not applied yet? Looking at the following two citations, it becomes clear that it was due to the manufacturing complications. Back then, it was not possible to make long glass tubes. When the tubes were longer than 1.5 metres, the tubes could be distorted during extrusion.

"My first idea was a circular tube, …. However, no producer (at that time) could produce that (6 metres tall columns, taking up 400 kN each)." (Bagger, A., et al. 2010).

''The biggest obstacle at this moment is the problems in the availability of long glass tubes and consistency of manufacture of these tubes." (Van Nieuwenhuijzen, E.J., et al. 2005).

In the current Bouwbesluit in the Netherlands, a building needs to have floors from at least 2.6 metres (Bouwbesluit; 2012). Due to new developments, it is possible to produce longer tubes. SCHOTT can produce glass tubes with a maximum height of 10 metres, named SCHOTT DURAN® profiles (see figure 7).

Borosilicate glass DURAN® SCHOTT tubes were used in an art project in Iceland. The tubes have a length of 2.9 metres and a diameter of 300 mm. Inside, the tubes are filled with water. The columns are resisting 260 kg of water. To prevent algae forming, the tubes are sealed by welded glass plates. The tubes were transported by ship to Iceland (Schwanke, H. n.d.). The tubes are not used as load-bearing columns, but it functions as art. The columns are shown in figure 6.

Figure 6 Tubular glass columns in Iceland (Schwanke, H. n.d.).

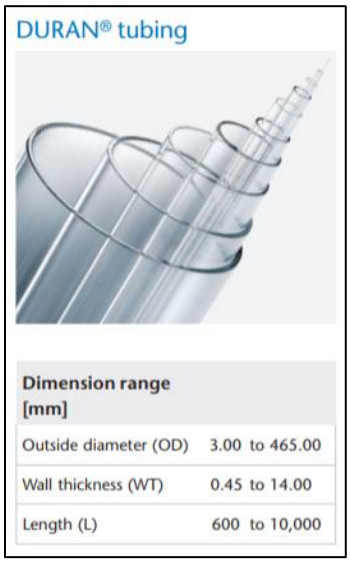

Figure 7 SCHOTT DURAN® glass profiles (SCHOTT. n.d.).

Furthermore, most of the tests performed on glass columns were compression tests. Other exposures onto glass columns, as fire or impact loads, are almost not tested. Even the existing columns of Danfoss Headquarter are only tested on compression and buckling (see citation below).

''However, as the problem of fire protection in particular remains unsolved (encasing glass members defeats the very object of their existence), such glass columns will continue to be isolated cases whose main purpose is to prove what is technically feasible.'' (Schittich, C., at al. 2017).

According to T. Wever, project manager at abt, and P. van de Rotten, head of structural engineering at Octatube, a column is a primary structural element in a building. It is part of the main load-bearing structure. If the column collapse, the impact is much larger than when

the façade collapse for example. If the column fails, the whole building can collapse. The applied glass columns or glass fins so far, only carries light-weight structures. A column in a building needs to be able to carry more floors. Furthermore, in the NEN-norm it is determined that when a structural element tends to break, it needs to give a sign to the people inside the building, so that the building can be evacuated on time. Glass is a brittle material, which results in a sudden failure. These aspects need to be taken into account while designing a glass column. In appendix 1.1. and appendix 1.4. the interviews are included.

1.2. Problem Statement

The resulting problem statement:

There are not yet well-established manufacturing methods with related checking and calculation methods for one of the most efficient shape of a glass column: the tubular. More knowledge is needed on the manufacturing, the fire safety, and the robustness.

1.3. Main Objective

The Main Objective for this thesis project is:

''To design and engineer a transparent tubular glass column as a structural element, which is robust and fireproof.''

1.4. Main Question

The Main Question for this thesis project is:

''What is the potential and what are limitations in designing and engineering a transparent tubular glass column as a structural element, which is robust and fireproof?''

1.5. Outline

In figure 8, the outline for this research is shown. Part I is the literature study. In part I some general information on glass is presented, like properties, types, etc. Furthermore, more information on the types of glass columns with applications and researches is shown. Lastly, design strategies for fire safety and robustness are given.

Part II is the design phase. In here the knowledge obtained in the literature study, is used to design and engineer designs for a tubular glass column which is robust and fireproof.

After part II, numerical and experimental tests were performed. In this part, hand calculations and numerical FEM-models were made to check the stresses due to temperature differences, and on the compression strength. After that, samples were manufactured. All of the components, to create the samples, were sponsored by external companies. Experimental tests were carried out on the compression strength and to check out the post-failure behaviour of the designed column.

In the last part, the discussion, the conclusion and recommendations are given.

1.6. Sub Objectives

The sub objectives are formulated per part.

Part I: Literature Study

- To obtain general information about properties, types, manufacturing methods, producers, tolerances, and limitations of glass.
- To obtain information about different types of glass columns, applications, other researches done, and already designed glass columns.

- To investigate glass design guidelines, failure mechanisms, and safety strategies for robustness, and fire safety for glass columns.

Part II: Design Phase

- To be able to point out design criteria and main concerns for the design of the column.
- To give some concepts for the glass column, which satisfies the design criteria.
- To give principles to design connections for the column.
- To give a way to replace the column when it is broken.
- To determine a case for the column.

Part III: Numerical and Experimental Investigations

- To verify the robustness and the transparency of the column and to check if cracks appeared during/after the lamination process.
- To set up the experimental test.
- To manufacture/arrange samples of the column for the experimental tests.
- To verify the designs on the compression strength and the post-failure behaviour by carrying out experimental tests.
- To explain the deviations from the numerical models/hand calculations with the experimental tests results.

1.7. Sub Questions

The sub objectives are formulated per part.

Part I: Literature Study

- What are main manufacturing methods and limitations to produce glass tubes?
- What are common designs for transparent tubular glass columns?
- What are principles to laminate tubular glass columns?
- Which failure mechanisms exists for glass columns?
- What are safety strategies for a robust and fireproof design?

Part II: Design Phase

- What are the design criteria and main concerns for designing a glass column?
- What are different concepts for the design of the column, which fulfils the design criteria?
- Which aspects for the end connections are from influence on the design and how are these aspects taken into account?
- Is it possible to replace to column when broken and how?
- For which case study will the glass column be designed?

Part III: Numerical and Experimental Investigations

- Are the samples transparent/robust and did cracks appear during/after the lamination process?
- How to manufacture samples for testing?
- How to set up the experimental test?
- What are results of the experimental tests regarding compression strength and the post-failure behaviour?
- How can the deviation between the numerical models/hand calculations and the experimental tests be explained?

The Outline

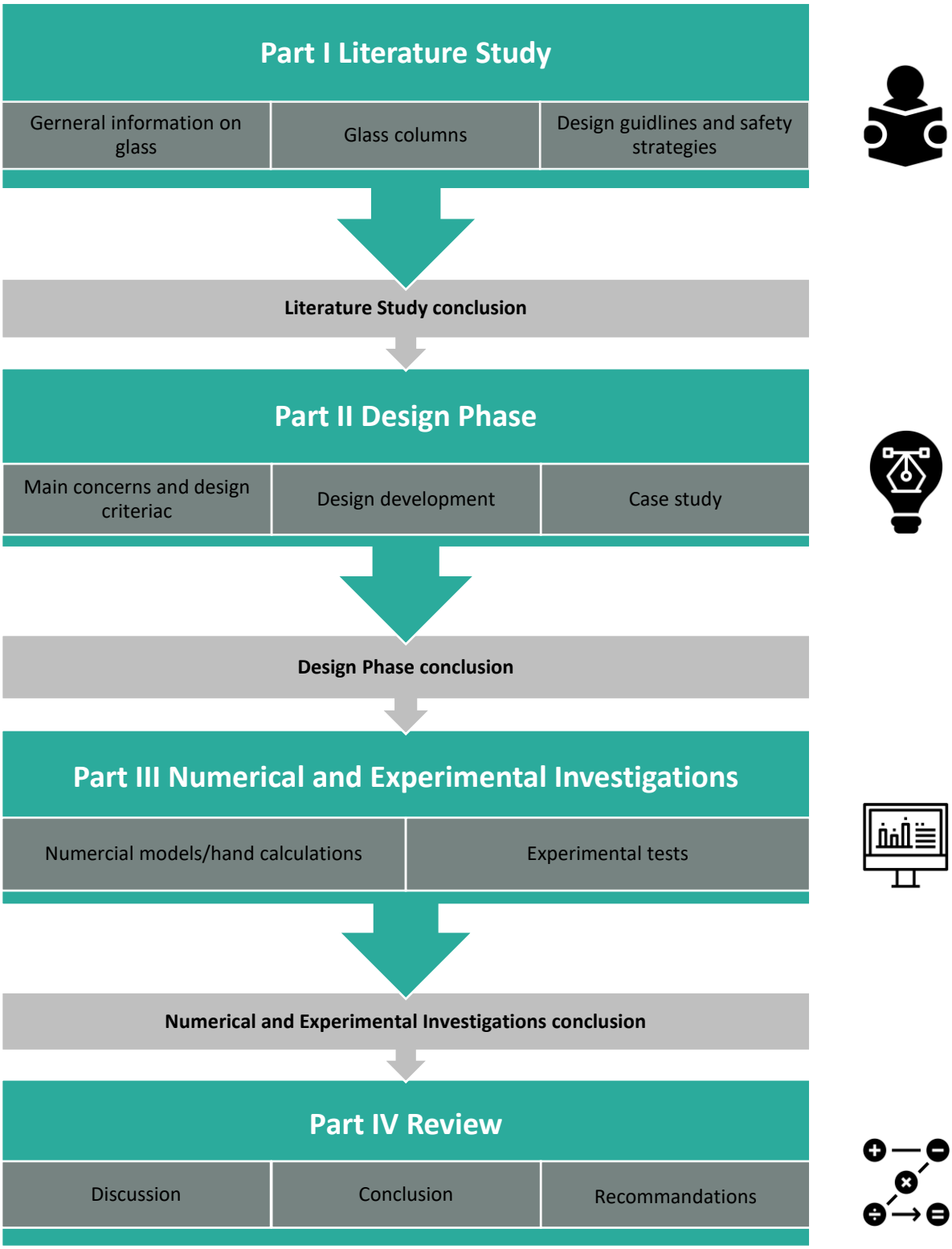

Figure 8 The Outline of this research (Own picture, with: Icons and Photos For Everything. n.d.).

Part I Literature Study

Part I Literature Study

2.1. General information on glass

2. Part I Literature Study

2.1. General information on glass

To understand how glass columns behave, first some research is done about the material glass.

2.1.1. History

As mentioned before, glass is one of the oldest manmade materials. The exact date of discovery is unknown, but it was discovered before BC. Some people say that the oldest glass found was made by Egyptians around 3500 BC (O'Regan, C. 2015). Others say that the first made glass came from Mesopotamia around 2000 BC (Corning Museum of Glass. 2002). They created small objects of glass. Around the 16th century, glass was used for jewellery or for hollow vessels. The Romans were the first who developed clear glass (O'Regan, C. 2015). Around 100 AD, a Roman writer wrote that glass was discovered by an accident by the Phoenicians. They stranded with their ship on a beach. They cooked dinner in a bronze pan on soda-lime rocks, on a fire. The next morning after the fire was extinguished, they found a glittering material, which is nowadays known as glass (Diehn, D. A. 1941). In appendix A2.1. a more extensive overview of the history on glass can be found.

2.1.2. Properties and types

Glass is transparent, and is made of non-transparent raw materials. It is an inorganic product. It has been cooled without crystallization. The liquids, to produce glass, are cooling fast that it avoids crystallization. So, glass is a non-crystalline (amorphous) product, and a crystalline product is named quartz (figure 9). When glass cools, the viscosity increases. This prevents the crystal growth. The silicon and oxygen ions are bonded together. These are the network formers. Network modifiers are ions of sodium, calcium, magnesium, etc. The molecular structure is complex, which makes glass unique and durable. Glass is an isotropic material without the crystalline lattice. It is a brittle material, because it is not yielding before fracture. (Overend, M. 2002). As can be seen in figure 10, glass gives a small decrease in the slope of the curve, this is the glass transition temperature (Tg). For crystalline materials, a discontinuous decrease of volume is shown when the melting temperature (Ts) is reached. Soda-lime glass is the most common group of glass. It consists of around 70% of silicone dioxide. Borosilicate glass is used for temperature-depending products (Haldimann, M., et al. 2008).

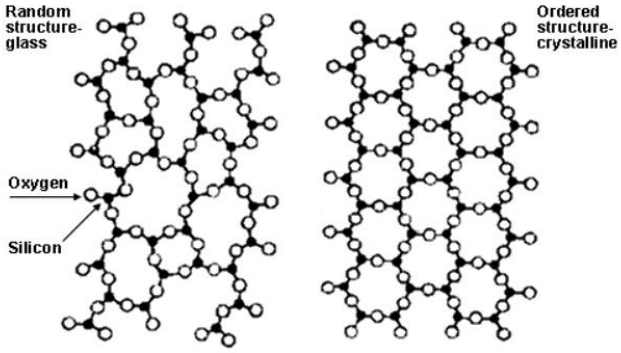

Figure 9 Amorphous and crystalline (TWI. 2020).

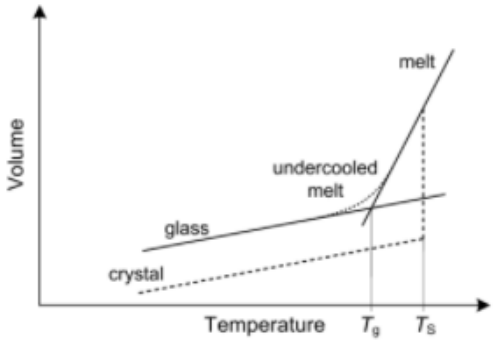

Figure 10 Comparison of volumes depending on temperature of glass vs crystalline material (Haldimann, M., et al. 2018).

The following raw materials are necessary to make glass: silica (SiO_2), lime (CaO) and sodium oxide (Na_2O). Silica is the main component. To obtain silica, several types of sand and rocks can be used. Silica has a melting temperature of approximately 1700 °C. In

addition to sand, lime needs to be included. Lime provides a certain hardness to the glass. To reduce the melting temperature, sodium oxide can be added. Furthermore, to obtain other properties of glass, several materials can be included to those three raw materials (Schittich, C., et al. 2017). Due to different compositions, there are several types of glass. In figure 11, different types of glass are given with its properties. Borosilicate glass has a good thermal shock and chemical resistance. It has a higher resistance for the occurring stresses by temperature changes, due to a lower coefficient of thermal expansion (Oikonomopoulou, F. 2019).

In figure 12, the viscosity versus temperature graph is shown for different types of glass. If the temperature changes, the viscosity of glass changes too. Glass becomes liquid at the melting point. The working point is when glass is deformed to a certain viscosity. This is important to know, when manufacturing the glass. The softening point is the maximum temperature that glass can be treated without changes in dimension. At the annealing point, the internal stresses can be relieved within 15 minutes. For soda-lime glass and borosilicate glass, this point is lower than for the other types. The transition temperature for glass is higher than the strain point. At the transition temperature, glass becomes rigid and can be fractured. Annealing is most time-consuming during manufacturing process (Elkersh, H. 2014).

Glass type	Approximate Composition	Observations	Typical applications
Soda-lime (window glass)	73% SiO_2 17% Na_2O 5% CaO 4% MgO 1% Al_2O_3	Durable. Least expensive type of glass. Poor thermal resistance. Poor resistance to strong alkalis (e.g. wet cement)	Window panes Bottles Façade glass
Borosilicate	80% SiO_2 13% B_2O_3 4% Na_2O 2.3% Al_2O_3 0.1% K_2O	Good thermal shock and chemical resistance. More expensive than soda-lime and lead glass.	Laboratory glassware Household ovenware Lightbulbs Telescope mirrors
Lead silicate	63% SiO_2 21% PbO 7.6% Na_2O 6% K_2O 0.3% CaO 0.2% MgO 0.2% B_2O_3 0.6% Al_2O_3	Second least expensive type of glass. Softer glass compared to other types. Easy to cold-work. Poor thermal properties. Good electrical insulating properties.	Artistic ware Neon-sign tubes TV screens (CRT) Absorption of X-rays (when PbO % is high)
Aluminosilicate	57% SiO_2 20.5% Al_2O_3 12% MgO 1% Na_2O 5.5% CaO	Very good thermal shock and chemical resistance. High manufacturing cost.	Mobile phone screens Fiber glass High temperature thermometers Combustion tubes
Fused-silica	99.5% SiO_2	Highest thermal shock and chemical resistance. Comparatively high melting point. Difficult to work with. High production cost.	Outer windows on space vehicles Telescope mirrors
96% silica	96% SiO_2 3% B_2O_3	Very good thermal shock and chemical resistance. Meticulous manufacturing process and high production cost.	Furnace sight glasses Outer windows on space vehicles

Figure 11 Glass types (Shand, E.B., et al. 1958).

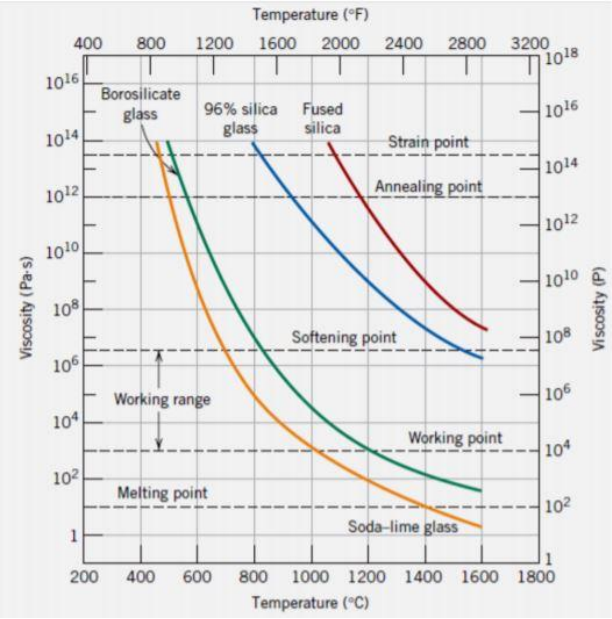

Figure 12 Viscosity vs temperature of different glass types (Elkersh, H. 2014).

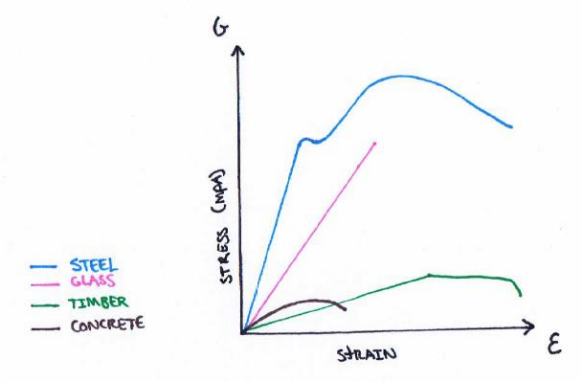

Figure 13 Stress-strain relation of glass, timber, concrete and steel

2.1.2.1. Mechanical properties

The mechanical properties for soda-lime and borosilicate glass are given in table 1:

Properties	Symbol	Unit	Soda-lime glass	Borosilicate glass
Density	ρ	kg/m^3	2500	2200-2500
Young's modulus	E	MPa	70000	60000-70000
Poisson's ratio	v	-	0.22-0.24	0.2
Coefficient of thermal expansion	α_T	10^{-6} K^{-1}	9	Class 1: 3.1-4.0 Class 2: 4.1-5.0 Class 3: 5.1-6.0
Thermal conductivity	λ	W/m*K	1	1
Emissivity	ε	-	0.837	0.837
Specific thermal heat capacity	c_p	J/kg*K	720	800

Table 1 Mechanical properties (Haldimann, M., et al. 2008).

Dislocating is prevented due to the lack of crystal lattice. In this way, there is no possibility that glass can have a plastic behaviour. The covalent bonding cannot be reshaped when it is broken. In this way, local stresses around the defect will result in a bond failure. The local stresses will increase. This means that if glass deforms, it deforms elastically, or it will break (Veer, F.A. 2007). In figure 13, the stress-strain relation is shown for glass in comparison with steel and timber.

2.1.3. Strength

As said before, glass has a large compressive strength, which can reach 1000 N/mm^2 (Saint-Gobain 2016). The theoretical tensile strength of glass 32 GPa. However, these strengths are not used in practise. The tensile strength of glass is depending on mechanical flaws on the surface, which means that lower strengths are used. In figure 14, the relation of flaw depth versus tensile strength is given. When the glass is loaded, flaws grow over the time. The tensile stress of glass is depending on many parameters, like: the condition of the surface, the size of the glass element, the duration of the load, the load actions, the residual stresses, the environmental conditions, etc. The surface flaw is not growing or failing due to

compression. Tensile stresses develop due to buckling and due to the Poisson's ratio effect at the loads. The compressive strength is much higher than the tensile strength, so the tensile strength will be reached far before the compressive strength (Haldimann, M., et al. 2008). The fracture tensile strength for soda-lime glass is 30-35 MPa, and for borosilicate glass is 22-32 MPa. The fracture compressive strength for soda-lime glass is 300-420 MPa, and for borosilicate glass is 260-350 MPa (Oikonomopoulou, F. 2019).

A crack results in a stress concentration on the glass surface. As shown in figure 15, the stress lines becoming curved due to the crack. By using the formula, which is shown in figure 15, an indication from stress concentrations can be determined.

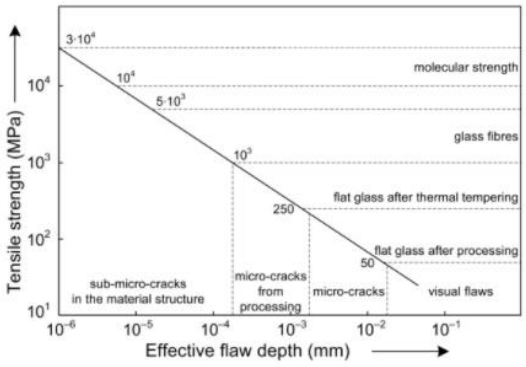

Figure 14 Flaw depth vs tensile strength of glass (Haldimann, M., et al. 2008).

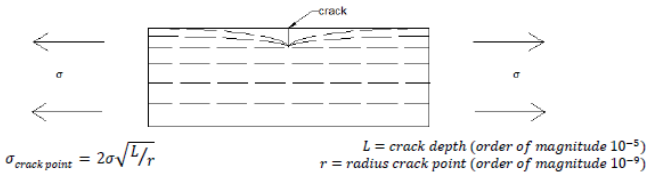

Figure 15 Crack and formula to determine stress concentrations (Ouwerkerk, E. 2011).

Figures 16 to 18 show the compressive strength, the tensile strength and the Young's modulus of soda-lime glass relative to other materials via CES Edupack. These figures are retrieved in 2017. As can be seen, the compressive strength of (soda-lime) glass is high comparing it to other materials. The tensile strength is lower compared to other materials, because it depends on many variables, which makes it difficult to determine.

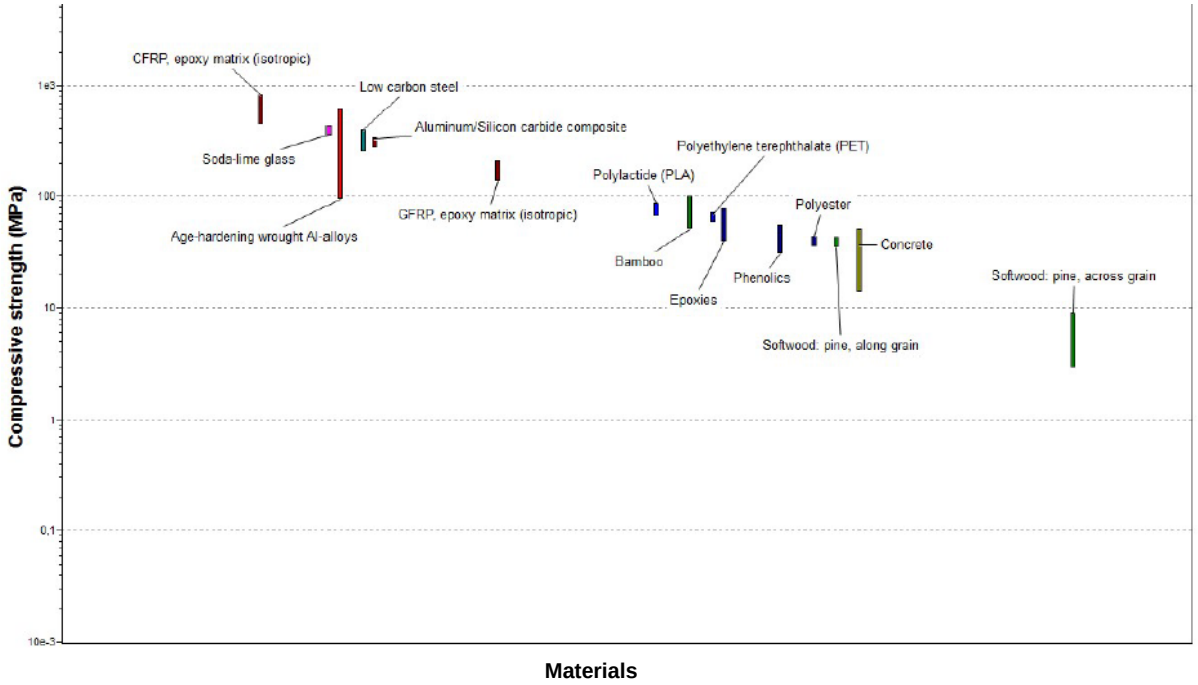

Figure 16 Compressive strength (Own picture via CES Edupack. 2017).

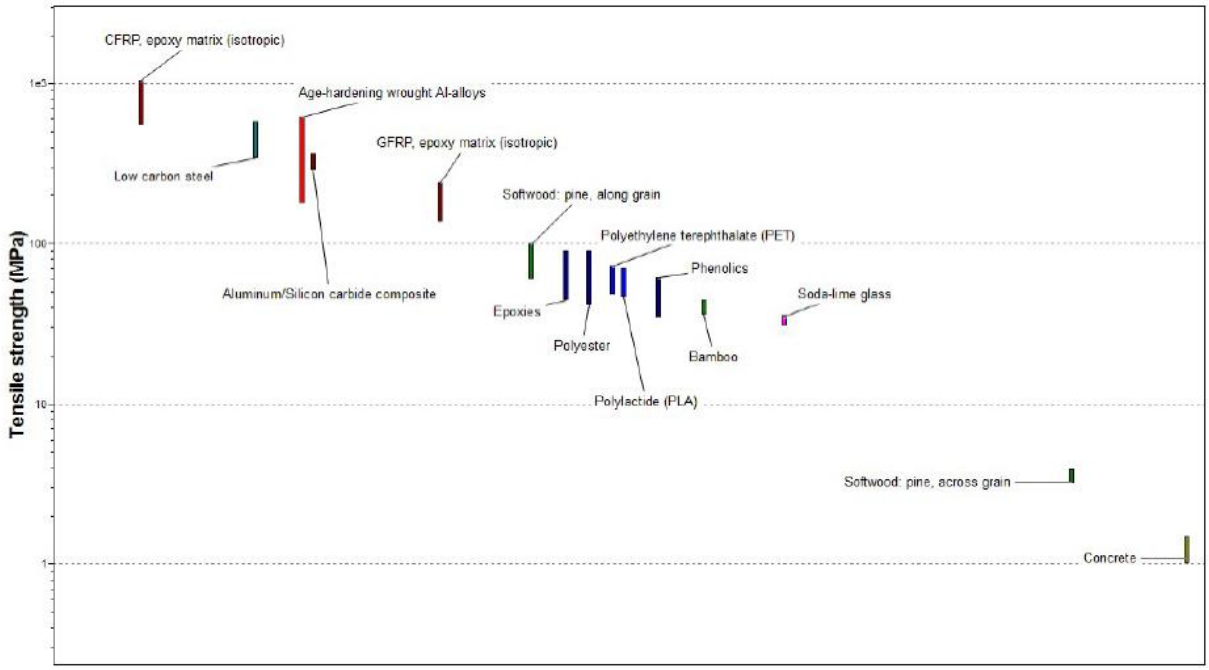

Figure 17 Tensile strength (Own picture via CES Edupack. 2017).

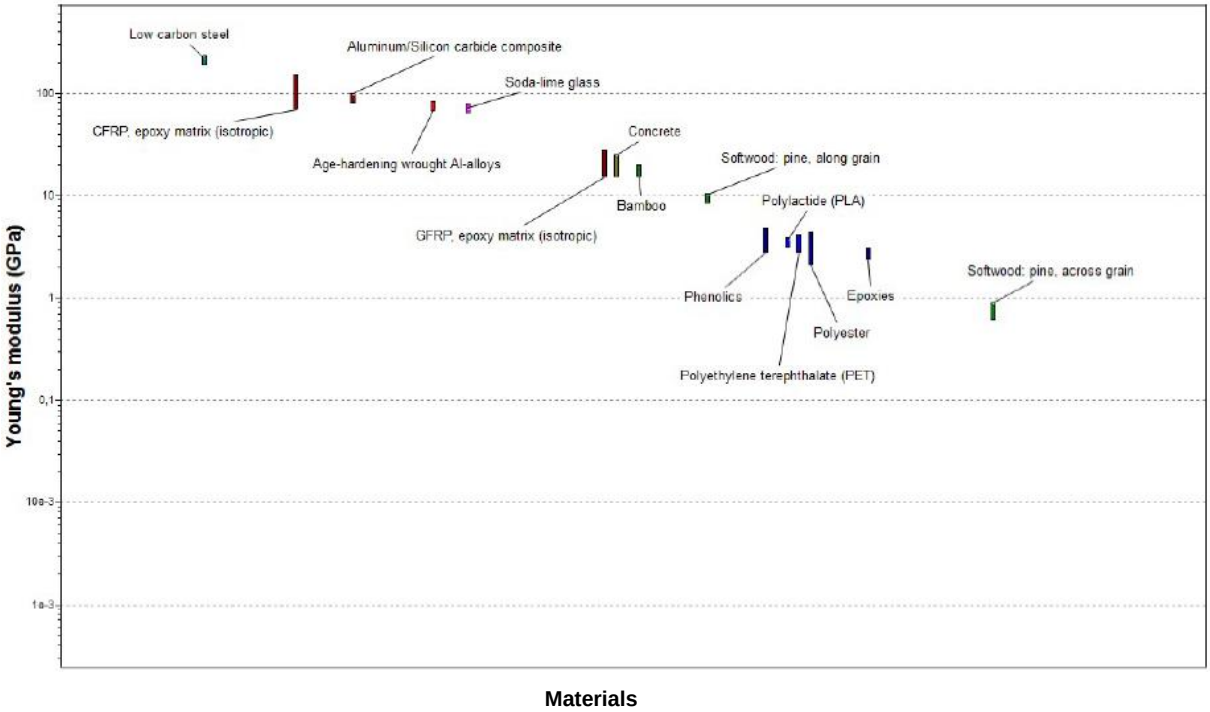

Figure 18 Young's modulus (Own picture via CES Edupack. 2017).

2.1.4. Manufacturing methods

There are two production processes: primarily and secondary. In chapter appendix A.2.2. different manufacturing methods are given, which are primarily processes. This research is focusing on glass tubes, so this chapter only elaborates on the extruding method.

2.1.4.1. Extruding

Extrusion is already used in plastic and metal industries, to create tubes and rod profiles. Glass tubes can also be made via the extrusion method (figure 20). There are two ways to

extrude glass: direct and inverted extrusion (figure 19). In figure a from 19, the direct method is presented for making rods. The material is contained by a cylinder, and is subjected to pressure due to the punch. The material is already heated up before going to be extruded, whereby its plasticity is increased. The shape of the die, determines the shape of the rod. The punch and the rod move in the same direction. Figure 19 b, schematised the direct method for tubes. The differences with a, is that a mandrel is fitted into the die. In figure 19 c, inverse extrusion is shown. A hollow punch is used, which is fixed to the die. The die will be pressured and it will move towards the material. In this way the material will go through the hollow punch. The compressed material is moving in the other direction than the punch. Direct extrusion is used more often, because inverse extrusion is more difficult (Roeder, E. 1971).

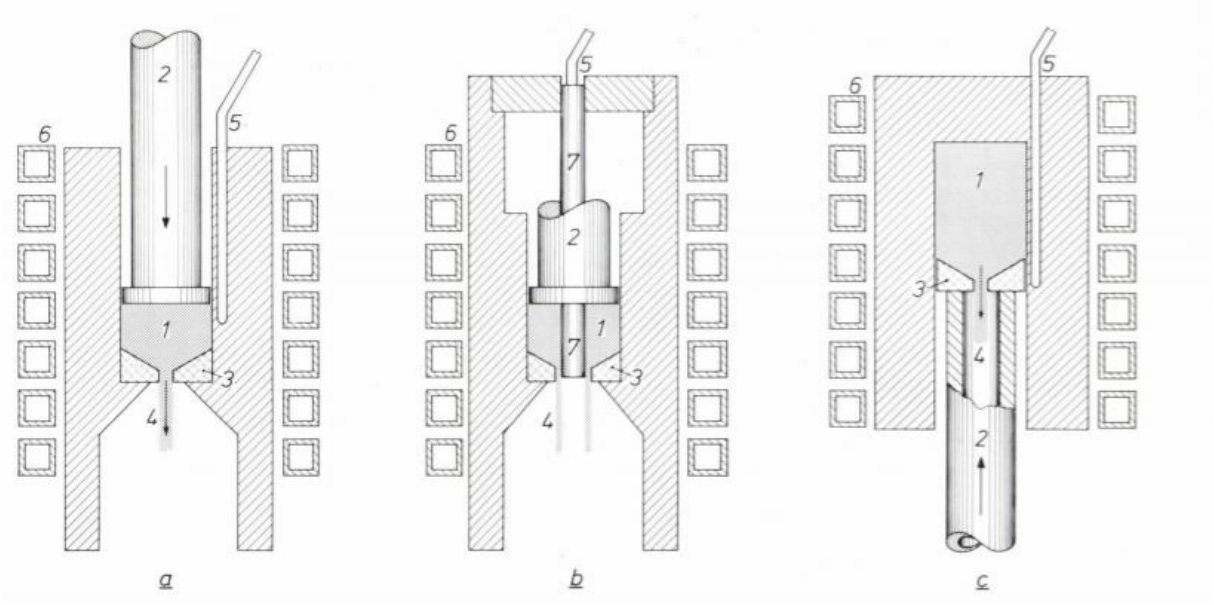

Figure 19 Direct and inverted extrusion. 1. Glass billet. 2. Punch. 3. Die. 4. Extruded product. 5 Thermocouple. 6. Coil for heat induction. 7. Hollow mandrel. (Roeder, E. 1971).

Figure 20 Extruded glass profiles (F&D Glass. 2014).

Not all types of glass are suitable for extrusion. This is depending on the viscosity of the glass. Figure 12, shows a viscosity versus temperature graph from different types of glass. Shaping processes have to take place within the 'working range'. Extrusion is only possible for a few types of glasses (Roeder, E. 1971).

The first type of glass which is suitable for extrusion is glass with a steep viscosity-temperature curve (short glasses). The small temperature range for working is inconvenient for shaping. Due to the extrusion pressure, shaping is possible with lower temperatures than usually needed, but then the glass is still very viscous. So, this means that the working range is extended for glasses with higher viscosities. For blowing, pressing and other manufacturing methods, it takes place in a working range with a viscosity of 10^3 and 10^7

poise. For extrusion, viscosities of 10^8 are manageable. These are called the short glasses (Roeder, E. 1971).

The second category of glasses suitable for extrusion, are glasses with a strong tendency to devitrify. Devitrification is the crystallization process in amorphous glass. Amorphous glass is free of crystals. The range of devitrification lies in the viscosity between 10^4 to 10^6 poise. This is the viscosity range where the common, manufacturing methods of shaping are happening. If the glass is unstable, devitrification can easily occur during the shaping process. Devitrification is undesirable. If the glass can easily devitrify can be shaped by extrusion by rapidly cooling of small pieces. In this way crystallization can be suppressed. When heating up the glass, before extruding, it is not needed to pass the critical ranges of crystallization, which lie above the softening temperature (the maximum temperature that glass can be treated without changes in dimension). However, due to the pressure, the temperature during extrusion, may stay below the maximum of crystallization. In this way the shaping is shifted into a range with lower crystallization rates (Roeder, E. 1971).

The crystallization of glass gives the maximum of the extrusion temperature. If the temperature is too low, glass is too viscous to extrude. If the temperature of the extrusion is above the softening point of the glass, grains are fusing. Air bubbles can be seen in the glass, due to evaporation during heating (figure 21). If the extrusion temperature is lower, the glass pieces do not entirely fuse, and crystallization is occurring at the grain boundaries (figure 22) (Roeder, E. 1971).

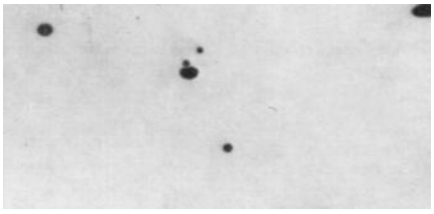

Figure 22 Air bubbles when the temperature is too high (Roeder, E. 1971).

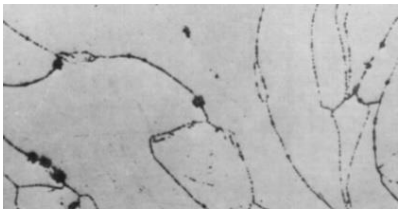

Figure 21 Crystallization when the temperature is too low (Roeder, E. 1971).

Furthermore, glasses with higher melting rates are suitable for extrusion. Shaping has to be done under higher temperatures. Lower pressing temperatures are needed for extrusion, so this can be better controlled (Roeder, E. 1971).

2.1.4.2. Producers

There are not many producers in the glass business, especially not with glass tubes. One leading company in the glass is SCHOTT AG. This company has firms worldwide. The one closest to the Netherlands is the branch in Mainz, Germany. The tubes that SHOTT produces are called DURAN® (SCHOTT. n.d.).

Besides the building industry, other industries are making more use of the applications of glass elements. Think about glass for art, lighting, electronics, labware, pharmaceutical products, bioreactors and for pneumatic conveying systems. The inventor of borosilicate glass is Otto Schott. This was used for gas street lamps. Soda-lime and lead glass was too weak for this application, so a new glass composition was invented, borosilicate glass. The name for these profiles became DURAN® in 1938. For now, it is still used for LED lamps, photovoltaic modules. Other glass types as aluminosilicate are used for halogen lamps and UV lamps. Nowadays in 2020 - 2021, they are busy with glass products to store the Corona vaccine in borosilicate glass containers (SCHOTT. 2020).

By 2021, SCHOTT wants to have 100% of its electricity from renewable energy sources (SCHOTT. 2020). In appendix A.2.4. more on sustainability is discussed.

2.1.5. Increasing strength

As said before, glass is brittle. So, it breaks easy when exposed to impact, external forces or temperature changes. Some treatments are given in this chapter to strengthen the glass to get higher strengths and decreasing chances of risks. Furthermore, there will be a look into breaking patterns. In this chapter the secondary processing is given. Within the secondary process, the product will be further shaped and the product can be made safer. Some of these are: cutting, edge working (arising, grinding, polishing), hole drilling, curving, coatings, thermal treatments, laminating of glass, etc. (Haldimann, M., et al. 2008). The treatments which were not used in this project, are descripted in appendix A.2.3.

2.1.5.1. Strengthening

There are four types of strengthened glass created by thermal treatment: annealing, tempered/fully tempered (fully toughened), heat strengthening, and chemical toughened (O'Regan, C. 2015).

In 1900 chemist Seiden R.A. secured a patent on thermal treatment. He invented that the glass became stronger by cooling the surface more rapidly than the centre. The strength of toughened glass comes from the surface compression strength (O'Regan, C. 2015).

Annealing is the most standard treatment which is implemented in most of today's production process (float glass). This is a process of gradually cooling of the glass element. In this way, the inside of the glass element cools the same way as the outside. This results in elastic behaviour during the cooling process until fracture. It prevents uneven stresses and formation of the glass. After the process, cutting of the glass is still possible. Furthermore, annealed glass is sensitive for thermal shock. It can result in cracking of the glass, because of the internal stresses due to temperature differences (O'Regan, C. 2015).

Heat-strengthen is also called semi-tempered or partially toughened. After producing annealed glass, it is heated up to 620 °C. Then it is re-heated to the same temperature and cooled rapidly by cool air. If the interior cools, it tries to shrink. This results in increasing tension stresses, which gives compression stresses to the surface of the glass element (figure 23). The surface compression stress for heat-strengthening glass varies between 24 to 52 N/mm^2. Because of nickel sulphide impurities, heat-strengthened glass is less sensitive to failure than tempered glass. Heat-strengthened glass and tempered glass has a better resistance to thermal shock than annealed glass (O'Regan, C. 2015).

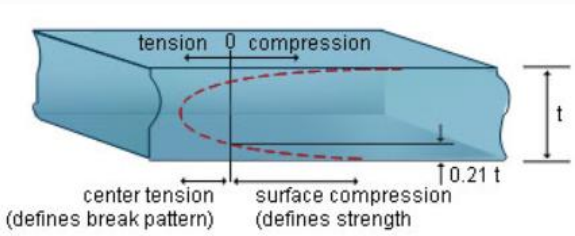

Figure 23 The internal stresses in a tempered glass pane (Glass Academy. 2016).

Tempering (toughening) has a similar process as heat-strengthened glass, but it is cooled more rapidly. First the surface is cooled and then the interlayers, which results in shrinkage. In this way tensile stresses are in the centre and the surface has compression stresses again. The surface stresses for tempered glass are between 80 and 150 N/mm^2. The glass has a better bending resistance. Surface compression can be measured by fragments. The higher the surface compression strength, the more fragments. Another technique to measure the surface compression strength is by using optical instruments. Cutting and grinding of the glass must be done before the toughening process. If the surface is scratched by 20% of

depth, the crack will go through the tensile zone, the glass pane will shatter. Surface cracks in the compression layer will be closed by the compression stresses until the external tensile stress exceeds internal the compression stress. Where the annealed glass pane breaks, the tempered glass does not break due to the higher compression strength (figure 24). So tempered glass has a better impact resistance than annealed glass (O'Regan, C. 2015).

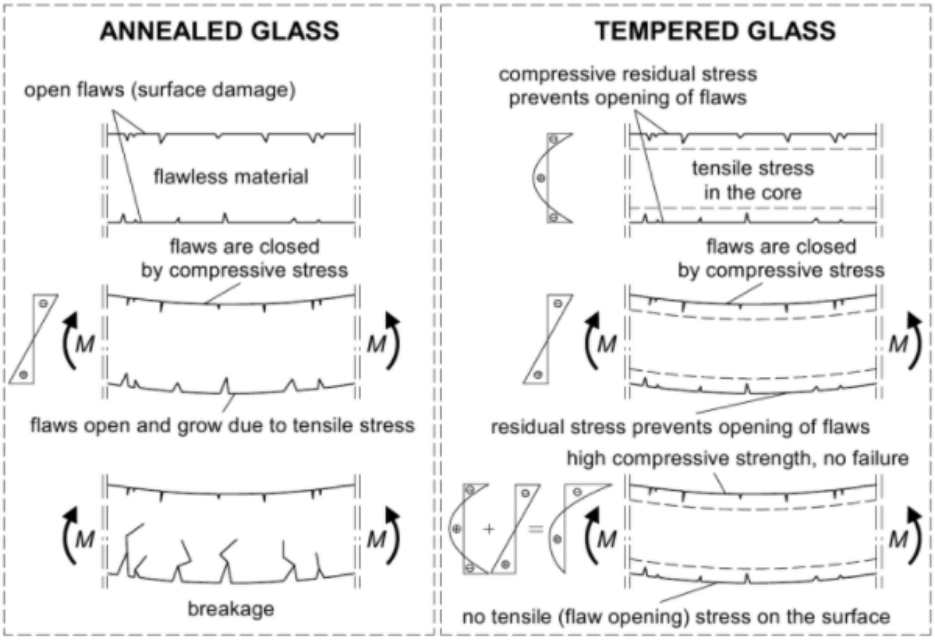

Figure 24 Crack development for annealed and tempered glass due to flaws in the surface (Haldimann, M., et al. 2008).

In order words, to prevent glass from breaking due to the low tensile strength, the glass is over-compressed by tempering. In this way, first the compressive strength needs to be dealt with, before the tensile stress can be built up in the glass. (Weller, B., et al 2009). In figure 23 an internal stress diagram is given for a tempered glass pane. The tensile stress is the stress in the centre and the compression is the surface stress. The compression stress determines the strength of the glass pane and the tensile stress defines the break pattern (O'Regan, C. 2015). In figure 25 the stress diagrams are given for the other treatments as well.

Chemically toughened glass is not often used in the building industry, but is more used for very thin panes and not common shapes of 3-dimensional objects. With this method, the glass object is dipped into an electrolysis bath. In here sodium ions on the surface are being exchanged for potassium ions. These potassium ions are three times bigger than the sodium ions. This results in compressive stresses. Advantage is less deformation during the process and thinner sheets can be treated. Disadvantages are thinner surface compressive layers. In this way the glass panes are less robust than with toughening the glass, and it is more expensive (O'Regan, C. 2015).

These different treatments results in different breaking patterns, which is shown in figure 25. On the left, annealed glass is shown, which breaks in large pieces. This can result in injuries. The second one, is heat-strengthen glass. At the third picture fully, tempered glass is shown. This type of glass breaks into small pieces. On the right, chemically tempered glass is shown. The breaking pattern of chemically tempered is not much different than from heat-strengthened glass, but the stress diagram is different. In the case of chemically tempered glass, there is more compressive stress, and almost no tensile stress anymore.

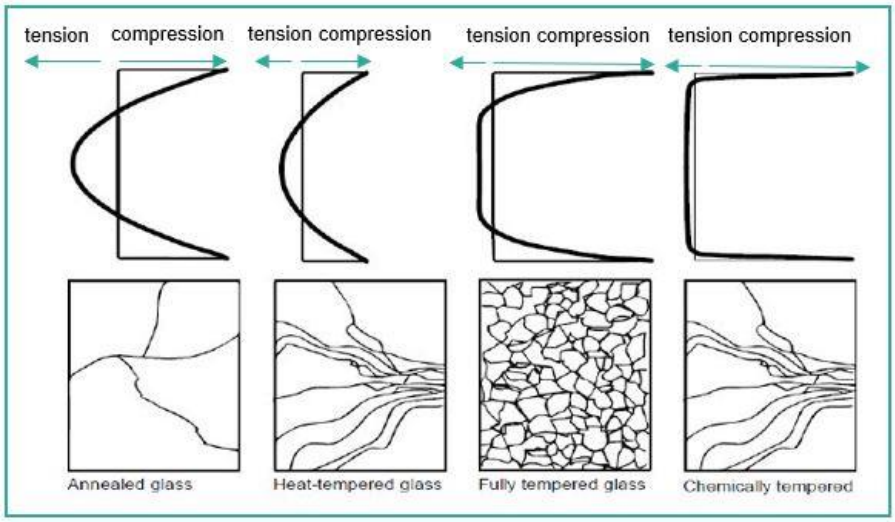

Figure 25 Breaking patterns with stresses (Van der Velden, M. 2019).

SCHOTT also produces heat-strengthened glass tubes, called DURATAN® (SCHOTT. 2021).

2.1.5.2. Lamination

Multiple layers of glass can be bonded together through lamination. Lamination can be done by a transparent glue/resin or by a foil interlayer between the glass panes. In figure 26, the different applications of glass products are shown. Without any lamination, it is a monolithic glass pane. There are three options:

- Air/gas, to insulate;
- foils/resin/glue, to make it safer;
- intumescent interlayers, for fire protection.

In chapter 2.2.2.5. and 2.3.3, the intumescent interlayers will be further explained. The IGU's are not relevant for this thesis project. In this chapter the principle of the laminated safety glass, and types of interlayers will be further explained.

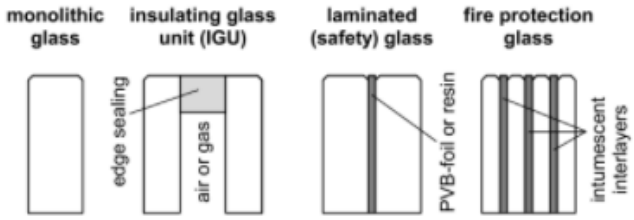

Figure 26 Glass products (Haldimann, M., et al. 2008).

The interlayer keeps the panes together. Even though the glass is stronger due to tempering, glass is still a brittle material. Lamination can improve the post-breakage behaviour. By these multiple layers, the strength can be increased of the element, as long as the adhesive or the foil can transfer the forces in the element, so that all the panes work as one (Haldimann, M., et al. 2008).

In figure 27, is shown that the layers are stronger while working together than separately. In this behaviour, there is an upper limit and a lower limit. In the upper limit the panes are working completely together (in here the adhesive/foil is working well), and in the lower limit the panes are not working together (in here there is no adhesive/foil present). The collaboration of the panes is depending on the shear stiffness of the interlayer. The interlayer

has a viscos-elastic property. Due to this, the load carrying behaviour is also depending on the temperature, the load duration, and the type of loading (Blaauwendraad, J. 2007). For short-term loading, there is a maximum cohesion between the layers. With long-term loading, sheet lamination between the glass panes will lose its maximum contact. If the temperature is above 50 °C, there will be no connection between the glass panes (O'Regan, C. 2015).

Interlayers can shrink, which can lead to void formation in the resin. This results into reduction of the optical quality, and shrinkage can give stresses in the glass which can lead to failure (Veer, F.A., et al. 1999).

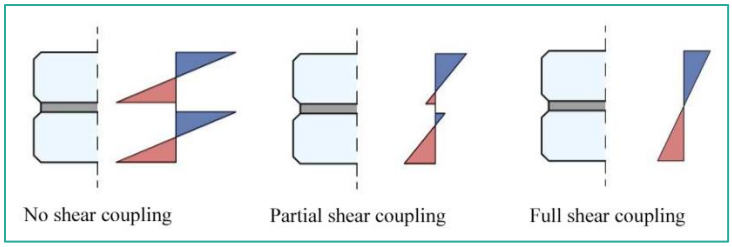

Figure 27 full coupling (upper limit) and no coupling (lower limit) for laminated glass panes (Hänig, J., et al. 2019).

It gives a redundancy to the glass element. If one pane breaks, the other(s) are still able to carry the loads. In figure 28, the breaking patterns are shown from annealed, tempered, and laminated glass panes. With laminated pane, the broken pieces are sticking to the interlayer, which results in less injuries, and the broken layer can protect the glass layers which are not broken. The layers can be put together in an autoclave. The autoclave heats the plates and takes the air out to bond them together (O'Regan, C. 2015).

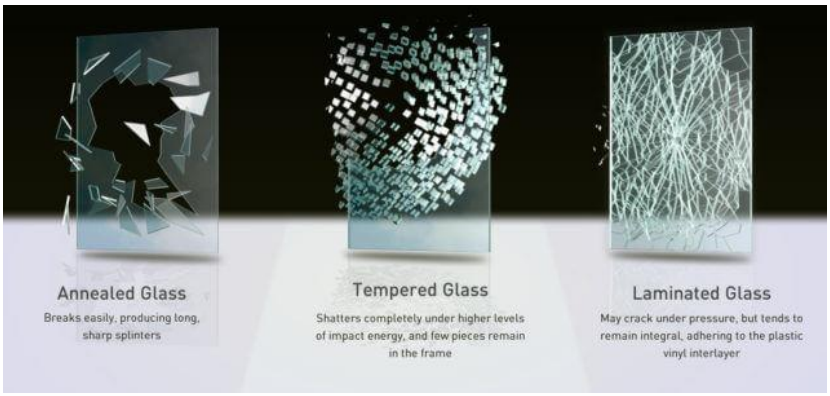

Figure 28 Breaking patterns of annealed, tempered, and laminated glass panes (Crystalia Glass Architectural glass & metal. 2020).

In 1910 laminated glass was developed. The oldest concept was with a celluloid plastic sheet in between to glass plates. Nevertheless, this plastic sheet had had a poor resistance against moisture. Due to the durability issues, the concept was not used anymore in the 1930s. Somewhere in 1950, a new interlayer was introduced: polyvinyl butyral (PVB). This material had a sufficient moisture resistant as was more durable. This was used in the automotive industry and in 1970 it was used in the building industry. After that another interlayer was developed: thermoplastic polyurethane (TPU). This is also used for trains and aircrafts, because of the high impact resistance. This resistance is created by using TPU to attach a layer of polycarbonate onto the glass. Furthermore, there is Ethyl vinyl acetate (EVA). This doesn't have to be cured into an autoclave. It is stiffer than PVB, but more expensive. In 1998 a new interlayer was created by DuPont, called SentryGlas Plus (SGP). Until now, this is the stiffest and the strongest interlayer material there is. However, for all of this interlayers, it has a reduced loading resistance. In 2004 polyester (PET) were developed. With this

material, it is possible to have light-emitting diodes (LED) within the glass (O'Regan, C. 2015).

So, there is sheet lamination: PVB, EVA, and ionoplast (SentryGlass). PVB is most commonly used. Furthermore, to laminate tubes for example, an interlayer resin can be used, like: acrylic, polyurethane (TPU) and polyester (PET). The glass elements are hold with a distance from each other and the resin will be poured in between. When the air is gone, the open edge is sealed. Curing of these resins can be done by a chemical reaction or via ultra violet light (O'Regan, C. 2015).

2.1.5.3. Surface treatment

In the production process, glass will be cut into pieces to obtain the right size, or holes will be drilled in the glass element. This can result in sharp edges or imperfections. The edges can be treated to reduce these imperfections. Glass can be treated to obtain decorative effects, for example by: enamelling, acid etching, and sand-blasting. Furthermore, glass can be treated for functional reasons by: edge finishing and coatings.

2.1.5.3.1. Enamelling, acid etching, and sand-blasting

By enamelling, a coloured layer will be applied to the glass surface. After that it will be baked into the glass during the toughened or the heat-strengthened process. The layer can also be sprayed onto the glass. A matt finish can be given to the glass by acid etching. The glass surface is treated by hydrofluoric acid. Patterns and figures can be etched into the surface. A degree of intensity of the etching process gives the roughness of etching the glass. The result of sand-blasting is comparable to the results from acid etching. The elements of glass are getting blasted by tiny sand particles at a high speed (Haldimann, M., et al. 2008) (Schittich, C., et al. 2017).

2.1.5.3.2. Edge finishing

After cutting the glass, the glass can be post-processed. In figure 29, different edge finishing works are shown. (In this figure, FT means fully tempered glass and HS means heat-strengthened glass.) The first one is the simplest. These edges are used if the glass is placed in a frame, where there is no danger of injuries by the sharp edges. The other edge types are obtained by polishing and grinding. Other applications where glass can be used are for: mirrors, balustrades, decorative furniture, structural glass elements, etc. (Schittich, C., et al. 2017).

2.1.5.3.3. Coatings

There are two types of coatings which can be used to change the properties of glass: hard coatings (on-line coating) and soft coatings (off-line coating). Hard coatings are burned on the glass and become part of the structure and soft coatings are coatings on the glass by ionized metals. These types of coatings can be used to modify properties as light and heat transmitting, or visual appearance. For the improvement of thermal performances, metal oxides or nitrides can be applied to the glass. This can be done by the use of magnetic sputtering (soft coatings). To improve the durability of the glass, pyrolytic coatings (hard coatings) can be applied. (Haldimann, M., et al. 2008) (Schittich, C., et al. 2017).

A hard coating can be applied to the glass in the annealing lehr, while the glass is still fluid. It is applied by using a chemical vapour deposition process. The hot glass is exposed to a gaseous chemical mixture, which results in a pyrolytic reaction. The used materials for the coatings can be pre metals and oxides. In this method, the coating has a stronger bond to the glass. Another alternative method for hard coating is dip coating. The coatings are hard, scratch resistance, and bendable. It reduces the light and energy transmittance through the glass. These types of coatings are more durable than soft coatings, but less flexible. These

coatings are used for reflective glass, solar controlled glass, thermally insulating glass and self-cleaning glass. (Haldimann, M., et al. 2008) (Schittich, C., et al. 2017).

With soft coating, the coating is applied in a secondary process, after cutting the glass. It can be done by dipping, chemical or physical vacuum deposition processes. The most common used method is magnetron sputtering, which is a physical coating process. These coatings cannot be used in aggressive environments, and it is not resistant to mechanical damage. This is why the coating often needs a protective layer. These coatings can be used to create low-emissivity glass (Haldimann, M., et al. 2008) (Schittich, C., et al. 2017).

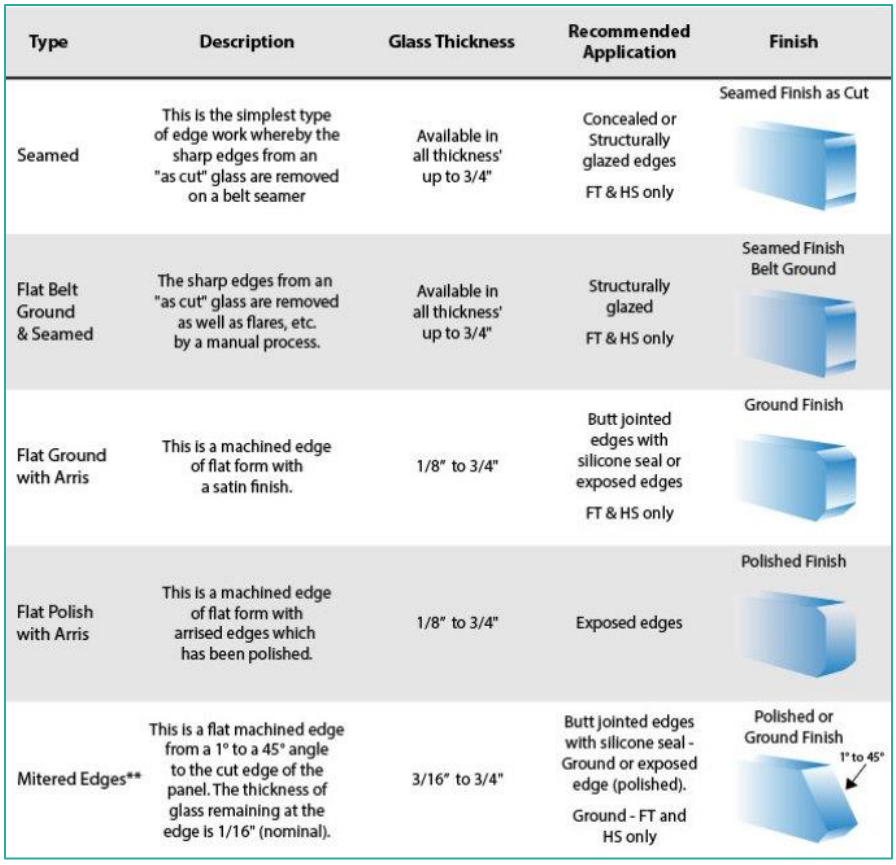

Figure 29 Edge finishing (Viracon. 2020).

2.1.6. Limitations and tolerances

Size limitations need to be taken into account, due to transportation limits. If special transport is needed, it will be more expensive. Furthermore, there are limitations for the lamination of glass panels. For panels longer than 16 metres, it will not fit in a standard autoclave.

Geometric tolerances need to be taken into account as well. Due to manufacturing tolerances, the thicknesses of (float) glass plates are often less. In the table below, tolerances are given for float glass plates. The tolerances on nominal dimensions for the length and the width are about 5 mm (BS EN 572-2. 2012).

Nominal thickness [mm]	3	4	5	6	8	10	12	15	19	25
Tolerances on thickness [mm] ±	0.2	0.2	0.2	0.2	0.3	0.3	0.3	0.5	1.0	1.0

Table 2 Tolerances of flat panes (BS EN 572-2. 2012).

For extruded profiles distortion play a role when profiles become longer. The longer the tubes become, the bigger the geometric tolerances will be. This needs to be taken into account.

Especially when the tubes need to be put into each other. The tolerances of the glass also are influencing the interlayer resin in between the tubes, because the thickness will vary.

2.1.7. Conclusion

Glass is a non-crystalline (amorphous) inorganic product, which is cooled before crystallization. Glass has a transition temperature. Glass is made from raw materials, which are the network formers. The raw materials needed for the composition are: silica, lime, and sodium oxide. To obtain certain properties other materials can be used. These are the network modifiers. Borosilicate glass has a higher resistance for the occurring stresses by temperature changes than soda-lime glass, due to a lower coefficient of thermal expansion. Glass has a large compressive strength, which can reach 1000 N/mm^2. The theoretical tensile strength for glass can reach 32 GPa. Nevertheless, the practical tensile strength is lower than the compressive strength, because the tensile is depending on the many parameters, as surface conditions (flaws), sizes of the element, load duration, residual stresses, and the environmental conditions.

There are several manufacturing methods to make products of glass, as: casting, blowing, pressing, floating, drawing, rolling, and extruding. This is called the primary process. The manufacturing method for glass tubes is the extrusion process. Suitable glass types for this are when they have a steep viscosity-temperature curve, a strong tendency to devitrify, or glasses with higher melting rates. One of the leading companies in producing glass tubes is SCHOTT AG.

Glass is a brittle material. There are a few methods to increase the strength of glass. A few methods are applicable for glass tubes: thermal treatment and lamination. Besides that, the glass product can be further shaped, by surface treatments, as cutting, edge working, hole drilling, curving, and by the use of coatings.

Part I Literature Study

2.2. Glass columns

2.2. Glass columns

First, columns in general and corresponding failure mechanisms were looked at. After that the different types of glass columns were researched. Then different types of (end) connections were looked at. Lastly several properties were compared between the different types of glass columns in a Multi-Criteria Analysis (MCA).

2.2.1. Columns

In the Encyclopaedia, the column is described as a supported vertical element. Most often it has a round shaft, a capital and a base (Britannica. n.d.). The difference with a wall and a column is that a column buckles about two axes, and a wall only on one axis. A column can be used as a structural or as a decorative element. Columns can be incorporated within walls or can be freestanding. Columns can create large open spaces. Nowadays columns are mostly made from steel, concrete, and wood. Glass is not much used as a structural material. In appendix A.2.5. more information is given on the history of columns.

2.2.2. Failure mechanisms

There are two types of failure: material failure and configuration failure. When the stresses exceed the allowable values, then material failure occurs. When the stresses are within the allowable values, but the structure is not capable of keeping its original configuration, configuration failure occurs. This type of failure can also be called buckling. (Gambhir, M.L. 2004). If a compression force is applied in axial direction on the glass column, the column deforms elastically and fails out of a sudden. The failure can be caused by elastic instability or by a lateral load, like imperfections. The lateral load can cause bending on the surface due to eccentricities. This can result in tensile stresses.

2.2.2.1. Stability

The stability is related to the reliability of the balance. If the balance is unreliable, the structure is unstable. The danger to instability is mainly the case of slender structures subjected to pressure. This pressure will increase the initial deformation. Instability can also occur as a result of shear forces and torsion. In this chapter, among other thing, different types of instability are given (Hartsuijker, C., et al. 2016).

In figure 30, three types of balance are shown: stable equilibrium, unstable equilibrium, and neutral equilibrium. The G in the figure, is an object with a weight. An equilibrium is stable if the system tends to return to its original equilibrium position (a). Dynamic events, which can lead to distortions in the balance, need to be within the limits. If it is within the limits, the system will return to its original position. If the system tends to go further away from its original position and does not come back, the equilibrium is unstable (b). When there is a neutral equilibrium, all equilibrium positions are possible (c). It will not return the original position by itself (Hartsuijker, C., et al. 2016).

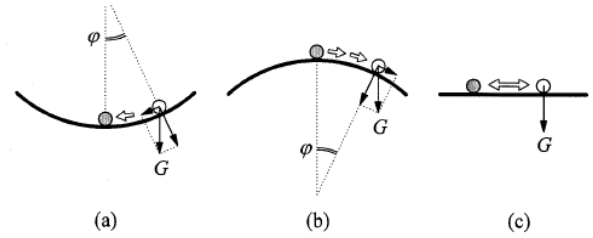

Figure 30 Types of equilibrium (Hartsuijker, C., et al. 2016).

In linear mechanics, the equilibrium equations are applied on the geometry of the undistorted construction. No deformation is occurring. This is a first order calculation. The stability

research needs to consider how the balance will change if the structure from the original position changes to another position. So, stability is depending on the relation between the load and the deformation. This is called non-linear mechanics, or second order calculation or a buckling analysis (Hartsuijker, C., et al. 2016).

2.2.2.2. Buckling

Columns are slender elements, which can bend. Due to its slenderness, columns can be exposed to buckling (bifurcation buckling). Due to a compression force, the column can become instable and can buckle. If the force becomes too large, the column can fail. This force is called the critical buckling load. In practise, the critical load can never be reached due to imperfections in the linearity of the column, and/or eccentricities of the applied load (imperfect column buckling). The larger the compression load, the more deformation occurs. When the maximum stresses in the material are reached due to the lateral deformation, the maximum load is obtained. Performing a buckling test, the load versus displacement graph (figure 31) can be obtained. Before the critical load (black dot in the curve) is reached, the curve shows a linear elastic behaviour. So as said before, the ultimate strength is can only be reached as the column is perfectly straight (Luible, A., et al. 2004).

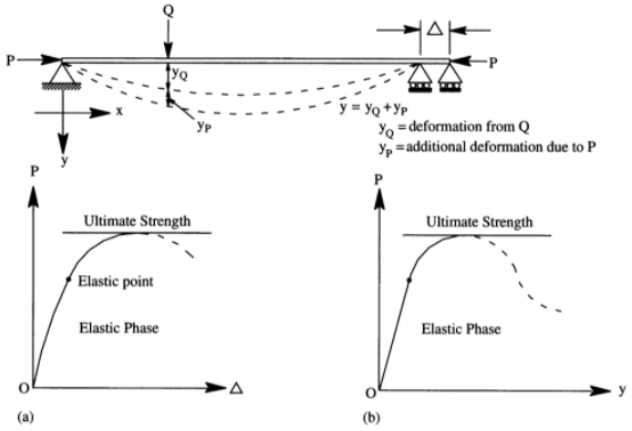

Figure 31 Load versus displacement curves (Gambhir, M.L. 2004).

In figure 32, the load versus displacement curve is represented for a glass laminated column. With a small imperfection the column will come closer to the ideal column line in the graph. So, a bigger imperfection will follow the imperfect column curve.

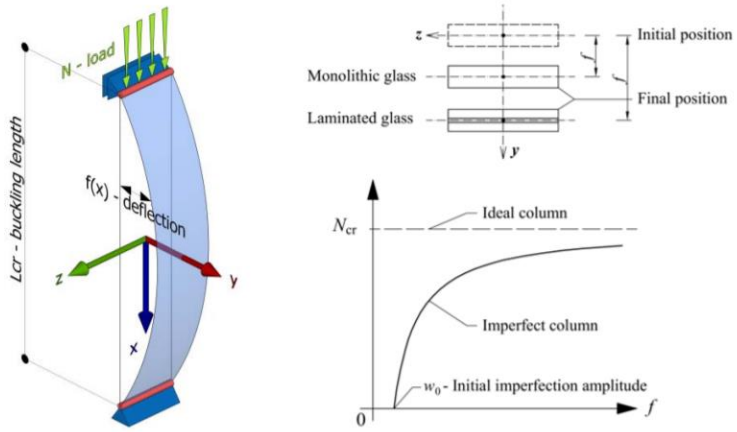

Figure 32 flexural buckling of a glass column and the load versus displacement curve for a perfect and imperfect column (Pešek, O., et al. 2017).

The elastic critical buckling load can be calculated with the following Euler formula:

$$F_{cr} = \frac{\pi^2 * E * I}{(K * L)^2} \qquad (1)$$

With:

- F_{cr} : critical buckling load [N]
- E : Young's modulus (depending on material properties/type of glass) [N/mm^2]
- I : moment of Inertia (depending on the cross-section) [mm^4]
- K : effective length factor (depending on boundary conditions/supports) [-]
- L : length of the column [mm]

So, when a glass column fails it is depending on: the glass thickness, the initial deformation, the viscoelastic interlayer used for laminated safety glass, and the load eccentricity, the breakage stress of glass, and the degree of damage of the glass surface. The viscoelastic interlayer acts as a shear connection between the glass layers with a certain shear modulus (G). The breakage stress of the glass depends on the type of glass. The embedded compressive surface stress due to tempering is different per type (Luible, A., et al. 2004).

A buckling curve can be created to investigate the relation between the slenderness versus the buckling load or the maximum compressive stress (figure 33). If the column is very slender, it will fail by buckling. If the column is not slender, the material failure is leading. The slenderness of the geometry can be determined by the following formula. For glass, the maximum tensile stress is leading, because the compression does not limit the buckling strength (Luible, A., et al. 2004):

$$\lambda_k = \pi * \sqrt{\frac{E * A}{F_{cr}}} \qquad (2)$$

With:

- λ_k : slenderness [-]
- E : Young's modulus [N/mm^2]
- A : cross-sectional area [mm^2]
- F_{cr} : critical buckling load [N]

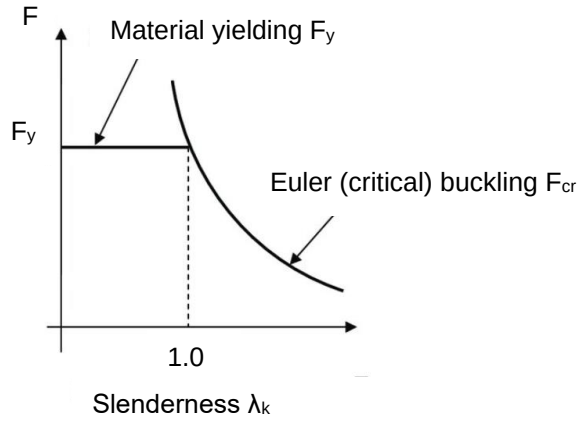

Figure 33 Buckling curve: load vs slenderness.

If the slenderness reached 1.0, the buckling stress is independent of geometry, but it depends on the material properties. This curve can also be determined for maximum compressive stress for the material. With the following formula, the force can be converted to the stress:

$$\sigma = \frac{F}{A} \qquad (3)$$

With:

- σ : stress [N/mm^2]
- F : force [kN]
- A : cross-sectional area [mm^2]

When calculating the critical buckling load for laminated glass with an interlayer, the shear connection from the interlayer has to be taken into account. In figure 45, the formulas are given (Luible, A., et al. 2004).

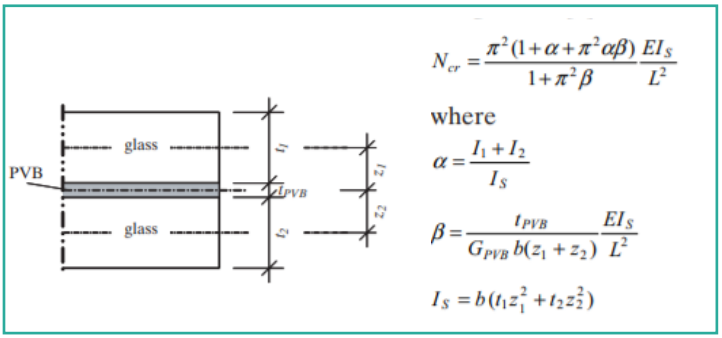

Figure 34 The formula for the critical buckling load for laminated glass (Luible, A., et al. 2004).

2.2.2.3. Torsional buckling

Torsional buckling can occur when the cross-section has a low torsional stiffness and a large bending stiffness. This can be the case for thin-walled cross-sectional profiles. Under a compression force, the column can twist (figure 35) (Hartsuijker, C., et al. 2016). Torsion is a different phenomenon than torsional buckling.

A cross-section with a maximum torsional rigidity is a circle, and closed cross-section profiles are stiffer to torsion than open cross-sections (Rees, D.W.A. 2009). In 2005, Overend, M., et al did research into torsional buckling on cruciform glass column, since a cruciform cross-section is susceptible to torsional buckling. In this article is also mentioned that tubular columns are more susceptible to flexural buckling (Overend, M., et al. 2005).

Torsion occurs without a compressive force, but it results in a twist due to a moment.

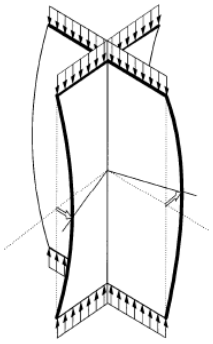

Figure 35 Twisting of a column (Hartsuijker, C., et al. 2016).

2.2.2.4. Thermal stresses

With thermal stresses, the material can fail. Due to temperature differences, internal forces can occur. There can be a temperature difference on the glass surface, and between the inner and outer surface of the glass. Besides that, a temperature difference can occur

between centre and the edge of the glass element. Glass can crack if the thermal stress exceeds the critical stress. Thermal stresses are depending on external and internal aspects. External factors could be the location and the orientation of the building, and internal factors could be the type of glass, the edge quality, the framing material, the size of the elements, etc. So, annealed glass can withstand a temperature difference limit of 40 °C, tempered glass can resist 200 °C, and heat-strengthen glass 100 °C (O'Regan, C. 2015).

When the temperature increases, the air pressure will increase as well. This relation is formulated in the ideal law of Boyle and Gay-Lussac (equation 4) (Hadiningrum, K., et al. 2018). If the differences in the air pressure becomes too large, internal stresses will occur and the glass will crack.

$$p * V = n * R * T \qquad (4)$$

With:

- p : absolute pressure of gas [N/m^2]
- V : volume [m^3]
- n : amount of gas [mol]
- R : universal gas constant [8.314472 $J*K^{-1}*mol^{-1}$]
- T : absolute temperature [K]

In a closed system, isochoric pressure can occur. If the air in this closed system is heated up, then it expands, and it wants to get out of the column. In this situation there is a low air pressure around the glass element. If the air is been cooled down, the pressure will be lower inside the closed system than outside (figure 36). In this case the risk of condensation increases, and it can result in stresses in the glass (GPD Glass Performance Days. 2020). If the warm air cools down below the dew point temperature, water vapour will begin to condense to a liquid phase (Van der Linden, A., C., et al. 2018). If the air is heated up, the pressure will be higher inside the column than outside. Due to this the air outside attracts air from the inside. Due to these temperature differences inside and outside, stresses occur in the glass. Cracks can occur due to these stresses. (GPD Glass Performance Days. 2020).

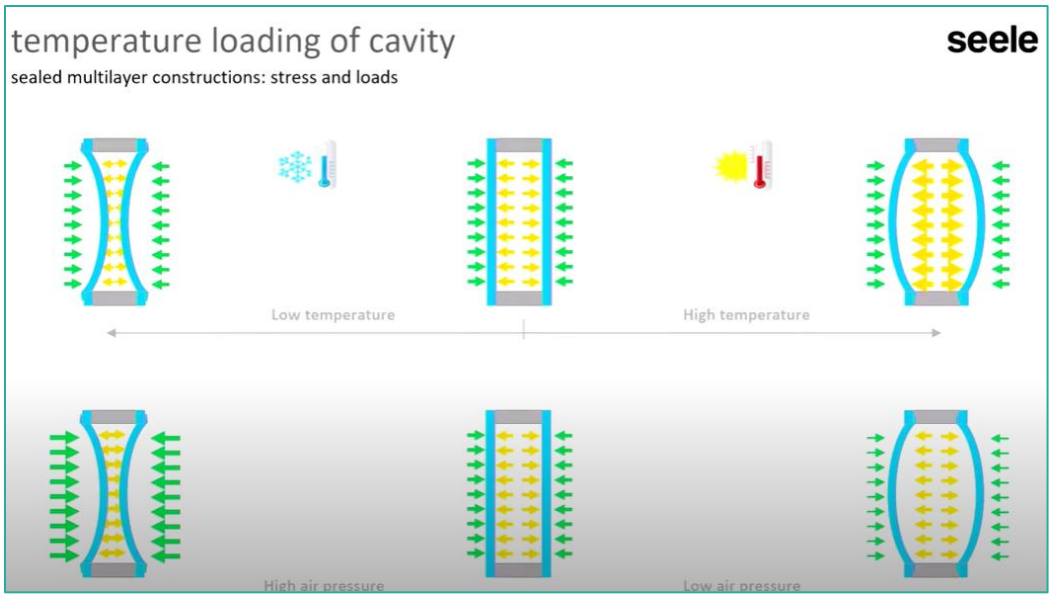

Figure 36 Isochoric pressure due to temperature differences (GPD Glass Performance Days. 2020).

Furthermore, if glass tubes are being laminated, heat will be used to do so. If glass, with the same thermal expansion coeffect, will be heated up, expansion occurs. If an interlayer resin

will be placed in between with another thermal expansion coefficient, will it not only result in expansion, but also in stresses. Besides, glass has tolerances in the glass, whereby the thickness of the interlayer will vary in length. The thicker the interlayer (>2mm) the more stresses will occur in the glass, after curing of the interlayer resin. The thinner the interlayer (<2mm), the less the glass tubes will be bonded.

These two phenomena need to be checked and taken into account while designing.

2.2.2.5. Fire

With a fire outbreak, the spread of flames and smoke (propagation of fire) need to be prevented, and it need to be possible to rescue people and animals out of the building. Fire resistance of a building, structure, or structural element, means that it is able to perform during a fire exposure. A minimum time (in minutes) is given in the NEN-norm that the structural element needs to withstand the fire. The ability of the elements to resist the fire can be divided in the groups: fire retardant, highly fire retardant and fire resistant. Building materials can be categorized in the following groups: incombustible, not readily flammable and flammable. Glass is an incombustible material (Weller, B., et al. 2009). The material that holds the fire glass in place needs to be made of an incombustible material as well. Some (sealing) strips can be used to create non-rigid supports. In case of fire, it can act as an insulating layer or it can foam up (O'Regan, C. 2015).

In general glass has a low resistance to thermal shock, which results in easily shattering of glass. Normal sheet glass has a low tensile capacity and a relatively high coefficient of thermal expansion. When the temperature differences in a fire are not leading to a glass failure, the temperature will reach a transition point at which glass starts to soften. This transition point is around 500 °C. When glass starts to soften, it loses its stiffness. When the temperature becomes higher the glass will melt. Nevertheless, glass has a lower thermal coefficient of thermal expansion compared to other materials (see table 3). Borosilicate glass even has a thermal expansion coefficient between 3.1 till $6*10^{-6}$ K^{-1}. This is the reason why borosilicate glass has a better thermal shock resistance. It increases the temperature differences at which the glass will crack, and it increases the softening temperature of the glass (O'Regan, C. 2015).

Material	Thermal expansion [K^{-1}]
Soda-Lime glass	$9*10^{-6}$
Steel	$12*10^{-6}$
Stainless steel	$17*10^{-6}$
Aluminium	$23*10^{-6}$
Concrete	$12*10^{-6}$

Table 3 Thermal expansion of glass compared to other materials (O'Regan, C. 2015).

Another way to increase the fire resistance of glass is by lamination. The lamination interlayer can be made from an intumescent material (see chapter 2.1.5.2.). The ply will act as a sacrificial layer in a two-ply laminated glass pane. First the outer layer fails due to the fire. Then the interlayer is exposed to fire, and expands into a foam. Due to its insulating behaviour, it will protect the layer(s) who are not exposed to the fire yet (O'Regan, C. 2015).

There are two approaches considering fire on glass: fire protection to glass, and a fire protection of glass. The first one is about the protection of glass from failing, and the second on concerns the glass protecting the structure, like compartmentation. For fire protection to glass, it needs to be isolated from the fire or the glass needs to have a resistance to the fire itself. So, the glass can be modified or it can be protected by sprinklers to reduce the temperature of the glass element (O'Regan, C. 2015).

As said before, borosilicate glass is mostly used for applications relevant to fire protection, due to the higher resistance of stresses caused by temperature changes and the lower thermal expansion which reduces stresses. Based on the BS EN 13051-2:2007, there are categories for glass: Class G (E), Class F (EI), Class EI and Class EW. In the table below, the different categories are shown with its properties. If openings occur in the glass due to cracks, fire can spread to the side which is not exposed to fire yet. In this case there is no reduced heat transmission anymore (O'Regan, C. 2015) (Weller, B., et al. 2009).

Type of glass	Properties when exposed to fire
Class G (E)	- Remains transparent and intact. - Prevents passage of smoke and flames. - Does not prevent transmission of heat radiation. - Single glazing: it doesn't shatter, but it deforms depending on the thermal load. - Two panes of float/toughened glass which are separated by a fire resistance layer/cavity filled with air/inert gas. The fire-resistant layer expands similar to intumescing paint which is used on steel elements.
Class F (EI)	- Provides additional protection against heat radiation, smoke and flames by a multi-ply layered element with special fire resistant interlayers (gel) that foams up when exposed to heat.
Class EI	- The surface of the side of the glass, which is not directly exposed to fire, may not rise above room temperature more than 140-180°C.
Class EW	- Prevents passage of smoke and flames. - Reduces transmission of heat radiation.

Table 4 Class types of glass for fire protection applications (O'Regan, C. 2015).

According to the Dutch regulations, there are requirements for the time (figure 37) the building or structural elements need to withstand the fire. So, for buildings with a height of 5 or 7 metres, the minimum time that the building needs to be withstand fire is 60 minutes. If the building needs to be safe for like 90 minutes, it can be reduced by other measurements, like sprinklers (Bouwbesluit. 2012).

woonfunctie	tijdsduur van de brandwerendheid met betrekking tot bezwijken in minuten	gebruiksfunctie niet zijnde een woonfunctie	tijdsduur van de brandwerendheid met betrekking tot bezwijken in minuten
Indien geen vloer van een verblijfsgebied hoger ligt dan 7 m boven het meetniveau	60	Indien geen vloer van een verblijfsgebied hoger ligt dan 5 m boven het meetniveau	60
Indien een vloer van een verblijfsgebied hoger ligt dan 7 m en geen vloer van een verblijfsgebied hoger ligt dan 13 m boven het meetniveau	90	Indien een vloer van een verblijfsgebied hoger ligt dan 5 m en geen vloer van een gebruiksgebied hoger ligt dan 13 m boven het meetniveau	90
Indien een vloer van een verblijfsgebied hoger ligt dan 13 m boven het meetniveau	120	Indien een vloer van een verblijfsgebied hoger ligt dan 13 m boven het meetniveau	120

Figure 37 Duration that buildings or structural elements need to be fire safe before failure (Bouwbesluit. 2012).

A required time of a resistance of 30 minutes can be subtracted, if the floor is not above 5 meters (non-residential), or not above 7 meters (residential), and the internal load is not higher than 500 MJ/m^2 (Bouwbesluit. 2012).

Heat-strengthen glass is heat-treated glass. This glass has surface residual stresses which can contribute to the resistance of thermal loads, but if the heat-treated glass is exposed too long to the fire, the glass will fail too. The glass type, but also the interlayer is from influence on the fire resistance. However, the temperature is not uniformly distributed over the surface,

which makes it possible that the glass will crack. It is necessary to check the behaviour of the interlayer when the glass has failed, to see if the glass was hold tighter properly by the interlayer or not. Most interlayers lose strength above a temperature of 100 °C. At approximately 250 °C, decomposition of the interlayer will start (O'Regan, C. 2015).

2.2.2.6. Impact loads

There are different action loads: wind, impact, explosion (bomb blast), and seismic (Haldimann, M., et al. 2008). Impact loads can be caused by people or by objects which can result in stresses and strains in the glass element. Heat-strengthened glass is stronger than annealed glass, which is better resist against impact loads. Glass in public areas needs to be safety glass to guarantee that it will not fall over which can cause injuries. It needs to bind the glass pieces together to protect the people next to it. If the glass breaks, it still needs to be able to carry residual loads for some time. The structural glass element needs to be able to resist a dynamic impact. To test impact, pendulum test can be performed (Weller, B., et al. 2009).

For a numerical robustness/ impact study, the effects of a rigid sphere can be simulated on a laminated glass element (figure 39). The sphere has a weight and a velocity. From this, a displacement versus time or acceleration versus time curve can be created. The influence of the mesh size is shown at the right of figure 39 (Timmel, M., et al. 2007).

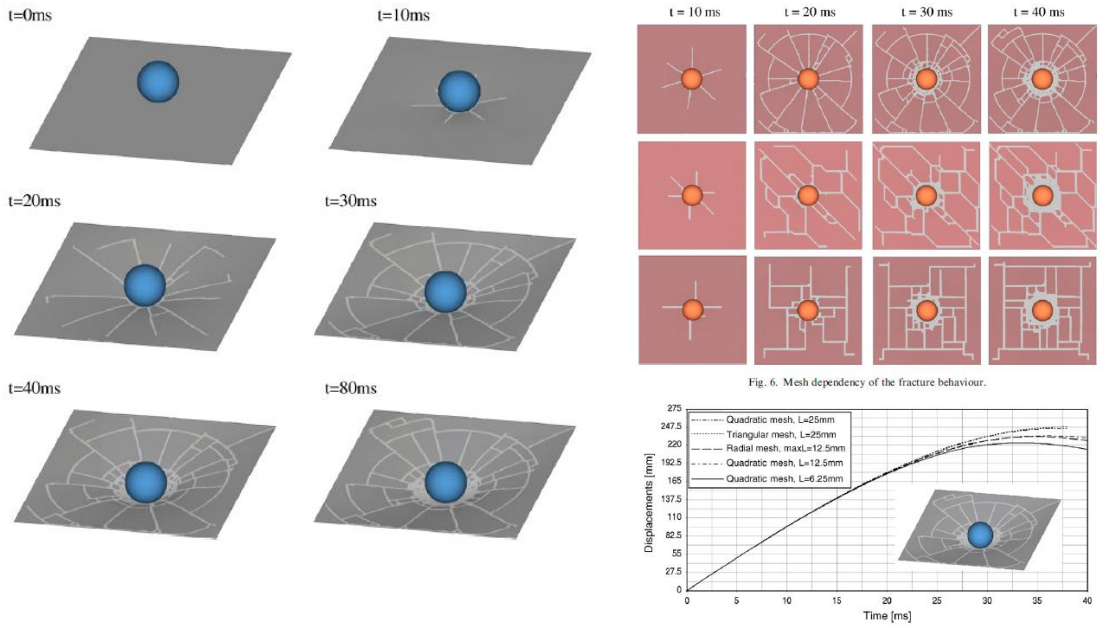

Figure 38 Evolution of impact on glass element (Timmel, M., et al. 2007).

2.2.3. Section properties

2.2.3.1. Moment of Inertia

The moment of inertia is influencing the mode of buckling and failure. The higher this value, the more buckling resistance. This is applicable for the y- and the z-direction. The three formulas are given in equations 5, 6 and 7 (Hartsuijker, C. 2005).

$$I_{yy} = \int_0^A y^2 * dA \qquad (5)$$

$$I_{zz} = \int_0^A z^2 * dA \qquad (6)$$

$$I_{yz} = \int_0^A yz * dA \qquad (7)$$

2.2.3.2. Open or closed profiles

Increasing or decreasing of thermal stresses can be influenced by open or closed profiles, by the use of the element, and by the orientation. In open profiles, the temperature differences could rise. Temperature differences could occur if cold air is blown inside the column, while the outside of the column is heated up by a fire or the sun. With open profiles, stresses could rise too, because of less external surface and a larger distance to the centre of the profile. In this case, temperature differences could occur due to the slowly changing temperature in the centre of the profile and the rapidly changing temperature on the surface. Furthermore, a closed cross-section profile has a better torsion resistance. Open profiles can be (hermetically) sealed to keep dirt out of the element and to keep the same air pressure inside the profile. In this case the connection is from influence while designing with an open profile (Ouwerkerk, E. 2011).

2.2.4. Connections

Connections need to introduce the forces into an element. Due to the elastic behaviour of glass, it is not capable of redistributing stresses. An intermediate material is needed between the glass element and the connection itself, to redistribute the forces, and to effect local imperfections in the glass. The intermediate material with is attached to the glass needs to be softer than the glass. So, it needs to have a lower Young's modulus than the glass itself to avoid local stresses which can result in cracks. Some intermediate materials are: POM, neoprene or an injectable mortar from Hilti (Hilti HIT-HY 70 for structural glass) (Hilti. 2008). There are mechanical, physical, and glued connections to connect glass with glass or glass with other materials (O'Regan, C. 2015). In appendix A.2.7. different examples are given for several connection types.

2.2.4.1. End connections

As mentioned in chapter 2.1.3. glass has a low tensile strength. It needs to be ensured that the glass column can only be loaded by compression forces without bending. This can be achieved by hinged connections. When the column wants to bend, eccentricities occur. This eccentricity gives bending moments in the glass column, and so tensile stresses occur.

''…and the failure behaviour of the glass columns is highly dependent on the way the column is supported.'' (Van Nieuwenhuijzen, E.J., et al. 2005).

As explained before, materials as PMMA, POM, soft aluminium, and wood, have lower Young's modulus than glass. This means that it can easily deform and function as a hinged connection between the support and the floor. Van Nieuwenhuijzen, E.J., et al. did research about the failure stresses of tubular layered glass tubes. They did tests with two end connections (figure 39) (Van Nieuwenhuijzen, E.J., et al. 2005):

- Prototypes with glass edges of the column resting on PMMA sheets (left, figure 39)
- Prototypes with PMMA heads/bases adhesively bonded to the inner tube (right, figure 39)

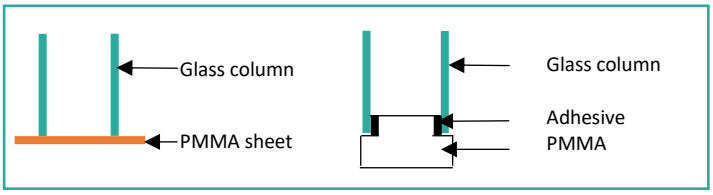

Figure 39 Two types of end connections of the glass column (Own picture, based on: Van Nieuwenhuijzen, E.J., et al. 2005).

From research can be concluded that both prototypes have a large initial crack strength and a safe failure behaviour. The glass columns which are placed directly a on PMMA sheet have much higher initial failure strengths and higher maximum strengths. A reason for this difference is that the adhesive used for the prototypes with glued endings is not properly divided along the circumference and therefore has weak and strong spots, which results in local peak stresses and so results in failure of the glass column (Van Nieuwenhuijzen, E.J., et al. 2005). This means that the left picture in figure 88 is a better choice for end support than the right one in figure 39. So, it is important to have a uniformly distribution of forces introduced in the glass column.

Another example of end connection for glass tubes is used in the project Bank in Bilbao. They built a wall of glass tubes in the building (figure 40). This wall is probably not load-bearing, because the soft layer used between the glass and steel is neoprene. This is such a soft material, that when the wall is compressed, the glass will punch through the neoprene onto the steel support. This can cause cracks (Van Nieuwenhuijzen, E.J., et al. 2005). The aim of this wall is to create a subtle separation between private and public spaces, which allowed light coming through in the spaces. Even the doors are included in these walls (figure 42). The wall is made of borosilicate glass tubes with a diameter of 150 mm and a thickness of 9 mm. In figure 41, a detail of the support is shown, where the glass wall is supported by the floor. In this figure (Best of Detail. 2014):

- 2 : borosilicate glass tube (diameter 150 mm, thickness 9 mm)
- 8 : brushed stainless steel profile bent to shape (dimensions: 170/50/5 mm) with in between the steel profile and the glass, a 5 mm thick neoprene seal
- 10 : 10 mm neoprene seal under glass tube as dust guard
- 19 : footplate: 10 mm stainless steel screwed to reinforced concrete floor slab
- 20 : floor finish: 5 mm epoxy resin, 200 mm reinforced concrete floor slab

Figure 40 Wall of glass tubes (Detail inspiration. 2009).

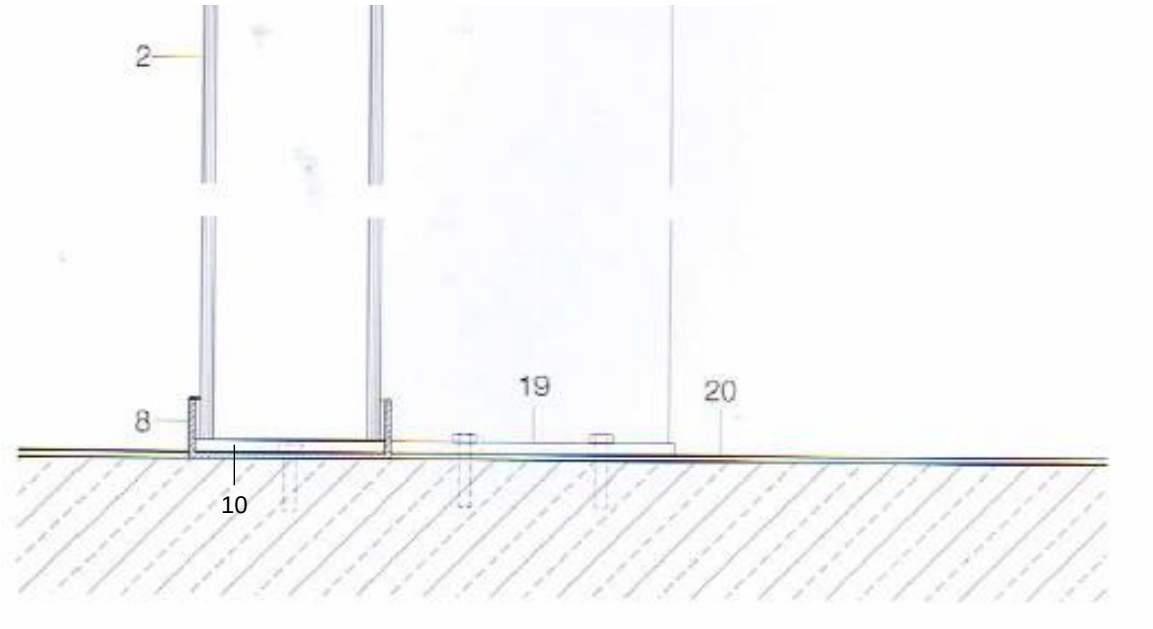

Figure 41 End support glass column supported by floor (Best of Detail. 2014).

Figure 42 Wall of glass tubes including a door built with the same principle (Detail inspiration. 2009).

The edges of the glass tubes need to be treated after producing to avoid sharp edges and to introduce the forces equally in the glass (chapter 2.1.5.3.). This needs to be discussed with the producer.

2.2.5. Types and applications

In figure 43, five different types of glass columns are shown: profiled, layered tubular, stacked, bundled and cast (Nijsse, R., et al. 2014).

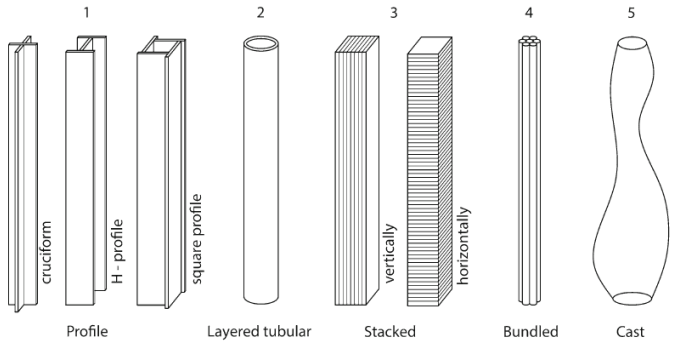

Figure 43 Type of glass columns (Nijsse, R., et al. 2014).

In table 5, an overview is made from applications and researches about the five types of columns. More about these projects is shown in this chapter. In appendix 3, a more extensive overview is given with findings and detail drawings of these researches.

Profiled columns	Layered tubular columns	Stacked columns	Bundles columns	Cast columns
Application of X-shaped columns in St-Germain-en-Laye in 1994	Glass tubes in Tensegrity Structure by Stuttgart University in 1996	Piece of art the Glazen Engel Michaël in Zwolle in 2010	Glass rods used in Zwiterleven Office in Amstelveen in 1996	Research on cast columns by Akerboom, R. in 2016
Research on X-shaped columns by Overend, M. in 2005	Glass tubes in Glasbaum in Aachen in 1998	Application of stacked glass walls in the Laminata house in Leerdam, the Netherlands in 2001	Research on bundled columns by Oikonomopoulou, F. in 2017	Research on cast columns in high-rise structures by Felekou, E. in 2016
Application of X-shaped columns in Dansfoss Headquarters in Denmark, 5.5 meter high in 2009	Research on laminated tubular glass columns by Veer, F. et al in 1999	Piece of art in Pompano Park water feature in 2006	Research on bundled columns by Van den Broek, E. in 2017	Research on cast columns by De Vries, E. in 2018
Research on H, T, and squared profile columns by Ouwerkerk, E. in 2011	Glass tubes used in the façade in Tower Place Office in London in 2002	Research on stacked columns by Van Heughten, R. in 2013	Application in the bridge at Green Village in Delft in 2017	
Research on X-shaped columns by Aiello, S. et al in 2011	Research on laminated tubular glass columns by Nieuwenhuijzen, E.J. et al in 2005	Piece of art The Glass Sphinx in 2013	Research on buckling performance of tubular glass bundled columns under compression by Kamarundin, M.K. et al in 2018	
Research on H, T, and squared profile columns by Campione and Rondello in 2014	Research on laminated tubular glass column by SCHOTT	Research on stacked columns in high-rise structures by Felekou, E. in 2016	Research on bundled columns by Verleg, K. in 2019	
Research on squared profile columns by Kalamar et al in 2017	Tubular glass columns filled with water in Iceland project as a piece of art in 2015	Research on cast columns by Akerboom, R. in 2016		
	Research on borosilicate glass tubes in 2020	Research on cast columns by De Vries, E. in 2018		
	Glastechnik Kirste got a patent on pressure-resistance glass tubes in 2020			

Table 5 Overview applications and researches of the different types of columns.

The different column types, are mostly manufactured in the following ways:

- Float glass: stacked, cast, and profiled columns
- Cast glass: cast and stacked columns
- Extruded glass: layered tubular and bundled columns

Due to the fact that this project is about tubular glass columns, there will be an elaboration on layered tubular columns. The other types of glass columns are descripted in appendix A.2.8.

2.2.5.1. Layered tubular columns

This type of column is not applied yet as free-standing column in buildings. Glass tubes are used as parts of façades or are integrated in art. Stuttgart University made a tensegrity structure of glass tubes in 1996 (Van Heughten, R.; 2013). Furthermore in 1998 'the Glasbaum' (glass tree) in Aachen was created with glass tubes as well (figure 44). So even in 1998 they were already busy with creating small and short glass tubes.

Figure 44 Glasbaum with glass tubes (facadeworld. 2013).

In 1999, Veer, F.A., et al did research into tubular laminated columns. They managed to make a prototype with a length of 0,55 metre, a diameter of 40 mm, and a wall thickness of 4 mm (figure 45 and 47). This prototype was made by laminating two glass tubes with an UV-light curing resin. Some critical aspects were: the fragility of the glass and the shrinkage of the resin during polymerisation. The shrinkage can result in void formation which decreases the transparency of the column. Furthermore, the shrinkage can lead to stresses in the glass, which results in decrease of strength and failure. Back then a new UV-light curing resin was developed where the process could be controlled. The resin is firstly hardened at the bottom. The shrinkage during polymerisation can be compensated by adding new resin at the top. To avoid bubbles, the right speed of hardening is needed (Veer, F.A., et al. 1999).

The following steps need to be taken into account during the polymerisation of the resin (Veer, F.A., et al. 1999):

- The tubes need to be put in a special holder that keeps them uniform along their axis.
- The space in between the tubes needs to be filled with a specially developed UV-curing resin.
- The resin needs to harden from the bottom by slowly (with the right speed) moving the UV-light to the top.
- During polymerisation, the resin can be added to the top to avoid shrinkage.

''This column is transparent but has a strength and failure behaviour comparable to a steel column of similar dimensions.'' (Veer, F.A., et al. 1999).

This column prototype was treated chemically with ion-exchange treatments to modify the cracks development, and it increases strength. Due to lamination, the glass pieces could be held together after cracks occurred, and it was still able to carry loads. Due to its elasticity, this resin was even capable of damping of shocks, which increased the resistance to more damage. Multiple compression tests have been carried out. First, they did compression tests with short prototypes which were rigidly clamped at the bases. The prototypes could be loaded to 35 kN before failure started, with a failure stress of 265 MPa. After that they column could still carry load while deforming. The tests were stopped after 35% of deformation. Slender columns, which could rotate at the bases, failed by buckling. They showed elastic behaviour till a load of 110 kN was reached, and a failure stress of over the 900 MPa. Then the prototypes started to buckle, and even though they were still able to carry

the maximum loads. Failure started at the compression zone at where the outer glass layer broke (figure 46). So, the glass columns had a similar behaviour as steel columns, but in the compression zone where glass breaks, steel would get plastic behaviour (Veer, F.A., et al. 1999).

Figure 45 The glass tube prototype from the research in 1999 (Veer, F.A., et al. 1999).

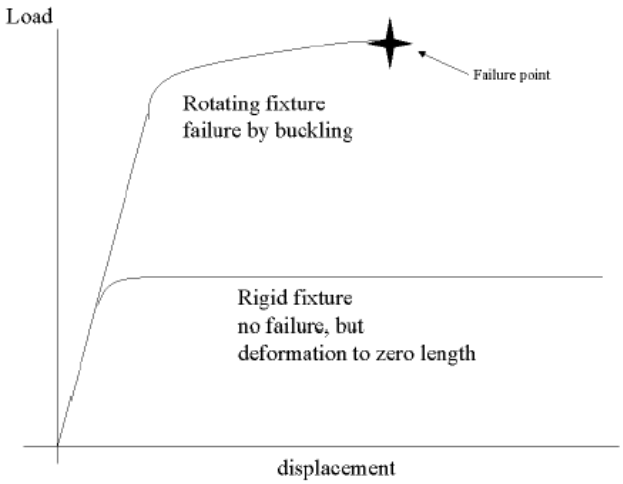

Figure 46 load versus displacement graph of tests from the prototypes (Veer, F.A., et al. 1999).

In 2005, Van Nieuwenhuijzen, E.J., et al continued with investigating tubular laminated glass columns. They used DURAN borosilicate glass tubes (annealed glass). In here they tried to design the column for a pavilion. The same principle was used as the engineered column from the research in 1999 (figure 47). They designed the connection in such a way that the column only could be compressed and not bend. The reason for this was that bending of the glass column resulted in local peak stresses and tension stresses. The prototypes were connected in bases of PMMA. In the table below the different test results are shown (Van Nieuwenhuijzen, E.J., et al. 2005).

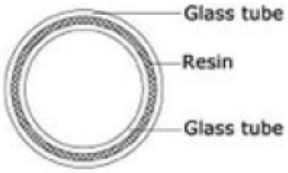

Figure 47 Principle of the cross-section of the laminated column (Van Nieuwenhuijzen, E.J., et al. 2005).

Prototype	Failure load	Maximum load	Failure stress	Maximum stress
1.2 m	73 kN	146 kN	28.9 MPa	57.8 MPa
1.5 m	61 kN	196 kN	18.0 MPa	57.9 MPa
1.5 m	40 kN	137 kN	11.8 MPa	40.6 MPa

Table 6 Results on the DURAN prototypes (Van Nieuwenhuijzen, E.J., et al. 2005).

The glass producer SCHOTT produced a tube column as well. The outer tube is made out of two half tubes. The outer and inner tube are laminated with a PVB foil. In this case, only the inner tube is load-bearing and the outer tube is only for protection of the inner tube. (Van Nieuwenhuijzen, E.J., et al. 2005).

As shown in figure 48, glass tubes are also used in Tower Place Office in London. In here the core tube is laminated to a split tube, which is used as a protecting shell. There is one inner tube is laminated with PVB to two half tubes. In figure 49, the principle is shown. The 3.6 metre borosilicate glass tubes are transporting the wind loads from the façade to the

steel columns which are supporting the roof. In the middle there is a tensioned steel cable included to resists wind suction. The end components are made of steel too. (Detail. 2003).

Figure 48 Tower Place London glass tubes (C|L. 1998-2003).

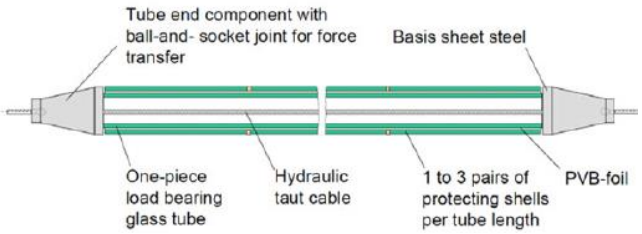

Figure 49 Principle of the glass tube system used in the Tower Place (Doenitz, F., et al. 2003).

As mentioned earlier (chapter 1.1), in 2015, glass tubular columns are used as a piece of art in Iceland in 'the Library of Water' (figure 6). The tube columns are filled with water. The columns can resist 260 kg of water (Schwanke, H. n.d.).

In 2020, Engels, S. investigated borosilicate glass tubes as well. The borosilicate glass tubes were coated by OPALFILM® produced by the company Haverkamp. He did research in the compression strength. Engels, S. tested 30 prototypes in total to determine the failure stress. The prototypes were DURAN® and DURATAN® profiles from SCHOTT. DURAN® is made of untreated borosilicate glass and DURATAN® is made of heat-treated borosilicate glass. Prototypes of 210 till 290 mm long, were clamped in steel plates with an interlayer of POM in between of 10 mm thick. The outer diameter was between 70 till 120 mm and the inner diameter 52 till 110 mm. The displacement method was used in the test with a displacement of 0.01 mm/s. During the test, the initial crack force and the ultimate force was noted. From this they calculated the stresses in N/mm^2. DURAN® had failure stresses between 3 till 45 N/mm^2, and DURATAN® had failure stresses between 14 till 105 N/mm^2. According to their conclusions, the interlayer had a major contribution to the failure strength of the tubes, because of the introduction of the tensile stresses. Another conclusion they made was that heat treatment of the tubes increased the strength 2 till 3 times. Due to Corona, the tensile strength tests were cancelled (Engels, S. 2020). In appendix 1.2. an interview is included with A. Snijder, researcher/teacher at the faculty of Architecture within the department of Structural Design and Mechanics at the Technical University of Delft, about this thesis project. Nowadays SCHOTT has DURAN® Tough / CONTURAX® Tough profiles (SCHOTT. n.d.) These are profiles with a polymer coating on the inside.

Furthermore, Glastechnik Kirste got a patent on a pressure-resistance laminated glass tubes in 2020 (Glastechnik Kirste. 2020).

2.2.6. Multi-Criteria Analysis

The aim of this research is to engineer and design a safe free-standing glass column. Therefore, in this chapter, the five types of columns are compared in the Multi-Criteria-Analysis (MCA) below (table 7). In appendix 4. more extensive arguments are given for the MCA.

For transparency:

- \+ transparent
- +- translucent
- \- not transparent

Fore form freedom:

- \+ completely form free
- +- relatively form free
- \- not form free

For buckling/ torsional resistance:

- \+ good resistant
- +- relatively good resistant
- \- not resistant

For safe failure:

- \+ safe failure
- +- it is depending on a lot of parameters
- \- not safe: it does not give a sign, and it fails suddenly

For production time:

- \+ fast production time
- +- the technique of gluing can slow down the time
- \- not fast, it cools very slowly

Fore production cost:

- \+ the primary and secondary manufacturing method is relatively cheap
- +- the primary manufacturing is cheap, the secondary manufacturing is not
- \- the whole manufacturing is expensive

		Profiled	Layered tubular	Stacked	Bundled	Cast
Architectural	*Transparency*	+-	+	-	-	-
	Form freedom	-	-	+	+-	+
Mechanical	*Buckling resistance*	+-	+	+-	+	+-
	Torsional resistance	-	+	+-	+-	+-
	Safe failure	-	+-	-	-	-
Financial	*Production time*	+-	+-	-	+-	-
	Production costs	+-	+-	+-	+-	+-
Total		**-**	**+**	**-**	**+-**	**-**

Table 7 MCA types of columns.

So, to concluded the scores in the MCA, the layered tubular glass column has the highest score. It is the most transparent option of all the types, because there are no edges. Furthermore, it has (as already mentioned in chapter 1.1. and 2.2.3.) a good cross-sectional shape to resist buckling and torsional buckling. For stacked and cast columns this is really depending on the shape. Profiled columns have a poor torsional resistance. Stacked and cast columns have the best form freedom. For most of the column, the primary manufacturing method can be standard via float glass or extruded profiles production.

Nevertheless, the lamination process or glued connections need to be done carefully, because it can be a weak point.

2.2.7. Conclusion

Columns are vertically structural elements, which supports other structural elements. Columns can create big open spaces, and are already an old phenomenon.

Failure mechanisms for columns are:

- buckling
- thermal stresses
- fire
- impact

Cross-sectional areas and so the moment of inertia does have large influences on the buckling and torsional buckling resistance of columns. If columns are slender, buckling can occur. The optimal cross-sectional shape for buckling and torsional buckling resistance is a circle.

Thermal stresses can occur due to temperature differences in the glass element. Due to different temperatures, isochoric pressure (differences in air pressure) can occur, which can result in condensation or stresses in the glass. When the stresses become too high, cracks can occur in the glass elements. Thermal stresses and expansion can also occur during/after the lamination process, due to the fact that glass and the interlayer material do have different coefficients of thermal expansion. Heat-strengthened glass is preferred, because it can resist higher thermal loads and temperature deviations.

According to Bouwbesluit, structures or buildings lower than 5 or 7 metres need to be able to withstand at least 60 minutes of fire. Based on the BS EN 13051-2:2007, there are categories for glass: Class G (E), Class F (EI), Class EI and Class EW. Differences in these types is the transparency in fire, prevention of smoke and flames, shattering or deforming, preventing against radiation, and fire-resistant layers. Besides, the glass type, nor the interlayer material are from influence on the fire resistance. Borosilicate glass has a higher resistance for the occurring stresses by temperature changes than soda-lime glass has, due to a lower coefficient of thermal expansion.

Impact loads can be caused by different actions: wind, impact, explosion (bomb blast), and seismic. Besides, impact loads can be caused by people too. Heat-strengthened glass has a better resistance against impact loads than annealed glass. Glass needs to be safe to guarantee that it will not fall over, which can cause injuries.

There are five types of glass columns: profiled, layered tubular, stacked, bundled and cast. The profiled column is so far the only free-standing type of column being applied in buildings. The MCA showed that the layered tubular glass column is most promising for further investigating, due to its transparency and its good buckling and torsional buckling resistance.

There are three types of connections: mechanically, physically, and glued. End connections have big influences on the failure behaviour of the column. If the connection is not well-designed, loads can be unevenly introduced into the column, which can result in local stresses. Furthermore, it is important to have a soft material with a lower modulus of elasticity between glass-to-glass connections or between the connection of glass to other materials, to avoid stresses and cracks. To avoid eccentricities, which result in tensile stresses, the end connection needs to be designed as a hinged connection so that only compression forces are introduced in the glass column.

Part I Literature Study

2.3. Design strategies for glass columns

2.3. Design strategies for glass columns

As mentioned before, glass is a brittle material, so it breaks without giving a sign. Because of this, glass needs to be engineered and designed safely to avoid high consequences for injuries. Therefore, the post-failure behaviour of glass needs to be researched. This can give an indication of the safety of the structural element. A structure is safe if it gives a warn to people. A risk analysis needs to be made to predict the risk and to give a value to consequences. In this chapter design guidelines for glass and some strategies are discussed.

2.3.1. Design guidelines

Some of the European Norms which are used now are:

- BS-EN 572: Glass in building - Basic soda-lime silicate glass products.
- NEN 2608: Glass in building - Requirements and determination method.
- NEN-EN 1627 - Pedestrian door sets, windows, curtain walling, grilles and shutters - Burglar resistance - Requirements and classification
- NEN-EN 1630 - Pedestrian door sets, windows, curtain walling, grilles and shutters - Burglar resistance - Test method for the determination of resistance to manual burglary attempts
- NEN-EN 356 - Glass in building - Security glazing - Testing and classification of resistance against manual attack

Knowledge which is not specified in the codes, is required from tests. The material safety factor for glass is depending on statistics, number of tests, probability, and on the scale of the prototype used for the tests. Due to lack of data, the safety factor for glass is higher than for other materials (The material safety factors for reinforced concrete are 1.7 and for steel it is 1.5.). Besides, glass is brittle and elements made from glass have a sudden failure. The values for glass are completely depending on the number of experiments, and on the scale of the prototypes. If the prototypes are tested on scale 1:1, the results from the test are more accurate. In that case, the material safety factor can be reduced. Due to the new technologies and the developments, more and more becomes known about the behaviour and the strength of glass. Through his multiyear long experiments in experimental testing of glass, according to Veer, F.A., a safety factor of 2 should be sufficient (Veer, F.A. 2014). Other applied columns in Danfoss Headquarter in Denmark had also a safety factor of above 2. The column failed with a compression load more than twice as large as the required load.

2.3.2. Design strategies on robustness

Before diving into robustness strategies for glass, first the meaning of robustness in general will be explained.

The definition for robustness:

''A quality in a structure/structural system that describes its ability to accept a certain amount of damage without that structure failing to any great degree. Robustness implies insensitivity to local failure. BS EN 1991-1-7 provides one definition of robustness as "the ability of a structure to withstand events like fire, explosions, impact or the consequences of human error without being damaged to an extent disproportionate to the original cause".'' (The Institution of Structural Engineers. 2010).

Every structure needs to be able to carry and transport horizontal and vertical loads to the ground via a load path. This load path needs to be defined. The longer the load path, the higher the stresses will be in the structural elements. If the horizontal loads are taken by the shortest route possible to the ground, the structure is stiffer. Redundancy can contribute to

help ensure the robustness of the structure. Furthermore, the more ductile the structure behaves, the more robust it will be (The Institution of Structural Engineers. 2010).

The definition for redundancy:

''A term used to signify that there are more load paths than strictly necessary to carry the load through the structure (or a part thereof). In structural analysis redundancy is associated with structural indeterminacy, but in the context of robustness the term has a wider meaning and interpretation.'' (The Institution of Structural Engineers. 2010).

If one load-bearing element leads to collapse of the entire structure, the structure has no redundancy. The degree of redundancy is depending on when the loads can be redistributed over the remaining structural elements. So, redundancy means that there are more load paths than needed. Besides, there is a second level of redundancy. If the elements are able of carrying more load than is actually demanded, then there is a margin. Margins are a difference between real material strength and specified strength. The loads on the structure during the event is less than used for design purpose. For a robust element, detailing is of influence too. If the support moves due to settlements or thermal movement over time, is it still able to carry loads? Structural ductility of the element, allows parts to deform, but these are still able to carry loads. It allows those overloaded parts of the structure can yield and redistribute the stresses. The connections and joints need to be able to deform too without fracture. Elements may only distort under accidental conditions if the structure stays intact and does not completely collapse. So, if the structure/structural elements are robust, it protects structures against the unforeseen (The Institution of Structural Engineers. 2010).

Glass is a brittle material, and therefore not robust itself. For designing with glass, first a risk analysis needs to be done, to take safety into account. To analyse the risks, the Fine and Kinney method can be used. This method is based on the probability that the damage will occur, the application and the damage. To determine the risk, equation 8 needs to be applied (NEN 2608. 2011). To determine the WS, BS and ES from equation 8, table 8 should be used.

$$RS = WS * BS * ES \qquad (8)$$

With:

- RS: risk of the damage
- WS: probability of the damage
- BS: exposure to the risk of the damage
- ES: consequence/ effect of the damage

Probability of damage with or without intent	WS	Exposure of structural element	BS	Consequence of complete break	ES
Virtually impossible	0.1	Very seldom	0.5	First aid	1
Practically impossible	0.2	A few times per year	1	Minor injury	3
Conceivable, but very improbable	0.5	Monthly	2	Serious injury	7
Only possible in the long term	1	Weekly	3	One death	15
Unusual, but possible	3	Daily	6	More than one death	40
Very possible	6	Constant	10	Catastrophe, many deaths	100
Can be expected	10				

Table 8 Determination of risk of breakage of structural element (NEN 2608. 2011).

If the RS is calculated, the damage of the risk can be determined via the following table:

Damage to structural element	Risk
Lateral breakage on one side	RS < 70
Lateral breakage on two sides	70 < RS < 400
Complete breakage of the structural element	RS > 400

Table 9 Determination of the degree of damage (NEN 2608. 2011).

''The goal is to achieve safe breakage and avoid collapse.'' (Honfi, D., et al. 2013).

According to Honfi, D., et al, there are three levels of redundancy in glass structures: material, component, and structural system. These three types need to be taken into account when designing.

The type of glass, has impact on the structural robustness, which makes it material dependent. Glass types have different properties, looking at the sensitivity for damage exposures.

On a component level, multiple layers of glass can be bonded together through lamination to ensure more safety. If one layer breaks, the other layers are taking care of the loads until repair or replacement. A disadvantage is that with lamination, delamination can occur. Another option for keeping the pieces together when a glass tube breaks, is by spraying a polymer coating on the inside of the glass tube. SCHOTT did a Semtex blast test on coated DURAN® tubes. In figure 50, the effects of this impact test are shown. The tubes are broken, but are held together in one piece. The glass shown on the floor is from previous tests. The tubes were 1.5 metres long, with an outer diameter of 120 mm, and a wall thickness of 5 mm. The tubes were fixed to a metal frame. For the explosion 50 g Semtex plus detonating coat is used, with a distance of 0.5 metre to the tubes. The coating is a polymer with a thickness of 300 µm (SCHOTT internal. 2019). However, probably only own weight of the tubs is included. From this test, it is not sure yet what happens with the glass when a compression load is applied.

Figure 50 Blast test on DURAN® tubes (left the outside view, right the inside view) (SCHOTT internal. 2019).

Strength is also depended on the failure patterns. Annealed and heat-strengthen glass breaks into large pieces and tempered glass breaks into small pieces. Connections and stiffness of interlayers can also influence component redundancy.

Furthermore, on a structural system level an additional load path can contribute to redundancy. If one structural element, like a column fails completely, then other structural elements can take over the loads until repair or replacement of the broken element. In this case, additional load needs to be taken into account on all of the surrounding structural elements. Some ways to increase robustness are: prevent consequences of failure, prevent failure (by protecting edges for example), use of reinforcement, and use of barriers like handrails (Honfi, D., et al. 2013). Acrylate can be used to protect the glass too. This material is less brittle than glass.

2.3.3. Design strategies on fire safety

Fire is one of the accidental load cases, which needs to be considered whether or not the element is robust enough in the event of fire. Relevant performance criteria of fire-resistant glass are: integrity, insultation, and radiation (Gravit, M., et al. 2019). Fire resistant glass can be divided into two categories: non-insulating and insulating glass. Insulated glasses can be distinguished in two types: laminated glass using intumescent interlayers, and gel-filled glass units (Gravit, M., et al. 2019).

An intumescent (inter)layer can be a safety strategy. When the first layer of glass breaks, the interlayer will foam up to protect the other glass layer which are still intact. In this way the glass is isolated from fire by the interlayer. A majority of fire-resistant glass is laminated glass with interlayers of an alkali metal silicate (sodium or potassium) based material. When the laminated glass pane is heated above 200 °C, the interlayer material starts to swell up to a volume which is 5-8 times bigger and it loses its transparency. After that it forms a foam which exists out of closed cells. With laminated glass in general, the greater the glass thickness, the more fire resistant the glass is (Gravit, M., et al. 2019).

H.B.Fuller Kömmerling, came with a new interlayer product, Ködiguard Conservation. This is a transparent colourless interlayer which needs to be cured with an UV-light. It is designed to safely laminate temperature sensitive, symmetric, tempered, flat and curved glass. It can also be used for solar control, fire, decorative and fire-resistant glass (Kömmerling. 2014).

Furthermore, there are glass panes filled with a special hydrogel (Gravit, M., et al. 2019). An example of this type of safety strategy is Contraflam, which is categorized in class EI (table 4, chapter 2.2.2.5.). It exists of tempered glass sheets with cavities filled with a transparent gel. This gel is made of sodium silicate and it reacts when exposed to fire. The gel will foam up and it isolates the glass from the fire (Vetrotech Saint-Gobain. 2020). It is also already applied in curved glass units by POLFLAM® (POLFLAM®. n.d.).

Unfortunately, most of these intumescent interlayers and gel-filled units are not existing for tubes or glass elements with a high curvature yet. Research should be done to see if this also works for laminated glass tubes. Communication with SCHOTT indicated that R&D process would be essential to apply such interlayers in tubing.

Fire resistant coatings were already used for structural elements made of timber and steel. In 2001, Veer, F.A., et al investigated structural glass beams on 4-point bending tests with weights to enforce a stress with a maximum of 24 MPa (Veer, F. A., et al. 2001). A constant flame with a temperature of 650 °C was applied on one side of the beam. On the other side of the beam, the temperature was measured. The beam prototypes were made of annealed glass, chemically toughened glass, and chemically toughened glass with polycarbonate foils and a special lamination with an insulating cavity. These beams were coated with an

intumescent coating/paint named Flameguard HCA-TR. From test results they could conclude that annealed glass was unsafe for structural use, and the toughened glass showed fire resistant behaviour. The coating showed an improvement of the failure time of a few beams. The coating slowed down the heating of the glass and the interlayer, and it slowed down the development of the thermal strain in the two materials. The best result for some of the beams was a fire resistance of >40 minutes (Veer, F. A., et al. 2001). Later on, Sturkenboom also investigated the fire resistance of glass beams (with and without HCA-TR), and Loman did research into the fire resistance of glass rods and flat glass panels. Results from the investigations of Sturkenboom were (Sturkenboom, J. 2018):

- It is better to cover the glass beam completely than partially with the coating.
- The fire-resistant coating was not fully transparent when it was painted on transparent glass.
- The glass beam element with the coating was fire resistant for around 23 minutes.

According to Veer, the coating is in principle transparent, but it must be applied properly. Results from investigations from Loman were (Loman, A.A.C. 2019):

- The Young's modulus for soda-lime glass decreased due to heating, whereas the Young's modulus for borosilicate glass increased first. After 400 °C both glass types show a decrease in stiffness.
- Glass rods it is observed that glass performs well up to temperatures of 500 °C. After 500 °C a sudden deformation occurred.
- Glass outperforms steel in terms of relative stiffness up to temperatures of 600 °C.
- The heating of a glass element can be delayed by the application of an intumescent coating and an improvement in fire resistance for the panels with low-E coating however is not proven.

These coatings (as HCA-TR) are investigated for laminated glass beams and for (laminated) flat panels, but never for laminated glass tubes. More research needs to be done on the behaviour of glass tubes with this kind of sprays and coatings when exposed to fire.

Another fire safety strategy can be the use of radiation-controlled glass. This is fire resistant glass categorized in class EW (table 4, chapter 2.2.2.5.). An example is the transparent glass elements Vetroflam ew60. A coating on the outer layer of the toughened glass can reflect some heat and so it can reduce the heat which will be going through the glass. This fire-resistant glass even remains transparent during a fire. It also protects against smoke, flames and toxic substances for 30 or 60 minutes and it is injury-proof (Vetrotech Saint-Gobain. 2020). According to 'Vetrotech Saint-Gobain Benelux', it is not available for tubes or glass elements with a high curvature yet.

The glass type itself can also have influence on fire resistance. As mentioned before, borosilicate glass has a better thermal resistance than soda-lime glass, and heat-strengthened glass is better resist to thermal loads than annealed glass (chapter 2.2.2.5.). Furthermore, sprinklers can be used to reduce temperature of the glass, or an element of glass can be filled with water, to keep the glass cool. This approach of using water inside the glass column to increase the fire-resistant behaviour is ones more introduced for the Samsung Museum in Seoul in Korea. This column is never been built due to a collapse of the Korean economy (Nijsse, R. 2003).

So according to the literature study and the conversations with H.B.Fuller Kömmerling, Vetrotech and SCHOTT, fire resistant coatings and intumescent interlayers are only existing for flat glass panes and not for glass tubes yet. More research needs to be done onto the behaviour of glass tubes with these intumescent coatings or interlayers. Transparent fire-

resistant coatings as HCA-TR can be applied to improve the failure time, and toughened glass is preferred to use over annealed glass, since toughened glass showed fire resistant behaviour. Moreover, borosilicate glass has a better thermal resistance than soda-lime glass. Nevertheless, more research is needed for these fireproof applications on (tubular) glass columns.

2.3.4. Conclusion

Some guidelines for glass are: BS-EN 572, NEN 2608, NEN-EN 1627, NEN-EN 1630, and NEN-EN 356. Knowledge which is not specified in the codes, is required from tests. The material safety factor for glass is depending on statistics, number of tests, probability, and on the scale of the prototype used for the tests. This means that higher safety factors for glass are demanded than for other materials.

Due to the brittleness of glass, structural elements made of glass needs to be designed and engineered safely. Firstly, a risk analysis needs to be performed to predict the risk of breakages, the consequences, and the degree of damage.

There are three levels of redundancy in glass structures: material, component, and structural system. Some methods to make a robust design are: laminating the glass elements, toughened glass to reduce the impact on injuries due to smaller pieces when it breaks, an additional load path, well-engineered connections, stiff interlayers, (polymer) coatings can be used, the use of acrylate, and the failure can be prevented by reinforcement or barriers.

Some methods to make a design resistant are: by the use of intumescent interlayers, fire resistant coatings, treated glass to fire reduce the strength, the use of fire-resistant insulation glass (several classes), the use of sprinklers or by filling the glass element with water to keep the glass cool. Moreover, borosilicate glass has a better thermal resistance than soda-lime glass, and heat-strengthened glass is better resist to thermal loads than annealed glass.

Part I Literature Study

2.4. Conclusion

2.4. Conclusion

In this chapter, the answers are given on the sub questions for part I Literature Study.

What are main manufacturing methods and limitations to produce glass tubes?

Glass tubes can be produced with the extrusion method. There are two methods: direct and inverted extrusion. The shape of the glass profile is created by the geometry of the opening of the container. When the temperature is too low, the glass is too viscous to extrude. Not all types of glass are suitable for extrusion. This is depending on the viscosity of the glass.

There are size limitations due to transport limitations. When laminating of panes is needed, the size of the panels must not be longer than 16 metres to fit in the autoclave. For extruded profiles geometric distortion play a role when profiles become longer, which means that the tubes are not entirely straight anymore. Geometric tolerances need to be taken into account. The thickness is often less due to manufacturing tolerances. For tubes, the longer the tube become, the bigger the tolerances will be.

What are common designs for transparent tubular glass columns?

There are three concepts for a tubular glass column studied (figure 51):

A. Two tubes laminated with a transparent UV-curing resin. Both tubes are contributing to the load-bearing capacity. The tubes were chemically treated, which increased the strength and toughness. This concept is designed by: Veer, F.A., et al. 1999 and Van Nieuwenhuijzen, E.J., et al. 2005.

B. A load-bearing inner tube protected by two half tubes that form an outer shell. Laminated via a PVB foil in between. These tubes were used in the Tower Place in London.

C. Borosilicate glass tubes from SCHOTT with an OPALFILM® coating to increase residual strength. The coating keeps the glass pieces together when it breaks. This tube can be the outer tube protecting an inner tube which can be placed inside. The tubes are not connected to each other, but both are contributing to the load-bearing capacity. Research is done about these tubes by Engels, S. 2020.

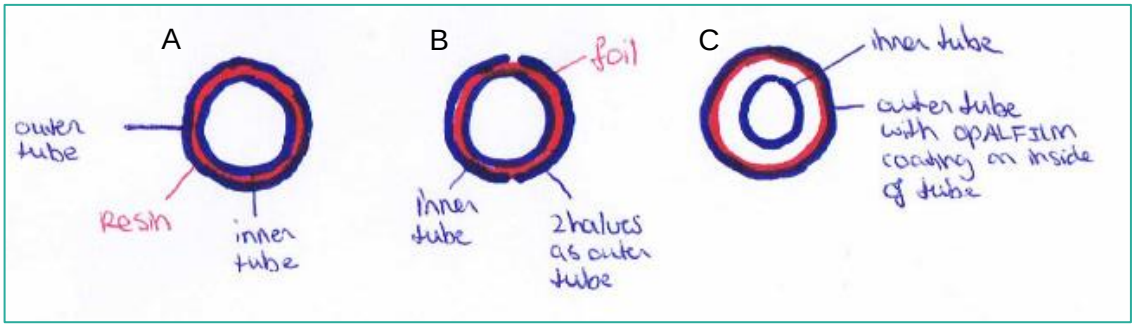

Figure 51 The cross-sections of three design options A, B and C, for tubular glass columns.

What are principles to laminate tubular glass columns?

Tubes glass profiles can be laminated via a transparent UV-curing interlayer resin. Putting a foil interlayer in between whole tubes is more difficult. This is actually only possible if the outer tube is made of two halves. Another way to keep glass pieces together when the glass element broke, is via the polymer coating like *Tough* from SCHOTT.

Which failure mechanisms exists of glass columns?

- Buckling
- Torsional buckling
- Thermal stresses
- Fire
- Impact

A circle shaped cross-section has a good buckling and torsional buckling resistance. The column needs to be designed so that it can be fire safe and robust. Due to this shape, it is not possible to clean the column inside. This means that the column needs to be sealed. Due to this, different air pressures can occur due to different temperatures.

What are safety strategies for a robust and fireproof design?

Some safety strategies for a robust glass design:

- Multiple layers of glass can be bonded together through lamination or by bonding layers together via an adhesive.
- The type of glass and the relevant breaking pattern has influence.
- Use of the polymer coating, like *Tough* on DURAN® profiles from SCHOTT.
- Use of a secondary load path.
- And/or use of acrylate. This is less brittle than glass.
- Prevent consequences of failure, or prevent failure by reinforcement, and by the use of barriers like handrails.

Some safety strategies for a fire safe design:

- There are different classes for fire resistant glass (E, F, EI and EW). These categorising depends on aspects from the glass element during a fire:
    - the transparency,
    - the prevention of smoke and flames,
    - shattering or deforming,
    - preventing against radiation.
- Furthermore, from glass composites, borosilicate glass is preferred, because of its lower coefficient of thermal expansion compared to soda-lime glass, which gives it higher resistance to thermal deviations. From glass types, heat-strengthened glass is preferred over annealed glass.
- Another option is by filling the glass tubes with water to keep the glass cool.
- By using a specialized fire-resistant coating or intumescent interlayers (this type of glass elements is categorized in the fire-resistant classes).
- Lastly the use of sprinklers can be applied to reduce the temperature of the glass.

Part II Design Phase

Part II Design Phase

3.1. Main concerns and design criteria

3. Part II Design Phase

The gained knowledge from the literature study will be used to design concepts for a tubular glass column which are fireproof and robust. First off, design criteria and main concerns are pointed out. Then the options A, B and C, from figure 51 are discussed. To design and engineer new design concepts, it can help to look at advantages and disadvantages of these options. During designing, it is important to think about end connections, and ways to replace the column when it is broken. So, possible failure mechanisms will be predicted for the new designs. After that, a case study was chosen for the column, so that a risk analysis could be performed and compression loads could be obtained.

3.1. Main concerns and design criteria

The column needs to satisfy design requirements. Some design requirements and main concerns emerged in the literature study. These aspects need to be taken into account while designing. The design criteria/main concerns for tubular glass columns are based on the following aspects, which will be elaborated on in this chapter:

- tubular shape
- thermal and residual stresses
- transparency
- fire resistance
- robustness
- manufacturing
- end connections
- restrictions to the case study
- ability to replace

3.1.1. Shape

The column, which will be investigated in this thesis, is the layered tubular glass column. This shape reduces the internal stresses, because there are no corners or angles. The circle-shaped cross-section contributes to resistance to buckling and torsional buckling of the column. However, it is not possible to clean the column on the inside. So, the column needs to be sealed to avoid that the column can become dirty.

3.1.2. Thermal and residual stresses

As said before, the column needs to be sealed. Due to this, it becomes a closed cavity. Thermal stresses can occur when there are temperature differences in the glass. Furthermore, isochoric pressure can occur, because different temperatures can result in different air pressures. Due to these air pressures, condensation can occur. All of these aspects need to be checked, to check if extra measurements are necessary. Thermal stresses can also occur during/after the lamination process. During the process the glass and the interlayer will be heated up. Due to the different thermal expansion coefficients of the glass and the interlayer material, it will result not only in expansion, but also in stresses. Besides, due to the tolerances in the glass, the thickness of the interlayer will vary. The thicker the interlayer, the more stresses occur. The thinner the interlayer, the less the tubes will bond.

3.1.3. Transparency

The column needs to be transparent, but visible. It is visible since the tubular shape results in visual distortion. In this way, no one runs into it, and it can contribute to the aesthetic value of the design. The more layers of glass, the less transparent it will become. If columns are made from other materials, for example steel, the column can be seen as an element that is blocking the view in space. Due to the transparency of glass, this experience can be

different. So, it is the intention that someone can look through the column, and that light can come through as well. Moreover, air inside the gaps, also plays a role in transparency, since this results in distortion.

3.1.4. Fire resistance

The time (in minutes) that a structural element must be fire resistant depends on the case and the application of the element (chapter 3.3.2.). The tubes for the column design will be made from borosilicate glass. This contributes to the fire resistance of the column, due to its lower thermal expansion value. Furthermore, if the tubes are made from heat-strengthened glass instead of annealed glass, it will contribute to the time that the column will be fire resistant as well.

3.1.5. Robustness

The column needs to be robust. For example, when the column is broken, forces still need to be transferred. One option is that the building is capable of transferring loads via a secondary load path, or another option is that the column itself is still capable of carrying the loads. If the column is exposed to an impact load, this can be caused by people or by objects, it can result in stresses and strains in the glass. As explained in chapter 2.3.2., there are three levels of redundancy: material, component, and structural system. For material redundancy the type of glass has influence on the strength of glass. Chemically tempered or heat threatened glass is stronger and can contribute to the robustness of the column (Veer, F.A., et al. 1999). Multiple layers of glass can be bonded together to have more safety in the component. For all structural glass elements, a risk analysis needs to be performed. To avoid injuries, SCHOTT *Tough* coating, or bonding of multiple layers together by lamination, will keep the pieces of glass together when the glass element breaks. Besides, the connections can also influence component redundancy, which is a point of attention during design. It needs to be investigated if a secondary load path is necessary or that the column is still capable of carrying the forces when broken.

3.1.6. Manufacturing

Extrusion is the manufacturing method for glass tubes. The tubes are produced by machines. After that the tubes are produced, the glass tubes need to be bonded together with a special transparent interlayer material. This needs to be done carefully, to avoid shrinkage. It can lead to void formation in the resin, and it increases the stresses in the glass. The glass is fragile, which means that cracks are introduced easily to the glass tubes. These stresses in the glass can lead to failure.

3.1.7. End connections

Furthermore, the end connections are of great influence. To avoid local peak stresses in the glass elements:

- The column needs to be designed as hinged, so that it will only take up normal forces.
- As said in chapter 2.2.4., a soft material, with a lower Young’s modulus, needs to be put in between the glass and the steel.
- The forces need to be introduced uniformly in the column.
- Not only the column, but the connections need to be designed fire safe.

While designing the connection, these aspects need to be considered. As said before, the column is only able to take up normal force due to the hinged connection. So only vertical

forces can be transferred via the columns. This means that in any case, the horizontal forces need to be taken up by other structural elements, like stability walls or bracing.

3.1.8. Restrictions to the case study

Furthermore, there are some restrictions to the case study, like the length of the column, and the loads. A risk analysis can only be performed according to a case. In chapter 3.3.2. these restrictions will be given.

3.1.9. Ability to replace

Finally, the column needs to be replaceable when partly or completely broken. Looking into the robustness of the designs, when the glass column is partly broken, it still needs to be able to carry the loads. When completely broken, a secondary load path is needed. For now, there can be assumed that due to bonding the glass tubes together by lamination, the column, is able to take part of the loads when damaged. This needs to be checked in the experiments, looking at the post-failure behaviour.

Part II Design Phase

3.2. Design development

3.2. Design development

3.2.1. Already designed concepts

In chapter 2.4, the three concepts for a tubular glass column designed so far are shown in figure 51. In the table below (table 10), the advantages and disadvantages are given for these three options.

In here:

- \+ Yes/not difficult/good
- +- Intermediate/it depends
- \- No, difficult/not good

	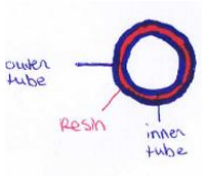	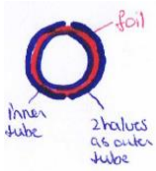	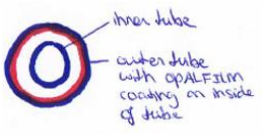
Property	**A. Veer, F. (1999)**	**B. Tower place (2003)**	**C. Engels, S. (2020)**
Outer tube load-bearing capacity?	+	-	+-
Collaboration between the layers	+	-	+-
Difficult to manufacture	+-	+-	+
Fire spray/coating possible?	-	-	+
Reusable	-	-	+-
Transparency	+-	-	+-

Table 10 Advantages and disadvantages for the options.

A. Veer, F. (1999):

+ The outer tube is load-bearing. Even when the outer layer is broken, it is still able to carry part of the loads. This is only possible when the layer is broken in large pieces of glass.
+ The collaboration between the tubes is probably best in option A, compared to the other options, due to the tubes which are bonded together.
+- The resin needs to be cured carefully, which makes the manufacturing process more difficult.
- The fire spray needs to be sprayed somewhere on the inside of the tubes, because it is sensitive to scratches. On the inside of the inner layer of the column it does not work anymore, because there the column is already exposed to fire. Which means, that for this option, a fire spray will not work. The column can also be filled with water to keep the column cooler during fire.
- Due to the connection between the layers, the tubes cannot be reused anymore.
+ Because there are no edges, it is transparent. The transparency is also depending on the numbers of layers. The more layers, the less transparent it will be.

B. Tower Place (2003):

- The outer tube, existing out of two halves, is not capable to carry loads. It is only a protective layer.
- There is no collaboration between the layers, because the outer layer is not capable of carrying loads.
+- In this system the layers will be bonded together by a foil in between the layers.

It is difficult to put a foil in between the tubes, because of the round shape.
- A fire spray is not possible (see argument option A).
- Due to the lamination foil in between the layers, it is not possible to reuse layers (see argument option A).
- Due to the fact that the outer layer exists of two half tubes, there are lines and edges visible, which means that this option is less transparent compared to the other options.

C. Engels, S. (2020):

+- As discussed in chapter 2.3.2., it is not certain what happens to the lamination behaviour of the coating if a compression force is put onto the outer layer. SCHOTT only did a blast test without a compression load. So, it can be possible that the outer layer is able to carry loads, but then the protective quality of the inner layer is probably less.
+- Due to the fact that the tubes are not bonded together, there is less collaboration between the layers for the load-bearing capacity than in option A. However, the outer tube can contribute to safety for the inner tube.
+ Spraying a *Tough* coating on the tube from SCHOTT is easier than bonding the tubes together by lamination.
+ It is possible to spray a fire spray on the outside of the inner tube. Then the outer tube can protect it from scratches. The fire spray can protect the inner tube. Besides, the cavity in between the outer and the inner layer can be filled with air, which may contribute to the fire resistance of the column. Water in between the outer and the inner layer is not possible. If the outer layer is broken, it keeps the glass pieces together, but water can probably come out.
+- Due to the fact that the tubes are not bonded to each other by lamination, maybe the inner tube can be reused if the outer tube is broken. However, this is also depending on the end connections.
+- See argument option A.

3.2.2. Design concepts

By looking into the already designed options (chapter 3.2.1.), advantages can be taken into account while designing new concepts:

- The glass column will be more redundant if the tubes will be bonded together by lamination. In this way, the column is able to carry part of the loads, even after fracture. Nevertheless, when bonding the tubes, it is not possible to delaminate the tubes.
- The *Tough* coating from SCHOTT can keep glass pieces together if the tube is not laminated.
- Two whole tubes are preferred instead of halve tubes, so as to offer load-bearing capacity.

Based on the above findings, the following two concepts have been developed:

- The MLA: two load-bearing borosilicate glass inner tubes which are bonded together, and a transparent fire coating applied on the outside. The inner tubes and the fire-resistant coating are protected by an outer tube with a *Tough* coating on the inside, which is not load-bearing.
- The SLW: two load-bearing borosilicate glass tubes which are bonded together. The column is filled with water to keep the temperature cooler for a certain time during fire.

In the following two chapters, the two new design concepts will be further explained. More research is needed on whether annealed or heat-strengthened glass will be used. In chapter 4, compression tests were performed on annealed and heat-strengthened samples.

3.2.2.1. Multi Layered with Air (MLA) - tube

In figure 52, the first new concept is shown, named the Multi Layered with Air (MLA). This column will be made of three glass tubes. The outer layer will be made from a borosilicate glass tube with a polymer coating inside the tube to keep the glass pieces together when the tube is broken. The outer layer is a protective layer, so it is not load-bearing. The two inner tubes are load-bearing and will be made borosilicate glass as well. These two inner tubes are bonded together by a transparent interlayer material. In this project, Ködistruct LG, LOCA material from H.B.Fuller Kömmerling is used. This is a thermoset, which is formed with cross-linked polymers. The first component is polyol and the second is isocyanate. This interlayer material cures/cools in room temperature. Due to this, no sudden cooling takes place, whereby no extreme stresses occur. Furthermore, this interlayer material has a low shrinkage value (3.5%).

The outside of the middle layer will be coated with a transparent fire resistance coating (like HCA-TR). However, as mentioned in chapter 2.3.3. this coating is only tested for flat glass panels and more research is needed to apply it to glass tubes. This coating is protected from scratches by the outer layer. Furthermore, it is advisable to use sprinklers in the building, to reduce the temperature of the glass for a certain time.

The column will be sealed to keep the dirt out of the column. As mentioned before, air pressure can occur due to temperature differences. This can result in condensation and stresses. If the shape of the cross-section of the glass column is not able to handle the stresses itself, the air pressure can be regulated by a ventilation system (figure 53). If the shape/glass is able to handle the stresses without breakage, the use of the ventilation system is not necessary. Nevertheless, condensation can still occur (see chapter 2.2.2.4.). In this case, silica grains are included in the design (figure 54). This principle is also used for double glazed units to avoid condensation.

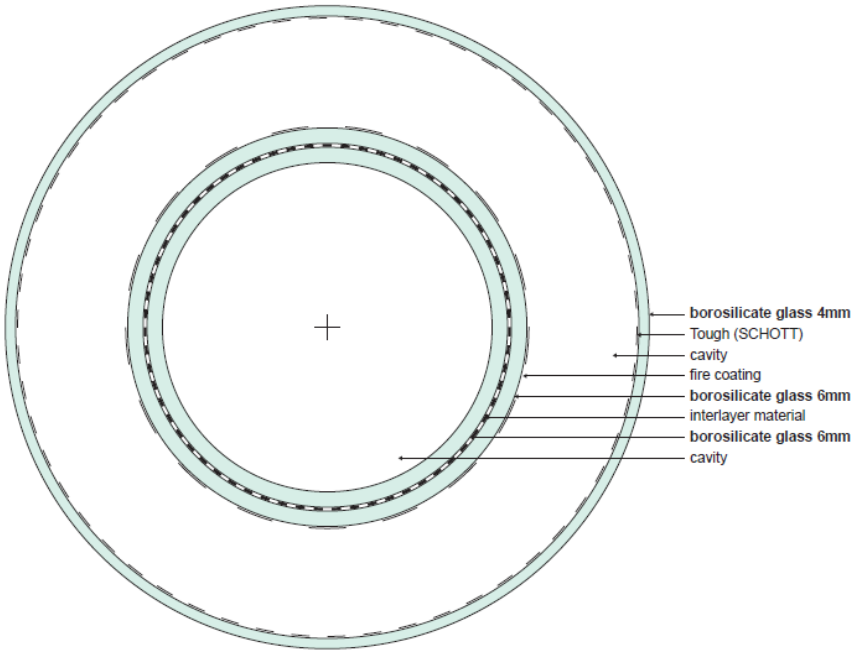

Figure 52 Cross-section of the concept Multi Layered with Air (MLA).

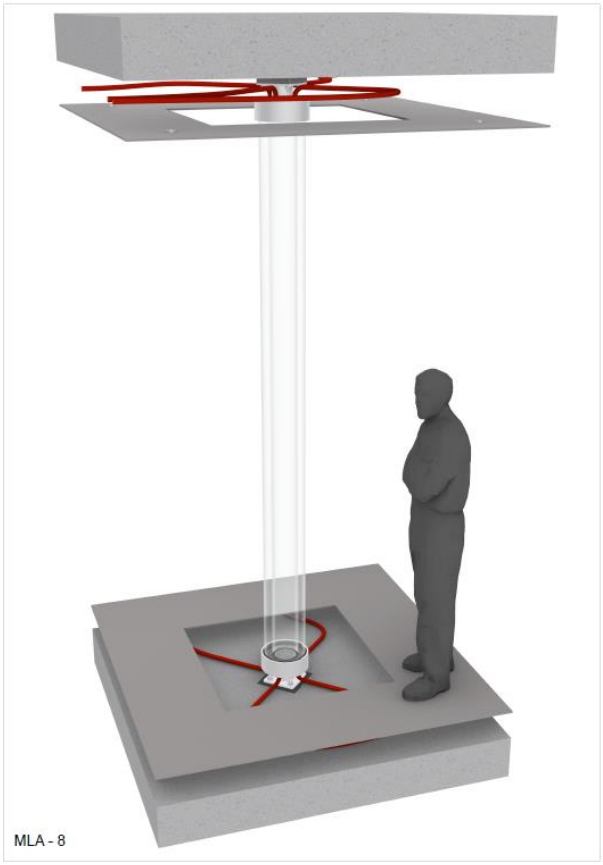

Figure 53 MLA (with air hoses).

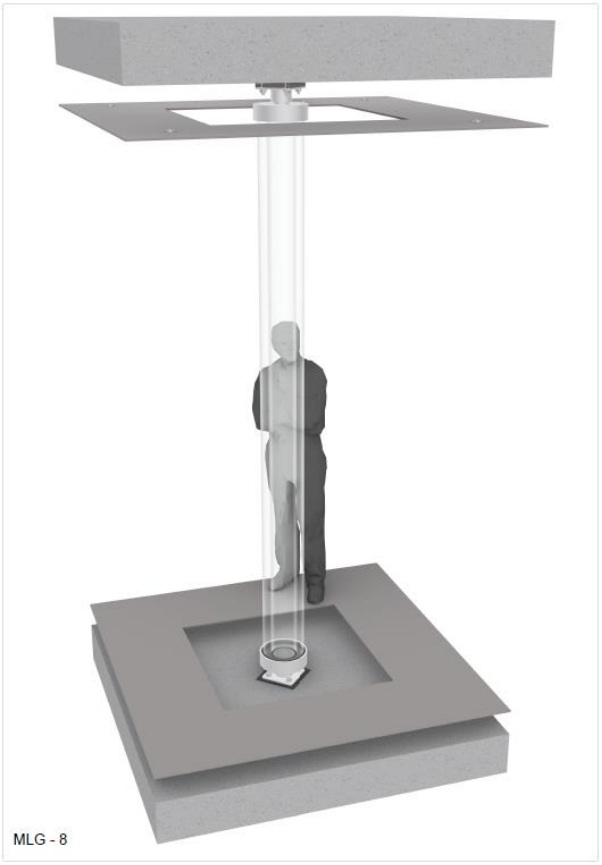

Figure 54 MLA (without air hoses).

Figure 55 SLW (with water hoses).

3.2.2.2. Single Layered with Water (SLW) - tube

In figure 55 (3D view) and 56 (plan view), the second concept is shown, named: Single Layered with Water (SLW). Two glass tubes are bonded together by an interlayer material (the same interlayer material as used for the MLA). The tube will be filled with water to keep the glass cool during fire. The water will be pumped through the column. Furthermore, it is advisable to use sprinklers in the building, to reduce the temperature of the glass for a certain time.

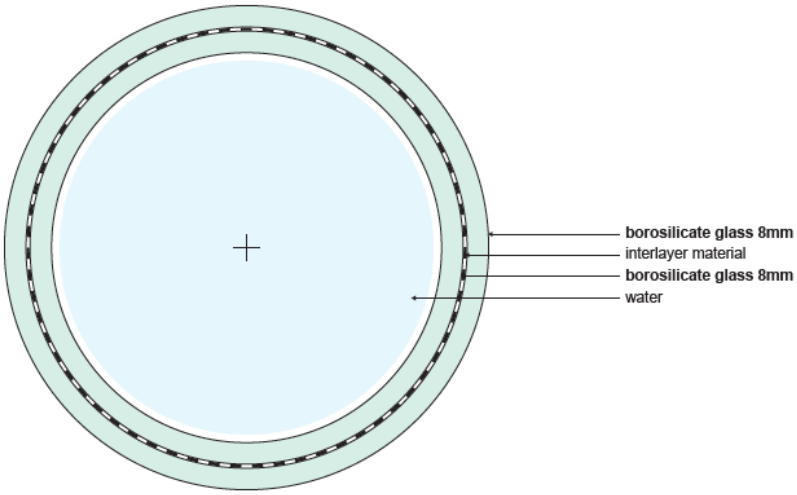

Figure 56 Cross-section of the concept Single Layered with Water (SLW).

3.2.3. End connections

From the literature study, a few points of attention emerged.

- The column needs to be designed as hinged connections, so that it will only take up normal forces.
- A soft material, with a lower Young's modulus, needs to be put in between the glass and the steel. A POM-block is designed with grooves, where the glass can be put in.
- The forces need to be introduced uniformly in the column. Under the glass tubes, in the groove in the POM-block, Hilti mortar will be injected. This Hilti mortar will distribute the forces into the glass tubes.
- Thermal expansion and isochoric pressure need to be taken into account due to temperature differences. For the MLA, filtered air will be regulated into the column. If this is not necessary, only silica grains can be put into the POM-block, which can take up water when condensation occurs. For the SLW, water will be pumped through the column. For these three designs, a POM-block is designed (explained in appendix 5).
- The column and the connections need to be designed to be fire resistant for 60 minutes.
- The edges of the glass need to be treated to avoid sharp edges, otherwise it is possible that forces are not uniformly distributed in the glass column, resulting in stresses.
- The column needs to be sustainable. This will be done by the following terms: durability and demountability.

Below a few aspects are mentioned which needed to be considered during designing of the end connections:

- How to pump the water/air from the hoses into the column, and how to make it water- or air tight?

- The Hilti mortar needs to be well-distributed into the POM-block grooves (under the glass).
- The POM-block and the column needs to be air- and water tight. Besides, the glass needs to stay clean during/after injecting of the Hilti.
- How to put silica grains in the POM-block?
- How to assemble the column? The parts are not bonded, but need to be held at the right place.
- How to replace the column?
- And when designing end connections, manufacturing tolerances need to be accommodated.

All of the abovementioned aspects, the design process and choices are further explained in appendix 5. In appendix 6, the drawing sheets are given, as 3D views, sections and details. In figure 57, a 3D cross section is shown of the MLA (with/without air hoses). These drawings are made for a concept column designed with fictive dimensions. This concept can be designed for every possible diameter according to the product list of SCHOTT, but the geometric tolerances of the glass tubes and the minimum/maximum width of the interlayer material needs to be taken into account. According to H.B.Fuller Kömmerling, the ideal interlayer material thickness is 2 mm, regarding the structural integrity of the column and the stresses occurring into the glass due to the resin. When the interlayer thickness is bigger than 2 mm, more stresses can occur in the glass. When the interlayer thickness is smaller than 2 mm, the structural integrity is not guaranteed. Lots of conversations with external companies have taken place to discuss the designs.

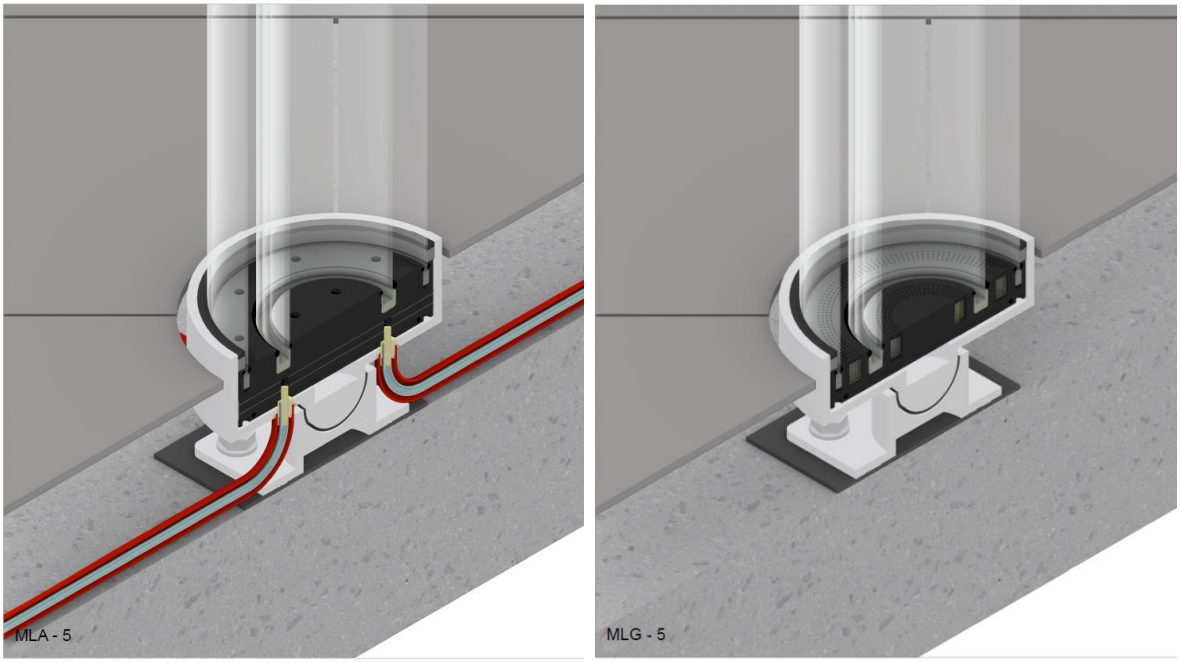

Figure 57 3D cross-section of the MLA (Left: with air hoses, right: without hoses).

3.2.4. Assembly sequence

An important aspect during detailing is the assembly sequence. If it is not possible to manufacture the column, then the details are incorrect. The assembly sequence for the MLA column (with air hoses) is presented in this chapter. Figure 58 shows the steps from the assembly sequence. This is a possibility for the assembly sequence, but other alternatives are not excluded. The intention is to show a possibility to present an efficient way to manufacture the column. The manufacturer also may come up with a way to assemble the

column. In appendix 7 is shown how to pre-assemble the POM-block, the steel shoe, the POM-ring, and the steel bracket.

- Step 00. This is the assembly machine. The glass tube(s) need(s) to be held and turned, because the Hilti mortar cannot be injected upside down.
- Step 01. The machine is ready.
- Step 02. While the glass inner tube is hanging in a crane, the first part of the ‘hands’ is placed around the inner tube. These ‘hands’ exist out of a clamp and a positioner.
- Step 03. After that the second ‘hand’ brace is placed around the glass.
- Step 04. To ensure the stability of the machine while rotating the glass, extra profiles are screwed to the machine.
- Step 05. Also, the second part will be attached to the machine, which makes the machine complete. The middle part at the top is screwed to both parts (step 4 and 5) by an equal angle.
- Step 06. Now the glass inner tube can be rotated 90 degrees to a vertical position. Next, POM braces will be screwed into the ‘hands’ and to the POM-block. Now the POM-block is hanging under the glass, and Hilti can be injected into the groove in the POM-block. In the POM-block the hoses are already attached (more on this in the assembly sequence from the POM-block itself, appendix 5 and 7).
- Step 07. After that the POM-block can be pushed under the glass inner tube at the right height, which is marked at the glass tube. Wait 30 minutes until the Hilti mortar is completely hardened.
- Step 08. Rotate the glass tube 180 degrees and repeat step 6 for the other side.
- Step 09. Repeat step 7 for the other side as well.
- Step 10. Attach braces for the steel shoe to the ‘hands’ with the steel shoe hanging in it. Under the steel shoe, studs are present to hang them in the braces.
- Step 11. Position the steel shoe under the POM-block and remove the braces which constrain the POM-block.
- Step 12. At the top connection, remove the POM-cap, and the POM braces. Replace the clamps from the glass ‘hands’ by bigger ones (so that it can hold the outer tube in step 13).
- Step 13. Remove the top parts from the machine (step 4 and 5) and slide over the outer glass tube. POM-rings are attached to both sides of the outer tube (more on this in the assembly sequence from the POM-block itself, appendix 5 and 7).
- Step 14. Attach the top parts of the machine again, and place back the POM-cap at the top connection.
- Step 15. At the top connection, attach the steel shoe with its braces. The braces need to be attached to the ‘hands’.
- Step 16. Apply the neoprene and the sealant to the bottom connection.
- Step 17. Rotate the glass tubes and repeat step 16 for the other side as well.
- Step 18. Rotate the glass to a horizontal position. Secondary parts need to be placed in between the braces to keep them together.
- Step 19. Now the pre-assembly of the column is finished. The glass needs to be hung into a crane again. The top parts of the machine can be removed again.
- Step 20. Now the glass ‘hands’ can be removed (first part).
- Step 21. The second part of the hands can be removed, and a general check must be carried out.
- Step 22. Place extra steel braces for safety during transport.

The pre-assembly is now finished, and all the components can be brought on-site and the column can be installed:

- Step 0. An overview is given of all the components that are needed to assemble the pre-assembly on-site.
- Step 1. The brackets need to be installed to the support (a floor or a beam) (more on this in the assembly sequence from the steel bracket itself, appendix 7).
- Step 2. Afterwards, the bottom connection can be placed in the bottom steel bracket.
- Step 3. Position the glass at the top.
- Step 4. Tighten the bolts to the top connection and place the shim plates at the top.
- Step 5. Remove the steel (protection) braces then the column is placed on-site. Connect the hoses to the system, and the column is finished.

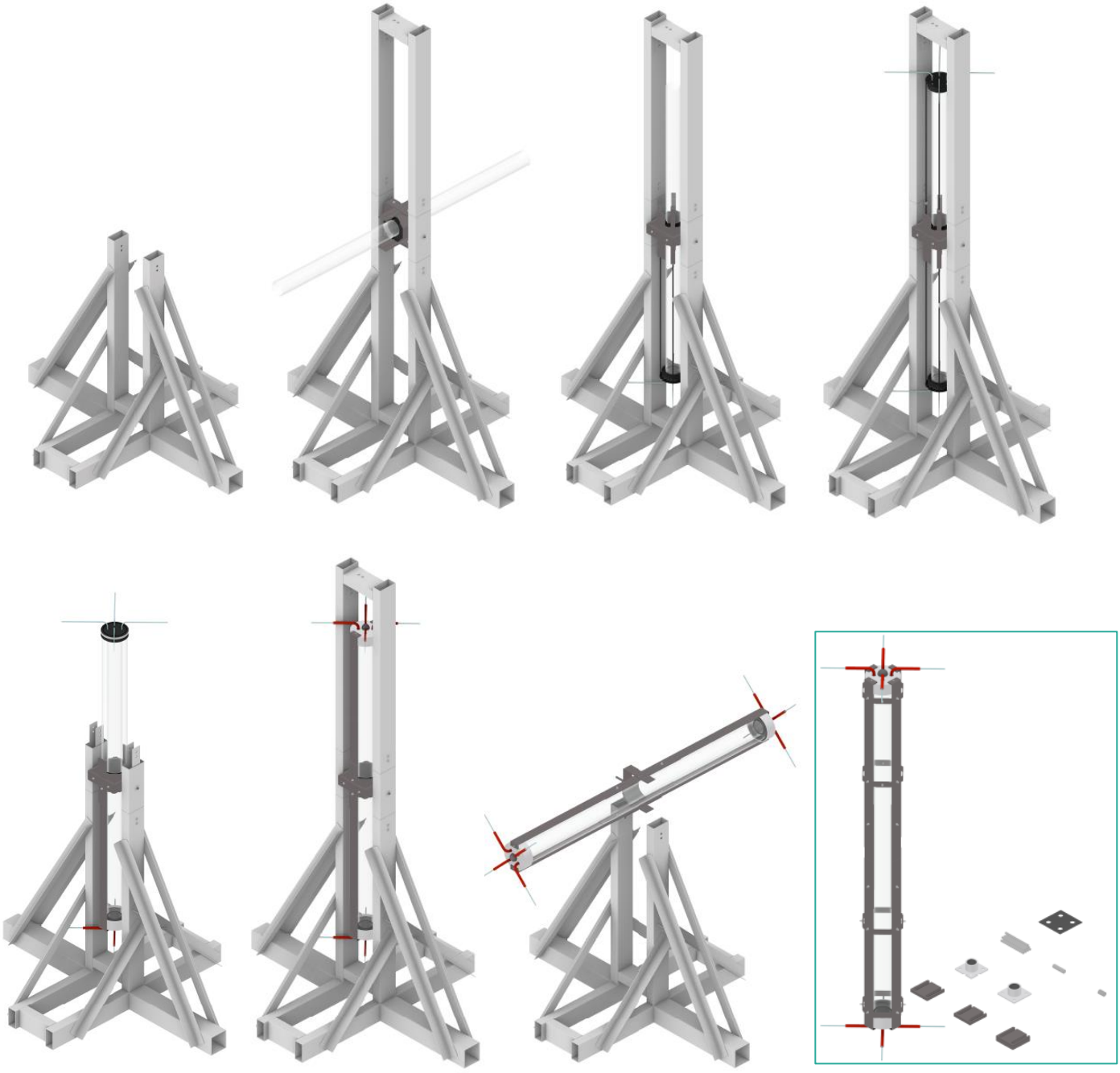

Figure 58 Steps to assemble the MLA with air hoses (step 1, 5, 7, 9, 13, 15, 20). The last picture is an overview of all the components ready for installation on-site.

3.2.5. Failure mechanisms

In chapter 2.2.2. possible failure mechanisms for columns are discussed. In this chapter, a prediction of the possible failure mechanisms for the MLA and the SLW are given.

3.2.5.1. Impact loads

3.2.5.1.1. MLA

If the column is loaded under impact loads, the outer layer will break first (see the dark red circles in figure 59, left). This outer layer will protect the inner layers for a while. If the impact load hits the column only once or a few times, only the outer layer is broken. The *Tough* coating on the inside of the outer tube will hold the glass pieces together. If the impact load continues, eventually the inner layer(s) will break too. So, to protect the inner layers, the column needs to be protected.

3.2.5.1.2. SLW

If the column is loaded under impact loads, the outer layer will break first (see the dark red circles in figure 59, right). Due to the fact that the tubes are bonded together, the glass will be kept in place when broken. In this way the outer layer is still capable of carrying part of the loads. If the impact load continues, eventually the inner layer will break too. So, the column needs to be protected, to keep the inner layer intact.

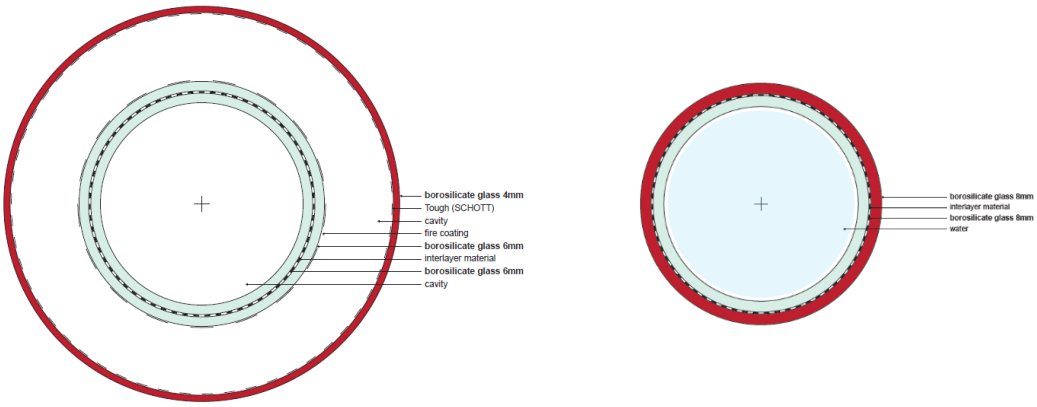

Figure 59 Failure mechanism at impact loads (left: MLA, right: SLW). The dark red circles will be hit by the impact loads and will break first.

3.2.5.2. Compression/buckling

The column needs to be robust, so that it gives a warning before total failure. If one of the columns fails, the glass cracks first as a warning, so that people can evacuate, before the glass starts shattering. There is assumed that no secondary load path is needed, which means that the glass column needs to be able to still carry the loads for the SLS situation even after fracture.

3.2.5.2.1. MLA

The MLA has an extra safety mechanism, because it can avoid glass shattering away whereby injuries occur. When the glass hits the outer tube, cracks can occur by the impact. The glass of the outer layer will be hold together by the *Tough* coating. The outer layer of the MLA is not load-bearing.

First off, the column will have an elastic behaviour. After that the column will start to deform. Buckling has started, due to the slenderness of the column, whereby the column wants to bend in the middle. Due to bonding the tubes together, the bending of one tube will be postponed because it is fixed to the other tube by lamination. After that, both tubes want to bend. The failure will start in the compression zone where the outer glass layer (of the inner

tubes) starts to disintegrate (Veer, F.A., et al. 1999). Then cracks will occur in the outer layer of the inner tubes first (see dark red in figure 60, left). After that, the crack formation continues, and the cracks will also occur in the most inner layer (light red in figure 60, left). Even when cracks appear, the column is able to carry loads for a certain time. After the critical buckling load, the column will completely fail (Van Nieuwenhuijzen, E.J., et al. 2005).

3.2.5.2.2. SLW

The inner layers of the MLA will react in the same why as the layers from SLW. So, first the column starts to deform, whereby buckling occurs, due to the slenderness of the column. Due to bonding the tubes together, the bending of one tube will be postponed because it is fixed to the other tube by lamination. After that, both tubes want to bend. Then cracks will occur in the outer layer first (see dark red in figure 60, right). After that, the crack formation continues, and the cracks will also occur in the inner layer (light red in figure 60, right). Even when cracks appear, the column is able to carry loads for a certain time. After the critical buckling load, the column will completely fail.

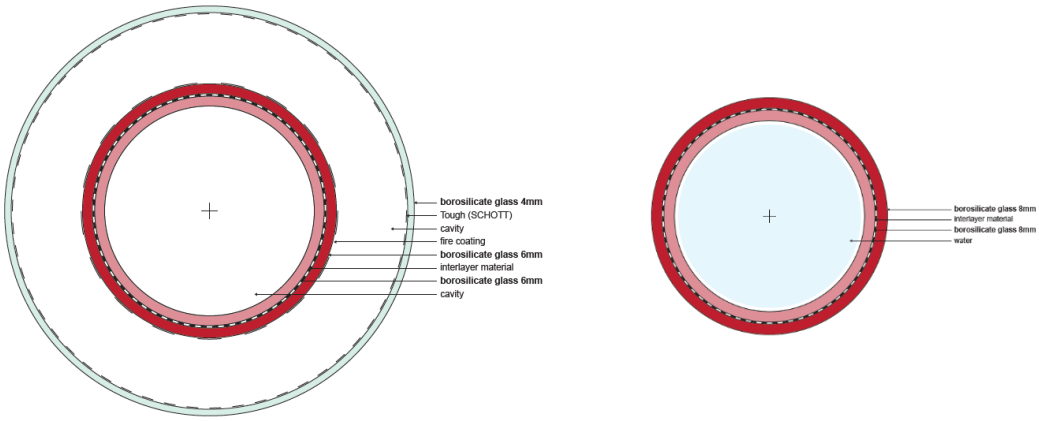

Figure 60 Failure mechanism at compression/buckling (left: MLA, right: SLW). Cracks will occur first in the outer layers (of the inner tubes), which is marked with dark red. After that, crack formation continues and cracks appae in the most inner layers too, which is indicated with light red.

3.2.5.3. Fire

Borosilicate glass has a better resistance against thermal stresses than other glass types, like soda-lime glass. At figure 61, the properties for temperature resistance and thermal expansion are given for DURAN® borosilicate glass tubes from SCHOTT.

3.2.5.3.1. MLA

The outer layer with the *Tough* coating from MLA starts to break/melt at a critical temperature (dark red in figure 62, left). Then it is not able to carry loads anymore, probably not even its own self-weight. This outer layer can keep the temperature of the inner layers below the critical temperature for a certain time. After that, the fire coating is exposed to a certain heat and this can protect the inner layers again for certain time (light red in figure 62, left). After that the column will fail completely. More research is necessary to investigate this principle.

3.2.5.3.2. SLW

The outer layer of the SLW will break first, due to temperature stresses (red dark circle in figure 62, right). This layer can protect the inner layer for a certain time. The water inside can keep the glass layer(s) cooler for a while. At a certain time, the column will fail completely. More research is necessary to investigate this principle.

Temperature resistance and thermal expansion	
Coefficient of mean linear thermal expansion α (20°C; 300°C) as per DIN ISO 7991	$3.3 \cdot 10^{-6}\ K^{-1}$
Transformation temperature T_g	525 °C
Glass temperature at viscosity η in dPa · s:	
10^{13} (annealing point)	560 °C
$10^{7,6}$ (softening point)	825 °C
10^{4} (working point)	1260 °C
Thermal conductivity λ_w at 90 °C	$1.2\ W \cdot m^{-1} \cdot K^{-1}$

Figure 61 Properties temperature resistance and thermal expansion for SCHOTT DURAN® tubes (SCHOTT. (n.d.).

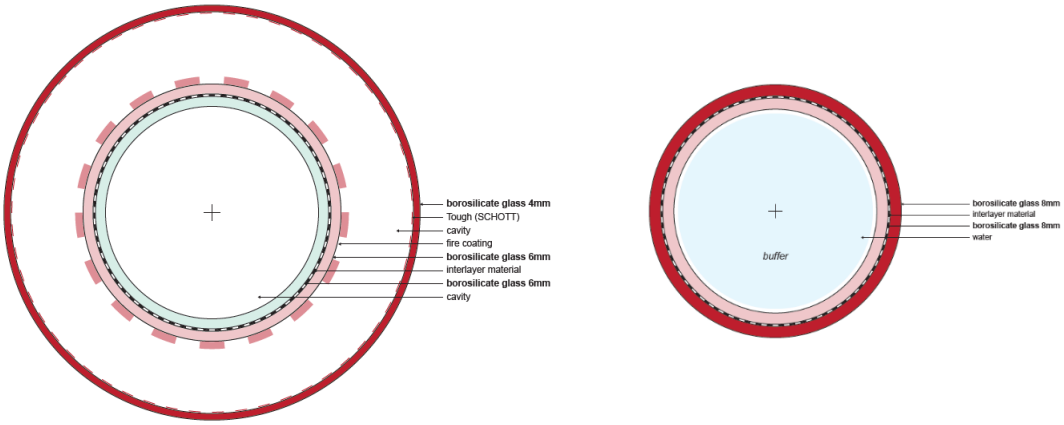

Figure 62 Failure mechanism at fire (left: MLA, right: SLW). The dark red circle is exposed to the fire and will break/melt first. After that, at the left (light red), the fire coating is exposed to fire and will foam up to protect the inner layers for a certain time. At the right (light red), due to the water inside, the temperature of the inner tube will be cooler for a certain time.

3.2.6. Replacement strategies

If the column fails due to one of the failure mechanisms given in chapter 3.2.5, it needs to be replaced. Replacement strategies are important to think off, while designing with glass. In the chapter below, the steps for the replacement strategy will be described. If the building was exposed to fire, it raises the question of whether replacement is still possible or whether it has to be built anew. If the column was loaded under too much compression force, all the glass layers are cracked, whereby it needs to be replaced. If the column is hit by an impact load, there is a possibility that for the MLA only the outer layer is broken. Then the same steps need to be carried out to replace the column, but only the outer layer needs to be reordered and the other parts can be reused, since none of the components are bonded together. The column needs to be designed so that it can handle impact loading. It is necessary that the column will be designed so that, when it is partly broken, it is still able to carry the SLS compression loads. For now, the assumption is made, that a secondary load path will not be necessary, because when the inner layers are partly broken, even then the column is capable of carrying part of the loads due to the fact that the glass is bonded together by an interlayer material.

Below the replacement strategy steps are described when all the layers are cracked:

- All the glass layers are cracked, but it is still able to carry the required SLS loads. However, these cracks are a warning that a temporary structure needs to be placed to support the floor/beam above the cracked column, so that if the glass column fails, no failure of the building can occur. These temporary columns can be placed at both sides next to the cracked column. The area around the column must be set off, so

that people cannot come close anymore to avoid injuries. In the meantime, new glass tubes need to be ordered.

- If the new glass tubes have arrived, the cracked column can be taken out of the building. First, the brackets need to be placed around the column (the same brackets that brought the column to the site can be used). These brackets keep the components together, since the components are not bonded. Afterwards, the hoses for the air/water regulation need to be unplugged from the system (figure 63, step 1).
- At the top, the shim plates can be removed, and the steel bracket can be moved to the top by tightening the bolts (figure 63, step 2).
- Now the column can be rotated in the lower steel bracket (figure 63, step 3).
- After that it can be taken out of the lower steel bracket. This needs to be done with a machine, because the column is too heavy to lift by hand.
- Now the column is ready to go on transport (figure 64, step 4).
- The column can be demounted in the factory. As said before, all the components can be reused, except for the cracked glass and the Hilti mortar. After that the column has been disassembled, the column can be pre-assembled again, in the same way a new column would be made (see the assembly sequence in appendix 7).
- After the pre-assembly of the column, it can be brought back on-site with the steel (protection) brackets attached to the column.
- Then steps 1 – 5 from the assembly sequence need to be repeated (chapter 3.2.4.).
- Lastly the temporary structure can be removed.

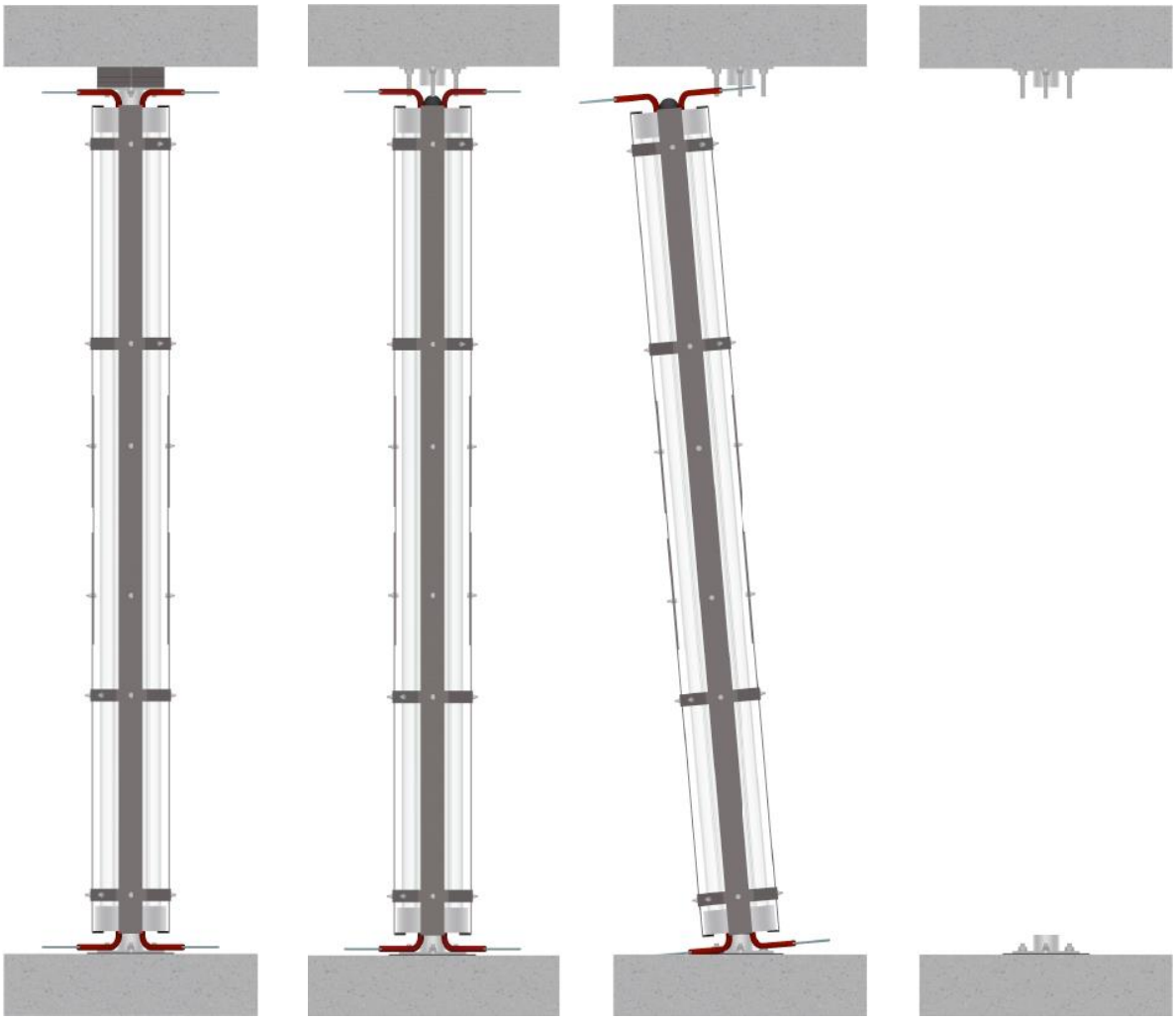

Figure 63 Replacement strategy.

Part II Design Phase

3.1. Case study

3.3. Case study

To design a column as realistic and practical as possible, it is crucial to show that the column will fit in a context. To determine loads, and to perform a risk analysis, a case is required. In this chapter the case study is explained, the starting points are given, the loads are determined for this case study, and the risk analysis is made.

3.3.1. Context and dimensions

For this project, the column will be placed in Bouwdeel D in Delft. Bouwdeel D is an extension of the office building of the architectural firm cepezed. This building is chosen for its light-weight structure. Nowadays, the existing glass columns are only able to carry one light-weight roof. In this project the column needs to be able to carry four light-weight floors from an office building. By replacing steel columns, standing in the middle of the building, with glass columns, it will suit the transparency and the modernity features of the building. According to Joost Heijnis, glass columns are a state of the art. It will probably not fit in a regular cheap building. Bouwdeel D is probably not as high end as other buildings, but it is modern. Due to its clear structure and its transplant look, Bouwdeel D can be a suitable case.

The employer of the project was cepezedprojects in Delft. The architect was cepezed. The constructor was cepezedbouwteam. IMd Raadgevende Ingenieurs in Rotterdam was structural engineer (Bouwdeel D(emontabel) Delft. 2020). The building Bouwdeel D is close to my home in Delft. I walked by the building many times, and I already became familiar with the building during my work as a structural engineer at IMd Raadgevende Ingenieurs. More information of Bouwdeel D will be given in this chapter.

As said, Bouwdeel D is an extension from the office building cepezed. The office is a former TU Delft building. In figure 64 the situation of the case is given. Bouwdeel D was nominated for ‘Kantoorgebouw van het jaar 2020’ and the office building won the ‘Nationale staalprijs 2020’. The complete building exists of parts A, B, C, and D (figure 65). The D in Bouwdeel D, stands for Demountable. This means that the building can be reused, so the building can be placed somewhere else without discard of parts. The extension is placed on the original foundation from the TU Delft (bouwdeel d(emontabel). 2019) (Bouwdeel D(emontabel) Delft. 2020).

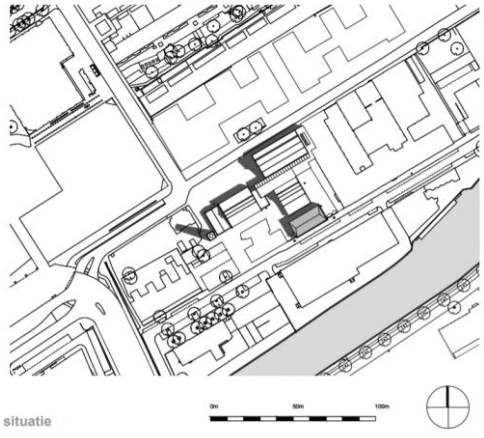

Figure 64 Situation case (Bouwdeel D(emontabel) Delft. 2020).

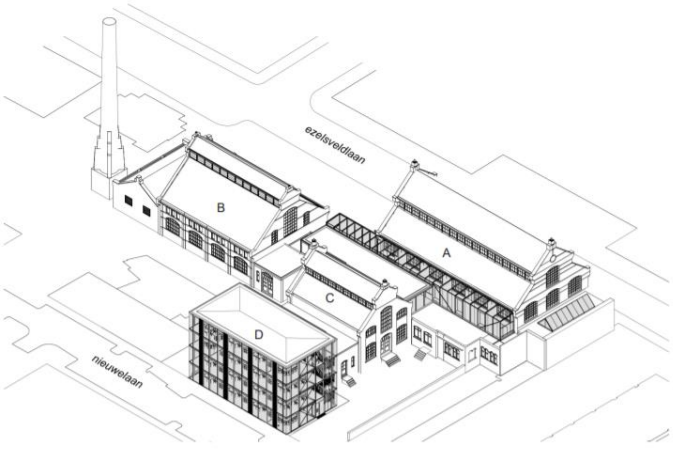

Figure 65 3D view from the situation of the case (Bouwdeel D(emontabel) Delft. 2020).

Bouwdeel D consists of 4 floors. The height of the floors is around 3.2 meters. The load-bearing structure exists of beams and columns, made from steel. Columns are placed in the

façade, and one row is placed in the middle of the floorplan. The columns in the façade are made out of one piece, the columns in the middle of the building are around 3.2 meters long. These columns in the middle are interrupted by steel beams. The floors are made of laminated Metsä Wood Kerto LVL timber elements of 11 meters long. These are spanning from façade to façade and are also supported by the beam in the middle of the floor. The façade is made of glass panels and a few metal panels are placed in between for ventilation. To carry the wind loads, bracings are placed in the façade and the floor panels do have diaphragm action. Due to the fact that the total building area is less than 1000 m^2, there are no fire requirements. The façade of Bouwdeel D which is close by the façade of part C has a requirement of 60 minutes, to avoid a fire flash-over. To keep the façade standing during a fire, the columns at the ground floor need to withstand the fire for 60 minutes, and extra bracing is placed in the first floor (Webinar Bouwdeel D(emontabel). 2020). In figure 66 a picture of Bouwdeel D is shown from the outside (left), and from the inside (right).

Figure 66 Bouwdeel D from the outside (left) and from the inside (right). (Bouwdeel D(emontabel) Delft. 2020).

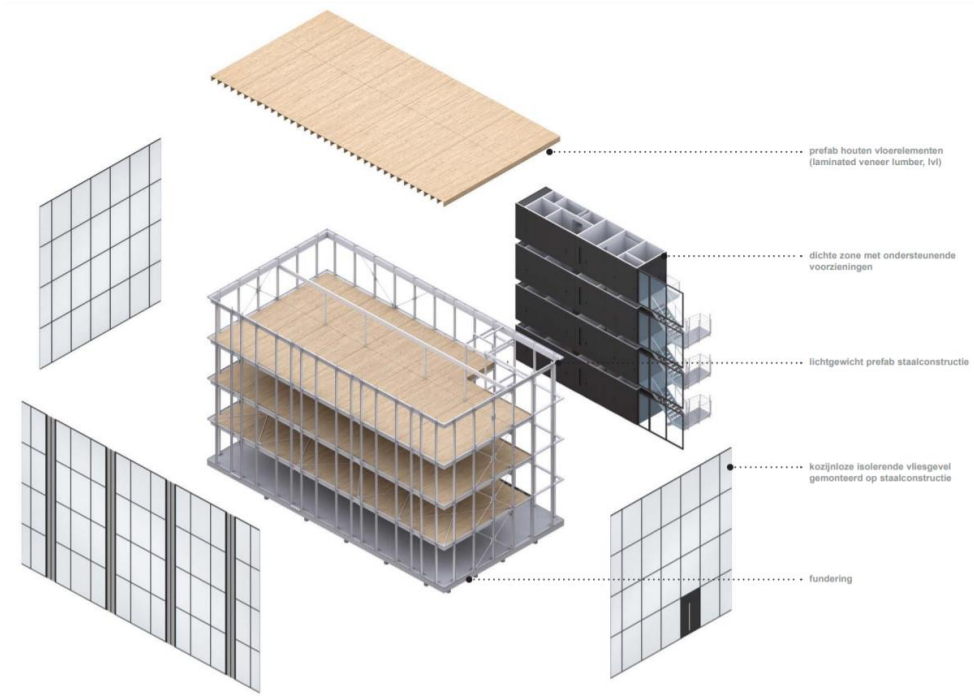

Figure 67 Explode view of Bouwdeel D (bouwdeel d(emontabel). 2019).

In figure 67 an explode view of the structure is shown. Bouwdeel D has a very clear grid of 1.8 by 1.8 meters (Webinar Bouwdeel D(emontabel). 2020). Most of the columns are placed in the façade, and there is only one row of columns in the middle of the building, standing further away from each other than the columns in the façade, to create a free layout. The

façade is made from glass. To give the building more transparency, it would be nice to replace the columns in the middle of the floorplan by glass columns.

3.3.2. Case restrictions

According to the case study, the building does not have fire requirements, because the building is smaller than 1000 m^2, which means that it is one fire compartment. Only the black part (figure 67), which is attached to part C of the building (figure 65), needs to be fire safe for 60 minutes, to avoid fire flash-over. One of the requirements from this thesis, is that the column needs to be fire resistant. In a regular office building with a hight of 12.5 meters, a column needs to be able to withstand fire for 90 minutes according to the regulations (figure 37). Due to extra measurements as sprinklers, this can be reduced to 30 or 60 minutes. So, for this project the columns need to withstand fire for 60 minutes. This is the same requirement as for the black part.

The project is known for its demountability. Due to the possibility of reusing the building, it is considered to be sustainable. The column is designed for this building, so it would be good if the column is demountable too. The whole building can be dismantled and been built up somewhere else. The whole column can be unscrewed from its support (floor/ beam) and can be removed from the building. When the building is going to be placed somewhere else, the column can be reused too, by screwing it back to its place in the building. Furthermore, all the components of the column can be demounted, because nothing is bonding the materials together. So, all components can be reused. Besides, glass is a durable material. The height of the columns needs to be around 3.2 meters.

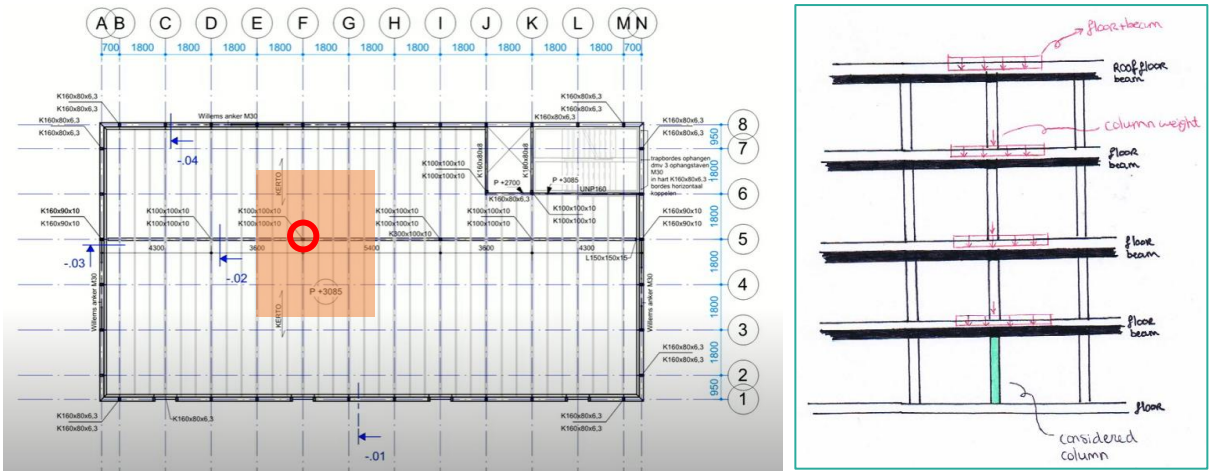

Figure 68 Floor plan with the considered column (left) (Webinar Bouwdeel D(emontabel). 2020). Cross section of the considered column (right).

In appendix 8, the compression loads are determined for this case. The starting points for the design are shown in appendix 8 as well. The considered column (shown in figure 68) is the one which needs to carry most of the loads (in the middle of the floor plan, on the ground floor). To include more safety, the glass column needs to be able to carry the loads for SLS situation even after fracture. In this case a higher safety factor is maybe not necessary. To determine a safety factor for the glass column, experimental tests need to be performed. These tests need to be carried out a few times to get a reliable value. For now, a safety factor of 1.5 will be considered. The compression load that needs to be considered on the column for ULS is around N_{ed} = 330 kN (the load is around 500 kN when a safety factor of 1.5 is taken into account). The compression load that needs to be considered on the column for ULS is around N_{ek} = 280 kN (the load is around 420 kN when a safety factor of 1.5 is taken into account).

The following dimensions are determined for this column:

- Outer tube with an outer diameter of 180 mm;
- Inner tube with an outer diameter of 160 mm;
- The wall thickness is 7 mm for the outer and the inner tube;
- This gives a cavity between the tubes of around 3 mm.

The column is slender, which means that buckling can be the cause of failure. The critical buckling force can be calculated with formula 1, which gives a critical buckling force of 1666,5 kN for the abovementioned dimensions (E_{glass} = 63000 N/mm^2). If the column needs to carry a compression force of 330 kN, then the Eigenvalue will be around 5. Also, the corresponding compression and tensile stresses can be calculated with formula 3 for these dimensions and compression forces.

- N_{ed} = 330 kN : compression stress = 46 N/mm^2 and tensile stress = 9.2 N/mm^2.
- N_{ed} = 500 kN : compression stress = 69 N/mm^2 and tensile stress = 13.8 N/mm^2.
- N_{ek} = 280 kN : compression stress = 39 N/mm^2 and tensile stress = 7.8 N/mm^2.
- N_{ek} = 420 kN : compression stress = 59 N/mm^2 and tensile stress = 11.7 N/mm^2.

The tensile stress is normative, because these values are lower than the allowable compression stress for glass. In appendix 9, the theoretical allowable tensile stress for annealed glass is 15.5 N/mm2 and for heat-strengthened glass is 36.3 N/mm2. This should mean that the occurring tensile stresses are lower than the allowable stresses, which is acceptable. The allowable compression stress for borosilicate glass is 260-350 N/mm^2 (chapter 2.1.3.), which is much higher than the occurring compression stresses due to the abovementioned forces.

Furthermore, in appendix 8, a risk analysis is performed, regarding to this office building. According to the risk analysis, one layer is needed, as an extra protective layer. So, in case this layer breaks, the other layer(s) are still able to take over the loads. In case of the MLA, there is an extra outer tube. Even though, if the inner layers are broken, it is still able to carry some load. For now, there will be assumed that the column can carry the loads, even when they are partly broken by an impact load, so no secondary load path is needed. This post-failure behaviour of the designs needs be checked in the experiments.

Since, only samples with a length of 300 mm were tested in this project, the safety factor for columns could not be determined. The case study gives a good example of loads and the stresses that the column needs to be able to carry for a light-weight (office) building with four floors.

In figure 69, top picture, a 3D view of Bouwdeel D is shown in the current situation with steel columns. In figure 69, bottom picture, the same 3D view is shown with the MLA (without air hoses). As can be seen, the glass columns are not blocking the view in space and the steel columns do. In appendix 6, more 3D perspectives are shown from the columns in Bouwdeel D. In here also the other columns are presented. In these pictures, the hoses are visible. The finishing is at the client's discretion.

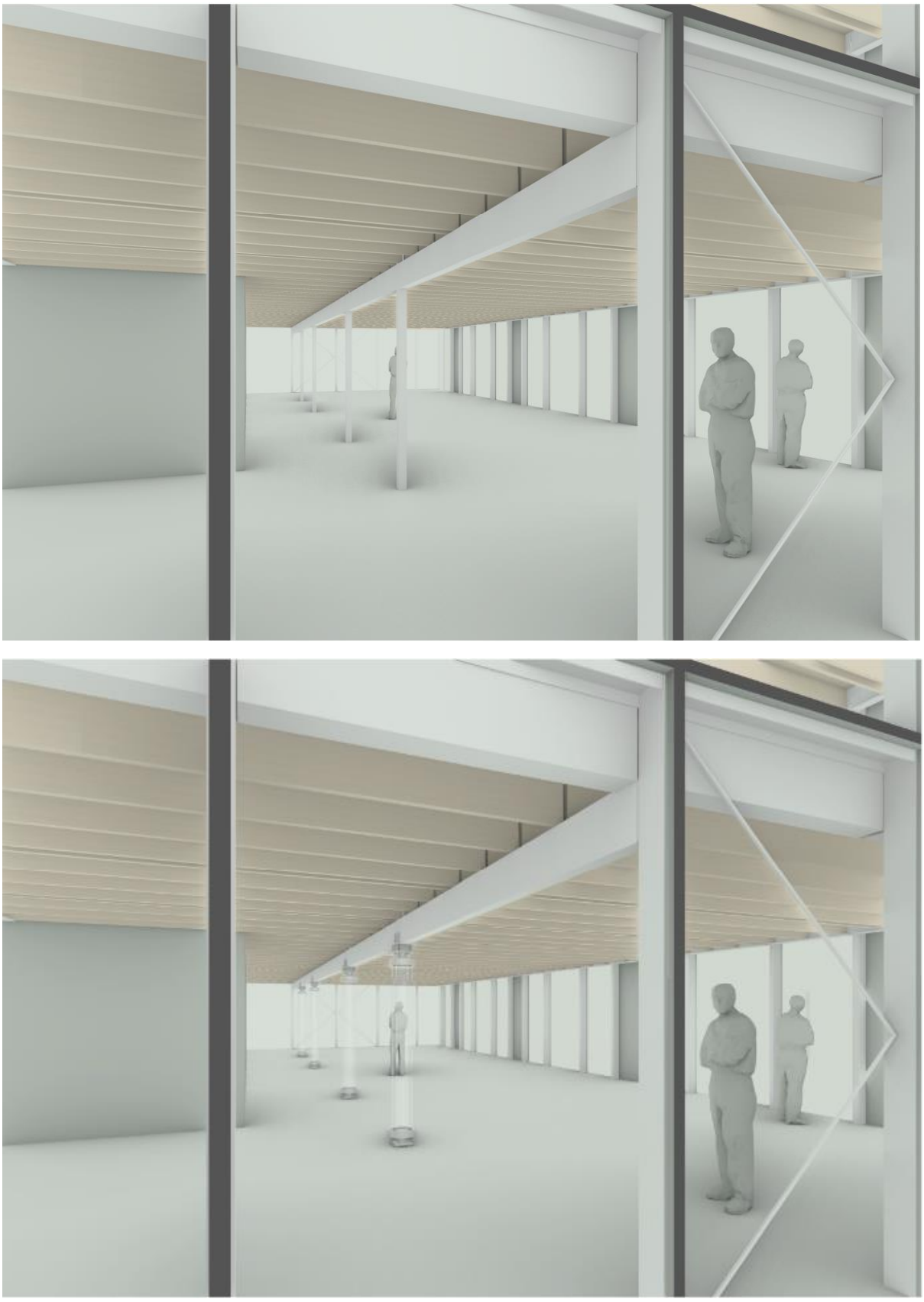

Figure 69 3D view of the column in Bouwdeel D.

In the figure 70, the tested sample is shown in Bouwdeel D to give an impression.

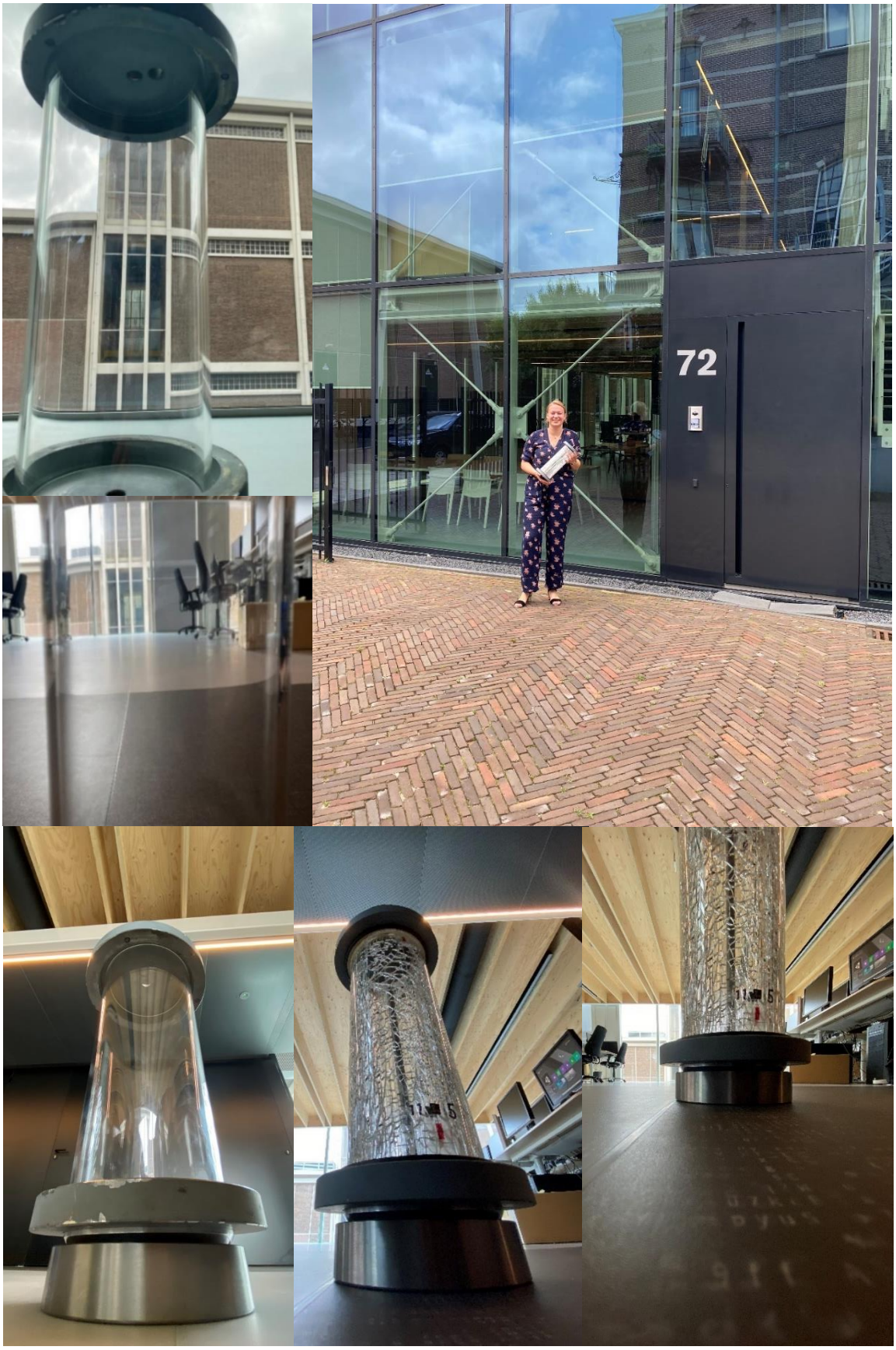

Figure 70 An impression of the sample in Bouwdeel D.

Part II Design Phase

3.4. Conclusion

3.4. Conclusion

In this chapter, the answers are given on the sub questions for part II Design Phase.

What are the design criteria and the main concerns for designing a glass column?

Design criteria and main concerns for the glass column are:

- Tubular shape:
  - Reduce of internal stresses due to the round shape, and the shape has a better resistance against buckling and torsional buckling.
- Thermal and residual stresses (condensation/dirt):
  - Due to the fact that the column needs to be sealed to avoid dirt coming into the column, isochoric pressure can occur. This can result in condensation, which needs to be avoided.
  - Thermal stresses can also occur during/after the lamination process. During the process the glass and the interlayer will be heated up. Due to the different thermal expansion coefficients of the glass and the interlayer material, it will result not only in expansion, but also in stresses.
  - Due to the geometric tolerances in the glass, differences in thickness in the interlayer material occur. The thicker the interlayer, the more stress resulting on the glass, the thinner the interlayer, the less it will bond the glass tubes.
- Transparent:
  - The ability to look through the column. Transparent, but visible, so that no one runs into it, and it contributes to the aesthetic value of the design. The more layers, the less transparent the column will be. Moreover, air inside the gaps, also plays a role in transparency, since this results in distortion.
- Fire resistance:
  - The case study has no specific requirements, but the column will be designed to withstand 60 minutes of fire. The tubes will be made of borosilicate glass, which contributes to the fire resistance.
- Robustness:
  - The column needs to be able to carry loads even after an impact load. If this is the case, a secondary load path is not necessary. This needs to be tested. Chemically tempered glass is stronger and contributes to the robustness of the column. Multiple layers bonded together are safer, and it results in less injuries, because glass pieces will be kept from falling. *Tough* coating from SCHOTT can keep glass pieces together too. Connections and stiffness of interlayers contributes to the robustness of the column.
- Manufacturing of the column:
  - The tubes are made by extrusion by machines. Curing of the resin needs to be done carefully, otherwise, void formation, shrinkage or stresses in the glass can occur.
  - Manufacturing tolerances need to be accommodated.
- End connections:
  - The column needs to be designed as hinged, so that it will only take up normal forces.
  - A soft material, with a lower Young's modulus, needs to be put in between the glass and the steel.
  - The forces need to be introduced uniformly in the column, to avoid local peak stresses.
  - Not only the column, but the connections need to be designed fire safe.
  - The column needs to be sealed to avoid dirt coming in.

- Restrictions to the case study:
    - The column needs to be demountable, because the case study is designed as demountable, which means that the building and all its components can be reused somewhere else. Reusing is a method to design in a more sustainable way.
    - Glass can contribute to this vision due to its high durability.
    - The columns in the building need to have a length of 3.2 meters.
    - It needs to be able to carry the calculated compression forces. (The forces are further explained in this chapter in the last question below.)
- Ability to replace:
    - The column needs to be replaceable when partly or completely broken.

What are different concepts for the design of the column, which fulfils the design criteria?

There are two new variations designed, which will be investigated in in part III of this project. All designs are made with borosilicate glass tubes, DURAN®/DURATAN® SCHOTT tubes.

In figure 71 (left), the first option is showed, named: Multi Layered with Air (MLA). The outer layer is a protective layer and is not load-bearing. The *Tough* coating on the inside of the outside tube will keep the pieces of the outer tube together when it is broken. The inner layers are bonded together by a transparent interlayer material. For this project a 2 PU-component, Ködistruct LG, LOCA material from H.B.Fuller Kömmerling is used. A fire coating is attached on the outside of the inner layers. The coating is protected by the outer layer. The cavities are filled with (clean) air. The tubes are sealed to avoid dirt getting in. Due to this, when there are temperature differences, air pressure differences will occur, which can result in condensation and stresses. So, a ventilation system is applied to regulate the air pressure. If this is not needed, only silica grains can be included in the POM-block. These grains can take up water when condensation occurs. Furthermore, when the outer layer is broken due to impact loads, and the inner layer is still intact, it is possible to reuse the inner layers, since the materials are not bonded together. An advice is to use sprinklers to reduce the temperature of the glass.

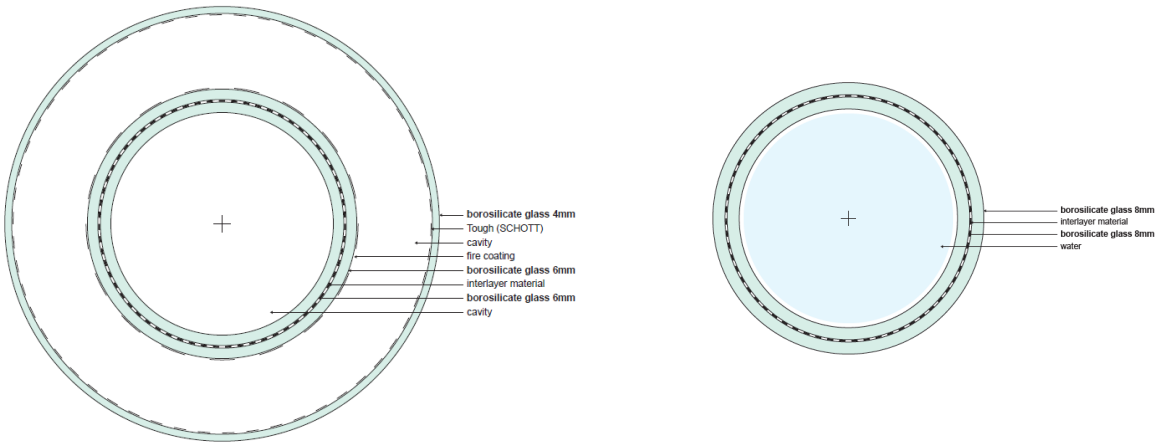

Figure 71 Plan views of principles of MLA (left), and SLW (right).

Concept 2 is shown in figure 71 (right), named Single Layered with Water (SLW). This concept is made of two glass tubes bonded together with a transparent interlayer material (the same interlayer material is used for the MLA). When the outer layer breaks, it is still able to carry part of the loads. If the outer layer is broken, it is not possible to reuse the inner layer. The tube will be filled with water to keep the column cooler when exposed to fire, so

that it can withstand the fire for a certain time. An advice is to use sprinklers to reduce the temperature of the glass.

Both designs fulfil the design criteria and main concerns: tubular shape, thermal stresses, transparency, fire resistance, robustness, manufacturing of the column, end connections, and restrictions to the case study.

Both designs have a tubular shape and are transparent. The thermal stresses and condensation are taken care of by the glass itself or by a regulated ventilation system, a regulated water system, or silica grains. The stresses from the lamination process need to be checked in the experimental investigations in project. Besides, the designs need to be fire resistant for 60 minutes. To make the design fire resistant for 60 minutes, sprinklers, a fire-resistant coating in the MLA and the water inside of the SLW, will be used. However, more research needs to be done on these principles. The column designs are robust due to the laminated tubes and the MLA even has an extra protective outer tube with a *Tough* coating on the inside. This lamination and the *Tough* coating, will keep the glass pieces together when broken, to avoid injuries. The post-failure behaviour will be checked in the experiments to conclude how robust the designs are. Manufacturing of the columns and the connections is possible. This is shown in the assembly sequences and are further described in the design process (appendix 5, 6 and chapter 3.2.4.). To be sure, lots of conversations have taken place to discuss the designs with external companies. Some restrictions to the case are: fire resistance of 60 minutes, the length of the column, the compression loads and the demountability. These are also aspects that could apply to other buildings. The designs are demountable, since all the parts are not bonding. So, all of the parts from the column can be reused. The designs for the end connections are dealing with a lot of these issues. The end connection will be elaborated in the next question.

Which aspects of the end connections have influence on the design and how are these aspects taken into account?

Some aspects that need to be taken into account in the connection:

1. Hinged connections, so that it will only take up normal forces.
2. A soft material, POM, will be put in between the glass and the steel.
3. Under the glass tubes, in the groove in the POM-block, Hilti mortar will be injected. This Hilti mortar will distribute the forces into the glass tubes, as uniformly as possible.
4. To avoid thermal stresses, isochoric pressures, and condensation, for the MLA, filtered air will be regulated into the column. If this is not necessary, only silica grains can be put into the POM-block, which can take up water when condensation occurs. For the SLW, water will be pumped through the column. Three POM-blocks are specially designed so that the water/air/silica grains are integrated in the end connections.
5. The column and the connection need to be designed to be fire resistant for 60 minutes. For the MLA this will be done by a fire coating, and water inside the SLW can keep the glass tubes cooler for a while. More research needs to be done for both systems. Besides, the steel components will be coated with a FR60 coating, the hoses will be covered by fire resistant hoses, connections are sealed off with a fire-resistant sealant, and sprinklers are advised.
6. The edges of the glass need to be treated to avoid sharp edges. Nevertheless, it will never be completely without irregularities.

7. The column needs to be sustainable. This will be done by the following terms: durability and demountability.

While designing the end connections, a few more aspects became from influence to deal with, concerning: the water/air tightness of the connection and the column, an efficient way of injecting the Hilti mortar, the assembly sequence, and the replacement strategy.

Is it possible to replace to column when broken and how?

The end connections of the column designs are engineered so that it is demountable. The connection is designed with a steel footplate. The plate can be unscrewed from the supports (floors/beams), and the glass column can be taken out in one piece. If the building will be placed somewhere else, it can be screwed back to its place. Furthermore, due to the fact that the Hilti mortar is not bonding, all the parts of the column are demountable and can be reused as well.

If one or more glass tubes are cracked or partly broken, the column needs to be replaced. If the column is able to carry part of the loads even after fracture, it still needs to be able to carry the loads for an SLS situation. When the column will be taken out, a temporary structure is needed. The steel brackets can be put around the column to keep the components together (during transport). In the top connection of the column, shim plates are placed, which create a tolerance into the top. These shim plates can be taken out, and the steel bracket can be moved to the top by tightening the bolts. Then the column can be rotated in the half hinge from the bottom end connection, and it can be taken out of the lower bracket. Then the column can be brought back to the factory. The parts that are not broken can be dismantled and reused (except for the Hilti mortar). The broken glass tubes need to be reordered. After that the column can be rebuild, in the same way as a new column will be pre-assembled. After that, the pre-assembly can be brought back on-site, it can be put in place, and after that the temporary structure can be removed.

For which case study will the glass column be designed?

The column will be place in Bouwdeel D, a four-floor extension from office building cepezed in Delft. The middle row of columns inside the building will be replaced by the glass columns designed and engineered in this project. The maximum required load for the ULS situation is N_{ed} = 330 kN (the load is 500 kN when an extra safety factor of 1.5 is taken into account, but this factor needs to be determined by carrying out experiments). This is calculated for the considered column, placed on the ground floor, which has to carry most of the loads. For the SLS situation, a load of N_{ek} = 280 kN needs to be considered (the load is 420 kN when a safety factor of 1.5 is included). The SLS situation needs to be taken into account when the column is broken. The corresponding compression stresses are between 39-69 N/mm^2 and the tensile stresses are between 7.8-13.8 N/mm^2. These values should be acceptable, because they are below the allowable tensile stress of 15.5-36.6 N/mm^2, and below the allowable compression stress of 260-350 N/mm^2.

Part III Numerical and Experimental Investigations

Part III Numerical and Experimental Investigations

4.1. Numerical models/hand calculations

4. Part III Numerical and Experimental Investigations

Based on the main concerns pointed out in Part II (chapter 3.1.), some numerical models and hand calculations are carried out to check if any of these concerns can cause problems to the design. The main problems which are checked are based on thermal stresses and compression/tensile stresses occurring due to a compression force onto the column.

By manufacturing samples, thermal stresses will occur during and after the curing process. H.B.Fuller Kömmerling will bond the tubes together. After that, the lamination process will be assed with H.B.Fuller Kömmerling and SCHOTT. Thermal stresses do not only occur during the manufacturing of the column. Due to the fact that the column is sealed, differences in air pressure occur due to differences in temperature inside and outside the column. More research is done on these stresses.

Furthermore, structural integrity needs to be verified from the designed structural glass columns. As said before, columns are primary structural elements, and if they fail, the consequences will be high. The manufactured samples are compressed by a compression load. The samples were compressed until failure. In this way, the post-failure behaviour of the design is researched, and compression/tensile stresses could be verified.

Next to these two aspects, more research is necessary for the fire resistance of the column designs. This will not be investigated in this research.

4.1 Numerical models/hand calculations

In this chapter, results of the numerical models and the hand calculations were defined for thermal and compression stresses.

4.1.1. Thermal stresses

As explained in chapter 2.2.2.4. and 3.1, thermal stresses occur due to temperature differences. The main concerns related to thermal stresses are listed below. These can happen in the manufacturing phase (the lamination/curing process) and during the user's phase.

- If the column is sealed it becomes a closed cavity. Differences in air pressure occur inside and outside the glass column due to temperature differences. These pressures are also called 'isochoric pressure'. It results in stresses in the glass and condensation inside the column.
- The glass can expand due to temperature differences.
- There are two types of interlayer material, the one which will be cured during UV-light and the other can cure in room temperature. If the interlayer material needs to be heated to cure, the glass and the interlayer material are exposed to a certain temperature. Glass has a lower thermal expansion coefficient than the interlayer material. This means that the interlayer material wants to expand more than the glass tubes, whereby stresses occur in the glass.

A few calculations were made of these phenomena in appendix 9 to check if it could cause any damage.

Due to temperature differences, overpressure and under pressure can occur. With overpressure the glass tube wants to expand and with under pressure the glass tube wants to contract. The occurring pressure in the tube can be calculated with equation 4 (chapter 2.2.2.4.). The allowable pressure in the glass tube depends on the wall thickness and the outer diameter of the glass tube. This is calculated according to the equation from SCHOTT (equation A.9.8). A small tube is checked with an outer diameter of 115 mm, a wall thickness

of 5 mm, and a length of 300 mm. It resulted in an allowable pressure of 636 MPa and an occurring pressure of 15.2 MPa (equation A.9.9). So, according to this calculation it will not give any problems.

Furthermore, when one glass tube is exposed to different temperatures, for example 20 °C inside the glass tube and 100 °C outside the glass tube, the tube wants to expand. The same dimensions were assumed for this calculation as before. According to the calculations the tube wants to expand with 0.03 mm. So, the new diameter would be 115.03 mm (equation A.9.14). The tube is free to expand 0.03 mm.

As explained, there are two types of interlayer material: the UV-light curved and the room temperature cured resin. If the UV-light curing resin materials will be used, then during the curing process the glass tube will be heated up to a certain temperature. The glass tubes and the interlayer material do have different thermal expansion coefficients. To check if any stresses occur that the glass cannot handle, a few calculations are made. The occurring tensile stress is leading. The allowable tensile stress for the annealed glass tubes (DURAN) is for long-term loading around 6 MPa (equation A.9.18) and for short-term loading around 15.5 MPa (equation A.9.17). For the heat-strengthened glass tubes (DURATAN) the allowable tensile strength for long-term loading is around 23 MPa (equation A.9.21) and for short-term loading is around 36.3 MPa (equation A.9.20). First a parametric model was made in Grasshopper (figure 72), and this is linked to Oasys GSA (figure 73). In appendix 9, the description is given how the Grasshopper-GSA model is made (chapter A.9.3.1.). The same dimensions were taken as used in the previous two calculations. The material properties for the glass and the interlayer material can be found in appendix 9 (chapter A.9.3.1.).

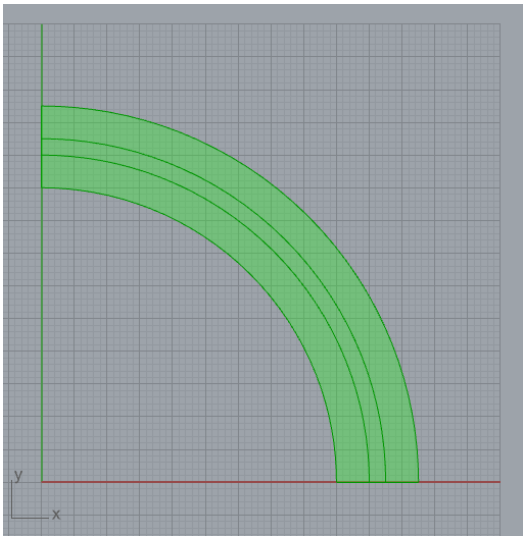

Figure 72 Grasshopper model of a quarter of the laminated glass tube shown in Rhino.

First an analysis was made for the situation that the sample only existed out of glass layers. In this way, the thermal expansion coefficient is the same for all layers, whereby only expansion should occur, and no stresses. The expansion/deformation for this situation is calculated via the numerical model in GSA and by hand calculations. The answers were almost the same. The deformation is around 0.0186 mm if all layers were made of glass, and almost no stresses occurred in the model.

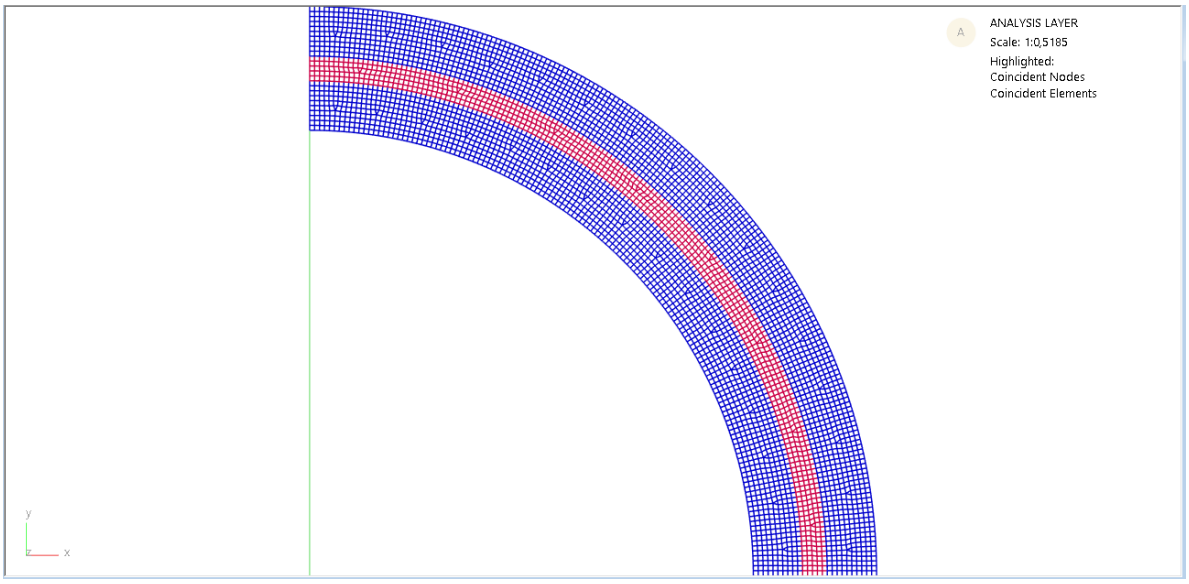

Figure 73 GSA model of the laminated glass tube.

Then a model was made as shown in figure 73 for two glass layers (figure 73, blue) and with an interlayer material (figure 73, red) in between the glass tubes. The deformation was the same as in the previous model, but now stresses are also present. The interlayer wants to expand, but the glass expands less. The interlayer material is not free to expand. It pushes onto both glass tubes, and this will give stresses. Compression stresses will occur in the inner glass layer and tensile stresses occur in the outer glass layer (figure 74).

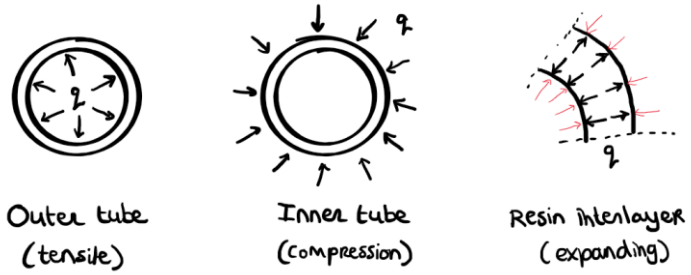

Figure 74 Stresses into the layers due to expansion of the interlayer resin.

These occurring stresses in the GSA-model were also checked with hand calculations. By comparing these results, it can be concluded that the stresses were in the same range. The stresses in the glass are around 0.002 MPa, which is quite low. So, in theory this will not result in problems, because the glass can handle these stresses. However, H.B.Fuller Kömmerling tried to bond two tubes with an interlayer resin before, ten years ago. Regarding to their experience back then, the glass tubes broke. They proposed to use an interlayer material which will reduce the impact of chemical induced reaction shrinkage, by shifting from van-der-Waals interactions to chemical bonds during curing and keeping the curing temperature as low as possible to avoid additional thermal shrinkage in the post-gelling phase. For this reason, they wanted to use an interlayer resin material which will cure/cool in room-temperature and not be cured by UV-light. Besides that, they wanted to use an interlayer material which has a lower shrinkage value. In the article of Veer, is also mentioned that shrinkage of the interlayer resin can cause stresses into the glass (Veer, F.A., et al. 1999). This lamination process will be tried out first on small samples (the same dimensions are used in the models and calculations) to see what happens to the interlayer

material and the glass tubes. More on the manufacturing of the samples can be found in chapter 4.2.1.

4.1.2. Compression stresses

4.1.2.1. Buckling value

In appendix 10 a few calculations were made on compression strength and buckling. First of all, models were made in DIANA FEA for a single glass tube with fixed and hinged connections. To get the most accurate values, a few tests were performed in DIANA of these models, by changing the mesh size, the imperfection load and/or the polynomial orders. For example, the lower the imperfection load applied on the glass tube, the less imperfect the column is (as explained in chapter 2.2.2.2. and A.10.2.3.). The values for the buckling load were verified with hand calculations. By performing a structural stability, eigenvalue analysis, the buckling value can be obtained. The values from DIANA were about the same as the values obtained from the hand calculations. This theses project will only test the 300 mm samples. These will first be assessed, and after that, longer tubes can be tested. The samples will be compressed, and due to the fact that the samples are small, global buckling will not occur. So, there were no more calculations/DIANA-models made for the laminated tubes. The setup of the model is working, which is verified with the buckling value by the comparison between hand calculations and the results from the numerical models. So, these models can be used and further developed when longer samples need to be verified.

4.1.2.2. Spring stiffness and deformation

To verify the compression tests (chapter 4.2.) a spring stiffness calculation was made (appendix 10). In here the load versus displacement curve is obtained during testing, which can be compared to the deformation calculated per force.

In figure 75, a 3D view is shown from one sample with a length of 300 mm. At the left the sample is shown with steel plates and at the right it is shown without the steel plates. One glass sample is made of:

- Two DURAN borosilicate glass tubes, (SCHOTT):
    - Outer tube:
        - OD: 115 mm
        - WT: 5 mm
        - L: 300 mm
    - Inner tube:
        - OD: 100 mm
        - WT: 5 mm
        - L: 300 mm
- Cavity filled with a transparent interlayer resin: Ködistruct LG, (H.B.Fuller Kömmerling):
        - Width: 2.5 mm (this can vary due to the tolerances in the glass)

And one of the heat-threated glass samples will be made of:

- Two DURANTAN borosilicate glass tubes, (SCHOTT):
    - Outer tube:
        - OD: 115 mm
        - WT: 5 mm
        - L: 300 mm
    - Inner tube:
        - OD: 100 mm
        - WT: 5 mm

        - L: 300 mm
- Cavity filled with a transparent interlayer resin: Ködistruct LG, (H.B.Fuller Kömmerling):
        - Width: 2.5 mm (this can vary due to the tolerances in the glass)

The connection for these small samples will be made of (the connection at the top will be the same as the bottom connection) (in figure 13 a sketch is shown of the cross section):

- POM-block, t=20 mm, ø=130 mm (with grooves to put in the glass tubes)
- HILTI HIT-HY 270 mortar (Hilti mortar), t =8mm (under the glass tubes)
- Steel bracket:
    - S355, cutting plate, t=20 mm, ø=165 mm (CNC-milling to create cambers to keep the POM-block and the hinge at its place)
- Steel hinge:
    - Standard product: GX50T

Furthermore, at the top and the bottom connection a steel plate is placed with a hole so that the wires from the sensors (placed at the inside of the glass), can go out of the glass tubes:

- Steel plate S3555, t = 10 mm, with hole for wires attached to the strain sensors inside the bonded glass tubes. *(Eventually, these were not used in the experimental tests, because a different compression machine was used. This machine had a hole in the top plate where the wires attached to the strain sensors could go through.)*

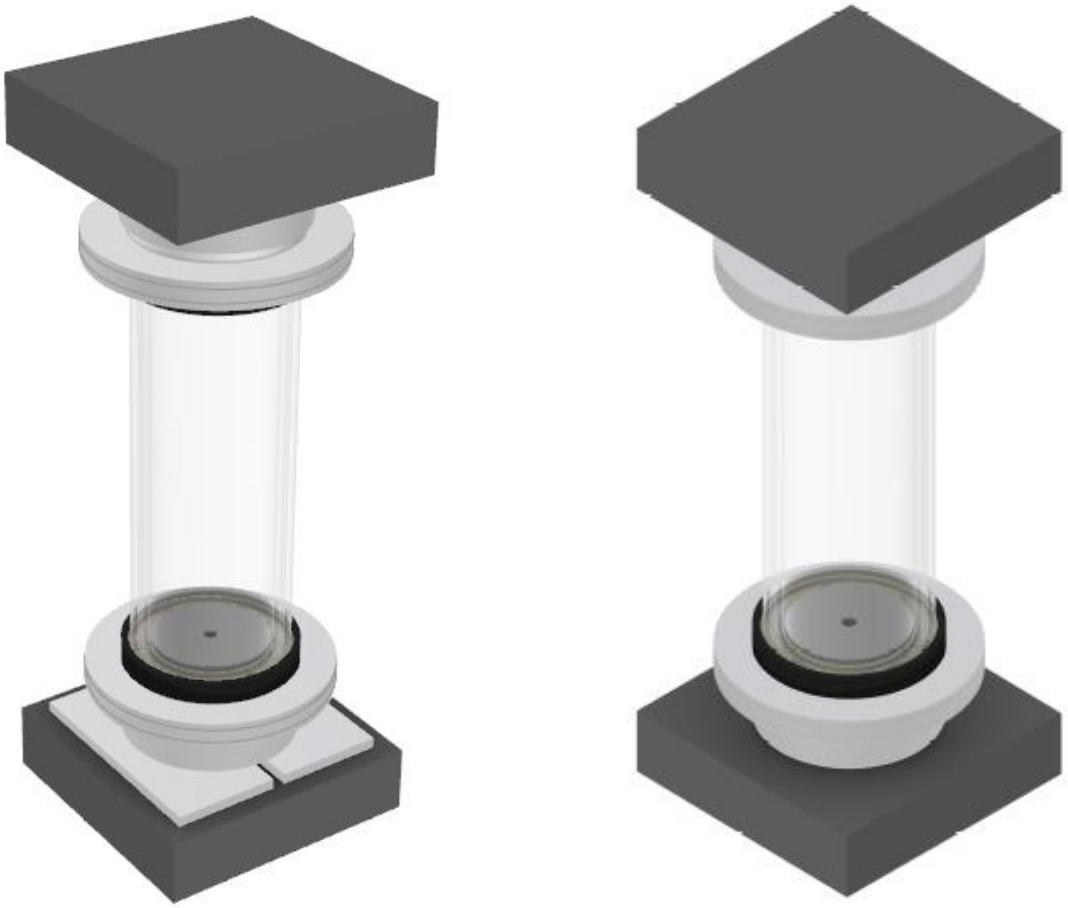

Figure 75 3D view of the sample with a length of 300 mm for the test setup (left). The sample without the steel plates (right).

Since both the MLA and the SLW have two laminated inner tubes which are load-bearing, so for both designs the same tests can be performed. With a load of 300 kN, the compression stress in the glass will be around 93 MPa (equation A.10.7). Due to the Poisson's ratio effects, transversal elongation will occur whereby tensile stresses occur. With a compression stress of 93 MPa, a tensile stress of 18.6 MPa will occur. For annealed glass, for short-term loading the allowable tensile strength is around 15.5 MPa. So, there is a change that the annealed glass tubes will break. For heat strengthened glass the tensile strength is higher, around 36.3 MPa. Besides, the allowable compression strength can reach 200 MPa for both samples. If 500 kN will be put onto the samples, the compression strength will be 155 MPa. According to the allowable compression strength this is still possible, but for the tensile stress it is not. In chapter A.10.3.2. the spring stiffness, the deformation and the strain values are calculated for the samples with a length of 300 mm. With equation A.10.11, the spring stiffness and the deformation can be calculated for a certain force. If the compression load of 500 kN will be assumed, then a deformation of around 2.5 mm will occur, and the strain in the glass will be around 0.00246 (table 11). In figure 11 the strain value is also been given times 1000000, because the values from the machine are also amplified with this factor.

Spring stiffness sample:

Components	Length or Thickness [mm]	A [mm2] =	A [mm^2]	E [N/mm^2]	F [kN]	σ [N/mm^2]	ε [-]	u or ΔL [mm]	k [N/mm]	ε*1000000 [-]
steel hinge GX50T	33	Pi*((120/2)^2-(50/2)^2)	9346,24	210000	500	53,497	0,00025	0,0084	59476060,92	254,7498089
steel bracket	3	Pi*((120/2)^2-(50/2)^2)	9346,24	210000	500	53,497	0,00025	0,0008	654236670,1	254,7498089
POM	6	Pi*((115/2)^2-(90/2)^2)	4025,17	2500	500	124,218	0,04969	0,2981	1677152,328	49687,39687
Hilti	8	Pi*((115/2)^2-(90/2)^2)	4025,17	1700	500	124,218	0,07307	0,5846	855347,6873	73069,70128
Two glass tubes	300	Pi*((100/2)^2-((90/2)^2)+Pi*((115/2)^2-((105/2)^2)	3220,13	63000	500	155,273	0,00246	0,7394	676227,8187	2464,652622
Hilti	8	Pi*((115/2)^2-(90/2)^2)	4025,17	1700	500	124,218	0,07307	0,5846	855347,6873	73069,70128
POM	6	Pi*((115/2)^2-(90/2)^2)	4025,17	2500	500	124,218	0,04969	0,2981	1677152,328	49687,39687
steel bracket	3	Pi*((120/2)^2-(50/2)^2)	9346,24	210000	500	53,497	0,00025	0,0008	654236670,1	254,7498089
steel hinge GX50T	33	Pi*((120/2)^2-(50/2)^2)	9346,24	210000	500	53,497	0,00025	0,0084	59476060,92	254,7498089
total							0,25	2,52	1433166690	248997,85

Table 11 The strain, the displacement, and the spring stiffness for the samples with a length of 300 mm.

In chapter 4.2.3. and in A.14.2. the results are given for the compression tests performed in the lab of the Technical University of Delft. The values from the experimental tests will be compared with the hand calculations/numerical models. The test results are shown in appendix 14.

Part III Numerical and Experimental Investigations

4.2. Experimental tests

4.2. Experimental tests

Six small samples with a length of 300 mm were produced to test the lamination process with regard to bubble formation and possible breakage of the glass by internal stresses. Three laminated DURAN (annealed) samples and three laminated DURATAN (heat-strengthened) samples were tested. Afterwards, these samples were tested on compression strength, to investigate the behaviour of the interlayer material, the post-failure behaviour of the designs, the differences between annealed and heat-strengthened glass samples, the behaviour of the connections under pressure, and the capacity of the glass tubes and the connections. The tests were performed at the Stevin lab II at the Technical University in Delft. In chapter 4.1.2.2. the build-up of the samples is described.

4.2.1. Manufacturing of the samples

Since bonding glass tubes together by lamination is a new process, smaller samples with a length of 300 mm will be produced first. Nowadays it is possible to produce tubes up to 10 m. However, the longer the tube, the more the tubes could be distorted during extrusion. The two tubes need to fit into each other, due to geometric tolerances it is difficult to determine if it will fit in front.

SCHOTT produced the glass, and they fit the tubes into each other in the factory. After that, the glass tubes were bonded together by H.B.Fuller Kömmerling (figure 77). As already mentioned in chapter 2.2.5.1. the interlayer material has some shrinkage, which can cause stresses into the glass. A two PU component, Ködistruct LG, interlayer material was chosen, because it can cure slowly in room temperature. In this way the glass is not exposed to extra stresses due to temperature to cure the interlayer material. This interlayer cures slowly due to the hydro-elastic nature of the interlayer material. After that, the interlayer material was tempered at 40 °C to make sure that the interlayer material was completely cured. Two types of glass were chosen to do so: DURAN (annealed glass) and DURATAN (heat strengthened) borosilicate glass tubes. The tubes are laminated while standing vertically. Furthermore, Octatube produced the steel and POM components for the connection (figure 76), Hilti arranged the HILTI HIT-HY 270 mortar, and the hinges were arranged by Techniparts. In appendix 11, the process is described with the producers to manufacture the components for the sample.

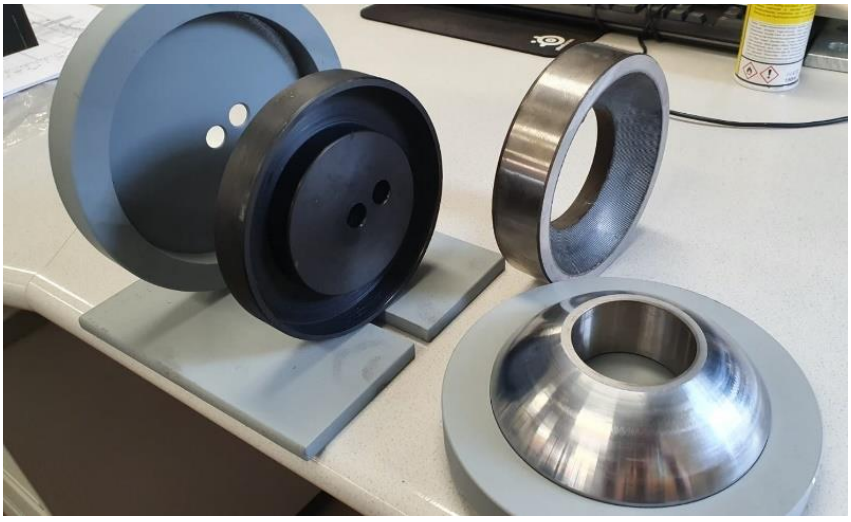

Figure 76 The steel and POM components for the connection (Octatube. 2021).

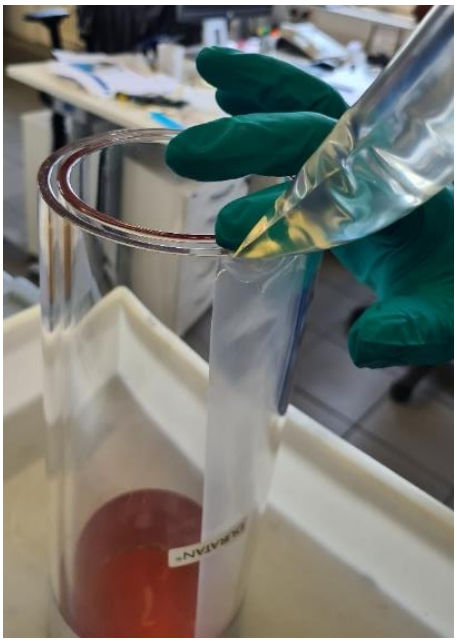

Figure 77 Putting the interlayer material between two glass tubes (H.B.Fuller Kömmerling. 2021).

4.2.2. Test set up for the experimental tests

Before testing, an experimental plan needs to be made to show the working method and the way to ensure safety. After a few meetings with Peter de Vries and Louis van den Breejen, the working method and schedule could be established. After approval of the experimental plan, a budget will become available. The plan is carried out as planned, except for a few things: another compression strength testing machine was used, and another way was found to ensure safety. The machine described in the experimental plan was in use, and only small samples were tested in this project, so another machine was possible too. A hydraulic displacement-controlled compression machine from Schenck was used (figure 78, left). The samples were clamped between the top and the base plate. The base plate moved up in z-direction with 1 mm per minute. Strain sensors were glued on the inside and the outside of the glass tubes. The wires attached to the sensors were amplified with a factor of 1 million. The schematic 3D view and the cross-section of the sample in the machine is given in figure 78 (middle and right). A larger format of these pictures is given in appendix 12 and 13.

In the first test a plexiglass enclosure was used to avoid injuries from shattering glass pieces, but a disadvantage was that the glass itself was not visible properly. In the other tests, we used plexiglass panels to stand behind. In this way injuries were avoided and the glass was visible. This experimental plan is attached in appendix 12. In here a few takes and measurements are established. These will be answered after the tests are performed in chapter 4.2.3.

When all the components were brought to the lab, the samples were prepared. Firstly, strain sensors were glued to the outside and the inside of the laminated glass tubes. Then wires were soldered to the inside sensors. These were pulled through the POM-block and the steel. After that, the Hilti mortar could be injected in the POM-blocks. In the POM-blocks three timber pieces were glued which kept the glass at the right position till the Hilti was hardened. The Young's Modulus of these timber pieces was lowered, by placing them perpendicular to the grain. The Hilti mortar started to harden already in approximately 5 minutes, so the Hilti needed to be injected, smoothed out, and directly afterwards the glass needed to be put on top of the Hilti mortar. After 30 minutes the Hilti was completely hardened. To be sure that there was enough Hilti, more Hilti was injected than needed. Then

the same procedure for injecting the Hilti was carried out for the other side. Lastly the wires needed to be soldered to the outside strain sensors. After that, the sample was placed in the compression machine. The hinges were put in its place, and the wires from the sensors needed to be set to zero with the computer of the machine. After that, the sample was ready for testing (figure 79). The Hilti is not bonding to the glass and the POM-block, but is sticks to it enough so that a threated rod is not necessarily needed to keep the components at the right place (as described in the experimental plan). The wires from the inside sensors, could be pulled through the hole of the top plate from the testing machine. This procedure is described in more detail in appendix 13.

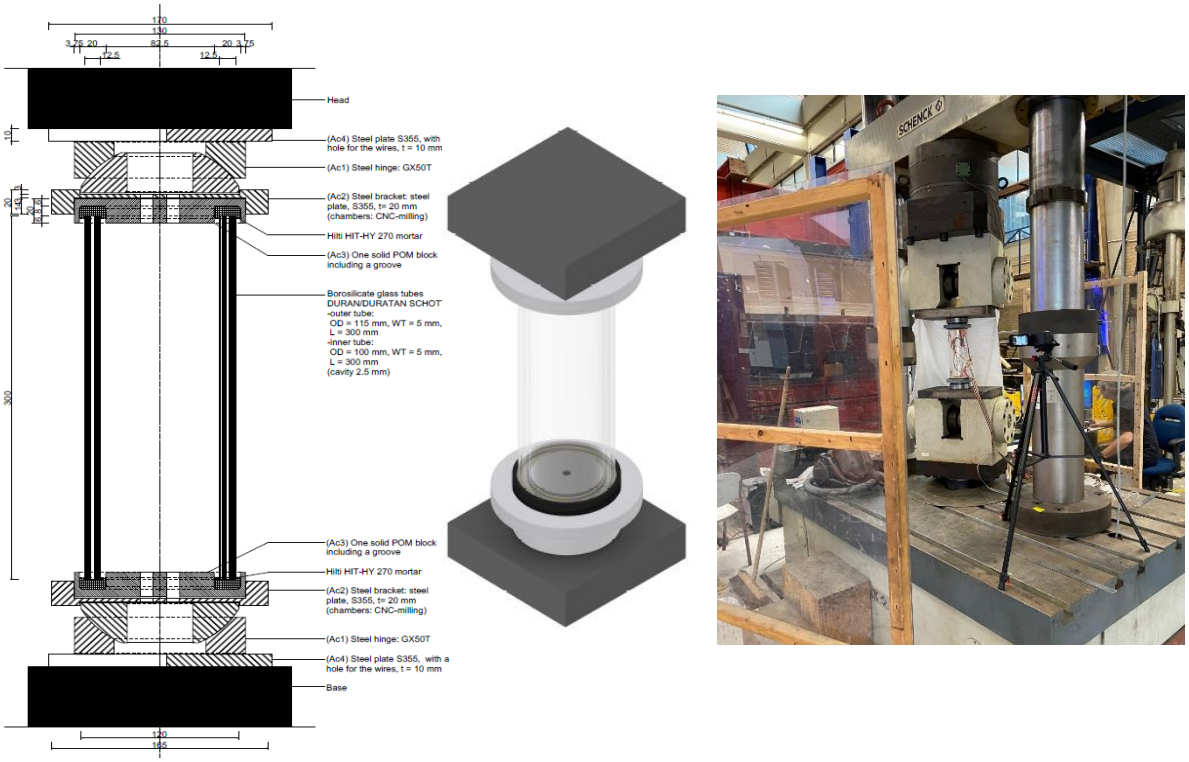

Figure 78 The set-up of the sample in the machine. Left: the schematic cross-section, middle: the schematic 3D view, and right: the sample in the machine.

Figure 79 Preparing the samples.

As can be seen in figure 79, a few air bubbles were present. Sample 4 had most air bubbles and samples 1, 5 and 6 had almost no bubbles. These bubbles occurred due to shrinkage and interaction with moisture during filling.

4.2.3. Results

In this chapter the estimations and hand calculations are verified with the results from the experimental tests. In the experimental plan a few tasks/measurements were drawn up, which were answered after the tests were performed. In the chapters below these aspects are explained and answered. All the results and pictures per sample are shown in more detail in appendix 14.

4.2.3.1. Injection of Hilti mortar

One of the aspects that needed to be checked was the procedure to inject Hilti mortar. To be sure that enough Hilti was present under the glass tubes, an extensive amount of Hilti was used. When using too much mortar, the Hilti squeezed up when the glass is put on top of it. At the outside of the tube, it could be easily wiped clean if the Hilti was not hardened yet, but on the inside, this was not possible anymore. After testing all the samples, one sample was properly made, with just enough Hilti on the glass (figure 80). In this way the glass could stay clean on the inside and the outside.

It is possible to inject the Hilti so that it is well-distributed into the groove of the POM-block. This is also shown in the figures in appendix 14.

Figure 80 The properly made sample.

4.2.3.1. Introduction of forces from the connection into the glass

The well-distributed introduction of compression forces into the glass tubes are depending on many aspects: the way the Hilti mortar is injected, but also on how the connection is placed related to the glass. By breaking out the Hilti by a few POM-blocks, it was visible that the Hilti was well-distributed into the grooves of the POM-block.

The even introduction of forces was checked by the values of the strain sensors. In the beginning most of the strain sensors were having the same value. Probably when cracks appeared, the stress field changed, whereby the strain values started to deviate from each other. What also stood out, some strain sensors were able to come back on after a moment of deviating or stopping. Perhaps the deviations of the values of the strain sensors were caused by the strain sensors not being positioned exact vertically. If the connection is not exactly perpendicular to the glass tubes, one side can receive more forces. Then an uneven stress distribution can occur, which results in peak stresses. Perhaps this could be another reason why the strain sensors deviated from each other. Besides, when only a small glass

splinter is attached to the glass, it already can cause an uneven introduction of the forces into the glass. The hinges GX50T performed as good hinged connections. However, quite large hinges were used, and perhaps this affected the functioning of the hinge as a hinged connection. In graph 1, a strain versus load curve is shown from sample 6. The strain versus load graphs from the other samples are shown in appendix 14.

In the tests, a few timber pieces were placed in the POM-block to keep the glass in its place when the Hilti was not hardened yet. Also, these timber pieces could have contributed to an uneven introduction of forces into the glass. This could be seen from the small cracks that appeared where the timber pieces were placed. These cracks did not propagate any further. For the heat-strengthened samples, not much deviation was visible at those spots compared to the other cracks in the glass tube. In the designs, attaching the connection to the glass will be done by machines, and due to the assembly sequence, it is possible to leave out the timber pieces (see chapter 3.2.4.).

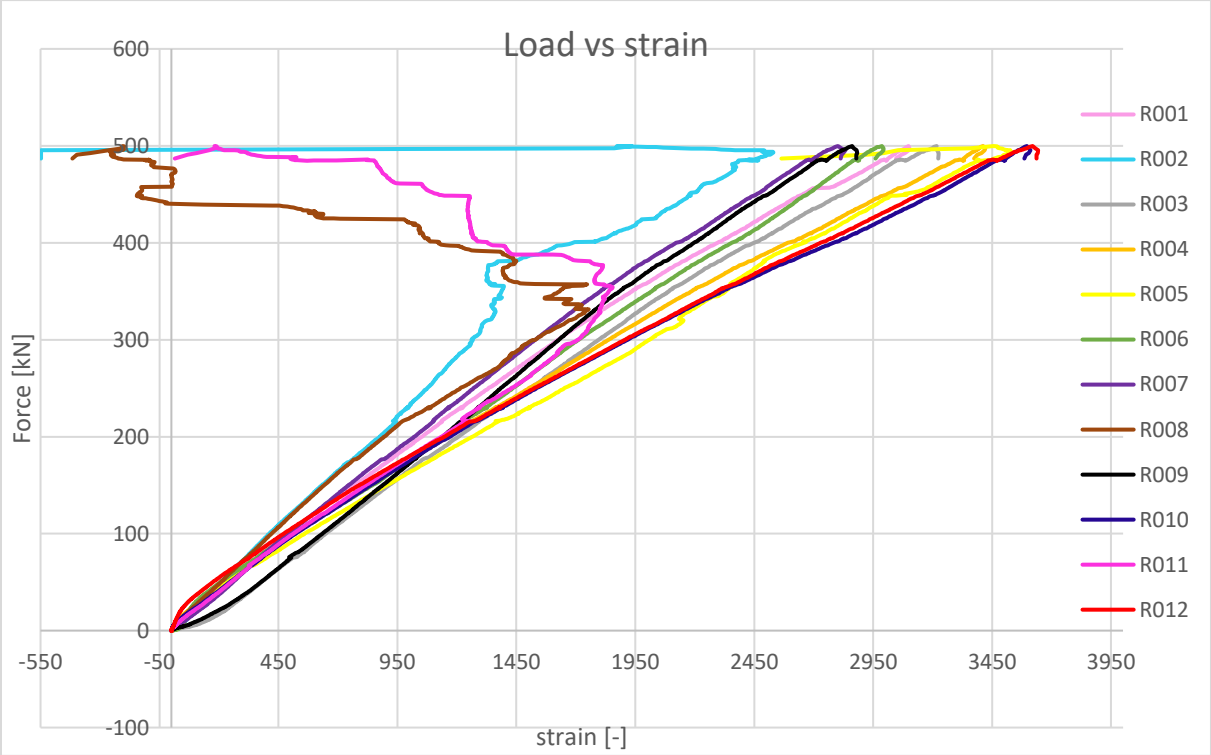

Graph 1Load versus strain curve till force was taken off - test 5 - sample 6.

4.2.3.1. Post-failure behaviour

The connections and the Hilti mortar remained intact, even after overstressing the Hilti mortar. Only the glass broke. The compression machine was stopped when the glass started to shatter and as can be seen in the load versus displacement curves (graph 2 and appendix 14), at that moment the curves started to decrease. The bullets in graph 2 represent the load at which the first crack appeared in the samples (the failure load).

The cracks appeared between 95-160 kN. This is at a compression stress of 29.5-49.5 N/mm^2, with corresponding tensile stresses of 5.9-9.9 N/mm^2 (equations A.14.1-A.14.4). According to equation A.9.17, the allowable practical tensile stress for annealed glass is 15.5 N/mm^2. This should mean that the first crack was expected at around 250 kN. Because, with a force of 250 kN, a tensile force of 15.6 N/mm^2 could be reached (with a compression stress of 78 N/mm^2). The tensile stress for heat-strengthened glass is higher, 36.3 N/mm^2 (equation A.9.20). Looking only at the compression strength for borosilicate glass, which is around 260-

350 N/mm^2 (chapter 2.1.3. and A.9.3.), then the sample would have been able to carry more loads before cracking.

So, the first crack appeared earlier in the glass than expected. In the calculations a perfectly hinged connection was taken into account. For the samples quite large hinges were used, and perhaps this affected the functioning of the hinge as a hinged connection. Besides, it could be that the glass had defects or that the tolerances in the glass affected the sample so that cracks appeared earlier than calculated. For example, the tolerances in the glass can result in different thicknesses of the interlayer whereby extra stresses can occur.

Furthermore, a few air bubbles were located in the cavity. Stresses were localised around these air bubbles. Sample 4 had the most bubbles, and it started shattering earlier than the other samples did.

Cracks started for all samples at the top or at the bottom. This means that it was probably not caused by bending, because those cracks would have started at the middle of the tube. The cracks could be caused by transversal elongation, which resulted in tensile stresses. After cracks appeared, local stresses were relieved. The tubes were kept together by the interlayer material. Due to the lamination, the tubes could not bend when cracks appeared. In this way it kept its load-bearing capacity. As can be seen the curve from the load versus displacement curves continued, which means that no strength was lost after fracture.

In table 12 and 13, the results are summed up at where the samples first cracked (failure load) and when the force was taken off (maximum load) with the corresponding stresses (calculated with equation 3). The force was taken off when the load versus displacement curve became less steep and when the glass started to shatter. The cross-sectional area of the two glass tubes is approximately 3220 mm^2.

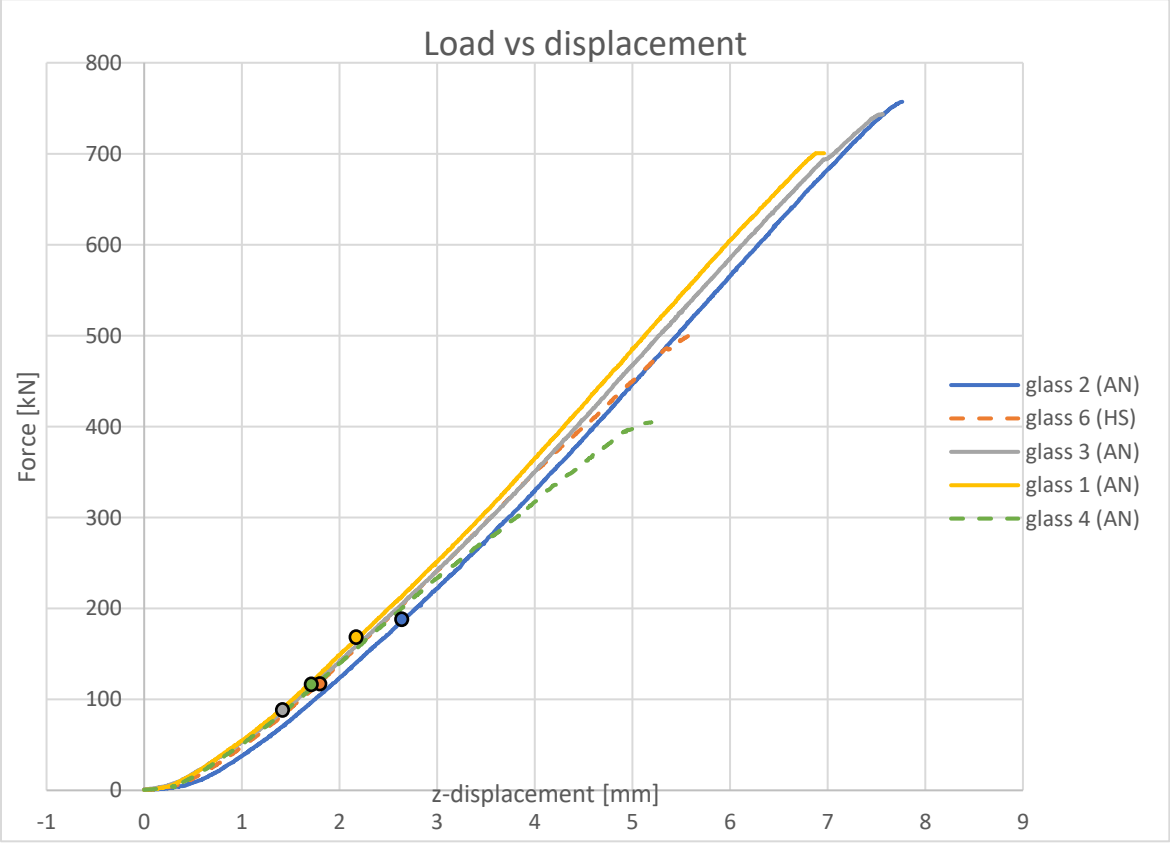

Graph 2 Load versus displacement curves of all samples. The bullets represent the load at which the first crack occurred in the samples.

test	sample	Failure load [kN]	failure stress (σ) [N/mm^2]	theoretical failure tensile stress [N/mm^2]	Maximum load [kN]	Maximum stress (σ) [N/mm^2]	theoretical maximum tensile stress [N/mm^2]	remarks
3	1	160	50	10	700	217	43	-
4	3	95	30	6	745	231	46	-
6	2	(second crack at 190)	-	-	750	233	47	Already had one crack before testing

Table 12 Test results for failure and maximum load with corresponding stresses – all annealed samples.

test	sample	Failure load [kN]	failure stress (σ) [N/mm^2]	theoretical failure tensile stress [N/mm^2]	Maximum load [kN]	Maximum stress (σ) [N/mm^2]	theoretical maximum tensile stress [N/mm^2]	remarks
1	5	>160	>50	>10	?	-	-	machine failed after 160 kN
2	4	120	37	7	390	121	24	a lot of air bubbles
5	6	120	37	7	490	152	30	-

Table 13 Test results for failure and maximum load with corresponding stresses – all heat-strengthened samples.

When the sample was compressed with a force of 750 kN, the stress was around 233 N/mm^2. This is close to the theoretical maximum strength for borosilicate glass of 260-350 N/mm^2 (chapter 2.1.3.).

In appendix 14, load versus strain curves were shown from all the samples. Some of the sensors deviated. A possible reason could be that the sensors were not exactly glued parallel to the force onto the glass, which gives an eccentricity.

The annealed samples had a few straight cracks parallel to the length of the tube. The cracks had a slow propagation. The first crack appeared between 95-160 kN and was able to carry a load of 700-750 kN. When the force was taken off, a few small perpendicular cracks appeared. Cracks appeared in both tubes, so there was a cooperation between them.

The heat-strengthened glass samples had a lot of straight cracks parallel to the length of the tube in the outer tube. The first cracks appeared at 120-160 kN. The cracks propagated quickly with a lot of speed. When the force was taken off around 390-490 kN, the inner tube exploded into small pieces at once. This sudden explosion made the samples less reliable than the annealed ones. The cooperation from the heat-strengthened samples was less as well.

At figure 81, both sample results are shown after the tests (left: annealed glass, right: heat-strengthened glass).

Only glass pieces of around 1 or 2 mm thick shattered off, so the glass did not shatter due to delamination of the glass tubes. This means that the interlayer had a good adhesion.

The samples had a structural integrity and were robust, because they were able to withstand loading without directly falling after a fracture. This means that the samples give a warning (the first crack) before failing, so that people can evacuate. After the first crack it was able to have around 4 times more load. After the first crack appeared, the local stresses were relieved, whereby the load versus displacement curve was continuing without deviations. This meant that the glass stayed stiff even after the first crack, so the samples do have a good safety mechanism.

Figure 81 Left a cracked annealed glass sample (sample 2) and right a heat-strengthened glass sample (sample 5).

After testing, the results were discussed with Veer, F. In 1999, he came up with a different way to create a lamination without air bubbles and shrinkage. An interlayer material was made with 90% of the catalyst taken out. Due to this it reacts and cures slowly. It is a UV-light cured interlayer, whereby the curing process could be controlled. The UV-light was placed 1 meter from the glass sample so that the glass would not become too warm. With a UV-light cured interlayer, the interlayer could be put in the cavity slowly and it could be cured locally. If the lamination material is put in at once, there is more chance on shrinkage, and so in air bubbles in the cavity, more stresses and more change on delamination. The glass was placed on a rotary table, and with a hose, the lamination material was dripped in the cavity, which was only a few microns thick. The next layer was put on top of the half-hardened layer, which gave a good adhesion. In this way there was only shrinkage in vertical direction, which could be refilled. The important thing was that there was no shrinkage in horizontal direction, which could cause extra stresses into the glass tubes. Unfortunately, the setup for this lamination process was burned down.

4.2.3.1. Compression force/stress

As already mentioned, the first cracks appeared earlier than expected. In the calculations a perfectly hinged connection is taken into account, which is not the case in practise. The strain values from the test results were deviating, because of the cracks in the glass. In the hand calculation cracks are not taken into account. For a compression force of 100 kN, both glass tubes need to have a strain of around 459-532 (appendix 14), for a compression force of 300 kN, a strain of around 1378-1560, and for a compression force of 500 kN, a strain of around 2297-2660. Almost all strains were in range with these numbers, only sensor 12 was deviating in sample 3, whereby the average strain value was a bit lower than calculated (table 14).

sample	type of glass	force [kN]	strain 1	strain 2	strain 3	strain 4	strain 5	strain 6	strain 7	strain 8	strain 9	strain 10	strain 11	strain 12	average strain
4	HS	100	561	624	439	481	648	563	518	454	333	528	573	0	520
4	HS	300	54	1881	1794	1302	1822	2268	1002	1249	698	1419	1964	0	1405
1	AN	100	507	276	608	498	497	603	497	330	476	491	511	388	474
1	AN	300	1509	1067	1490	1581	1851	2049	1347	556	1240	1570	1766	1086	1426
1	AN	500	2360	1525	2394	2844	3206	3581	1111	616	2010	2902	3089	1588	2269
3	AN	100	457	525	580	304	406	426	494	447	512	257	481	-144	395
3	AN	300	1567	2010	2033	1081	1132	1031	1036	1679	1091	662	1125	376	1235
3	AN	500	2593	3159	3414	1692	1929	1510	947	2190	1697	1193	1929	846	1925
6	HS	100	485	411	648	512	559	509	491	421	635	523	513	472	515
6	HS	300	1624	1261	1795	1837	2008	1711	1529	1527	1628	1916	1707	1905	1704
2	AN	100	496	415	523	407	459	446	481	461	478	449	467	446	461
2	AN	300	1576	1280	1607	1381	1262	1416	1692	1398	1599	1751	1510	1495	1497
2	AN	500	2424	2376	2885	2519	2006	2765	2130	2586	2937	3379	1793	2728	2544

Table 14 The strain values (sensor 1-12) for the glass tubes at 100, 300 and 500 kN – samples 1,2,3,4, and 6.

In the load versus displacement curves, the displacement from the components from the machine are included as well. Nevertheless, the displacement of the glass tubes can be calculated with the required strain from the sensors (equation A.14.8). For 100 kN, the glass should have a displacement of around 0.1479 mm, for 300 kN around 0.4436 mm, and for 500 kN around 0.7394 mm. All the displacements from the tests are in the same range as calculated by hand (table 15).

sample	type of glass	force [kN]	average strain (*1000000)	average strain	Length or Thickness [mm]	u or ΔL [mm]
4	HS	100	520	0,0005	300	0,1561
4	HS	300	1405	0,0014	300	0,4215
1	AN	100	474	0,0005	300	0,1421
1	AN	300	1426	0,0014	300	0,4278
1	AN	500	2269	0,0023	300	0,6807
3	AN	100	395	0,0004	300	0,1186
3	AN	300	1235	0,0012	300	0,3706
3	AN	500	1925	0,0019	300	0,5775
6	HS	100	515	0,0005	300	0,1545
6	HS	300	1704	0,0017	300	0,5112
2	AN	100	461	0,0005	300	0,1382
2	AN	300	1497	0,0015	300	0,4492
2	AN	500	2544	0,0025	300	0,7632

Table 15 The displacement obtained from the average strain values from the tests at 100, 300 and 500 kN – samples 1,2,3,4, and 6.

4.2.3. Comparison of the results from other researches

In this chapter other researches from laminated tubular glass column were compared with the results from this project.

Veer and Van Nieuwenhuijzen did also research into tubular laminated glass tubes (DURAN) in 1999. Below a table is given with the tested tube dimensions. Furthermore, a sketch is given in figure 39 of the connections used. A hinged connection was created with PMMA sheets (Van Nieuwenhuijzen, E.J., et al. 2005).

Specimens/ Length [mm]	Outer diameter [mm]	Inner diameter [mm]	Wall thickness [mm]	Cavity width [mm]
Small samples	40	31	1.5 and 1.5	1.5
1.2 m	110	90	5 and 3	2
1.5 m	120	95	5 and 5	2.5

Table 16 Dimensions of laminated tubular glass tubes tested by Van Nieuwenhuijzen (Van Nieuwenhuijzen, E.J., et al. 2005).

The results were only given for the 1.2 and the 1.5 m samples (table 16). The failure load for the 1.2 and the 1.5 meters samples was between 137-196 kN and the first crack appeared at

40-73 kN. After the first crack the specimens were able to have around 2-3 times more load after the first crack.

The diameter and the wall thickness of the samples tested during this thesis are almost the same as Veer and Van Nieuwenhuijzen tested. Only their samples were longer. Nevertheless, the samples only failed due to compression and not on buckling (see the citation below). The samples from this thesis project failed due to compression forces as well.

''All specimens failed due to compression. Buckling didn't occur, because the buckling strength was significantly higher than the compression strength'' (Van Nieuwenhuijzen, E.J., et al. 2005).

As said before, the first crack appeared between 95-160 kN in the DURAN samples tested in this thesis, and after that the samples were still able to carry a load of 700-750 kN. So, after the first crack the specimens were able to have around 4-5 times more load after the first crack.

The failure and maximum stresses from this thesis (table 12 and 13) are summed up and compared to the values from Van Nieuwenhuijzen (table 6) in table 17 below. Van Nieuwenhuijzen tested three DURAN samples and in this research three DURAN and three DURATAN samples were tested. Since all samples failed on compression the values can be compared.

	Van Nieuwenhuijzen Annealed	Veenstra Annealed	Veenstra Heat-strengthened
Lowest failure stress [N/mm^2]	12	30	37
Highest failure stress [N/mm^2]	29	50	>50
Lowest maximum stress [N/mm^2]	41	217	121
Highest maximum stress [N/mm^2]	58	233	152

Table 17 Comparison failure and maximum stresses from this thesis and from the results from Van Nieuwenhuijzen.

As can be seen in table 17, is that in this thesis, much higher stresses were arrived compared to the values of Van Nieuwenhuijzen. Perhaps the improvements achieved in this project can be attributed to better detailing. Van Nieuwenhuijzen used PMMA sheets to create a hinged connection between the support and the glass column, because of the lower Young's modulus of PMMA compared to glass, and in this thesis, steel hinges and Hilti mortar were used for a better introduction and distribution of the forces into the glass tubes.

Part III Numerical and Experimental Investigations

4.3. Conclusion

4.3. Conclusion

In this chapter, the answers are given on the sub questions for part III Numerical and Experimental Investigations.

Are the samples transparent/robust and did cracks appear during/after the lamination process?

As mentioned before, due to the lamination process, thermal stresses could occur during/after curing. The interlayer material was cured in room-temperature. After that the interlayer material was tempered at 40 °C to make sure that the interlayer material was completely cured. Only in sample 2 (annealed) one crack out of a sudden, before testing. A grain was visible inside the glass, and probably due to stresses from shrinkage of the interlayer material, a crack appeared. The interlayer material is transparent, but there were a few air bubbles inside the cavity, especially sample 4 had more air bubbles in the cavity than the other samples. Samples 1 and 6 were almost without bubbles.

The sample is very robust, because after the first crack it is able to have around 4-5 times more load (the annealed samples). So, after the crack the samples are still having a large load-bearing capacity. The annealed sample is a bit more reliable, because: the inner tube of the heat-strengthened samples cracked out of a sudden after the force was taken off, there were more cracks, it failed while exposed to less compressive force, and the cracks propagated faster.

How to manufacture samples for testing?

First of all, the dimensions were determined, and the glass tubes were ordered. The tubes were extruded and were cut into the right lengths afterwards. The outer and the inner tubes were fitted into each other by the glass producer (SCHOTT). Then the tubes were bonded together by an interlayer material (done by H.B.Fuller Kömmerling). As mentioned, the interlayer material was cured at room-temperature and after that, the interlayer material was tempered to cure completely. Furthermore, steel and POM components were designed and discussed with the producer (Octatube). The steel parts were made from steel rods and chambers were created into the steel rods by CNC-milling. In these chambers, the POM-block and the steel hinges (Techniparts) were placed. The POM-blocks were made from solid POM-rods. Grooves were created into the POM-rods by CNC-milling as well. All these components were brought to the lab. Strain sensors were glued to the inner and the outer glass tubes. Lastly, Hilti mortar (Hilti) was injected into the grooves of the POM-blocks and the laminated glass tubes were put on top of that. The Hilti mortar was well-distributed into the grooves and it was possible to inject it properly, whereby the glass stayed clean.

How to set up the experimental test?

When all the components were present in the lab from the Technical University of Delft, first strain sensors were glued to the glass tubes, which were soldered to the connectors. The glass was made rough by sanding, at the locations where the sensors were glued, to make sure that the strain sensors were not falling off. After that the wires could be soldered to the connectors as well. Timber pieces were glued inside the grooves of the POM-blocks to hold the glass at the right height when the Hilti was not hardened yet. Then the Hilti could be injected. It started to harden within 5 minutes, which is quite fast. Within these 5 minutes, the Hilti needed to be injected, smoothened out, and the glass needed to be placed on top at the right height. Afterwards, the wires needed to be set to zero with the machine and then the samples were ready for testing. A hydraulic displacement-controlled compression machine from Schenck was used. The samples were clamped between the top and the base plate.

The base plate moved up in z-direction with 1 mm per minute. The wires attached to the strain sensors were amplified with a factor of 1 million.

What are results of the experimental tests regarding compression strength and the post-failure behaviour?

The samples are robust, because it still has a large load-bearing capacity after the first cracks appeared. In this way the sample gives a warning at the first cracks, before failure. After a crack, the local stresses were relieved, and the sample stayed strong. The load versus displacement curve kept continuing with the same slope, even when cracks appeared.

The annealed samples had a few straight cracks parallel to the length of the tube. The cracks had a slow propagation. The first crack appeared between 95-160 kN and after that the samples were still able to carry a load of 700-750 kN. When the force was taken off, a few small perpendicular cracks appeared. Cracks appeared in both tubes, so there was a cooperation between them. The heat-strengthened glass samples had a lot of straight cracks parallel to the length of the tube in the outer tube. The first cracks appeared at 120-160 kN. The cracks propagated quickly with a lot of speed. When the force was taken off around 390-490 kN, the inner tube exploded into small pieces at once. This sudden explosion makes the samples less reliable than the annealed ones. The cooperation from the heat-strengthened samples is less as well.

The tubes were kept together by the interlayer material. Due to the lamination, the tubes cannot bend when cracks appear. The glass pieces were kept together by the lamination material. At failure, glass started to shatter into pieces of 1 or 2 mm thick. The tubes were 5 mm thick, so the interlayer material is performing well.

How can the deviation between the numerical models/hand calculations and the experimental tests be explained?

As mentioned, cracks appeared earlier than calculated by hand. For the samples quite large hinges were used, and perhaps this affected the functioning of the hinge as a hinged connection. Besides, it could be that the glass had defects or that the tolerances in the glass affected the sample so that cracks appeared earlier than calculated. For example, the tolerances in the glass can result in different thicknesses of the interlayer whereby extra stresses can occur. Furthermore, a few air bubbles were located in the cavity. Stresses were localised around these air bubbles. Sample 4 had the most bubbles, and it started shattering earlier than the other samples did.

The strain values from the test results were deviating, probably because of the cracks in the glass whereby the stress field changed. In the hand calculation cracks were not taken into account. Perhaps the deviations of the values of the strain sensors were caused by the strain sensors not being positioned exact vertically. Another reason could be that if the connection is not exactly perpendicular to the glass tubes, one side can receive more forces. Then an uneven stress distribution can occur, which results in peak stresses. Besides, when only a small glass splinter is attached to the glass, it already can cause an uneven introduction of the forces into the glass. Nevertheless, the strain and displacement values form the experimental tests and the hand calculations were in the same range.

The large load-bearing capacity after the first cracks was not expected. This makes the samples robust with a strong structural integrity.

Part IV Review

Part IV Review

5.1. Discussion

5. Part IV Review

5.1. Discussion

The glass was sanded so that the strain sensors could not fall off. This was advised by the staff of the lab. If the sensors did fall off, it was not possible to reach the sensors on the inside of the glass. Sanding of the glass may have affected crack formation. As mentioned in chapter 2.1.3. the tensile strength of glass is depending on mechanical flaws on the surface. When the glass is loaded, flaws grow over the time. So, it will probably have more influence on the long-term loading than on short-term loading. There are more methods to test if strains are equal in the glass. Other methods to verify this could be by the use of special cameras.

Furthermore, in the tests, a few timber pieces were placed in the grooves of the POM-block to keep the glass in its place when the Hilti was not hardened. There is a possibility that these timber pieces could have contributed to an uneven introduction of forces into the glass. Small cracks appeared where the timber pieces were placed. These cracks did not propagate any further. For further research, perhaps it is better to not use these timber pieces, to be sure that the forces are uniformly introduced in the glass.

As mentioned in chapter 4.2.3. in this thesis, much higher stresses were arrived compared to the values of Van Nieuwenhuijzen. Van Nieuwenhuijzen tested three DURAN samples and in this research three DURAN and three DURATAN samples were tested. Since all samples failed on compression the values can be compared. In this thesis the failure stress was between 30-50 N/mm^2, and the failure stress from the tests of Van Nieuwenhuijzen was between 12-29 N/mm^2. The maximum stress in this research was between 217-233 N/mm^2, from Van Nieuwenhuijzen was between 41-58 N/mm^2. In this project steel hinges and Hilti mortar were used for a better introduction and distribution of the forces into the glass tubes. Van Nieuwenhuijzen used PMMA sheets to create a hinged connection between the support and the glass column, because of the lower Young's modulus of PMMA compared to glass. Perhaps the hinged connection used in this project functioned better as a hinge.

In this project one particular method is described to assemble the column. An assembly machine has been designed for this purpose. Nevertheless, perhaps more alternatives can be devised. It could be that the manufacturer knows an easier method to assemble the column with different (already existing) machines.

Stress corrosion cracking can happen in glass. It happens when the element is exposed to corrosive environment (Wiederhorn, S.M., et al. 1970). The designs from the MLA are protected against water occurring on the inside of the column by silica grains or by the filtered air that will be pumped through the column. Perhaps the glass has a higher strength when loaded under long-term loading. This is not applicable for the SLW, since water will be pumped through the column.

Part IV Review

5.2. Conclusion

5.2. Conclusion

From the literature study it became clear that glass has a large compressive strength and that glass can be a viable material for a column, despite the fact that it is a brittle material with a sudden failure. This results in the following research question:

"What is the potential and what are limitations in designing and engineering a transparent tubular glass column as a structural element, which is robust and fireproof?"

5.2.1. Literature study

Glass tubes are produced with the extrusion method. The longer the tubes become, the bigger the geometric tolerances. So, when the dimensions were determined for the glass tubes, the producer first had to fit the tubes into each other to check if they would fit. By bonding the tubes together, a structural integrity can be integrated in the structural element. The ideal thickness for the interlayer material for the samples is around 2 mm. If it becomes thicker, more shrinkage and therefore stresses can occur, and when it becomes less, the structural integrity is less guaranteed due to the interlayer curing process in which cross links are formed.

Some safety strategies for a robust glass design:

- Multiple layers of glass can be bonded together through lamination or by bonding layers together via an adhesive.
- The type of glass and the relevant breaking pattern has influence.
- Use of the polymer coating, like *Tough* on DURAN® profiles from SCHOTT.
- Use of a secondary load path.
- Prevent consequences of failure by the use of barriers.

Some safety strategies for a fire safe design:

- There are different classes for fire resistant glass (E, F, EI and EW) which can be used.
- Furthermore, from glass composites, borosilicate glass is preferred, because of its lower coefficient of thermal expansion compared to soda-lime glass, which gives it higher resistance to thermal deviations. From glass types, heat-strengthened glass is preferred over annealed glass.
- Another option is by filling the glass tubes with water to keep the glass cool.
- By using a specialized fire-resistant coating or intumescent interlayers (this type of glass elements is categorized in the fire-resistant classes).
- Lastly the use of sprinklers can be applied to reduce the temperature of the glass.

Three common designs for transparent tubular glass were studied:

- Two tubes laminated with a transparent UV-curing resin. Both tubes are contributing to the load-bearing capacity.
- A load-bearing inner tube protected by two half tubes that form an outer shell. Laminated via a PVB foil in between.
- Borosilicate glass tubes (DURAN and DURATAN) from SCHOTT with an OPALFILM® coating to increase residual strength. The coating keeps the glass pieces together when it breaks.

5.2.2. Design phase

After studying manufacturing possibilities, different common designs for glass tubes, and several safety strategies, design criteria and main concerns (as failure mechanisms) were

determined which need to be taken into account while designing free-standing structural glass tubular columns:

- buckling
- thermal and residual stresses
- robustness
- transparency
- ability of manufacturing/assembling
- ability to replace it when broken
- end connections
- restrictions to the case study
- fire resistance

There were two options to laminate a tube within a tube: a 2 PU-component (Ködistruct LG) material which cured slowly by room-temperature, or a UV-light cured material (Acrylate UV). The UV-light cured material had a lower Young's modulus, but a higher shrinkage value. For the 2 PU-component material this was vice versa. Thermal and residual stresses can occur during/after the lamination process. If the interlayer material cures too fast, more stresses will occur in the glass tubes, especially around air bubbles. In this project the 2 PU-component (Ködistruct LG) was used. It is slowly cured at room temperature, and after that it was tempered to make sure that the interlayer was completely cured. The impact of chemical induced reaction shrinkage was reduced, by shifting from van-der-Waals interactions to chemical bonds during curing and the curing temperature was kept as low as possible to avoid additional thermal shrinkage in the post-gelling phase. Moreover, when the interlayer material becomes too thick, due to variations in the thickness of the glass tubes, extra stresses can occur. If the interlayer becomes too thin, the structural integrity is less guaranteed.

Three designs were engineered in this project: the MLA (2x) and the SLW. Both designs are made from laminated tubular borosilicate glass tubes from SCHOTT. Due to the tubular shape, internal stresses are reduced, and it has a better resistance against buckling. Furthermore, there are no edges in the glass tube, which improves the transparency of the column. The columns need to be sealed to avoid dirt coming in whereby isochoric pressure can occur due to temperature differences. This can result in condensation, which needs to be avoided. This had influence on the design for the end connections. Filtered air will be regulated in the MLA by a ventilation system. If the pressures can be handled by the glass itself, the MLA without the ventilations system can be applied. In this design, only silica grains are included to take up the water when condensation has occurred. This same system is used for double glazed units. In the SLW, water will be regulated into the column. Furthermore, for both designs, hinged connections are used, to make sure only axial compression forces can be taken up by the glass column. A POM-block is placed in between the steel foot and the glass tubes, because it has a lower Young's modulus than glass, and Hilti mortar needs to be injected under the glass tubes into the groove of the POM-block to distribute the compression loads from the connection into the glass tubes.

The water inside the SLW is also a safety mechanism to keep the glass cooler during fire. A transparent fire coating will be applied to the outside of the inner tubes of the MLA, which is protected from scratches by the outer tube. This outer tube of the MLA is coated with *Tough* on the inside, which is a polymer coating created by SCHOTT. When the tube breaks, the *Tough* coating keeps the glass pieces together. In both cases the use of sprinklers is advised. More research needs to be done on both of these principles for the fire resistance.

A column is a primary structural element, so it needs to be robust. The column needs to be designed so that even after fracture, it is able to carry the loads for SLS situation. The crack will give a warning and people can evacuate. So, it may not lead to a sudden failure. Bonding multiple glass layers together is safer, because tubes can cooperate with each other, and glass pieces will be kept from falling whereby injuries can be avoided.

Furthermore, some restrictions to the case study were taken into account while designing. The column is in this project designed for Bouwdeel D in Delft, which is a four-storey office building. The building is demountable, so the column is designed to be demountable as well. This means that the column can be taken out of the building in one piece and can be placed somewhere else. Dry connections are used, so all components can be reused as well. Only the Hilti mortar is not reusable and delamination of the glass tubes is not possible. In this way, it is also possible to replace the column when broken. Temporary struts need to be placed next to the broken column on both sides, and the column can be taken out to replace it. So, because of the possibility to reuse the column, sustainability is taken into account. Moreover, glass is a durable material. So next to demountability, other restrictions to the case were that the column needs to be:

- fire resistant for 60 minutes (the glass column nor the end connections);
- 3.2 meters long;
- able to carry the following compression loads:
    - Ned=300 kN (Ned=500 kN including a safety factor of 1.5)
    - Nek=280 kN (Nek=420 kN including a safety factor of 1.5)

Regarding to the above-mentioned restrictions, the following dimensions were determined for this column: an outer tube with an outer diameter of 180 mm and a wall thickness of 7 mm, and an inner tube with an outer diameter of 160 mm and a wall thickness of 7 mm. Then the corresponding compression stresses are between 39-69 N/mm^2 and the tensile stresses are between 7.8-13.8 N/mm^2. These values should be acceptable, because they are below the allowable tensile stress of 15.5-36.6 N/mm^2, and below the allowable compression stress of 260-350 N/mm^2. The critical buckling force for this column is 1666,5 kN. If the column needs to carry a compression force of 330 kN, then the Eigenvalue will be around 5.

Lastly, to show that it is possible to manufacture the column designs, the assembly sequence is engineered for the MLA column (with air hoses).

5.2.3. Numerical and experimental investigations

To ensure the designs fulfil the design criteria/main concerns, some numerical models, hand calculations and experimental tests were performed. First six small samples (three annealed samples and three heat-strengthened samples) with a length of 300 mm were tested to try out the lamination process of a tube within a tube. Only in sample 2 (annealed) one crack out of a sudden, before testing. The interlayer material is transparent, but there were a few air bubbles inside the cavity, especially sample 4 had more air bubbles than the other samples. Samples 1 and 6 were almost without bubbles.

After that, the same six samples were used for compression strength tests to investigate the behaviour of the interlayer material, the post-failure behaviour of the designs, the differences between annealed and heat-strengthened glass samples, the behaviour of the connections under pressure, and the capacity of the glass tubes and the connections.

To manufacture the samples, first of all, the dimensions were determined. The tubes were extruded and were cut into the right lengths afterwards. The outer and the inner tubes were fitted into each other by the glass producer (SCHOTT). Afterwards, the tubes were bonded together by an interlayer material (H.B.Fuller Kömmerling). Furthermore, steel and POM

components had to be made (Octatube). The steel parts were made from steel rods and chambers were created into the steel rods by CNC-milling. In these chambers, the POM-block and the steel hinges (Techniparts) were placed. The POM-blocks were made from solid POM-rods. Grooves were created into the POM-rods by CNC-milling as well. Strain sensors were glued to the inner and the outer glass tubes. The glass was made rough by sanding, to make sure that the strain sensors were not falling off. These sensors were soldered to the connectors. Wires were soldered to the connectors, and these wires were amplified with a factor of 1 million. Timber pieces were glued inside the grooves of the POM-blocks to hold the glass at the right height when the Hilti was not hardened. Lastly, Hilti mortar (Hilti) was injected into the grooves of the POM-blocks and the laminated glass tubes were put on top of that. It started to harden within 5 minutes, which is quite fast. Within these 5 minutes, the Hilti needed to be injected, smoothened out, and the glass needed to be placed on top at the right height. Afterwards, the wires needed to be set to zero with the machine and then the samples were ready for testing. A hydraulic displacement-controlled compression machine from Schenck was used. The samples were clamped between the top and the base plate. The base plate moved up in z-direction with 1 mm per minute.

Resulting from the compression tests, it can be concluded that the samples were very robust, especially the annealed samples. Nevertheless, in annealed sample a crack appeared out of a sudden before testing. The annealed (DURAN) samples were able to carry around 4-5 times more load after the first crack appeared and the heat-strengthened (DURATAN) samples around 3 times. In this way the sample gives a warning at the first cracks, before failure. The load versus displacement curves from all samples were continuing with the same linearity, even when the cracks appeared and further propagated. Local stresses were relieved after the cracks, but the samples kept their strength and stiffness. The glass pieces that shattered off, had a thickness of 1 or 2 mm.

All cracks started at the top or the bottom connection. These cracks were probably caused due to transversal elongation which results in tensile forces. The annealed glass samples cracked differently than the heat-strengthened glass samples. The annealed samples had a few straight cracks parallel to the length of the tube. Some of these cracks were slowly propagating, and some cracks did not propagate at all. The first crack appeared between 95-160 kN and the samples were able to carry a load of 700-750 kN before shattering started and the load versus displacement curve became less steep. When the force was taken off, a few small perpendicular cracks appeared. The cooperation was good between the tubes, because cracks appeared in both tubes. In the heat-strengthened samples a lot of parallel cracks appeared in the outer tube parallel to the length of the tube. The cracks occurred very fast. The first cracks appeared between 120-160 kN and the glass started shattering at around 390-490 kN. When the force was taken off, the inner tube exploded into small pieces at once. For all samples, the connections and the Hilti remained intact.

The heat-strengthened glass sample are less reliable than the annealed samples: the heat-strengthened samples had a sudden explosion at the inner tube at the end, the cracks slowly propagated in the annealed tubes, and the annealed tubes had a bigger load-bearing capacity after the first cracks. Moreover, the cooperation between the annealed tubes was better than for the heat-strengthened samples, because cracks appeared in both annealed tubes. In the heat-strengthened samples, first only cracks appeared in the outer tube, and the inner tube broke when the force was taken off.

The first cracks appeared earlier in the samples (between 95 and 160 kN) than calculated by hand. The hand calculation was based on 250 kN, whereby the tensile stress is 15.6 N/mm^2 and the compression stress is 78 N/mm^2. The allowable tensile stress for annealed glass for short-term loading is 15.5 N/mm^2 (calculation A.9.17.). The corresponding compression

stress for 95 kN is 29.5 N/mm^2 with a tensile stress of 5.9 N/mm^2. The corresponding compression stress for 160 kN is 49.7 N/mm^2 with a tensile stress of 9.9 N/mm^2. So, 5.9 and 9.9 N/mm^2 are lower than the allowable stress of 15.5 N/mm^2. The allowable tensile stress for heat-strengthened glass is even higher, 36.3 N/mm^2. The tensile stress is normative, since the allowable compression stress for borosilicate glass is higher, between 260-350 N/mm^2.

A reason that cracks appeared earlier than expected could be that for the samples quite large hinges were used, and perhaps this affected the functioning of the hinge as a hinged connection. Besides, it could be that the glass had defects or that the tolerances in the glass affected the sample so that cracks appeared earlier than calculated. For example, the tolerances in the glass can result in different thicknesses of the interlayer whereby extra stresses can occur. Furthermore, a few air bubbles were located in the cavity. Stresses were localised around these air bubbles. Sample 4 had the most bubbles, and it started shattering earlier than the other samples did.

The strain values from the test results were deviating, probably because of the cracks formation in the glass, which were not taken into account with the hand calculations. Perhaps the deviations of the values of the strain sensors were caused by the strain sensors not being positioned exact vertically. Another reason could be that if the connection is not exactly perpendicular to the glass tubes, one side can receive more forces. Then an uneven stress distribution can occur. Nevertheless, the strain and displacement values form the experimental tests and the hand calculations were in the same range.

The large load-bearing capacity after the first cracks was not expected. This makes the samples robust with a strong structural integrity.

5.2.4. Main question

To come back to the main question, three designs were designed and engineered for a transparent tubular glass column as a structural element, which are robust and fireproof!

Some limitations of the designs were:

- Geometric tolerances in the glass tubes.
- It is a challenge to laminate a tube within a tube.
- It is a challenge to assemble the glass column(s).
- Failure mechanisms need to be taken into account, especially while designing end connections.

In this project six samples were used for compression strength tests to investigate the behaviour of the interlayer material, the post-failure behaviour of the designs, the differences between annealed and heat-strengthened glass samples, the behaviour of the connections under pressure, and the capacity of the glass tubes and the connections. Nevertheless, more research is needed on the long-term loading and on the fire safety principles designed for the designs.

Part IV Review

5.3. Recommendations

5.3. Recommendations

In this project it is proven that the designs were very robust, but as already mentioned, more research needs to be done on the fire safety mechanisms designed in this project. Furthermore, a case study was used to determine the compression loads, which gives a good estimation for a light-weight (office) building. The next step would be to perform more compression tests on longer samples (1.5 or 3 meter) to determine the safety factor of the designs and to check the behaviour of the design when exposed to buckling. On these longer tubes, also the behaviour of the designs needs to be checked when loaded under impact loads. Besides, in this thesis only compression tests were performed on short-term loading. To create layered tubular glass columns in the future, more research needs to be done on long-term loading as well.

First small samples where tested due to the fact that the lamination process of a tube within a tube was new and a lot of undertenancies were present. So, one of the main challenges was to laminate such a geometry. In this project, there were a few samples with almost no air bubbles located in the cavity, but also some samples with air bubbles. To further improve the transparency of the interlayer material between these tubes to create an interlayer without air bubbles, and to reduce the shrinkage in the interlayer material, so that less stresses occur during/after the lamination process, more research needs to be done on the lamination process of such a geometry.

In this project, only samples of annealed/annealed and heat-strengthened/heat-strengthened were tested. Maybe a combination could work as well. In the literature study, it emerged that heat-strengthened glass has a better resistance against impact loads and has a better resistance against thermal shock. It can be interesting to try out the combination of a heat-strengthened tube on the outer layer and an annealed glass tube on the inner layer. The heat-strengthened glass tubes had less load-bearing capacity after the first cracks than the annealed glass tubes. This different distribution of the loads can be integrated in the design of the end connection, for example by the use of hard and soft rubber. If the hard rubber is placed under one glass tube and the soft rubber is placed under the other glass tube, then the tube with the hard rubber gets more load then the other one. In this way, if the annealed inner tube cracks first, it gives the warning, and because it is the inner tube, no glass pieces can shatter so no injuries can be caused.

During tests, strain sensors were used which were glued in a vertically position to the glass. The values of the strain sensors were deviating, so perhaps other, more reliable, methods are possible to use to check if the strains are equal in the glass. When the strains are equal, the forces are equal, and that means that the forces are well-distributed introduced in the glass. Other methods to verify this could be by the use of special cameras.

Furthermore, it could be interesting to do further research in the photo-elastic stresses from the pictures taken with the polarised light. This can be done by the use of the stress optical law formula to estimate the approximate stress in the glass, especially around the air bubbles.

Lastly, the tubes were tested in room temperature. The tubes can also be tested in a climate chamber. In this way, tests could be performed at different temperatures or with a different humidity, to investigate thermal expansion of the glass tubes laminated with an interlayer material of which coefficient of thermal expansion (CTE) is much higher.

References

References

Achintha, M. (2016). Sustainability of Construction Materials (Second Edition): 5 - Sustainability of glass in construction. Woodhead Publishing Series in Civil and Structural Engineering, pp. 79-104. University of Southampton, Southampton, United Kingdom. DOI: 10.1016/B978-0-08-100370-1.00005-6.

Aiello, S., Campione, G., Minafò, G., Scibilia N. (2011). Compressive behaviour of laminated structural glass members. Engineering Structures 33, pp. 3402-3408.

Bagger, A., Petersen, R.I. (2009). Structural use of glass: Cruciform columns and glass portals with bolted connections subjected to bending. Proceedings Glass Performance Days. Tampere: GPD, pp. 381-385.

Best of Detail. (2014). Glas Glass. Edition Detail. 1st Edition. Werbedruck GmbH Horst Schreckhase, Spangenberg, pp. 81-83.

Blaauwendraad, J. (2007). Buckling of laminated glass columns. Faculty of Civil Engineering and Geosciences, Delft University of Technology.

Bouwbesluit. (2012). Hoofdstuk 4: Technische bouwvoorschriften uit het oogpunt van bruikbaarheid. Afdeling 4.1. Verblijfsgebied en verblijfsruimte. Artikel 4.3. Afmetingen verblijfsgebied en verblijfsruimte. From: https://www.bouwbesluitonline.nl/docs/wet/bb2012/hfd4

Bouwbesluit. (2012). Hoofdstuk 2. Technische bouwvoorschriften uit het oogpunt van veiligheid. Afdeling 2.2. Sterkte bij brand. Artikel 2.10. Tijdsduur bezwijken. From: https://rijksoverheid.bouwbesluit.com/Inhoud/docs/wet/bb2012/hfd2/afd2-2

bouwdeel d(emontabel). (2019). cepezed. From: https://www.cepezed.nl/files/publications/bouwdeel-demontabel-nl.pdf

Bouwdeel D(emontabel) Delft. (2020). Nationale Staalprijs 2020. Bouwdeel D(emontabel)_tekeningen_cepezed. From: https://www.nationalestaalprijs.nl/project/bouwdeel-demontabel

Britannica. (n.d.). Column architecture. From: https://www.britannica.com/technology/column-architecture

BS EN 572-2. (2012). Glass in building - Basic soda lime silicate glass products: Part 2: Float glass. BSI Standards Publication.

Checkmate Fire. (2018). Specifying Fire Resistant Glass. From: https://www.checkmatefire.com/news/specifying-fire-resistant-glass#

Corning Museum of Glass. (2002). TIMELINE OF GLASS HISTORY. From: https://www.cmog.org/visit/schools-groups-and-scouts/school-tours/resources/timeline-glass-history

Detail. 2003. Structural Glass Tubes - Tower Place in London. From: https://www.detail-online.com/magazine/structural-glass-tubes-tower-place-in-london-15407/

Eekhout, M. (2019). TUBULAR STRUCTURES IN ARCHITECTURE. 17th International Symposium on Tubular Structures (ISTS17)

Elkersh, H. (2014). Innovative Cleaner Production Technique: Foam Glass Production From Lead Crystal Glass Sludge. The American University In Cairo, School of Sciences and Engineering. MSc Mechanical Engineering. DOI: 10.13140/RG.2.1.4850.9849.

Engels, S. (2020). Structures from Borosilicate glass tubes: From experimental data to structural design. MSc, Technical University of Delft.

Gambhir, M.L. (2004). Stability Analysis and Design of Structures. Berlin, Springer.

Glastechnik Kirste. (2020). Precision in glass: news. From: https://www.glastechnik-kirste.de/en/menu/news/einzalansicht-en/article/glastechnik-kirste-receives-patent-on-laminated-glass-tube/

GPD Glass Performance Days. (2020). Martien Teich | Development of a Novel CCF Glass Tube Façade in Hong Kong. YouTube. From: https://www.youtube.com/watch?v=1OppxZS4zuU

Gravit, M., Klimin, N., Dmitriev, I., Karimova, A., Fedotova, E. (2019). Fire technical properties of intumescent and ablative fire resistant glass. IOP Conference Series: Materials Science and Engineer 666 012095. DOI:10.1088/1757-899X/666/1/012095.

Hadiningrum, K., Muldani, R.F. (2018). Optimization of the Amount of Gas Moles Determination through Boyle's Law and Gay-Lussac's Law Experiments. (no. 02, vol. 2). Journal of Physics: Theories and Applications, pp.53-63. DOI: 10.20961/jphystheor-appl.v2i2.30666.

Haldimann, M., Luible, A., Overend, M. (2008). Structural Engineering Document 10: Structural Use of Glass. Zürich, Switzerland: International Association for Bridge and Structural Engineering.

Hartsuijker, C. (2005). Toegepaste Mechanica. Deel 2: Spanningen, Vervormingen, Verplaatsingen. Academic Service, Den Haag.

Hartsuijker, C, Welleman, J.W. (2016). Constructiemechanica 3. Module: Stabiliteit van het evenwicht. Deel 1: Theorie. CTB2210. Civiele Techniek TU-Delft.

Hilti. (2008). Hilti HIT-HY 70 for structural glass. Its advantages are crystal clear. From: https://www.hilti.co.nz/media-canonical/ASSET_DOC_LOC_2871327_APC_RAW/ASSET_DOC_LOC_2871327
Honfi, D., Overend, M. (2013). Glass structures – learning from experts. COST Action TU0905, Mid-term Conference on Structural Glass.

Kömmerling. 2014. Kommerling's new liquid composite for glass, Ködiguard Conservation, significantly reduces UV light damage. From: http://www.kommerlinguk.com/uploads/news/20141016113315-Kodiguard%20conservation24.9.14.pdf

Loman, A.A.C. (2019). Performance of structural glass at elevated temperatures. MSc, Technical University of Delft.

Luible, A., Crisinel, M. (2004). Buckling Strength of Glass Elements in Compression. Structural Engineering International, pp. 120-125. DOI: 10.2749/101686604777964107.

NEN 2608. (2011). Annex D: Structural safety according to the Fine and Kinney method, pp. 37-38.

Nijsse, R. (2003). Glass in Structures: Elements, Concepts, Designs. Birkhauser, Germany, pp. 71.

Nijsse, R. (2003). Glass in Structures: Elements, Concepts, Designs. Birkhauser, Germany. In: Oikonomopoulou, F., van den Broek, E.A.M., Bristogianni, T., Veer, F.A., & Nijsse, R. (2017). Design and experimental testing of the bundled glass column. Glass Structures & Engineering. DOI: 10.1007/s40940-017-0041-x.

Nijsse, R., Ten Brincke, E.H.J. (2014). Glass columns. In: Oikonomopoulou, F., van den Broek, E.A.M., Bristogianni, T., Veer, F.A., & Nijsse, R. (2017). Design and experimental testing of the bundled glass column. Glass Structures & Engineering. DOI: 10.1007/s40940-017-0041-x.

Oikonomopoulou, F. (2019). Unveiling the third dimension of glass: Solid cast glass components and assemblies for structural applications. (Doctor). Delft University of Technology, Delft.

Oikonomopoulou, F., van den Broek, E.A.M., Bristogianni, T., Veer, F.A., & Nijsse, R. (2017). Design and experimental testing of the bundled glass column. Glass Structures & Engineering. DOI: 10.1007/s40940-017-0041-x.

O'Regan, C. (2015). Structural use of glass in buildings (Second edition). The Institution of Structural Engineers.

Ouwerkerk, E. (2011). Glass columns. MSc, Technical University of Delft.

Overend, M. (2002). THE APPRAISAL OF STRUCTURAL GLASS ASSEMBLIES: Submitted for the degree of PhD to the Department of Civil Engineering of the University of Surrey.

Overend, M., Vassallo, C., Camillieri, K. (2005). The Design, Assembly & Performance of Glass Columns. Proceedings Glass Performance Days 2005. GPD, pp. 1-5.

POLFLAM®. (n.d.). Our technology. From: https://polflam.pl/en/our-technology/

Promat. (n.d.). PROMADUR®. From: https://www.promat.com/en/construction/products-systems/products/intumescent-paints/promadur/

Rees, D.W.A. 2009. Mechanics of optimal structural design. Chichester: John Wiley & Sons. In: Ouwerkerk, E. (2011). Glass columns. MSc, Technical University of Delft.

Roeder, E. (1971). EXTRUSION OF GLASS. Journal of Non-Crystalline Solids 5, pp. 377-388. From: https://www.sciencedirect.com/science/article/pii/0022309371900391

Saint-Gobain. (2016). Mechanical properties. From: https://www.saint-gobain-sekurit.com/glossary/glassproperties#:~:text=The%20main%20characteristics%20of%20glass,breakage%20resistance%20and%20chemical%20resistance

Schittich, C., Staib, G., Balkow, D., Schuler, M., Sobek, W. (2017). Glass Construction Manual 2nd Revised and Expanded Edition Ed. Birkhauser, Basel.

SCHOTT. (2021). Shock-resistant and durable: pre-stressed DURATAN® special glass tubing. From: https://www.schott.com/tubing/english/products/duratan.html

SCHOTT. (2020). Climate-neutral by 2030. From: https://www.schott.com/english/company/environment/climate-neutral-by-2030.html?WTC=corporate_en_linkedIn_social_post

SHOTT. (2020). Applications: Glass Tubing solutions for your applications. From: https://www.schott.com/tubing/english/applications/index.html

SCHOTT. (2020). Glass Tubing for Lamp Design. From: https://www.schott.com/tubing/english/special_glass/lighting.html

SCHOTT. (2020). Three out of every four COVID-19 vaccine projects across the globe rely on SCHOTT vials. From: https://www.schott.com/english/news/press.html?NID=com5812

SCHOTT internal. (2019). COATED TUBES – glass types DURAN® and CONTURAX®. Semtex blast test.

SCHOTT. (n.d.). DURAN®. Tubing, rods and capillaries made of borosilicate glass 3.3. Retrieved on January, 20, 2021, from: SCHOTT.

SCHOTT. (n.d.). DURATAN®. Thermally prestressed tubing of special glass. Retrieved on May, 10, 2021, from: SCHOTT.

SCHOTT. (n.d.). DURAN® Tough / CONTURAX® Tough. From: https://www.schott.com/d/tubing/3887a1d0-e951-4133-b81d-035b905726da/1.0/schott-conturax-tough-duran-tough-tubing-flyer-en-english-03032021.pdf

Schwanke, H. (n.d.). SCHOTT. Art with Glass: Complex Glass Artworks of Great Depth. From: https://www.schott.com/magazine/english/sol207/sol207_12_glassartworks.html

Sturkenboom, J. (2018). Fire Resistant Structural Glass Beams. Developing design recommendations for future development and fire certification of structural glass beams. MSc, Technical University of Delft.

The Architect's Newspaper: I.M. Pei's JFK in Terminal Trouble. (2010). From: https://www.archpaper.com/2010/06/im-peis-jfk-in-terminal-trouble/

The Institution of Structural Engineers. (2010). Practical guide to structural robustness and disproportionate collapse in buildings (October 2010). The Institution of Structural Engineers.

Timmel, M., Kolling, S., Osterrieder, P., Du Bois, P.A. (2007). A finite element model for impact simulation with laminated glass. International Journal of Impact Engineering 34, pp. 1465–1478

Van Heughten, R. (2013). Load-bearing glass columns: the stacked column. MSc, Technical University of Eindhoven.

Van Nieuwenhuijzen, E.J., Bos, F.P., Veer, F.A. (2005). The Laminated Glass Column. Proceedings Glass Performance Days, pp. 1-4

Veer, F.A. (2007). The strength of glass, a non-transparent value. Heron. pp. 87-104.

Veer, F.A. (2014). Glass safety factor and reinforcement. Delft, Delft University of Technology.

Veer, F.A., Pastunink., R.J. (1999). Developing a Transparent Tubular Laminated Column. Proceedings Glass Performance Days, pp. 277-280.

Veer, F.A., Van Der Voorden, M., Rijgersberg, H., & Zuidema, J. (2001). Using Transparent Intumescent Coatings to Increase the Fire Resistance of Glass and Glass Laminates. Glass Processing Days, (June), 18–21. https://doi.org/10.1016/S1353-8020(11)70040-2. In:

Vetrotech Saint-Gobain. (2020). VETROFLAM. From: https://www.vetrotech.com/nl-nl/vetroflam

Vetrotech Saint-Gobain. (2020). CONTRAFLAM. From: https://www.vetrotech.com/nl-nl/contraflam

Webinar Bouwdeel D(emontabel). (2020). Bouwen met staal. YouTube. From: https://www.youtube.com/watch?v=YOdKu9nGJ-0

Weller, B., Unnewehr, S., Tasche, S., Härth, K. (2009). Glass in Building: Principles Applications Examples. Birkhäuser Edition Detail.

Wiederhorn, S.M., Bolz, L.H. (1970). Stress Corrosion and Static Fatigue of Glass. (no. 10, vol. 53). Journal of The American Ceramic Society. Institute for Materials Research, National Bureau of Standards, Washington, D. C. 20234, pp. 543-548.

Figure list

Figure 1 - ©ERIETA ATTALI PHOTOGRAPHIC ARCHIVE. (2016). DIVISARE: KENGO KUMA AND ASSOCIATES 隈研吾建築都市設計事務所 WATER GLASS. Retrieved on November, 30, 2020, from: https://divisare.com/projects/326306-kengo-kuma-and-associates-erieta-attali-water-glass

Figure 2 - iDesignArch. (2010-2021). Apple Store Fifth Avenue New York. Retrieved on November 12, 2020, from: https://www.idesignarch.com/apple-store-fifth-avenue-new-york/

Figure 3 - Own picture. Delft. Retrieved on November 30, 2020.

Figure 4 - Nijsse, R., Ten Brincke, E.H.J. (2014). Glass columns. In: Oikonomopoulou, F., van den Broek, E.A.M., Bristogianni, T., Veer, F.A., & Nijsse, R. (2017). Design and experimental testing of the bundled glass column. Glass Structures & Engineering. DOI: 10.1007/s40940-017-0041-x. Retrieved on November, 10, 2020.

Figure 5 - Schmidt Hammer Lassen Architects. (n.d.). Architectour.net. Danfoss Domicil Danfoss Head Office. Retrieved on November 13, 2020, from: https://www.architectour.net/opere/opera.php?id_opera=6473&nome_opera=Danfoss%20Domicil&architetto=Schmidt%20Hammer%20Lassen

Figure 6 - Schwanke, H. (n.d.). SCHOTT. Art with Glass: Complex Glass Artworks of Great Depth. Retrieved on November, 23, 2020, from: https://www.schott.com/magazine/english/sol207/sol207_12_glassartworks.html

Figure 7 - SCHOTT. (n.d.). DURAN®. Tubing, rods and capillaries made of borosilicate glass 3.3. Retrieved on November 11, 2020, from: https://www.schott.com/en-gb/products/duran/downloads

Figure 8 - Own picture. Delft. Retrieved on November 28, 2020. With: Icons and Photos For Everything. (n.d.). Noun Project. Retrieved on November, 28, 2020, from: https://thenounproject.com/

Figure 9 - TWI. (2020). HOW ARE GLASS, CERAMICS AND GLASS-CERAMICS DEFINED? Retrieved on December, 14, 2020, from: https://www.twi-global.com/technical-knowledge/faqs/faq-how-are-glass-ceramics-and-glass-ceramics-defined

Figure 10 - Haldimann, M., Luible, A., Overend, M. (2008). Structural Engineering Document 10: Structural Use of Glass. Zürich, Switzerland: International Association for Bridge and Structural Engineering, pp.5. Retrieved on December, 14, 2020.

Figure 11 - Shand, E.B., Armistead, W.H. (1958). Glass Engineering Handbook. McGraw-Hill Book Company. In: Oikonomopoulou, F. (2019). Unveiling the third dimension of glass: Solid cast glass components and assemblies for structural applications. (Doctor). Delft University of Technology, Delft. Retrieved on November, 23, 2020.

Figure 12 - Elkersh, H. (2014). Innovative Cleaner Production Technique: Foam Glass Production From Lead Crystal Glass Sludge. The American University In Cairo, School of Sciences and Engineering. MSc Mechanical Engineering. pp. 13. DOI: 10.13140/RG.2.1.4850.9849. Retrieved on December, 14, 2020.

Figure 13 - Own picture. Delft. Retrieved on January, 18, 2021. Based on: Ali, R.B., Islam, M. M., Billah, M. (2019). Sophisticated Developments and Advanced Applications of Glass Structure: Summary of Recent Research. World Scientific New: An International Scientific Journal, WSN 124(1) (2019) 1-93. Department of Civil Engineering, Bangladesh University of Engineering & Technology. Retrieved on December, 14, 2020, from: http://www.worldscientificnews.com/wp-content/uploads/2019/02/WSN-1241-2019-1-93-2.pdf AND Felekou, E. (2016). Glass Tower in high-rise buildings. MSc, Technical University of Delft, pp. 31

Figure 14 - Haldimann, M., Luible, A., Overend, M. (2008). Structural Engineering Document 10: Structural Use of Glass. Zürich, Switzerland: International Association for Bridge and Structural Engineering, pp. 8. Retrieved on December, 14, 2020.

Figure 15 - Ouwerkerk, E. (2011). Glass columns: A fundamental study to slender glass columns assembled from rectangular monolithic flat glass plates under compression as a basis to design a structural glass column for a pavilion. In: SIMONIS, F. 1997. Van veilig construeren in glas tot veiligheidsglas. Delft: Stichting Postacademisch Onderwijs. pp. GL 3.

Figure 16 - Own picture from: Granta's CES Edupack 2017. Retrieved on 2017.

Figure 17 - Own picture from: Granta's CES Edupack 2017. Retrieved on 2017.

Figure 18 - Own picture from: Granta's CES Edupack 2017. Retrieved on 2017.

Figure 19 - Roeder, E. (1971). Extrusion of Glass. Philips tech. Rev. 32, No. ¾, pp. 97. Retrieved on May, 5, 2021, from: https://www.pearl-hifi.com/06_Lit_Archive/02_PEARL_Arch/Vol_16/Sec_53/Philips_Tech_Review/PTechReview-32-1971-096.pdf

Figure 20 - F&D Glass. (2014). Friedrich & Dimmock, inc. Simax Glass Tube & Rod. Retrieved on November, 23, 2020, from: https://fdglass.com/our-products/simax-glass-tubing-rod/?gclid=Cj0KCQiAhs79BRD0ARIsAC6XpaWukDCbgmKTH6ORshmFwwvbXu_Cl3LTqojFdy_CDXjyt4_FBrRcAuQaAmsiEALw_wcB

Figure 21 - Roeder, E. (1971). EXTRUSION OF GLASS. Journal of Non-Crystalline Solids 5, pp. 383. Retrieved on November, 23, 2020, from: https://www.sciencedirect.com/science/article/pii/0022309371900391

Figure 22 - Roeder, E. (1971). EXTRUSION OF GLASS. Journal of Non-Crystalline Solids 5, pp. 383. Retrieved on November, 23, 2020, from: https://www.sciencedirect.com/science/article/pii/0022309371900391

Figure 23 - Glass Academy. (2016). Tempered Glass. Retrieved on December, 16, 2020, from: http://www.glass-academy.com/tempered-glass-2/

Figure 24 - Haldimann, M., Luible, A., Overend, M. (2008). Structural Engineering Document 10: Structural Use of Glass. Zürich, Switzerland: International Association for Bridge and Structural Engineering, pp. 10. Retrieved on December, 14, 2020.

Figure 25 - Van der Velden, M. (2019). CIE4285 Structural Glass Reader. Delft University of Technology, pp. 27. Retrieved on December, 16, 2020.

Figure 26 - Haldimann, M., Luible, A., Overend, M. (2008). Structural Engineering Document 10: Structural Use of Glass. Zürich, Switzerland: International Association for Bridge and Structural Engineering, pp. 9. Retrieved on December, 14, 2020.

Figure 27 - Hänig, J., Bukieda, P., Engelmann, M., Stelzer, I., Weller, B. (2019). Examination of Laminated Glass with Stiff Interlayers – Numerical and Experimental Research. (vol. 3). International Journal of Structural Glass and Advanced Materials Research, pp.2. DOI: 10.3844/sgamrsp.2019.1.14.

Figure 28 - Crystalia Glass Architectural glass & metal. (2020). What Is the Difference between Laminated Glass and Tempered Glass? Retrieved on December, 16, 2020, from: https://crystaliaglass.com/what-is-the-difference-between-laminated-glass-and-tempered-glass/

Figure 29 - Viracon. (2020). Enhancements: Edgework. BIG GLASS CONFIGURATIONS AVAILABLE UP TO 130” x 236. Retrieved on December, 22, 2020, from: https://www.viracon.com/edgework/

Figure 30 - Hartsuijker, C., Welleman, J.W. (2016). Constructiemechanica 3. Module: Stabiliteit van het evenwicht. Deel 1: Theorie. CTB2210, pp.3. Civiele Techniek TU-Delft. Retrieved on January, 6, 2021.

Figure 31 - Gambhir, M.L. (2004). Stability Analysis and Design of Structures. Berlin, Springer, pp.4. Retrieved on January, 6, 2021.

Figure 32 - Pešek, O., Melcher, J. (2017). Shape and Size of Initial Geometrical Imperfections of Structural Glass Members. Civil Engineering Series. (no. 1, vol. 17). De Gruyter Open. Transactions of the VŠB – Technical University of Ostrava. Retrieved on January, 6, 2021.

Figure 33 - Own picture. Delft. Retrieved on January, 6, 2021.

Figure 34 - Luible, A., Crisinel, M. (2004). Buckling Strength of Glass Elements in Compression. Structural Engineering International, pp. 122. DOI: 10.2749/101686604777964107. Retrieved on January, 6, 2021.

Figure 35 - Hartsuijker, C., Welleman, J.W. (2016). Constructiemechanica 3. Module: Stabiliteit van het evenwicht. Deel 1: Theorie. CTB2210, pp.9. Civiele Techniek TU-Delft. Retrieved on January, 6, 2021.

Figure 36 - GPD Glass Performance Days. (2020). Martien Teich | Development of a Novel CCF Glass Tube Façade in Hong Kong. YouTube, minute: 7:15. Retrieved on February, 3, 2021, from: https://www.youtube.com/watch?v=1OppxZS4zuU

Figure 37 - Bouwbesluit. (2012). Hoofdstuk 2. Technische bouwvoorschriften uit het oogpunt van veiligheid. Afdeling 2.2. Sterkte bij brand. Artikel 2.10. Tijdsduur bezwijken, table 2.10.1 and 2.10.2. Retrieved on January, 8, 2020, from: https://rijksoverheid.bouwbesluit.com/Inhoud/docs/wet/bb2012/hfd2/afd2-2

Figure 38 - Timmel, M., Kolling, S., Osterrieder, P., Du Bois, P.A. (2007). A finite element model for impact simulation with laminated glass. International Journal of Impact Engineering 34, pp. 1473–1474. Retrieved on January, 12, 2021.

Figure 39 - Own picture. Delft. Retrieved on January, 25, 2021. Based on: Van Nieuwenhuijzen, E.J., Bos, F.P., Veer, F.A. (2005). The Laminated Glass Column. Proceedings Glass Performance Days, pp. 3.

Figure 40 - Detail inspiration. (2009). Bank in Bilbao. DETAIL 07-08/2009. Retrieved on January, 25, 2021, from: https://inspiration.detail.de/bank-in-bilbao-103420.html

Figure 41 - Best of Detail. (2014). Glas Glass. Edition Detail. 1st Edition. Werbedruck GmbH Horst Schreckhase, Spangenberg, pp. 83. Retrieved on January, 25, 2021.

Figure 42 - Detail inspiration. (2009). Bank in Bilbao. DETAIL 07-08/2009. Retrieved on January, 25, 2021, from: https://inspiration.detail.de/bank-in-bilbao-103420.html

Figure 43 - Nijsse, R., Ten Brincke, E.H.J. (2014). Glass columns. In: Oikonomopoulou, F., van den Broek, E.A.M., Bristogianni, T., Veer, F.A., & Nijsse, R. (2017). Design and experimental testing of the bundled glass column. Glass Structures & Engineering. DOI: 10.1007/s40940-017-0041-x. Retrieved on November, 10, 2020.

Figure 44 - facadeworld. (2013). Glasbaum. Retrieved on November 13, 2020, from: https://facadeworld.com/2013/10/06/glasbaum/

Figure 45 - Veer, F.A., Pastunink., R.J. (1999). Developing a Transparent Tubular Laminated Column. *Proceedings Glass Performance Days*, pp. 278. Retrieved on November 13, 2020.

Figure 46 - Veer, F.A., Pastunink., R.J. (1999). Developing a Transparent Tubular Laminated Column. *Proceedings Glass Performance Days*, pp. 279. Retrieved on November 13, 2020.

Figure 47 - Van Nieuwenhuijzen, E.J., Bos, F.P., Veer, F.A. (2005). The Laminated Glass Column. Proceedings Glass Performance Days, pp. 1. Retrieved on January, 11, 2021.

Figure 48 - C|L. (1998-2003). GLASS TUBE FIELD. Retrieved on November 12, 2020, from: https://carpenterlowings.com/portfolio_page/glass-tube-field/

Figure 49 - Doenitz, F., Jung. H., Behling, S., Achenbach, J. (2003). Laminated glass tubes as structural elements in building industry. Glass Processing Days, (pp. 275-278). Tampere, Finland.

Figure 50 - SCHOTT internal. (2019). COATED TUBES – glass types DURAN® and CONTURAX®. Semtex blast test.

Figure 51 - Own picture. Delft. Retrieved on January, 12, 2021.

Figure 52 - Own picture. Delft. Retrieved on February, 3, 2021.

Figure 53 - Own picture. Delft. Retrieved on March, 3, 2021.

Figure 54 - Own picture. Delft. Retrieved on March, 3, 2021.

Figure 55 - Own picture. Delft. Retrieved on March, 3, 2021.

Figure 56 - Own picture. Delft. Retrieved on February, 3, 2021.

Figure 57 - Own picture. Delft. Retrieved on June, 10, 2021.

Figure 58 - Own picture. Delft. Retrieved on June, 8, 2021.

Figure 59 - Own picture. Delft. Retrieved on March, 3, 2021.

Figure 60 - Own picture. Delft. Retrieved on March, 3, 2021.

Figure 61 - SCHOTT. (n.d.). DURAN®. Tubing, rods and capillaries made of borosilicate glass 3.3. Retrieved on January, 20, 2021.

Figure 62 - Own picture. Delft. Retrieved on March, 3, 2021.

Figure 63 - Own picture. Delft. Retrieved on June, 12, 2021.

Figure 64 - Bouwdeel D(emontabel) Delft. (2020). Nationale Staalprijs 2020. Bouwdeel D(emontabel)_tekeningen_cepezed, pp, 1. Retrieved on January, 21, 2021, from: https://www.nationalestaalprijs.nl/project/bouwdeel-demontabel

Figure 65 - Bouwdeel D(emontabel) Delft. (2020). Nationale Staalprijs 2020. Bouwdeel D(emontabel)_tekeningen_cepezed, pp, 2. Retrieved on January, 21, 2021, from: https://www.nationalestaalprijs.nl/project/bouwdeel-demontabel

Figure 66 - Bouwdeel D(emontabel) Delft. (2020). Nationale Staalprijs 2020, pp, 2. Retrieved on January, 21, 2021, from: https://www.nationalestaalprijs.nl/project/bouwdeel-demontabel

Figure 67 - bouwdeel d(emontabel). (2019). cepezed, pp. 3. Retrieved on January, 21, 2021, from: https://www.cepezed.nl/files/publications/bouwdeel-demontabel-nl.pdf

Figure 68 - Left: Webinar Bouwdeel D(emontabel). (2020). Bouwen met staal. YouTube, minute: 52:51. Retrieved on January, 20, 2021, from: https://www.youtube.com/watch?v=YOdKu9nGJ-0. Right: Own picture. Delft. Retrieved on January, 21, 2021.

Figure 69 - Own picture. Delft. Retrieved on August, 9, 2021.

Figure 70 - Own picture. Delft. Retrieved on July, 16, 2021.

Figure 71 - Own picture. Delft. Retrieved on March, 3, 2021.

Figure 72 - Own picture. Delft. Retrieved on May, 3, 2021.

Figure 73 - Own picture. Delft. Retrieved on May, 4, 2021.

Figure 74 - Own picture. Delft. Retrieved on May, 12, 2021.

Figure 75 - Own picture. Delft. Retrieved on May, 31, 2021.

Figure 76 - Made by Octatube. Delft. Retrieved on June, 4, 2021.

Figure 77 - Made by H.B.Fuller Kömmerling. Delft. Retrieved on June, 8, 2021.

Figure 78 - Left and middle: Own picture. Delft. Retrieved on May, 31, 2021. Right: Own picture. Delft. Retrieved on June, 24, 2021.

Figure 79 - Own picture. Delft. Retrieved on June, 25, 2021.

Figure 80 - Own picture. Delft. Retrieved on July, 1, 2021.

Figure 81 - Own picture. Delft. Retrieved on June, 30, 2021.

Table and graph list

Table 1 - Haldimann, M., Luible, A., Overend, M. (2008). Structural Engineering Document 10: Structural Use of Glass. Zürich, Switzerland: International Association for Bridge and Structural Engineering, pp. 7. Retrieved on December, 14, 2020.

Table 2 - BS EN 572-2. (2012). Glass in building - Basic soda lime silicate glass products: Part 2: Float glass. BSI Standards Publication, pp. 6. Retrieved on December, 22, 2020.

Table 3 - O'Regan, C. (2015). Structural use of glass in buildings (Second edition). The Institution of Structural Engineers, pp. 21. Retrieved on January, 7, 2020.

Table 4 - O'Regan, C. (2015). Structural use of glass in buildings (Second edition). The Institution of Structural Engineers, pp. 75. AND Weller, B., Unnewehr, S., Tasche, S., Härth, K. (2009). Glass in Building: Principles Applications Examples, pp. 27. Birkhäuser Edition Detail. Retrieved on January, 8, 2020.

Table 5 - Own made overview. Delft. Retrieved on November, 2020.

Table 6 - Van Nieuwenhuijzen, E.J., Bos, F.P., Veer, F.A. (2005). The Laminated Glass Column. Proceedings Glass Performance Days, pp. 4. Retrieved on January, 11, 2021.

Table 7 - Own made overview. Delft. Retrieved on January, 11, 2021.

Table 8 - NEN 2608. (2011). Annex D: Structural safety according to the Fine and Kinney method, pp. 37-38.

Table 9 - NEN 2608. (2011). Annex D: Structural safety according to the Fine and Kinney method, pp. 37-38.

Table 10 - Own made table. Delft. Retrieved on January, 22, 2021. With Own pictures. Delft. Retrieved on January, 12, 2021.

Table 11 - Own made table. Delft. Retrieved on July, 6, 2021.

Table 12 - Own made table. Delft. Retrieved on July, 10, 2021.

Table 13 - Own made table. Delft. Retrieved on July, 10, 2021.

Table 14 - Own made table. Delft. Retrieved on July, 9, 2021.

Table 15 - Own made table. Delft. Retrieved on July, 9, 2021.

Table 16 - Van Nieuwenhuijzen, E.J., Bos, F.P., Veer, F.A. (2005). The Laminated Glass Column. Proceedings Glass Performance Days, pp. 2. Retrieved on January, 11, 2021.

Graph 1 - Own made graph. Delft. Retrieved on July, 4, 2021.

Graph 2 - Own made graph. Delft. Retrieved on July, 8, 2021.

Appendix

Appendix

Part I - Introduction/Literature Study

Part II - Design

Part III - Numerical and Experimental Investigations

Appendix 1 – Interviews

During the literature study and the design phase, interviews were held with a few professionals in the working field, to get a clear view of the current state of the material glass, of the development of glass as a structural material in practise, and of the opinions about the application of glass columns.

Appendix.1.1. Interview Thomas Wever (abt)

Thomas Wever is a project manager/ structural engineer at ABT. This interview was held on 6-12-20.

1. What projects have you worked on in relation to glass (columns)?

I have been working on a bundled glass column for at the entrance for the office building abt in Velp. Due to circumstances, it is never built. We have tested a few prototypes at compression strength in the lab in Delft back then.

Furthermore, I worked on the glass bridge in Rurlow. We designed the glass floor in this bridge. Besides, I worked on a project in Gouda with glass elements to support wind loads from a canopy (beams/ lateral torsional buckling elements).

2. What are developments on structural glass (columns) at the moment in practise?

Columns are a primary structural element. If the column fails, the building fails. This is more critical compared to a part of a façade for example. According to the norm, a structural element needs to give a sign before failing. Glass has a sudden failure, so this is more difficult with glass. The structural glass elements as beams and fins are designed for light-weighted structures so far. A glass façade only needs to carry/ transport wind forces. The building industry is conservative, so it can take a lot of years when something innovative and new will be allowed at the market.

3. What are reasons according to you why glass columns are not much applied yet in buildings?

The building industry is conservative, so it can take a lot of years when something innovative and new will be allowed at the market. Furthermore, to develop something new is expensive.

4. According to Rob Nijsse, there are five types of glass columns. What is the most ideal one in your point of few, considering cross-section shape/ (fire-)safety/ robustness/ etc?

The laminated tubular glass column, due to its stability against buckling. If I were you, I would design it so that the tubes will collaborate with each other for a higher strength.

5. Which finite element program should you use to check buckling forces?

SCIA or DIANA.

Appendix.1.2. Interview Ate Snijder (TU Delft)

Ate Snijder is researcher/teacher at the faculty of Architecture within the department of Structural Design and Mechanics at the Technical University of Delft. This interview was held on 18-12-20.

1. You was one of the committee members in both researches from Steven Engels and Arjan Boonstra about borosilicate glass tubes. Why did you used hollow glass tubes for the design?

A disadvantage of rod glass columns is that rods can fall. This is not safe and less transparent. There are two ways of insuring structural safety, namely load-bearing capacity and safety of people (injuries).

2. How is the strength increased in these designs?

We tested singular tubular glass profiles with a length of 400 mm. On the inside of the tubes, a OPALFILM coating was attached. The coating has a strength and contributes to the load-bearing capacity and it decreases injuries, because the failing glass pieces are kept in place by the coating.

If you design two tubes into each other, then the coating is not contributing to the collaboration of these tubes. It is only attached to the inside of the outer tube (shown in the figure below). The inner tube is protected by this outer tube, who is made safe by itself.

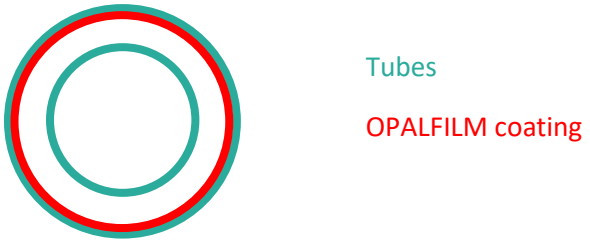

Figure 1 Cross-section of two tubes with a OPALFILM coating.

3. How is the coating attached to the glass tube?

SCHOTT did this is collaboration with another firm. How they did this exactly is not known.

4. Which tests were performed in these two researches?

We did only tests on tubes with a length of 400 mm. Steven Engels did research into axial forces for buckling on single tubes of 400 mm and Arjan Boonstra did research into bending forces on the same size tubes.

5. What where tests that you were planning to do but did not do in the end?

We did only tests on tubes with a length of 400 mm. Compression and bending strength tests were performed. We wanted to test longer profiles and wanted to do impact tests. These tests were not performed due to Corona.

6. Were the results from the tests as desired?

The test results were different, which is not preferable. If profiles were not completely clamped, the tube broke completely. Profiles who were better clamped didn't broke.

7. How were the connections be designed?

For the tests we used a compression set-up. The glass tube was clamped between MFD/ wood ply. For the application they designed connections with POM. This is a good material due to the fact that it will doesn't show creep behaviour and it has a low Young's modulus. In this way, no stress concentrations occur in the glass.

8. How did you obtained the glass tubes?

SCHOTT sponsored them.

9. Why is there not much research done into glass columns?

Mostly due to: high costs, production failures, etc.

10. Why wouldn't the producer have done much research on it?

They do more business in the pharmaceutical industry. It is costly to do tests themselves. They only perform tests if a client wants a lot of something.

For example, SCHOTT performed a Semtex blast test on glass tubes with OPALFILM for an airport project in the Middle-East. There they are afraid of bomb attacks. So, they wanted a wall, but they needed to show that it didn't break into 1000 flying pieces. It could break, but the glass pieces needed to stick to the coating.

References

Figure 1 - Own made picture. Retrieved on December, 19, 2020.

Appendix.1.3. Interview Joost Heijnis (cepezed)

Joost Heijnis is a building engineer at cepezed. Cepezed is an architectural firm. This interview was held on 26-1-2021.

1. If it would be possible to design with glass columns, would cepezed design with it or not?

This is depending on the project. If the project needs to have a luxury appearance, then glass columns will fit definitely. I am thinking of projects like a perfume shop, a court house, etc. The designs of cepezed are most of the time showing the structural elements too. So, columns by itself are not ugly, but the slimmer they can be the more space is left in the floorplan. So, glass or not, the slimmer the better.

In this research, the glass columns will be round. This will suit best in the middle of a building. Due to its round shape, people can walk around it, and it has a more friendly look.

2. For the case study in this thesis, Bouwdeel D will be used, because of its clear grid and its sustainability aspect demountability. Furthermore, the middle row of columns is different comparing to the columns in the façade, so the columns in the middle row will be made out of glass. The building is modern and it has a transparent façade, these features will fit looking to glass columns. What do you think of glass columns in Bouwdeel D? Is this case suitable?

Bouwdeel D has something that looks a bit cheap, due to the fact that the finishing level is low. If the finishing in this building would have been more, than glass columns can suit into the building. It is understandable that you choose this building looking at the low weight of the building, and its modern and transparent appearance.

Looking at your designed connection, it looks good! And really nice that you are trying something new to expand the toolkit of materials we can use to design with. This is innovative.

Appendix.1.4. Interview Peter van de Rotten (Octatube)

Peter van de Rotten is one of the heads of the structural department of Octatube. This interview was held on 9-2-2021.

1. Which projects did you worked on related to glass tubes?

We ones worked on a façade designed by OMA with glass tubes, but it is not built. Furthermore, we worked on a project with curved glass panels.

2. What are reasons according to you why glass columns are not much applied yet in buildings?

Because it is difficult to make sure that the glass column is robust enough. If not, a secondary load path needs to be included in the design.

3. According to Rob Nijsse, there are five types of glass columns. What is the most ideal one in your point of few, considering cross-section shape/ (fire-)safety/ robustness/ etc?

The laminated tubular glass column will be best according to buckling, but a lot of other difficulties needs to be taken into account in this concept, like thermal expansions due to temperature differences. Of course, it is depending on a lot of variables. In the end it is depending on what the client wants.

4. The article you send about isochoric pressure is interesting! So, to avoid this effect, it is possible to use a ventilation system. Show details to discuss:

POM is a plastic material. Creep can occur in POM if stresses become too high (>20 N/mm^2). Hilti injection mortar can take over a little bit higher stresses from the glass. You can use spacers under the glass. In the empty spots you can inject Hilti mortar under the glass. Furthermore, if the stresses are not too high in the glass due to temperature differences, maybe a simpler solution can be used instead of the ventilation system, like with a bellow (balg). If this is not necessary too, you can maybe use silica grains to take out the water if condensation is occurring. This principle is also used in double glazed units.

5. Which finite element program would you use to check the buckling behaviour of laminated glass tubes?

DIANA.

Appendix 2 – Literature Study

A.2.1. History glass

Glass is an old material. The exact date of discovery is unknown, but it was discovered before BC. Some people say that the oldest glass found was made by Egyptians around 3500 BC (O'Regan, C. 2015). Others say that the first made glass came from Mesopotamia around 2000 BC (Corning Museum of Glass. 2002). They created small objects of glass. Around 16th century glass was used for jewellery or for hollow vessels. The Romans were the first who developed clear glass (O'Regan, C. 2015). Around 100 AD, a Roman writer wrote that glass was discovered by an accident by the Phoenicians. They stranded with their ship on a beach. They cooked dinner in a bronze pan on soda-lime rocks, on a fire. The next morning after the fire was extinguished, they found the glittering material, which is nowadays known as glass (Diehn, D. A. 1941).

The first used glass in windows was in the Roman Age in villas in Pompeii and Herculaneum. Small glass panes were used as part of the façade of the building. The sizes of the panes were 300 by 500 mm and 30 or 60 mm thick. The panes were cast and drawn. Most of these panes were coloured green and were not totally transparent yet (Schittich, C., et al. 2017).

Manufacturing of glass was labour intensive, that was why glass was seen as a luxury product. If owners had glass in the window frames of their building, they were seen as rich, because it was difficult to install glass in window frames. In the Middle Ages, the most important manufacturing techniques were the blown cylinder sheet and the crown glass process (figure 1). These techniques were the basis until the 20th century. In the blown technique, molten glass was attached to a hollow pipe. The makers were blowing on the pipe to make a bubble of the molten glass. This process was the same for the crown technique, but by spinning the pipe, they created a circular flat glass pane (Schittich, C., et al. 2017). In the middle of the panes, a bubble was visible. This bubble was called: 'bullseye' (figure 2). They could produce panes of 0.5 by 0.75 metres. Mostly glass panes were used for windows in cathedrals (O'Regan, C. 2015). In the 17th century not only glass panes were used in cathedrals, but also for palaces and houses. Glass was used in buildings, because it let daylight through, but it protected the inside from weather conditions (Schittich, C., et al. 2017). In the cylinder method (or broad method), a hollow pipe is used as well with molten glass. A bubble is blown in the molten glass and by swinging a cylinder is made. Then the ends were cut off and the middle part was opened as a flat sheet (figure 11). Plates were made of 1 by 1.3 metres. In 1871, Pilkington created a drawing machine to automate the production by using the cylinder method. The first mechanical cylinder drawing machine was invented in 1910 (O'Regan, C. 2015).

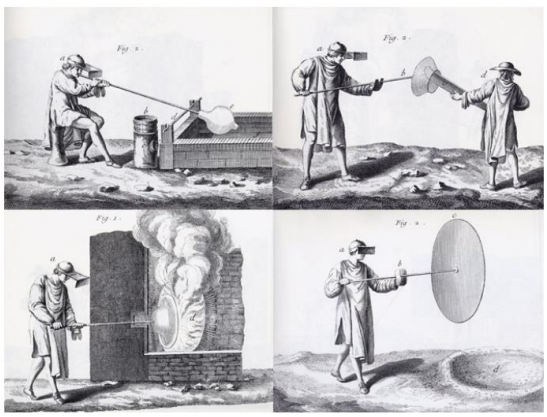

Figure 1 Crown method (Hermens, E. 2017).

Figure 2 Bullseye glass panes (Glashütte Lamberts. n.d.).

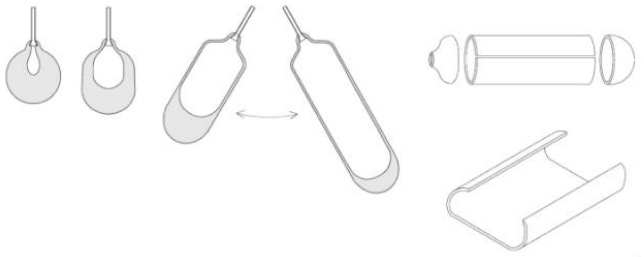

Figure 4 Cylinder method (Schittich, C., et al. 2017).

Figure 3 Crystal Palace (Shower Talk. n.d.).

In the 1687 Bernard Perrot developed the manufacturing process for cast glass. With this method they could make panes up to 1.2 by 2 metres. Less labour was required, which reduced costs (Schittich, C., et al. 2017). In the 1856 the Siemens-Martins method was invented. It made higher temperatures possible to create better glass qualities, by using the heat from waste gases (O'Regan, C. 2015). In 1839, the Chance brothers had new developments in cutting, polishing and grinding techniques of the blown cylinder process (figure 3). It resulted in less breakages and improvements on the surface finish. This better quality made it possible to design large glass panes in glasshouses, like the Crystal Palace (figure 4) from Joseph Paxton in 1851. It was built in a few months (Schittich, C., et al. 2017). Paxton used 84000 m^2 of glass (O'Regan, C. 2015). In 1900 Lubbers developed a mechanical process to combine drawing and blowing. It was now possible to make 12 metres of length and diameters of 800 mm. In 1919 the Bicheroux process was invented, a casting, polishing and rolling method. Glass panes of 3 by 6 metres were possible to produce with this method (Schittich, C., et al. 2017).

In the 20th century several drawn methods were invented to make flat sheets (by Belgian Fourcault and the American Colburn Processes). From the furnace, molten glass was drawn in a thin stream, flattened and cooled. The cooling process was done by pulling it between rollers. It was possible to make panes of 1.9 metres. In this century, float glass processes were invented by Pilkington. Furthermore, they experimented in the 20th century with ways to make the glass safer (O'Regan, C. 2015). In chapter 2.1.2. - 2.1.5. more information about glass types and surface treatments is given.

So, the material glass exists for a long time, as well as some manufacturing processes to create the different objects of glass, like: cast, drawn, blown, crown, cylinder (or broad), rolled, and float. Due to these technologies over time, the use of glass changed as well. From small round shaped glass panes, to cut rectangular panes to machine-made glass panes. In de Industrial Revolution, new building materials were discovered as wrought-iron and cast-iron. With this new material, new building methods were made possible. Solid stone walls were replaced by slender skeleton structures with columns and beams. Bigger rooms and larger openings were possible, and so larger glass panes were placed in building envelopes to create lighter. Later on, glass flat panels were used in skyscrapers. Then curtain walls were used in office buildings and high-rises. In the 1926 Le Corbusier wrote five points to create new architecture, with free plans and free façades with long horizontal windows. Besides, long glass panes, walls of glass bricks were used as well (Schittich, C., et al. 2017).

Nowadays glass is also used as a structural building material. Trough experiments and temporary buildings, the use of glass as a load-bearing material was and is still being investigated. The first experiments were with glass balustrades. After that, glass roofs, staircases and floors were designed and engineered. The next phase is the use of primary

load-bearing elements, like walls, fins, mullions, beams, and columns (Schittich, C., et al. 2017). Terminal 6 at JFK airport was one of the first buildings with the use glass mullions, which was built in 1970 (The Architect's Newspaper. 2010). The glass column is still in development, but in 1994 the first free-standing type of load-bearing glass column was built in St.-Germain-en-Laye in France. Thus, even today, the use of glass is still in development. In figure 5, an overview is given from the use of glass in buildings (Schittich, C., et al. 2017).

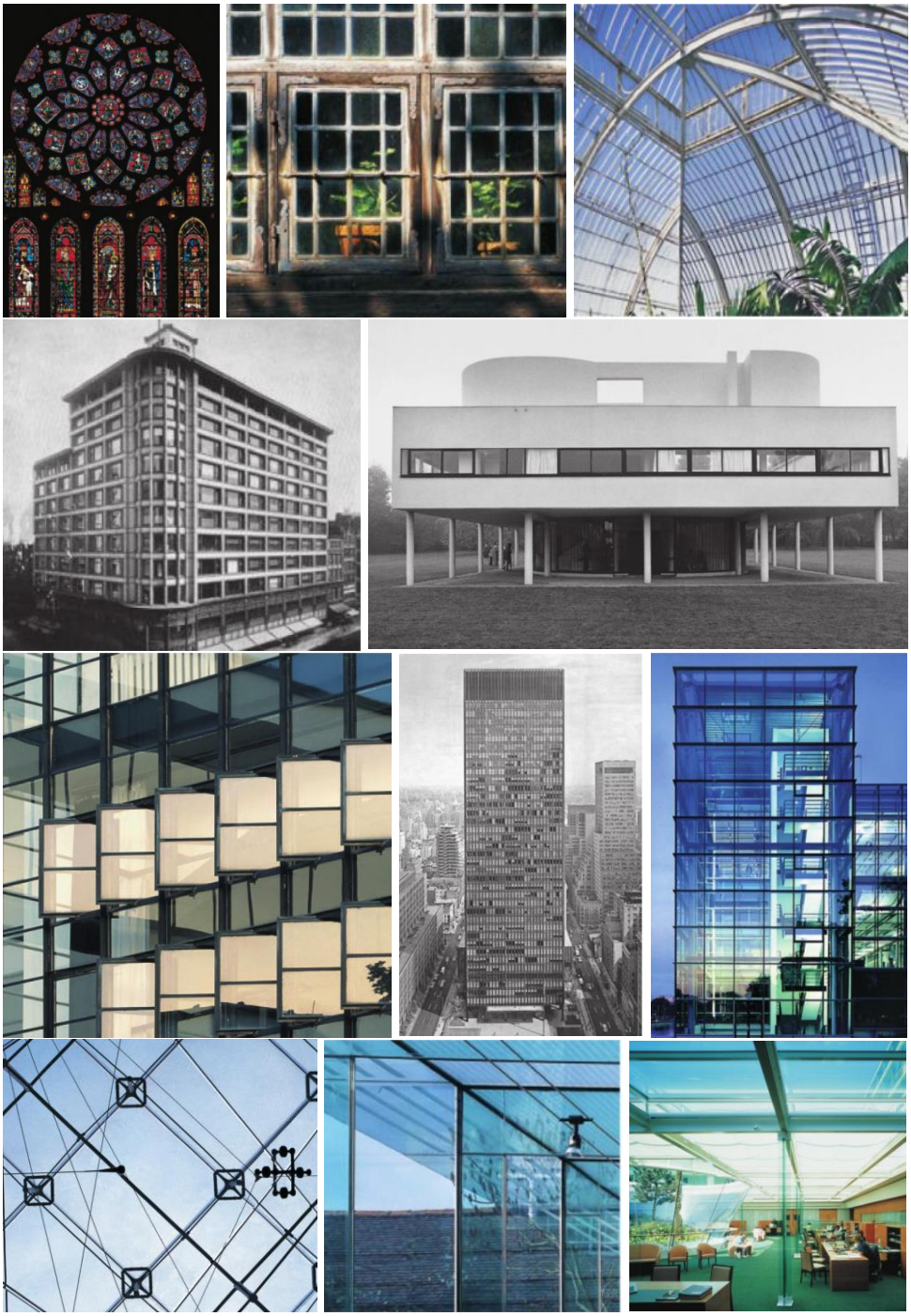

Figure 5 Development of the use of glass in buildings (Schittich, C., et al. 2017).

A.2.2. Manufacturing methods

In this chapter, different manufacturing methods are given. In appendix A.2.1. the history of most methods is mentioned. In this chapter, the descriptions of the processes are explained and common applications are given. There are two production processes: primarily and secondary. The primarily processing of glass are given in this chapter. In chapter 2.1.5. examples for secondary processing are given.

A.2.2.1. Casting

To create 3-dimensional products, the casting method can be used. Molten glass is poured into a mould and almost every shape can be created. The thicker the element, the more cooling time is needed. Solid and decorative items can be made, like glass bricks and sculptures. The cooling process takes often more time, but this is depending on the desired shape. There are two methods which can be used for casting of glass: hot pour (figure 19) and kiln casting (figure 20). In the Crystal Houses in Amsterdam (figure 21), the façade is made out of glass bricks (Oikonomopoulou, F. 2019). In the faculty of Architecture and the Built Environment from the TU in Delft, some cast glass elements are presented (figure 22).

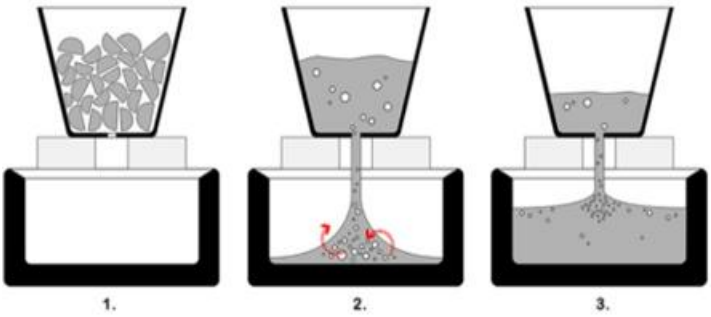

Figure 6 Hot pour (Oikonomopoulou, F. 2019). *Figure 7 Kiln-casting (Bristogianni, T., et al. 2017).*

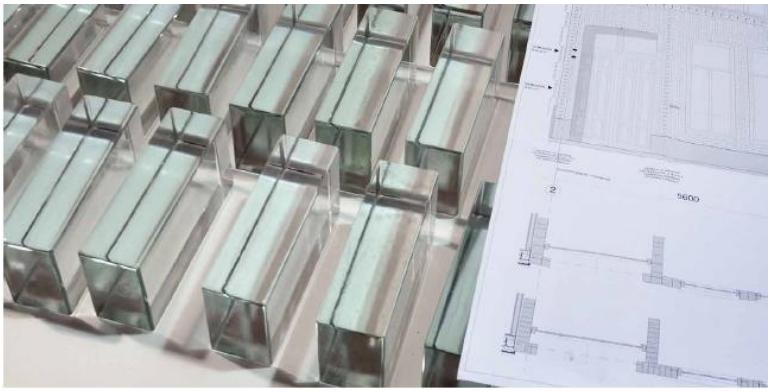

Figure 8 Glass bricks for the façade of Crystal Houses (Oikonomopoulou, F. 2019).

Figure 9 Cast glass elements.

A.2.2.2. Blowing

As mentioned in chapter 2.1.1. this method is old and invented BC. Nowadays this method is not used for building elements anymore. More common products are bowls and bottles. Firstly, glass will be molten in a furnace. Then the molten glass will be attached in the shape of a bulb to a hollow pipe. By rolling the pipe and by blowing the glass will be shaped (figure 23). Nowadays also automatic blowing production is possible. There are two methods: blow-blow and press-blow. With the blow-blow method, the molten glass is put into a mould and blown into a general shape. Then it is transferred into a second mould where it is further blown. The press-blow method is almost the same process as the blow-blow method, but

than it is first pressed into a shape in the mould, before blowing it further in its shape (Haldimann, M., et al. 2008).

Figure 10 Glass blow factory in Biot in France.

A.2.2.3. Pressing

Molten glass is put in a mould and is pressed by a plunger. With this method, decorative items are made, like bowels, or bottles (Haldimann, M., et al. 2008).

A.2.2.4. Floating

Floating glass is the most used method to produce flat glass. Windows, fins and other objects are created with this method. Due to the large availability, the costs are relatively low. Furthermore, it is possible to make large sizes. In figure 24, the process is shown. Firstly, the raw materials are molten. Then the molten glass is pushed onto a thin bath. Due to the floating, the glass will form in a continuous plate with a certain thickness. It has smooth surfaces. After that the glass will be cooled in the annealing lehr. After the visual inspection, it is cut to the right size. The thickness can vary from 2 to 25 mm. Profiled glass can be made by rolling too (Weller, B., et al. 2009). With this method the most common sheet dimensions are Jumbo plates of 3 by 6 metres (O'Regan, C. 2015).

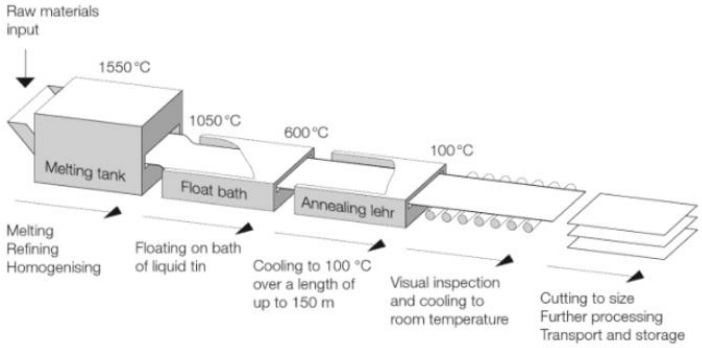

Figure 11 Float glass process (Weller, B., et al. 2009).

A.2.2.5. Drawing

Flat sheets are made with this method. The productivity is less than using the floating method. Some distortions like waves are visible on the surface. Therefore, it is not often used in the building industry. In old buildings, the method was used to make window panes. Furthermore, this method is used to restore buildings. The thickness varies from 2 till 12 mm (Weller, B., et al. 2009). In the production, molten glass rolls out of the melting tank through rollers. The rollers give the glass the patterns. The glass can be down-drawn or up-drawn (figures 25 and 26).

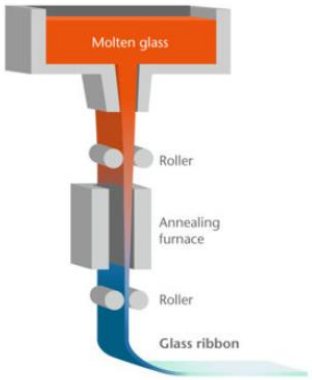

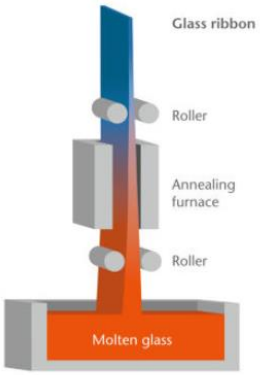

Figure 12 Down-drawn glass (SCHOTT. 2020). *Figure 13 Up-drawn glass (SCHOTT. 2020).*

A.2.2.6. Rolling

Common applications of rolled glass are window panes. After the raw materials are molten, it will be rolled through two contra-rotation rollers, which are cooled by water. The thickness can be determined by the distance between the rollers. After rolling, the glass is cooled in the annealing lehr (figure 27). The rollers can be put closer together if a thinner size is required. The surface is less transparent than with the floating glass method. By rolling also a texture can be given to the glass to create patterned or wired glass. The thickness varies between 3 and 15 mm (Weller, B., et al. 2009).

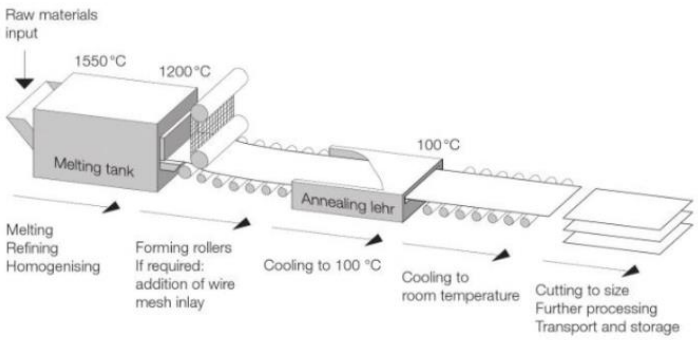

Figure 14 Rolling process (Weller, B., et al. 2009).

A.2.2.7. Extruding

There are two ways to extrude glass: direct and inverted extrusion (figure 28). In direct/ forward extrusion, the shape of the profile is created by the geometry of the die opening of the container (figure 29). The punch and the extruded profile are moving in the same direction. In the container, the billet is compressed, and the punch is giving direction to the extrusion die. The force increases when the billet is set up to fill the container and even more when the billet needs to break through the opening at the die. When the billet has broken through to being extruded, the force decreases for a while. The length of extrusion is now

increasing. When the minimum force is reached, and the billet thins out, the force increases again to the die opening. In inverted extrusion, the punch is hollow, and is giving support to the die, who is being pushed against the billet. The extrusion profile in the punch, moves in opposite to this movement. For the invented method, the pressure needed, can be lower than with the direct method, but the method it is more difficult to do, and more impurities at the surface of the profile. To increase the plasticity, the billet is heated before the extrusion starts (Roeder, E. 1971).

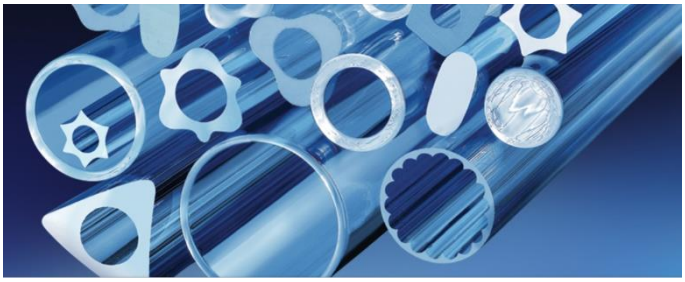

Figure 15 Extruded glass profiles (F&D Glass. 2014).

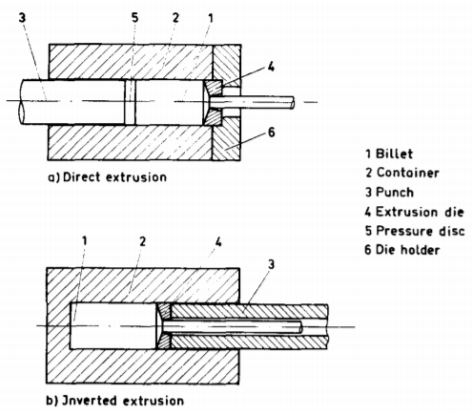

Figure 16 Extrusion methods (Roeder, E. 1971).

If the glass begins to crystalize, extrusion is not possible anymore. The crystallization of glass gives the maximum of the extrusion temperature. If the temperature is too low, glass is too viscous to extrude. If the temperature of the extrusion is above the softening point (viscosity) of the glass, grains are fusing. Air bubbles can be seen in the glass, due to evaporation during heating. If the extrusion temperature is lower, the glass pieces do not entirely fuse, and crystallization is occurring at the grain boundaries (Roeder, E. 1971).

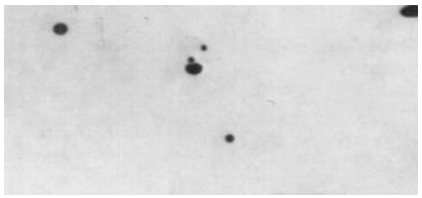

Figure 18 Air bubbles when the temperature is too high (Roeder, E. 1971).

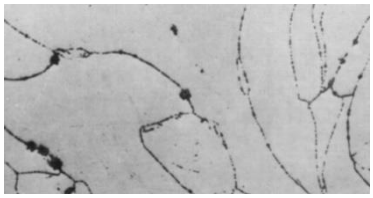

Figure 17 Crystallization when the temperature is too low (Roeder, E. 1971).

A.2.3. Increasing strength

The increasing methods which are not be used in this project, are descripted in this chapter.

A.2.3.1. Curving of glass

By curving the glass, the stiffness can be increased. This is because the moment of inertia can be increased. Curved glass is less flexible and so less able to deform under loading (Schittich, C., et al. 2017). Curving can be done by hot, cold, or warm bending. With cold bending, the glass will be curved by room temperature in a mould. The glass will be forced into a shape. The glass is permanently deformed due to bending stresses. Radius is limited by cold bending, and this method is inducing stresses in the glass. However, glass can be bend in the x-direction and/or the y-direction, and it is cheaper than hot or warm bending (Datsiou, K. 2017).

With hot bending, every shape can be created, and no internal stresses are occurring, which makes it stronger. Firstly, the mould will be preheated. After that, the flat glass will be placed

on the mould. Then the temperature rises up to 600°C in the oven, and the glass will meld into the mould with the required shape due to the gravity. If the glass is cooled, it can be taken from the mould. The stiffness of the glass will be determined by the radius of the shape. A disadvantage is that glass might not have the same thickness everywhere (Datsiou, K. 2017).

If the hot bending takes place in the autoclave, the glass plate will be heated and forced into a curve. During curving, it will be cooled again. Due to this process, the glass keeps the curved shape. With this method, only cylindrical shapes are possible. Due to the tempering, the strength is increased. Lamination is possible afterwards (Datsiou, K. 2017).

With warm bending (or cold lamination bending) glass panes and interlayers are piled up on a mould. Then the glass is forced into the shape of the mould and will keep its shape. After that, it will be put into the autoclave, which will heat the glass. The glass panes and the interlayers will join. After cooling the glass, it will curve back into a less curved shape, but it is still curved. It creates a good coherent behaviour between the glass and the interlayers. As well as cold bending, this method induces stresses in the glass (Datsiou, K. 2017).

A.2.3.2. Reinforcement

As said before, glass has a high compressive strength and can take less tension. By reinforced concrete, the steel is working together with the concrete. This creates a hybrid structural element. The steel is attached to the concrete. For glass elements, steel can only work as a back-up structure. Direct contact of steel with glass, can result in failure of the glass. So, if the glass breaks, the steel can take over as a second load path. A disadvantage is that the steel is decreasing the transparency of the element (Louter, P.C. 2011).

A.2.4. Sustainability

Sustainability is to divide into two aspects: environmental impact and durability. Nowadays with the worldwide increase of CO_2 emissions, more buildings need to be energy-efficient. In order to protect the environment, more careful use of natural products should be taken into account. A reduction of carbon emission is needed, and the building industry contributes to a large amount of the total carbon emission. Designing an energy-efficient and low carbon building is different from the 20th century. Embodied carbon encounters a few aspects: the carbon of the materials, from the construction process, and operational carbon from operation and maintenance. Reduction in embodied carbon can be obtained by: reducing the number of materials, minimise of waste, reducing the use of energy-intensive manufacturing methods, less transport of materials, reuse and recycling of materials. Most of the buildings built in the 20th century are based on fossil fuel energy. So can glass be used in solar energy technologies in solar thermal collectors. In this way, daylight and solar can be gained, while energy can be conserved (Achintha, M. 2016).

In table 4, the embodied energy and carbon values of glass are compared with other materials. As can be seen, float glass has a lower embodied energy/carbon value than steel, but a higher value than concrete. The largest proportion of the glass embodied energy/ carbon value is due to the high temperature during the production process. So, concrete has a lower value per unit mass than glass, but concrete has a bigger share on the global impact, due to the fact that concrete is used a lot in the building industry. However, the mass of glass needed for building elements is less than for concrete. Furthermore, glass is more durable than steel and concrete (Achintha, M. 2016). Glass that is made BC is still intact. Glass has a great resistance against: non-oxidant and oxidant acids, salt, water, aliphatic, aromatic and chlorinated hydrocarbons, alcohol, ester, oil, fat, UV radiation (sunlight) and it is non-flammable (Haldimann, M., et al 2008).

Material	Embodied energy [MJ/kg]	Embodied carbon [MJ/kg]
Float glass	15	0.232
Toughened glass	23.5	0.346
Reinforced concrete	1.39	0.057
Steel (bars or rods)	24.6	0,466

Table 1 Embodied energy and carbon of glass, concrete and steel (Achintha, M. 2016).

It is possible to recycle glass, like glass bottles. However, it is not (yet) common to recycle glass sheets. It is difficult to separate coatings and interlayers from the glass panes. Furthermore, only a low energy (5%) can be saved from the recycling of glass. Glass will be crushed into small pieces, then it will be mixed with the original raw materials. After that, it will be heated and annealed in the same way that new glass will be produced with pure raw materials (Achintha, M. 2016). In 2020 there were some new developments on the recycling of glass. The glass type, like bottles, has reached a considerable recycling rate, but other applications on glass are wastes or downgraded for the use as aggregate or fillers in concrete. Cast glass bricks has lower restrictions than other structural elements due to its monolithic shape. At a research at the TU Delft, different recycling mixtures have been casted to study possible combinations of glass types (Anagni, G.A., et al. 2020).

SCHOTT is a glass manufacturer. High temperatures are needed for the production of glass, fossil fuels are used for heating, and a lot of energy is required. By 2021, SCHOTT wants to have 100% of its electricity from renewable energy sources (SCHOTT. 2020).

''We want to become a climate-neutral company by 2030 and thus make an active contribution to climate protection.'' (Dr. Heinricht, F. SCHOTT. 2020)

The plan to become more sustainable has four levels (SCHOTT. 2020):

- Continuous improvement of energy efficiency
- Switch to 100% green electricity
- Technology change
- Compensation of technology unavoidable emissions

A.2.5. History columns

The first column was only supporting the roof from small buildings. From 3000-1000 BC more advanced columns were used in Egypt, the Assyrian Empire and in the Minoan civilization. Columns were made of stone and wood. Later on, the Mycenaeans were using columns as well. In Archaic Greece, columns made from wood were replaced. First columns were made out of one piece, but the buildings become bigger. So, columns were made from more pieces and were connected via wooden dowels or metal pegs. These pieces were called drums (see figure 6). Columns made of more drums had a better resistance against earthquakes, but had less resistance against wind forces. In the 1st century BC. Romans were able to standardise columns as well. As can be seen at figure 7, the first column design was marked as the Egyptian column. After the Egyptian column, three principal column designs were designed in the Greek world: Doric, Ionic, and Corinthian. The Doric columns were the first ones used. These columns are wider at the bottom and had a simple design. The Ionic column stands on a base. The capital is in the form of a double scroll. The Corinthian columns are slimmer and were more decorated. In the Roman Empire, there were also three principal columns designs: Tuscan, Doric and Composite. The Tuscan column is simple and without flutes. The difference with Tuscan and Doric columns, are the flutes on the shaft. The Composite column is a mix of different styles. Later on, the Solomonic column was designed. This column has a twist shaft (Cartwright, M. 2012).

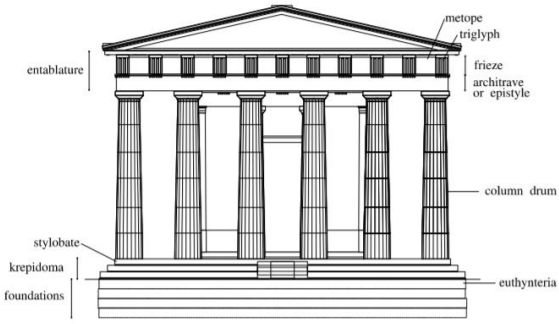

Figure 19 Terms for an old building façade (Pakkanen, J. 1998).

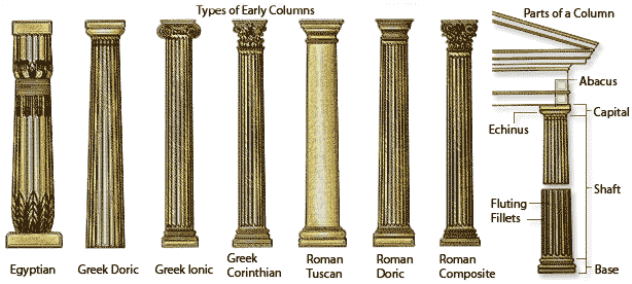

Figure 20 Order of columns (Cartwright, M. 2012).

A.2.6. Fire regulations and tests

When testing elements on its resistance for fire, the standard temperature in fire chamber increases according to a temperature-time curve. In table 5, the values are given (O'Regan, C. 2015).

Temperature [°C]	Time [min]
700	15
825	30
900	45
920	60
>1000	90

Table 2 Temperature versus time in a fire chamber (O'Regan, C. 2015).

There are NEN-norms according to materials as steel and concrete, but nowadays there are no specific regulations for fire on glass yet. Some general NEN-norms about fire and test set-ups are:

- NEN-EN 1991-1-2 Actions on structures – Part 1-2: General actions – Actions on structures exposed to fire
- NEN-EN 13501-1 Fire classification of construction products and building elements - Part 1: Classification using data from reaction to fire tests
- NEN-EN 13501-2 Fire classification of construction products and building elements - Part 2: Classification using data from fire resistance tests, excluding ventilation services
- NEN-EN 1363-1 Fire resistance tests - Part 1: General requirements
- NEN-EN 1365-4 Fire resistance tests for loadbearing elements - Part 4: Columns

In the NEN-norm 1991-1-2, there is made a difference between thermal load and mechanical loads. A nominal temperature-time curve is the thermal calculation from structural elements for a prescribed time. A fire model is the thermal calculation of structural elements due to a complete fire with the cooling time included. For the mechanical calculation the same time needs to be taken as for the thermal calculation. Fire-resistance needs to satisfy the following formulas. Equation A.2.1 is a check for time, equation A.2.2 is a check for strength, and equation A.2.3 for temperature (NEN-EN 1991-1-2. 2019).

$$t_{fi,d} \geq t_{fi,requ} \qquad \text{(A.2.1)}$$

$$R_{fi,d,t} \geq E_{fi,d,t} \qquad \text{(A.2.2)}$$

$$\Theta_d \leq \Theta_{cr,d} \qquad \text{(A.2.3)}$$

With:

- $t_{fi,d}$: design value for fire-resistance
- $t_{fi,requ}$: required time for fire-resistance
- $R_{fi,d,t}$: design value for the resistance of the element exposed to fire at time (t)
- $E_{fi,d,t}$: design value for the load effect applied in the fire situation on time (t)
- Θ_d : design value for the temperature of the material
- $\Theta_{cr,d}$: design value for the critical temperature of the material

The thermal load is expressed in net heat flux density ($\dot{h}_{net}$ in W/m^2) on the surface that is exposed to fire as a function of the heat transfer due to convection and radiation. Next to thermal loads, mechanical loads due to fire can be determined. The expansions and deformations due to temperature changes when exposed to fire leads to load effects as forces and bending moments (NEN-EN 1991-1-2. 2019).

The design value for a fire load is (NEN-EN 1991-1-2. 2019):

$$q_{f,d} = q_{f,k} * m * \delta_{q1} * \delta_{q2} * \delta_n \qquad \text{(A.2.4)}$$

$$\delta_n = \prod_{i=1}^{10} \delta_{ni} \qquad \text{(A.2.5)}$$

With:

- $q_{f,d}$: design value for the fire load [MJ/m^2]
- $q_{f,k}$: characteristic value for the fire load [MJ/m^2]
- m : combustion factor
- δ_{q1} : the risk factor for the occurrence of a fire due to the size of the fire
- compartment
- δ_{q2} : the risk factor for the occurrence of a fire due to the use
- δ_n : the factor which takes different active fire security systems (i) into account

In appendix E in NEN-EN 1991-1-2 can be used to determine the abovementioned parameters (NEN-EN 1991-1-2. 2019).

In NEN-EN 13501-2 a general fire classification of building materials is given. When new building materials are used, manufactures needs to prove the fire-resistance of the loadbearing elements by experimental testing. Next to the spread of fire and smoke, the loadbearing capacity of the structural element/ structure needs to be addressed. The fire-resistance of load-bearing shall be addressed using five levels of thermal attack (NEN-EN 13501-2. 2016). These are nominal fires (NEN-EN 1991-1-2. 2019):

- the standard temperature-time curve (post flash-over fire)
- the slow heating curve (smouldering fire)
- the semi-natural fire
- the external fire exposure curve
- the constant temperature attacks

The standard temperature-time curve relationship is applied for a full duration of the test (figure 21). This curve can be determined via the following formula (NEN-EN 13501-2. 2016):

$$T = 20 + 345 * log_{10} * (8 * t + 1) \qquad \text{(A.2.6)}$$

With:

- T : the mean furnace temperature [°C]
- t : time (from the start of the test) [min]

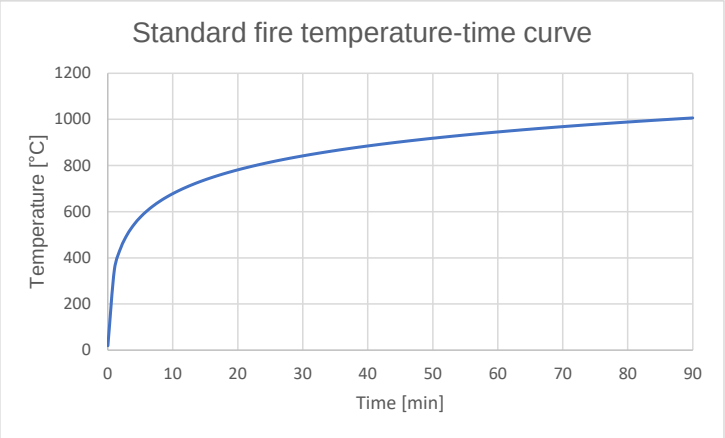

Figure 21 Standard temperature-time curve.

A smouldering fire test only needs to be done when it is expected that the fire-resistance of an element will be affected by the temperatures in the growth stage of fire. Especially when the element is affected by temperatures which are lower than 500 °C.

In a semi-natural fire, the temperature of gases in the test will rise to 1000 °C within 10 to 20 minutes. This test can be performed because of the difficulties in achieving the thermal attack in conventional furnace. The attack is provided by fire from wooden cribs from softwood.

The external fire exposure curve is representing an external face of a wall which is exposed to an external fire or fire that emerge through windows.

With a constant temperature attack, the elements are loaded by a constant temperature. Depending on the application, the values are 20, 200, 500, or 1000 °C (NEN-EN 13501-2. 2016).

In NEN-EN 1363-1, the performance criteria for failure of the element which is exposed to fire is given. The required time in minutes needs to be lower than the time which the test specimen continues to be able to carry the loads. For loadbearing vertical elements, failure is occurred when one of the following equations have been exceed. In equation A.2.7, the limiting vertical contraction (C_{limit}) is given in mm and in equation A.2.8, the limiting rate of vertical contraction is given ($(dC/dt)_{limit}$) in mm/min (NEN-EN 1363-1. 2020).

$$C_{limit} = \frac{h}{100} \quad \text{(A.2.7)}$$

$$\left(\frac{dC}{dt}\right)_{limit} = \frac{3*h}{1000} \quad \text{(A.2.8)}$$

With:

- h : the initial height of the test specimen once the load has been applied [mm]

For load-bearing elements exposed to fire, NEN-EN 1365 is applicable. For column design the required NEN-norm is NEN-EN 1365-4. Fire tests for load-bearing structural columns needs to be performed according to NEN-EN 1363-1 and NEN-EN 1365-4. In this case the column is fully exposed to fire on all sides. In these norms the following aspects are

described: the test equipment, test conditions, test specimen (size, number, design, construction, verification), installation of test specimen (supporting constructions, end conditions), application of instrumentation (furnace thermocouples, pressure, axial deformation), test procedure, and performance criteria (NEN-EN 1365-4. 1999).

A.2.7 Connections

Continuous linear supports are the most used methods. This support is mostly used for cladding systems, where the glass edges are supported by frames. The frame is mostly made from steel, timber, plastic or aluminium. The out-plane loading (lateral forces) is transmitted via structural sealants to transport the lateral loads from the glass pane to the frame. The in-plane loading is transmitted via setting blocks. For the sealings, ethylene propylene diene monomer (M-class) (EPDM) rubber, silicon, or gaskets are used. Furthermore, loads from diaphragm action can be transmitted via continuous linear supports. The corners of the glass panel need to be isolated from the in-plane loading (vertical loads) and from the effects due to thermal movement of the supporting frame. Besides this, the stress distribution is not constant along the line support. These aspects need to be taken into consideration (O'Regan, C. 2015).

To create cladding systems where the glass surface is more visible, isolated clamps can be created. In this situation, frames are placed behind the glass panes. The clamps can carry out-of-plane loads or both in-plane and out-plane loads. A metal clamp is used with a layer of neoprene, EPDM rubber or another soft material that needs to distribute the loads uniformly. The fixing system needs to be able to carry friction to transfer in-plane loading from the pane to the clamp. To create a friction connection, steel plates are clamped together with a bolt. The holes of the bolt are oversized to avoid contact between the bolt and the glass (O'Regan, C. 2015).

With bolt connection for glass elements, the bolts have contact with the glass surface. This can result in high local stresses. So, for these type of connections, only tempered glass is used. The stresses around the bolt are never uniform. To avoid these varying local stresses a reliance is placed on the bolt which can yield locally, or by articulating the connections. The material between the bolt and the glass surface has a lower modulus of elasticity than glass. Normally soft aluminium, plastics or resins can be used. A risk of bolt fixings is the connection can be loosed due to vibrations. For this aspect, spring washers and lock-nuts can be used that are resistant to vibration effects. Furthermore, edge distances, the thickness of the glass pane, and the isolating material between the bolt and the glass needs to be taken into account. Bolt fixings resist in-plane loading or are capable to take in-plane movement. Expanding of the plane, due to temperature differences, needs to be taken into consideration (O'Regan, C. 2015).

There are two types of adhesives for glass structures available: soft elastic materials and stiff materials. Soft materials are materials as structural silicones, and stiff materials are made of epoxy adhesives and polyester resins. Silicones are used to bond glass panes to each other of with other materials as supporting frames. These bonds can distribute the forces uniform over the length. The connection is homogeneous, because there are no holes and notches anymore. In this way the local stresses are reduced. Silicone-based adhesives are well resisting against tension, but not well against shear loads. When they are exposed to long-term loading, they can break. Still a lot is unknown about stiff adhesives in glass structures. Stiff adhesives can achieve a composite behaviour. Due to the low shear stiffness of soft adhesives, soft adhesives are not able to achieve this composite behaviour. Lucio Blandini's Glass Dome in Stuttgart is an example of a structure made with adhesive connections (table 3). By using stiff connections, the surface area, the temperature needed for the adhesive,

and the time it takes to cure needs to be taken into consideration. Thickness variations in the stiff adhesive can result in stress concentrations. To avoid this, the sharp edges of the glass panes need to be removed first. Voids against the glass in the adhesive needs to be avoid too, since these results in big stresses as well. Stiff adhesive connections can resist thermal movement more than soft adhesives can. A disadvantage of stiff adhesives is that it is difficult to repair or replace. Soft adhesives are viscoelastic materials, which means that creep can occur in the adhesive. Normally soft adhesives only need to be able to carry short-term loading as wind. Stiff adhesives are less affected by creep. Especially with adhesive-based structures, redundancy needs to be taken into account, since a failure of the connection must not result in a collapse of the structure (O'Regan, C. 2015).

Type of connection	Example
Continuous linear support	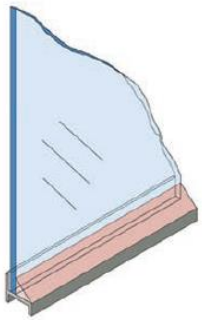
Clamp fixing	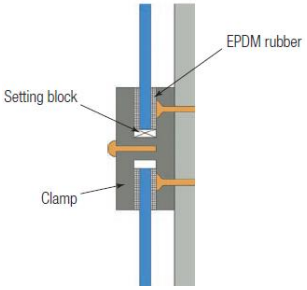
Friction clamp fixing	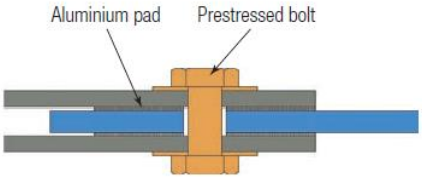
Bolt fixing	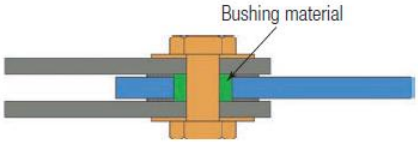
Adhesive connection *(Lucio Blandini's Glass Dome)*	

Table 3 Types of connections with examples (O'Regan, C. 2015).

A.2.8. Types and applications

A.2.8.1. Profiled columns

So far, the only type of free-standing structural glass columns applied in buildings, are the glass profiled columns with cruciform cross-sections. The cruciform columns are used in St-Germain-en-Laye in 1994, and in Danfoss Headquarters (figure 52). The Danfoss columns are 5.5 metres high. They performed 1:1 scale tests to demonstrate that the column could carry much higher compressive loads than required. Even after the column was damaged, it could still carry two times the axial load than the maximum expected load. So, the safety factor for this case is higher than 2. Even though, the roof is designed with extra redundancy to take over the forces if one of the columns would fail. The axial failure load, from tests, was 575 kN. The failure stress was 18.53 MPa (Bagger, A., et al. 2009). The columns in the St-Germain-en-Laye project are 3,3 m high. Compressive loading tests are done to demonstrate that the column could withstand six times the required load. The failure load was 430 kN and the failure stress was 16.06 MPa (Schittich, C., et al. 2017).

Overend, M. also did research into X-columns in 2005 (Oikonomopoulou, F., et al. 2017). Alternative cross-sections for profiled columns are H, T and squared profiles. Earlier research about these profiled columns is done by E. Ouwerkerk in 2011 at the TU in Delft. The length of the tested columns was one metre. Compression tests have been performed, and the founded failure load was around 215 till 255 kN. The failure stresses were approximately 88.4 till 106.6 MPa (Ouwerkerk, E. 2011). Furthermore, research is done by Campione and Rondello in 2014. They analysed the effects and the load carrying capacity of transverse cross-section shape columns and glued connections between single laminated multi-layered glass columns. They concluded that the glued connections were the weakest parts of the columns, and that the buckling strength of laminated multi-layered glass columns could be predicted accurately with analytical models (Campione, G., et al. 2014):

Furthermore, research has been done about the compression behaviour of laminated structural glass members by Aiello, S., et al in 2011. They performed compression strength tests on cruciform and T profiled columns. The length of the column prototypes was around 400 till 600 mm. The failure loads were around 116 till 135 kN (Aiello, S., et al. 2011). In 2017, Kalamar, R., et al did research into squared profiled glass columns with a length of 3 m. They performed impact tests. The failure load was between 630-780 kN and the failure stress was 54.2 till 65 MPa (Kalamar, R., et al. 2017).

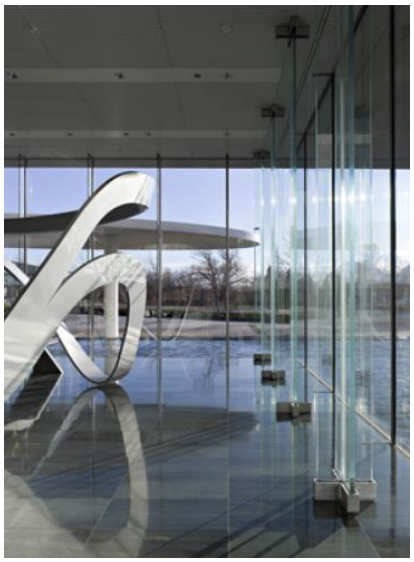

Figure 22 Profiled column Danfoss Denmark (Schmidt Hammer Lassen Architects. n.d.).

A.2.8.2. Stacked columns

As well as for the tubular columns, the stacked columns are also not used as structural columns in buildings. Stacking of glass is used for other structural elements, like the walls in the Laminata house in the Netherlands, built in 2001 (figure 60). Stacking of glass can be done vertically and horizontally. Furthermore, this principle of stacking glass is used to create pieces of art. In Zwolle the 'Glazen Engel Michaël' is made of stacked glass (figure 59). It is a statue, named 'The glass angel Michaël'. Two other projects, were stacked glass is used, is The Pompano Park water feature (realized in 2006), and The Glass Sphinx (created in 2013) (Van Heughten, R.; 2013).

Furthermore, some research is done about stacked columns by Felekou, E. in 2016. Felekou, E. did compression tests on elements of 615 mm long. The column existed out of 50 horizontally stacked elements. The compression failure load was around 525 kN and the failure stress 52.5 MPa (Felekou, E. 2016).

Figure 23 Glazen Engel (Glazen Engel Michaël, beschermheilige van Zwolle (HDR). n.d.).

Figure 24 Laminata house (Pinterest. n.d.).

A.2.8.3. Bundled columns

Bundled columns, are more used as pieces in trusses than as columns. These types of columns are more translucent than transparent. Glass rods are used as truss elements in Zwitserleven office in Amstelveen in the Netherlands in 1996, designed by ABT, Nijsse, R. (Van Heughten, R. 2013).

The concept of bundled columns was first designed by ABT in Arnhem, with approval of Nijsse, R. (Nijsse, R. 2003). This prototype was not realized due to difficulties with the bonding method. The research continued for this concept by Oikonomopoulou, F., et al. in 2017. The prototypes they tested were made of 6 rods of DURAX® glass, and in the middle a hollow star-shaped CONTURAX® glass profile, which were bonded all together by a clear UV-curing adhesive Delo Photobond 4468. Different lengths were tested on compression strength. With a length of 1500 mm, and a clamped connection, the failure load was 331 till 508.8 kN, and the failure stress was 129.7 till 199.36 MPa. The slenderness ratio of this column was 47. The first crack was observed at 260 and 120 kN. Then a few pinned connected columns, with a length of 2400 mm and a slenderness ratio of 151, were tested. The failure load was between 62.7 and 90 kN and the failure stress was between 24.6 and 35.3 MPa. It is possible to have a steel rod in the middle of this column, to create a secondary failure mechanism. If the glass breaks, the steel rod can take over the loads. This steel rod is almost not visible in the column (Oikonomopoulou, F., et al. in 2017). A disadvantage is that the steel cannot collaborate with the glass rods. As mentioned earlier, there needs to be a soft material in between.

Kamarudin, M.K., et al did also research about the buckling performance of tubular glass columns under compression. According to his research, glass columns with a slenderness ratio below 40, can be classified as slender and are expected to fail due to buckling. The prototypes were made of three hollow glass tubes, with an outer diameter of 24 mm, bonded together by a structural silicone. The wall thickness of the tubes was 2.5 mm. The column had a length of 1,5 m. The failure load was 13.37 kN and the failure stress was 26.4 MPa (Kamarudin, M.K., et al. 2016).

On the Green Village (figure 25) in Delft a truss is made for a bridge with bundled columns. Next the bridge, there was a bench where a bundled column was used as support. A visible disadvantage was that the glue become dirty and coloured green over time.

Figure 25 The bridge with bundled glass and a bundled glass column (which became dirty) in Green village in Delft.

A.2.8.4. Cast columns

Casting of glass is similar to the stacking system. In 2016, Felekou, E. did also tests on cast/stacked columns with a length of 650 mm existed out of 10 elements. The thickness per element was 65 mm. The elements were stacked and were bonded together with Delo Photobond 4468. The failure load was 1412 kN and the failure stress was 128 MPa (Felekou, E. 2016).

Furthermore, some research has been done by Akerboom, R. in 2016. With these thesis projects, the cast elements were stacked due to an interlocking system. Akerboom, A. performed compression tests (figure 62). The stacked hollow elements are curved (interlocking shape), with an VIVAK interlayer in between. At the connection steel shoes are used. For the test 54 bricks were stacked, this was in total 6 metres high. The expectation was that the prototype would fail at 10 tons of load. Nevertheless, at 1.65 tons, the first crack was introduced in the prototype. After that they stopped testing. The early failure probably occurred because the layer in between the steel connection and the glass was not thick enough. No cracks occurred from the VIVAK interlayer connection with the glass (Akerboom, A. 2016).

In 2018, De Vries, E. did also research in the compression strength of cast columns. In figure 63, elements of the column are shown. She used the interlocking system too, with VIVAK interlayers. From DIANA FEM models the failure load was 78 kN and the failure stress was 28 MPa. In the experiment analysis, 8 sugar glass components were tested in shear forces. A failure load of 1136 till 3369 kN. The deflection at the failure load was between 6.96 and 11.16 mm (De Vries, E. 2018).

Cast glass is not used as columns in buildings, but cast elements are used for other structural elements as walls. In figure 64, cast glass bricks are shown. These were used for the façade of the Chanel store building in Amsterdam (Oikonomopoulou, F. 2019).

Figure 26 Compression test set up (Akerboom, R. 2016).

Figure 27 Cast elements of a column.

Figure 28 Chanel glass house. (Oikonomopoulou, F. 2019).

References

Achintha, M. (2016). Sustainability of Construction Materials (Second Edition): 5 - Sustainability of glass in construction. Woodhead Publishing Series in Civil and Structural Engineering, pp. 79-104. University of Southampton, Southampton, United Kingdom. DOI: 10.1016/B978-0-08-100370-1.00005-6.

Akerboom, R. (2016). Glass columns: exploring the potential of free-standing glass columns assembled from stacked cast elements. MSc, Technical University of Delft.

Anagni, G.A., Bristogianni, T., Oikonomopoulou, F., Rigone, P., Mazzucchelli, E.S. (2020). Vol.7. Challenging Glass 7: Conference on Architectural and Structural Applications of Glass. Ghent University: Recycled Glass Mixtures as Cast Glass Components for Structural Applications, Towards Sustainability. DOI: 10.7480/cgc.7.4482

Campione, G., Rondello, V. (2014). Effects of shape of transverse cross-section on the load carrying capacity of laminated glass columns. Construction and Building Master 61, pp. 349-359.

Cartwright. M. (2012). Ancient History Encyclopedia: Column. From: https://www.ancient.eu/column/

Corning Museum of Glass. (2002). TIMELINE OF GLASS HISTORY. From: https://www.cmog.org/visit/schools-groups-and-scouts/school-tours/resources/timeline-glass-history

Datsiou, K. (2017). DESIGN AND PERFORMANCE OF COLD BENT GLASS. (Doctor). Department of Engineering: Lucy Cavendish College, University of Cambridge.

De Vries, E. (2018). The stackable glass column. MSc, Technical University of Delft.

Diehn, D. A. (1941). History of Glass (no. 4, vol. 24). Ohio State, United States: Ohio State University, College of Engineering.

Felekou, E. (2016). Glass Tower in high-rise buildings. MSc, Technical University of Delft.

Haldimann, M., Luible, A., Overend, M. (2008). Structural Engineering Document 10: Structural Use of Glass. Zürich, Switzerland: International Association for Bridge and Structural Engineering.

Kalamar, R., Bedon, C., Eliášová, M. (2017). Assessing the structural behaviour of square hollow glass columns subjected to combined compressive and impact loads via full-scale experiments. Engineering Structures 143, pp. 127-140.

Kamarudin, M.K., Disney, P., Parke, G.A.R. (2016). Structural performance of single and bundled glass columns. ARPN J. Eng. Appl. Sci. 11(3), pp. 355–369. In: Oikonomopoulou, F., Van den Broek, E.A.M., Bristogianni, T., Veer, F.A., & Nijsse, R. (2017). Design and experimental testing of the bundled glass column. Glass Structures & Engineering. DOI: 10.1007/s40940-017-0041-x.

Louter, P.C. (2010). Fragile yet Ductile: Structural Aspects of Reinforced Glass Beams. (Doctor). Delft University of Technology, Delft.

NEN-EN 1363-1. (2020). Fire resistance tests - Part 1: General requirements.

NEN-EN 1365-4. (1999). Fire resistance tests for loadbearing elements - Part 4: Columns.

NEN-EN 13501-2. (2016). Fire classification of construction products and building elements - Part 2: Classification using data from fire resistance tests, excluding ventilation services.

NEN-EN 1991-1-2. (2019). Eurocode 1: Actions on structures – Part 1-2: General actions – Actions on structures exposed to fire.

Oikonomopoulou, F. (2019). Unveiling the third dimension of glass: Solid cast glass components and assemblies for structural applications. (Doctor). Delft University of Technology, Delft.

Oikonomopoulou, F., van den Broek, E.A.M., Bristogianni, T., Veer, F.A., & Nijsse, R. (2017). Design and experimental testing of the bundled glass column. Glass Structures & Engineering. DOI: 10.1007/s40940-017-0041-x.

O'Regan, C. (2015). Structural use of glass in buildings (Second edition). The Institution of Structural Engineers.

Ouwerkerk, E. (2011). Glass columns. MSc, Technical University of Delft.

Schittich, C., Staib, G., Balkow, D., Schuler, M., Sobek, W. (2017). Glass Construction Manual 2nd Revised and Expanded Edition Ed. Birkhauser, Basel.

Van Heughten, R. (2013). Load-bearing glass columns: the stacked column. MSc, Technical University of Eindhoven.

Figure list

Figure 1 - Hermens, E. (2017). Looking through art: 16th-century stained glass, crown, cylinder, silver stain and more. Retrieved on December, 9, 2020, from: https://lookingthroughartblog.wordpress.com/2017/10/20/16th-century-stained-glass-crown-cylinder-silver-stain-and-more/

Figure 2 - Glashütte Lamberts. (n.d.). Genuine Rondels. Retrieved on December, 9, 2020, from: http://www.lamberts.de/en/products/genuine-rondels.html

Figure 3 - Schittich, C., Staib, G., Balkow, D., Schuler, M., Sobek, W. (2017). Glass Construction Manual 2nd Revised and Expanded Edition Ed. Birkhauser, Basel, pp. 11. Retrieved on December, 11, 2020.

Figure 4 - Shower Talk. (n.d.). CRYSTAL PALACE. Retrieved on December, 9, 2020, from: https://blog.inoxstyle.com/en/crystal-palace/

Figure 5- Schittich, C., Staib, G., Balkow, D., Schuler, M., Sobek, W. (2017). Glass Construction Manual 2nd Revised and Expanded Edition Ed. Birkhauser, Basel, pp. 13-57. Retrieved on December, 11, 2020.

Figure 6 - Oikonomopoulou, F. (2019). Unveiling the third dimension of glass: solid cast glass components and assemblies for structural applications, pp. 68. Retrieved on December, 16, 2020.

Figure 7 - Bristogianni, T., Oikonomopoulou, F., Veer, F. A., Snijder, A., & Nijsse, R. (2017). Production and Testing of Kiln-cast Glass Components for an Interlocking , Dry-assembled Transparent Bridge. Glass Performance Days 2017 Conference Proceedings, pp. 25–30.

Figure 8 - Oikonomopoulou, F. (2019). Unveiling the third dimension of glass: solid cast glass components and assemblies for structural applications, pp. 122. Retrieved on December, 16, 2020.

Figure 9 - Own picture. Delft. Retrieved on November 13, 2020.

Figure 10 - Own picture. Biot, France. Retrieved on July, 2008.

Figure 11 - Weller, B., Unnewehr, S., Tasche, S., Härth, K. (2009). Glass in Building: Principles Applications Examples. Birkhäuser Edition Detail, pp. 12. Retrieved on December, 16, 2020.

Figure 12 - SCHOTT. (2020). Down-Draw Process. Retrieved on December, 16, 2020, from: https://www.schott.com/advanced_optics/english/capabilities/down-draw-process.html?com-origin=en-GB

Figure 13 - SCHOTT. (2020). Up-Draw Process. Retrieved on December, 16, 2020, from: https://www.schott.com/advanced_optics/english/capabilities/up-draw-process.html?com-origin=en-GB

Figure 14 - Weller, B., Unnewehr, S., Tasche, S., Härth, K. (2009). Glass in Building: Principles Applications Examples. Birkhäuser Edition Detail, pp. 13. Retrieved on December, 16, 2020.

Figure 15 - F&D Glass. (2014). Friedrich & Dimmock, inc. Simax Glass Tube & Rod. Retrieved on November, 23, 2020, from: https://fdglass.com/our-products/simax-glass-tubing-rod/?gclid=Cj0KCQiAhs79BRD0ARIsAC6XpaWukDCbqmKTH6ORshmFwwvbXu_Cl3LTqojFdy_CDXjyt4_FBrRcAuQaAmsiEALw_wcB

Figure 16 - Roeder, E. (1971). EXTRUSION OF GLASS. Journal of Non-Crystalline Solids 5, pp. 378. Retrieved on November, 23, 2020, from: https://www.sciencedirect.com/science/article/pii/0022309371900391

Figure 17 - Roeder, E. (1971). EXTRUSION OF GLASS. Journal of Non-Crystalline Solids 5, pp. 383. Retrieved on November, 23, 2020, from: https://www.sciencedirect.com/science/article/pii/0022309371900391

Figure 18 - Roeder, E. (1971). EXTRUSION OF GLASS. Journal of Non-Crystalline Solids 5, pp. 383. Retrieved on November, 23, 2020, from: https://www.sciencedirect.com/science/article/pii/0022309371900391

Figure 19 - Pakkanen, J. (1998). The Temple of Athena Alea at Tegea A Reconstruction of the Peristyle Column. Department of Art History at the University of Helsinki, no. XVIII in Co-operation with the Finnish Institute at Athens, pp. 82. Retrieved on December, 27, 2020.

Figure 20 - Cartwright, M. (2012). Ancient History Encyclopedia: Column. Retrieved on December, 27, 2020, from: https://www.ancient.eu/column/

Figure 21 - Own graph. Delft. Retrieved on January, 19, 2021.

Figure 22 - Schmidt Hammer Lassen Architects. (n.d.). Architectour.net. Danfoss Domicil Danfoss Head Office. Retrieved on November 13, 2020, from: https://www.architectour.net/opere/opera.php?id_opera=6473&nome_opera=Danfoss%20Domicil&architetto=Schmidt%20Hammer%20Lassen

Figure 23 - Glazen Engel Michaël, beschermheilige van Zwolle (HDR). (n.d.). Retrieved on January 11, 2021, from: https://mapio.net/pic/p-42781314/

Figure 24 - Pinterest. (n.d.) Retrieved on November 13, 2020, from: https://nl.pinterest.com/pin/308496643196576126/

Figure 25 - Own picture. Delft. Retrieved on November, 13, 2020.

Figure 26 - Akerboom, R. (2016). Glass columns: exploring the potential of free standing glass columns assembled from stacked cast elements. MSc, Technical University of Delft, pp. 131. Retrieved on January, 11, 2020.

Figure 27 – Own picture. Delft. Retrieved on November, 13, 2020.

Figure 28 - Oikonomopoulou, F. (2019). Unveiling the third dimension of glass: solid cast glass components and assemblies for structural applications, pp. 121. Retrieved on November 13, 2020

Table list

Table 1 - Achintha, M. (2016). Sustainability of Construction Materials (Second Edition): 5 - Sustainability of glass in construction. Woodhead Publishing Series in Civil and Structural Engineering, pp. 79-104. University of Southampton, Southampton, United Kingdom. DOI: 10.1016/B978-0-08-100370-1.00005-6, pp. Retrieved on December, 23, 2020.

Table 2 - O'Regan, C. (2015). Structural use of glass in buildings (Second edition). The Institution of Structural Engineers, pp. 75. Retrieved on January, 8, 2020.

Table 3 - C). Structural use of glass in buildings (Second edition). The Institution of Structural Engineers, pp. 13-15. Retrieved on January, 9, 2020. AND Building With Glass. (n.d.). Lucio Blandini used adhesives to create a glass dome in Stuttgart, Germany. Retrieved on January, 9, 2020, from: https://www.nytimes.com/slideshow/2009/07/06/science/070709GLASS_index/s/070709GLASS_slide9.html

Appendix 3 – Overview applications

In this table, an overview is given from earlier researches into glass columns.

Project	Year	Type	Design	Safety strategy	Tests	Failure load at axial compression loading*	Average compressive failure stress*	Application
St-Germain-en-Laye France *(Schittich, C., et al. 2017)* *(Oikonomopoulou, F. et al; 2017)*	1994	Profiled column: X	Length: 3300 mm Thickness: 10/15/10 mm Layers: 3 Cross-section: 400x400 mm	One continuous laminated glass panel and one glass panel split in two bonded with clear silicone. The panels are laminated with Poly Vinyl Butyral (PVB) foil.	Comprehensive loading tests to demonstrate that the column could carry the compressive strength. X-shape to overcome buckling. Fire protection not solved. They could withstand 6x the required load.	430 kN	16.06 MPa	Columns
Dansfoss Headquarters Denmark *(Bagger, A., et al. 2009)* *(Oikonomopoulou, F. et al; 2017)*	2009	Profiled column: X	Length: 5500 mm Thickness: 12/12/12 mm Layers: 3 Cross-section: 449x449 mm	One continuous laminated glass panel and one glass panel split in two bonded with clear silicone. The panels are laminated with PVB foil.	Performed tests on 1:1 scale prototypes. They demonstrated that the column could carry much higher compressive loads than required. Even after the column was damaged, it could still carry 2x the axial load than the maximum expected load (safety factor >2). Even though, the roof was designed with extra redundancy to take over if a column would fail.	575 kN (was subjected to a soft and hard body impact test, while loaded at 190 kN)	18.53 MPa	Columns in office building
E. Ouwekerk *(Ouwekerk, E. 2011)*	2011	Profiled column: H (also tested other profiled columns, but H had the best results)	Length: 1000 mm Thickness: 8 mm Layers: 1 Cross-section: 116x100 mm	Single glass panes bonded with Hercuseal polymer sealer 302. The Hercuseal polymer sealer had higher load-bearing capacity than the prototypes with Araldite 2000 Plus 2013.	Compression strength tests.	212-255 kN	88.4 - 106.6 MPa	Research
Aiello, S., et al. *(Aiello, S., et al. 2011)*	2011	Profiled column: X	Length: 400-600 mm Thickness: 4/4 mm Layers: 2 Cross-section: 300x300 mm	Two 4 mm thick float glass layers bonded together with a PVB layer with a thickness of 1 mm. The pieces were glued with structural silicone.	Compression strength tests (and 4 point bending tests) on laminated glass members.	116-135 kN	-	Research
Aiello, S., et al. *(Aiello, S., et al. 2011)*	2011	Profiled column: T	Length: 600 mm Thickness: 4/4 mm Layers: 2 Cross-section: 300x150 mm	Two 4 mm thick float glass layers bonded together with a PVB layer with a thickness of 1 mm. The pieces were glued with structural silicone.	Compressive tests (and 4 point bending tests) on laminated glass members.	132 kN	-	Research
Kalamar, R., et al. *(Kalamar, R., et al. 2017)*	2017	Profiled column: squared	Length: 3000 mm Thickness: 10/10 mm Layers: 2 Cross-section: 150x150 mm	Laminated glass panels of floated glass layers which were adhesively bonded with a PVB foil (t_{int} = 0.76 mm). Two pads composed of Poly-Methyl Methacrylate (PMMA) were made from one piece of material at the base/top restraints.	Performed tests on 1:1 scale prototypes. They performed impact tests. The specimens were subjected to compressive load increase until collapse (200 N/s the loading speed)	630 - 780 kN	54.2 - 65 MPa	Research
Veer, F., et al. *(Veer, F., et al. 1999)*	1999	Layered tubular column	Length: 550 mm Diameter outer: 40 mm Thickness wall: 1.5/1.5 mm Layers: 2	2 borosilicate glass tubes laminated with a UV curing clear resin (low-shrinkage). Both tubes are load-bearing.	Compression strength tests.	110 kN (hinged con. HC) 30 kN (rigid con. RC)	> 900 MPa (HC) 265 MPa (RC)	Research
Nieuwenhuijzen, E., et al. *(Van Nieuwenhuijzen, E.J., et al. 2005)* *(Oikonomopoulou, F. et al; 2017)*	2005	Layered tubular column	Length: 1500 mm Diameter outer: 120 mm Diameter inner: 95 mm Thickness wall: 5/5 mm Layers: 2	2 borosilicate glass tubes laminated with a UV curing clear resin (low-shrinkage). Both tubes are load-bearing.	Compression strength tests.	137-196 kN	40.6 – 57.9 MPa	Research
Engels, S. *(Engels, S. 2020)*	2020	Tubular profiles	Length: 210-290 mm Diameter outer: 70 - 120 mm Diameter inner: 60 - 110 mm Thickness per tube wall: 5 - 9 mm Layers: 1	Two types of borosilicate glass were tested: borosilicate glass DURAN SCHOTT and heat-treated borosilicate glass DURATAN SCHOTT. These tubes were sprayed with OPALFILM coating on the inside of the tubes, which keeps the glass pieces together after breakage.	Compression strength tests. (Tensile strength tests were not performed due to the Corona virus.)	-	DURAN: 3-45 MPa DURATAN: 14-105 MPa	Research
Felekou, E. *(Felekou, E. 2016)* *(Oikonomopoulou, F. et al; 2017)*	2016	Stacked column	Length: 615 mm Thickness per element: 12 mm Number of stacked elements: 50 Cross-Section: 100x100 mm	50 horizontally stacked float panels bonded with SilverTape 8502.	Compression strength tests.	525 kN	52.5 MPa	Research
Felekou, E. *(Felekou, E. 2016)* *(Oikonomopoulou, F. et al; 2017)*	2016	Cast column	Length: 650 mm Thickness per element: 65 mm Number of stacked elements: 10 Cross-section: 105x105 mm	10 horizontally solid cast glass blocks bonded with Delo-Photobond 4468	Compression strength tests.	1412 kN	128 MPa	Research
Kamarudin, M.K., et al. *(Kamarudin, M.K. et al. 2016)* *(Oikonomopoulou, F. et al; 2017)*	2016	Bundled column	Length: 1500 mm Diameter of tubes: 24 mm Thickness per tube wall: 2.5 mm	3 borosilicate glass tubes bonded by a structural silicon (density: 1542 kg/m^3, Young's modulus: 1,72 MPa, Poisson's ratio:0.5, tensile strength: 2.65 MPa).	Compression strength tests.	13.37 kN	26.4 MPa	Research
Oikonomopoulou, F., et al. *(Oikonomopoulou, F. et al; 2017)*	2017	Bundled column	Length: 1500 mm Diameter of rods: 22 mm Diameter outer star-rod: 30 mm Diameter inner star-rod: 17 mm	6 glass DURANA SCHOTT rods bonded by clear adhesive UV-curing with a CONTURAX SCHOTT star-shaped central profile. (In the middle, a steel rod which can be included for a secondary failure mechanism.)	Compression strength tests. Clamped connections.	331 - 508.8 kN	129.7 - 199.4 MPa	Research
Oikonomopoulou, F., et al. *(Oikonomopoulou, F. et al; 2017)*	2017	Bundled column	Length: 2400 mm Diameter of rods: 22 mm Diameter outer star-rod: 30 mm Diameter inner star-rod: 17 mm	6 glass DURANA SCHOTT rods bonded by clear adhesive UV-curing with a CONTURAX SCHOTT star-shaped central profile. (In the middle, a steel rod which can be included for a secondary failure mechanism.)	Compression strength tests. Pinned connections.	PT: 62.7 - 69 kN Not PT: 63 - 90 kN (PT: post-tensioned)	PT: 24.6 - 27 MPa Not PT: 24.7 - 35.3 MPa	Research

Table 1 Overview researches into glass columns.

* Some of these tests were performed on one specimen, so then only one value is obtained, or only one value is given in the literature.

To make the descriptions from the projects in the table 1 clearer, figures and details are given in the table below.

Project	Details	3D/ section
St-Germain-en-Laye France	 [1] (Van Heughten, R. 2013).	 [2] (Schittich, C., et al. 2017).
Dansfoss Headquarters Denmark	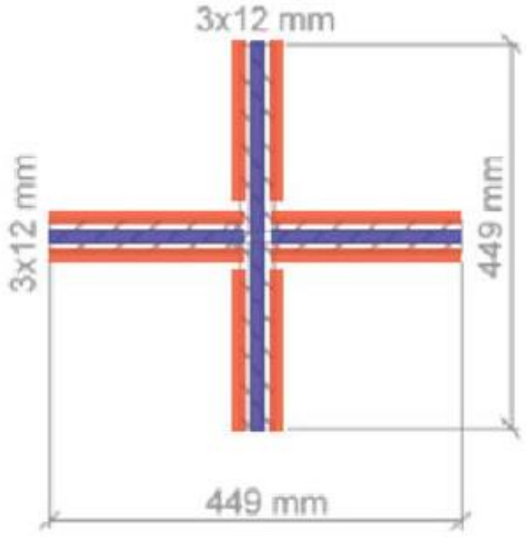 [3] (Van Heughten, R. 2013).	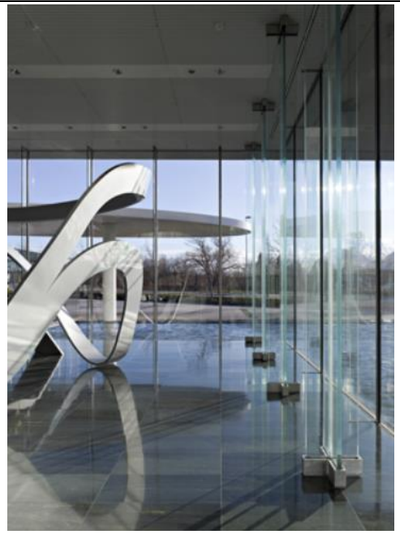 [4] (Schmidt Hammer Lassen Architects. n.d.).
E. Ouwekerk	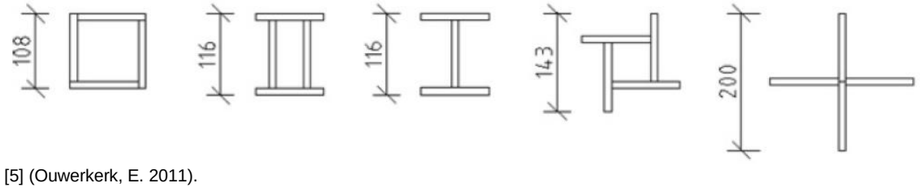 [5] (Ouwerkerk, E. 2011).	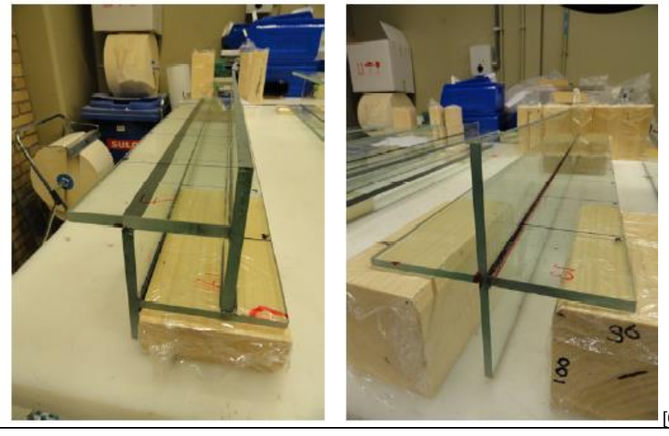 [6] (Ouwerkerk, E. 2011).

Aiello, S., et al.	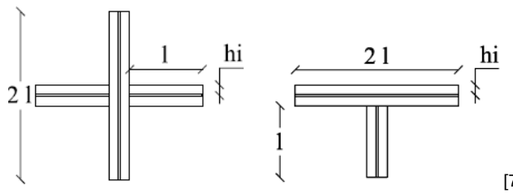 [7] (Aiello, S., et al. 2011).	 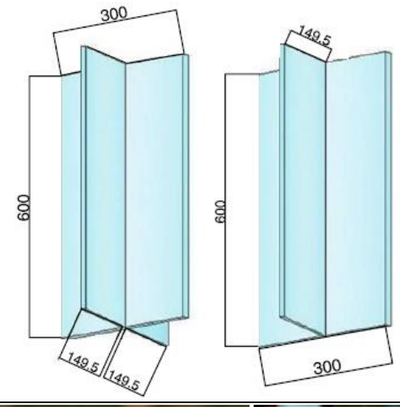 [8] (Aiello, S., et al. 2011).
Kalamar, R., et al.	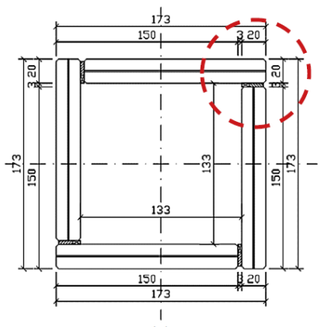 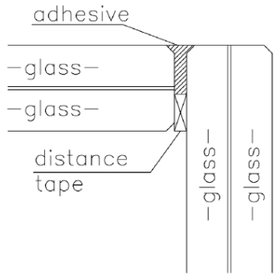 [9] (Kalamar, R., et al. 2017).	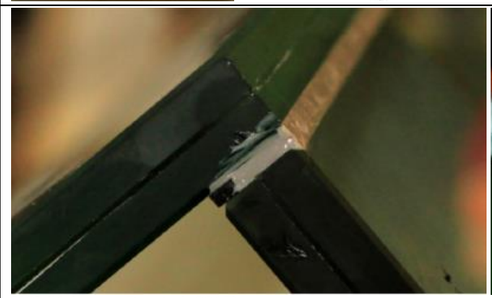 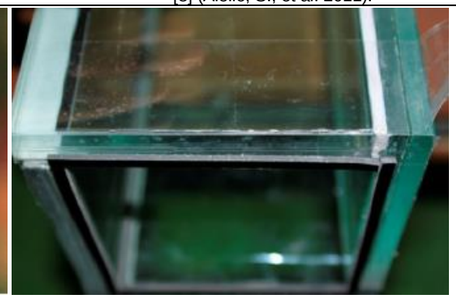 [10] (Kalamar, R., et al. 2017).
Veer, F., et al. and Nieuwenhuijzen, E., et al.	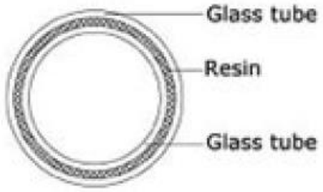 [11] (Van Nieuwenhuijzen, E.J., et al. 2005).	 [12] (Veer, F.A., et al. 1999).

Engels, S.	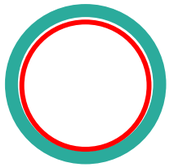 Tubes OPALFILM coating [13]	 [14] (Engels, S. 2020).
Felekou, E.	 [15]	 [16] (Felekou, E. 2016).
Felekou, E.	 [17]	 [18] (Felekou, E. 2016).

Kamarudin, M.K., et al. *(Kamarudin, M.K. et al. 2016)*	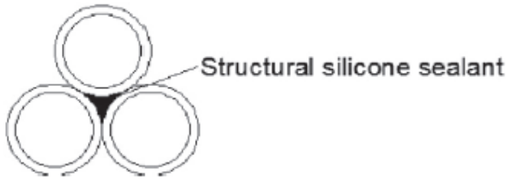  [19] (Kamarudin, M.K., et al. 2016).	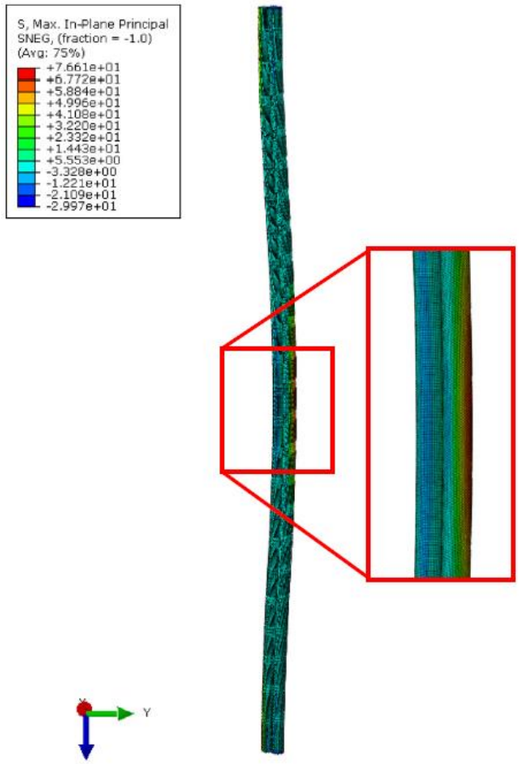 [20] (Kamarudin, M.K., et al. 2016).
Oikonomopoulou, F., et al. *(Oikonomopoulou, F. et al; 2017)*	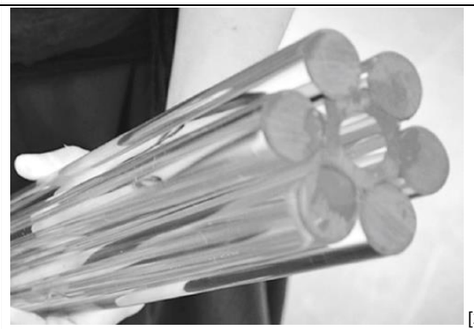 [21] (Oikonomopoulou, F., et al. 2017). 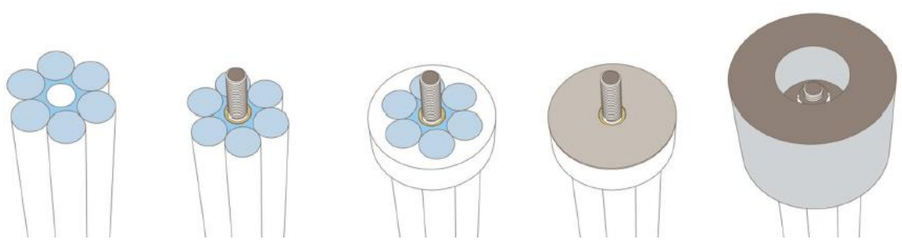	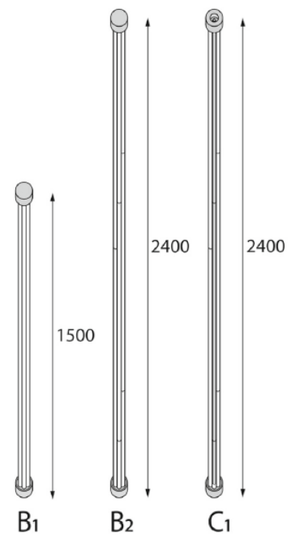  [22] (Oikonomopoulou, F., et al. 2017).

References

Aiello, S., Campione, G., Minafò, G., Scibilia N. (2011). Compressive behaviour of laminated structural glass members. Engineering Structures 33, pp. 3402-3408.

Bagger, A., Petersen, R.I. (2009). Structural use of glass: Cruciform columns and glass portals with bolted connections subjected to bending. Proceedings Glass Performance Days. Tampere: GPD, pp. 381-385.

Engels, S. (2020). Structures from Borosilicate glass tubes: From experimental data to structural design. MSc, Technical University of Delft.

Felekou, E. (2016). Glass Tower in high-rise buildings. MSc, Technical University of Delft.

Kalamar, R., Bedon, C., Eliášová, M. (2017). Assessing the structural behaviour of square hollow glass columns subjected to combined compressive and impact loads via full-scale experiments. Engineering Structures 143, pp. 127-140.

Kamarudin, M.K., Disney, P., Parke, G.A.R. (2016). Structural performance of single and bundled glass columns. ARPN J. Eng. Appl. Sci. 11(3), pp. 355–369.

Oikonomopoulou, F., van den Broek, E.A.M., Bristogianni, T., Veer, F.A., & Nijsse, R. (2017). Design and experimental testing of the bundled glass column. Glass Structures & Engineering. DOI: 10.1007/s40940-017-0041-x.

Ouwerkerk, E. (2011). Glass columns. MSc, Technical University of Delft.

Schittich, C., Staib, G., Balkow, D., Schuler, M., Sobek, W. (2017). Glass Construction Manual 2nd Revised and Expanded Edition Ed. Birkhauser, Basel.

Van Nieuwenhuijzen, E.J., Bos, F.P., Veer, F.A. (2005). The Laminated Glass Column. Proceedings Glass Performance Days, pp. 1-4

Veer, F.A., Pastunink., R.J. (1999). Developing a Transparent Tubular Laminated Column. Proceedings Glass Performance Days, pp. 277-280.

Figure list

[1] Van Heughten, R. (2013). Load-bearing glass columns: the stacked column. MSc, Technical University of Eindhoven, pp. 55. Retrieved on February, 20,2021.

[2] Schittich, C., Staib, G., Balkow, D., Schuler, M., Sobek, W. (2017). Glass Construction Manual 2nd Revised and Expanded Edition Ed. Birkhauser, Basel, pp. 54. Retrieved on December, 11, 2020.

[3] Van Heughten, R. (2013). Load-bearing glass columns: the stacked column. MSc, Technical University of Eindhoven, pp. 55. Retrieved on February, 20,2021.

[4] Schmidt Hammer Lassen Architects. (n.d.). Architectour.net. Danfoss Domicil Danfoss Head Office. Retrieved on November 13, 2020, from: https://www.architectour.net/opere/opera.php?id_opera=6473&nome_opera=Danfoss%20Domicil&architetto=Schmidt%20Hammer%20Lassen

[5] Ouwerkerk, E. (2011). Glass columns. MSc, Technical University of Delft, pp. 55. Retrieved on January, 20, 2021.

[6] Ouwerkerk, E. (2011). Glass columns. MSc, Technical University of Delft, pp. 57. Retrieved on January, 20, 2021.

[7] Aiello, S., Campione, G., Minafò, G., Scibilia N. (2011). Compressive behaviour of laminated structural glass members. Engineering Structures 33, pp. 3408. Retrieved on December, 21, 2020.

[8] Aiello, S., Campione, G., Minafò, G., Scibilia N. (2011). Compressive behaviour of laminated structural glass members. Engineering Structures 33, pp. 3403. Retrieved on December, 21, 2020.

[9] Kalamar, R., Bedon, C., Eliášová, M. (2017). Assessing the structural behaviour of square hollow glass columns subjected to combined compressive and impact loads via full-scale experiments. Engineering Structures 129. Retrieved on February, 4, 2021.

[10] Kalamar, R., Bedon, C., Eliášová, M. (2017). Assessing the structural behaviour of square hollow glass columns subjected to combined compressive and impact loads via full-scale experiments. Engineering Structures 130-131. Retrieved on February, 4, 2021.

[11] Van Nieuwenhuijzen, E.J., Bos, F.P., Veer, F.A. (2005). The Laminated Glass Column. Proceedings Glass Performance Days, pp. 1. Retrieved on January, 11, 2021.

[12] Veer, F.A., Pastunink., R.J. (1999). Developing a Transparent Tubular Laminated Column. *Proceedings Glass Performance Days*, pp. 278-279. Retrieved on November 13, 2020.

[13] Own picture. Delft. Retrieved on December, 22, 2021.

[14] Engels, S. (2020). Structures from Borosilicate glass tubes: From experimental data to structural design. MSc, Technical University of Delft, pp. 3. Retrieved on January, 10, 2021.

[15] Own picture. Delft. Retrieved on March, 20, 2021.

[16] Felekou, E. (2016). Glass Tower in high-rise buildings. MSc, Technical University of Delft, pp. 91. Retrieved on March, 20, 2021.

[17] Own picture. Delft. Retrieved on March, 20, 2021.

[18] Felekou, E. (2016). Glass Tower in high-rise buildings. MSc, Technical University of Delft, pp. 91. Retrieved on March, 20, 2021.

[19] Kamarudin, M.K., Disney, P., Parke, G.A.R. (2016). Structural performance of single and bundled glass columns. ARPN J. Eng. Appl. Sci. 11(3), pp. 356.

[20] Kamarudin, M.K., Disney, P., Parke, G.A.R. (2016). Structural performance of single and bundled glass columns. ARPN J. Eng. Appl. Sci. 11(3), pp. 367.

[21] Oikonomopoulou, F., van den Broek, E.A.M., Bristogianni, T., Veer, F.A., & Nijsse, R. (2017). Design and experimental testing of the bundled glass column. Glass Structures & Engineering. DOI: 10.1007/s40940-017-0041-x, pp. 5, 9. Retrieved on November, 10, 2020.

[22] Oikonomopoulou, F., van den Broek, E.A.M., Bristogianni, T., Veer, F.A., & Nijsse, R. (2017). Design and experimental testing of the bundled glass column. Glass Structures & Engineering. DOI: 10.1007/s40940-017-0041-x, pp. 4, 6. Retrieved on November, 10, 2020.

Appendix 4 – Arguments for the column MCA

A.4.1. Profiled columns

Architectural	Transparency	A green flow is on the edges of the column due to the use of flat float glass. Profiled columns have edges and glued connections the column is not completely transparent.
	Form Freedom	The column is created by flat laminating pieces. Due to this, the form is already a bit prescribed, with not much form freedom.
Mechanical	Buckling resistance	These profiled columns like T and H profiles have 1 clear weaker direction. These profiles are not optimal at for buckling resistance.
	Torsional resistance	The profiled columns are not able to resist torsional buckling.
	Safe failure	The column performs badly under buckling and torsional forces. The thin sizes of for example H-profiles are vulnerable to vandalism or impact loads. The glue connection of the flat panes can be weak too. Even though the planes are laminated, if one pane breaks or cracks at the glued connection, it can fail out of plane. This gives higher risk consequences for injuries.
Financial	Production time	The manufacturing (float glass) and laminating of the glass planes has been produced many times, which makes it known. This method can be done automatically so this not time-consuming. The glued connection of the planes needs to be done more carefully which can be time-consuming.
	Production costs	The float glass manufacturing method is already commonly product, as well as laminating of the panes, which makes is cheaper. The glued connection of the panes needs to be done carefully which can make it more expansive.

A.4.2. Layered tubular columns

Architectural	Transparency	Because the tube doesn't have edges and lines, it is really transparent.
	Form Freedom	The form is already prescribed, so there is not much form freedom.
Mechanical	Buckling resistance	A circular cross-section is the most optimal cross-section to resist buckling.
	Torsional resistance	Just like the buckling-resistance, the tubular column has a good torsional buckling resistance.
	Safe failure	This column exists of two or more tubes laminated to each other. If one (the outer) break, even than it still can have a load carry capacity.
Financial	Production time	The tubes can be made by the extruded manufacturing method. This can be done by machines. This is not really time-consuming. Lamination of the columns needs to be done carefully, this can be time-consuming. The adhesive needs to cure on the right way and in the right speed to avoid shrinkage and voids.

	Production costs	The primary method is in between cheap and expensive, because it is done more times. The lamination process is more time-consuming and needs to be done carefully which can be more expensive.

A.4.3. Stacked columns

Architectural	Transparency	This is not transparent (looking at the figures in the report at appendix A.2.8.2.) Only light can come through.
	Form Freedom	It has a good form freedom. A lot of shapes are possible to create.
Mechanical	Buckling resistance	It can have a good buckling resistance. This depends on the shape.
	Torsional resistance	It can have a good torsional buckling resistance. This depends on the shape.
	Safe failure	It probably has a high failure load, but showed at the report from Akerboom, A. a crack development is depending on the interlayer and the connection design. After the first crack is introduced, the column is less stable and can fail in any direction, which gives a higher risk at injuries.
Financial	Production time	This is really time-consuming due to the different shapes.
	Production costs	This is really time-consuming due to the different shapes, which makes it expensive. If float glass is used it will be cheaper.

A.4.4. Bundled columns

Architectural	Transparency	This type is not transparent. It can let light come through.
	Form Freedom	The column consists of glass rods. The amount is giving the shape, this can differ. There are a many different types of profiles which can be used. Nevertheless, the general shape is the same.
Mechanical	Buckling resistance	Just as tubular glass columns, the bundled column can have a good buckling resistance.
	Torsional resistance	Depending on the symmetry, but in general the bundled column can have a good buckling resistance.
	Safe failure	If one rod fails it can fall to any direction, which gives high consequences for injuries. For extra redundancy a steel rod can be included in the middle of the column. If the glass rods failed, the steel rod can take over the loads.
Financial	Production time	Just as the tubular glass column, the profiles are made of extruded profiles. This is done more times, which makes it less time-consuming. Bonding of the rods can make it more expensive, because it is an essential part of the column.
	Production costs	The primary costs are relatively low, because it is done by a machine. The bonding process needs to be done carefully, which can make it more expensive.

A.4.5. Cast columns

Architectural	Transparency	This is not really transparent, due to distortions. It can let light come through.
	Form Freedom	Just as the stacked columns. It has a good form freedom. Many shapes are possible to cast.
Mechanical	Buckling resistance	It depends on the shape.
	Torsional resistance	It depends on the shape.
	Safe failure	It depends on the shape. If it fails, it is probably due to crack development. The same as for stacked columns: after the first crack is introduced, the column is less stable and can fail in any direction, which gives a higher risk at injuries.
Financial	Production time	This is really time-consuming due to the different shapes. Furthermore, the cooling time can be really long if the cast element is big/large.
	Production costs	This is really time-consuming due to the different shapes, which makes it expensive. If float glass is used it will be cheaper.

Appendix 5 – Design process of the end connections

A.5.1. Aspects from the literature study

From the literature study, a few points of attention came forward:

1. The column needs to be designed as hinged, so that it will only take up normal forces.
2. A soft material, with a lower Young's modulus, needs to be put in between the glass and the steel.
3. The forces need to be introduced uniformly in the column.
4. Thermal expansion and isochoric pressure need to be taken into account due to temperature differences.
5. How to deal with fire safety (FR60): coatings/fire-resistant interlayers/water?
6. The edges of the glass need to be treated to avoid sharp edges, otherwise it is possible that forces are not uniformly distributed in the glass column, resulting in stresses.
7. The column needs to be sustainable.

From these points of attention, needed materials were chosen and it was put together:

1. For a hinged connection, two half spheres will be introduced (figure 1). Between the two spheres, Teflon will be placed.

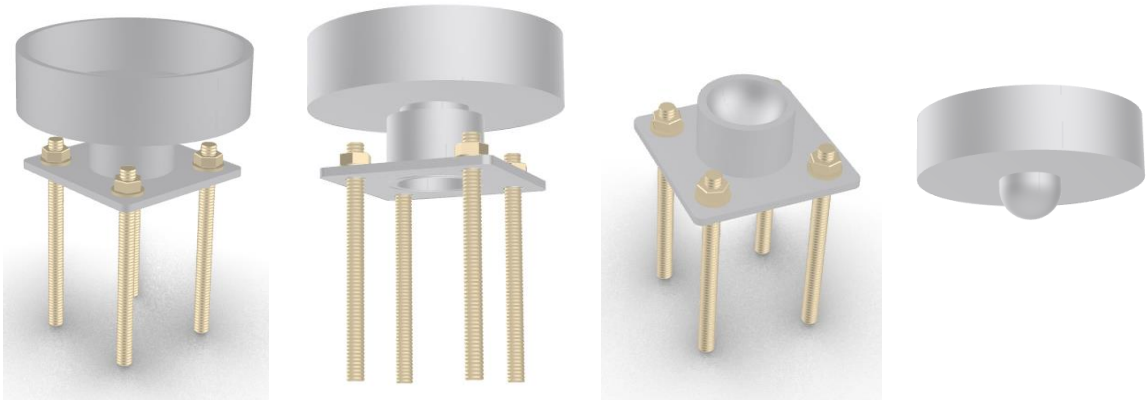

Figure 1 The hinged connection with a steel shoe, two half spheres with Teflon, and a steel footplate.

2. The soft material with a lower Young's modulus than glass can be POM. The glass tubes will be placed in the POM-block and this POM-block will be placed in the steel shoe (figures 2, 3 and 4).

Figure 2 No direction connection between glass and steel

Figure 3 The glass will be placed in a POM-block.

Figure 4 The POM-block will be placed in the steel shoe.

3. This POM will not introduce the forces uniformly and it cannot take up the stresses from the glass, so another material is needed to cover these issues. Hilti mortar (HILTI HIT-HY 270 mortar) will be used (figure 5). The mortar will be injected under the glass, to take over the stresses from the connection when loaded. The Hilti mortar will be injected when it is liquid and when it is hardened, it has the same shape as the surface edges of the glass tubes (where they were cut and treated). According to the literature study, it is able to distribute compression forces into the glass element (Pascual, C., et al. 2021). However, this mortar is for now only used for balustrades and not for applications like this. Furthermore, it is once used for another research to test the compression strength of laminated glass plates (Pascual, C., et al. 2021). Hilti mortar can take higher stresses then POM, it is water resistant, and it does not bond materials. In the POM-block, grooves are included. The Hilti will be hardened in 30 minutes.

First, studs were included in the design (figure 6) to keep the glass at the right height when the Hilti is not hardened, but this will influence the uniform distribution of forces into the glass. So, this will not be used anymore. The glass will be marked at the right height and it will be held at the right position by a machine.

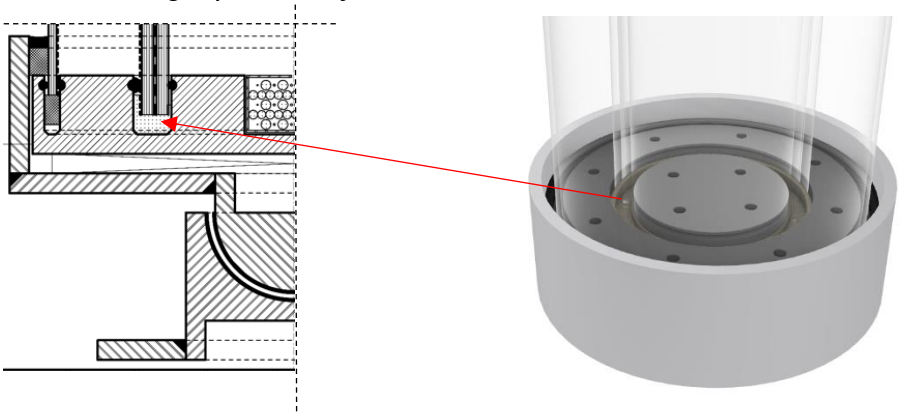

Figure 5 Section of the end connection with the Hilti shown.

First, as shown in figure 6 the POM-block should be included with grooves and studs, but these studs will influence the well/distributed introduction of the forces into the glass tubes. So, these were taken out of the design.

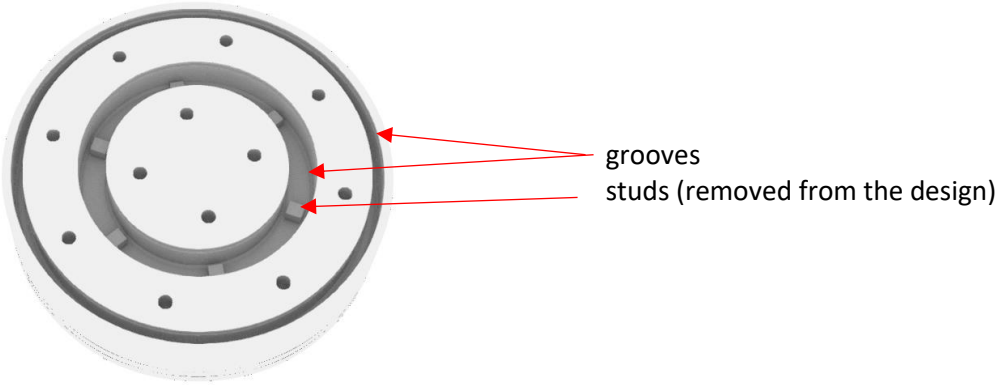

Figure 6 POM-block with studs and the grooves.

4. The column will be sealed to avoid dirt coming in. This will be done by a sealant and a neoprene gasket, resting on the POM edge (figure 7). This POM edge can serve at the same time as an extra protection for the glass during manufacturing.

In this way it is a closed system, which can lead to pressures. If these pressures become too high, stresses can occur in the glass. The MLA with air hoses can regulate the air to avoid air pressures and condensation. If the glass is able to resist the stresses, the MLA without air hoses is designed. Silica grains are included to take up water when condensation occurs, which is the same principle as used in double glazed units (IGU's). For the SLW, water will be regulated into the system.

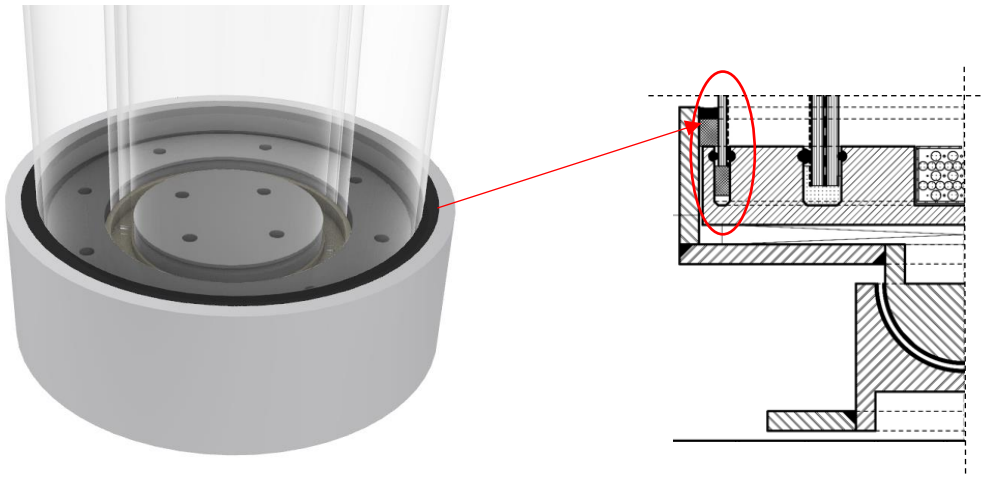

Figure 7 The sealant with neoprene at the edges to seal to column.

5. The column needs to be designed fire safe for 60 minutes (FR60). This means that both, the glass column and the connections, need to be fire safe. Water will be pumped inside of the SLW column to keep the temperature of the glass cooler for a while. For the MLA a special transparent fire-resistant coating can be used. To make the connection fire safe as well, the steel components will be coated with a FR60 coating, and the hoses will be enclosed by fire resistant hoses (figure 8). These fire hoses will be connected via a threated connection into the steel shoe (figure 9). This will be covered by a fire-resistant sealant (figure 10). These aspects are discussed with a fire officer in Dordrecht.

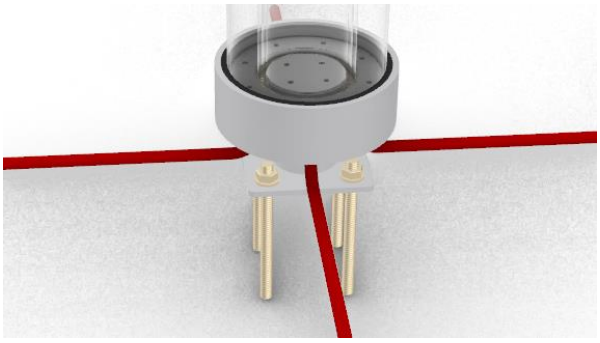

Figure 8 Fire hoses to enclose the air/water hoses.

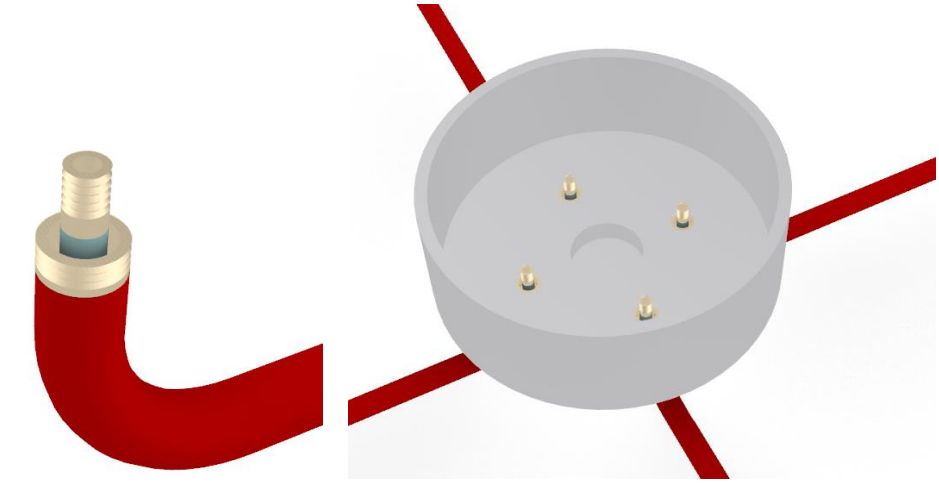

Figure 9 Threated connection to plug in the fire hoses in the steel shoe, and threated connections to plug in the water/air hoses into the POM.

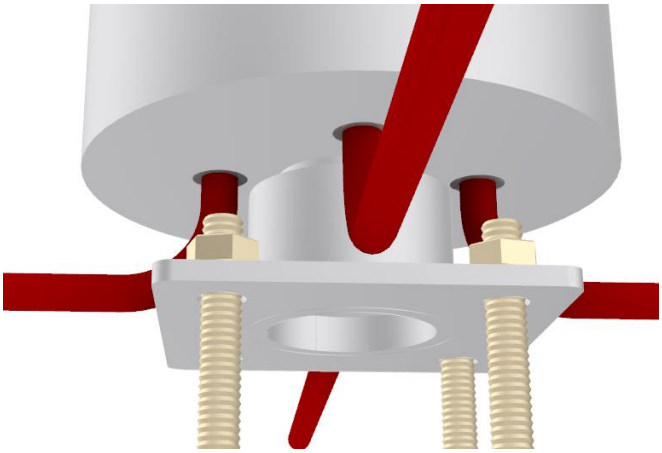

Figure 10 Fire sealant

6. The edges of the glass tubes will be threated. The producer SCHOTT decided how. After cutting the tubes in the right length, the edges of the glass tubes will be fire-polished. This was confirmed in the order confirmation from the tubes made by SCHOTT.

Nevertheless, the glass edges will always have a few irregularities.

7. The column is sustainable by the fact that glass is durable and the complete column is demountable. Which means that the column can be dissembled from the building and it can be placed somewhere else. Moreover, all the components can be reused in other

constructions as well, because the components are not bonded. Only dry connections were used in the designs.

A.5.2. Considerations on the design of the end connections

Other problems occurred during designing which needed to be solved:

1. How to pump the water/air from the hoses into the column, and how to make it water- or air tight?
2. The Hilti mortar needs to be well-distributed into the POM-block grooves.
3. The POM-block and the column needs to be air- and water tight. Besides, the glass needs to stay clean during/after injecting of the Hilti.
4. How to put silica grains in the POM-block?
5. How to assemble the column? The parts are not bonded, but need to be held at the right place.
6. How to replace the column?

1. If air or water needs to be pumped through the column. Hoses need to be plugged into the POM-block, and the POM-block needs to regulate this from the hoses into the column. Therefore, the POM-block needs to be air- and watertight. Figure 11 shows the POM-block that regulates air (MLA), and figure 12 shows the POM-block that regulated the water (SLW).

A system needs to be designed for this. Plugs will be screwed into the with a threated connection into the first layer of POM (figures 11, and 12, left) (figure 13). Then hoses can be plugged. The air/water will go through the holes, via the canals to the branches in the second layer of the POM-block (figures 11 and 12, middle). Then in the third layer of the POM-block, the water/air will go through the holes into the column (figures 11 and 12, right). This threated connection is used in plastics before, for example in a Bose- sound speaker (figure 14). An extra foil will be placed around the POM-block to make sure it is air/water tight (figure 15).

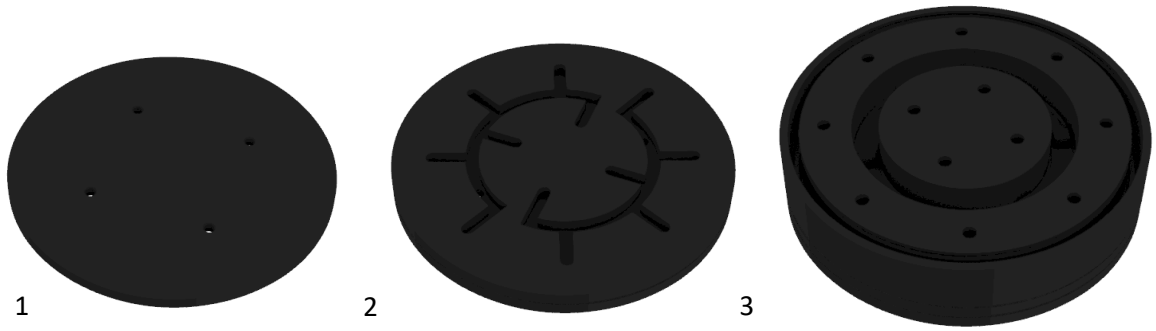

Figure 11 POM-block to regulate air with three layers

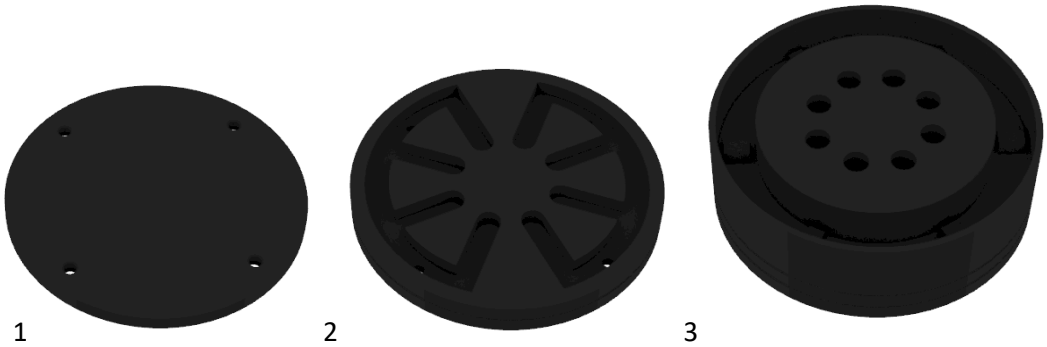

Figure 12 POM-block to regulate water with three layers

So as explained above, patterns were designed in different POM-layers. More layers are needed, to make sure that it can be produced. To make sure that all these grooves and shapes are possible in the POM, a company was contacted, which makes/processes POM, named Ridderflex.

According to Ridderflex, it is possible to make the sleeves in the POM, POM is water resistant, it is possible to make threated connections in the POM, the smallest whole which can be made in POM is around Ø 2 mm, and geometric tolerances of POM are around 0.1 mm. Furthermore, according to Ridderflex, the different layers can be put together with a special glue (like Araldite 2010). To do so, the side where the glue will be attached, needs to be treated with phosphoric acid. In this way the POM-block is sealed to avoid water coming out of the POM-block.

An alternative for this glued connection, are pinned connections. This is not water- and air tight, but it only keeps the layers attached to each other. This is way the preference goes to the glued connection.

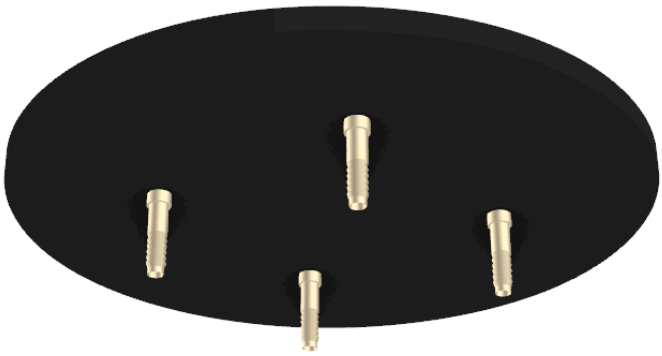

Figure 13 Threated connection for the hoses into the first layer of the POM-block

Figure 14 Bose-sound speaker with a threated connection into plastic.

When there is a water/air failure in the column, the water/air leakage could only appear on top of the connection, which is above floor level so it is always visible. In this way, the leakage can be repaired in an early state.

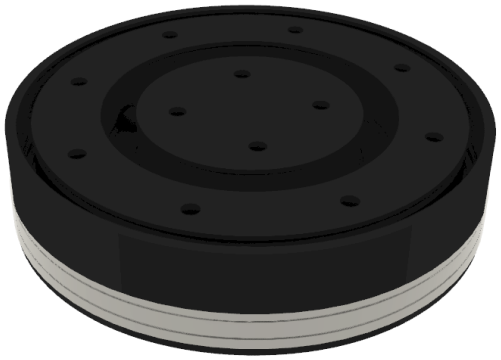

Figure 15 Tape to make the POM-block air- and water tight.

A plug for the threated connection is shown in figure 16 below (plastic/copper).

Figure 16 Plugs for a threated connection.

2. To ensure that the mortar is well-distributed in the grooves in the POM-block, small chamfers were placed into the grooves (figure 17).

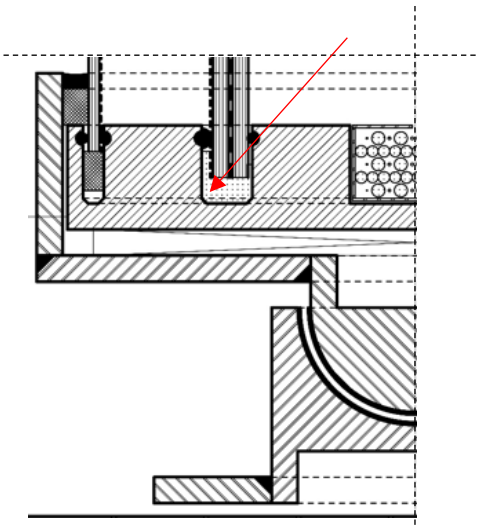

Figure 17 Small chamfers into the grooves of the POM-block.

3. The make the column air- and watertight and to make sure that the mortar will not make the glass tubes dirty during injecting, gaskets will be placed in the POM. These gaskets will be placed into sleeves in the POM-block. In figure 18 and 19, the sleeves in the POM-block

are shown. This idea came from a doorstop (figure 20). According to Ridderflex, it is possible to make the sleeves in the POM.

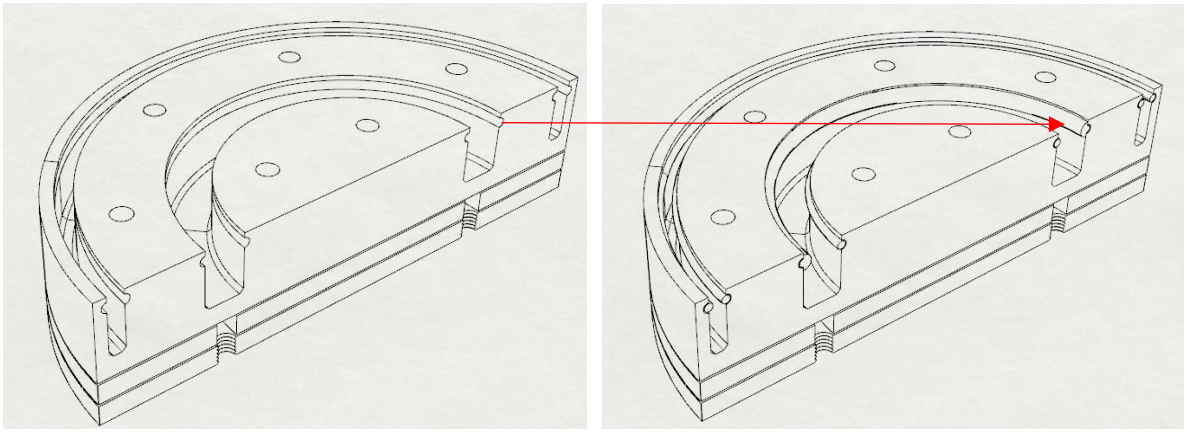

Figure 18 The sleeves in the POM-block where the gasket can be placed in.

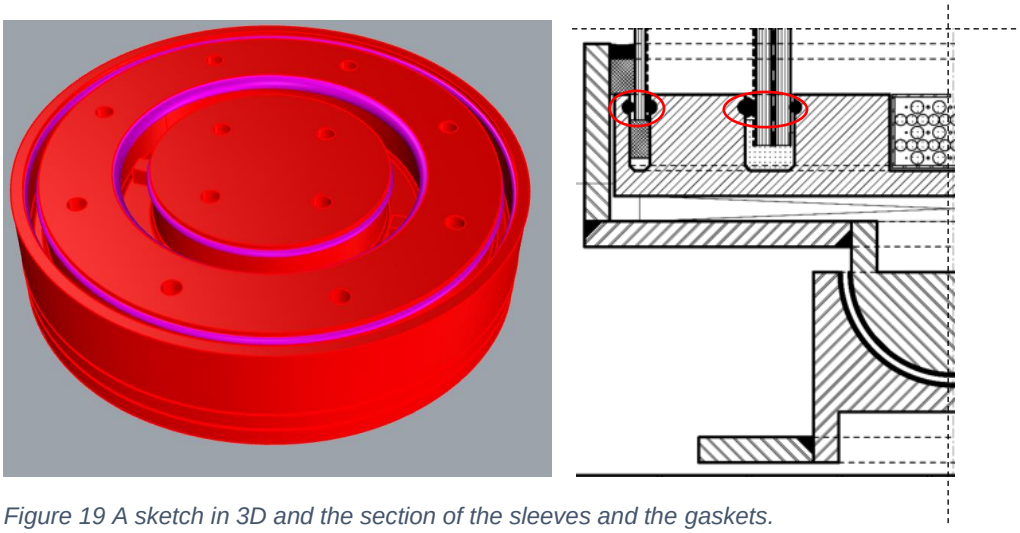

Figure 19 A sketch in 3D and the section of the sleeves and the gaskets.

Figure 20 the doorstop with the sleeves and the gasket.

4. For the MLA without air hoses, only one layer of POM is enough, due to the fact that the different abovementioned patterns are not needed. As said before, in this design silica grains need to be put inside the POM-block, to avoid condensation. In figure 22, the POM-block is shown with the silica grains and the holes in the POM. The same principle is used in double glazed units.

Actually, all the glass designs are based on the system used in double glazed units:

Double glazed unit (figure 21) – tubular glass design:

- Window frame – Steel shoe
- Glass – Glass
- Air cavity – Air/water cavity
- Spacer – POM-block
- Silica grains (desiccant) – silica grains/filtered air/ water
- Sealant – sealant

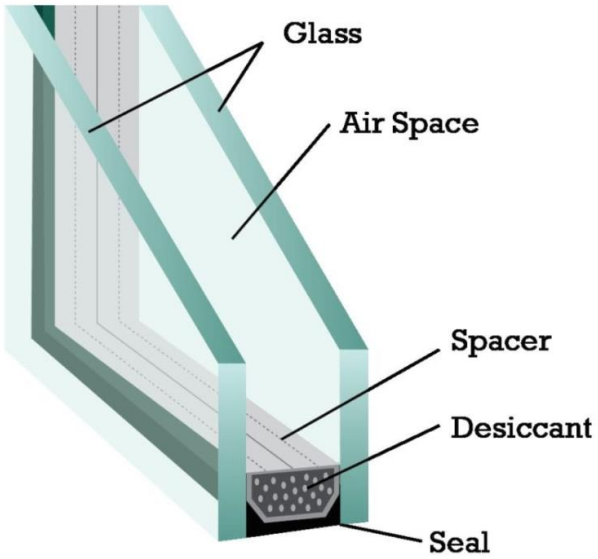

Figure 21 Double glazed unit (GLASSDOCTOR. n.d.).

The grains are placed inside holes in the POM-block, and a POM-cover is glued on top. The cover needs to have a pattern so that the grains do not fall out, and it needs to be partly open so that the water can be taken up by the grains. The double glazed unit has holes in the spacer as well (figure 21).

Figure 22 The POM-block with silica grains for the MLA (without air hoses).

5. The POM-block is later on adjusted, otherwise it was not possible the assemble the column. There are a few difficulties for the assembly:

- The glass needs to be held and rotated: this will be done in an assembly machine, specially designed for this.
- The components are not bonded, but it needs to be held together at the right position.
- If the outer tube (MLA) is held in the machine, without the bottom connection, the inner tube will fall out. So, it would be better to first assemble the connections to the inner tube and to connect the outer tube later on. (The SLW does not have an outer tube.) In chapter 3.2.4. the full assembly sequence is given (only for the MLA with hoses because this one is the most difficult to assemble).

First of all, the glued POM-block (MLA with hoses), shown in figure 11, is divided into two parts: the inner part where also the Hilti will be injected, and the outer part, named: POM-ring. It was necessary to divide this into two parts, otherwise, it was not possible to slide over the outer glass tube. First off, the assembly machine will only hold the inner tube. If it holds the outer tube, the inner tube falls out, because there are no connections yet.

First the inner part of the POM-block will be assembled with the Hilti and the inner glass tube. To keep the POM-blocks at its place after injecting the Hilti, the POM-blocks will be constrained via four POM-braces (figure 24). These braces are screwed with threated connections to ‘hands’ in the machine, which are holding the glass inner tube, and to the POM-cap (figure 23 and 25). These POM-braces can be tightened up when the Hilti is injected and when it needed to be placed against the glass tubes (figure 24). A gasket ring will be placed around the inner POM-block in the sleeves of the POM-cap, to make sure that the inner POM-block and the POM-cap are air/water tight (figure 23 and 25).

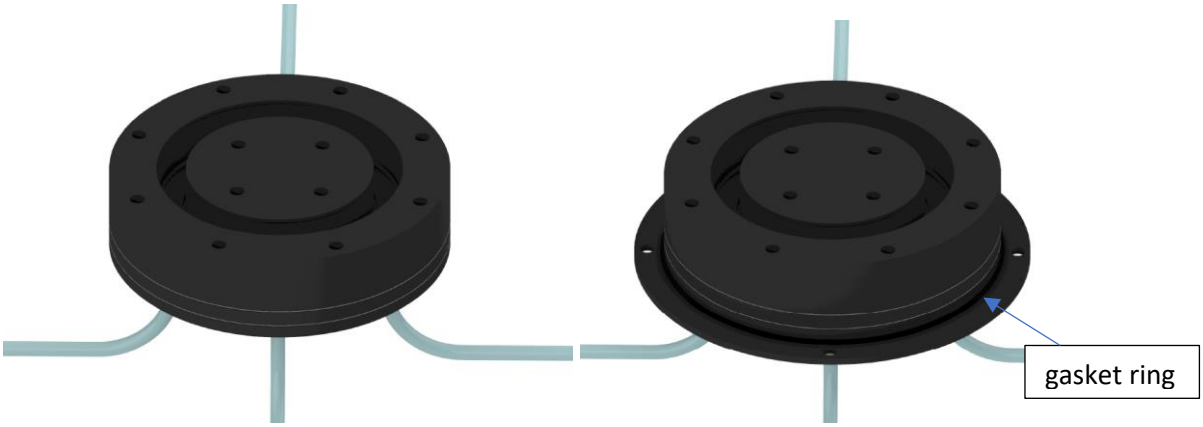

Figure 23 Glued POM-block (left). The POM-block with the POM-cap under it (right).

At figure 25, The POM-cap is shown from the top side (without the inner POM-block on top). The cap will be screwed to the inner POM-block from the bottom side and later on the POM-cap will be screwed to the POM-ring from the top side (figure 26 and 27). With the gasket ring attached to the POM-cap and the inner POM-block, and with the extra foil at the outside of the POM-ring, the total POM-block is water/air tight (figure 27).

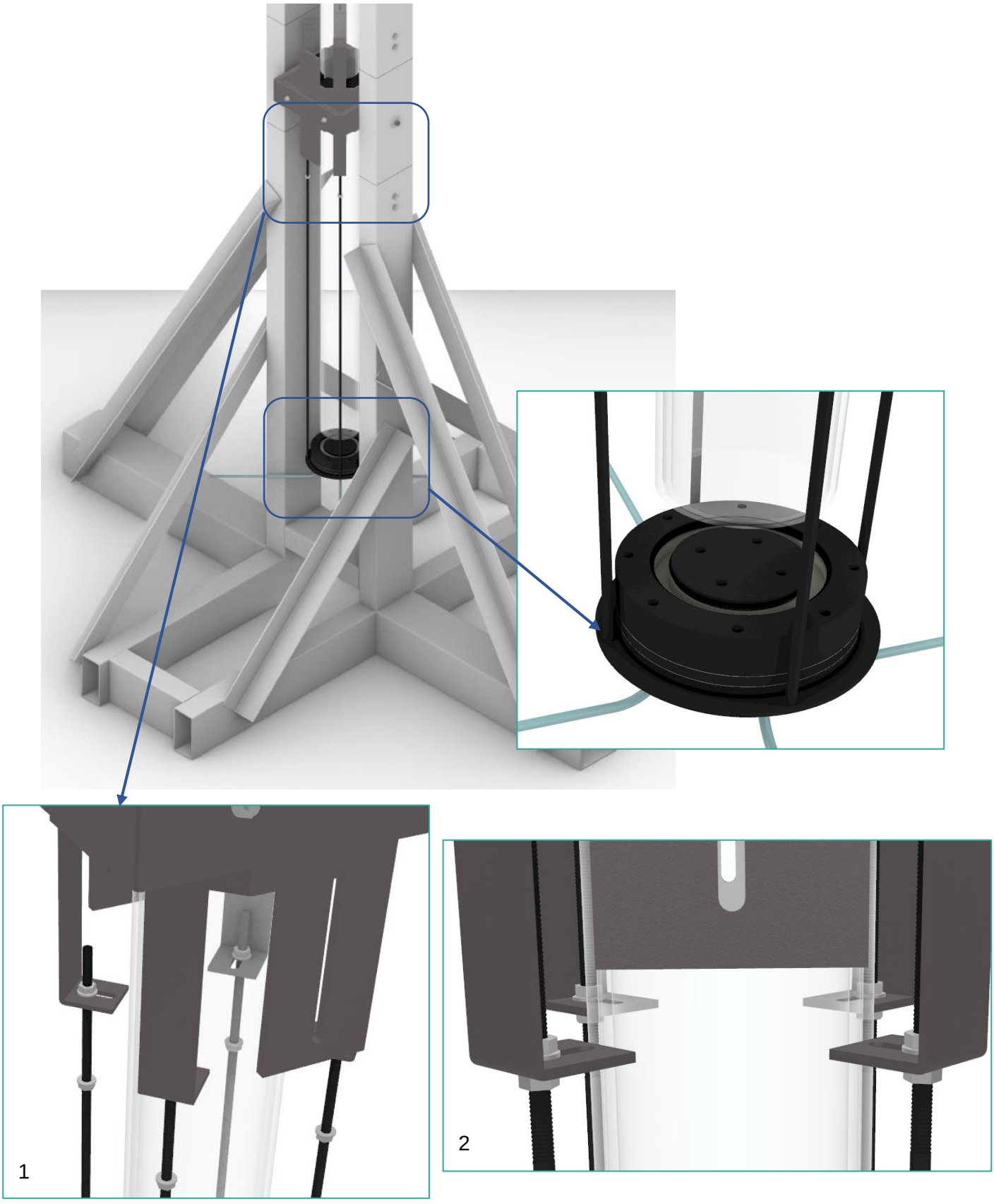

Figure 24 The POM-block is attached with the POM-cap by braces to the machine to constrain the POM-block. When the POM-block hangs under the glass before the Hilti is injected the bolts are not tightened up yet (1), and when the Hilti is injected and the POM-block needs to be attached to the glass, the bolts are tightened up to move the POM-block with the braces up (2).

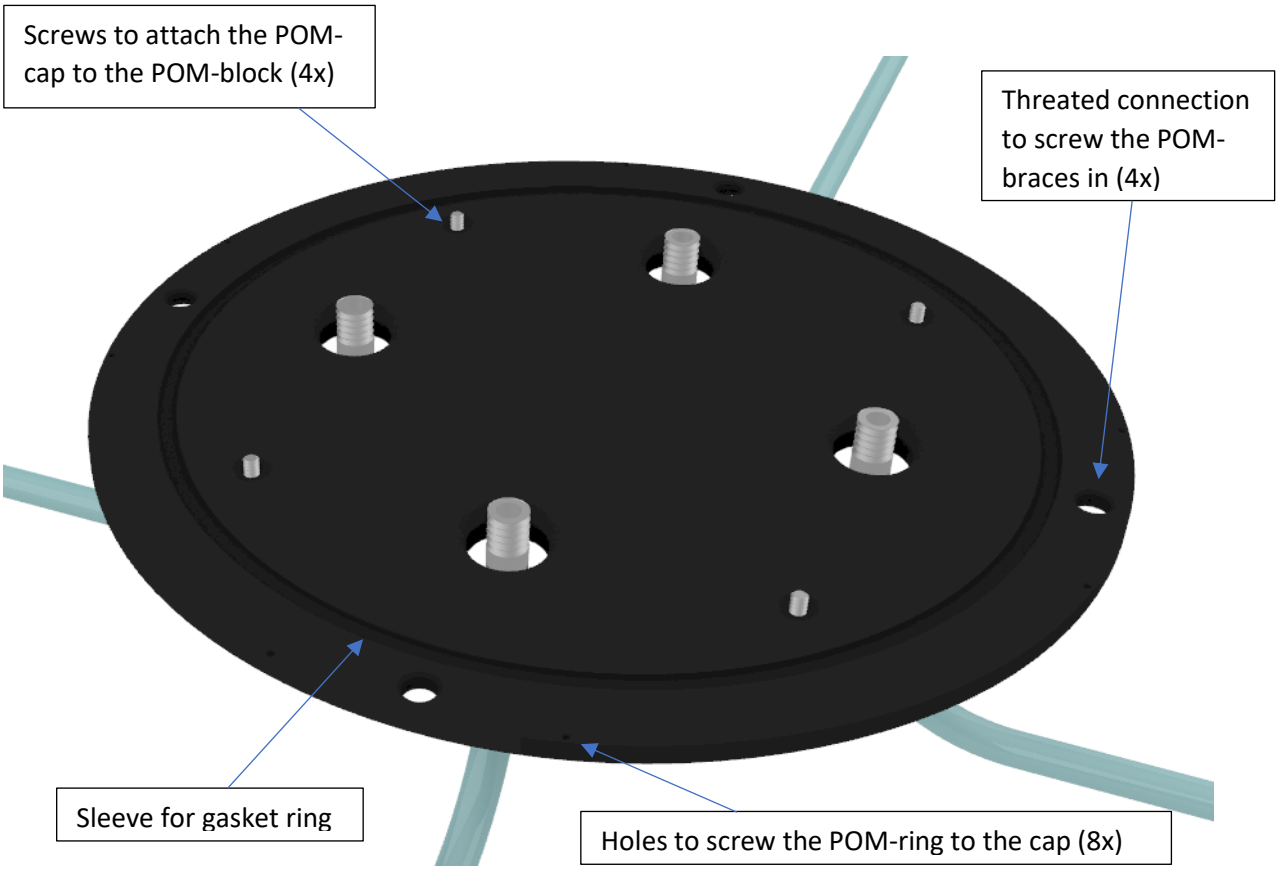

Figure 25 The POM-cap (shown from the top).

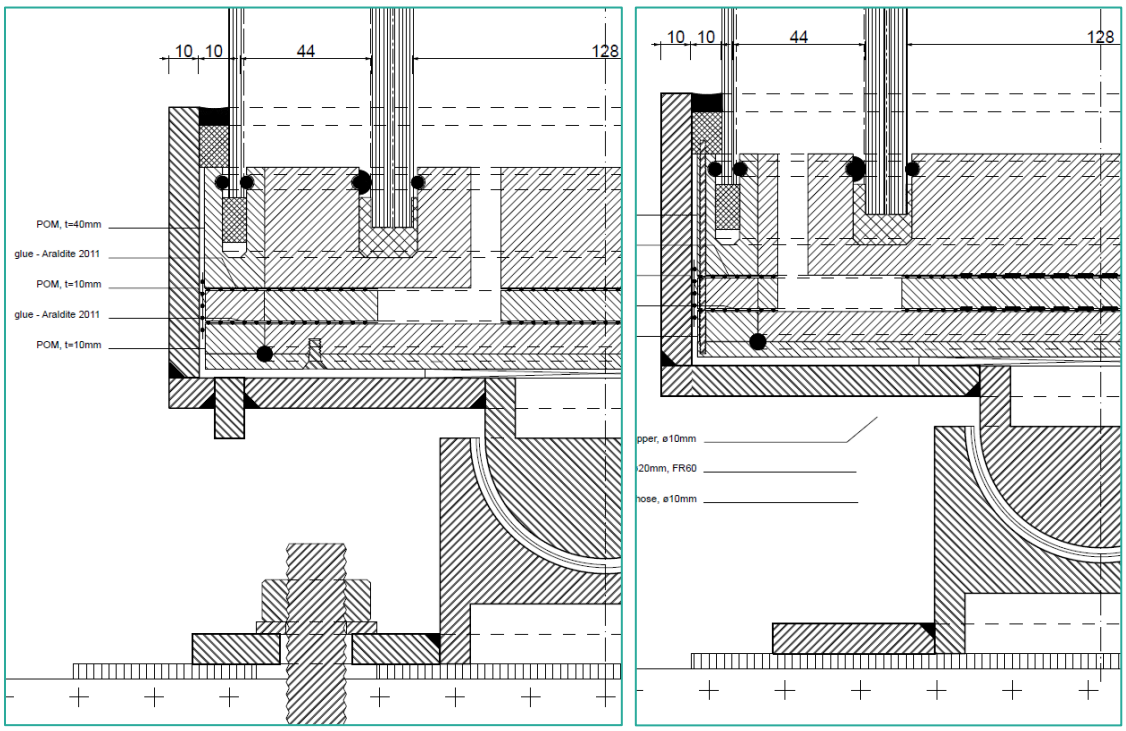

Figure 26 The POM-cap will be screwed to the inner POM-block from the bottom side (left) and to the POM-ring from the top side (right) (MLA).

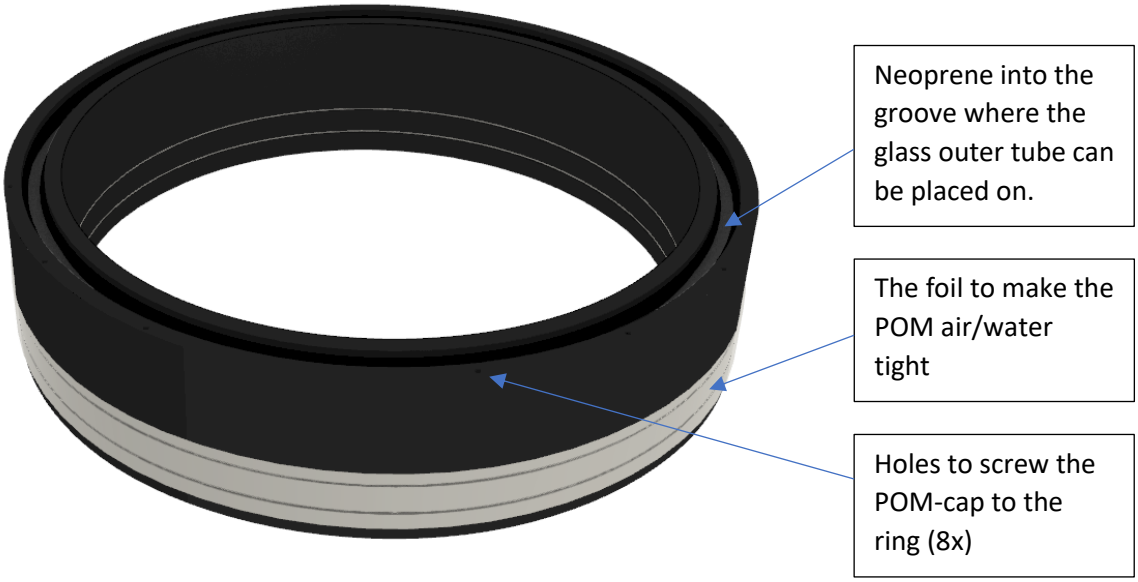

Figure 27 The POM is water/air tight by the gasket attached to the POM-cap (figure 23) and the extra foil attached outside the POM-ring.

Steel braces will be placed at the steel shoe to keep all the components together during assembly and transport. It also serves as an extra protection during transport. The steel brackets are attached to the studs under the steel shoe (figure 28). When the steel shoe is attached to the steel braces, the POM-braces can be removed from the assembly machine (appendix 7 an chapter 3.2.4.).

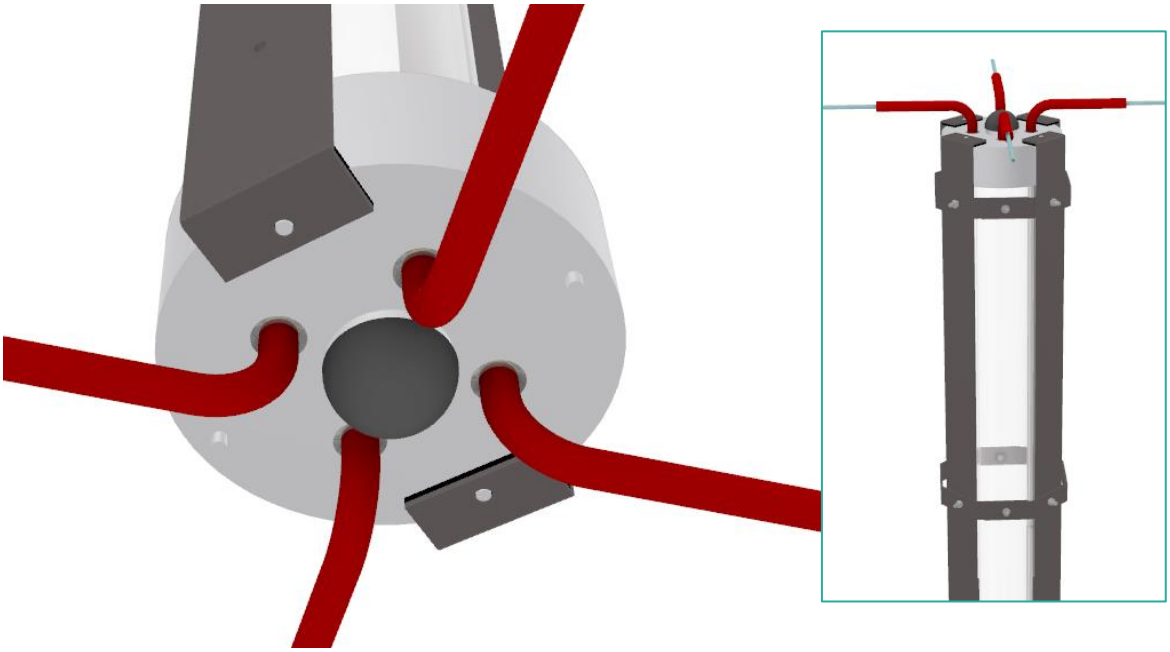

Figure 28 The studs under the steel shoe where the steel brackets can be attached to.

The assembly machine exists out of three parts: the lower part, and two upper parts. The upper parts must ensure the stability of the machine, when the column will be turned into the machine. Figure 29 shows the lower part of the machine. In between the lower and the upper parts, an extra part of steel is placed. Figure 30 shows the middle part between the lower and the upper parts. When different lengths/diameters will be used, the machine needs to be changed, but the middle parts do not need to be adjusted. Then the first upper part can be

screwed to the middle part (figure 31). Lastly, the second upper part can be screwed to the middle part, which makes the assembly machine complete (figure 32). The first and the second upper parts are screwed to each other with an equal angle (figure 32).

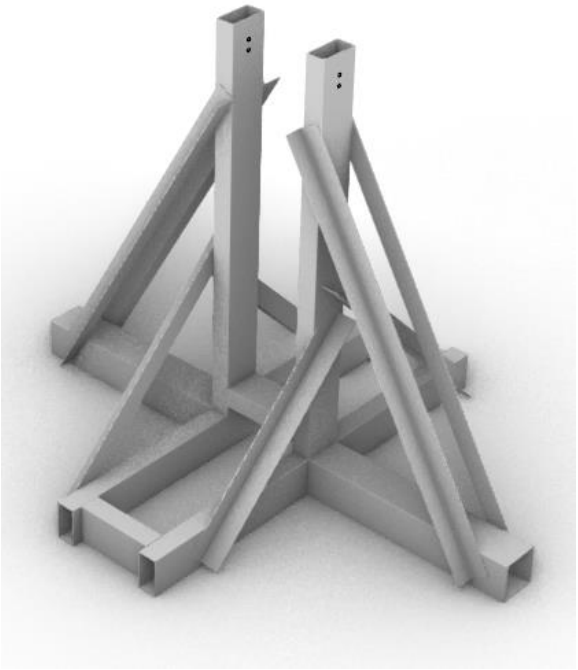

Figure 29 Lower part of the assembly machine.

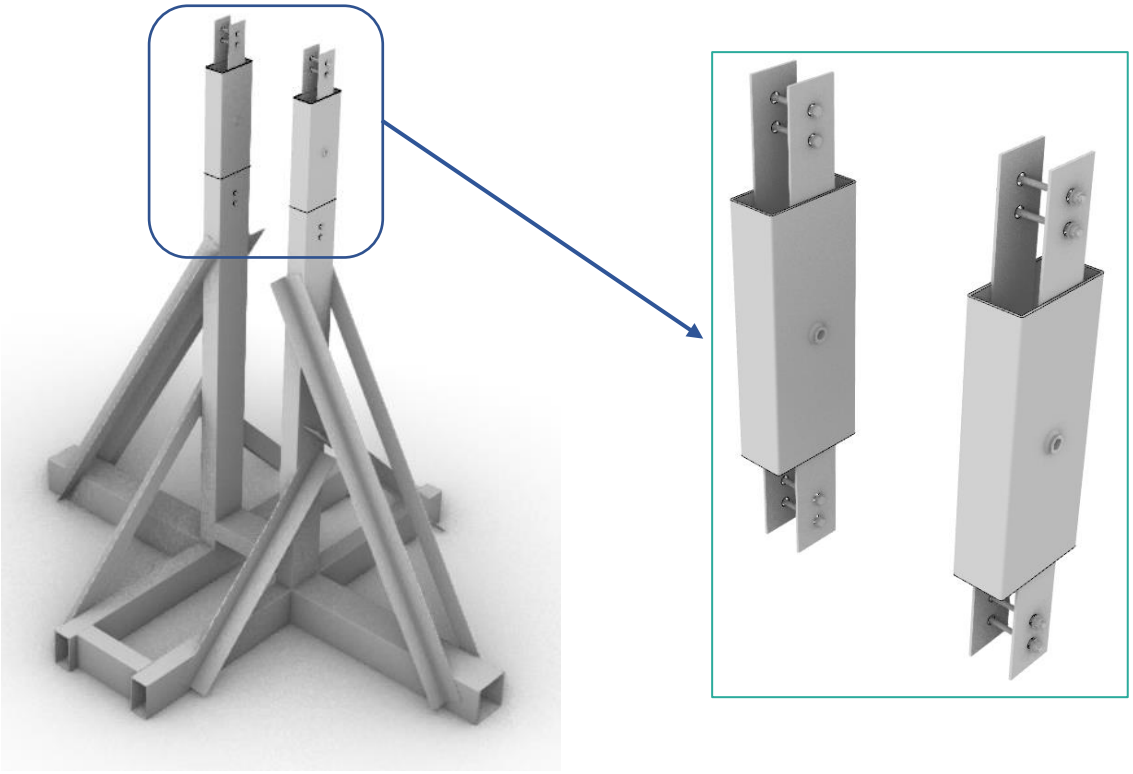

Figure 30 The lower and the middle parts.

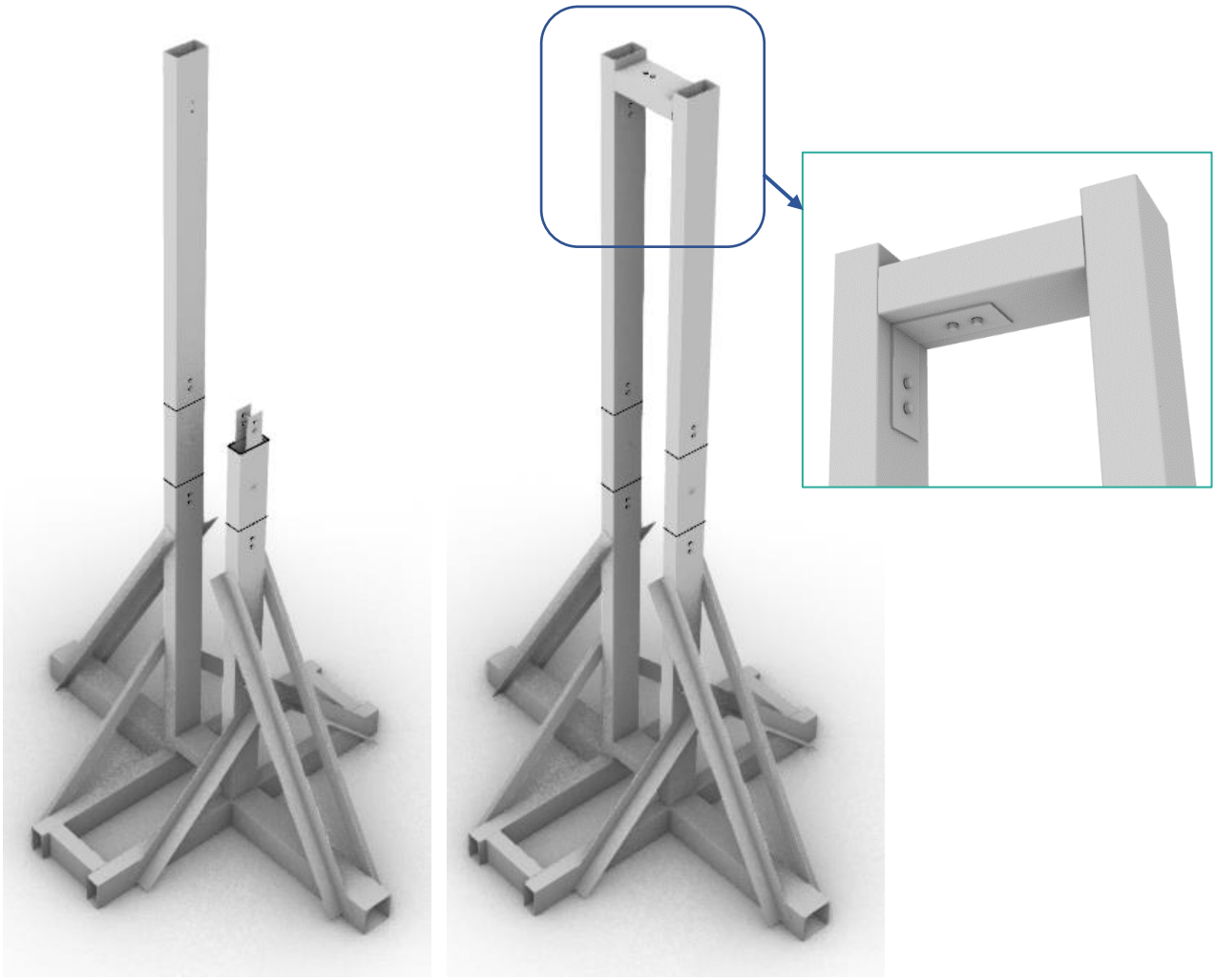

Figure 31 Lower, middle and one upper part. *Figure 32 The complete machine.*

In the machine ‘hands’ are present. These hands hold the inner tube and later on the outer tube. The hands are placed with a pin in the middle part of the machine, so that the column can be rotated (figure 34). The black part can be taken out of the ‘hands’ and can be replaced for bigger ones when the outer tube needs to be held (figure 33).

Furthermore, a slotted hole is attached to the hand, where the steel braces are screwed to (figure 34). In this way, the steel braces can be set to the right position for the steel shoe.

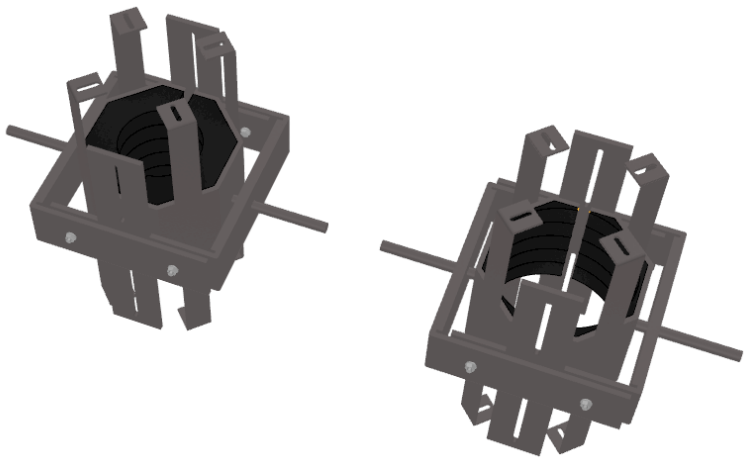

Figure 33 Left: the hands with the black part to hold the inner tube. Right: to hold the outer tube.

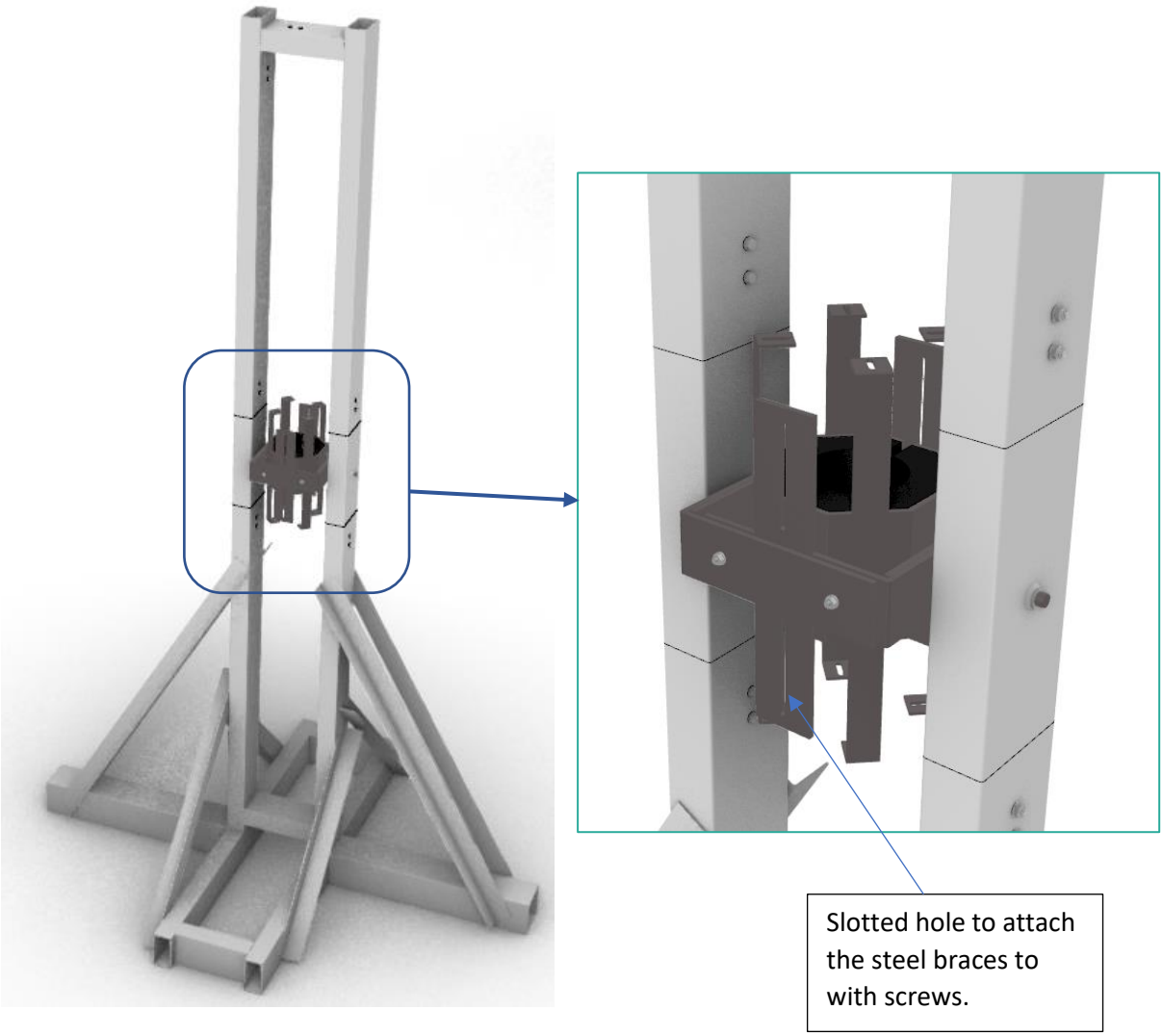

Figure 34 The 'hands' in the machine with a pin.

When hands can be removed from the glass tube when finished, an extra piece of steel needs to be placed in between the steel braces. When, the upper and the lower steel braces are attached to each other with the extra part, the hands can be removed (figure 35).

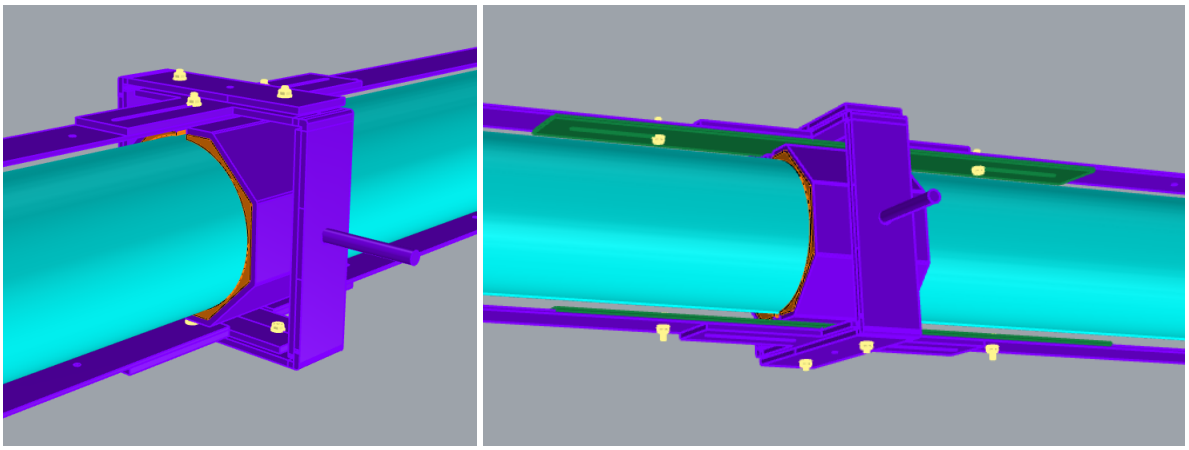

Figure 35 Left: the steel braces are only screwed to the hands. Right: the steel braces are also screwed on the inside to the extra parts (green) that keeps the lower and the upper steel braces together as one.

6. The steel footplate will be screwed onto the support (floor/beam). In this way the whole column is demountable. To be able to replace the column, shim plates are used at the top of the column to create a tolerance. These can be taken out, the steel footplate can be moved to the top by tightening the bolts, so that the column can be rotated and can be taken out of the steel brackets (figure 36). The replacement strategy is further explained in chapter 3.2.6.

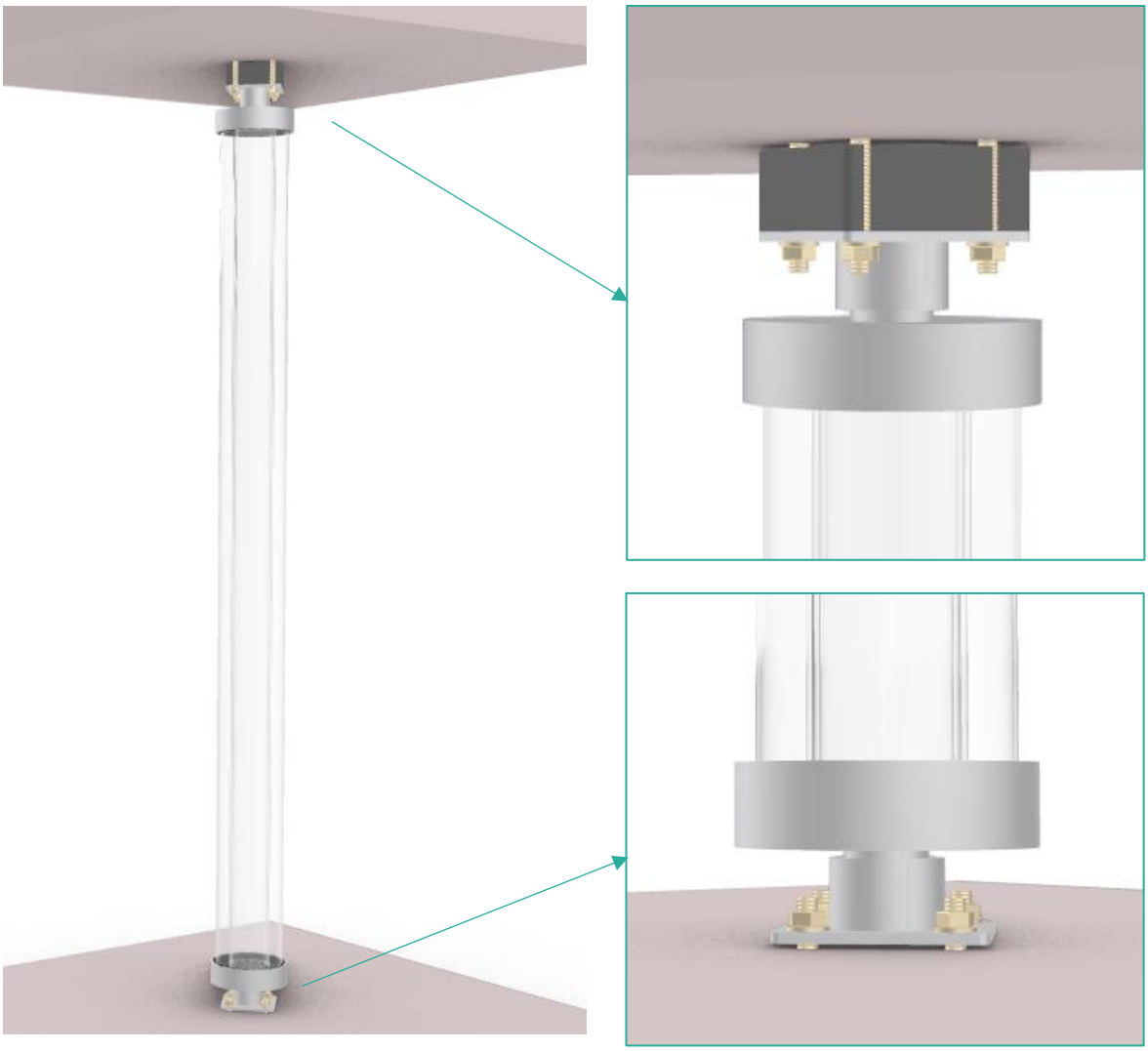

Figure 36 The column (MLA without air hoses), shown the top connection with the shim plates and the top bracket, and the bottom connection with the lower bracket.

Furthermore, the steel connection will be placed under the finishing floor, because the column needs to be as transparent as possible. To be able to repair or replace the column, there are removable tiles in the finishing floor around the connection (figure 37).

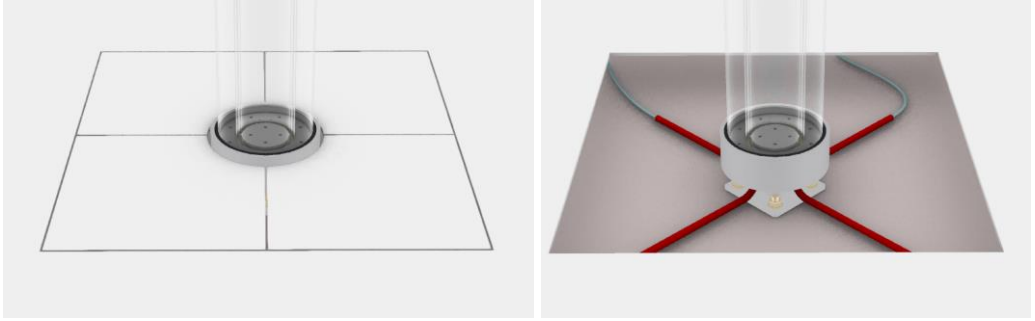

Figure 37 the removable tiles.

The same principle is used for example around trees (figure 38, right), and at the columns for the Moreelse Brug bridge at train station in Utrecht (figure 38, left).

Figure 38 Projects/samples with the same principle with the removable tiles.

References

Pascual, C., Overend, M. (2021). Buckling of sandwich struts with a particular application in composite multi-layer glazing. Engineering Structures 230 (111545), pp. 1-14.

Figure list

All figures except figure 21 - Own pictures.

Figure 21 – GLASSDOCTOR. (n.d.). How to Fix Moisture & Condensation Between Double Pane Windows. Retrieved on March, 10, 2020, from: https://glassdoctor.com/expert-tips/all-about-window-glass/condensation-between-window-panes

Appendix 6 – Drawing sheets

The drawings made for this project for the designs are listed below and are shown in this chapter.

MLA (with air hoses):

1. 2D-cross-section + 2D-detail of the bottom connection
2. 2D-cross-section + 2D-detail of the bottom connection
3. 2D-cross-section + 2D-detail of the bottom connection
4. 3D-view + 3D-cross-section 1 of the bottom connection
5. 3D-view + 3D-cross-section 1 of the bottom connection
6. 3D-view + 3D-cross-section 1 of the bottom connection
7. 3D-view
8. 3D-view

MLA (with silica grains):

1. 2D-cross-section + 2D-detail of the bottom connection
2. 2D-cross-section + 2D-detail of the bottom connection
3. 2D-cross-section + 2D-detail of the bottom connection
4. 3D-view + 3D-cross-section 1 of the bottom connection
5. 3D-view + 3D-cross-section 1 of the bottom connection
6. 3D-view + 3D-cross-section 1 of the bottom connection
7. 3D-view
8. 3D-view

SLW (with water hoses):

1. 2D-cross-section + 2D-detail of the bottom connection
2. 2D-cross-section + 2D-detail of the bottom connection
3. 2D-cross-section + 2D-detail of the bottom connection
4. 3D-view + 3D-cross-section 1 of the bottom connection
5. 3D-view + 3D-cross-section 1 of the bottom connection
6. 3D-view + 3D-cross-section 1 of the bottom connection
7. 3D-view
8. 3D-view

scale - 1:25

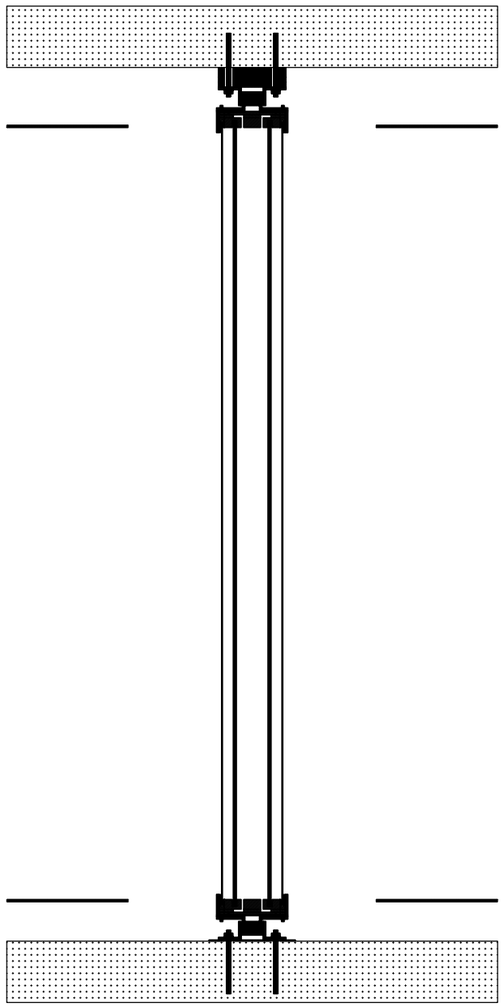

scale - 1:2

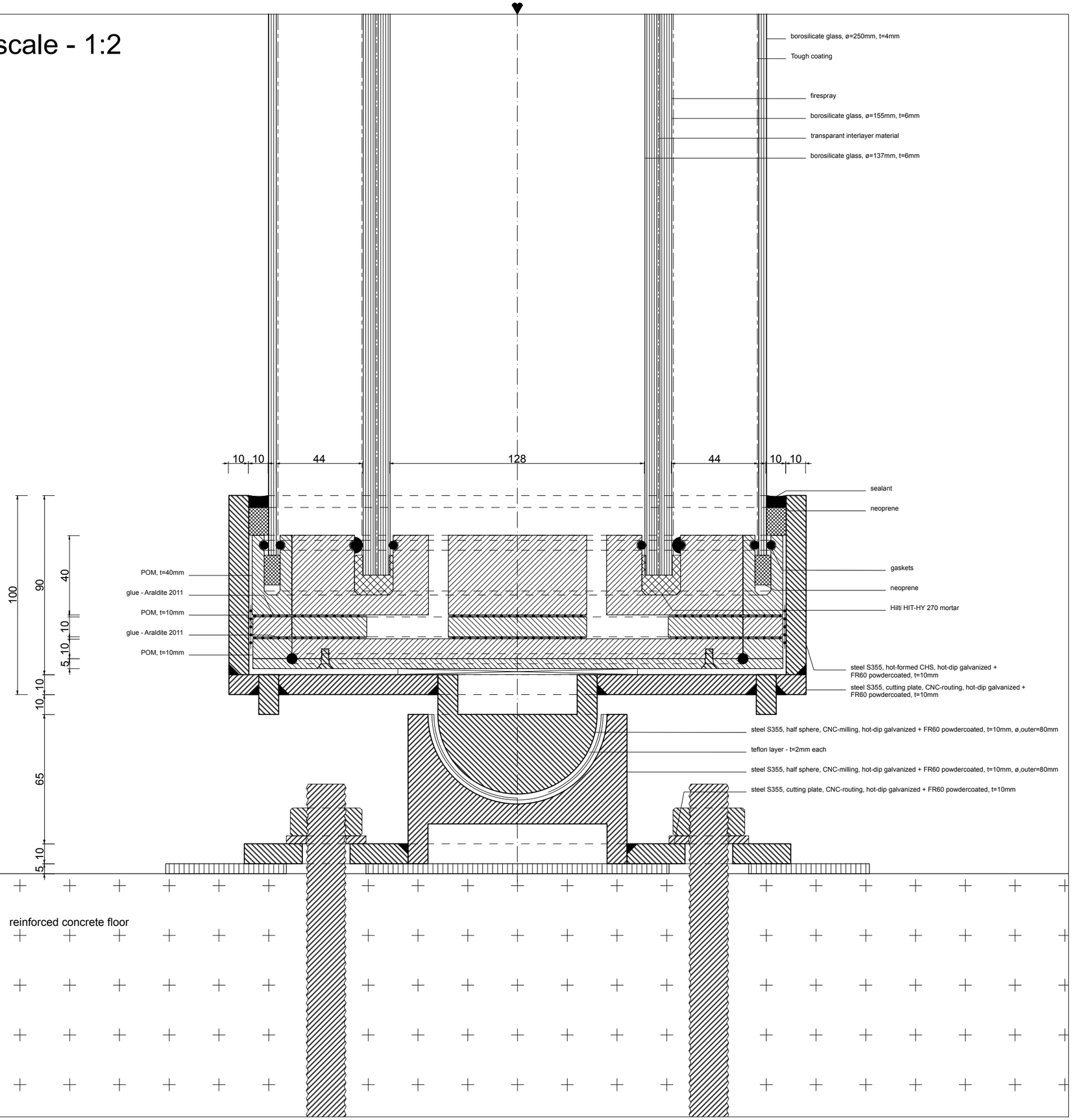

MLA - 1

scale - 1:25

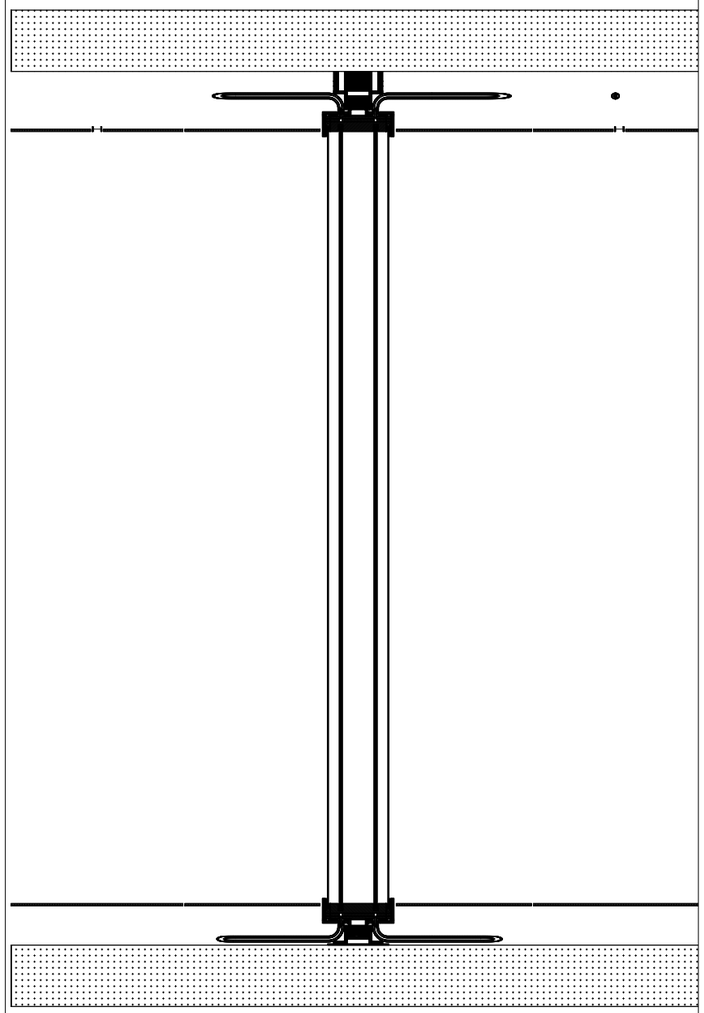

scale - 1:2

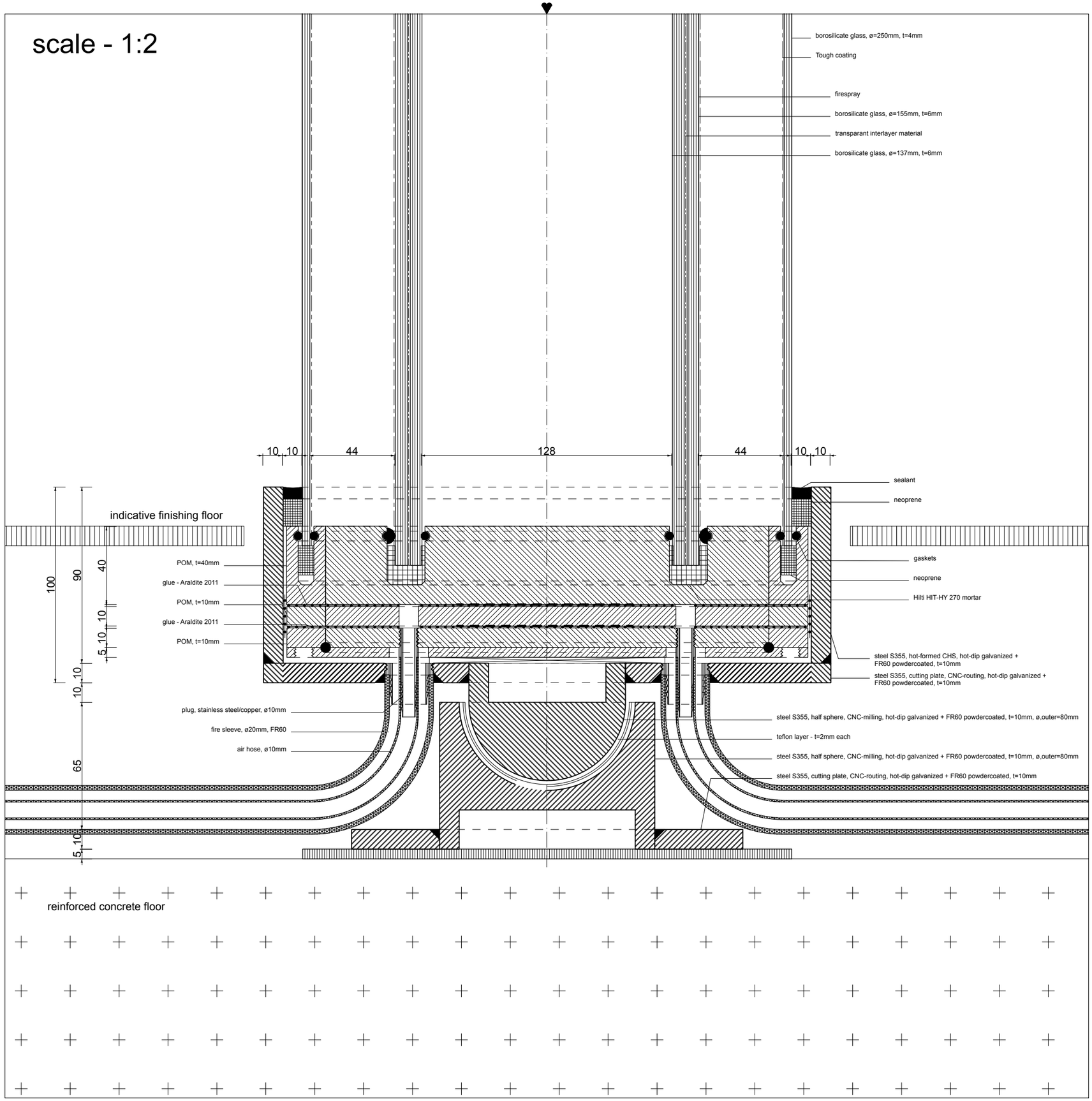

MLA - 2

scale - 1:25

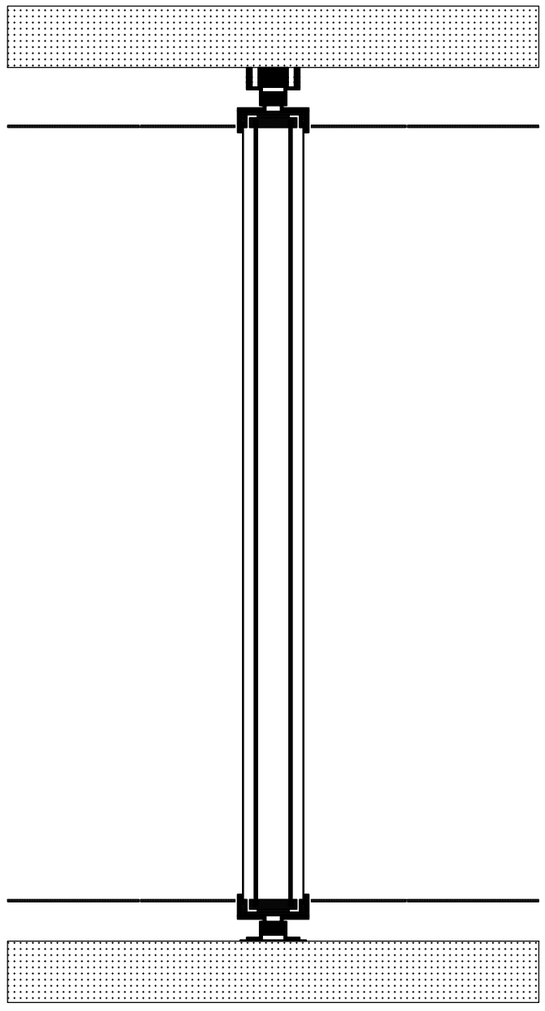

scale - 1:2

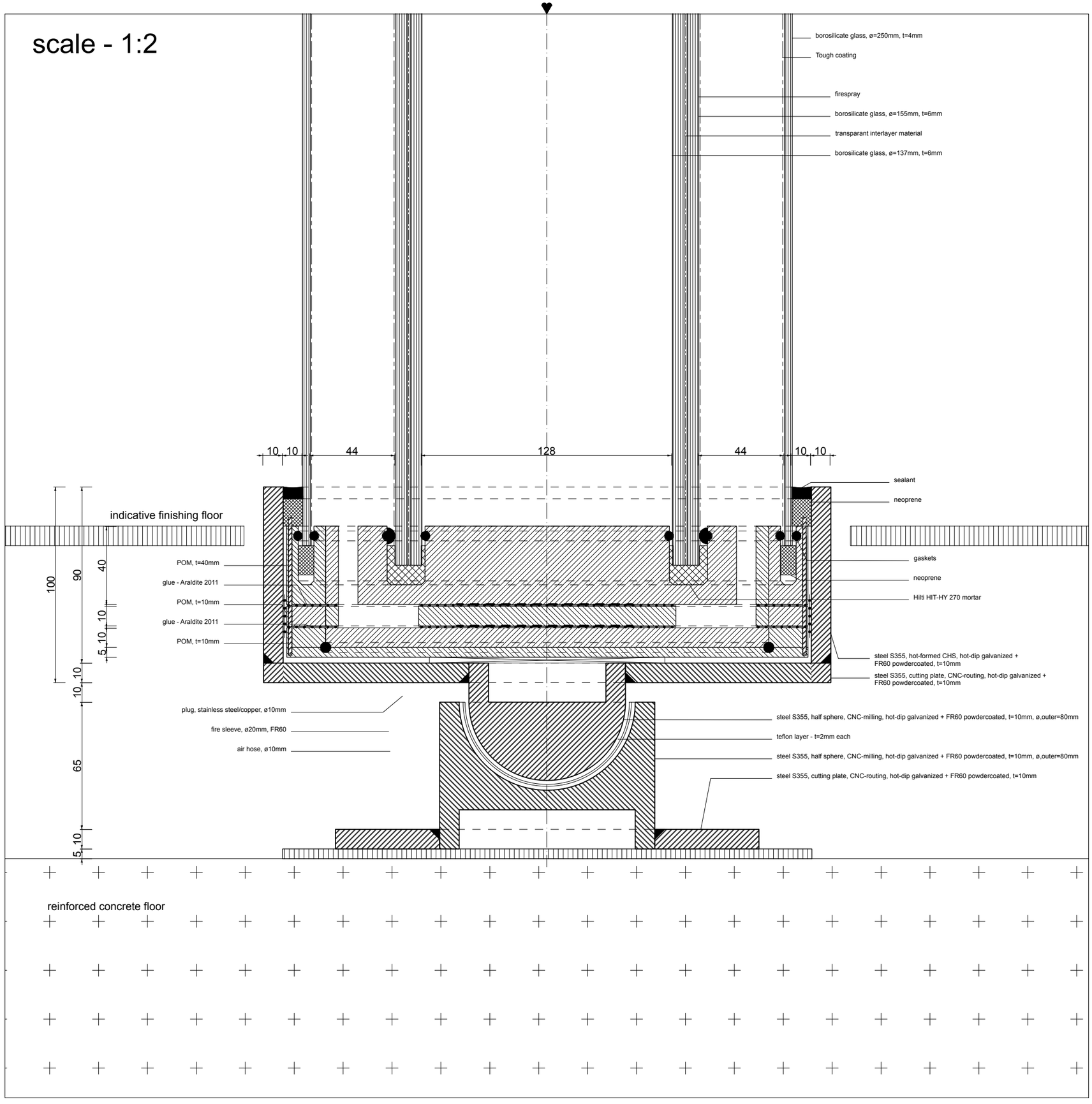

MLA - 3

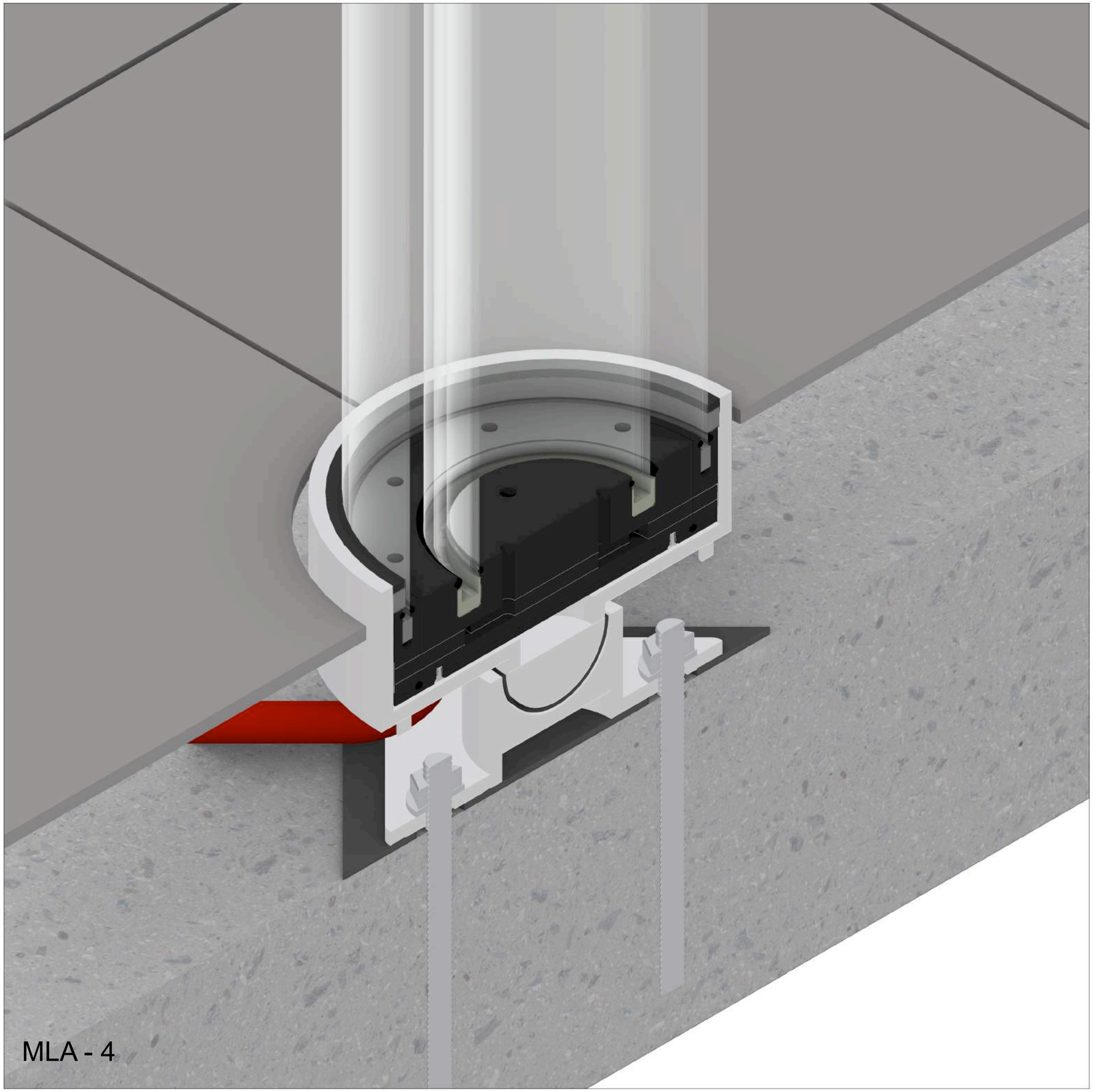

MLA - 4

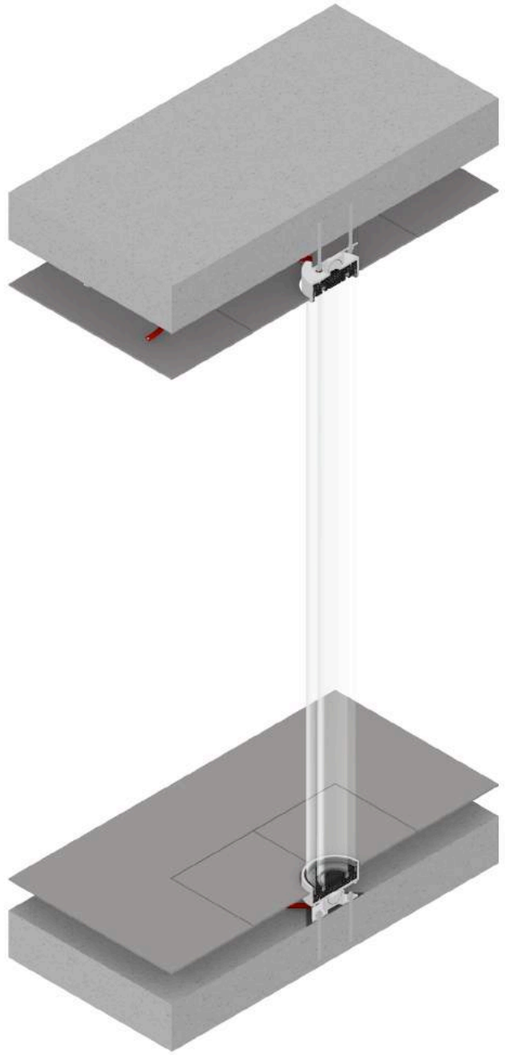

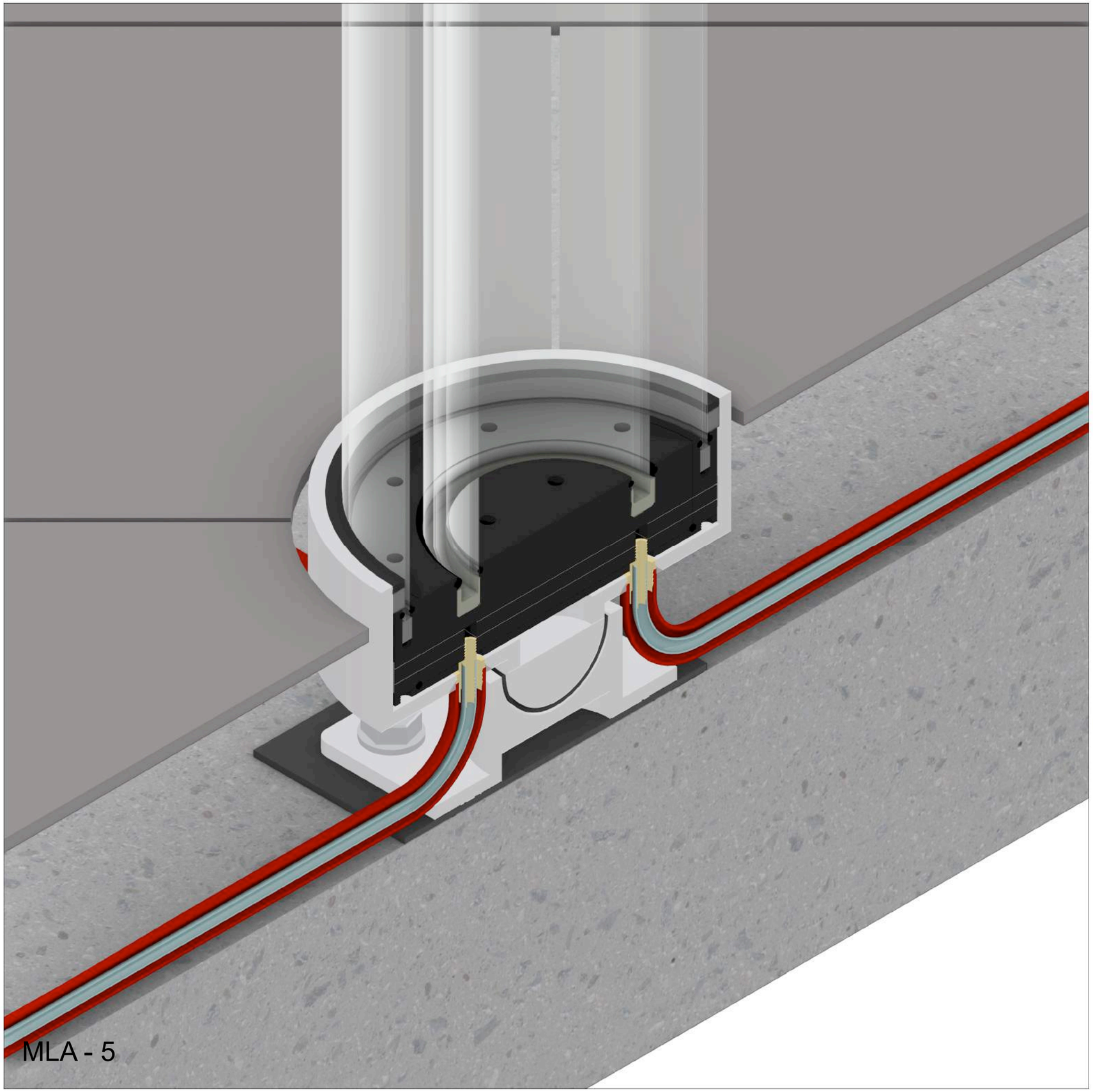

MLA - 5

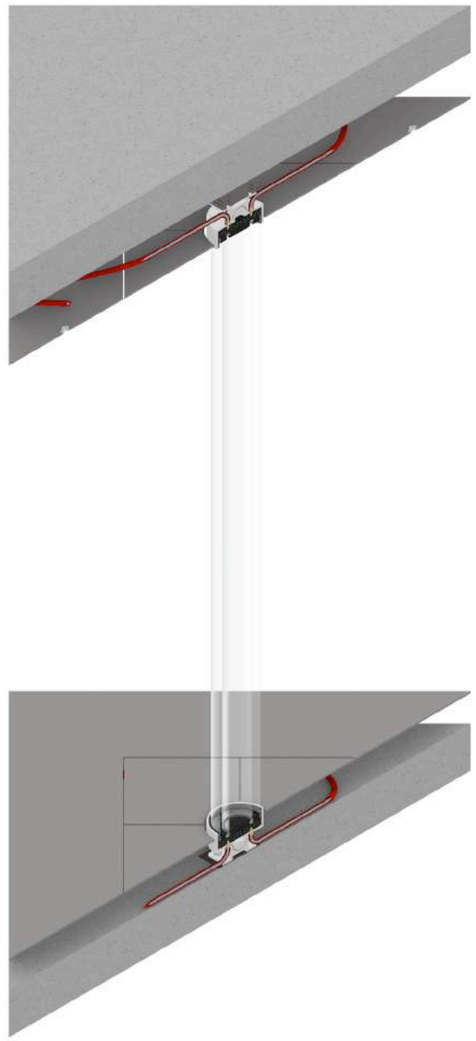

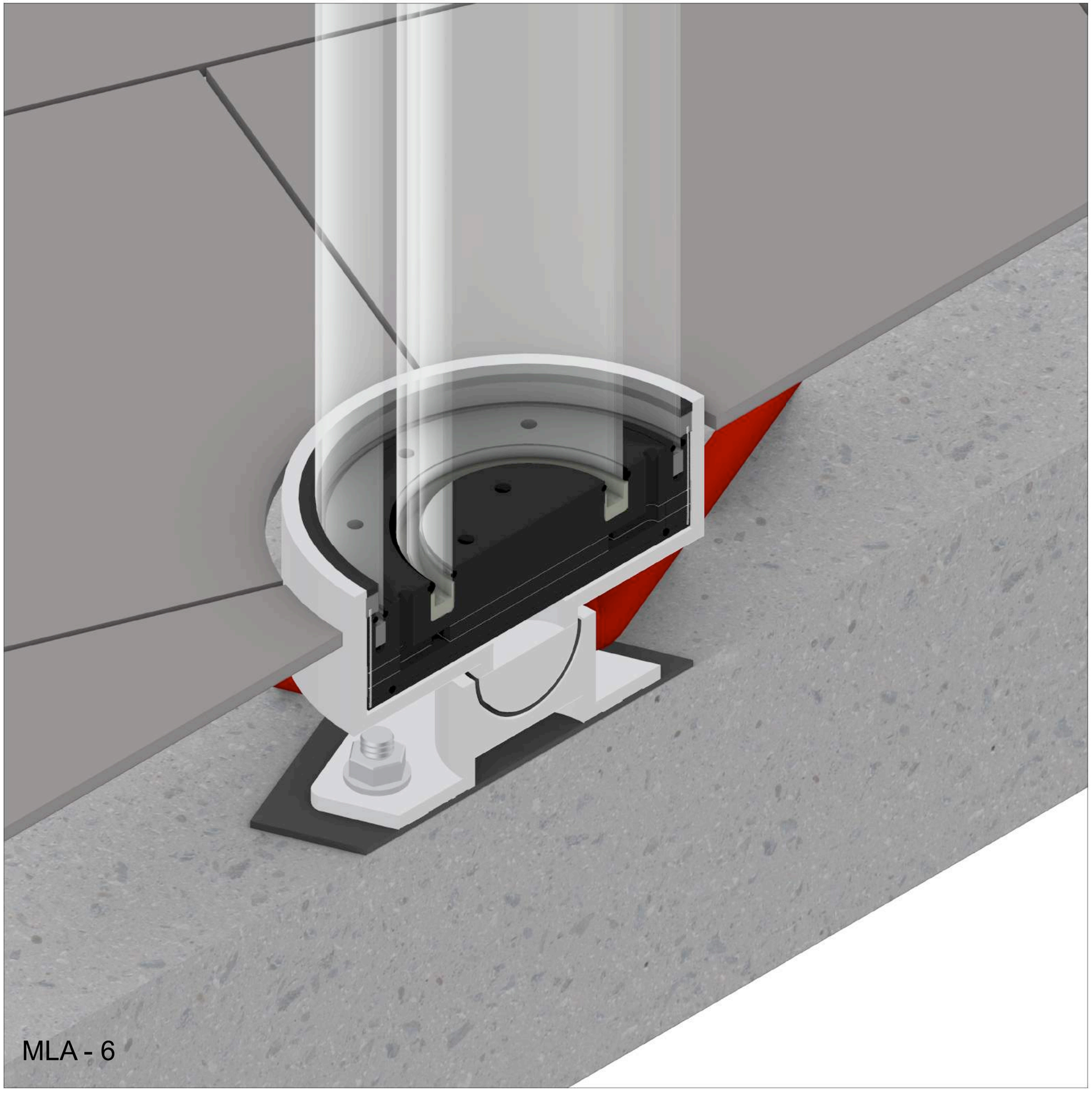

MLA - 6

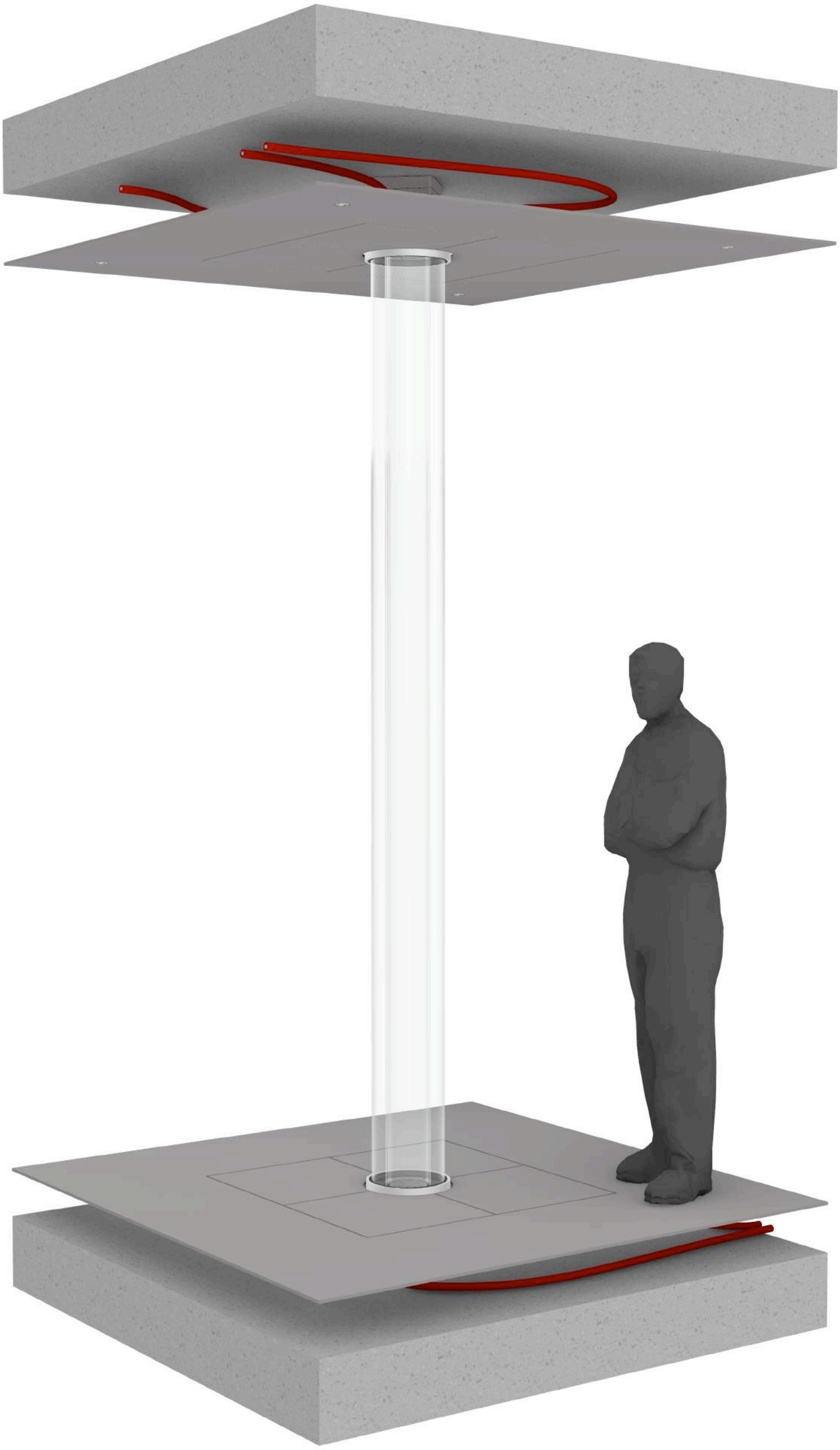

MLA - 7

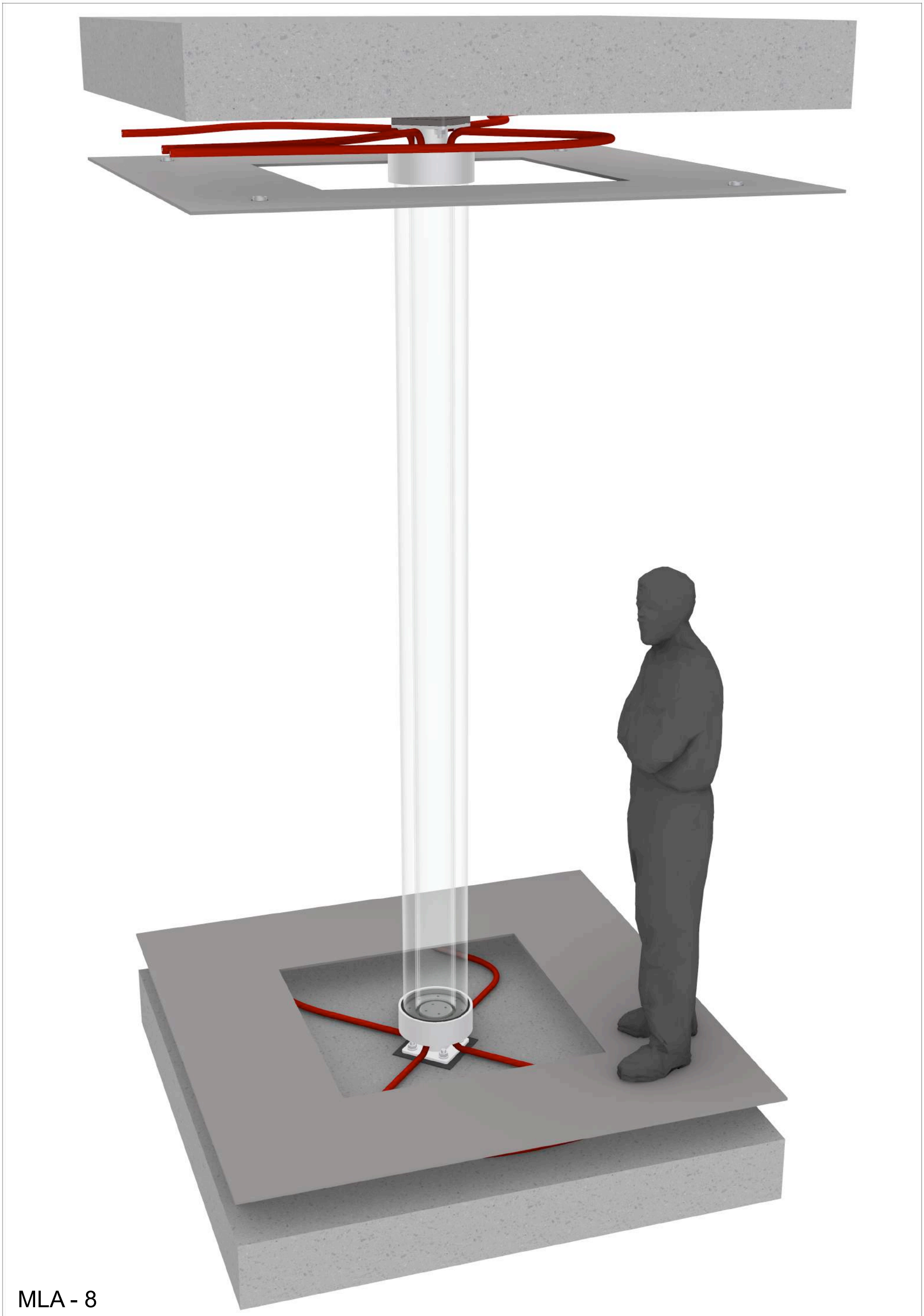

MLA - 8

scale - 1:25

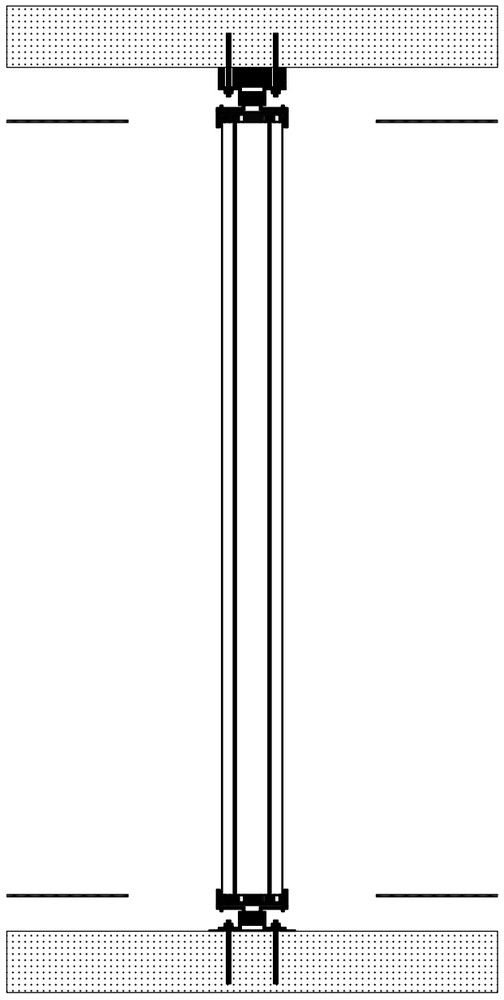

scale - 1:2

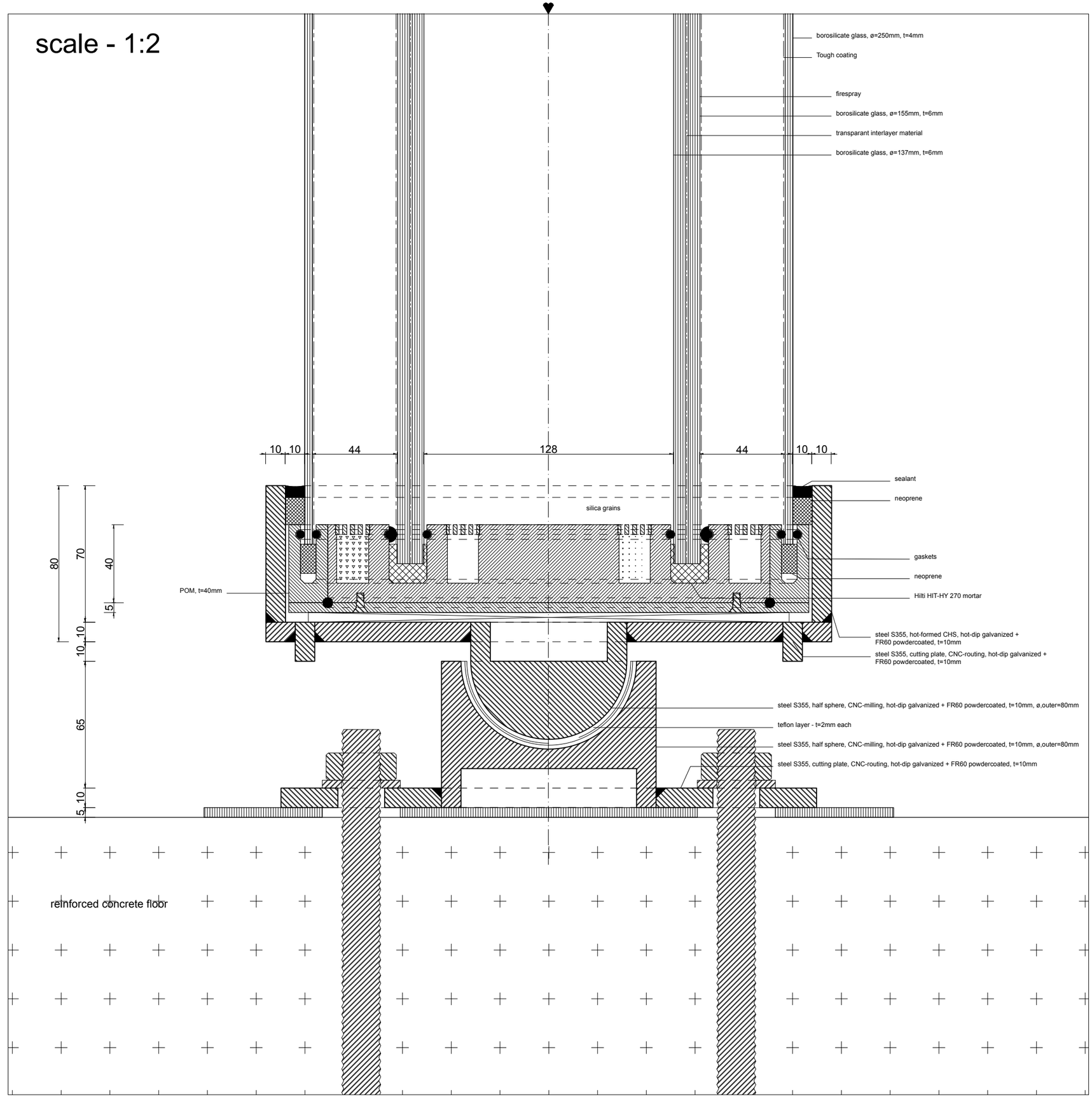

MLG - 1

scale - 1:25

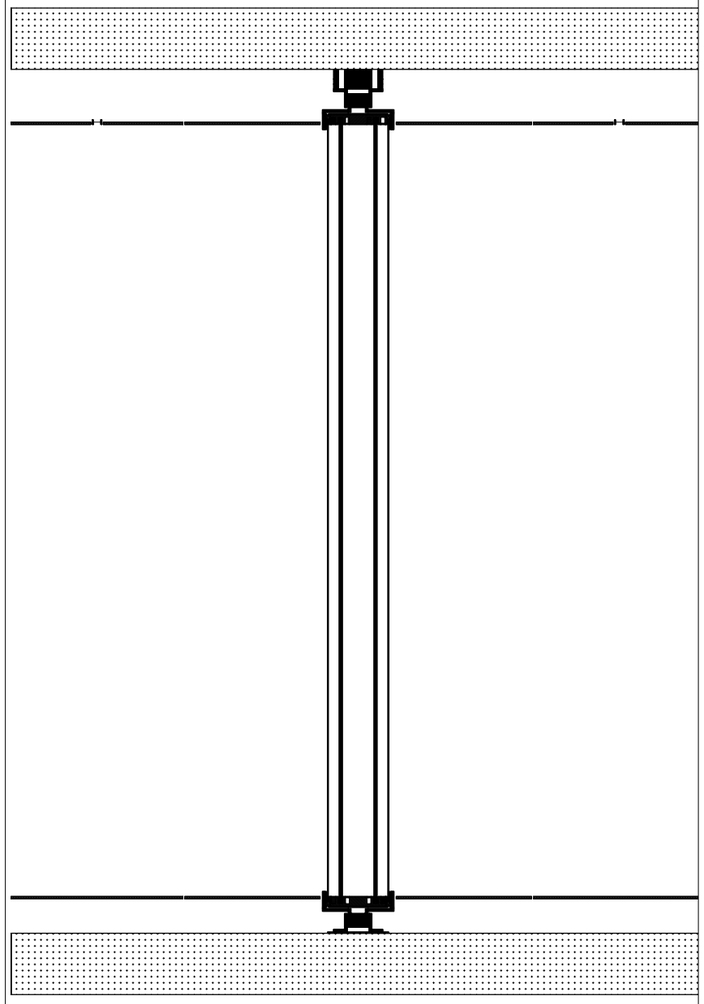

scale - 1:2

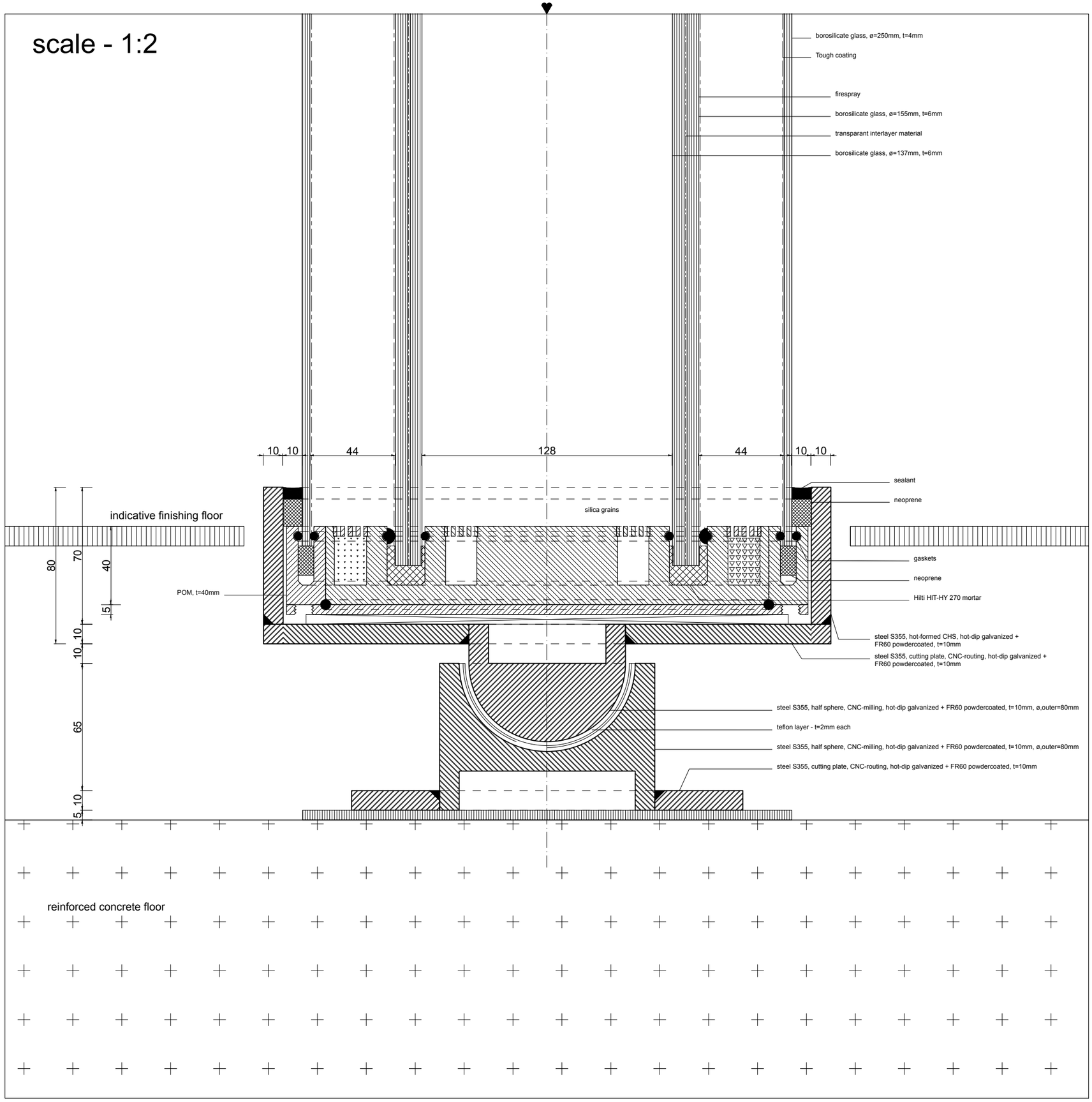

MLG - 2

scale - 1:25

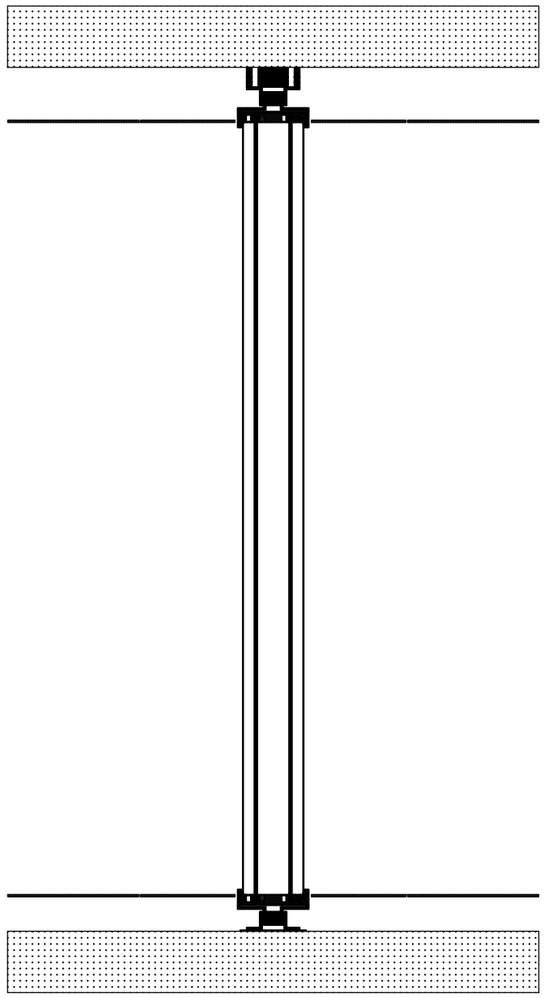

scale - 1:2

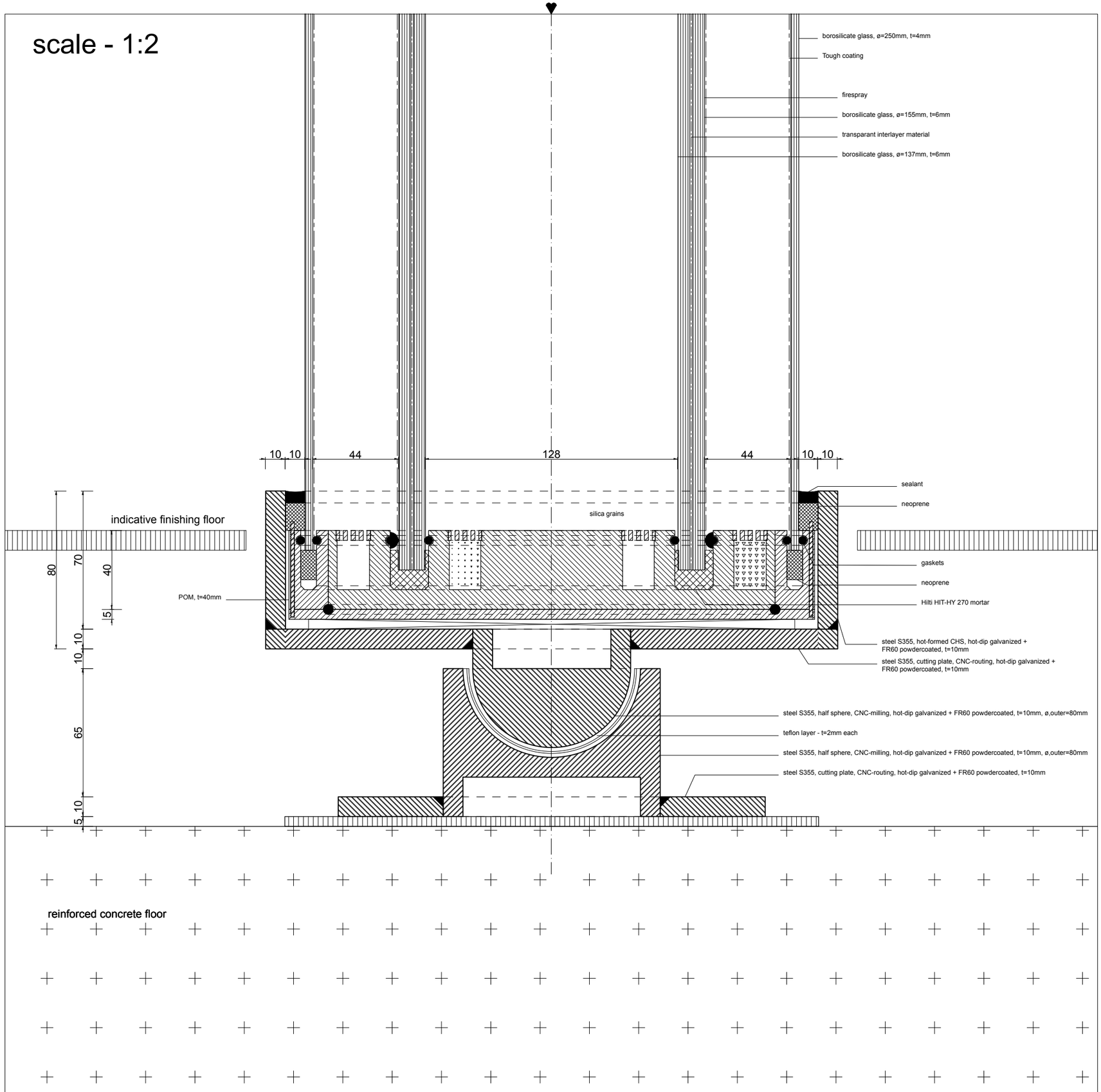

MLG - 3

MLG - 4

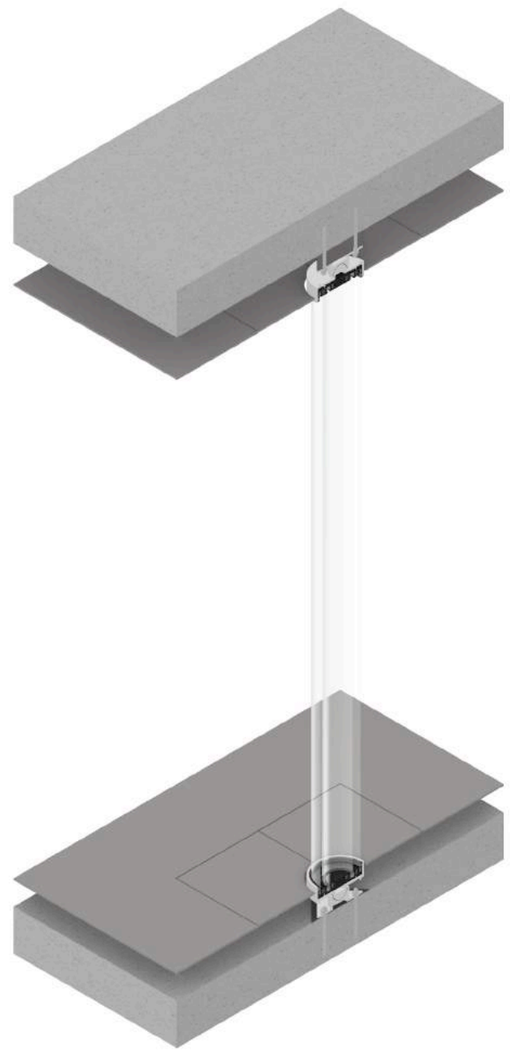

MLG - 5

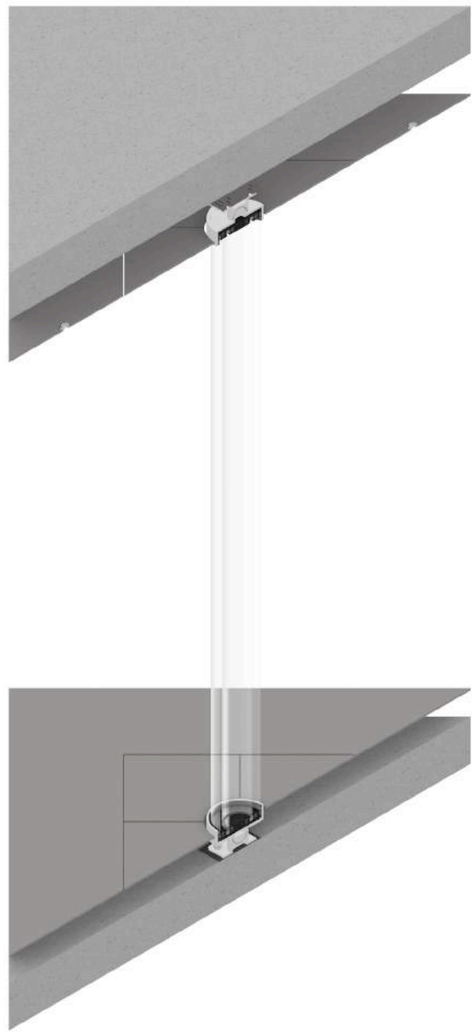

MLG - 6

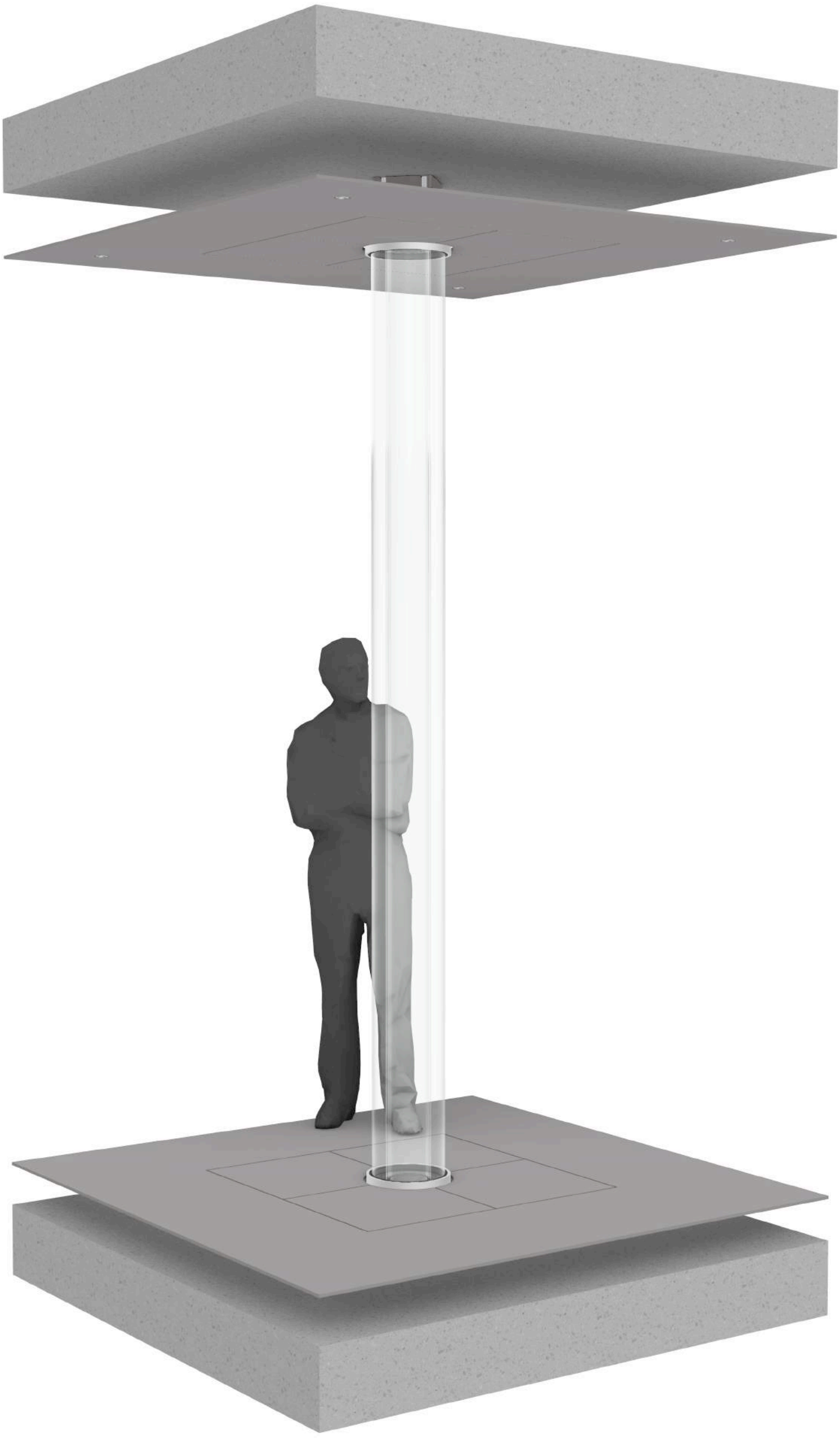

MLG - 7

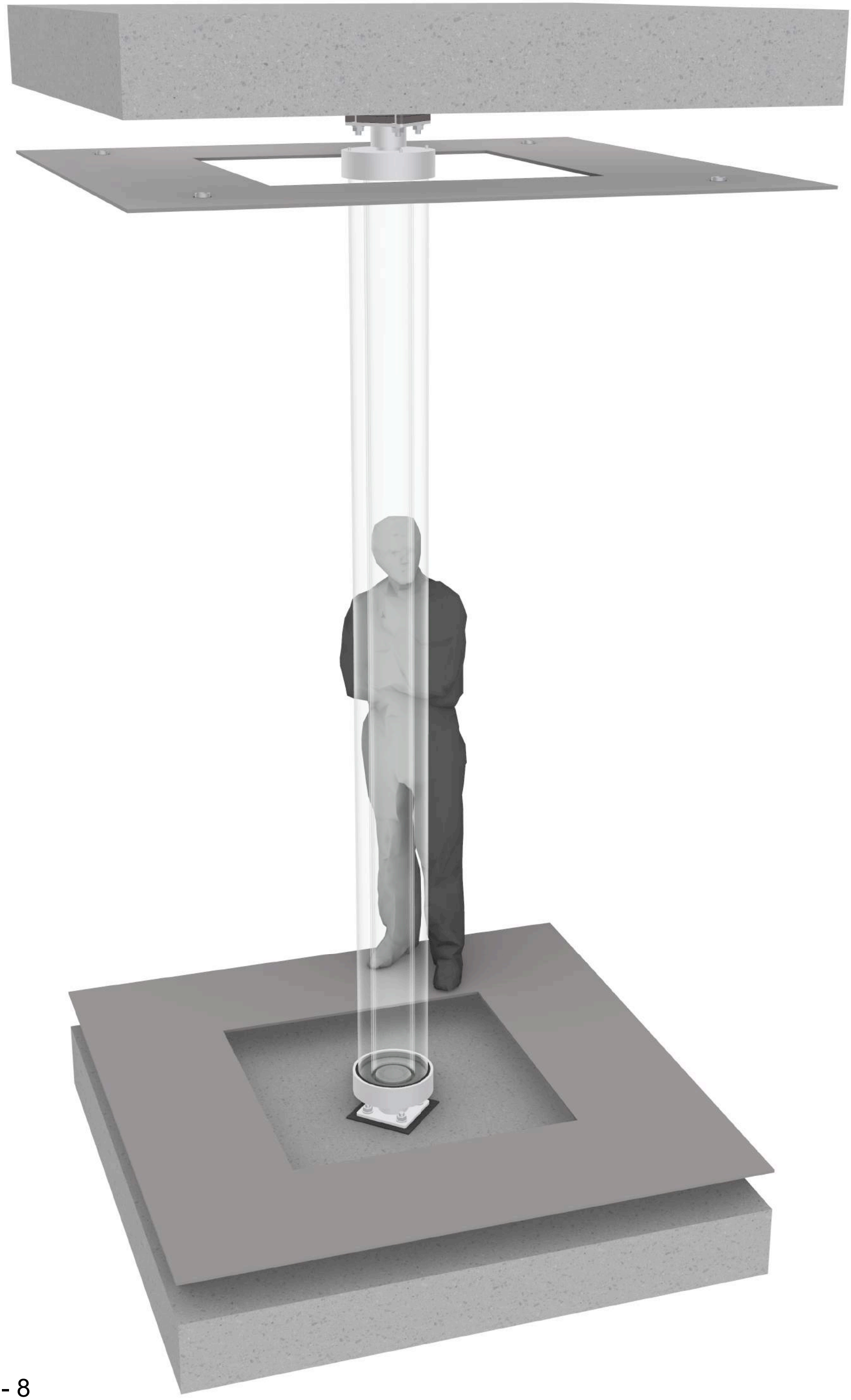

MLG - 8

scale - 1:25

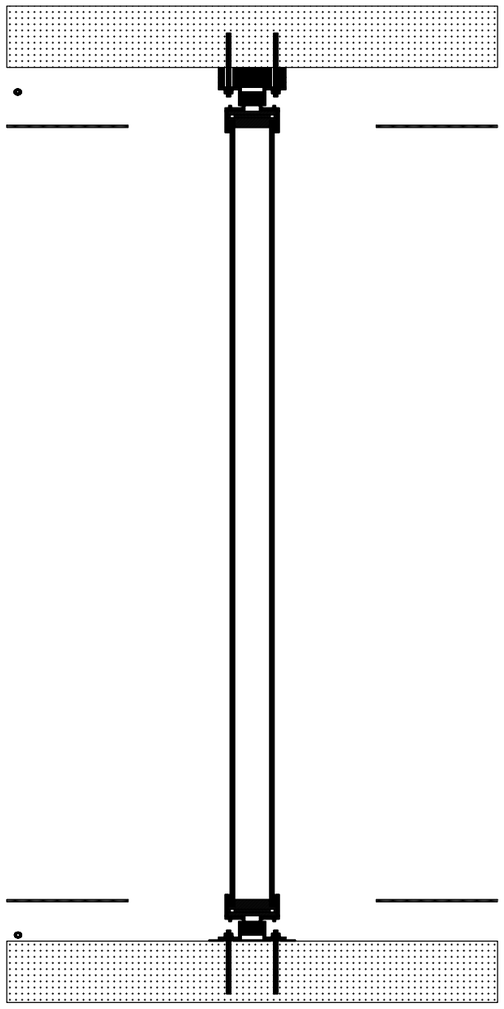

scale - 1:2

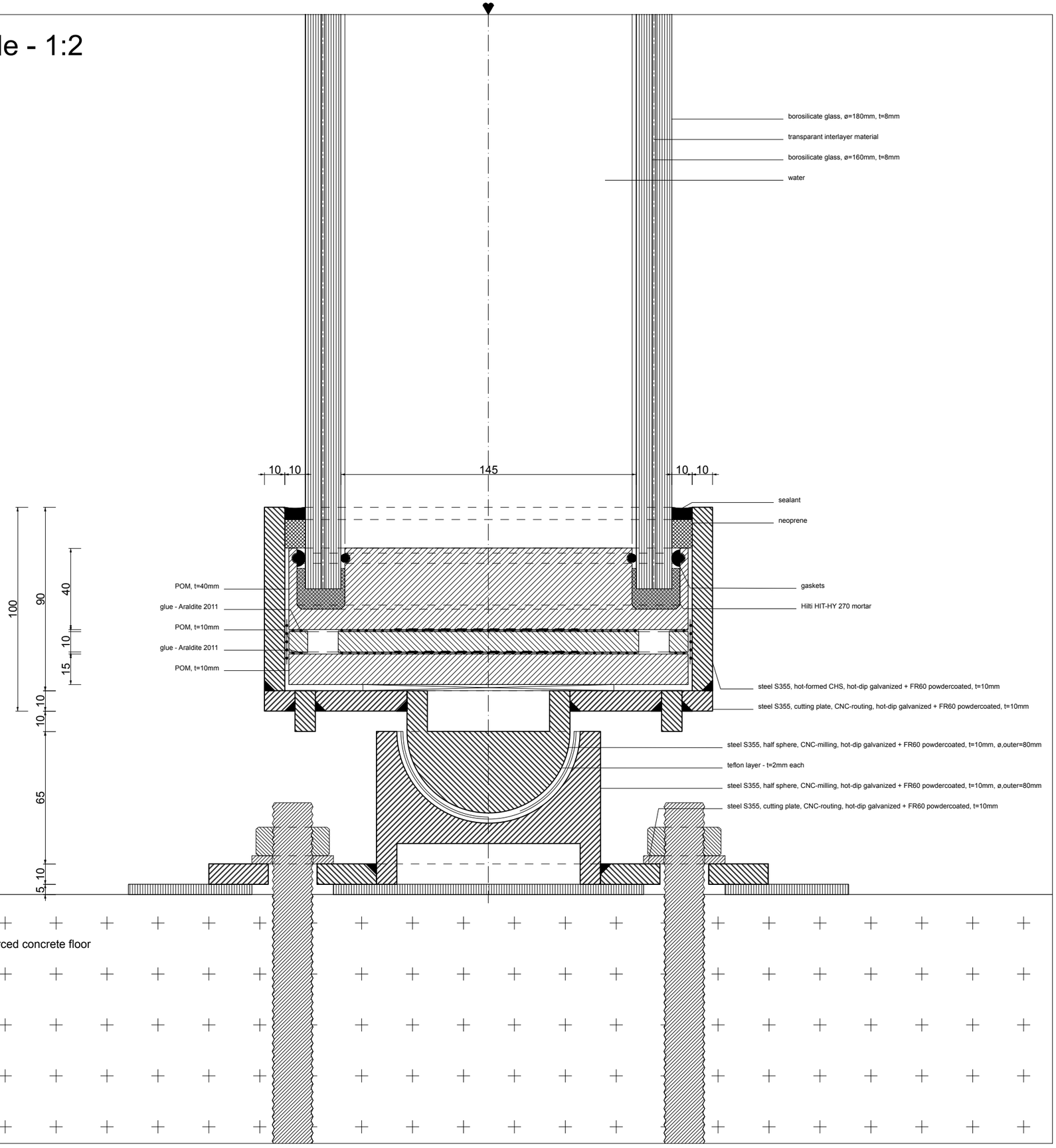

SLW - 1

scale - 1:25

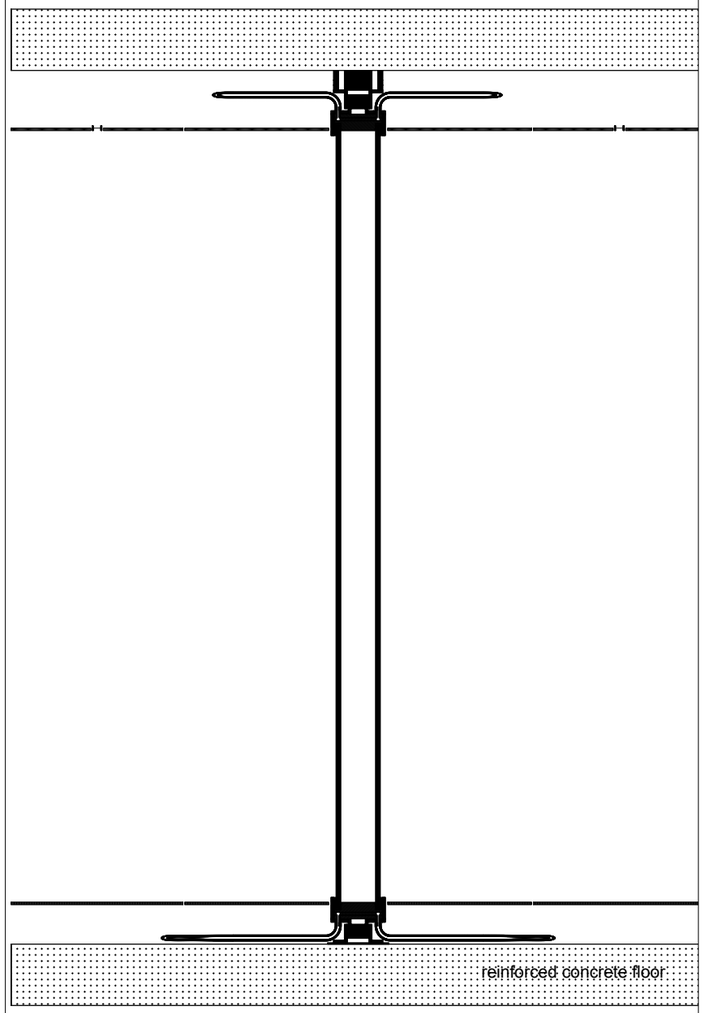

scale - 1:2

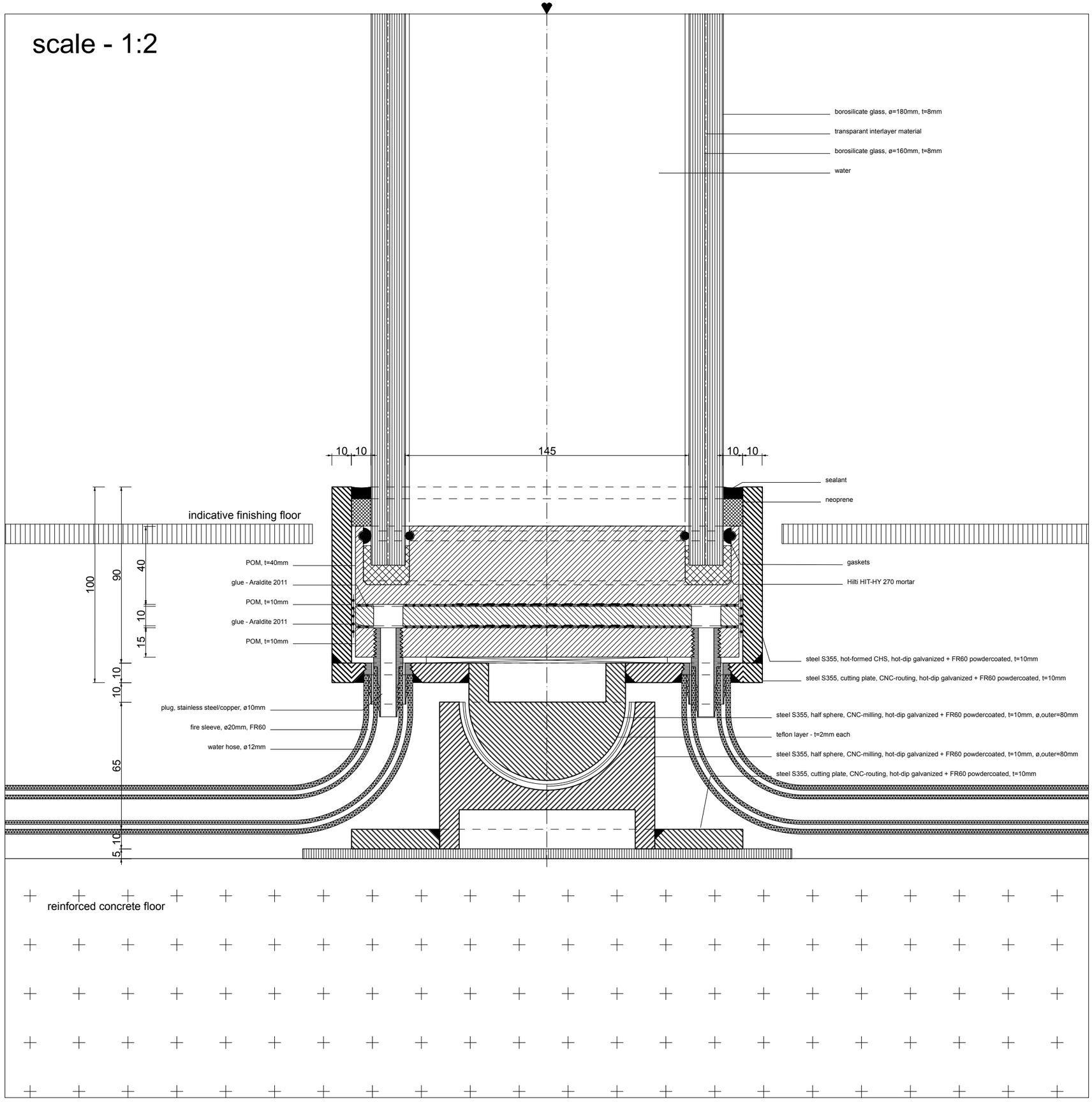

SLW - 2

scale - 1:25

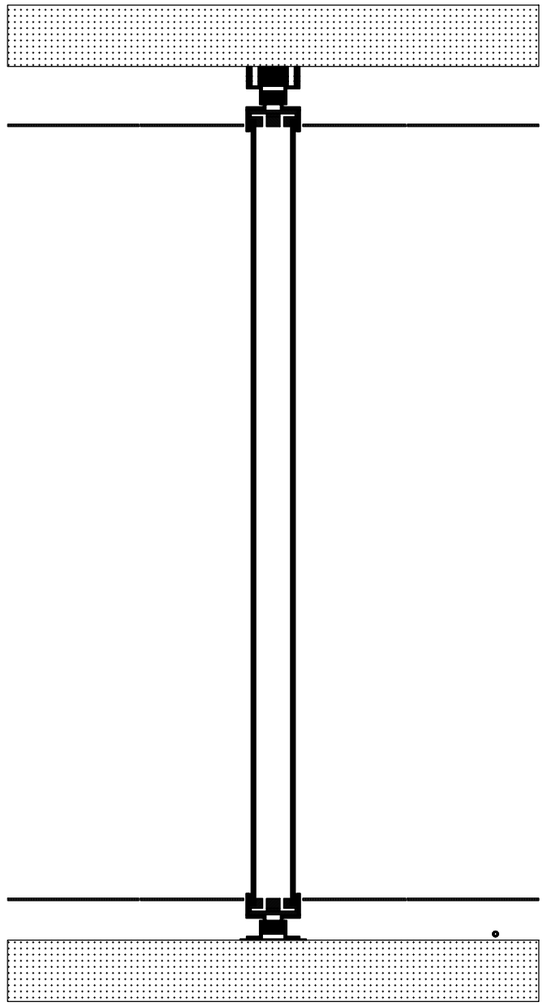

scale - 1:2

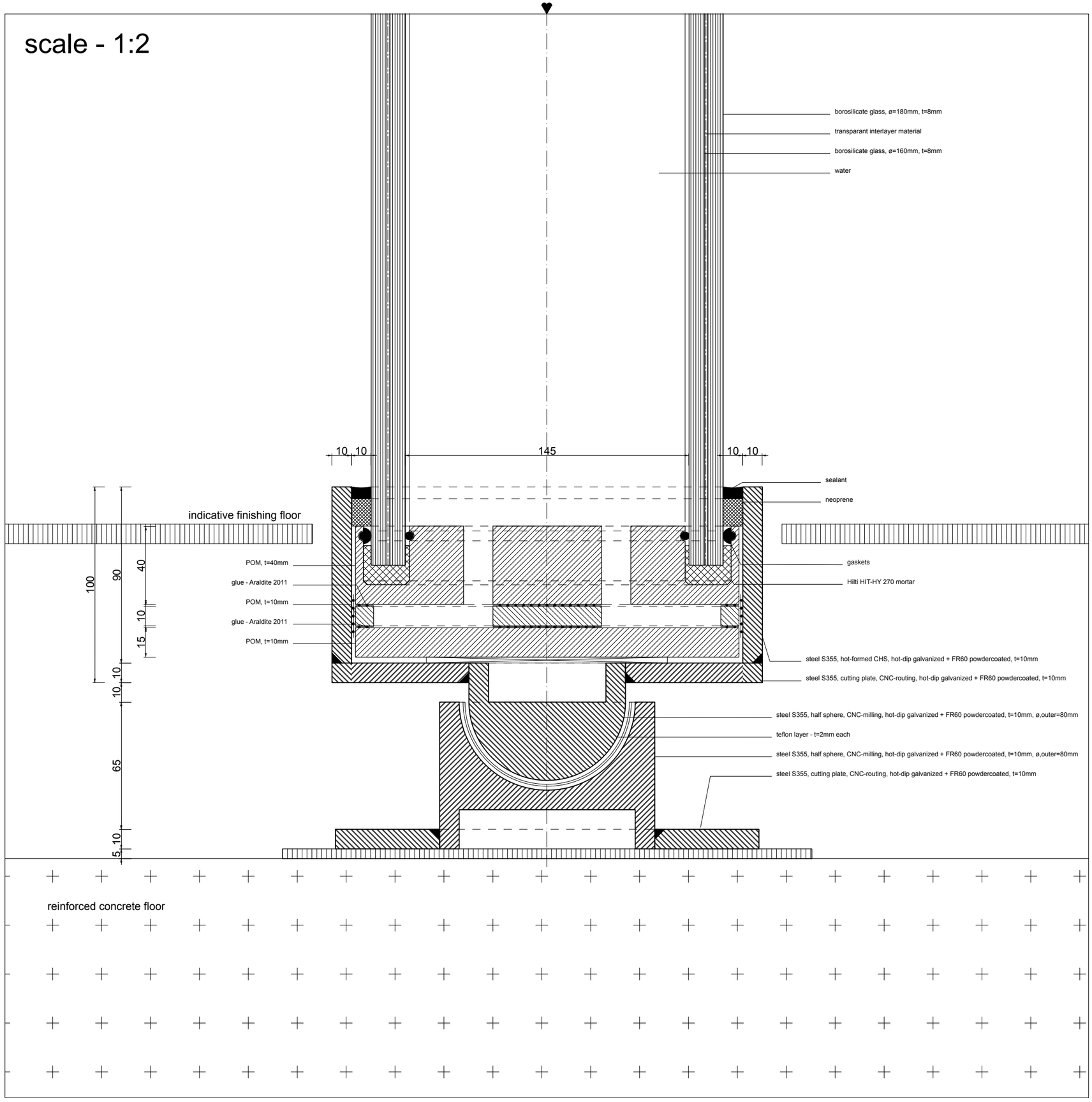

SLW - 3

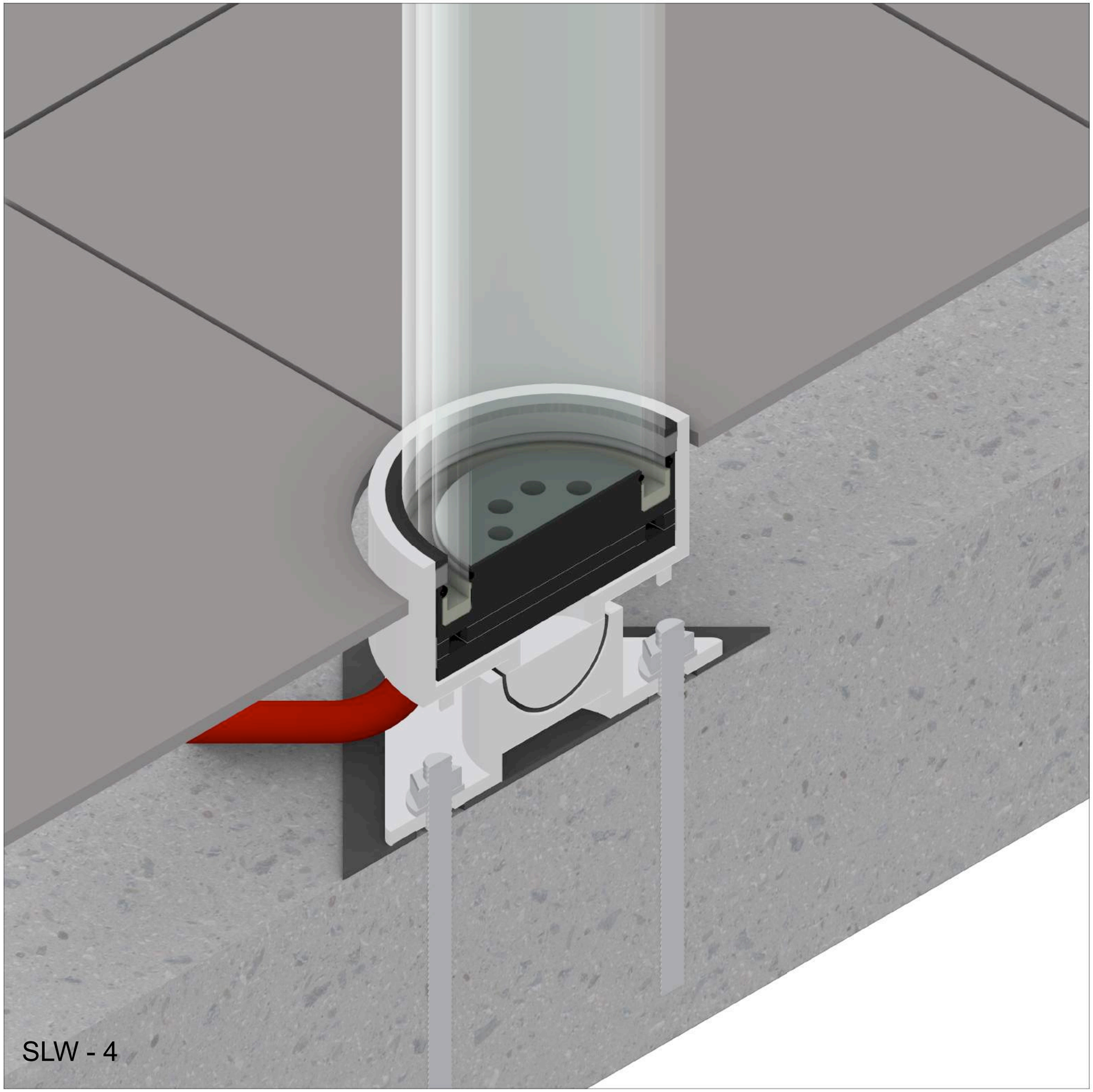

SLW - 4

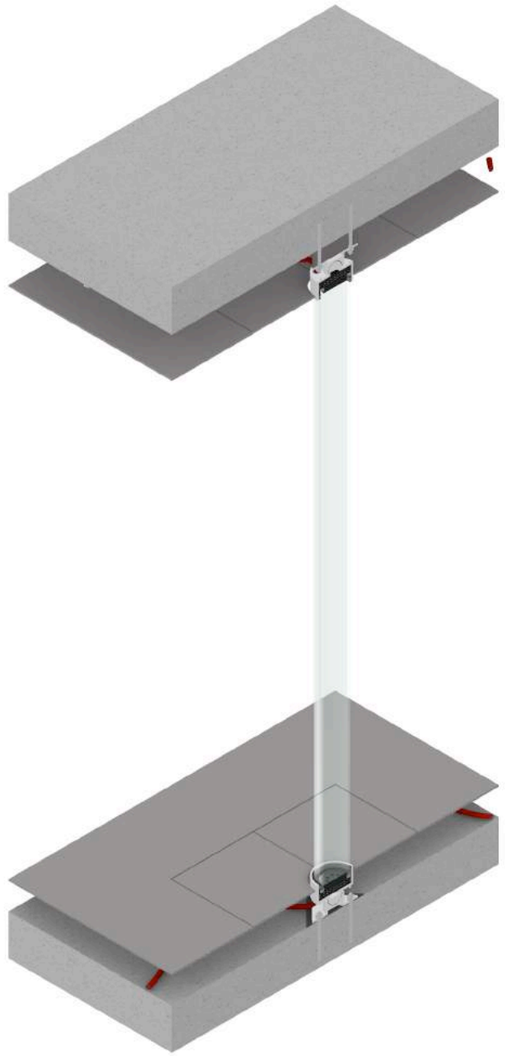

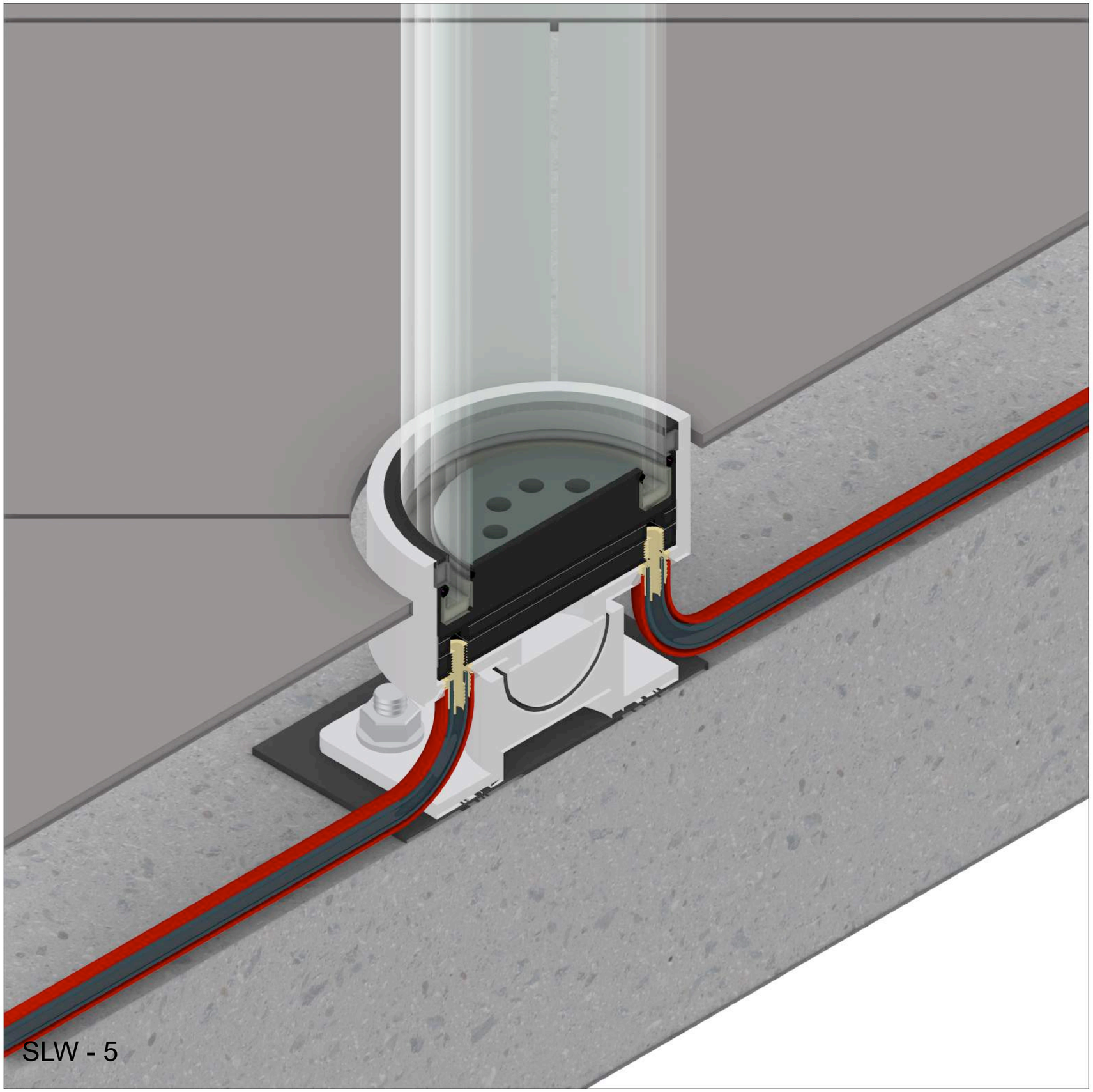

SLW - 5

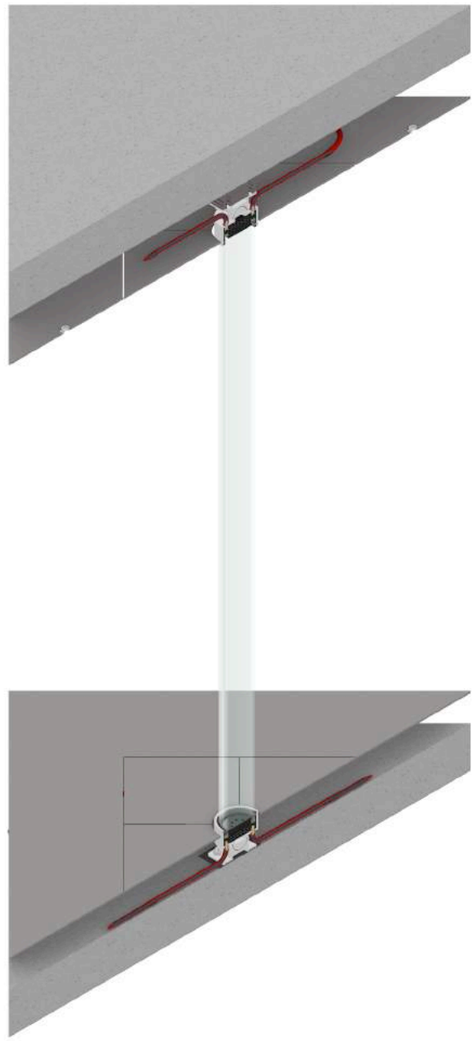

SLW - 6

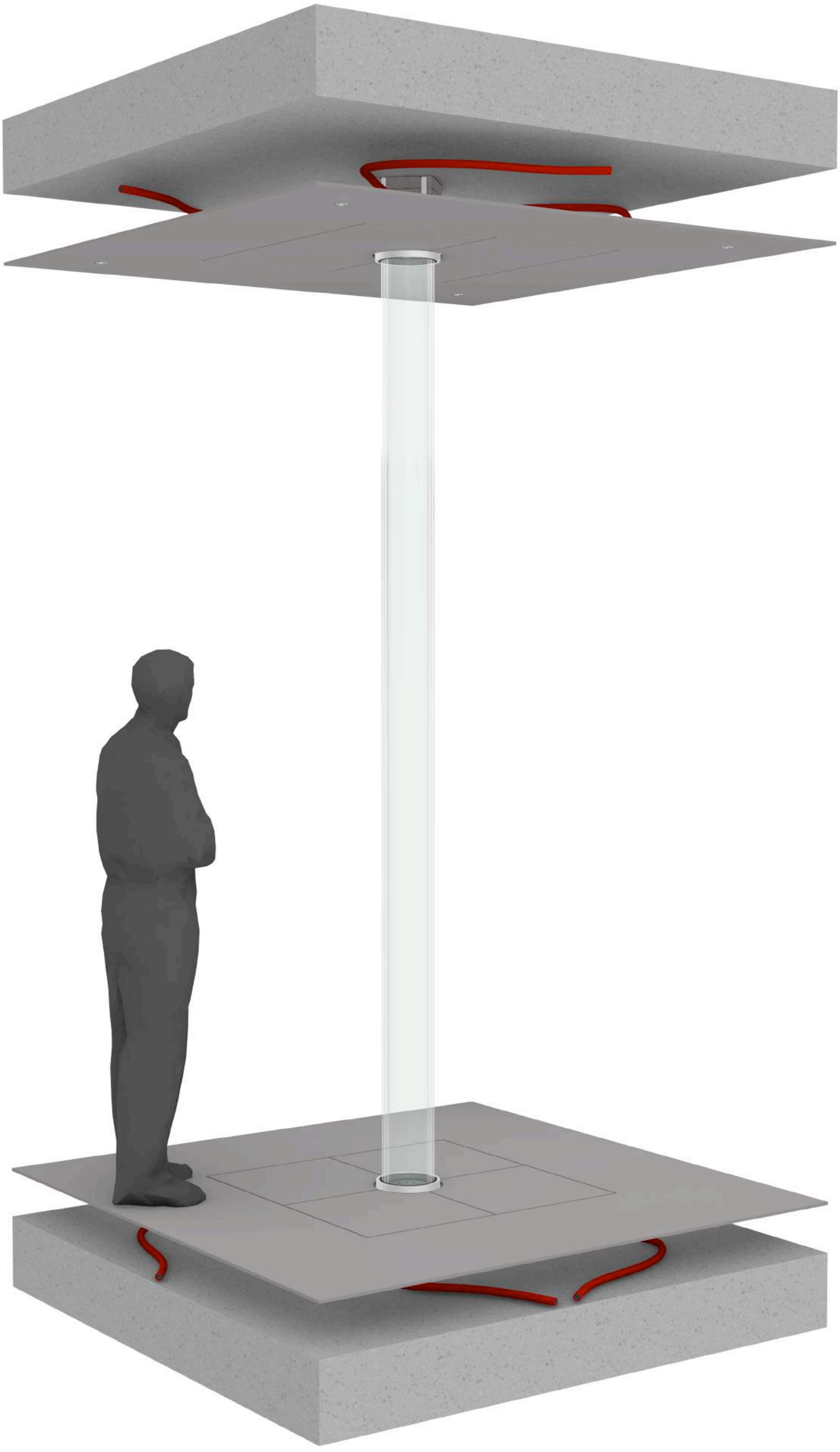

SLW - 7

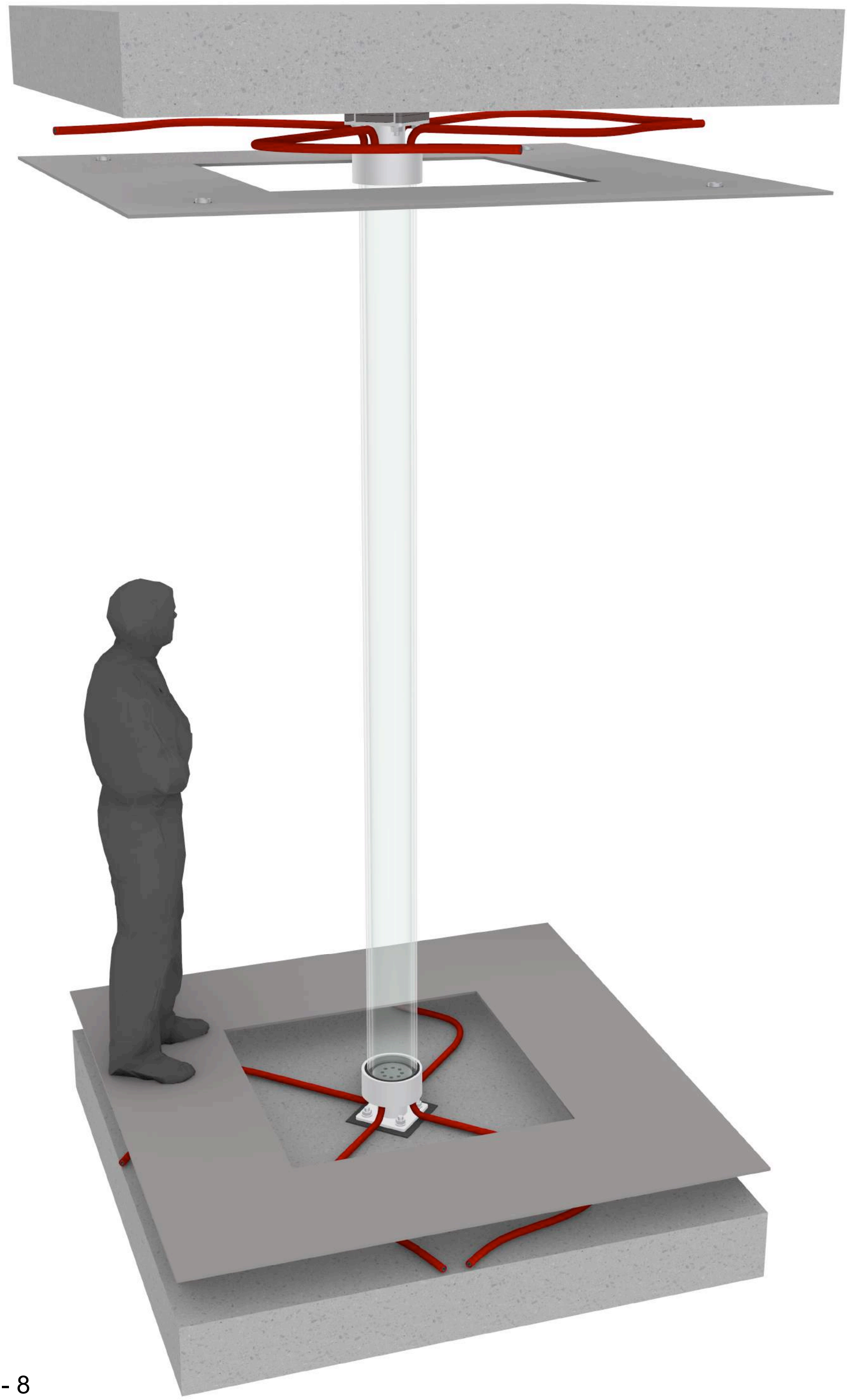

SLW - 8

Case Study Bouwdeel D:

3D view of the Bouwdeel D:

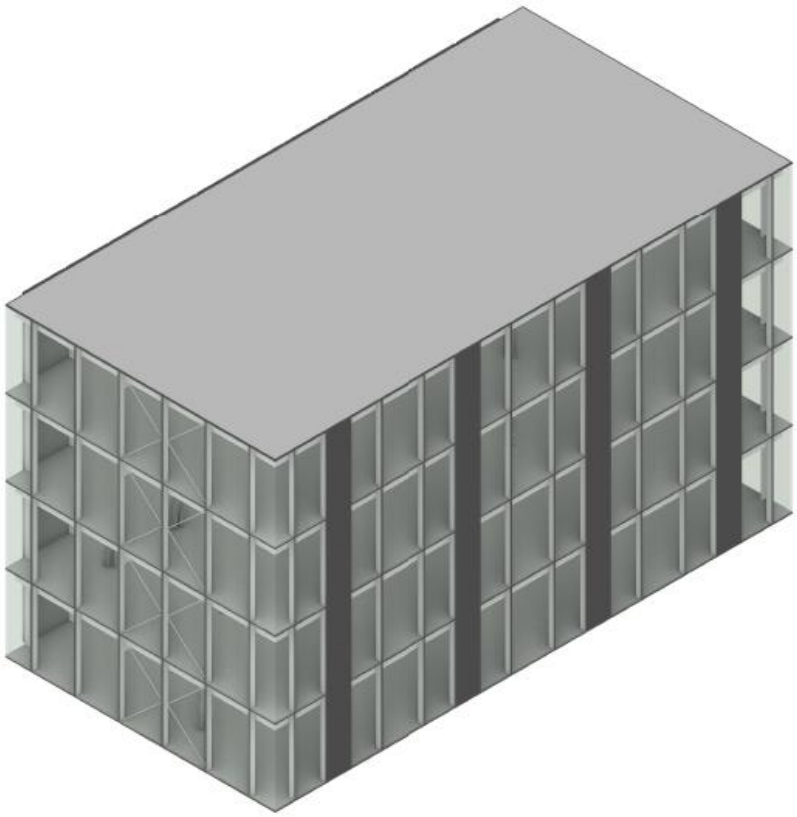

3D view: steel columns (current situation)

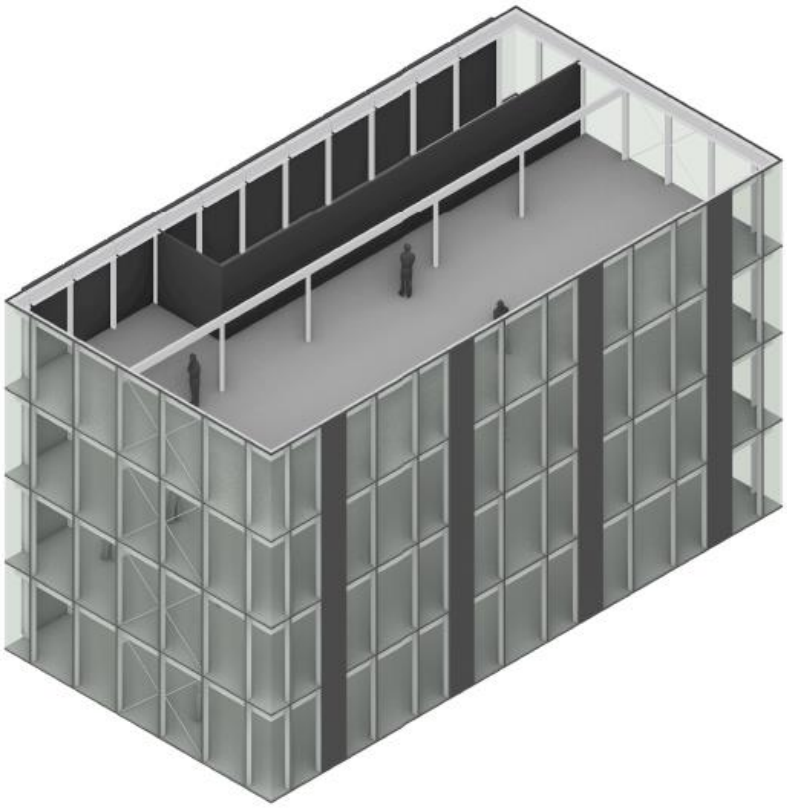

3D view: MLA (with air hoses)

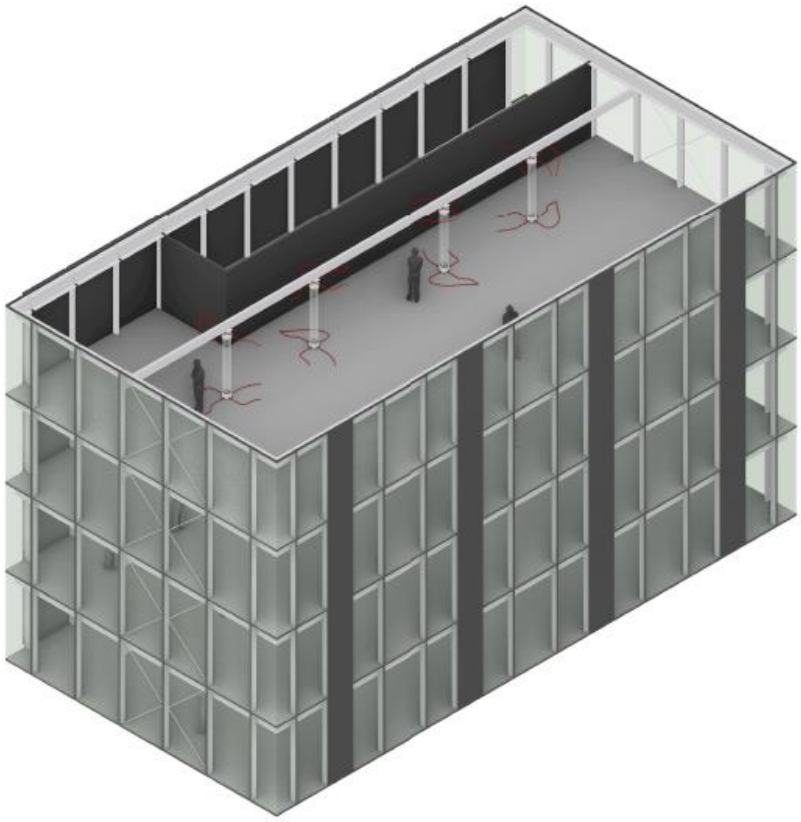

3D view: MLA (without air hoses)

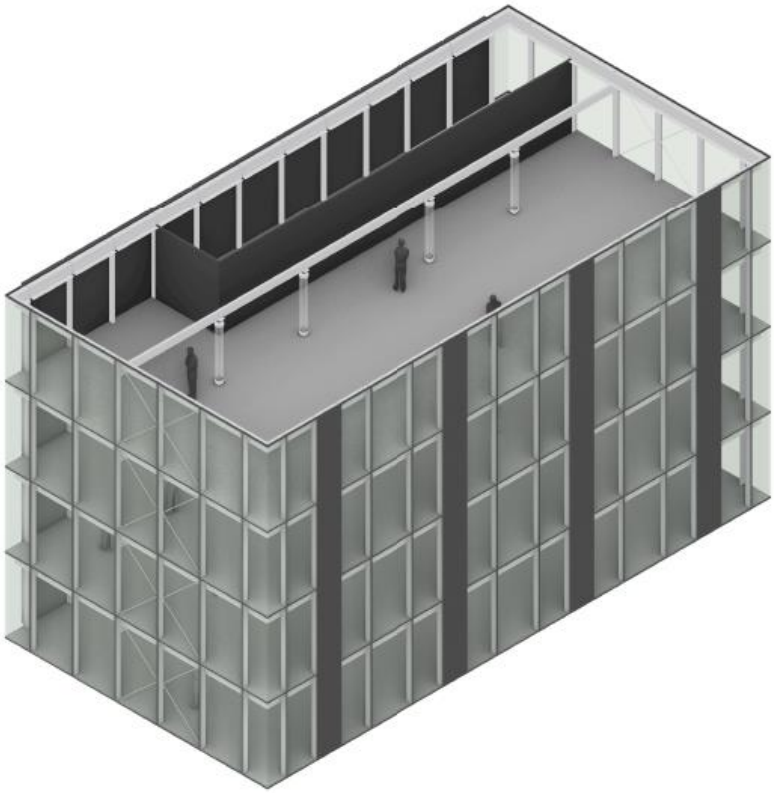

3D view: SLW (with water hoses)

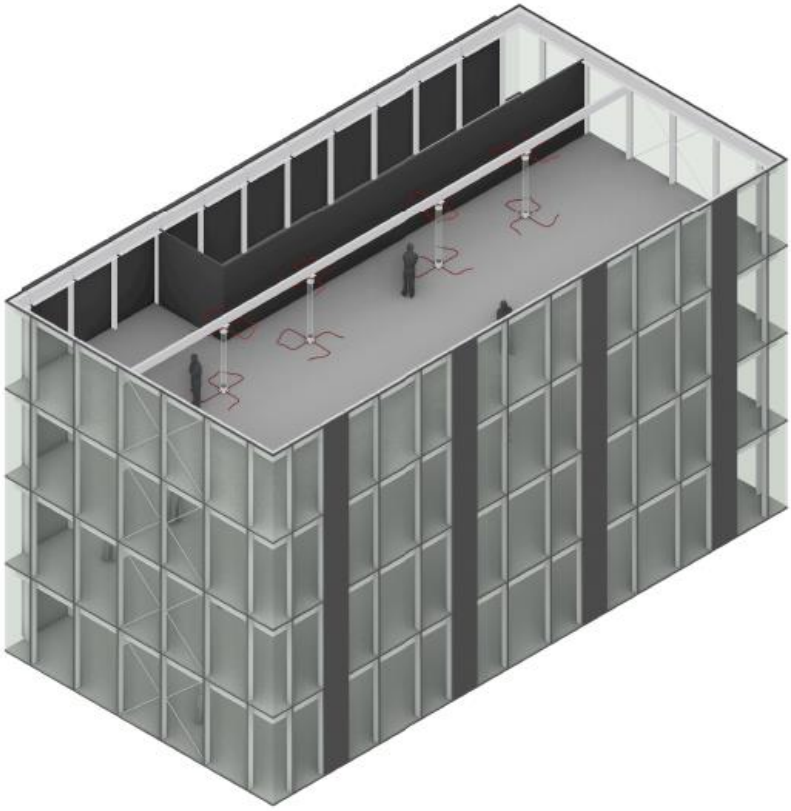

Perspective 1: steel columns (current situation)

Perspective 1: MLA (with air hoses)

Perspective 1: MLA (without air hoses)

Perspective 1: SLW (with water hoses)

Perspective 2: steel columns (current situation)

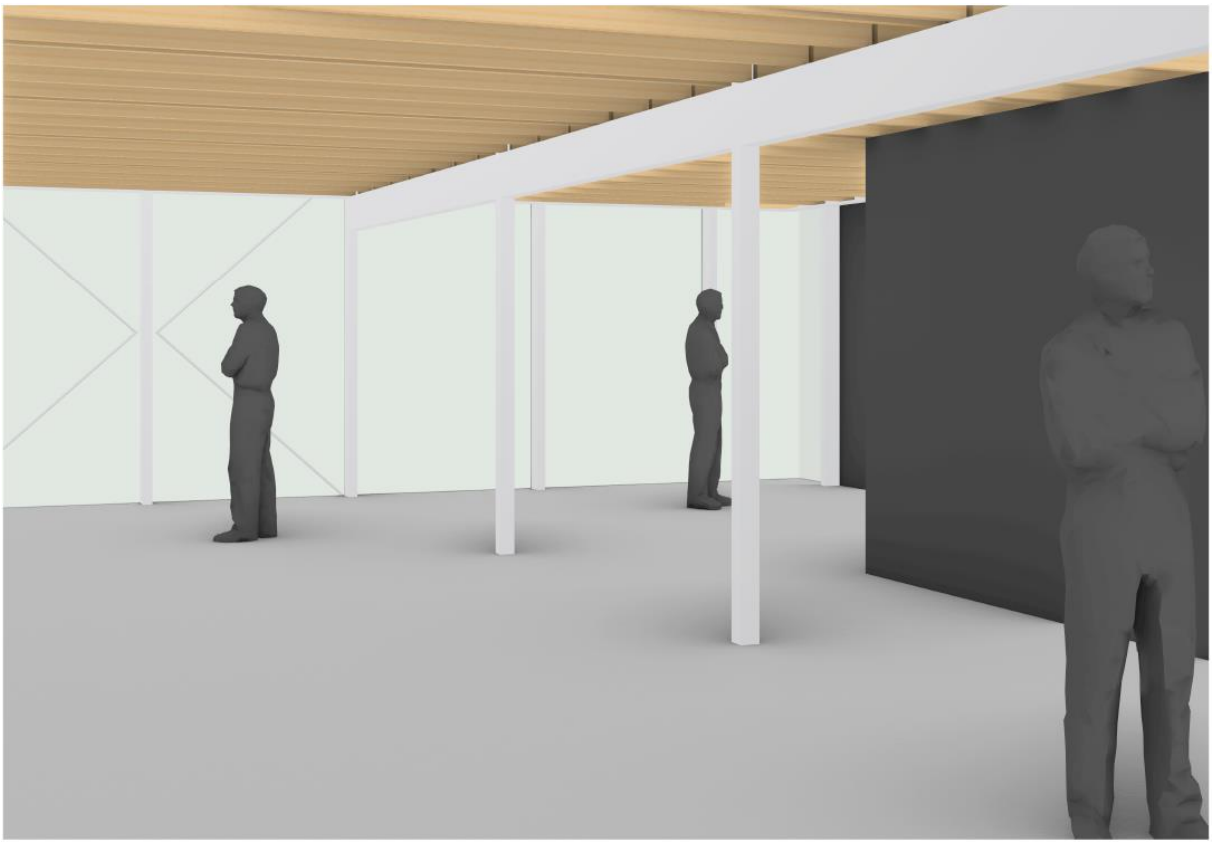

Perspective 2: MLA (with air hoses)

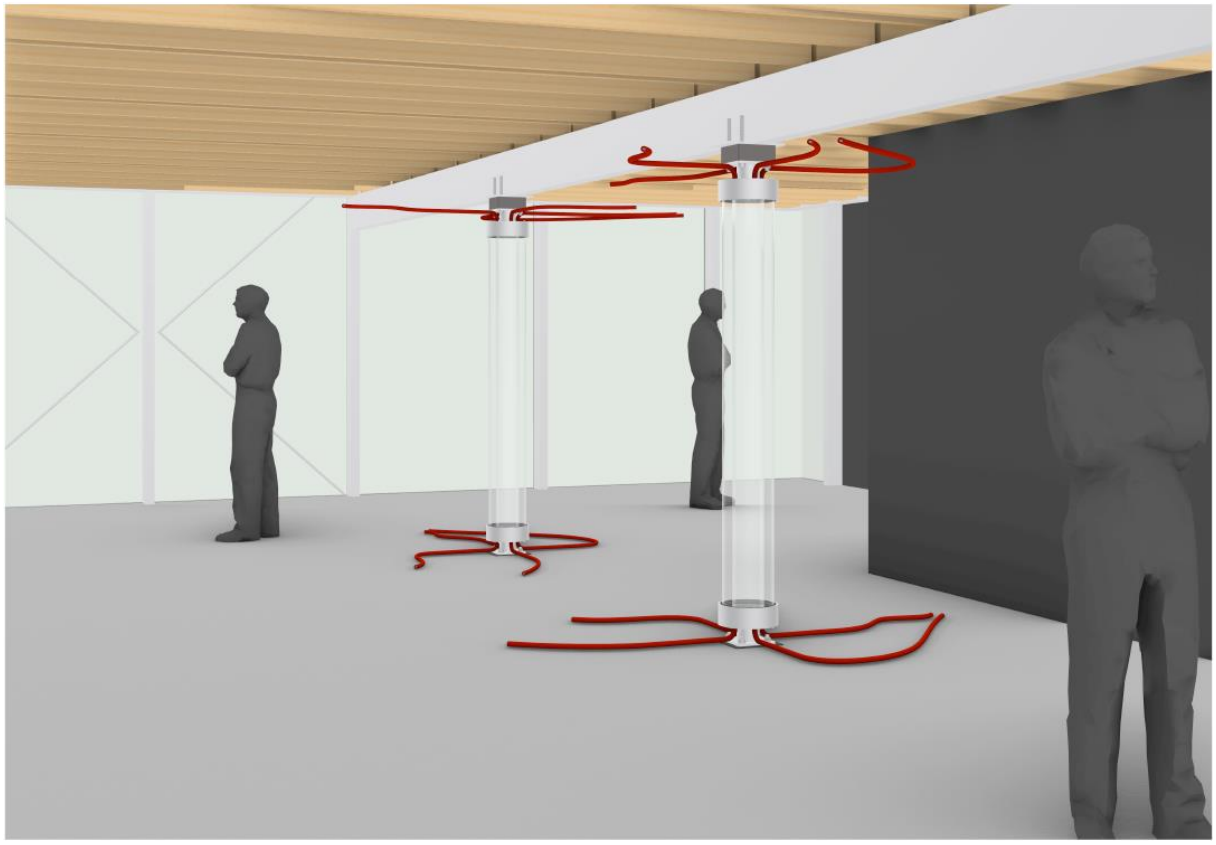

Perspective 2: MLA (without air hoses)

Perspective 2: SLW (with water hoses)

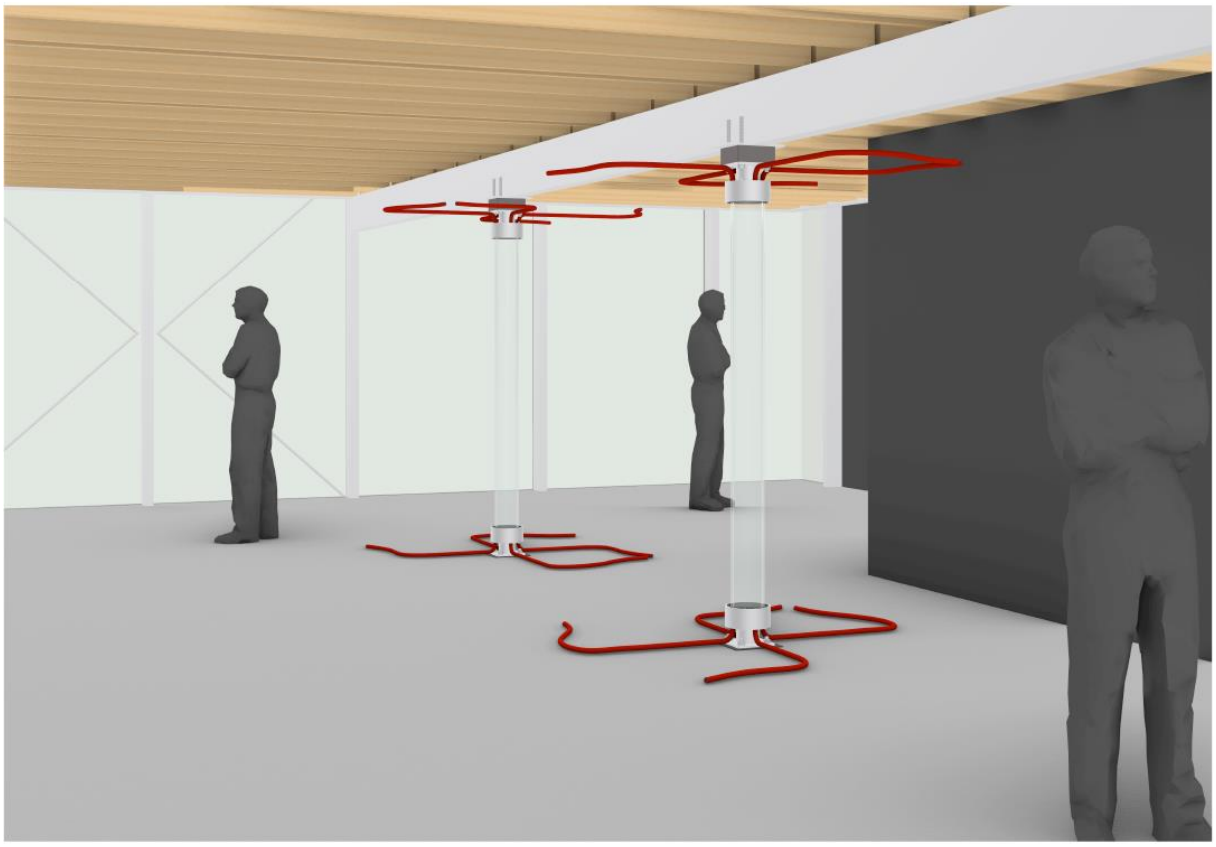

Perspective 3: steel columns (current situation)

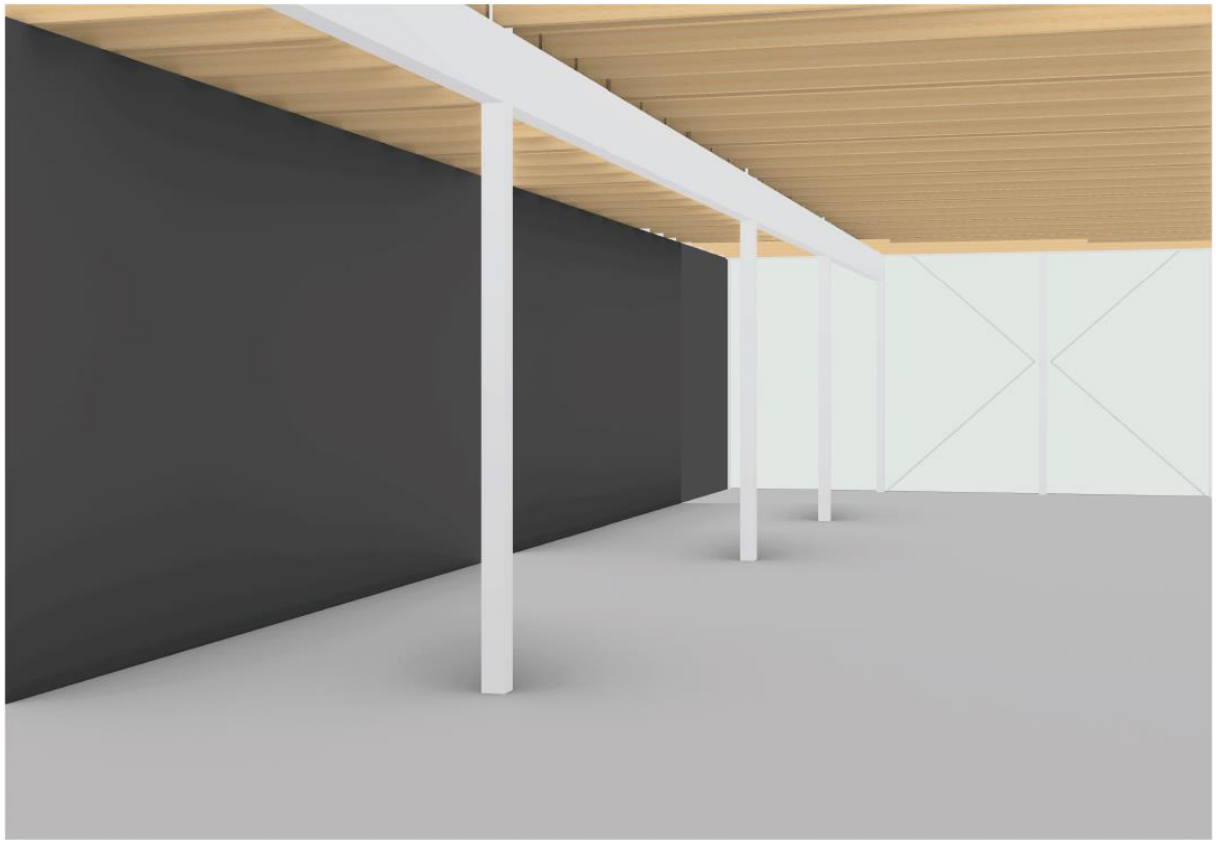

Perspective 3: MLA (with air hoses)

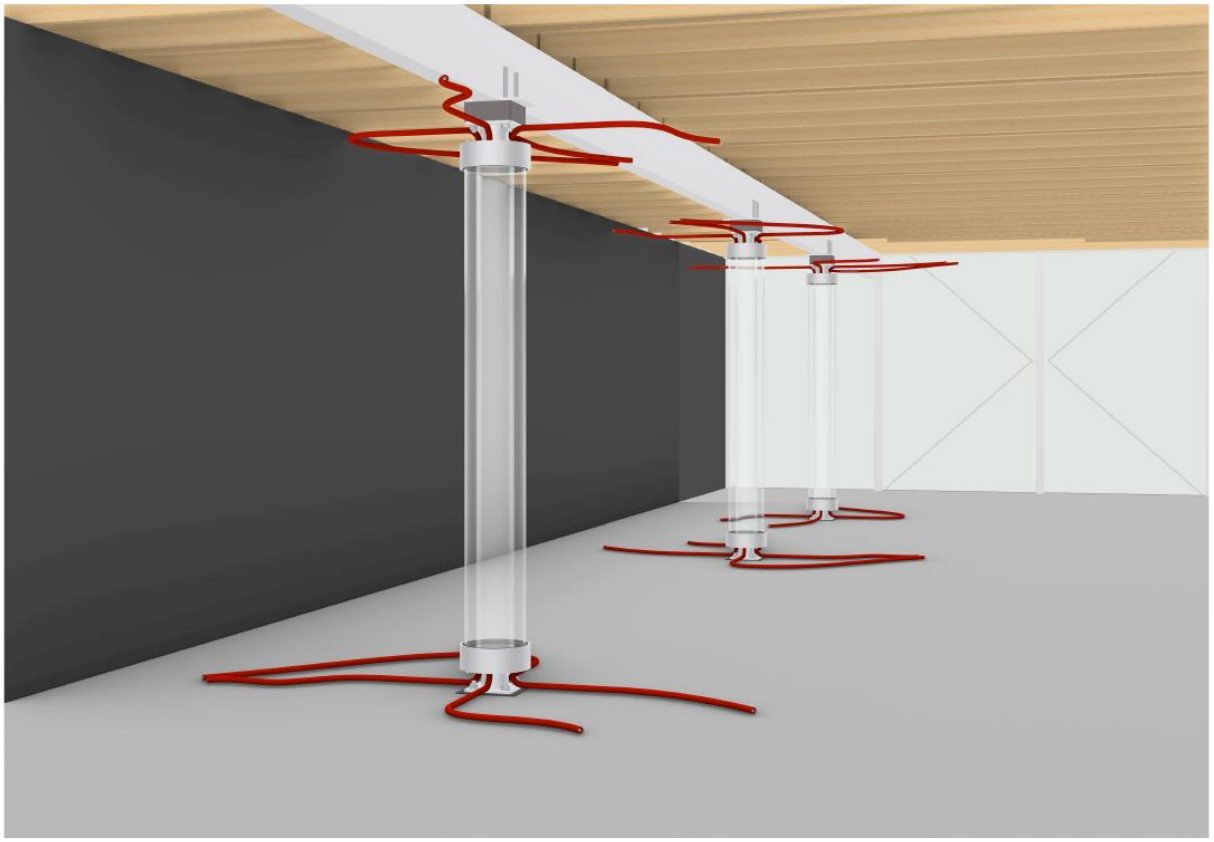

Perspective 3: MLA (without air hoses)

Perspective 3: SLW (with water hoses)

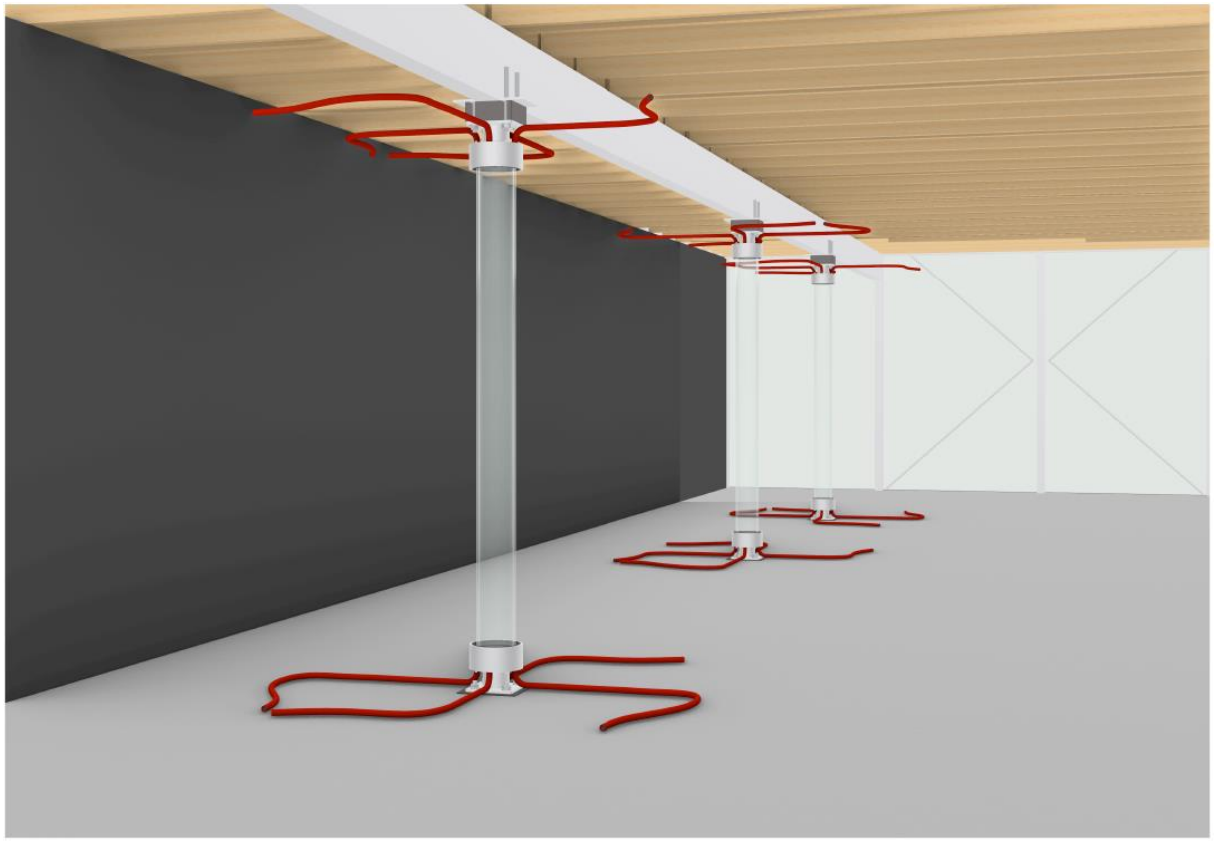

Appendix 7 – Pre-assemblies

- Steps to pre-assemble the:
  - The POM-block, which is attached to the POM-cap.
  - The POM-socks.
  - The steel shoe.
  - The steel bracket.

A.7.1. The assembly of the POM-block

The steps to assemble the POM-block are shown below. This is shown for the MLA with air hoses. This POM-block is attached to the POM-cap.

- Step 1. - The first (bottom) layer of the POM-block is shown.
- Step 2. - In this layer threated holes are included. In here the plugs for the hoses needs to be screwed.
- Step 3. - Apply a layer of glue on top of first the POM-layer
- Step 4. - Attach the second layer (middle layer) of POM to the block.
- Step 5. - Apply another layer of glue.
- Step 6. - Attach the third layer (top layer) of POM to the block. Now the inner POM-block is finished.
- Step 7. - Plug the hoses to the plugs.
- Step 8. - The POM-cap can now be screwed to the inner POM-block.
- Step 9. - In the POM-cap a sleeve is included next to the POM-block. Now the gasket can be placed in this sleeve.

Step 1:

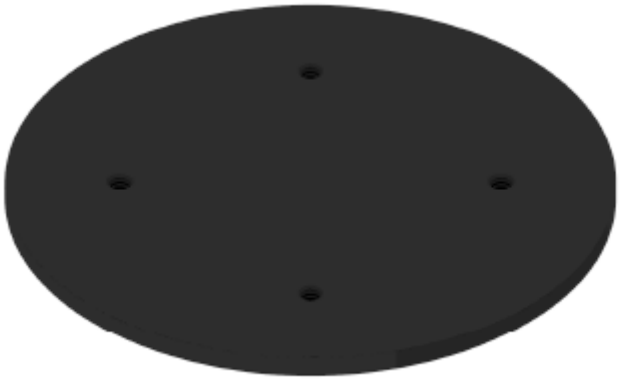

Step 2:

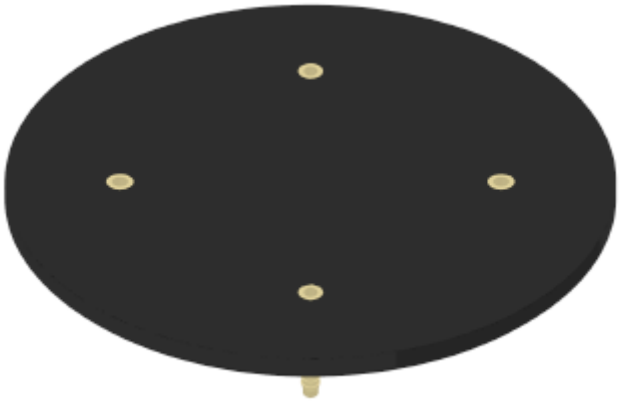

Step 3:

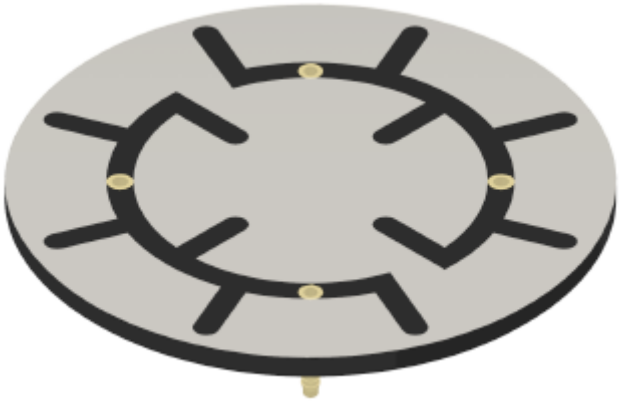

Step 4:

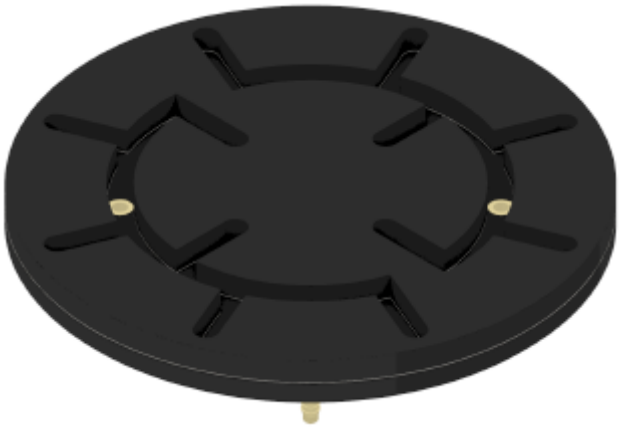

Step 5:

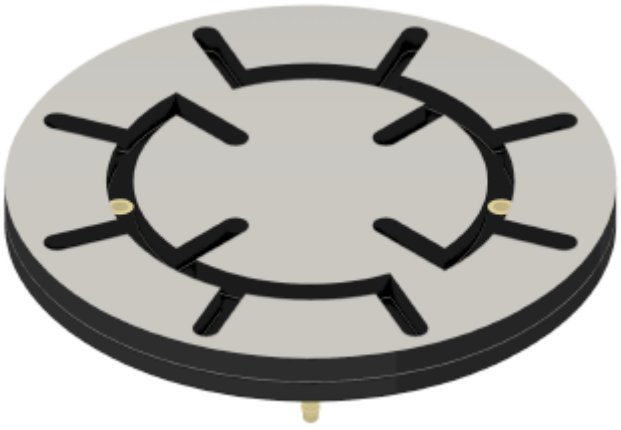

Step 6:

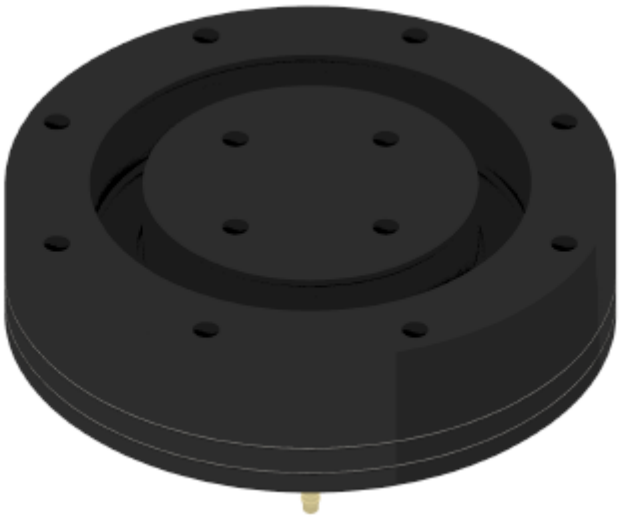

Step 7:

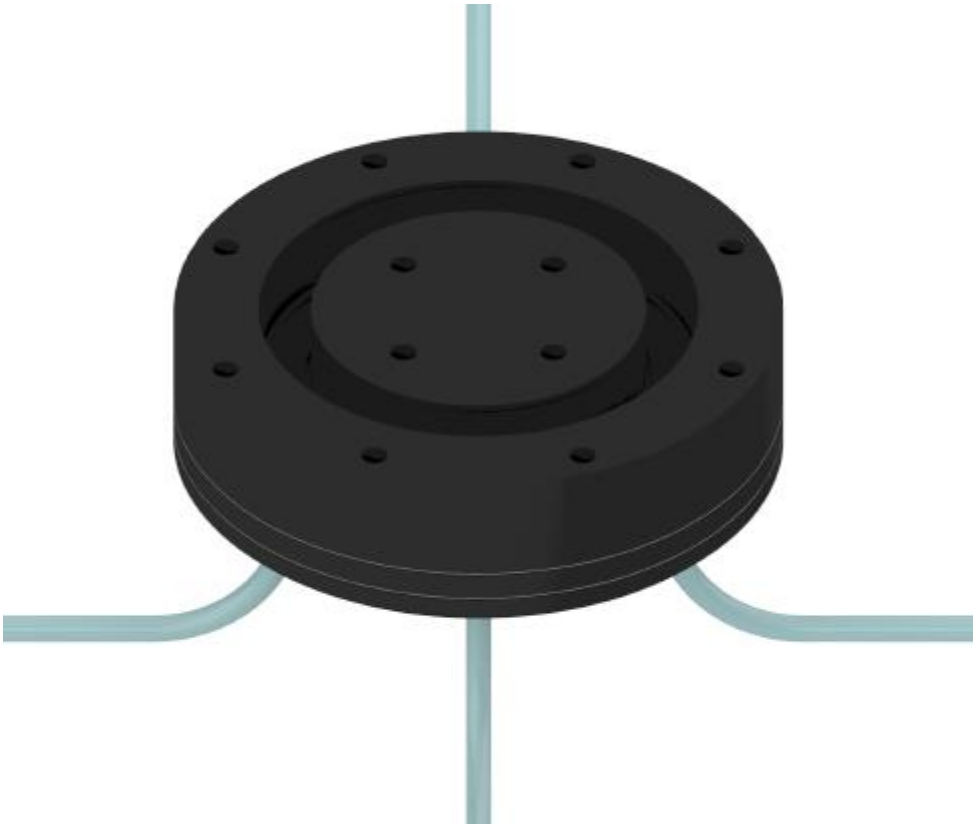

Step 8:

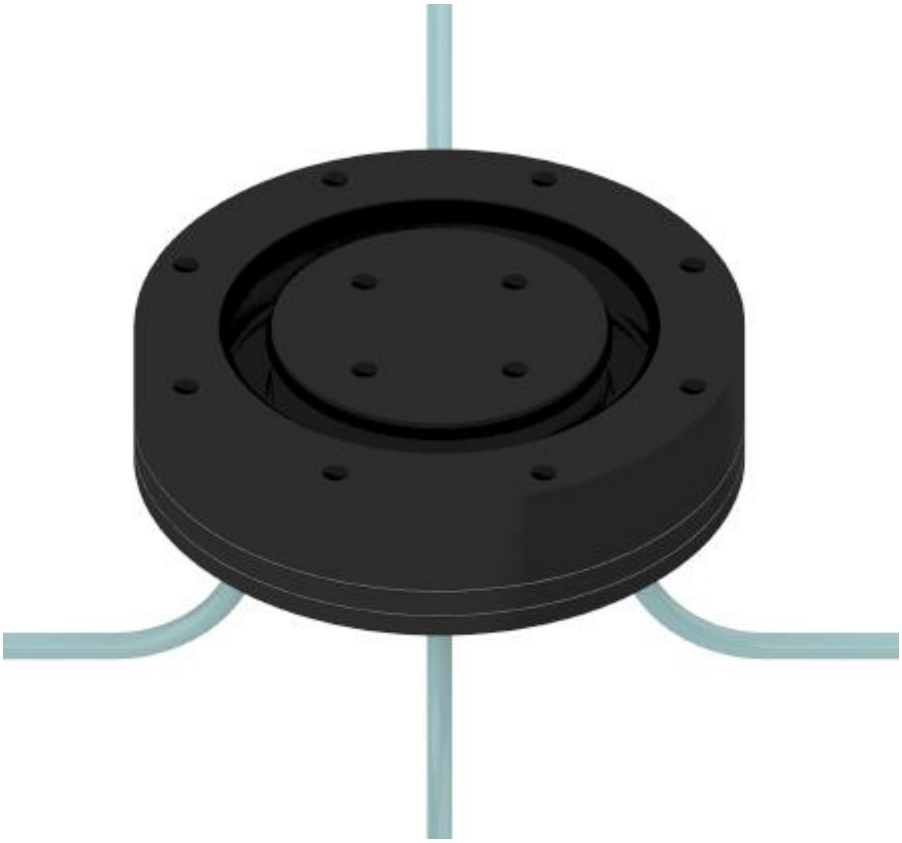

Step 9:

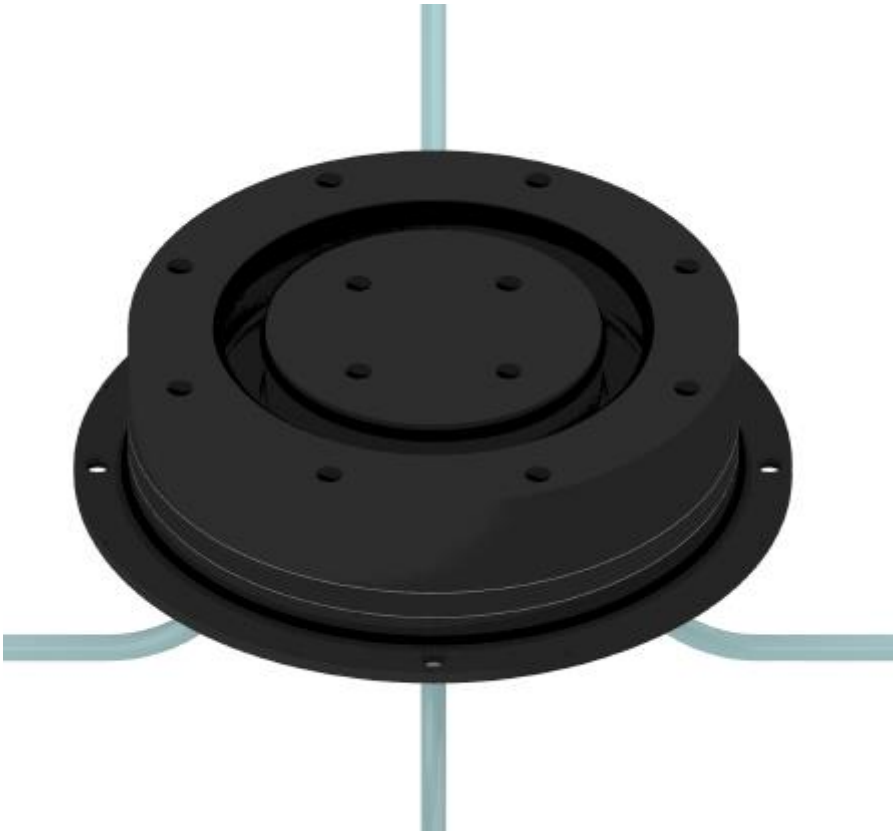

A.7.2. The assembly of the POM-sock

The steps to assemble the POM-socks are shown below (for the MLA). These are placed at the top and the bottom of the outer glass tubes and are attached to the POM-cap later on in the assembly sequences.

- Step 1. - The first layer (bottom) of POM is shown.
- Step 2. - Apply a layer of glue on top of first POM-layer.
- Step 3. - Attach the second layer (middle layer) of POM.
- Step 4. - Apply another layer of glue.
- Step 5. - Attach the third layer (top layer) of POM.
- Step 6. - Now attached an air/water-tight foil around the POM-sock.
- Step 7. - In the groove included in the top layer of POM, neoprene needs to be placed.
- Step 8. - In the same groove, sleeves are inserted. In these sleeves, gaskets can be placed. Now the POM-sock is finished, so that (in the assembly sequence) the outer tube can be placed in the groove on top of the neoprene.

Step 1:

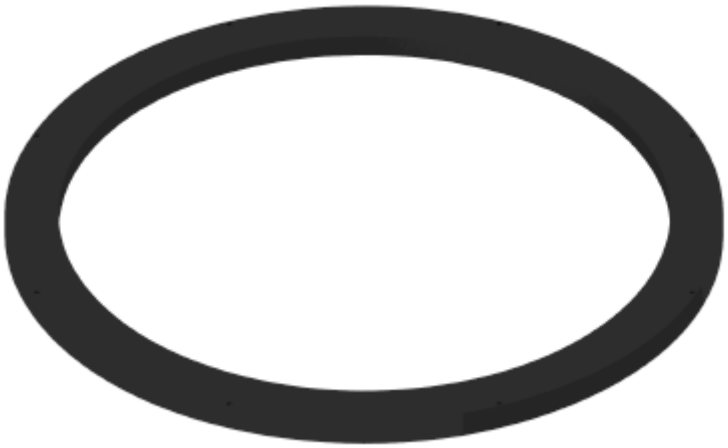

Step 2:

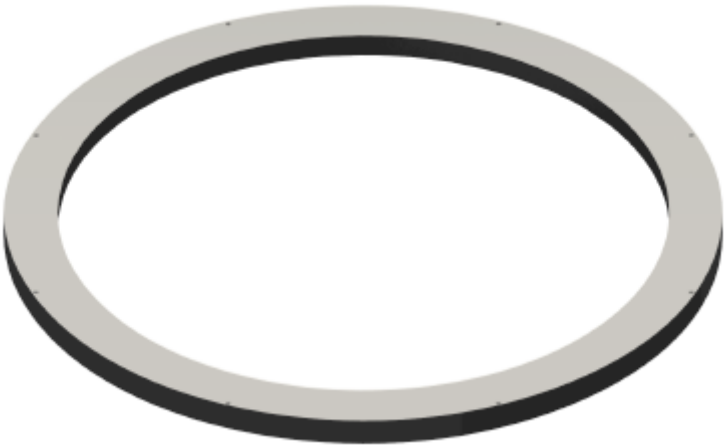

Step 3:

Step 4:

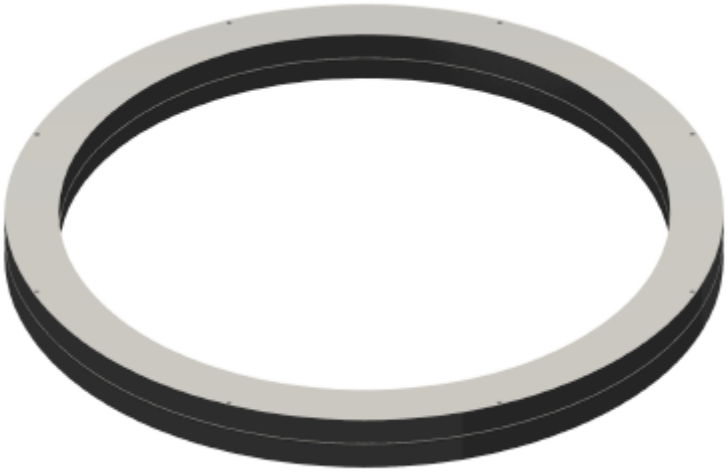

Step 5:

Step 6:

Step 7:

Step 8:

A.7.3. The assembly of the steel shoe

The steps to assemble the steel shoe are shown below.

- Step 1. - The base plate is shown with a chamfer.
- Step 2. - Pins need to be welded under this base plate (to be able to attach the steel braces).
- Step 3. - Then the CHS needs to be cut and it can be placed on top of the base plate.
- Step 4. - The CHS needs to be welded on top of the base plate. The weld needs to be placed in the chamfer.
- Step 5. - Place the route element (the half sphere) to the base plate.
- Step 6. - Weld the half sphere to the base plate.
- Step 7. - This element needs to be hot-dipped galvanized and a FR60 coating needs to be coated on the element.
- Step 8. - Apply the Teflon under the half sphere.
- Step 9. - Insert the plugs in the steel base plate (threated connection).
- Step 10. - Apply fire hoses around the hoses.
- Step 11. - Apply the fire sealant at where the plugs are placed in the base plate.

Step 1:

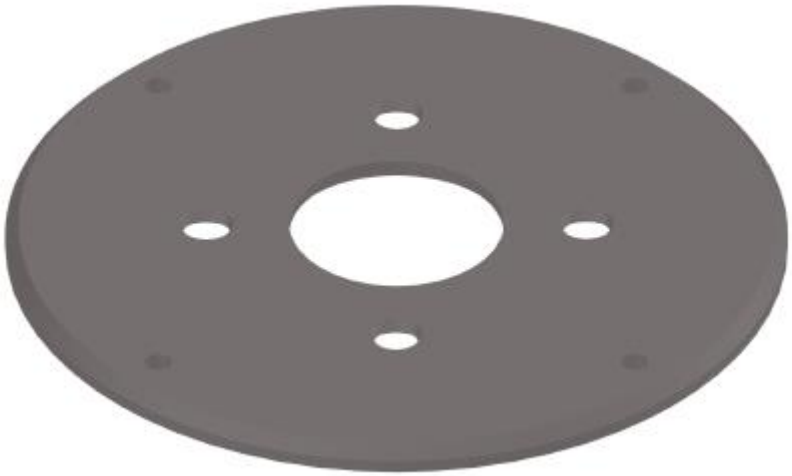

Step 2:

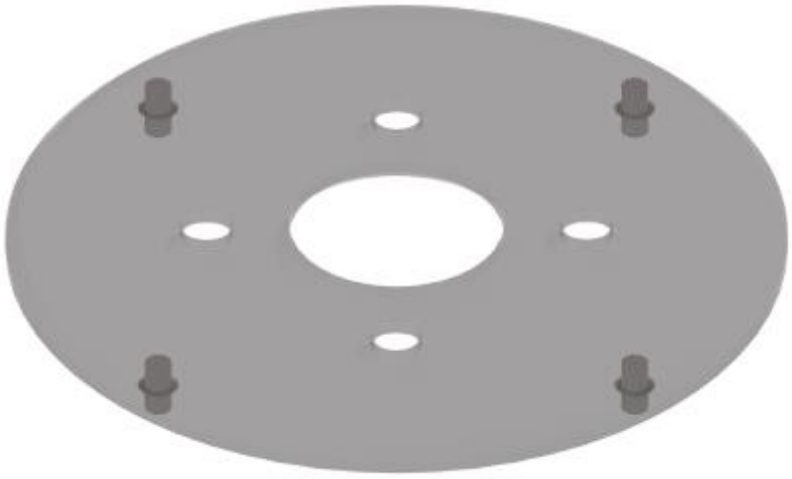

Step 3:

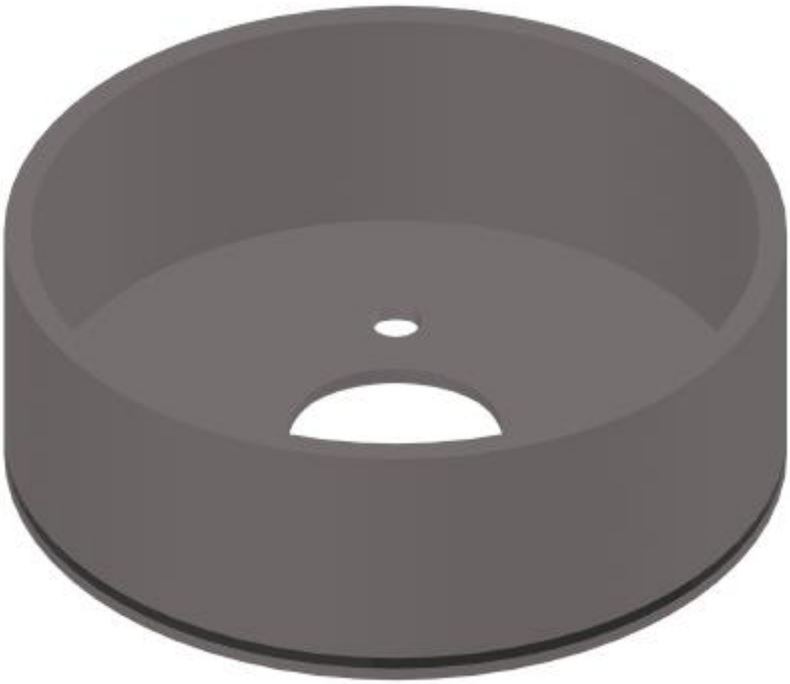

Step 4:

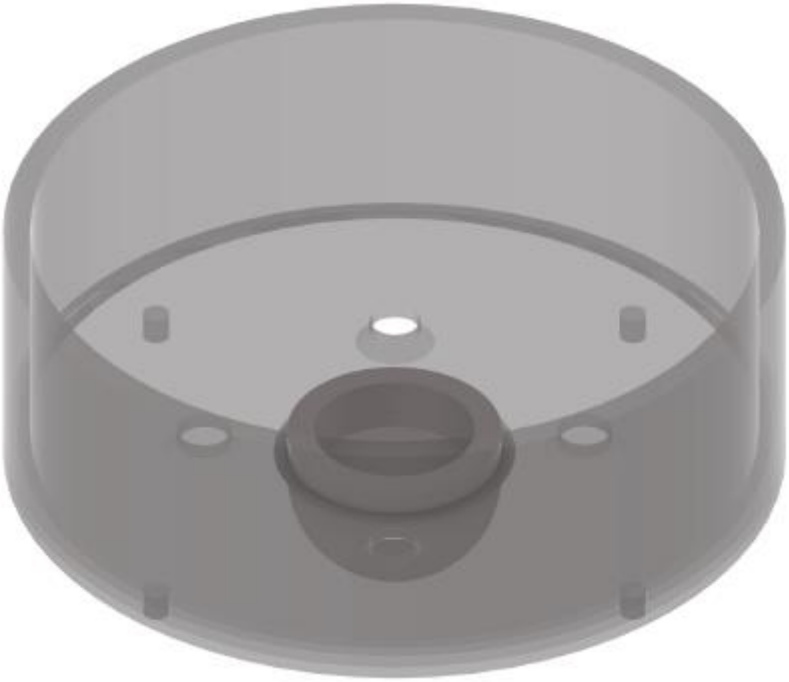

Step 5:

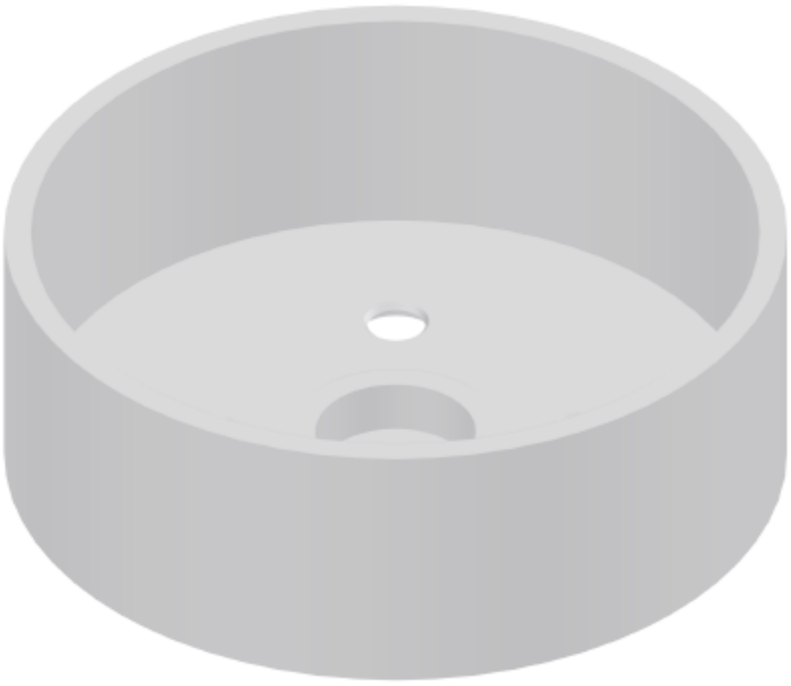

Step 6:

Step 7:

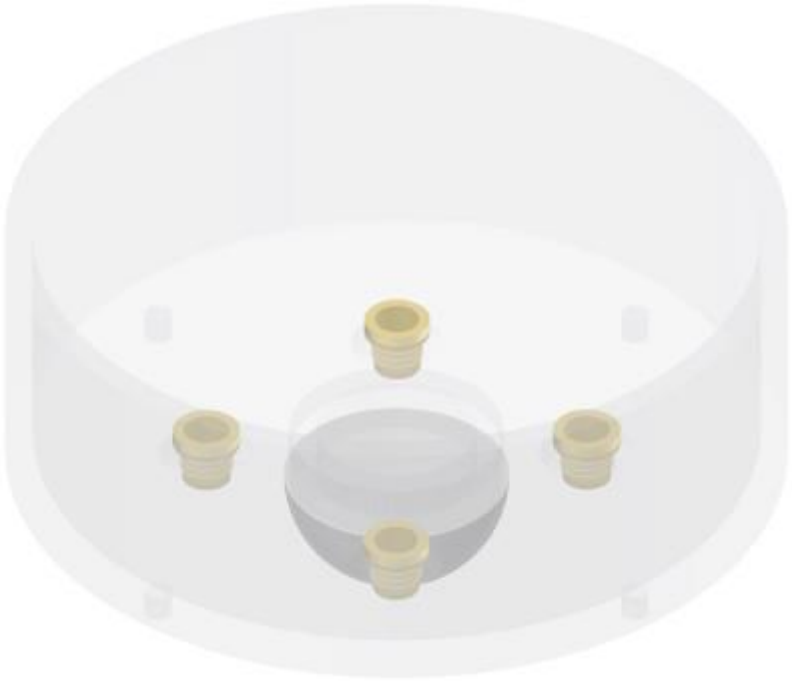

Step 8:

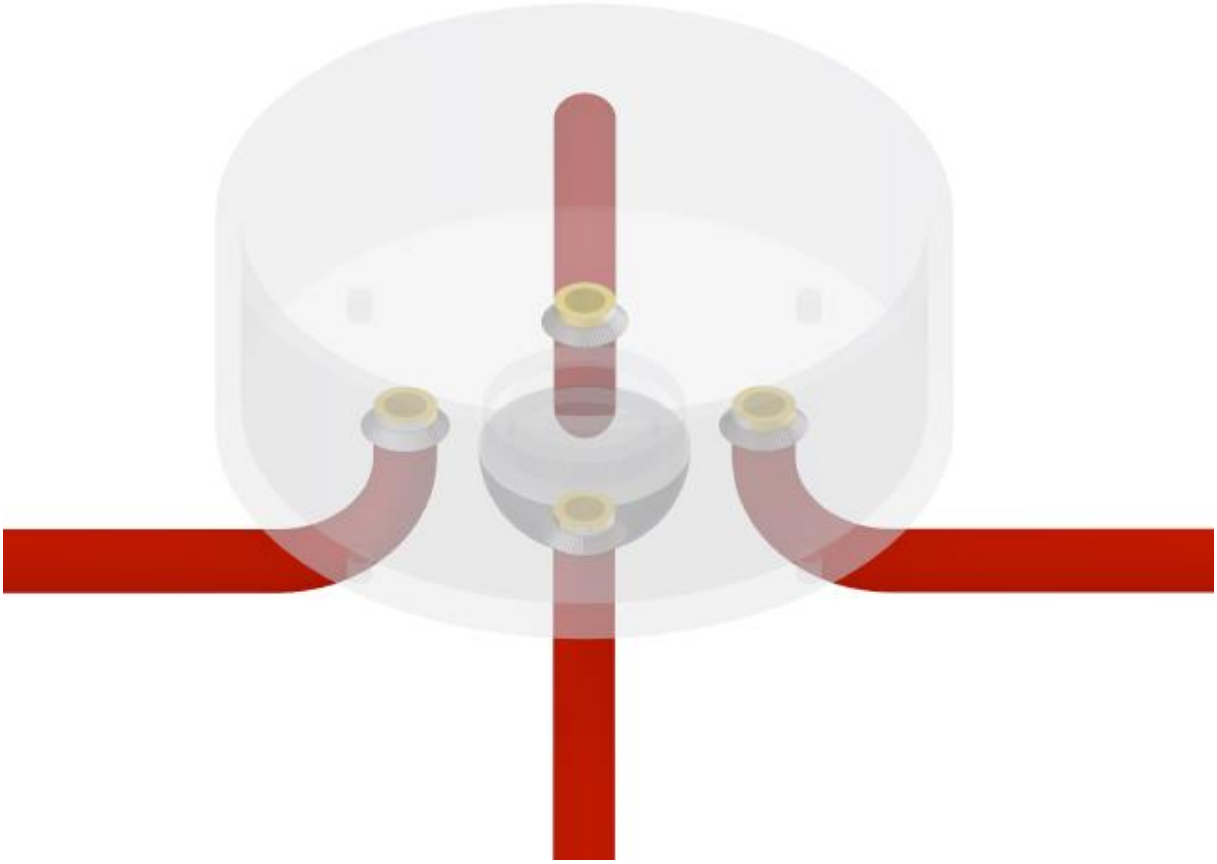

A.7.4. The assembly of the steel bracket

The steps to assemble the steel bracket are shown below.

- Step 1. - The base plate is shown of the bracket.
- Step 2. - A routed element (the other half sphere) needs to be placed in the base plate and weld the base plate and the sphere to each other.
- Step 3. - This element needs to be hot-dipped galvanized and a FR60 coating needs to be coated on the element.
- Step 4. - Apply the Teflon under the half sphere.

Step 1:

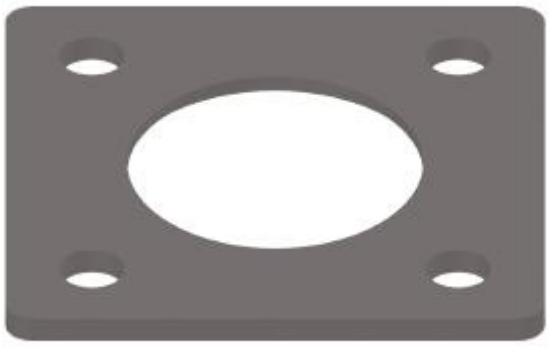

Step 2:

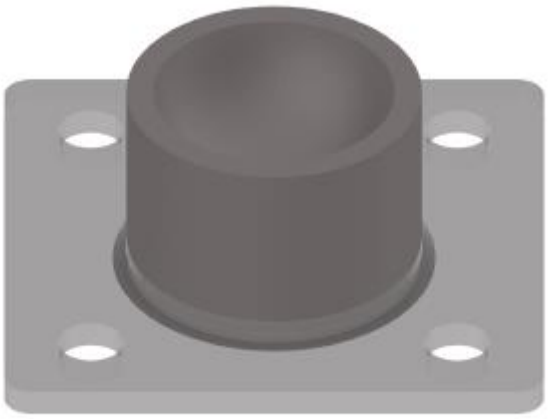

Step 3:

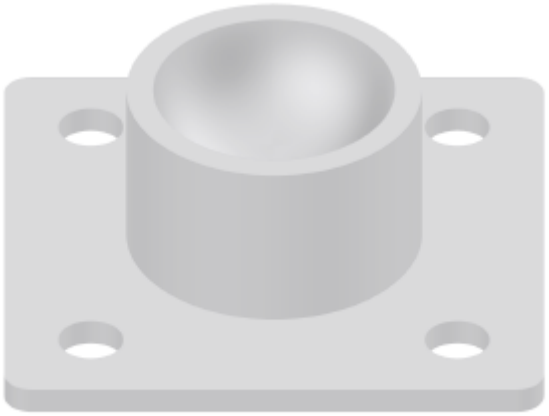

Step 4:

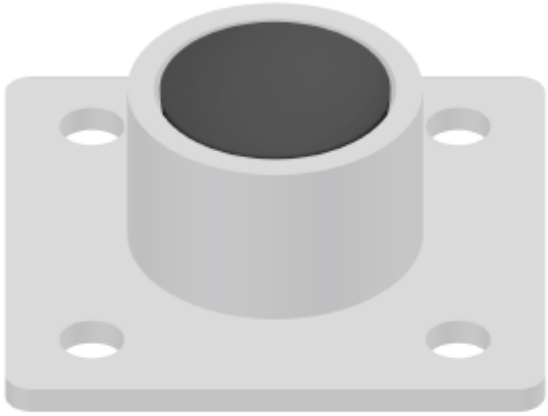

Appendix 8 – Compression loads (case study)

A.8.1. Starting points

For the design, the following starting points will be applied (these starting points are according to NEN-EN 1990):

- Consequence class: CC2
- Reliability class: RC2
- k_{FI} : 1.0
- Reference period: 50 years

Used load combinations:

$$ULS1 = 1.35 * G + 1.5 * Q_{main} * \psi_0 + 1.5 * Q_{other} * \psi_0 \quad \text{(A.8.1)}$$

$$ULS2 = 1.2 * G + 1.5 * Q_{main} + 1.5 * Q_{other} * \psi_0 \quad \text{(A.8.2)}$$

A.8.2. Determining of the compression loads

Firstly, the floor loads are determined. In table 1, an overview of the floor loads is given.

Project: Bouwdeel D cepezed
date: 20-01-21

Overview loads

	Thickness (m)	Weight (kN/m^3)	Dead load (kN/m^2)	Permanent (kN/m^2)	Live load (kN/m^2)	Variable (kN/m^2)	Psi	
Roof terrace				**1**		**1**		**0.00**
Metsä Wood Kerto LVL		-	0.5					
Finishing			0.5					
Live Load					1			
Total			1		1			
Storey floors				**1**		**3.3**		**0.58**
Metsä Wood Kerto LVL			0.5					
Finishing			0.5					
Seperation walls					0.8			
Live Load					2.5			
Total			1		3.3			

Table 1 Overview floor loads

Furthermore, to indicate the weight per glass column, an indication is given according to the values below, given in table 2. To conclude also the weight of the connections, a rough estimation is made. Per glass column, the permanent load that will be considered is around 2.5 kN.

	thickness wall (mm)	diameter outer (mm)	diameter inner (mm)	A (m^2)	weight (kN/m^3)	Permanent load (kN)
Glass column					**23**	
glass layer 1 (inner)	6	137	125	0,002469	23	0,0568
glass layer 2	6	155	143	0,002809	23	0,0646
glass layer 3 (outer)	4	250	242	0,003091	23	0,0711
				0,01		**0,19**

Table 2 Estimation for weight of the glass column.

All of the columns in the middle row of the building will be made out of glass, but in this thesis, only the column which receives most load will be considered. In figure 1, a cross section is given from the building. In here, the green coloured column is the standing on the ground floor and is receiving most of the load. In figure 2, a floor plan is shown of the building. In this plan view, the column which carries most of the load per floor is the one marked with the red circle. The orange area (5.45 m * 4.5 m) is the area which will be carried by this column. If this is too much, then it is possible to place an extra column in the row, then the area (3 m * 5.45 m) and so the force will be lower. The total loads on the column are given in table 3, based on the extra column. The compression loads are determined by equations A.8.1 and A.8.2 for ULS and SLS situation. The compression load in ULS

situation, is the force which needs to be carried by the column. If the column is broken, the column must be able to carry the compression loads in SLS situation.

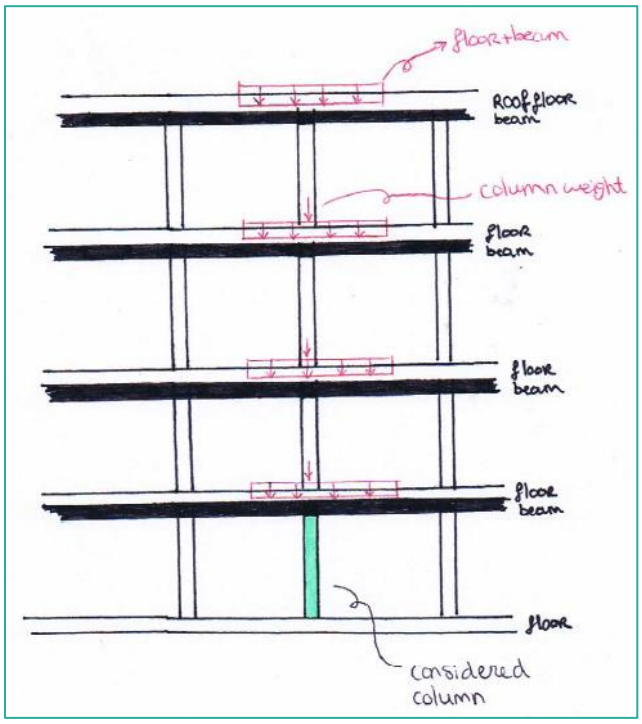

Figure 1 Cross section of the considered column.

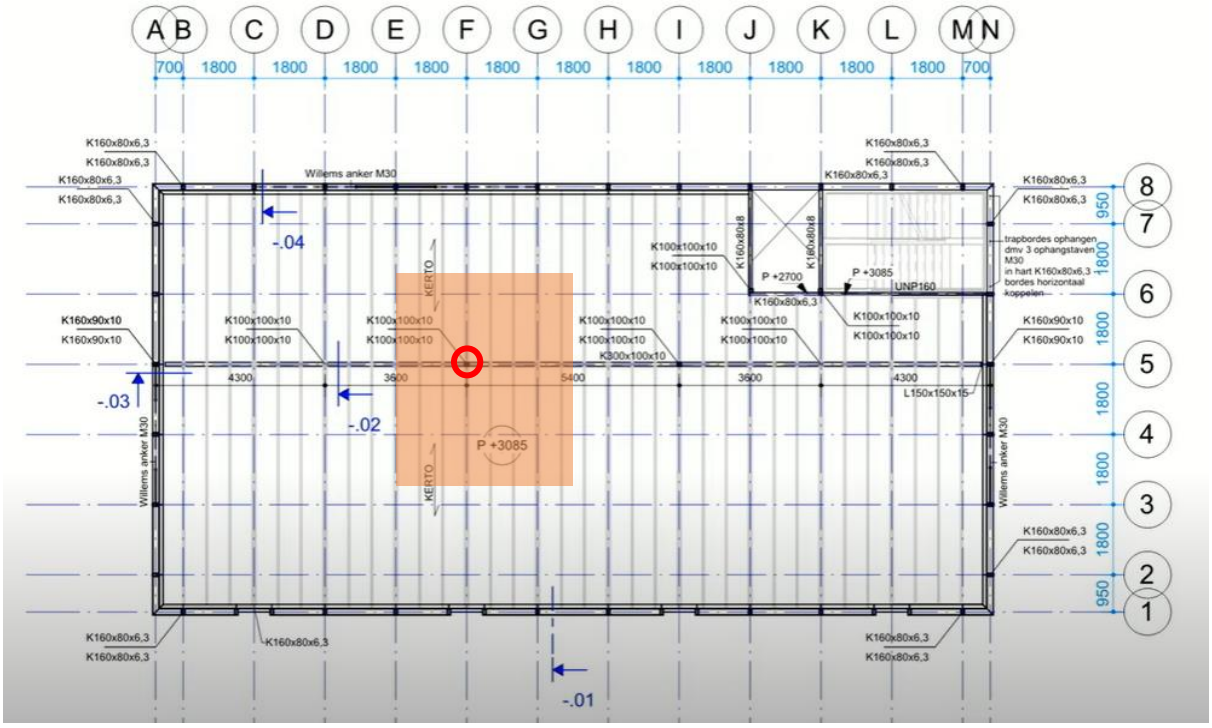

Figure 2 Floor plan with the considered column (Webinar Bouwdeel D(emontabel). 2020).

Column loads

floor nr from above	height (m)	length (m)	surface (m2)	Permanent load (kN/m)	Permanent load (kN/m2)	Live load (kN/m2)	Psi	P (kN)	LL (kN)	ULS1 Design value (kN)	ULS2 Design value (kN)	SLS Characteristic value (kN)
	3,2	4,5	16,35									
1 roof												
roof floor			16,35		1	1		0,00	16,35	16,35		
beam K300x100x10		4,5		0,56				0,00	2,52	0		
column weight	3,2			2,50				0,00	8,00	0		
total									**26,87**	**16,35**	36,27	32,24	43,22
2 story floor (extreme)												
floor			16,35		1	3,3		0,58	16,35	53,96		
beam K300x100x10		4,5		0,56				0,00	2,52	0		
column weight	3,2			2,50				0,00	8,00	0		
total									**26,87**	**53,96**	83,22	113,18	80,83
3 story floor (extreme)												
floor			16,35		1	3,3		0,58	16,35	53,96		
beam		4,5		0,56				0,00	2,52	0		
column weight	3,2			2,50				0,00	8,00	0		
total									**26,87**	**53,96**	83,22	113,18	80,83
4 story floor												
floor			16,35		1	3,3		0,58	16,35	53,96		
beam K300x100x10		4,5		0,56				0,00	2,52	0		
total									**18,87**	**53,96**	72,42	69,58	72,83
TOTAL LOAD											275,12	**328,18**	**277,70**
										required for:	strength test 492 (328*1,5)	impact test 417 (278*1.5)	

Table 3 Calculation of compression force onto the column for ULS and SLS situation.

This means that the compression load that needs to be considered on the column for ULS is around N_{ed} = 330 kN. Due to the fact that the column in a primary structural element and due to the fact that glass is brittle, perhaps more safety needs to be included. The safety factor needs to be determined by carrying out multiple experiments, but for now a safety factor of 1.5 will be considered. This means that the column needs to be able to carry approximately N_{ed} = 500 kN in ULS situation. For the SLS situation, so when broken, it still needs to be able to carry around N_{ek} = 280 kN. When taken the safety factor of 1.5 into account, the column needs to be able to carry N_{ek} = 420 kN.

The column is only able to take up normal force due to the hinged connection. So only vertical forces can be transferred via the columns. This means that in any case, the horizontal forces need to be taken up by other structural elements, as walls or bracing.

A8.3. Risk analysis

Next to including a higher safety factor, a risk analysis needs to be performed to guarantee safety. In chapter 2.3.2. the equations are already discussed. Due to the brittleness of glass, safety needs to be considered during designing. Three aspects are from influence in this risk analysis: probability (WS), exposure (BS), and consequences (ES). To determine the risk (RS), values can be filled in the equation 16. To determine these values, table 8 is needed:

- WS: 3
- BS: 1
- ES: 7

The probability of damage is most likely without intent. It would be unusual that the column would fail in an office building, but it is possible. Someone can walk against it or the columns can be hit by something which causes an impact load. It can be possible as well that there is damage with intent. For example, when someone breaks in the office building. Most of the time, offices building have an alarm system, then thieves do have only a few minutes to steal or break something. When they only have a few minutes, they probably are more interested in stealing, and not in damaging the columns, but it is possible. This is why the value for WS is determined to be 3. Furthermore, the column could also be exposed to fire which can bring damage to the column. It is unusual, but it can happen.

The exposure of the column (the structural element) will be somewhere between ‘very seldom’ and ‘a few times per year’. This is the same explanation as for the probability. Possible exposures in office buildings in Delft are mostly fire and impact. This can happen,

but is unusual. To be on the safe side, a few times per year will be assumed, which means that the value for ES is 1.

Lastly when the column is completely broken, the consequence of injuries will be quite low. First of all, a few glass tubes will be used in the column design. When one glass tube break, other(s) are still able to carry loads. Furthermore, when a layer of the column breaks, the glass pieces will be hold together by lamination (interlayer resin) or by a coating (as Tough coating). Besides that, when a column breaks completely, by fire for example, the structural elements only need to be able to carry the loads for around 60 minutes. After that probably the hole building will not be safe anymore. The column will be designed to be able to carry more compression force then needed. In this case it will not fail if there is a bit more compression load then calculated. So, the consequences for injuries will probably be minor. This gives a value of 3 for ES. To be sure, an ES of 7 will be taken into account (serious injury).

By filling in the equation 16, the RS will be 21. Looking at table 9, the RS is below 70, which means that there only would be lateral breakage on one side. So, with a tubular layered column, only the outer tube will break. The column needs to be designed in such a way that the column is still able to carry the loads even when the outer tube is completely broken. When the outer layer breaks, and the pieces will be hold together, research showed that even then the outer tube can carry some loads. To be sure, this structural integrity and post-failure behaviour will be checked in the experimental tests. The design for the MLA has an extra non load-bearing, protective tube. Nevertheless, the designs for the MLA and the SLW will be considered, so that the columns are able to take up more force then needed (looking at the safety factor). This means that when the outer layer is broken, it is still able to carry the loads needed in SLS situation.

References

NEN-EN 1990+A1+A1/C. (2019). Eurocode: Basis of structural design.

Figure list

Table list

Appendix 9 – Thermal stresses

A.9.1. – Temperature differences - Isochoric pressure

There are two concerns due to temperature differences: stresses in the glass and condensation. Due to the fact that the column needs to be sealed properly, it becomes a closed cavity system. Air is inside the cavities of this sealed column and this air will be exposed to isochoric pressure due to climatic loading (chapter 2.2.2.4.). If the air is cooled down, the pressure will be lower inside the glass column than outside. This means that it attracts air from the outside, and this results in airflow towards the cavity. Hereby the risk of condensation increases. Condensation occurs, when the temperature of the object is below the dew point of the air of the surrounded area. If the warm air cools down below the dew point temperature, water vapour will begin to condensate to a liquid phase (Van der Linden, A., C., et al. 2018). Due to condensation, water will be inside of the column for a certain time, which results in the growth of mould for example. It is not possible to clean the column inside, so condensation should be avoided. If the air is heated up, the pressure will be higher inside the column than outside. Due to this the air outside attracts air from the inside. The air cannot flow in or out the glass, because the column is a closed system. So, these differences in air pressures from the inside and outside will result in stresses in the glass. This needs to be taken into account while designing, and it needs to be calculated if extra measurements are necessary.

A closed cavity façade (CCF) system is designed for the New art museum in Hong Kong, K11 Art and Cultural Centre designed by Eckersley O'Callaghan. For this project the façade is made of connected half glass tubes (figures 1 and 2). CCF makes use of a pressurized air supply, or a ventilation system known from the concept of pressurized multilayer ETFE-film cushion systems (Glass on Web. 2020).

Figure 1 The façade tubes of K11 Art and Cultural Centre in Hong Kong (CCF) (Glass on Web. 2020).

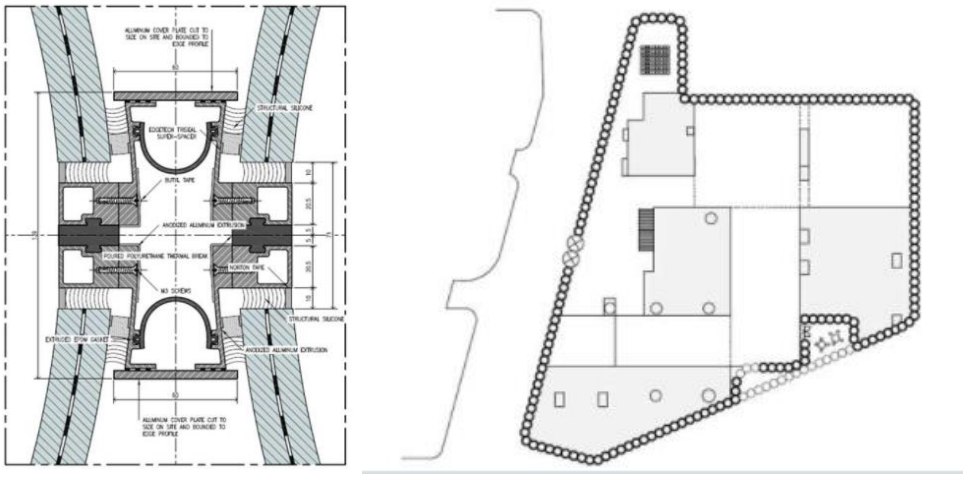

Figure 2 Left: connection of the glass tubes, right: plan view of K11 Art and Cultural Centre in Hong Kong (Eckrsley O'Callaghan. 2021).

A.9.1.1. – The two inner tubes of MLA & SLW

Due to the fact that the column needs to be sealed to avoid dirt coming in, differences in air pressure between the inside and the outside will occur if there are differences in temperature. These air pressures result in stresses. To check if the column can take over these stresses without breakage, the formula of Boyle and Gay-Lussac will be used (equation 4 in chapter 2.2.2.4.).

$$p * V = n * R * T \qquad \text{(A.9.1)}$$

The pressure can be rewritten as:

$$p = \frac{n*R*T}{V} = \frac{R*T}{V_M} \qquad \text{(A.9.2)}$$

With:

- p : absolute pressure of gas [N/m^2]
- V : volume [m^3]
- n : amount of gas [mol]
- R : universal gas constant [8.314472 $J*K^{-1}*mol^{-1}$]
- T : absolute temperature [K]
- V_M : molar volume air [$24.4*10^{-3}$ m^3]

The column will be placed in the Netherlands in Delft. The following temperatures are assumed:

- T1 = -20°C = 253.15 K
- T2 = 40°C = 313.15 K

These temperatures are giving pressures of:

$$p1 = \frac{8.314472*253.15}{24.4*10^{-3}} = 86.3\ kN/m^2 \qquad \text{(A.9.3)}$$

$$p2 = \frac{8.314472*313.15}{24.4*10^{-3}} = 106.7\ kN/m^2 \qquad \text{(A.9.4)}$$

The average pressure in the Netherlands is (NEN2608):

$$p_{NL;av} = 101.5\ kN/m^2 \qquad \text{(A.9.5)}$$

The difference in pressures:

$$\Delta p1 = 101.5 - 86.3 = 15.2\ kN/m^2 \qquad \text{(A.9.6)}$$

$$\Delta p2 = 101.5 - 106.7 = -5\ kN/m^2 \qquad \text{(A.9.7)}$$

The air pressure is equal on the entire glass surface, due to the round shape. If the air is pressing on the inside of the glass tube, it gives tensile stresses in the tube. This air pressure results in expansion (figure 3, left). If the air pressure is too low, the tube will shrink (figure 3, right). It will give compression stresses in the tube itself. The pressures from inside the tubes are different than the pressures from the outside. This will give a difference in pressure. So, it needs to be checked if the borosilicate DURAN® tubes are able to resist these stresses.

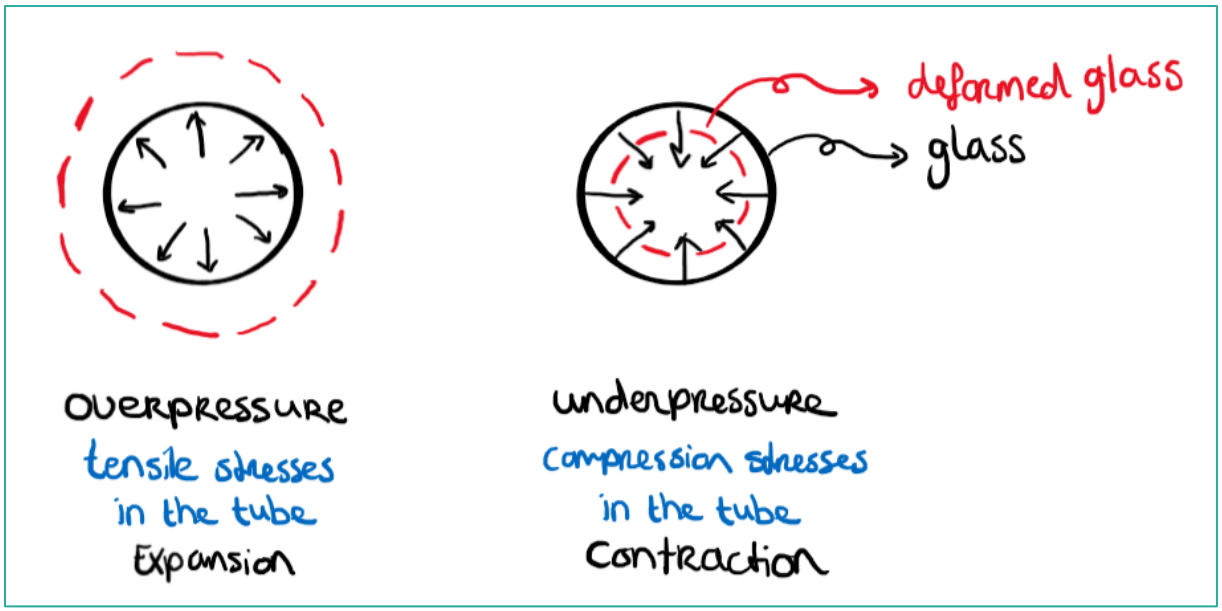

Figure 3 Differences in air pressure.

Processing notes

Compressive strength of DURAN® borosilicate glass 3.3 tubing

The following formula applies to stress-free tubing and hollow cylindrical bodies with rounded profile, consistent wall thickness and open ends, free of thermal loads under positive interior and negative exterior pressure.

Calculating resistance to pressure (p)	Calculating wall thickness (WT)
$p = \frac{WT \cdot 140\ bar}{OD - WT}$	$WT = \frac{OD \cdot p}{140\ bar + p}$

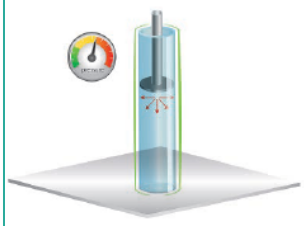

OD = outside diameter in mm
WT = wall thickness in mm
p = pressure in bar

The formula stems from the AD 2000 specifications N4, Issue 2000-10: Pressure vessels of glass with Annex 1, Issue 2000-10: Assessment of errors in pressure vessel walls of glass and B1, Issue 2000-10: Cylinder and spherical shells under excess interior pressure, whereby approved strain under DIN EN 1595: Pressure equipment made from borosilicate glass 3.3 – General rules for design, manufacture and testing of 7N/mm² were established.
Under DIN EN 1595: Pressure equipment of borosilicate glass 3.3 – General rules for design, manufacture and testing, DURAN® is an approved material and can be used in the manufacture of pressure equipment.

Thermal-shock resistance

The thermal-shock resistance of glass tubing can be estimated with, for example, a GIT publication (data and process sheets, Process sheet GIT 6 [1962] booklet 12 [Dec.]). Thermal-shock resistance refers to the mechanical resistance of glass tubing against cracking or breaking under extreme thermal shock. The values in this publication are based on theoretical research and practical experience and should show temperature differences which the glass bodies can withstand in practice. Breakage is thereby not expected until temperature differences are 1.2 to 2 times higher.

Figure 4 Notes SCHOTT DURAN tube (SCHOTT. n.d.).

The allowable possible interior and negative exterior pressure [bar] for the inner tube (OD: 115 mm, WT = 5 mm) (figure 4):

$$p = \frac{5*140}{115-5} = 6.36\ bar \quad \text{(A.9.8)}$$

So, the resistance to the pressure is 6.36 bar = 636 kN/m^2.

$$636 > 15.2\ kN/m^2 \qquad \text{(A.9.9)}$$

This means that there are no extra measures necessary. Due to the round shape, the air pressures resulting by temperature changes can be taken up by the glass column itself.

A.9.2. – Temperature differences - Expansion

What will be the expansion of the glass tubes due to temperature differences in the glass? For example, if the temperature at the outside of the glass is 100 °C and at the inside of the glass is 20 °C, then the glass tube will expand (figure 6). According to SCHOTT, as can be seen in figure 5, it is recommended not to exceed a temperature difference of 120 °C.

The table below gives two maximum temperature differences each for some dimensions. The publication for glass tubing distinguishes between two types of temperature change.
1. Temperature change to the tubing occurs only form the outside, without direct influence on the interior atmosphere.
2. Temperature change occurs simultaneously from the outside and on the inside of the tubing. This case is less critical and represents the higher value of the table.

Tubing	Rod
OD 50.5/WT 5.00 mm: 100/140 °C	OD 24.0 mm: 75 °C
OD 133.0/WT 7.00 mm: 90/120 °C	
OD 120.0/WT 8.00 mm: 85/110 °C	

The thermal-shock resistance of tubing, capillaries and rods depends on wall thickness, shape and size of the quenched surface, surface condition, existing stresses and end finish. It is recommended not to exceed a temperature difference of 120 °C.

Figure 5 Notes SCHOTT DURAN tube (SCHOTT. n.d.).

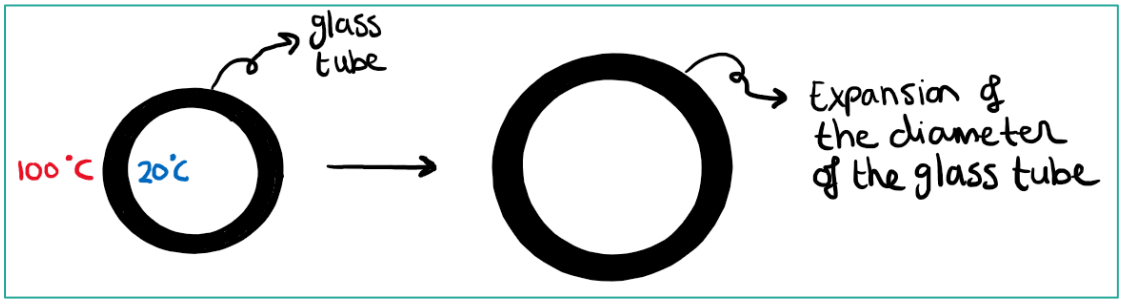

Figure 6 Left: one glass tube with different temperatures, right: thermal expansion due to temperature differences in the glass.

What is the new diameter (orange, figure 6 right) of the tube from the example of figure 5?

Borosilicate glass (DURAN® SCHOTT) (SCHOTT. n.d.):

- Young's modulus (E) : 63 000 N/mm^2
- Thermal expansion coefficient (α_T) : 3.3*10^{-6} 1/°C
- Outer diameter of the outer tube (OD) : 115 mm
- Area cross-section : 11608 mm^2

The temperature difference (d_T) is: 100-20 = 80 °C

The circumference of the tube can be expressed as (Engineering ToolBox. 2010):

$$c = 2 * \pi * r \quad \text{(A.9.10)}$$

The change in diameter due to temperature difference can be calculated as follows (Engineering ToolBox. 2010):

$$d_c = c_{fin} - c_{ini} = 2 * \pi * r_{ini} * d_T * \alpha_T \quad \text{(A.9.11)}$$

$$d_c = 2 * \pi * r_{fin} - 2 * \pi * r_{ini} = 2 * \pi * r_{ini} * d_T * \alpha_T \quad \text{(A.9.11)}$$

This can be written as (Engineering ToolBox. 2010):

$$r_{fin} = r_{ini} * d_T * \alpha_T + r_{ini} = r_{ini} * (d_T * \alpha_T + 1) \quad \text{(A.9.12)}$$

Instead of the radius, it can also be written down for diameter (Engineering ToolBox. 2010):

$$d_{fin} = d_{ini} * (d_T * \alpha_T + 1) \quad \text{(A.9.13)}$$

With:

- c_{ini} = initial outer diameter [mm]
- c_{fin} = final outer diameter [mm]
- d_c = change in diameter [mm]
- r_{ini} = initial radius [mm]
- r_{fin} = final radius [mm]
- d_T = temperature difference [K]
- α_T = linear expansion coefficient [1/K]
- d_{fin} = final diameter [mm]
- d_{ini} = initial diameter [mm]

So, with the last equation the final diameter can be calculated due to the temperature differences:

$$d_{fin} = 115 * [80 * 3.3 * 10^{-6} + 1] = 115.03\, mm \quad \text{(A.9.14)}$$

So, the new diameter of the outer tube will be 115.03 mm, so the expansion is 0.03 mm. The tube is free to expand 0.03 mm.

A.9.3. Temperature - Expansion and stresses

During curing of the interlayer resin between the glass tubes, the tubes and the resin will be heated up. In the glass tubes, geometric tolerances need to be taken into account. This results in different interlayer thicknesses. Due to these different thicknesses and the different thermal expansion coefficient between the glass and the interlayer, not only expansion, but stresses can also occur. If all the materials had the same thermal expansion coefficient, then only expansion will occur without stresses.

H.B.Fuller Kömmerling will cure the interlayer. Both DURAN and DURATAN tubes will be tested in this process. DURATAN is heat threated and is resistant against higher stresses.

As mentioned before, the tensile stresses are normative. The tensile stress is difficult to determine for glass, because this is depending on many parameters (as flaws). For annealed glass (DURAN tubes), the tensile strength is around 7 MPa (Kasunic, K.J. 2015). To determine an estimation of the tensile strength of annealed glass for the DURAN tubes, the following formula can be used (NEN 2608. 2014):

$$f_{mt;u;d} = \frac{k_a * k_e * k_{mod} * k_{sp} * f_{g;k}}{\gamma_{m;A}} \qquad \text{(A.9.15)}$$

$$k_{mod} = (\frac{5}{t})^{\frac{1}{c}} \qquad \text{(A.9.16)}$$

With:

- k_a: factor for the surface effect
- k_e: factor for the edge quality of the pane
- k_{mod}: factor which is depending on the load duration and the reference period
- k_{sp}: factor for surface structure
- $f_{g;k}$: characteristic value of bending tensile strength in MPa (45 MPa)
- $\gamma_{m;A}$: material factor of the pane
- c: corrosion factor
- t: the load duration in seconds

For the DURAN tubes, the following values are assumed:

- k_a= 1 (typically)
- k_e= 0.8 (annealed glass)
- t_s= 5 minutes * 60 = 300 s (short term loading)
- t_l= 25 years * 31556926 = 788923150 s (long term loading)
- c= 16
- $k_{mod;s}$= 0.774 (short term loading, according to equation A.9.17)
- $k_{mod;l}$= 0.307 (long term loading, according to equation A.9.18)
- k_{sp}= 1 (not patterned glass)
- $f_{g;k}$= 45 Mpa (NEN 2608. 2014)
- $\gamma_{m;A}$= 1.8 (for all situations)

This results in an approximately design strength for short term loading of:

$$f_{mt;u;d} = \frac{1*0.8*0.774*1*45}{1.8} = 15.5\ MPa \qquad \text{(A.9.17)}$$

This results in an approximately design strength for long term loading of:

$$f_{mt;u;d} = \frac{1*0.8*0.307*1*45}{1.8} = 6.1\ MPa \qquad \text{(A.9.18)}$$

So, for short term loading, the tensile strength of the annealed glass tubes (DURAN) will be around 15.5 MPa and for load term loading around 6 MPa.

Heat tempered glass (DURATAN tubes) has a higher tensile stress. The surface is subjected to compressive stress during the tempering process. The inside of the tube is subjected to tensile stress. In this way, the tube will only break at a compressive stress up to 50 MPa on the surface (figure 7) (SCHOTT. n.d.). The design tensile strength of thermally prestressed glass can be determined by the following formula (NEN 2608. 2014):

$$f_{mt;u;d} = \frac{k_a * k_e * k_{mod} * k_{sp} * f_{g;k}}{\gamma_{m;A}} + \frac{k_e * k_z * (f_{b;k} - k_{sp} * f_{g;k})}{\gamma_{m;V}} \qquad \text{(A.9.19)}$$

With the same components as for annealed glass and:

- $\gamma_{m;V}$: material factor of prestressed glass (1.2)
- $f_{b;k}$: characteristic value of bending tensile strength for prestressed glass in MPa
- k_z: factor

For the DURATAN tubes, the following values are assumed:

- k_a= 1 (typically)
- k_e= 0.8 (heat-strengthened)
- t_s= 5 minutes * 60 = 300 s (short term loading)
- t_l= 25 years * 31556926 = 788923150 s (long term loading)
- c= 16
- $k_{mod;s}$= 0.774 (short term loading, according to equation A.9.20)
- $k_{mod;l}$= 0.307 (long term loading, according to equation A.9.21)
- k_{sp}= 1 (not patterned glass)
- $f_{g;k}$= 45 Mpa (NEN 2608. 2014)
- $\gamma_{m;A}$= 1.8 (for all situations)
- $\gamma_{m;V}$= 1.2 (for all situations)
- k_z= 1 (for heat-strengthened, centre zone)
- $f_{b;k}$= 70 MPa (float glass, heat-strengthened)

This results in an approximately design strength for short term loading of:

$$f_{mt;u;d} = \frac{1*0.8*0.774*1*45}{1.8} + \frac{1*1*(70-1*45)}{1.2} = 36.3\ MPa \qquad \text{(A.9.20)}$$

This results in an approximately design strength for long term loading of:

$$f_{mt;u;d} = \frac{1*0.8*0.307*1*45}{1.8} + \frac{1*1*(70-1*45)}{1.2} = 23.0\ MPa \qquad \text{(A.9.21)}$$

So, for short term loading, the tensile strength of the heat-strengthened glass tubes (DURATAN) will be around 36.3 MPa and for load term loading around 23 MPa.

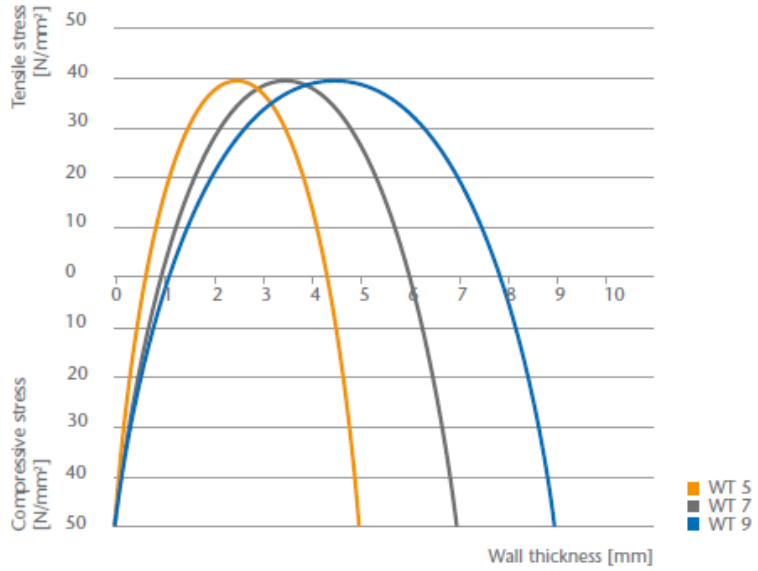

Figure 7 Stress profile for a tube with a diameter of 120 mm for several wall thicknesses (SCHOTT. n.d.).

To check that the tubes can resist the stresses due to the curing process, a GH-GSA (Grasshopper- Oasys GSA) model is made. In the following chapter a description will be given on how to make the model. After that, the results will be discussed.

A.9.3.1. Making the GH-GSA model

As described above, the purpose of the model is to analyse the stresses due to thermal expansion of materials with different expansion coefficients. Firstly, a parametric 2D model is made in Grasshopper of the cross section from the 300 mm samples. Due to the fact that it is parametric, thicknesses of the glass/interlayer can be changed quickly. In figure 9, the script

made in Grasshopper is shown. This will be explained by steps in this chapter. In figure 8, the model is displayed in Rhino.

The model is based on samples with a length of the 300 mm:

- Outer tube: OD = 115 mm, WT = 5 mm, L = 300 mm
- Inner tube: OD = 100 mm, WT = 5 mm, L = 300 mm
- Cavity = 2.5 mm

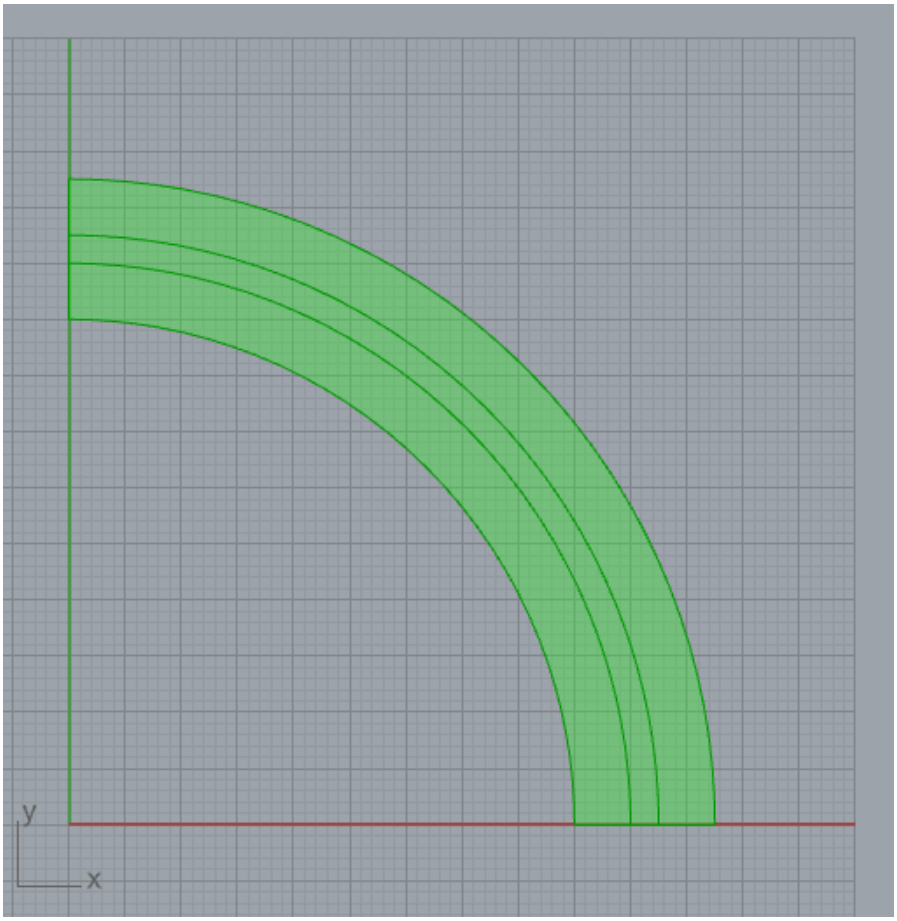

Figure 8 The Rhino model of the script in GH with a quarter of the 2D cross-section of the two tubes with the interlayer in between.

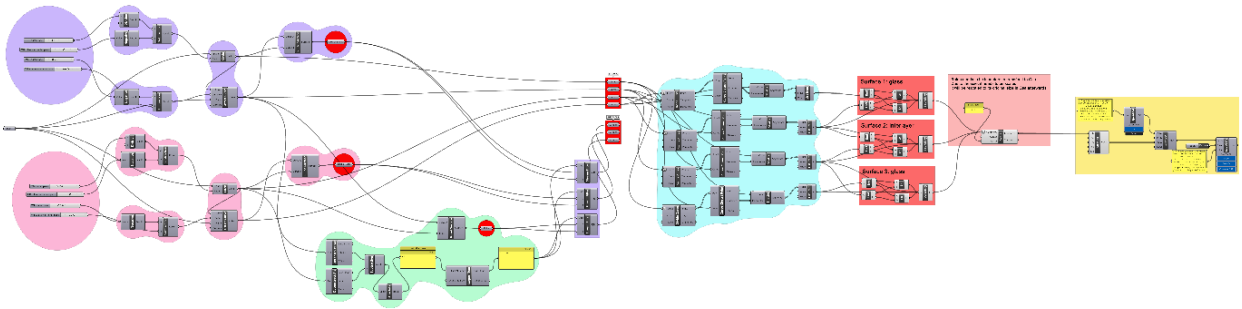

Figure 9 Overview of the GH-model

In the beginning of the script the parameters are given for the glass, and circles are made (figure 10).

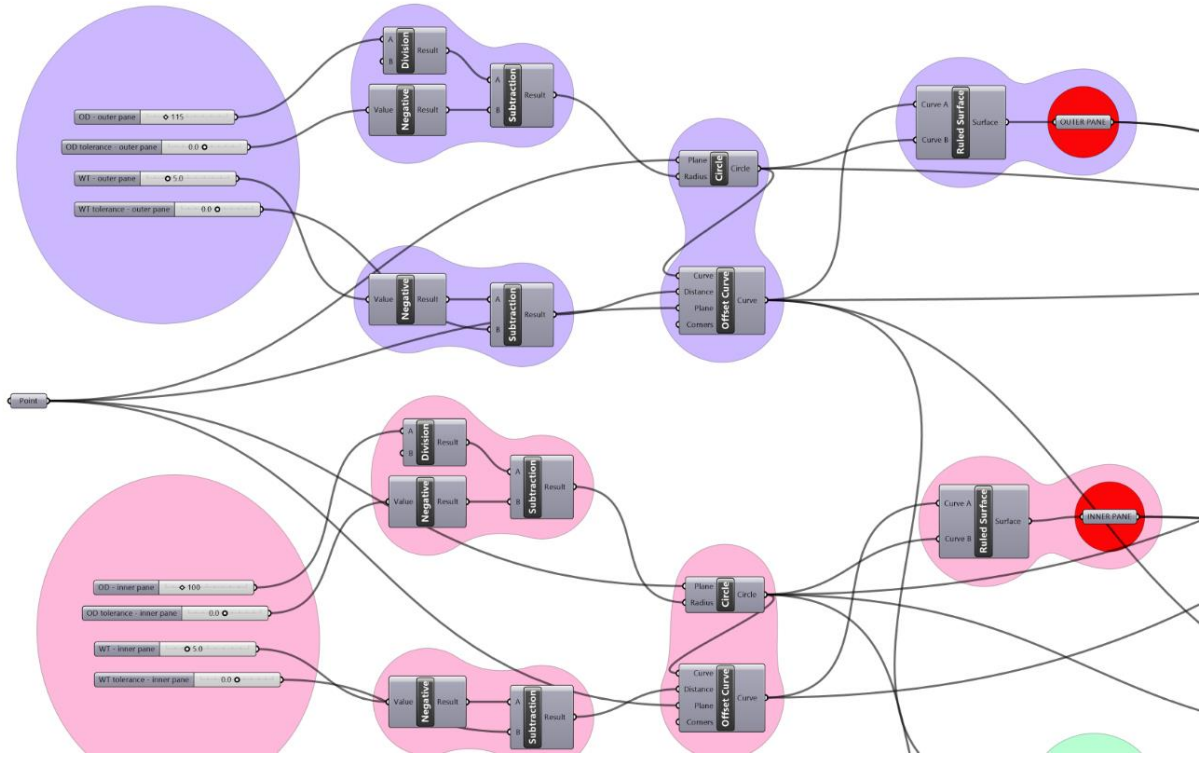

Figure 10 Parameters of the glass and making of the circles for the inner and outer tubes

From the circles, the interlayer resin can be made (figure 11).

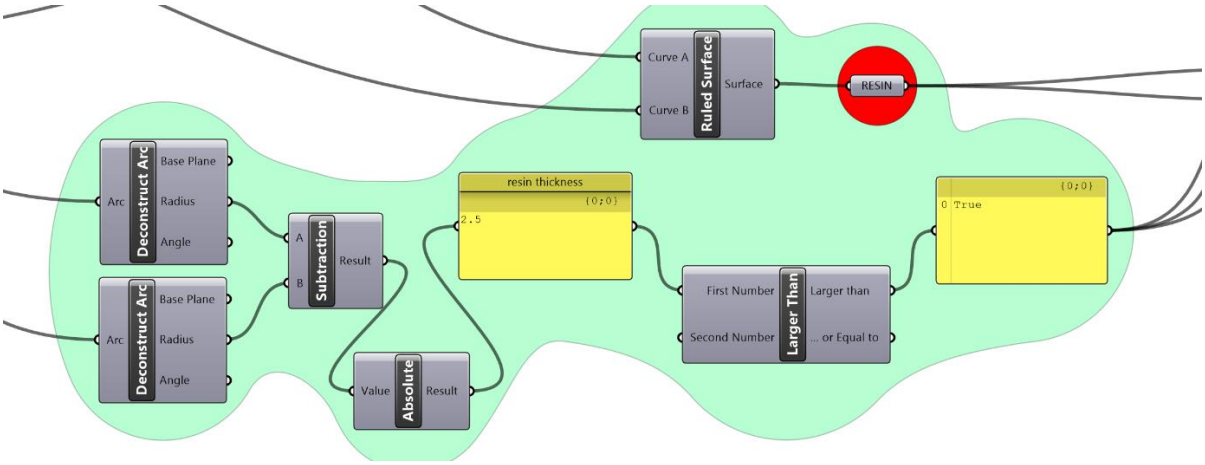

Figure 11 making of the interlayer resin

From these values, surfaces and curves can be made (figure 12).

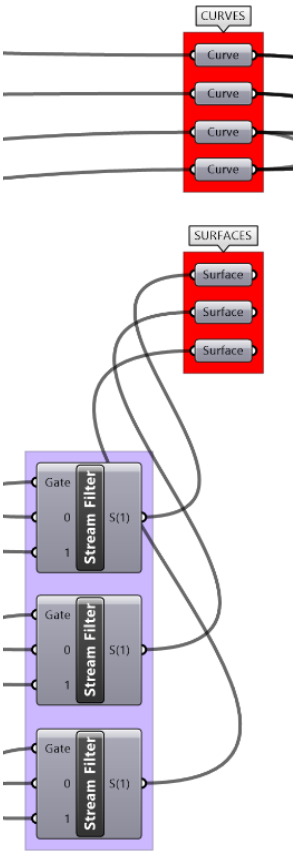

Figure 12 surfaces and curves from the obtained values

The model can also be calculated with a quarter. It is even faster if only a quarter is given in the GSA-model. From the components in figure 13, curves are given.

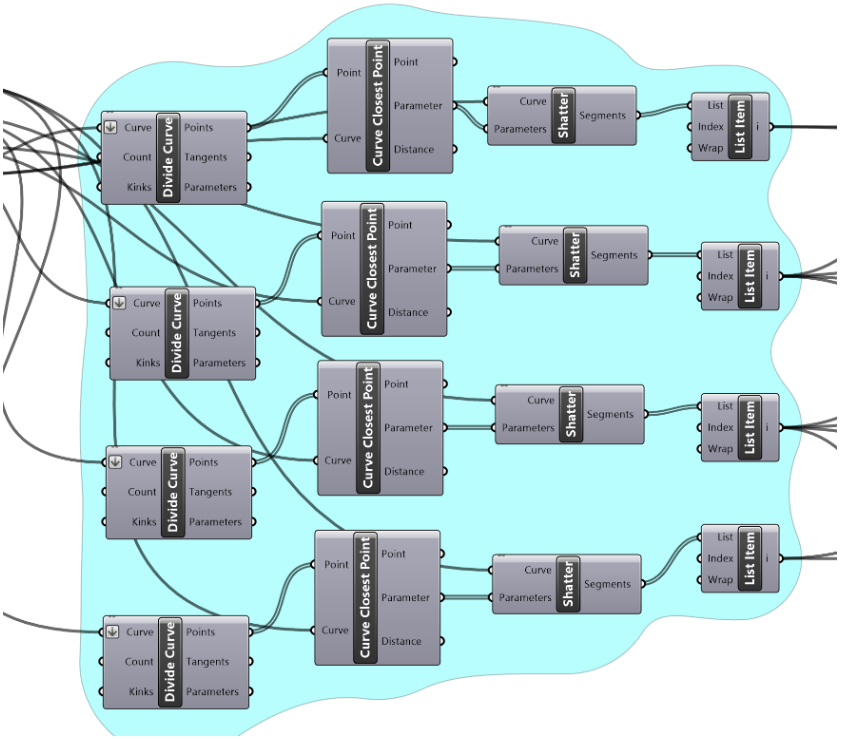

Figure 13 To make a quarter of the circle

From the lines, surfaces need to be made again (figure 14).

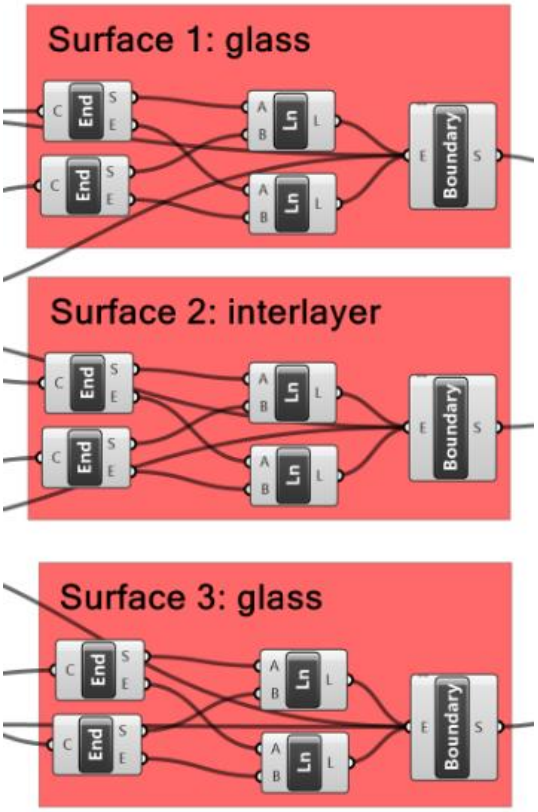

Figure 14 Making surfaces from the lines

In this GH-model, the model is scaled with a factor of 100. The model is made in mm and it needs to be in meters, so to go from mm to meters and to scale times 100, a factor of 0.1 is implemented (see figure 15). If the model is not scaled by 100, it is too small to transfer it to GSA. If it is transferred into GSA, it will be scaled back into GSA.

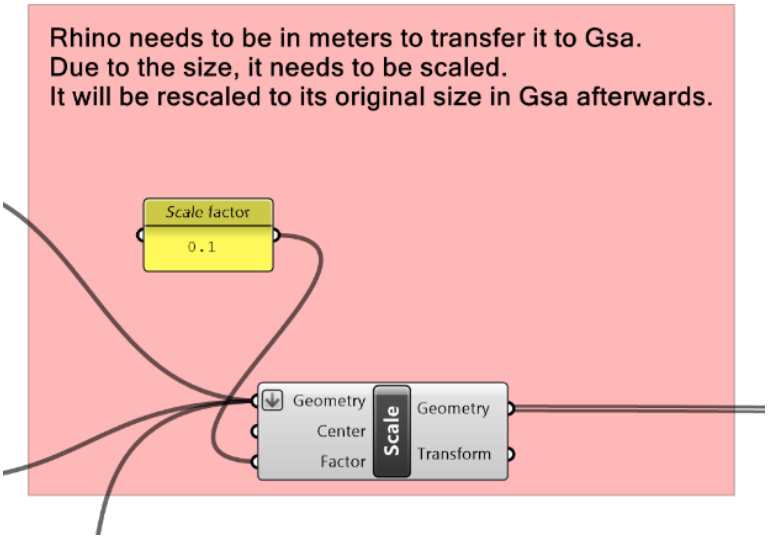

Figure 15 Scaling the model

The last step is transferring the model into GSA. Via the command ‘TestPackageManager’ the plugin for GSA can be downloaded. The components in figure 16 are needed to transfer the model into GSA. In ‘OpenGSA’ an empty GSA file can be plugged in. With the ‘Save GSA’ component the GH-model will be uploaded into the empty file and will be saved as a new file.

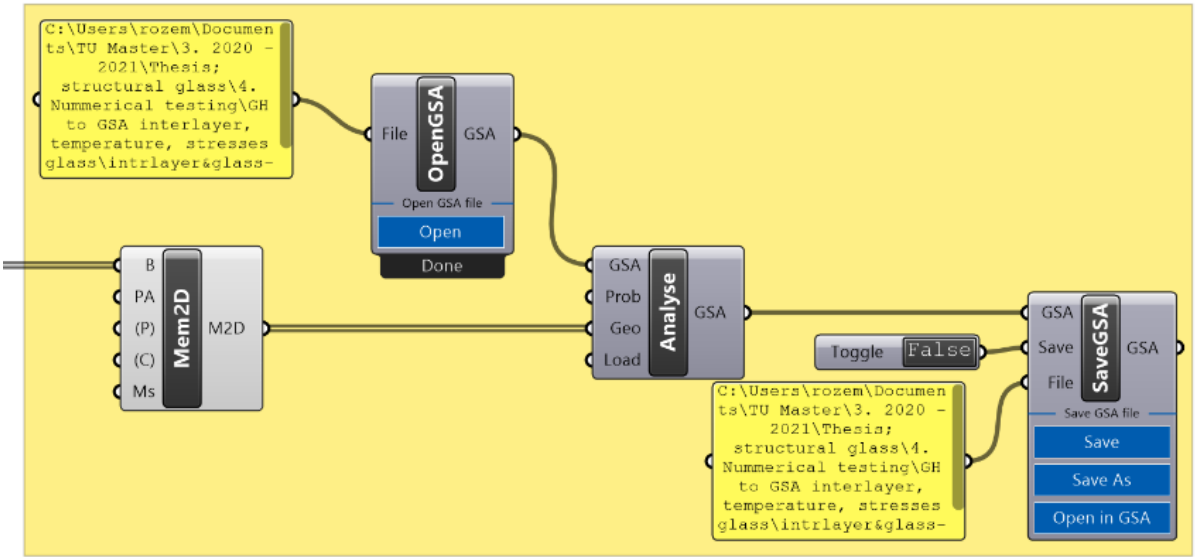

Figure 16 Open and Save the GH-model into GSA

The file where the GH-model will be placed in, need to be prepared:

- In ‘specifications’ the right ‘units’ needs to be set.
- In ‘specifications’ to ‘general’, the tolerances need to be adjusted to 0.1 mm.
- In ‘members’ three times a member needs to be set with 2D generic, and with a ‘target mesh size’ of 0.1 mm.

Furthermore, the material properties can already be given. For glass, (standard) borosilicate glass is used with the following values (these values are given by SCHOTT):

- Density: 2.23 t/m^3
- Young’s modulus: 64000 N/mm^2
- Poisson’s ratio: 0.2
- Thermal expansivity: 3.25*10^{-6} 1/°C

For the interlayer resin, two materials were considered. The first one is a UV-curing transparent interlayer resin, named the Koedilan LED UV curing LOCA material (these values are given by H.B.Fuller Kömmerling):

- Density: 1.02 t/m^3
- Young’s modulus: 0.18 N/mm^2
- Poisson’s ratio: 0.495
- Thermal expansivity: 70*10^{-6} 1/°C
- Shrinkage: 12%

And the second is: 2 PU component Ködistruct LG LOCA material (these values are given by H.B.Fuller Kömmerling):

- Density: 1.05 t/m^3
- Young’s modulus: 65 N/mm^2

- Poisson's ratio: 0.495
- Thermal expansivity: 200*10^{-6} 1/°C
- Shrinkage: 2%

The material is created in 'advanced material properties' in GSA.

After the materials are made, these could be assigned to the '2D properties'. Element type 'shell' is used. It is necessary to give it a thickness. This value does not matter, due to the fact that the model that has been created is 2D. Nevertheless, the program is set in 3D, so a thickness is required. In '2D properties', also a colour can be assigned to the different materials.

After the model is saved from GH to GSA, the scaling factor of 100 needs to be undone and the mesh size needs to be adjusted. The 'nodes' (x, y, z) from GSA can be copied into Excel, where the values can be divided by 100. After that the Excel values can be copied back into the GSA 'nodes'. Then the mesh size can be adjusted in the analyse layer:

- Select the mesh and delete it
- Select the nodes and delete it
- Use 'coordination tools' to create a mesh from members

After this in 'members', the 'target mesh size' need to be changed in 0.005 mm.

Now the constrains can be set:

- All nodes need to be constrained in the z-direction
- The nodes at the end at the top, need to be constrained in the x-direction
- The nodes at the end at the bottom, need to be constrained in the y-direction

In 'Label and Display methods', then 'colour entities', 'by property' need to be checked, so that the model with its different material properties can be displayed by a colour. This colour is given in 2D properties.

Lastly a load can be assigned. In 'loading' going to '2D element loading', in 'Thermal', a temperature is given from 100 °C, set to all elements. This load is set into Load Case 1 thermal (LC1).

Now the analysis can start. In figure 17 The GSA-model is shown in the analyse layer.

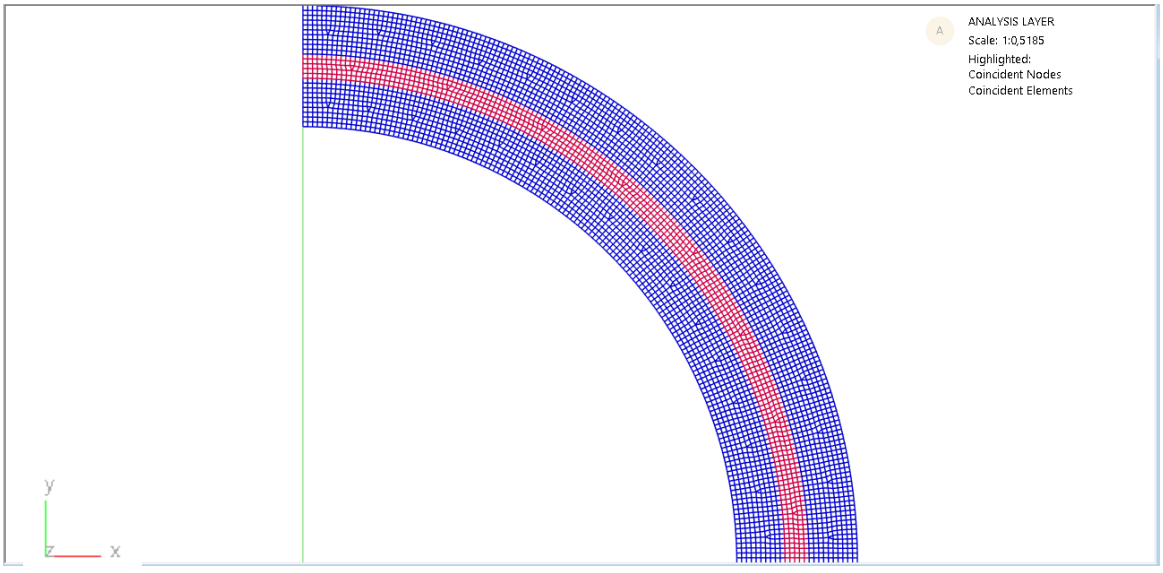

Figure 17 The GSA-model Analyse layer

A.9.3.2. Analyses of the GSA-model

A.9.3.2.1. All glass layers

From the model made in A.4.3.1, first the model will be analysed in the case that all the three layers are made out of glass. In this way, all the layers have the same thermal expansion coefficient. This means that due to the temperature, it will only expand. Almost no stresses may occur.

In figure 18 and, the deformation is shown, and in figure 20, the stresses are shown. As can be seen, almost no stresses are occurring as expected (around 0,01 MPa).

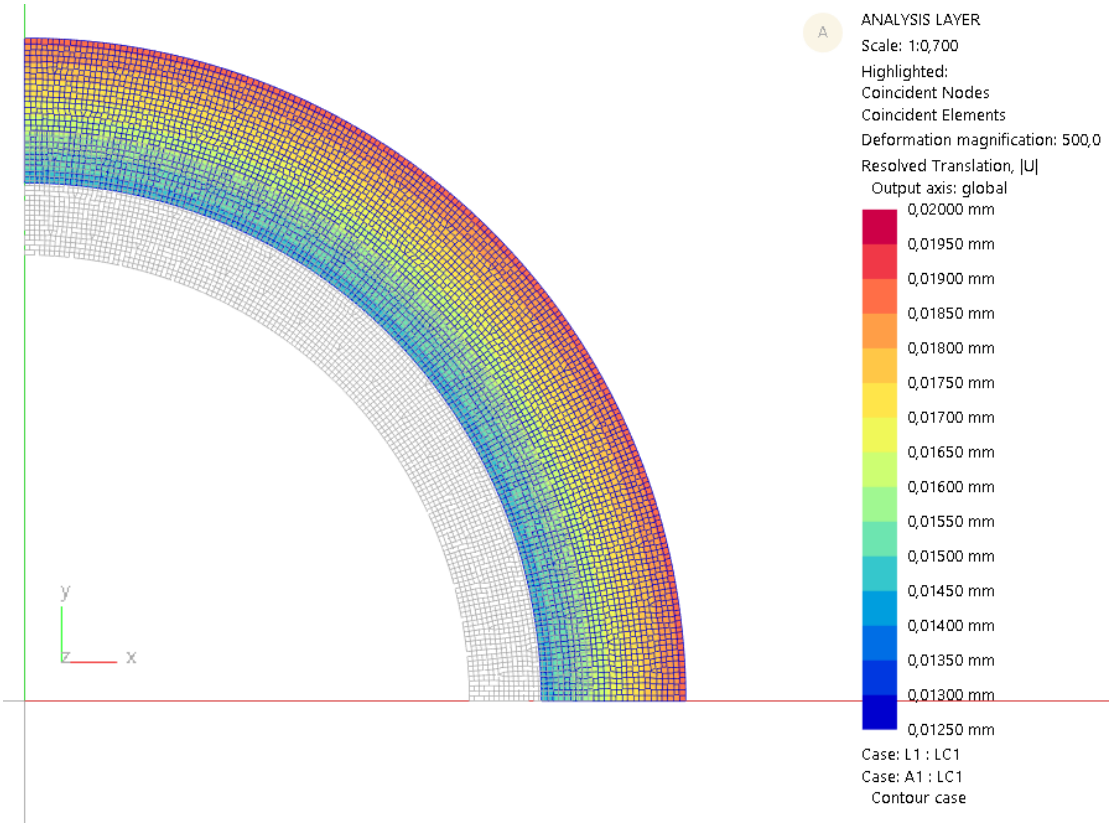

Figure 18 Deformation of the tube (only glass) in the deformed view.

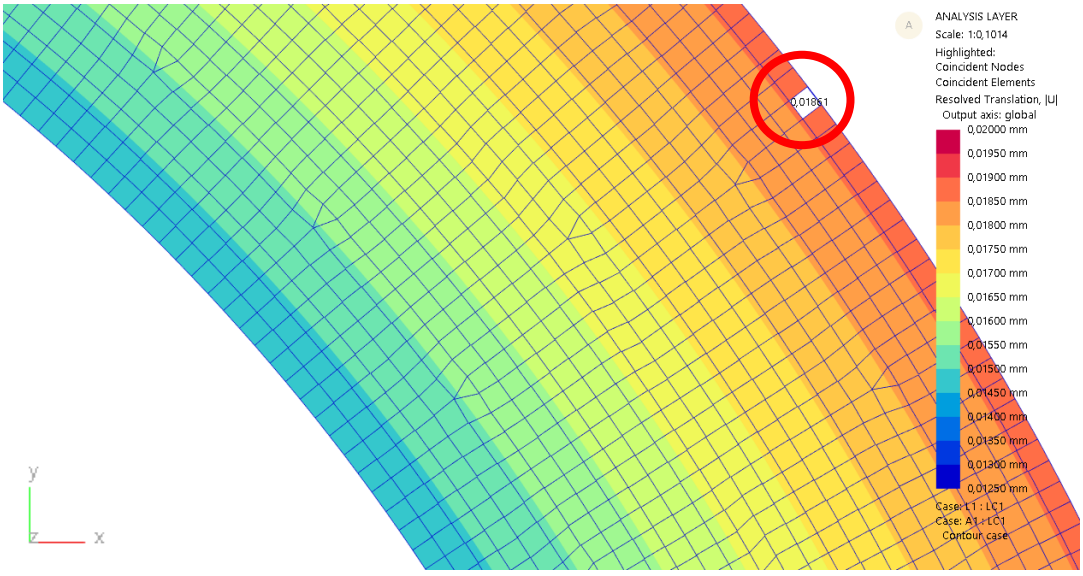

Figure 19 Deformation of the tube (only glass) zoom-in (value: 0.01861 N/mm^2).

To verify the model, equation A.9.13. can be used again.

$$d_{fin} = 115 * [100 * 3.3 * 10^{-6} + 1] = 250.037\ mm \quad \text{(A.9.22)}$$

With:

- d_{ini} = 115 mm
- ΔT = 100 °C
- α_T = 3.3*10^{-6} 1/°C

So, the expansion of the diameter from one side is:

$$\frac{0.037}{2} = 0.0185 \quad \text{(A.9.23)}$$

As can be seen in figure 19, the expansion is around 0.0186 mm. So, the model is correct.

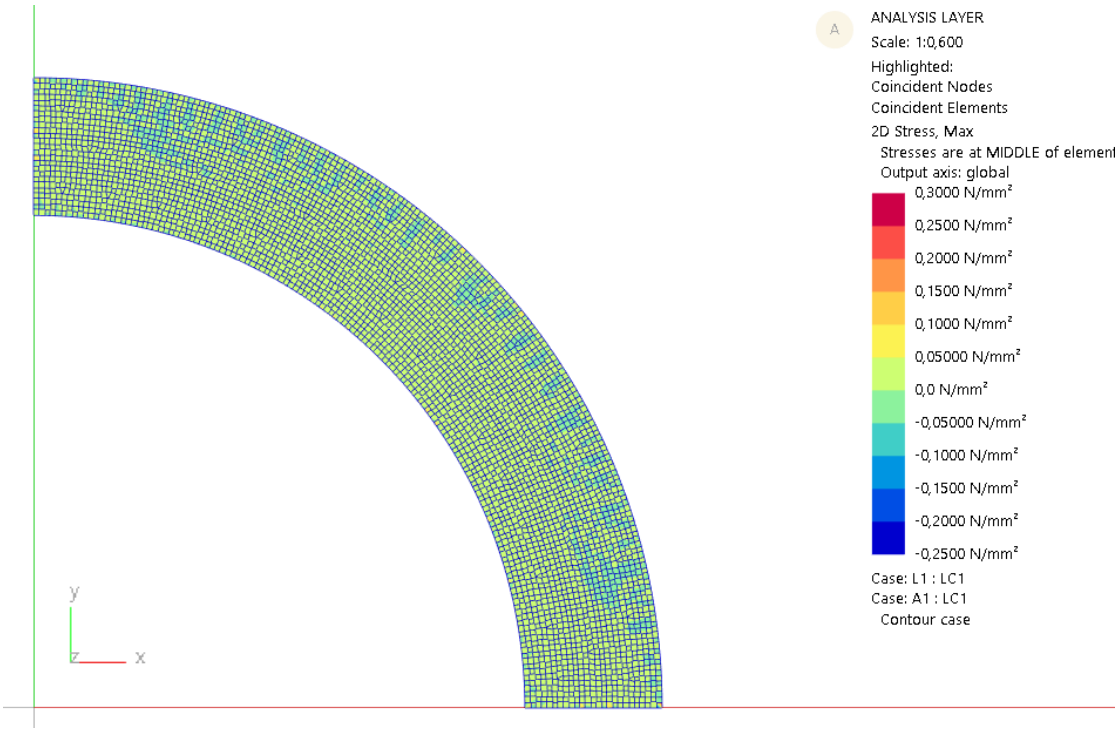

Figure 20 Main stresses in the tube (only glass).

A.9.3.2.1. Glass outer layers with interlayer Koedilan LED UV curing LOCA material

Now the middle layer will be changed into the interlayer resin material Koedilan LED UV curing LOCA material (as shown in figure 17). Next to expansion, also stresses need to occur. In figure 21 and 22, the deformation is given. As can be seen not much is changed here compared to the model with only glass. The expansion is still around 0.0186 mm. In figure 23 the stresses are given.

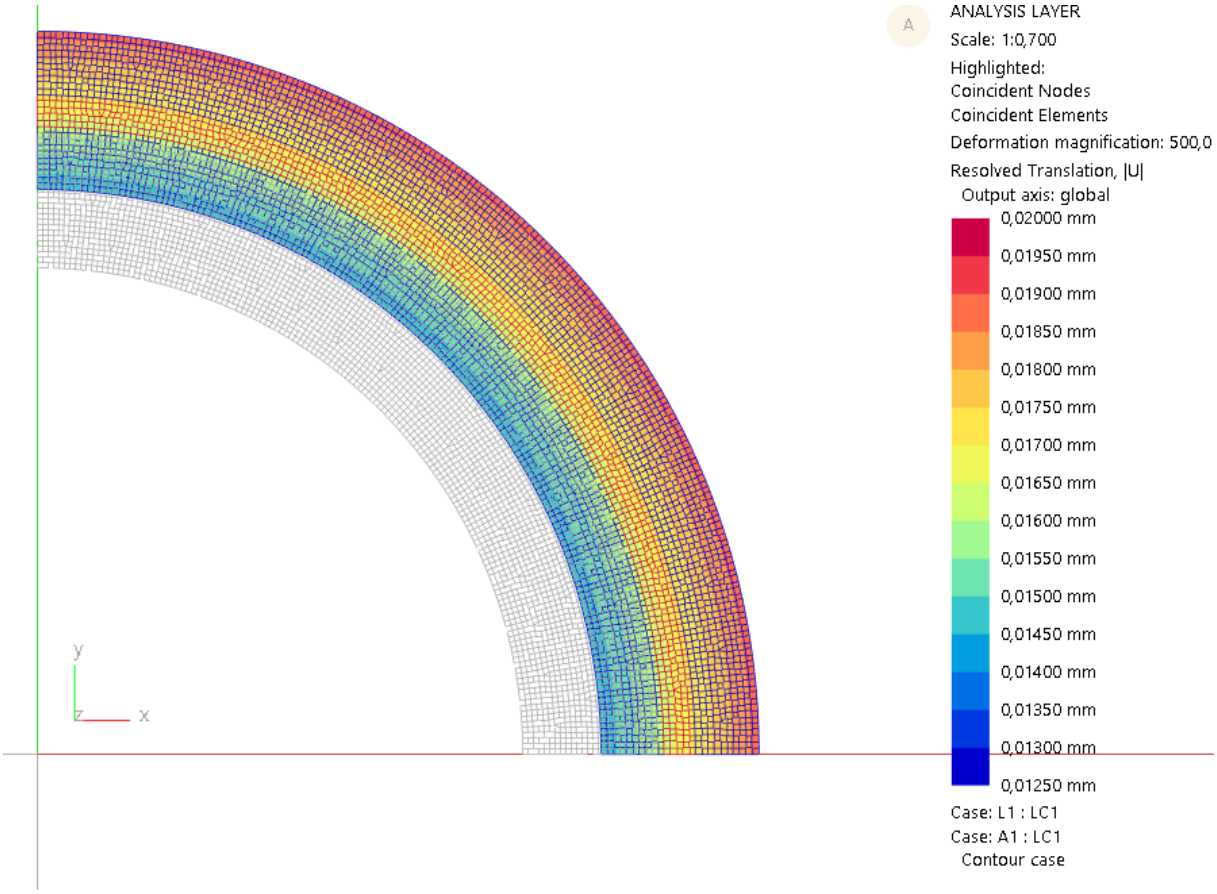

Figure 21 Deformation of the tube (glass-interlayer-glass) in the deformed view.

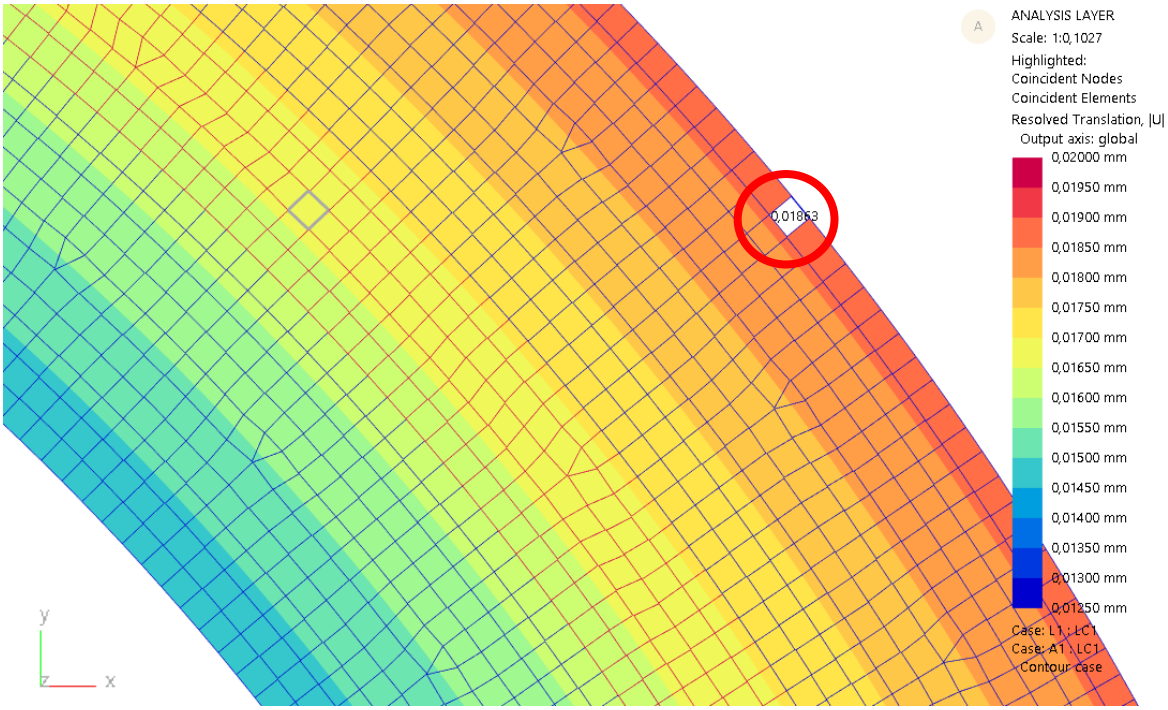

Figure 22 Deformation of the tube (glass-interlayer-glass) zoom-in (value: 0.01863 N/mm^2).

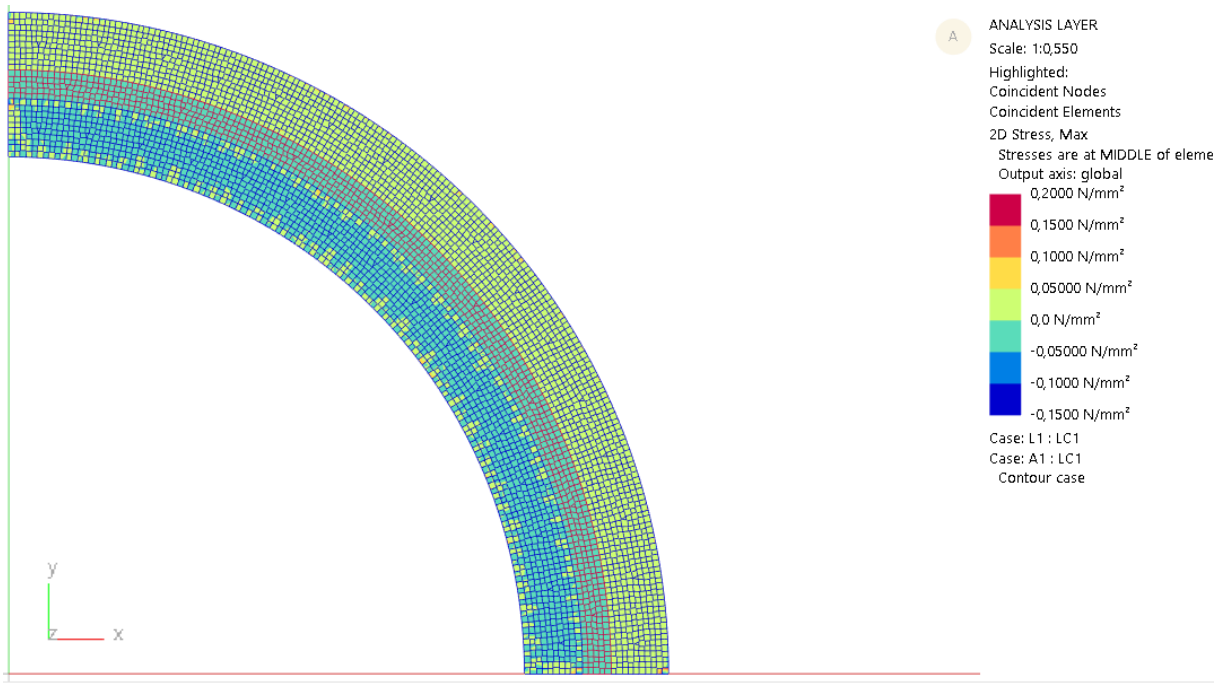

Figure 23 Main stresses in the tube (glass-interlayer-glass).

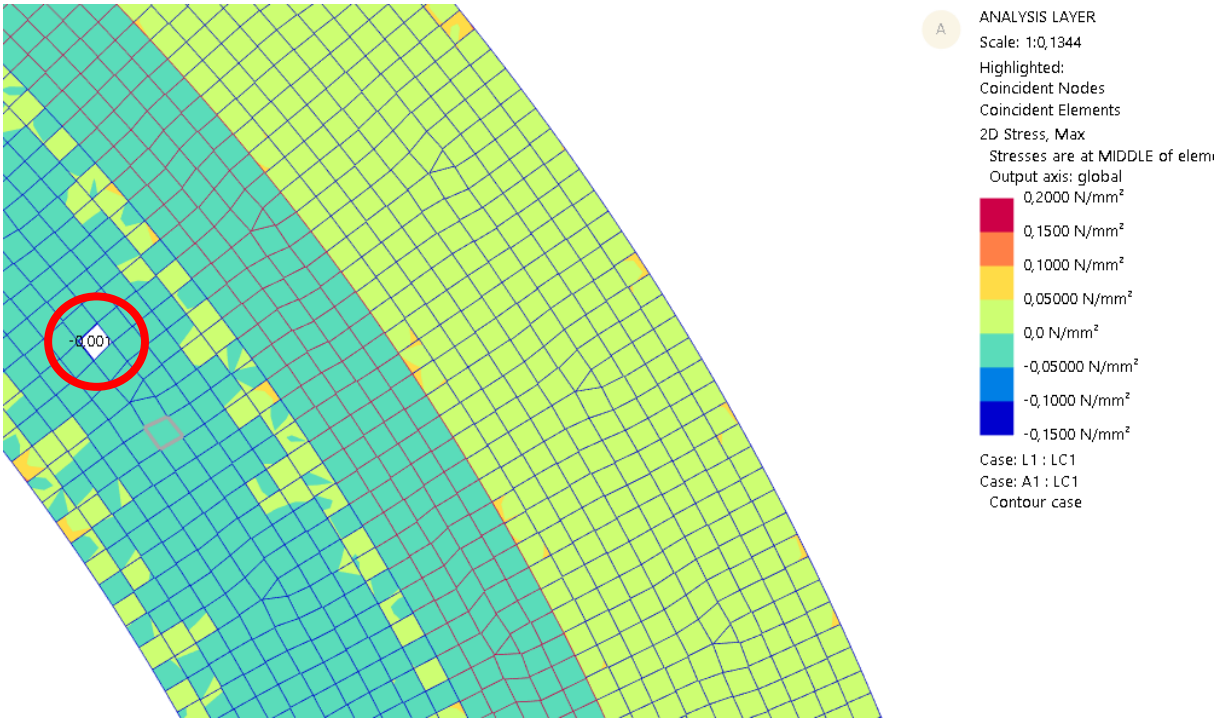

Figure 24 Main stresses of the tube (glass-interlayer-glass) zoom-in on the inner glass layer (compression stresses) (value: -0.001 N/mm^2).

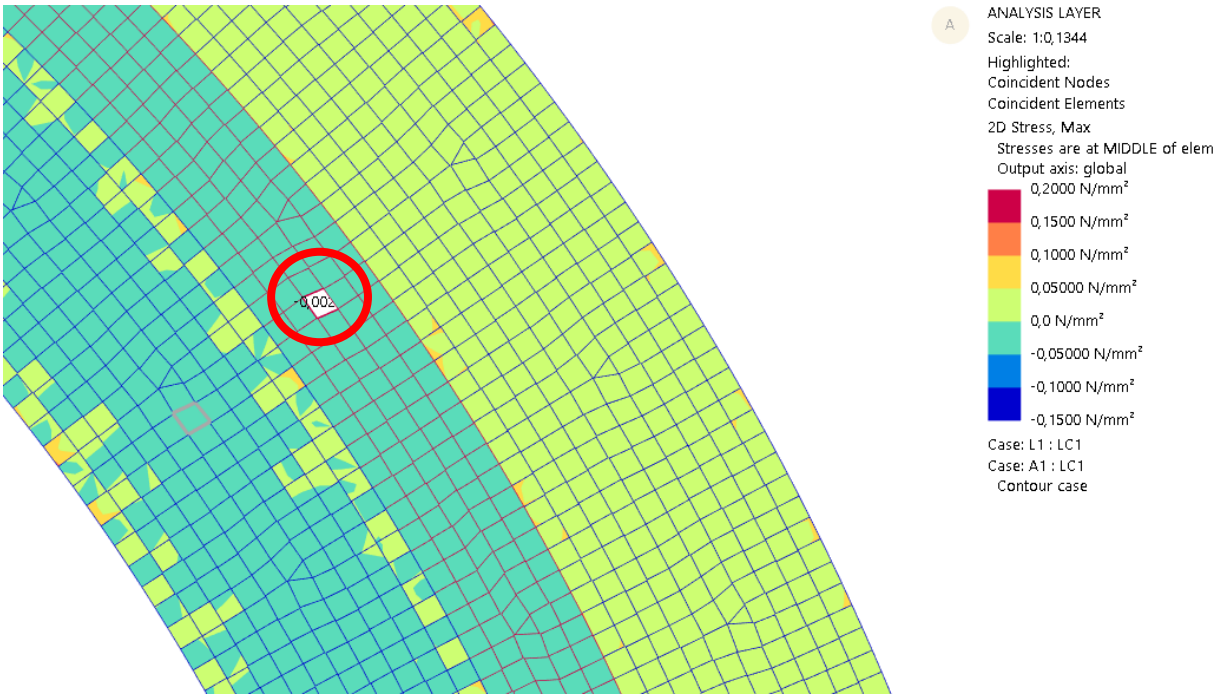

Figure 25 Main stresses of the tube (glass-interlayer-glass) zoom-in on the interlayer (compression stresses) (value: -0.002 N/mm^2).

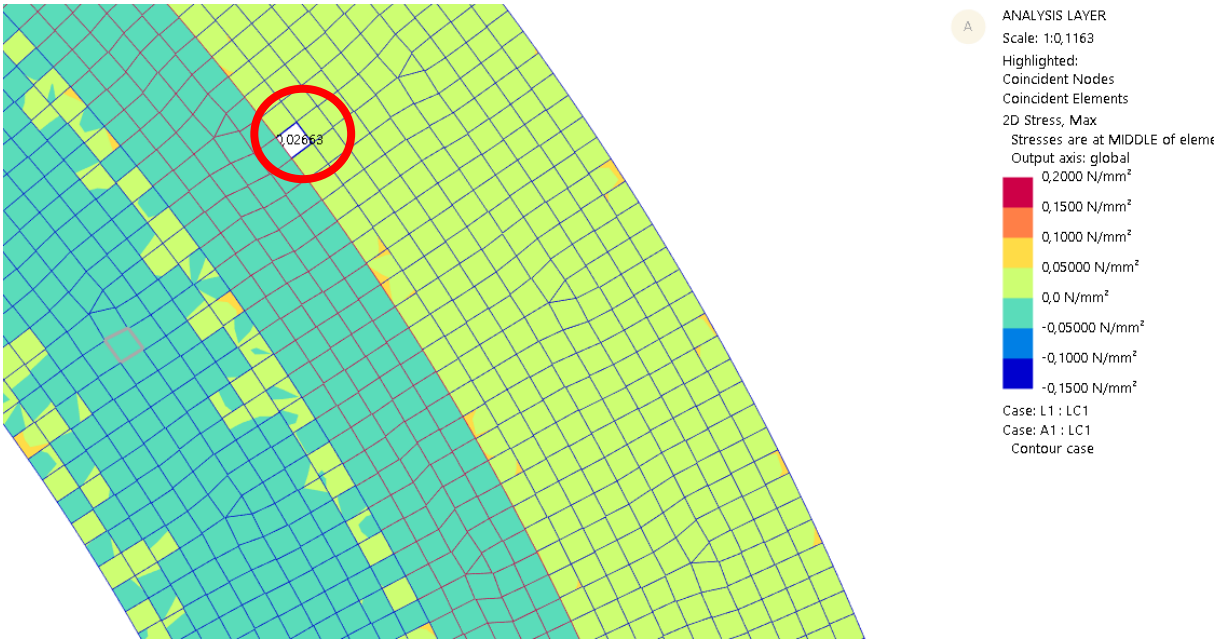

Figure 26 Main stresses of the tube (glass-interlayer-glass) zoom-in on the outer glass layer (tensile stresses) (value: 0.02663 N/mm^2).

As can be seen, the interlayer resin material wants to expand with a high thermal expansion coefficient, but it is enclosed into the two glass layers with low thermal expansion coefficients. So, the interlayer is not free to expand, and this will give stresses. This interlayer material pushes onto both glass tubes, which results in compression stresses into the inner glass layer, and in tensile stresses into the outer glass layer (see figure 27).

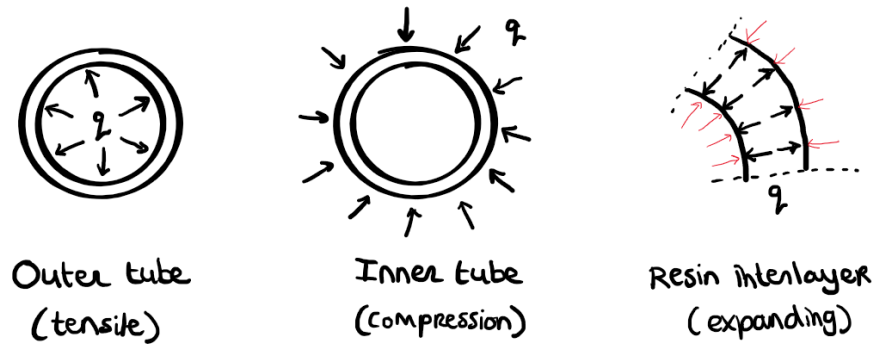

Figure 27 Stresses into the layers due to expansion of the interlayer resin.

In the figure 23-26, the GSA model is shown for this situation. In the inner tube and the interlayer resin compression stresses occur, and in the outer tube tensile stresses occur.

To measure the values of these stresses, the following formula can be used. This is based on cylinder thin-walled hoop stresses (Wikipedia. 2021):

$$\sigma_h = \frac{p*r}{t} \qquad \text{(A.9.24)}$$

With:

- p: pressure [Mpa]
- r: radius [mm]
- t: thickness [mm]

To determine the pressure, formula A.9.25, can be rewritten into A.9.26 and in A.9.27:

$$\Delta L = \frac{F*L}{E*A} \qquad \text{(A.9.25)}$$

$$F = \alpha * \Delta T * E * A \qquad \text{(A.9.26)}$$

$$p = \Delta\alpha * \Delta T * E_{resin} \qquad \text{(A.9.27)}$$

To determine the stresses in the glass, equation the formulas above can be rewritten as:

$$\sigma_{glass} = \Delta\alpha * \Delta T * E_{resin} * (\frac{t_r}{t_g}) \qquad \text{(A.9.28)}$$

- t_r: thickness of the resin layer [mm]
- t_g: thickness of the glass layer [mm]
- F: force [kN]
- L: length [mm]
- α: thermal expansion coefficient [1/°C]
- E: Yong's modulus [MPa]
- A: area [mm^2]
- ΔT: temperature difference [°C]

The following values will be applied (the same values are used in the GSA model):

- Radius: 115/2 = 57.5 mm
- α_{resin}: $7.0*10^{-5}$ 1/°C
- α_{glass}: $3.25*10^{-6}$ 1/°C
- Δα: $6.68*10^{-5}$ 1/°C
- E_{resin}: 0.18 Mpa

- ΔT: 100 °C
- t_r: 2.5 mm
- t_g: 5 mm

Filling in equations A.9.27 and A.9.24 it will give the following hoop stresses:

$$p = 6.68 * 10^{-5} * 100 * 0.18 = 0.001\ MPa \qquad \text{(A.9.29)}$$

$$\sigma_h = \frac{0.001*57.5}{5} = 0.0138\ MPa \qquad \text{(A.9.30)}$$

The stresses in the glass will can be determined by filling in equation A.9.28:

$$\sigma_{glass} = 6.68 * 10^{-5} * 100 * 0.18 * \left(\frac{2.5}{5}\right) = 0.001\ MPa \qquad \text{(A.9.31)}$$

Looking at figures 24-26, the stresses determined in GSA are in the same range as the stresses determined in equations A.9.30 and A.9.31. These stresses are quite low, so in theory this will not result in problems during/after curing. H.B.Fuller Kömmerling tried to bond two tubes with an interlayer resin before, ten years ago. Regarding to their experience back then, the glass tubes broke. They proposed to use an interlayer material which will reduce the impact of chemical induced reaction shrinkage, by shifting from van-der-Waals interactions to chemical bonds during curing and keeping the curing temperature as low as possible to avoid additional thermal shrinkage in the post-gelling phase. For this reason, they want to use an interlayer resin material which will cure/cool in room-temperature and not cured by UV-light. Besides, they want to use an interlayer material which has a lower shrinkage value. In the article of Veer, he also mentioned that shrinkage of the interlayer resin can cause stresses into the glass (Veer, F.A., et al. 1999).

References

Glass on Web. (2020). Development of a CCF Glass Tube Façade in Hong Kong. From: https://www.glassonweb.com/article/development-ccf-glass-tube-facade-hong-kong

Kasunic, K.J. (2015). Optomechanical Systems Engineering. John Wiley & Sons.

NEN 2608. (2014). Glass in building - Requirements and determination method, pp.

SCHOTT. (n.d.). DURAN®. Tubing, rods and capillaries made of borosilicate glass 3.3. Retrieved on January, 20, 2021.

SCHOTT. (n.d.). DURATAN®. Thermally prestressed tubing of special glass. Retrieved on May, 10, 2021, from: SCHOTT.

Engineering ToolBox. (2010). Thin Circular Ring - Temperature and Expanding Radius. Retrieved on March, 20, 2021, from: https://www.engineeringtoolbox.com/thin-circular-ring-radius-temperature-change-d_1612.html

Van der Linden, A.,C., Kuijpers-van Gaalen, I., M., Zeegers, A. (2018). Building Physics (2nd ed.). Thiememeulenhoff BV.

Veer, F.A., Pastunink., R.J. (1999). Developing a Transparent Tubular Laminated Column. Proceedings Glass Performance Days, pp. 277-280.

Wikipedia. (2021). Cylinder stress. Retrieved on April, 10, 2021, from: https://en.wikipedia.org/wiki/Cylinder_stress

Figure list

Figure 1 - Glass on Web. (2020). Development of a CCF Glass Tube Façade in Hong Kong. Retrieved on February, 6, 2021, from: https://www.glassonweb.com/article/development-ccf-glass-tube-facade-hong-kong

Figure 2 - Eckrsley O'Callaghan. (2021). K11 Art and Cultural Centre. Retrieved on April, 13, 2021, from: https://www.eocengineers.com/en/projects/k11-art-and-cultural-centre-310

Figure 3 - Own picture. Delft. Retrieved on February, 19, 2021.

Figure 4 - SCHOTT. (n.d.). DURAN®. Tubing, rods and capillaries made of borosilicate glass 3.3, pp. 16. Retrieved on November 11, 2020, from: https://www.schott.com/en-gb/products/duran/downloads

Figure 5 - SCHOTT. (n.d.). DURAN®. Tubing, rods and capillaries made of borosilicate glass 3.3, pp. 17. Retrieved on November 11, 2020, from: https://www.schott.com/en-gb/products/duran/downloads

Figure 6 - Own picture. Delft. Retrieved on April, 7, 2021.

Figure 7 - SCHOTT. (n.d.). DURATAN®. Thermally prestressed tubing of special glass, pp. 7. Retrieved on May, 10, 2021, from: SCHOTT.

Figure 8 - Own picture. Delft. Retrieved on May, 3, 2021.

Figure 9 - Own picture. Delft. Retrieved on May, 3, 2021.

Figure 10 - Own picture. Delft. Retrieved on May, 3, 2021.

Figure 11 - Own picture. Delft. Retrieved on May, 3, 2021.

Figure 12 - Own picture. Delft. Retrieved on May, 3, 2021.

Figure 13 - Own picture. Delft. Retrieved on May, 3, 2021.

Figure 14 - Own picture. Delft. Retrieved on May, 3, 2021.

Figure 15 - Own picture. Delft. Retrieved on May, 3, 2021.

Figure 16 - Own picture. Delft. Retrieved on May, 3, 2021.

Figure 17 - Own picture. Delft. Retrieved on May, 4, 2021.

Figure 18 - Own picture. Delft. Retrieved on May, 10, 2021.

Figure 19 - Own picture. Delft. Retrieved on May, 10, 2021.

Figure 20 - Own picture. Delft. Retrieved on May, 10, 2021.

Figure 21 - Own picture. Delft. Retrieved on May, 11, 2021.

Figure 22 - Own picture. Delft. Retrieved on May, 11, 2021.

Figure 23 - Own picture. Delft. Retrieved on May, 11, 2021.

Figure 24 - Own picture. Delft. Retrieved on May, 11, 2021.

Figure 25 - Own picture. Delft. Retrieved on May, 11, 2021.

Figure 26 - Own picture. Delft. Retrieved on May, 11, 2021.

Figure 27 - Own picture. Delft. Retrieved on May, 12, 2021.

Appendix 10 – Compression calculations

A.10.1. Numerical Analyses

There are some types of analyses to test the behaviour of the glass element (O'Regan, C. 2015):

- Linear elastic
- Geometrically non-linear
- Materially/ Physically non-linear
- Non-linear boundary conditions

A linear elastic analysis is a structural model analysis. In here the material stress-strain relationship is linear and structural deflections needs to be small (half a thickness of the glass plane). So, with small deflections, linear elastic analysis is accurate enough. A FEM computer model which this type of analysis can calculate the result fast. However, it is not suitable for every situation (O'Regan, C. 2015).

If there are small deformations, and the element is subjected to high stresses, it is more accurate to test the model by a geometrically non-linear analysis. If stresses are equal to the plate thickness, a transition occurs. Then the deformation increases and the stresses are being redistributed. At larger deflections, a linear analysis will over-estimate the stresses which can lead to inaccuracies. Furthermore, if there are initial support movements, or element imperfections, which can influence the structural stiffness, a non-linear analysis is needed. A stability analysis is required, also known as a second order theory (O'Regan, C. 2015). In chapter 2.2.2.1. and 2.2.2.2. more information is given on stability analyses and buckling.

For non-linear elastic materials, a non-linear or a hyper-elastic material model is required. Glass is a linear elastic material till fracture. The modulus of elasticity is constant without plastic deflections or yielding point. Interlayers, silicone adhesives and steel connections, are not linear elastic. To get an accurate model, a physically or a materially non-linear model needs to be analysed. This is especially the case when the element is subjected to high strains (O'Regan, C. 2015).

Lastly, if boundary conditions are based on the applied load (elastic bedding, soft sub-frames, contact capturing problems, or compression/tension only supports), the effects need to be incorporated in the model. For this situation, spring models with a stiffness or compression only supports can be used. Normal boundary conditions remain rigid under applied loads, then a non-linear boundary condition analysis is not necessary (O'Regan, C. 2015).

Furthermore, advanced FEM models can be considered for the following analysis:

- Dynamic
- Viscoelastic
- Creep
- Probabilistic
- Fragmentation

When loads are different over a certain time, like with impact loads, dynamic analysis should be performed. Impact loads can be subdivided into soft-body and hard-body impact loads. People and objects can introduce vibrations to the glass element. For structural elements which have time-dependent stress-strain properties, viscoelastic or creep analysis can be

done. A failure probability can be required by a probabilistic analysis. When a material is brittle, and breaks into pieces when the limited stress is reached, fragmentation analysis can be performed. Nevertheless, fragmentation analysis is still in development. In this analysis the cracks and the propagation can be obtained (O'Regan, C. 2015).

With FEM modelling, reliable results are depending on a converged solution. To verify the convergence, more solutions are needed. When the result is too different from the original solution, it is for sure that the result did not converged. When the result is not changing much anymore, then the result is converged correctly. The two methods to show that the solution has been converged are: p-refinement and h-refinement. These methods are two different approaches where degrees of freedom (dof) are added to the FEM model (figure 1). The h-refinement method is also known as the sensitivity mesh study. In here the use of a finer mesh needs to give a more accurate result, while the degree of elements used is fixed (figure 2). The mesh must be changes when a more accurate result is wanted. The FEM model runs again and gives a new solution. When this solution is still too different compared to the solution required before, the mesh needs to be finer. This needs to be repeated until the results are almost not changing from each other anymore. With p-refinement, the mesh is fixed and the polynomial degree of elements is increased. By increasing the polynomial degree, the complexity of the shape function is upgraded (figure 3) (Toogood, R. 2001).

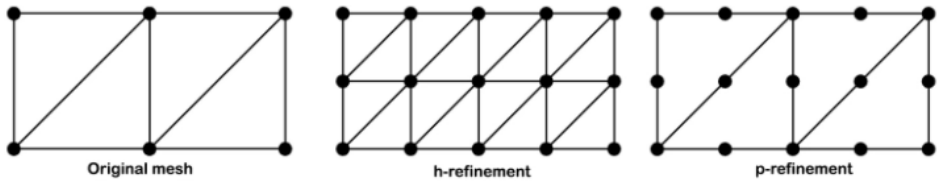

Figure 1 Degrees of freedom (Everyone is Number One. 2014).

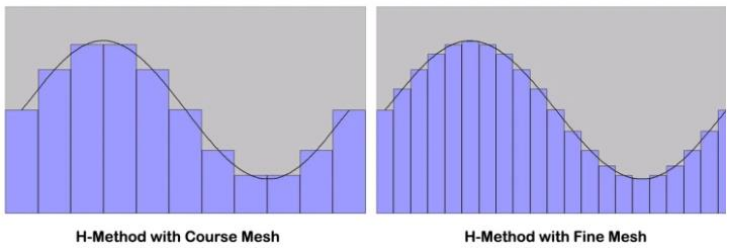

Figure 2 Effects of the h-refinement method (Everyone is Number One. 2014).

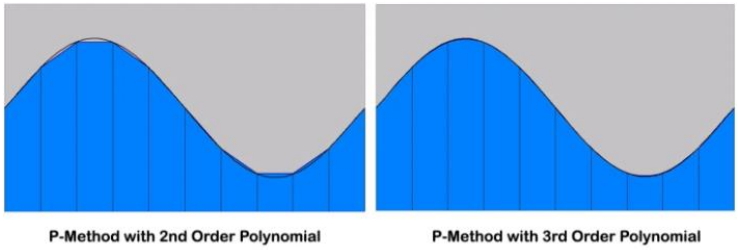

Figure 3 Effects of the p-refinement method (Everyone is Number One. 2014).

A.10.2. Buckling

The Euler's buckling formula is given in the report in equation 1. To calculate the second moment of inertia for hollow circular cross sections, the following equation can be used (figure 4):

$$I_{circle} = \frac{1}{4} * \pi * (r_{outside}^4 - r_{inside}^4) \qquad \text{(A.10.1)}$$

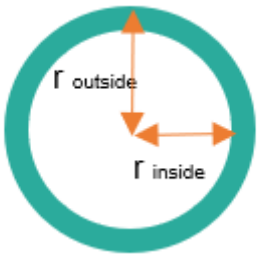

Figure 4 The cross section of a hollow circle

A.10.2.1. Buckling calculation DIANA model single tube fixed

For the critical buckling load, formula 1 can be used.

With:

- E = 70000 N/mm^2
- I = ¼ * π * ($r_{out}^4 - r_{in}^4$) = ¼ * π * ($25^4 - 24.1^4$) = 41850 mm^4
- L = 1500 mm
- K = 0.5 (fixed)

$$F = \frac{\pi^2 * 70000 * 41850}{(0.5 * 1500)^2} = 51.4\ kN \qquad \text{(A.10.2)}$$

A.10.2.2. Buckling calculation DIANA model single tube hinged

For the critical buckling load, formula 1 can be used.

With:

- E = 70 000 N/mm^2
- I = ¼ * π * ($r_{out}^4 - r_{in}^4$) = ¼ * π * ($25^4 - 24.1^4$) = 41850 mm^4
- L = 1500 mm
- K = 1 (hinged)

$$F = \frac{\pi^2 * 70000 * 87001}{(1 * 1500)^2} = 12.9\ kN \qquad \text{(A.10.3)}$$

The difference in critical load of the hinged column should be ¼ of the fixed column, this is correct.

A.10.2.3. DIANA FEA column models fixed

The parameters used in DIANA were:

- Young's modulus: 70 000 N/mm^2
- Poisson's ratio: 0.2
- Mass density: 2500 T/mm^3

At figure 5, the model for the fixed column is shown.

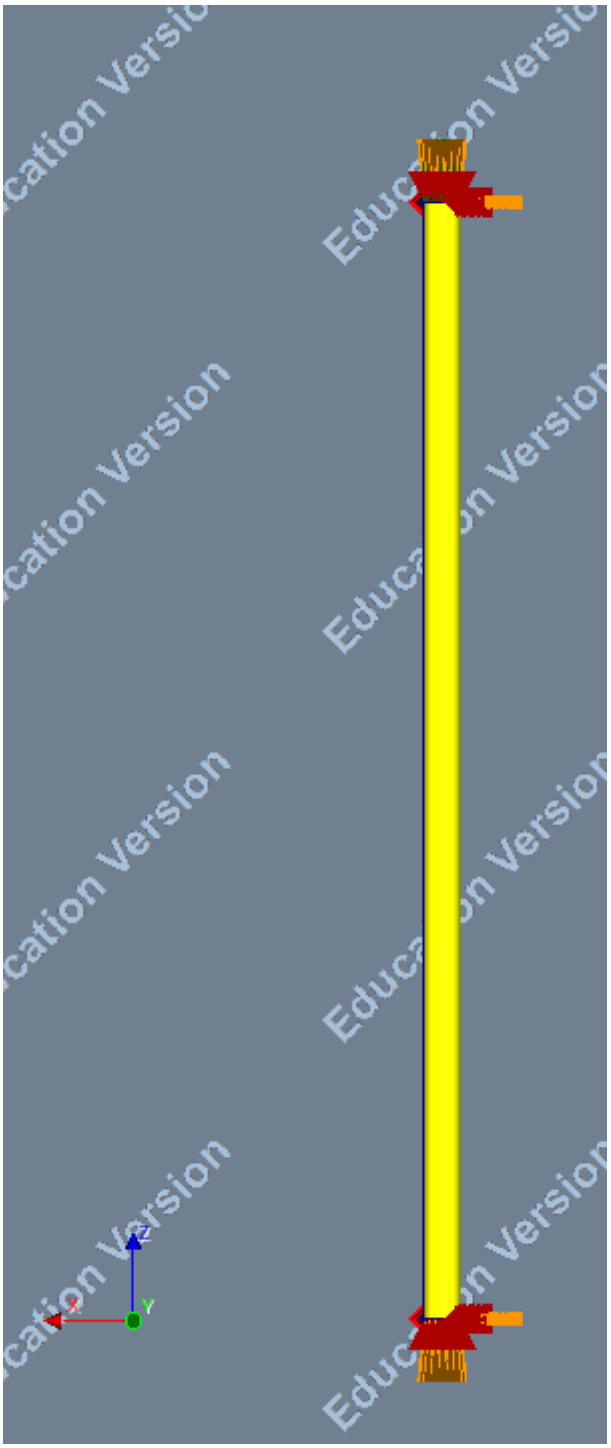

Figure 5 DIANA model of the fixed column

A few models were made, to play with the imperfection loads, finer meshes, and polynomial orders:

Test_fixed column_1:

- Geometrically non-linear analysis (quadratic)
- Imp. load: 0.01 N/mm^3 (x-direction)
- Prescribed displacement: -20 mm (z-direction)

Test_fixed column_2:

- Geometrically non-linear analysis (quadratic)
- Imp. load: 0.01 N/mm^3 (x-direction)
- Prescribed displacement: -10 mm (z-direction)

Test_fixed column _3:

- Geometrically non-linear analysis (quadratic)
- Imp. load: 0.001 N/mm^3 (x-direction)
- Prescribed displacement: -10 mm (z-direction)

Test_fixed column _4:

- Geometrically non-linear analysis (quadratic)
- Imp. load: 0.0001 N/mm^3 (x-direction)
- Prescribed displacement: -10 mm (z-direction)

Test_fixed column _5:

- Geometrically non-linear analysis (linear)
- Imp. load: 0.0001 N/mm^3 (x-direction)
- Prescribed displacement: -10 mm (z-direction)

In figure 6, the x- and the z-displacement output models are given from test 4.

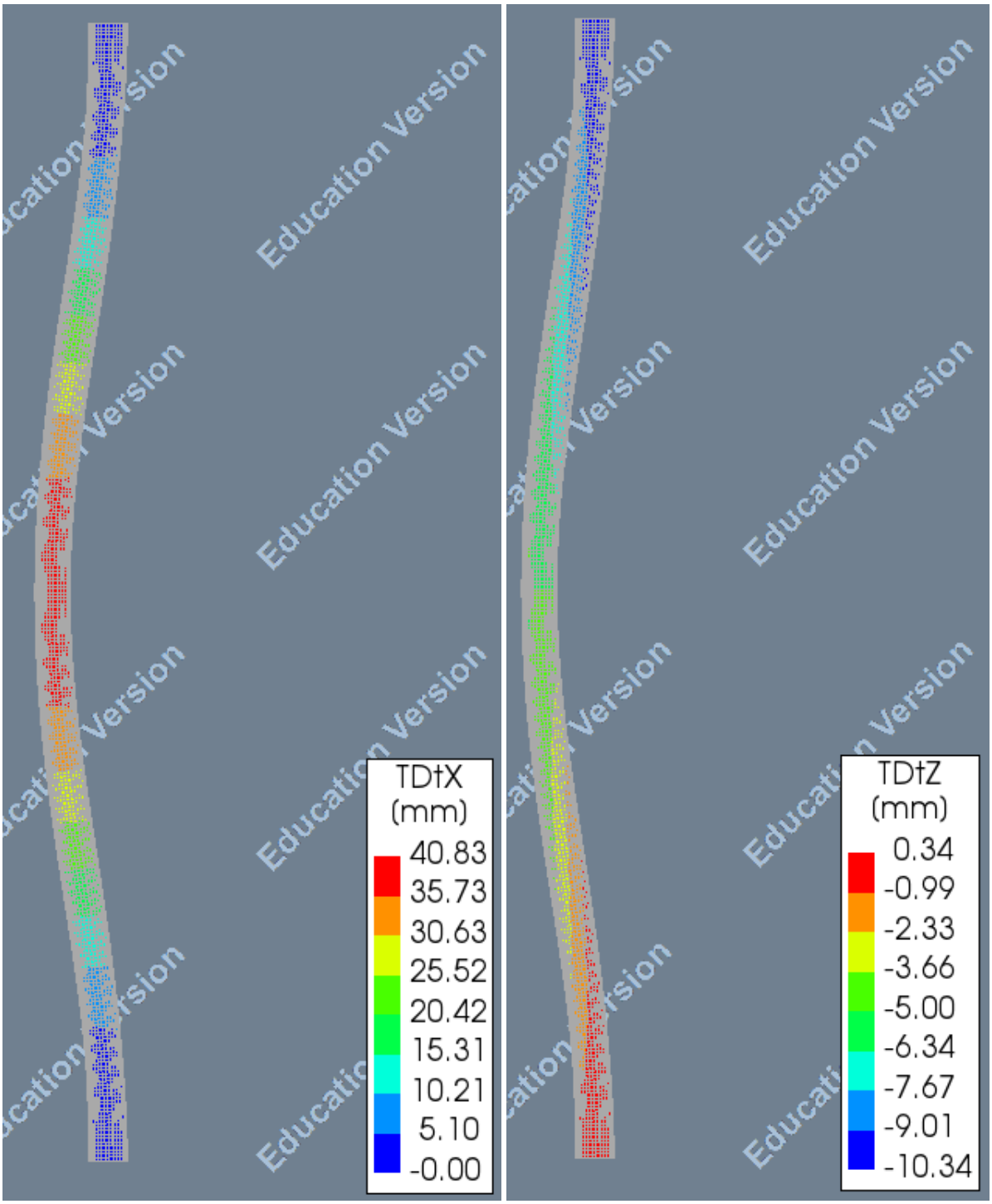

Figure 6 x- and z-displacement of the fixed column of test 4

The values from DIANA were used in Excel to get the load versus displacement curves: graph 1 and 2. As you can see in graph 1 and figure 7, is that when the imperfection load becomes lower (0.0001 N/m^3), the curve of the column goes to an ideal column (blue lines in graph 1 and figure 7). So according to the theory, the curves in graph 1 are correct. Changing the polynomial order, from linear to quadratic, not much is changing in the curves.

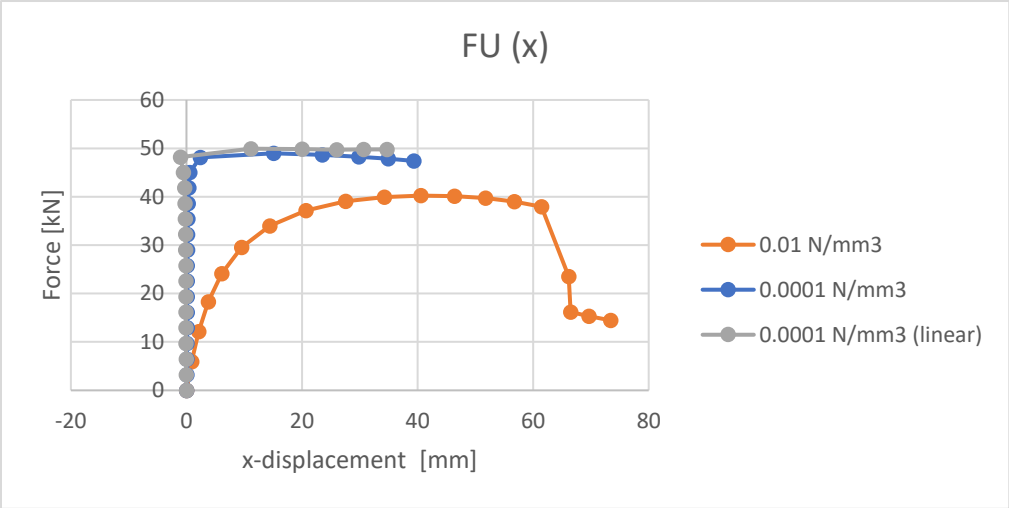

Graph 1 load versus displacement curve (x-direction)

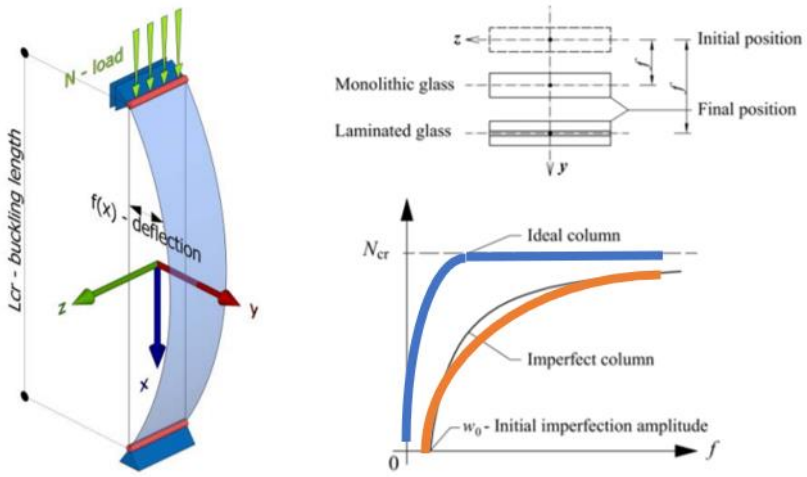

Figure 7 The ideal and the imperfect column, load versus displacement curve (Pešek, O., et al. 2017).

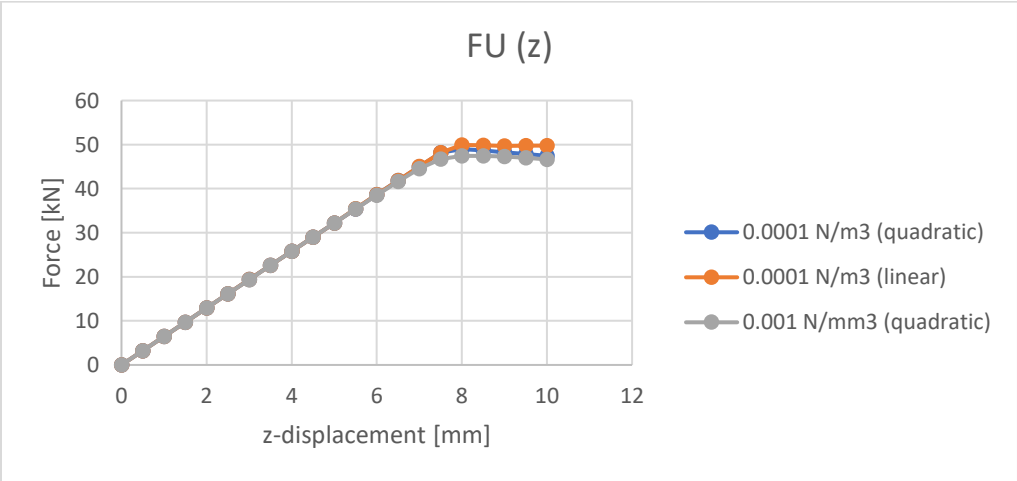

Graph 2 load versus displacement curve (z-direction)

To compare the DIANA model to the Euler buckling formula, a structural stability, eigenvalue analysis is done in DIANA. The obtained buckling value from DIANA is: 357.7 (figure 8).

A distributed pressure force of 1 N/mm^2 is put onto the column. The approximately area where the force is put onto is 138.8 mm^2.

$$\text{Euler buckling value} = (1 * 357.7 * 138.8)/1000 = 49.7 \text{ kN} \qquad \text{(A.10.4)}$$

The calculated buckling value from the Euler formula in chapter A.10.2.1. was 51.4 kN. So, 49.7 kN is almost the same value as the buckling value from DIANA. This model is correctly modelled.

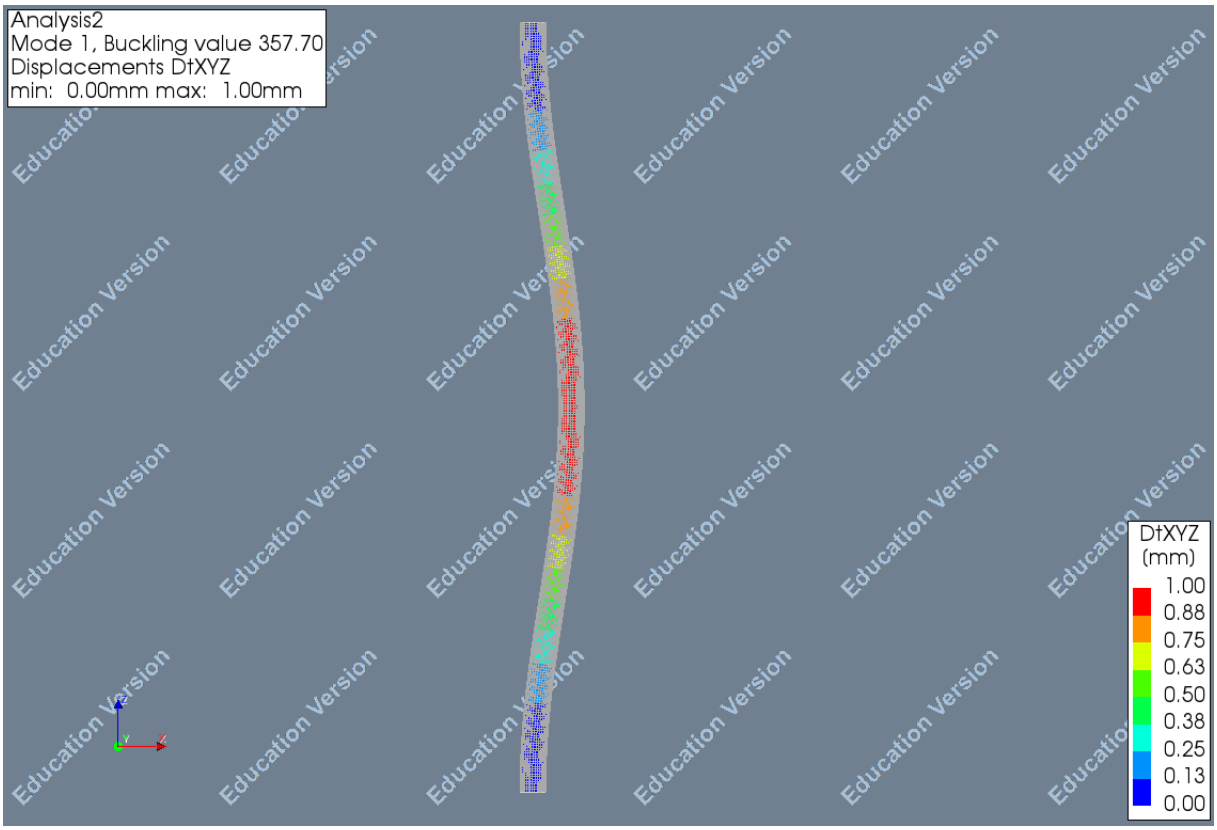

Figure 8 Buckling value of the fixed single tube

A.10.2.4. DIANA FEA column models fixed versus hinged

After the fixed column, a hinged model was made. The hinged column has to have ¼ of the buckling load of the fixed column, according to the formula of Euler.

For the hinged column the same parameters were used as for the fixed column. At figure 9, the DIANA model for the hinged column is shown.

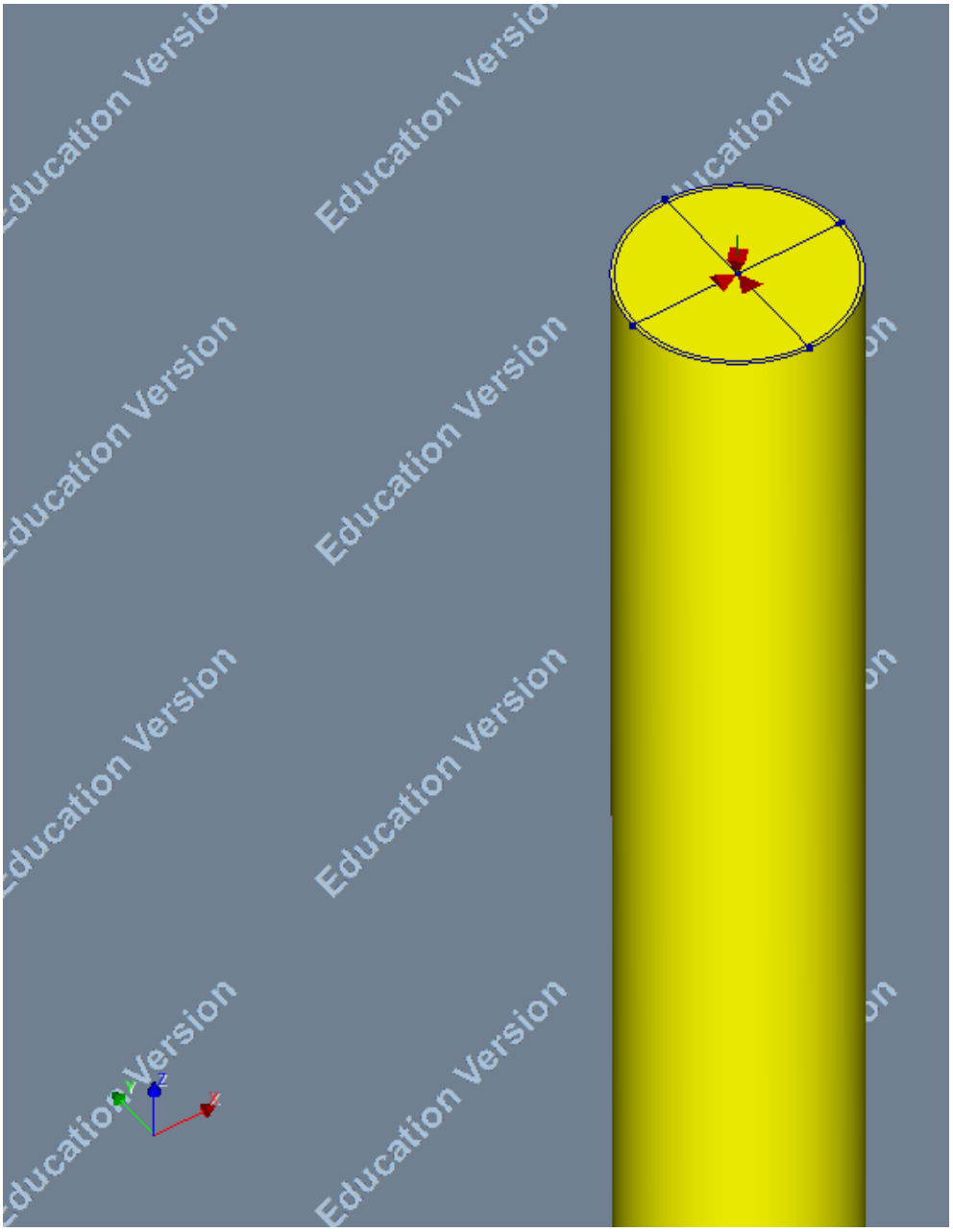

Figure 9 DIANA model hinged column

The performed test:

Test_hinged column_1:

- Geometrically non-linear analysis (quadratic)
- Imp. load: 0.0001 N/mm^3 (x-direction)
- Prescribed displacement: -10 mm (z-direction)

In figure 10, the x- and z-displacements are shown for test 1 of the hinged column.

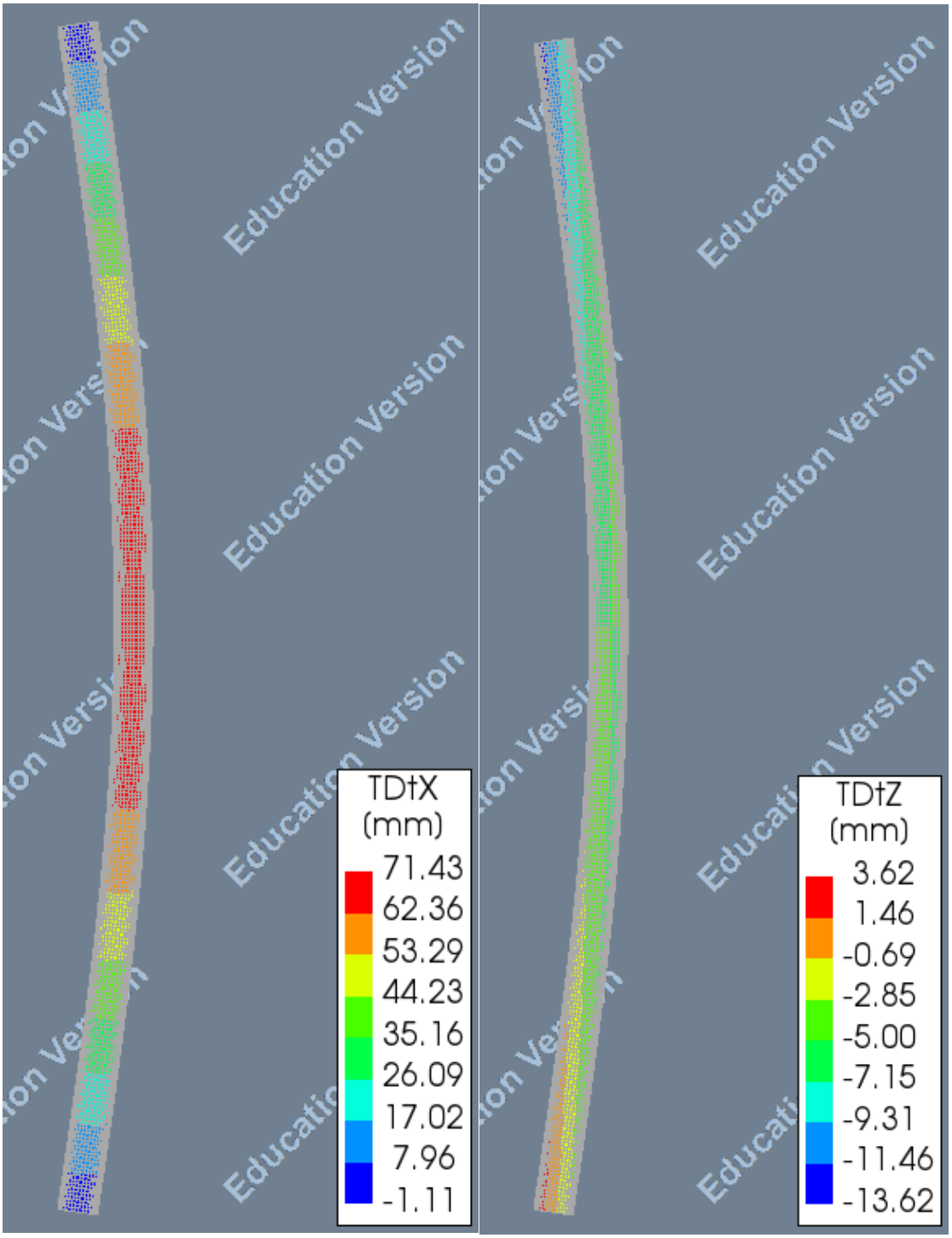

Figure 10 x- and z-displacement of the hinged column (test 1)

To compare the DIANA model to the Euler buckling formula, a structural stability, eigenvalue analysis is done in DIANA. The obtained buckling value from DIANA is: 12597 (figure 11).

A distributed pressure force of 1 N is put onto the column.

$$\text{Euler buckling value} = (1 * 12597)/1000 = 12.6\ \text{kN} \qquad \text{(A.10.5)}$$

The calculated buckling value from the Euler formula in chapter A.10.2.2. was 12.9 kN. So, 12.6 kN is almost the same value as the buckling value from DIANA. This model is correctly modelled.

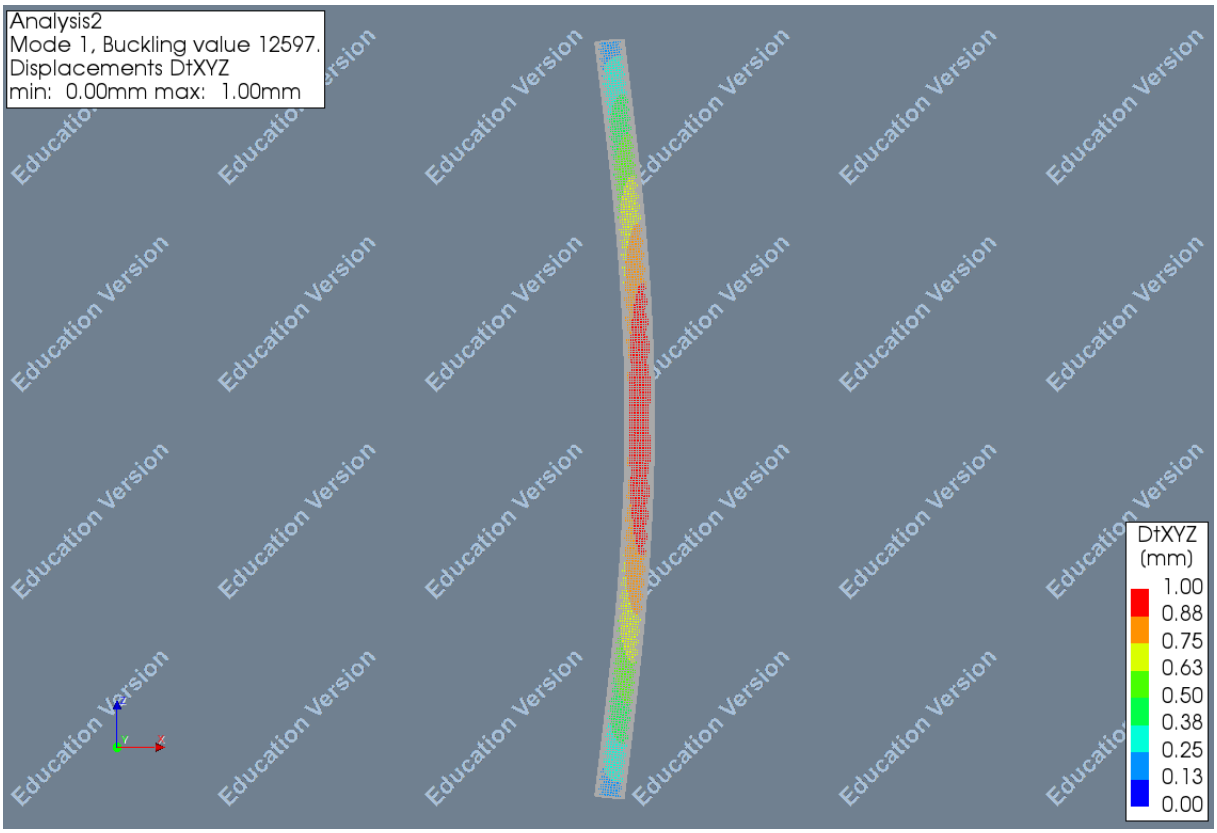

Figure 11 Buckling value of the hinged single tube

Comparing the fixed and the hinged columns in the Excel graphs (graph 3 and 4), there can be seen that the critical load for the fixed column is around ¼ of the buckling load of the fixed column, so this is correct.

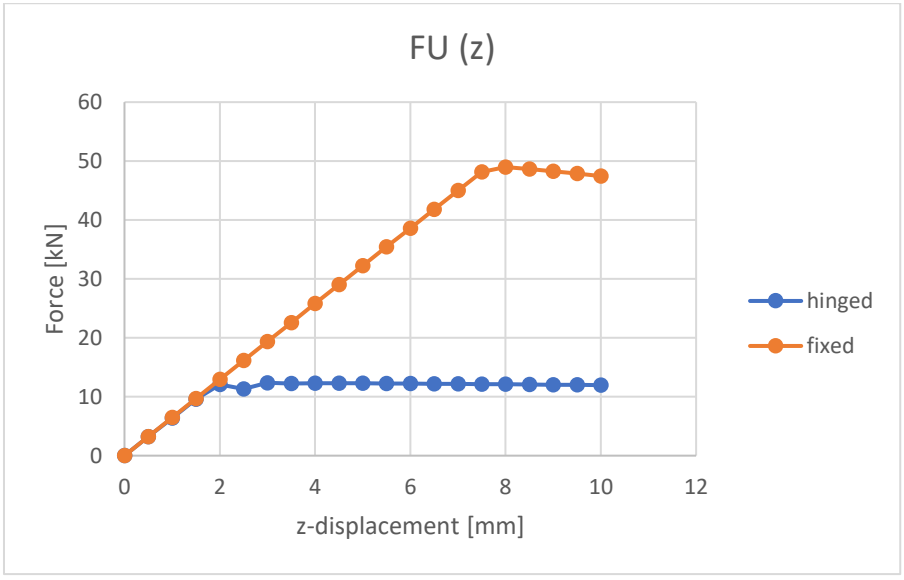

Graph 3 Load versus z-displacement curve

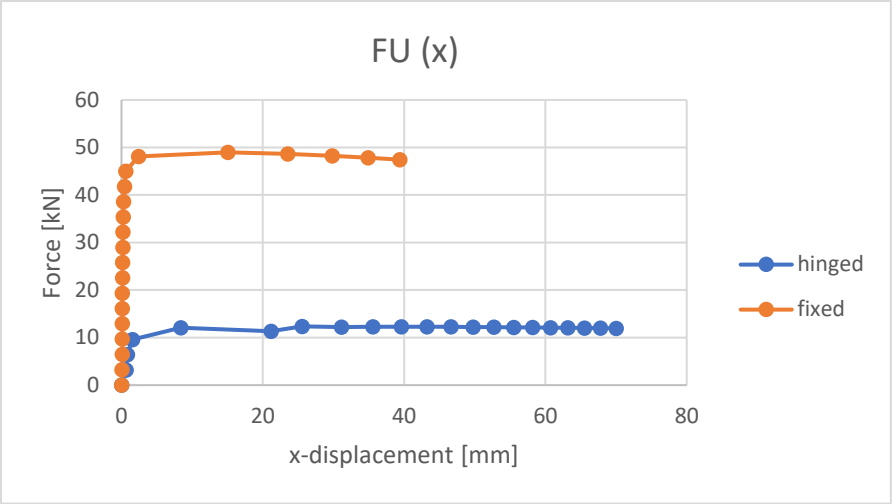

Graph 4 Load versus x-displacement curve

A.10.3. Samples to test

This theses project will only test the 300 mm samples. These will first be assessed, and after that, longer tubes can be tested. The samples will be compressed, and due to the fact that the samples are small, buckling will probably not occur. So, for this, the spring stiffness will be calculated to compare it with the load versus z-displacement curves resulting from the tests. The parts for one sample are given below. In figure 12 and 13, a 3D view and a cross section of one sample with a length of 300 mm is shown for the test setup.

One glass sample will be made of:

- Two DURAN borosilicate glass tubes, (SCHOTT):
    - Outer tube:
        - OD: 115 mm
        - WT: 5 mm
        - L: 300 mm
    - Inner tube:
        - OD: 100 mm
        - WT: 5 mm
        - L: 300 mm
- Cavity filled with a transparent interlayer resin: Ködistruct LG, (H.B.Fuller Kömmerling):
        - Width: 2.5 mm (this can vary due to the tolerances in the glass)

And one of the heat-threated glass samples will be made of:

- Two DURANTAN borosilicate glass tubes, (SCHOTT):
    - Outer tube:
        - OD: 115 mm
        - WT: 5 mm
        - L: 300 mm
    - Inner tube:
        - OD: 100 mm
        - WT: 5 mm
        - L: 300 mm
- Cavity filled with a transparent interlayer resin: Ködistruct LG, (H.B.Fuller Kömmerling):

- Width: 2.5 mm (this can vary due to the tolerances in the glass)

The connection for these small samples will be made of (the connection at the top will be the same as the bottom connection) (in figure 13 a sketch is shown of the cross section):

- POM-block, t=20 mm, ø=130 mm (with grooves to put in the glass tubes)
- HILTI HIT-HY 270 mortar (Hilti mortar), t =8mm (under the glass tubes)
- Steel bracket:
  - S355, cutting plate, t=20 mm, ø=165 mm (CNC-milling to create cambers to keep the POM-block and the hinge at its place)
- Steel hinge:
  - Standard product: GX50T

Furthermore, at the top and the bottom connection a steel plate is placed with a hole so that the wires from the sensors (placed at the inside of the glass), can go out of the glass tubes:

- Steel plate S3555, t = 10 mm, with hole for wires attached to the strain sensors inside the bonded glass tubes. *(Eventually, these were not used in the experimental tests, because a different compression machine was used. This machine had a hole in the top plate were the wires attached to the strain sensors could go through.)*

Figure 12 3D view of the sample with a length of 300 mm for the test setup.

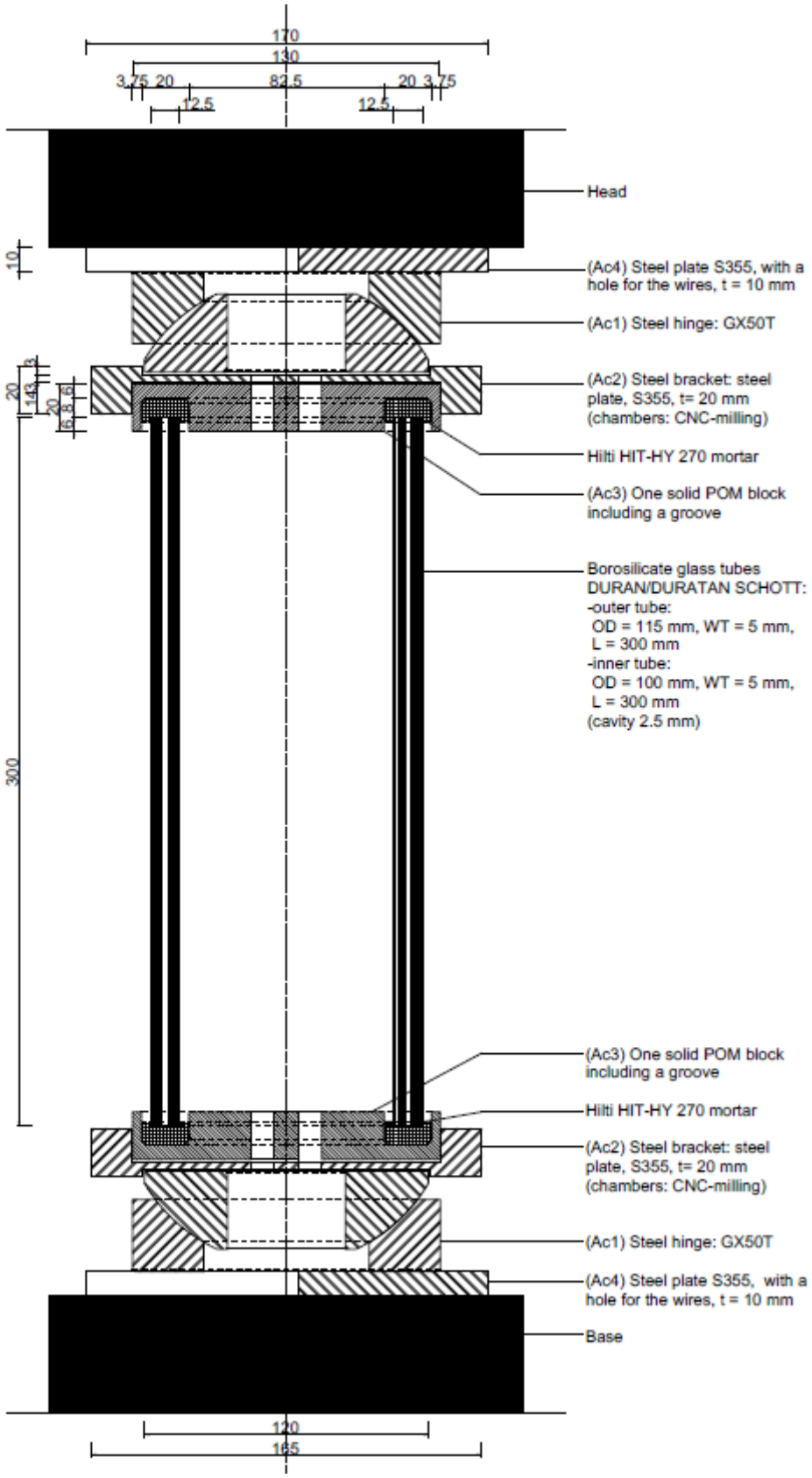

Figure 13 One sample with a length of 300 mm test setup

A.10.3.1. Buckling calculation and compression and tensile stresses

To calculate the critical buckling load of the samples, equation 1 can be used (chapter 2.2.2.2.). The two inner tubes are load-bearing, so the MLA will behave in the same when loaded with a compression force as the SLW. The dimensions of the samples are given in the chapter above (chapter A.10.3.).

With:

- E_{glass} = 63 000 N/mm^2
- $A_{two\_glass\_tubes}$ = 3220 mm^2
- L = 300 mm
- K = 1 (hinged)

There are two ways to calculate the second moment of Inertia: when fully collaborating with each other and when there is no collaborating between the tubes. In reality it will be somewhere in between.

- $I_{no\_collaboration}$ = ¼ * π * ($r_{out}^4 - r_{in}^4$) = ¼ * π * ((115/2)^4 - (105/2)^4) + ¼ * π * ((100/2)^4 - (90/2)^4) = 4306927 mm^4
- $I_{full\_collaboration}$ = ¼ * π * ($r_{out}^4 - r_{in}^4$) = ¼ * π * ((115/2)^4 - (90/2)^4) = 5364791 mm^4
- $I_{between\_collaboration}$ = (5364791 + 4306927) / 2 = 4835859 mm^4

Filling in equation 1 the critical buckling force can be calculated:

$$F = \frac{\pi^2 * 63000 * 4835859}{(1*300)^2} * \frac{1}{1000} = 33409.6\ kN \qquad \text{(A.10.6)}$$

So, the two glass (inner) tubes can handle a buckling load around 33409 kN according to the Euler formula.

The compression strength of glass can go up to 1000 MPa, and the fracture compressive strength for borosilicate glass is 260-350 MPa (mentioned before in chapter 2.1.3.). If a force of 250 kN will be put onto the glass, a compression stress of 78 N/mm^2 will occur (equation A.10.7), which is lower than 260-350 N/mm^2.

$$\sigma = \frac{F}{A} = \frac{250 * 10^3}{3220} = 78\ N/mm^2 \qquad \text{(A.10.7)}$$

According to the Euler buckling formula, this will give an Eigenvalue of:

$$\frac{33409}{250} = 133.6 \qquad \text{(A.10.8)}$$

This is really high, so buckling will not the cause of failure in this situation.

Furthermore, tensile stresses can occur when the sample will be compressed. If the column will be compressed in the y-direction, then it will give tensile stresses in the x-direction (figure 14). This will be the Poisson's ratio times the compression force. The glass would break earlier on tensile stresses than on compression stresses.

$$\sigma_{tensile} = \sigma_{compression} * Poisson's\ ratio \qquad \text{(A.10.9)}$$

For the borosilicate glass samples:

$$\sigma_{tensile} = 78 * 0.2 = 15.6\ N/mm^2 \qquad \text{(A.10.10)}$$

For annealed glass, the allowable tensile stress is around 6 N/mm^2 for long-term loading and 15.5 N/mm^2 for short-term loading. For heat tempered glass this will be higher, for short-term loading around 36.3 N/mm^2 and for long-term loading around 23 N/mm^2 (chapter A.9.3.).

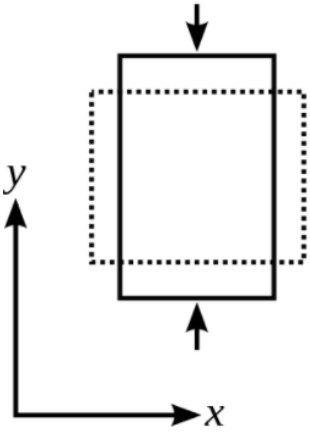

Figure 14 Transversal elongation due to the Poisson's ratio effect (Wikipedia. 2021).

A.10.3.2. Spring stiffness

Looking at the high Eigenvalue of the glass sample (equation A.10.8), the sample will probably not fail by buckling. To verify compression forces and compression stresses, the spring stiffness will be calculated and will be compared to the load versus displacement curve from the experimental tests.

$$F = k * u \qquad \text{(A.10.11)}$$

$$k = \frac{F}{u} \qquad \text{(A.10.12)}$$

With:

- F = Force [kN]
- k = spring stiffness [N/mm]
- u = displacement [mm]

The sample will be loaded with a compression force (F). This will result in a z-displacement (u). To calculate the total spring stiffness of the whole column, the spring stiffness of all the components can be summed up, according to equation A.10.13.

$$k_{tot} = \frac{F}{u_1} + \frac{F}{u_2} + \frac{F}{u_3} + \cdots \qquad \text{(A.10.13)}$$

Another annotation for u=Δl. Then the following formulas can be applied:

$$\Delta l = \frac{F*L}{E*A} \qquad \text{(A.10.14)}$$

$$\varepsilon = \frac{\Delta l}{l} \qquad \text{(A.10.15)}$$

$$\sigma = E * \varepsilon \qquad \text{(A.10.16)}$$

$$\sigma = \frac{F}{A} \qquad \text{(A.10.17)}$$

The sample is built up out of the components given in table 1 and in figure 15. In figure 15 an indication is given how the force will flow through the connections and the laminated glass tubes. These lengths and areas are taken into account in table 1. With an axial compression force of 500 kN, the z-displacement is around 2.5 mm and the spring stiffness is around 2609616090 N/mm.

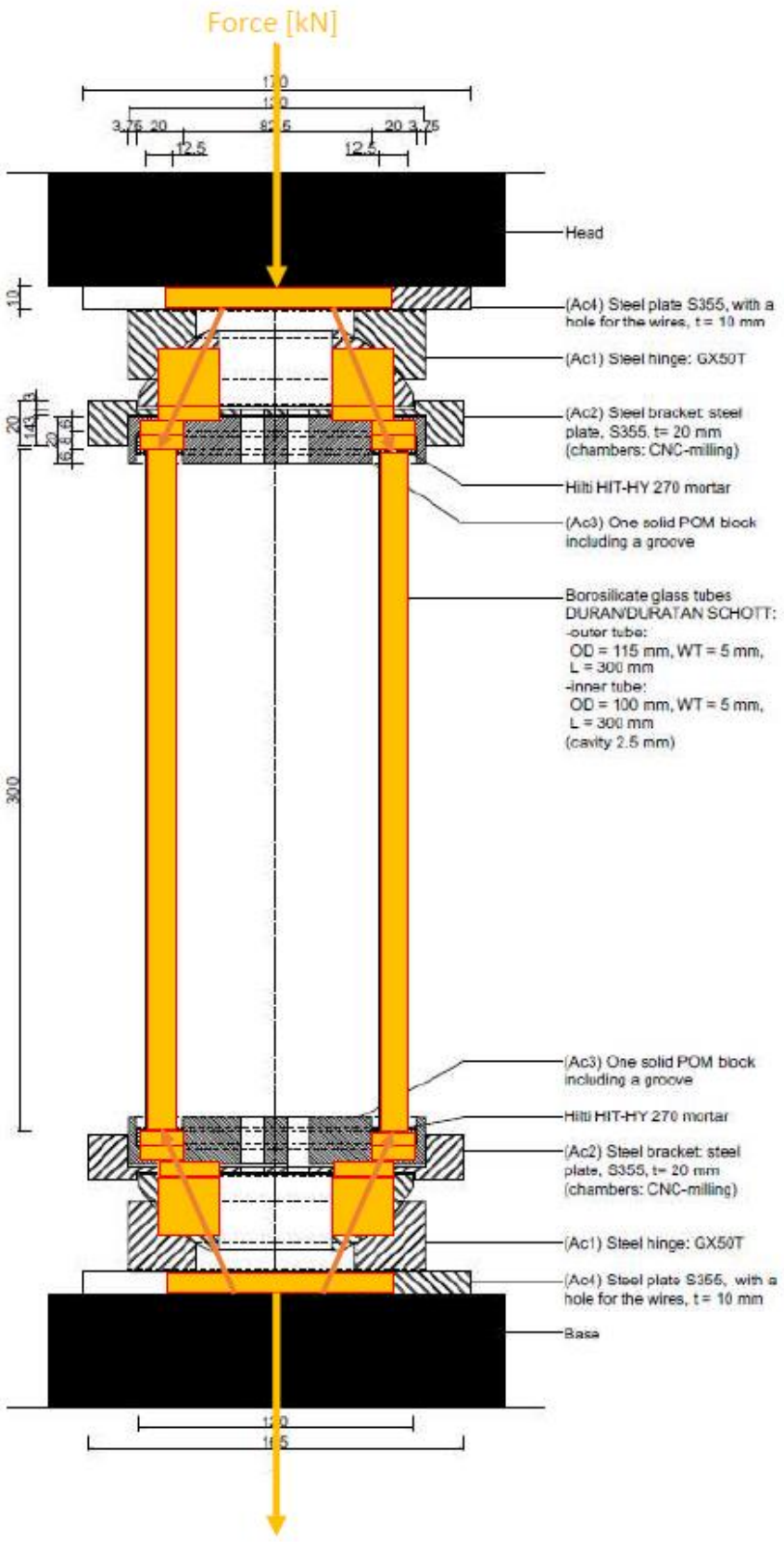

Figure 15 The force flow into the column and the connections

Spring stiffness sample:								
Components	Length or Thickness [mm]	A [mm2] =	A [mm^2]	E [N/mm^2]	F [kN]	σ [N/mm^2]	u or ΔL [mm]	k [N/mm]
steel plate	10	(170*170)-hole	28010,7	210000	500	17,850	0,0009	588224700
steel hinge GX50T	33	Pi*((120/2)^2-(50/2)^2)	9346,24	210000	500	53,497	0,0084	59476060,92
steel bracket	3	Pi*((120/2)^2-(50/2)^2)	9346,24	210000	500	53,497	0,0008	654236670,1
POM	6	Pi*((115/2)^2-(90/2)^2)	4025,17	2500	500	124,218	0,2981	1677152,328
Hilti	8	Pi*((115/2)^2-(90/2)^2)	4025,17	1700	500	124,218	0,5846	855347,6873
Two glass tubes	300	Pi*((100/2)^2-((90/2)^2)+Pi*((115/2)^2-((105/2)^2)	3220,13	63000	500	155,273	0,7394	676227,8187
Hilti	8	Pi*((115/2)^2-(90/2)^2)	4025,17	1700	500	124,218	0,5846	855347,6873
POM	6	Pi*((115/2)^2-(90/2)^2)	4025,17	2500	500	124,218	0,2981	1677152,328
steel bracket	3	Pi*((120/2)^2-(50/2)^2)	9346,24	210000	500	53,497	0,0008	654236670,1
steel hinge GX50T	33	Pi*((120/2)^2-(50/2)^2)	9346,24	210000	500	53,497	0,0084	59476060,92
steel plate	10	(170*170)-hole	28010,7	210000	500	17,850	0,0009	588224700
total							2,52	2609616090

Table 1 The spring stiffness (k) and z-displacement (u) of the sample with all components, due to a compression force of 500 kN.

As already mentioned, in the experimental tests, the steel plates where not necessary anymore, because a different compression machine was used as firstly assumed. Holes were included in the base and top plate of the compression machine itself. These holes were necessary so that the wires attached to the strain sensors on the inside could go to the computer of the machine. In table 2, the spring stiffness and deformation is calculated for the samples without the two steel plates. The deformation is almost not changed.

Spring stiffness sample:								
Components	Length or Thickness [mm]	A [mm2] =	A [mm^2]	E [N/mm^2]	F [kN]	σ [N/mm^2]	u or ΔL [mm]	k [N/mm]
steel hinge GX50T	33	Pi*((120/2)^2-(50/2)^2)	9346,24	210000	500	53,497	0,0084	59476060,92
steel bracket	3	Pi*((120/2)^2-(50/2)^2)	9346,24	210000	500	53,497	0,0008	654236670,1
POM	6	Pi*((115/2)^2-(90/2)^2)	4025,17	2500	500	124,218	0,2981	1677152,328
Hilti	8	Pi*((115/2)^2-(90/2)^2)	4025,17	1700	500	124,218	0,5846	855347,6873
Two glass tubes	300	Pi*((100/2)^2-((90/2)^2)+Pi*((115/2)^2-((105/2)^2)	3220,13	63000	500	155,273	0,7394	676227,8187
Hilti	8	Pi*((115/2)^2-(90/2)^2)	4025,17	1700	500	124,218	0,5846	855347,6873
POM	6	Pi*((115/2)^2-(90/2)^2)	4025,17	2500	500	124,218	0,2981	1677152,328
steel bracket	3	Pi*((120/2)^2-(50/2)^2)	9346,24	210000	500	53,497	0,0008	654236670,1
steel hinge GX50T	33	Pi*((120/2)^2-(50/2)^2)	9346,24	210000	500	53,497	0,0084	59476060,92
total							2,52	1433166690

Table 2 The spring stiffness and the displacement due to a compression force of 500 kN (without the steel plates).

During the tests, strain sensors are attached to the glass. In this way the values of the strain in the glass can be checked by the values from the tests. Due to the fact that not all samples were able to carry a force of 500 kN (table 3), it is also calculated for a compression force of 300 kN (table 4). To have at least two strain values per sample, also the graph for 100 kN is given in table 5. In appendix 14, the comparison is been made between these strain values and the strain values from the sensors obtained during tests.

Spring stiffness sample:										
Components	Length or Thickness [mm]	A [mm2] =	A [mm^2]	E [N/mm^2]	F [kN]	σ [N/mm^2]	ε [-]	u or ΔL [mm]	k [N/mm]	ε*1000000 [-]
steel hinge GX50T	33	Pi*((120/2)^2-(50/2)^2)	9346,24	210000	500	53,497	0,00025	0,0084	59476060,92	254,7498089
steel bracket	3	Pi*((120/2)^2-(50/2)^2)	9346,24	210000	500	53,497	0,00025	0,0008	654236670,1	254,7498089
POM	6	Pi*((115/2)^2-(90/2)^2)	4025,17	2500	500	124,218	0,04969	0,2981	1677152,328	49687,39687
Hilti	8	Pi*((115/2)^2-(90/2)^2)	4025,17	1700	500	124,218	0,07307	0,5846	855347,6873	73069,70128
Two glass tubes	300	Pi*((100/2)^2-((90/2)^2)+Pi*((115/2)^2-((105/2)^2)	3220,13	63000	500	155,273	0,00246	0,7394	676227,8187	2464,652622
Hilti	8	Pi*((115/2)^2-(90/2)^2)	4025,17	1700	500	124,218	0,07307	0,5846	855347,6873	73069,70128
POM	6	Pi*((115/2)^2-(90/2)^2)	4025,17	2500	500	124,218	0,04969	0,2981	1677152,328	49687,39687
steel bracket	3	Pi*((120/2)^2-(50/2)^2)	9346,24	210000	500	53,497	0,00025	0,0008	654236670,1	254,7498089
steel hinge GX50T	33	Pi*((120/2)^2-(50/2)^2)	9346,24	210000	500	53,497	0,00025	0,0084	59476060,92	254,7498089
total							0,25	2,52	1433166690	248997,85

Table 3 The spring stiffness, the displacement and the strain (without the steel plates) due to a compression force of 500 kN.

Spring stiffness sample:										
Components	Length or Thickness [mm]	A [mm2] =	A [mm^2]	E [N/mm^2]	F [kN]	σ [N/mm^2]	ε [-]	u or ΔL [mm]	k [N/mm]	ε*1000000 [-]
steel hinge GX50T	33	Pi*((120/2)^2-(50/2)^2)	9346,24	210000	300	32,098	0,00015	0,0050	59476060,92	152,8498853
steel bracket	3	Pi*((120/2)^2-(50/2)^2)	9346,24	210000	300	32,098	0,00015	0,0005	654236670,1	152,8498853
POM	6	Pi*((115/2)^2-(90/2)^2)	4025,17	2500	300	74,531	0,02981	0,1789	1677152,328	29812,43812
Hilti	8	Pi*((115/2)^2-(90/2)^2)	4025,17	1700	300	74,531	0,04384	0,3507	855347,6873	43841,82077
Two glass tubes	300	Pi*((100/2)^2-((90/2)^2)+Pi*((115/2)^2-((105/2)^2)	3220,13	63000	300	93,164	0,00148	0,4436	676227,8187	1478,791573
Hilti	8	Pi*((115/2)^2-(90/2)^2)	4025,17	1700	300	74,531	0,04384	0,3507	855347,6873	43841,82077
POM	6	Pi*((115/2)^2-(90/2)^2)	4025,17	2500	300	74,531	0,02981	0,1789	1677152,328	29812,43812
steel bracket	3	Pi*((120/2)^2-(50/2)^2)	9346,24	210000	300	32,098	0,00015	0,0005	654236670,1	152,8498853
steel hinge GX50T	33	Pi*((120/2)^2-(50/2)^2)	9346,24	210000	300	32,098	0,00015	0,0050	59476060,92	152,8498853
total							0,15	1,51	1433166690	149398,71

Table 4 The spring stiffness, the displacement and the strain (without the steel plates) due to a compression force of 300 kN.

Spring stiffness sample:										
Components	Length or Thickness [mm]	A [mm2] =	A [mm^2]	E [N/mm^2]	F [kN]	σ [N/mm^2]	ε [-]	u or ΔL [mm]	k [N/mm]	ε*1000000 [-]
steel hinge GX50T	33	Pi*((120/2)^2-(50/2)^2)	9346,24	210000	100	10,699	0,00005	0,0017	59476060,92	50,94996177
steel bracket	3	Pi*((120/2)^2-(50/2)^2)	9346,24	210000	100	10,699	0,00005	0,0002	654236670,1	50,94996177
POM	6	Pi*((115/2)^2-(90/2)^2)	4025,17	2500	100	24,844	0,00994	0,0596	1677152,328	9937,479374
Hilti	8	Pi*((115/2)^2-(90/2)^2)	4025,17	1700	100	24,844	0,01461	0,1169	855347,6873	14613,94026
Two glass tubes	300	Pi*((100/2)^2-((90/2)^2)+Pi*((115/2)^2-((105/2)^2)	3220,13	63000	100	31,055	0,00049	0,1479	676227,8187	492,9305245
Hilti	8	Pi*((115/2)^2-(90/2)^2)	4025,17	1700	100	24,844	0,01461	0,1169	855347,6873	14613,94026
POM	6	Pi*((115/2)^2-(90/2)^2)	4025,17	2500	100	24,844	0,00994	0,0596	1677152,328	9937,479374
steel bracket	3	Pi*((120/2)^2-(50/2)^2)	9346,24	210000	100	10,699	0,00005	0,0002	654236670,1	50,94996177
steel hinge GX50T	33	Pi*((120/2)^2-(50/2)^2)	9346,24	210000	100	10,699	0,00005	0,0017	59476060,92	50,94996177
total							0,05	0,50	1433166690	49799,57

Table 5 The spring stiffness, the displacement and the strain (without the steel plates) due to a compression force of 100 kN.

Furthermore, in the load versus displacement curve from the experimental tests, also the displacement of the components of the compression machine are included. The strain values are known from the samples (at loads 100, 300 and 500 kN). From this strain, the displacement can be calculated from the glass tubes. These values can be compared to the values calculated by hand (table 3, 4 and 5). In appendix 14, the comparison is been made between these displacements obtained during tests and from the hand calculations.

References

GoodFellow. (2021). Your Global supplier for materials. Polyoxymethylene – Homopolymer (Acetal – Homopolymer POMH) Material Information. From: http://www.goodfellow.com/A/Polyoxymethylene-Homopolymer.html

O'Regan, C. (2015). Structural use of glass in buildings (Second edition). The Institution of Structural Engineers.

Toogood, R. (2001). Pro/MECHANICA Tutorial Structure. Release 2001 - Integrated Mode. Schroff Development Corporation.

Figure list

Figure 1 - Everyone is Number One. (2014). Explore, Discover, Improve… h-Method & p-Method. Retrieved on January, 12, 2021, from: https://deust.wordpress.com/2014/11/30/h-method-p-method/

Figure 2 - Everyone is Number One. (2014). Explore, Discover, Improve… h-Method & p-Method. Retrieved on January, 12, 2021, from: https://deust.wordpress.com/2014/11/30/h-method-p-method/

Figure 3 - Everyone is Number One. (2014). Explore, Discover, Improve… h-Method & p-Method. Retrieved on January, 12, 2021, from: https://deust.wordpress.com/2014/11/30/h-method-p-method/

Figure 4 - Own picture. Delft. Retrieved on January, 21, 2021.

Figure 5 - Own picture. Delft. Retrieved on January, 6, 2021.

Figure 6 - Own picture. Delft. Retrieved on January, 8, 2021.

Figure 7 - Pešek, O., Melcher, J. (2017). Shape and Size of Initial Geometrical Imperfections of Structural Glass Members. Civil Engineering Series. (no. 1, vol. 17). De Gruyter Open. Transactions of the VŠB – Technical University of Ostrava. Retrieved on January, 6, 2021.

Figure 8 - Own picture. Delft. Retrieved on January, 26, 2021.

Figure 9 - Own picture. Delft. Retrieved on January, 27, 2021.

Figure 10 - Own picture. Delft. Retrieved on January, 28, 2021.

Figure 11 - Own picture. Delft. Retrieved on February, 25, 2021.

Figure 12 - Own picture. Delft. Retrieved on May, 31, 2021.

Figure 13 - Own picture. Delft. Retrieved on May, 31, 2021.

Figure 14 - Wikipedia. (2021). Poisson's ratio. Retrieved on May, 20, 2021, from: https://en.wikipedia.org/wiki/Poisson%27s_ratio

Figure 15 - Own picture. Delft. Retrieved on May, 31, 2021.

Graph and table list

Graph 1 – Own made graph. Delft. Retrieved on January, 8, 2021.

Graph 2 – Own made graph. Delft. Retrieved on January, 9, 2021.

Appendix 11 – Process with the producers

A.11.1 Process

In this chapter the process is given to get all the parts of the samples together at the Stevin lab II at the Technical University of Delft. I started with this process at the beginning of March, and all the components of the samples were present at the lab at the end of June. After this, the components needed to be put together to make the samples ready for testing. Due to Corona, all meetings were held via Zoom or Teams.

The companies who sponsored this thesis project are listed below:

- SCHOTT sponsored the glass tubes. The tubes were cut into the right length and were fit into each other. They delivered the tubes to H.B. Fuller Kömmerling.
- H.B. Fuller Kömmerling sponsored the interlayer material and carried out the lamination process.
- Octatube sponsored the connections (steel and POM). I was also allowed to borrow the tool needed to inject the Hilti mortar.
- Techniparts delivered two steel hinges for the connections.
- Hilti sponsored the Hilti mortar.
- TU Delft Stevin lab II sponsored a few aspects needed for testing, like the strain sensors. Furthermore, I could use the compression machine in the lab and staff from the lab was able to help during the experimental tests.

While designing the concepts, I e-mailed Hilti a few times for information on the product. The Hilti mortar is most often used for balustrades. To test the capacity of the Hilti mortar under pressure for a column and to check if the mortar could be injected efficiently, samples with a length of 300 mm samples were tested. H.B. Fuller Kömmerling used these 300 mm samples first to try out the lamination process. Furthermore, the samples were used to check out the post-failure behaviour of the laminated tubes and to check if the connection capacity of the end connection.

At the 8th of March, Chris Noteboom contacted Frank Muntz (owner) at Techniparts to ask if it was possible to get two steel hinges, the same ones which were used in the Markthal in Rotterdam. We got an e-mail back saying that this was possible.

After the first big steps were made with the design concepts, Faidra Oikonomopoulou e-mailed her contacts at SCHOTT at 17th of February, and the first meeting was planned at the 3th of March. At this day, Kerstin Kohl (customer service/sales), Klaas Roelfsma (regional sales director), Folker Steden (head of department Scientific Services) from SCHOTT were present, and Chris Noteboom and Faidra Oikonomopoulou from the committee were present. The presentation went well and they were enthusiastic about the designs. After this I got some information about the DURAN® SCHOTT tubes on tolerances and possible dimensions.

The covering values to determine the dimensions are the compression loads from the case, the allowable Hilti stresses, and the tensile stresses in the glass due to compression and Poisson's ratio. After calculating these values, dimensions were chosen. The glass tubes need to be put into each other. This depends on the tolerances in the glass and on the thickness of the lamination interlayer. After a few e-mails about tolerances, at the 17th of March, I gave the order list to SCHOTT. Then, SCHOTT cut the profiles into the right lengths. After that they fitted the tubes into each other by hand. From that point on, we could make sure that the tubes would fit into each other with enough space left for the resin. At the 23th of March I got an e-mail from SCHOTT that the tubes were in stock. Before, SCHOTT cut the

profiles, we had to send an address for delivery first, which was depending on H.B. Fuller Kömmerling.

At the 3th of March, I e-mailed Roel Schipper with questions about budget for testing in the Stevin lab, and what the right machine was for these kind of compression tests. Roel Schipper stated that I should contact Peter de Vries (coordinator of the Stevin lab II) about the test possibilities and the machines. Peter de Vries gave an indication about the costs, and Roel Schipper submitted this to the department chairman of the faculty Civil Engineering Bert Sluys. Roel Schipper also sent me a few draft versions of an experimental plan that needed to be written and discussed with Peter de Vries.

At the 11th of March I sent Peter de Vries an e-mail, about the test setup and possible dates for testing. He confirmed that the tests setup was acceptable. I had to think everything through and had to describe it in the experimental plan. Possible dates were at the beginning of April (which was too early), or probably around June. This was depending on SCHOTT, H.B. Fuller Kömmerling, Octatube and Hilti. As soon as there was more known about the planning, I could give the experimental plan to Peter with the planning included.

In 1999 Fred Veer laminated glass tubes himself at the lab from the TU in Delft. Since the fire at the faculty of Architecture, the set-up to bond the tubes together, burned down. This meant that it was not possible to laminate the tubes ourselves anymore and we needed to arrange another company who could help us with this. At the 22th of February, I contacted Chris Davis (composites manager) from H.B. Fuller Kömmerling. I was curious about possible fire interlayers/coatings. After this, Mauro Overend thought of H.B.Fuller Kömmerling to laminate the tubes for us, so I e-mailed Chris Davis for an appointment to explain my thesis to him. For this I changed the presentation from SCHOTT, because dimensions and some small details had changed in the meantime. On the 9th of March we had a meeting. Chris Davis from H.B. Fuller Kömmerling was present, and from the committee, Mauro Overend and Faidra Oikonomopoulou were present. I presented the design concepts and goals for the tests, and Chris Davis was enthusiastic too. Although he first wanted to discuss the possibilities internally. For this I wrote an overview with phases and I sent a draft overview to Chris Davis at the 23th of March.

I interviewed Peter van de Rotten from Octatube at the 9th of February. He gave good feedback on my details from the design concepts. At the 23th of March Chris Noteboom e-mailed Peter van de Rotten to ask if they would help to develop the connections, so that we could test the glass tubes on compression strength and robustness. At the 31th of March we had a meeting to brainstorm about the connections. I made drawings for Octatube, sent them at the 7th of April, and Peter van de Rotten wanted to first discuss this internally as well. He had some questions about the drawings of the connections and about the thickness of the steel shoe. We discussed a few of these points at another meeting at the 14th of April. At the 16th of April Peter responded. At that moment they had no material in stock to make the connections, but we had another meeting to see if some simplifications were possible.

At the 12th of April, I went to Stevin lab II at the TU Delft to have a conversation with Peter de Vries. We talked about methods for testing, and other aspects necessary that needed to be arranged by the TU. Furthermore, we looked at some products that were maybe in stock. Besides, I got a tour at the lab. It was useful to see the machine. Now I could finish a large part of the experimental plan. At the 19th of April, I got an email from Peter de Vries. The contact person for the lab would be Louis den Breejen. He would help me make the samples ready and during the tests. A meeting was planned with Louis to show the test setup of the project at the 3th of May.

At the 6th of April, I got an e-mail back, from H.B.Fuller Kömmerling, with material options for the interlayer material with pros and cons. Another meeting was planned at the 16th, to discuss the sponsorship and the materials. This meeting was held with Chris Davis from H.B. Fuller Kömmerling, and with Chris Noteboom and Faidra Oikonomopoulou. As a result, they wanted to sponsor. This was really good news. Moreover, it would be good to compare the 300 mm DURAN® samples with DURATAN® sample. Stresses can be quite high during and after the curing process. H.B.Fuller Kömmerling already tested something familiar 10 years ago, and then the annealed glass broke after the curing process. If the tolerances in the glass became too large, the interlayer might become too thick, this will give more stresses onto the glass. So, we asked SCHOTT to send also 3x DURATAN® samples, with the same length. At the 19th of April, Chris Davis sent the delivery address for these 6x 300 mm samples.

On the 20th of April, Faidra Oikonomopoulou sent an email to SCHOTT with the delivery address, so that they could send the 6x 300 mm samples to H.B.Fuller Kömmerling. After another phone call and meeting with H.B.Fuller Kömmerling, it became clear that it would be good to test tubes with a larger diameter as described now, this would be easier to work with during testing, to bonded them together and to make connections for. Due to all new insights, I sent SCHOTT a new list with required tube sizes. I suggested another meeting with SCHOTT and H.B.Fuller Kömmerling, before sending the tubes to H.B.Fuller Kömmerling. To be sure that unfortunate mistakes would be avoided. At the 23th of April we had this suggested meeting, with: Chris Davis, Klaas Roelfsma, Folker Steden, Chris Noteboom. I explained the planning with the revised order list. After this meeting, I sent an email to SCHOTT with the revised order list. Katrin Djuric (customer service/sales) helped us further with this revised order list, because Kerstin Kohl was out of office for a while.

Another meeting was held at the 30th of April with Chris Noteboom and Peter van de Rotten (Octatube), to discuss simplification for the connections. It was indeed better to take samples with a larger diameter (around 100 mm instead of 50 mm). These sizes are more standard. Furthermore, we discussed options for the POM-block and some simplifications for the steel connections. I updated the drawings for the test set up. These were discussed at a new meeting, which was directly planned at the 12th of May.

At the 29th of April, I called Katrin Djuric from SCHOTT to get more information on the progress of the 300 mm samples for the first order. To arrange everything, a few phone calls were held and e-mails were sent. On the 3th of May I received an email with the correct order confirmation, and SCHOTT let us know that the required 300 mm length tubes were in stock. After that, they started with cutting the profiles in the right length, fitting them into each other, and gave them specimen numbers. They sent the 300 mm samples (6x) tubes to H.B. Fuller Kömmerling at the 11th of May. After this I sent the order confirmation to Chris Davis and I gave him the delivery date when they would receive the tubes, and I asked for an update on their planning.

On the 23th of April, I got an email form Peter de Vries. He indicated that the machine will be available the whole month of June. At the 3th of May I went to the lab to meet Louis van den Breejen. We discussed the test set-up. The enclosure was already available at the lab. Only the strain sensors needed to be arranged. I came across Peter, and he said that I could also use sensors inside of the glass. For this the detail needed to be adjusted. At the 17th of May, I sent the drawings to Peter van de Rotten and Chris Noteboom.

At the 12th of May, I had another meeting with Peter van de Rotten and Chris Noteboom to discuss the drawings. The drawings were correct in this way. Peter van de Rotten sent the drawings to their technical service to start the production of the connection parts.

Furthermore, to inject Hilti, a tool was necessary. Since Octatube used Hilti before, I could borrow it. The goal was to deliver the connections parts at the beginning of June. Peter van de Rotten gave me an update on the 19th of May. The steel bracket would be made by CNC-milling. Peter sent two options. We discussed these options on the 20th of May. I confirmed the sizes and the amounts on the 21th of May. After that the production was started.

After a few phone calls with Chris Davis, it was confirmed that they received the tubes from SCHOTT. Due to the fact that this lamination process was so new, a meeting was planned at the 12th of May with technical service of H.B.Fuller Kömmerling and the TU committee: Wolfgang Wittwer, Christian Scherer, Jens Wolthaus, Chris Davis, Mauro Overend. It was a discussion about the shrinkage values, the temperature influences, and the heating and cooling process. At this meeting, the interlayer material was chosen. First a UV-curing interlayer was chosen, but it was changed into a 2 PU component interlayer material, due to a lower shrinkage value and due to the fact that this interlayer would cool more slowly (and cure) in room-temperature. After this meeting a few e-mails were sent between the TU committee and the technical service of H.B.Fuller Kömmerling. I called Chris Davis a few times about their planning, which was difficult to determine, because the interlayer material was not in stock and needed to be made first.

At the 20th of May, I called Frank Muntz about the delivery date and address for the hinges. These were delivered at my address at the 9th of June.

At the 17th of May, Chris Noteboom had a conversation with Thomas Goedegebuure (Technical adviser/engineer) at Hilti about sponsoring of the Hilti mortar. They were happy to help, and after a few more e-mails and phone calls, the patrons with Hilti mortar were delivered to Octatube. Now all the components for the connections were arranged, and could be brought to the lab at once. At the 4th I had contact with Peter. He mentioned that the components for the connections were made. I visited Octatube at the 16th of June to have a look at the results. At the 21th I picked up all the components and Willem Poot taught me how to use the Hilti tool.

At the 26th of May, I send Peter de Vries an e-mail about the schedule and the experimental plan. He confirmed that the planning was acceptable, and he gave me a budget indication at the 31th of May for the sensors and the staff hours. At the 31th of May I sent an email to Roel Schipper with the budget indication, so that he could discuss this with prof. Bert Sluys. At the 3th of June, I got a response back with an approval. Directly after that, I emailed Louis van den Breejen to order the sensors.

On the 20th of May I got an update about the planning form H.B. Fuller Kömmerling. They would laminate the tubes in week 22 and 23. The expected delivery week would be in week 24. At the 21th of May I responded to their planning. At the 31th of May, I got an email that they received the interlayer material and that they would start in week 22 as planned. In week 23 the tubes were cured and monitored. At the 8th of June I got an update from Chris Davis with pictures of the lamination process. We discussed the possibilities for transportation. At the 22th of June, I picked up the tubes in Antwerp by car. Benjamin from H.B.Fuller Kömmerling took them from Pirmasens to Antwerp. At figure 1, all the components were visible gathered together.

Figure 1 All the components were gathered together at the evening of 22th of June.

At 23th of June, all the components were brought to the lab to prepare the samples for the tests so that the compression strength tests could be performed afterwards. The tests were finished at the 30th of June. Louis van den Breejen helped preparing the samples and Fred Schilperoort helped during the tests. At the 25th of June I contacted Thomas Goedegebuure if it was possible to get 2 or 3 more Hilti mortar patrons. At the 27th of June, I picked them up at the store in Berkel en Rodenrijs.

At the 2nd and the 6th of July, I went to the microlab at the faculty of Architecture to analyse the cracks with Telesilla Bristogianni. At the 8th I had another look at the cracks with Fred Veer in the microlab at the faculty of Architecture.

After bonding the 300 mm samples and carrying out of the experiments, another meeting was planned with SCHOTT, the TU Delft committee and H.B. Fuller Kömmerling to assess the samples. At the 14th of July, I presented the test results shortly and afterwards the results were discussed.

A.11.2 Lessons learned

In this chapter I have written out my lessons learned, with the intention that this may help others during a similar process. The process was sometimes stressful, but I also learned a lot form it:

- Don’t panic if something goes wrong. There are more possibilities.
- Calling is way more efficient than e-mailing.
- Keep good contact with all the producers during the project and during the manufacturing time.
- The presentations, which I held for producers in between, were useful, because due to presenting, all the information needed to be summarized constantly.
- Producers ask questions if something is unclear. In this way, you keep looking at your work with a critical eye.
- It was good to meet people from the field of work to get new insights on the subject.
- Good pictures in the presentations are important for explaining the topic and to make people enthusiastic.
- At the end, when everything is planned and when it has worked out, you get a satisfied feeling.
- My Linked-In network has grown during this thesis project.

Appendix 12 – Experimental plan

Experimental plan: Tubular Glass Columns

To: Peter de Vries and Louis den Breejen (Stevinlab II TU Delft)

Table of Contents

1. Introduction

This thesis project is focussed on designing and engineering of a structural, robust and fire-resistant tubular structural glass column. To validate the design concepts, compressive tests need to be carried out, and the post/failure behaviour needs to be checked in the lab of the Technical University of Delft. To show the principle of the designs, one of the models is shown in 3D in figure 1.

This document contains the experimental plan for the research on compression strength and the behaviour of tubular glass columns after breakage.

1.1. Problem Statement

The problem statement of this research is:

There are not yet well-established manufacturing methods with related checking and calculation methods for one of the most efficient shape of a glass column: the tubular. More knowledge is needed on the manufacturing, the fire safety, and the robustness.

1.2. Main Question

Which results in the main question:

How to design and engineer a transparent tubular glass column as a structural element, which is robust and fireproof?

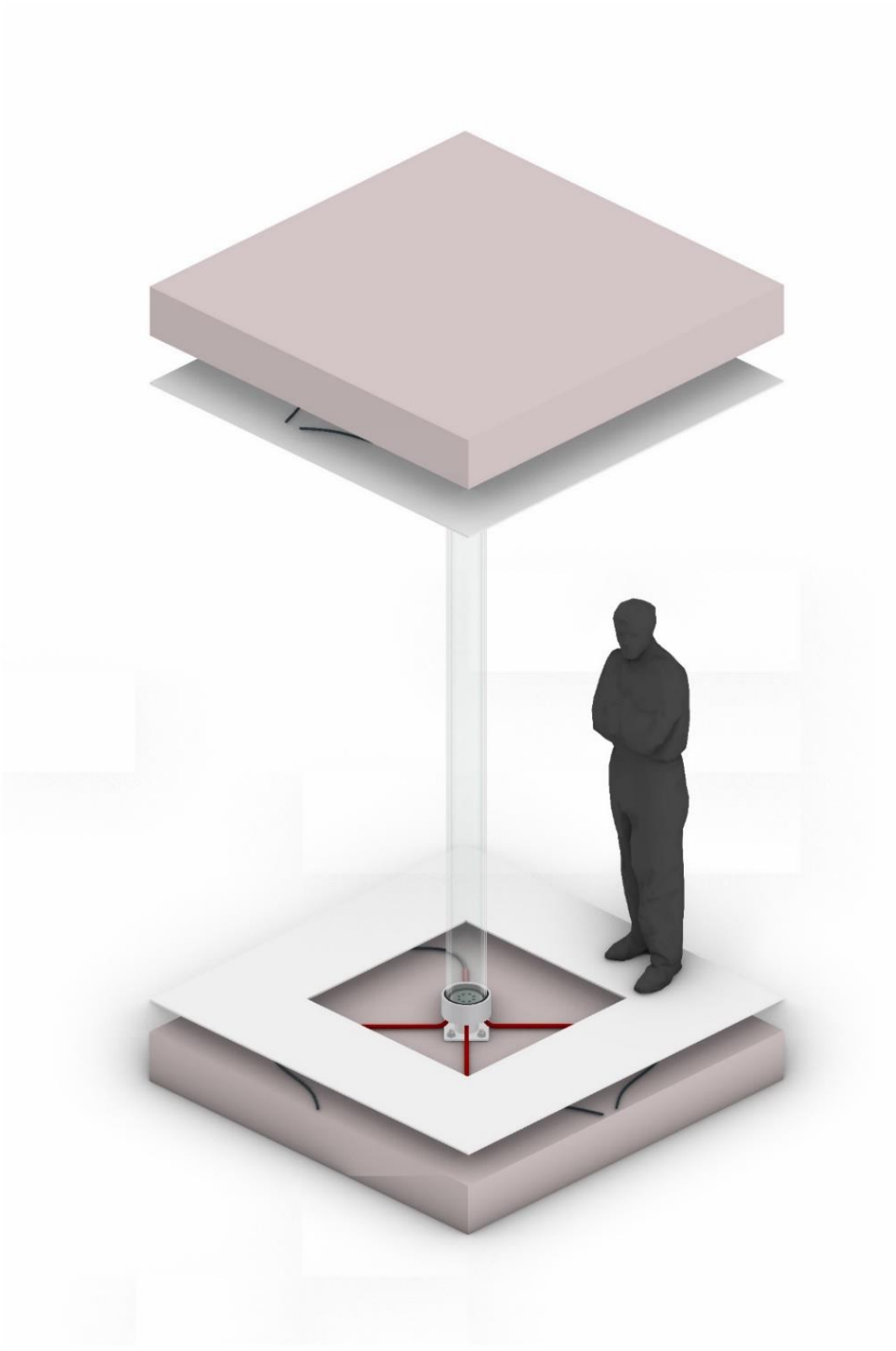

Figure 1 One of the models of the glass column shown in 3D

2. Experiments part 1 (June)

2.1. Goals

The goals of this experiment are:

- To verify the stresses in the glass and the connection due to the compression force.
- To investigate the post-failure behaviour/robustness on the designs for a tubular glass column.
- To check which part fails first: the connection or the glass.

2.2. Prototypes and manufacturing

2.2.1. Small samples of 300 mm

To try out curing the interlayer resin (2 PU-component, Ködistruct LG, LOCA material), Kömmerling H.B.Fuller needs 6 samples of 300 mm long, 3x the DURAN and 3x the DURATAN tubes. These samples can be used as well to try out the most efficient way of injecting the Hilti mortar, to figure out what happens to the Hilti mortar if it will be overstressed, and to check the post-failure behaviour of the glass column.

One glass sample will be made of:

- Two DURAN borosilicate glass tubes, (SCHOTT):
    - Outer tube:
        - OD: 115 mm
        - WT: 5 mm
        - L: 300 mm
    - Inner tube:
        - OD: 100 mm
        - WT: 5 mm
        - L: 300 mm
- Cavity filled with a transparent interlayer resin: Ködistruct LG, (H.B.Fuller Kömmerling):
        - Width: 2.5 mm (this can vary due to the tolerances in the glass)

And one of the heat-threated glass samples will be made of:

- Two DURANTAN borosilicate glass tubes, (SCHOTT):
    - Outer tube:
        - OD: 115 mm
        - WT: 5 mm
        - L: 300 mm
    - Inner tube:
        - OD: 100 mm
        - WT: 5 mm
        - L: 300 mm
- Cavity filled with a transparent interlayer resin: Ködistruct LG, (H.B.Fuller Kömmerling):
        - Width: 2.5 mm (this can vary due to the tolerances in the glass)

The connection for these small samples will be made of (in figure 2 the sketch is shown for the cross section of the connection):

- POM-block, t=20 mm, ø=130 mm (with grooves to put in the glass tubes)
- HILTI HIT-HY 270 mortar (Hilti mortar), t =8mm (under the glass tubes)
- Steel bracket:

    - S355, cutting plate, t=20 mm, ø=165 mm (CNC-milling to create cambers to keep the POM-block and the hinge at its place)
- Steel hinge:
    - Standard product: GX50T

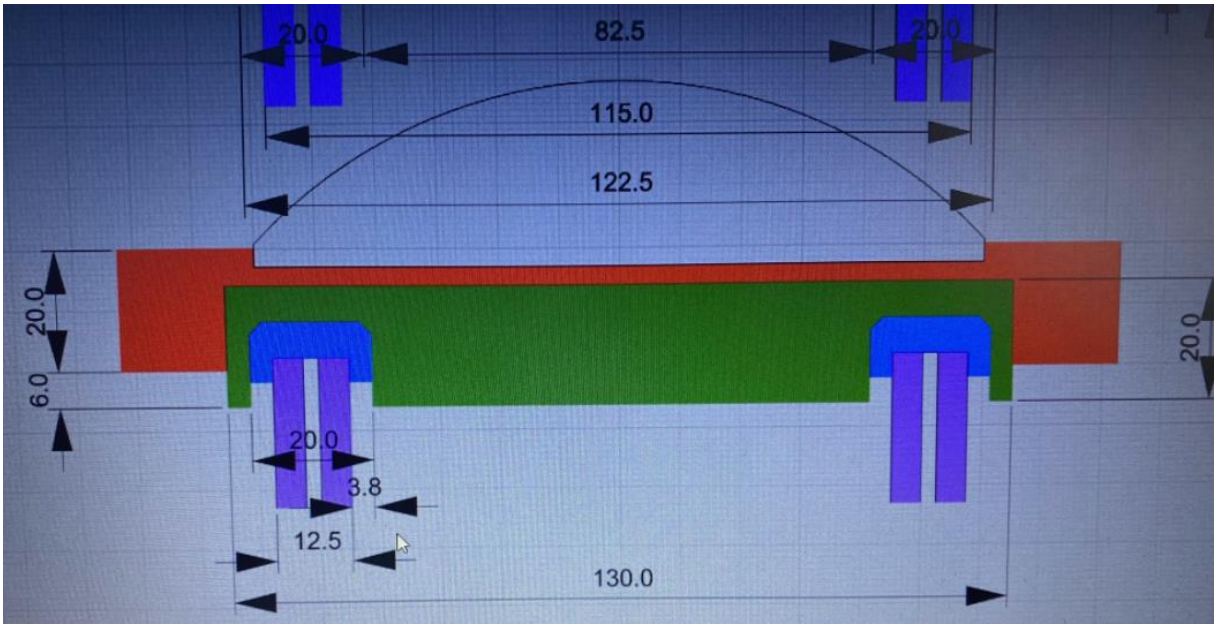

Figure 2 Sketch cross section of the connection with; red: steel bracket, green: POM-block, blue: Hilti mortar, purple: glass tubes, circle: the hinge (Octatube. 2021).

Furthermore, at the top and the bottom connection a steel plate is placed with a hole so that the wires from the sensors (placed at the inside of the glass), can go out of the glass tubes:

- Steel plate S3555, t = 10 mm, with hole for wires attached to the strain sensors inside the bonded glass tube (see the plan view of this plate in figure 5).

SCHOTT will sponsor the glass tubes and delivers them to Kömmerling H.B.Fuller (11th of May). These tubes need to be bonded together by a transparent UV-curing resin. This will be done by H.B.Fuller Kömmerling. The POM-block, the steel parts (from the connections) and some threated rods with fixation materials will be made/arranged by Octatube at the beginning of June. The Hilti mortar patrons are already delivered at Octatube as well. All the parts will be at the Technical University of Delft at the 23th of June (the starting date).

Before testing, the strain sensors need to be attached to the glass tubes (inside and outside), and the Hilti mortar needs to be injected in the lab. We can borrow the tools needed to inject the Hilti mortar from Octatube. In figure 3 and 4, details are shown for one sample with a length of 300 mm. The one/two hole(s) in the middle of Pom-block and the steel, is for the threated rod (figure 5) and for the wires attached to the strain sensors (figure 6).

Figure 3 3D view of the samples with a length of 300 mm.

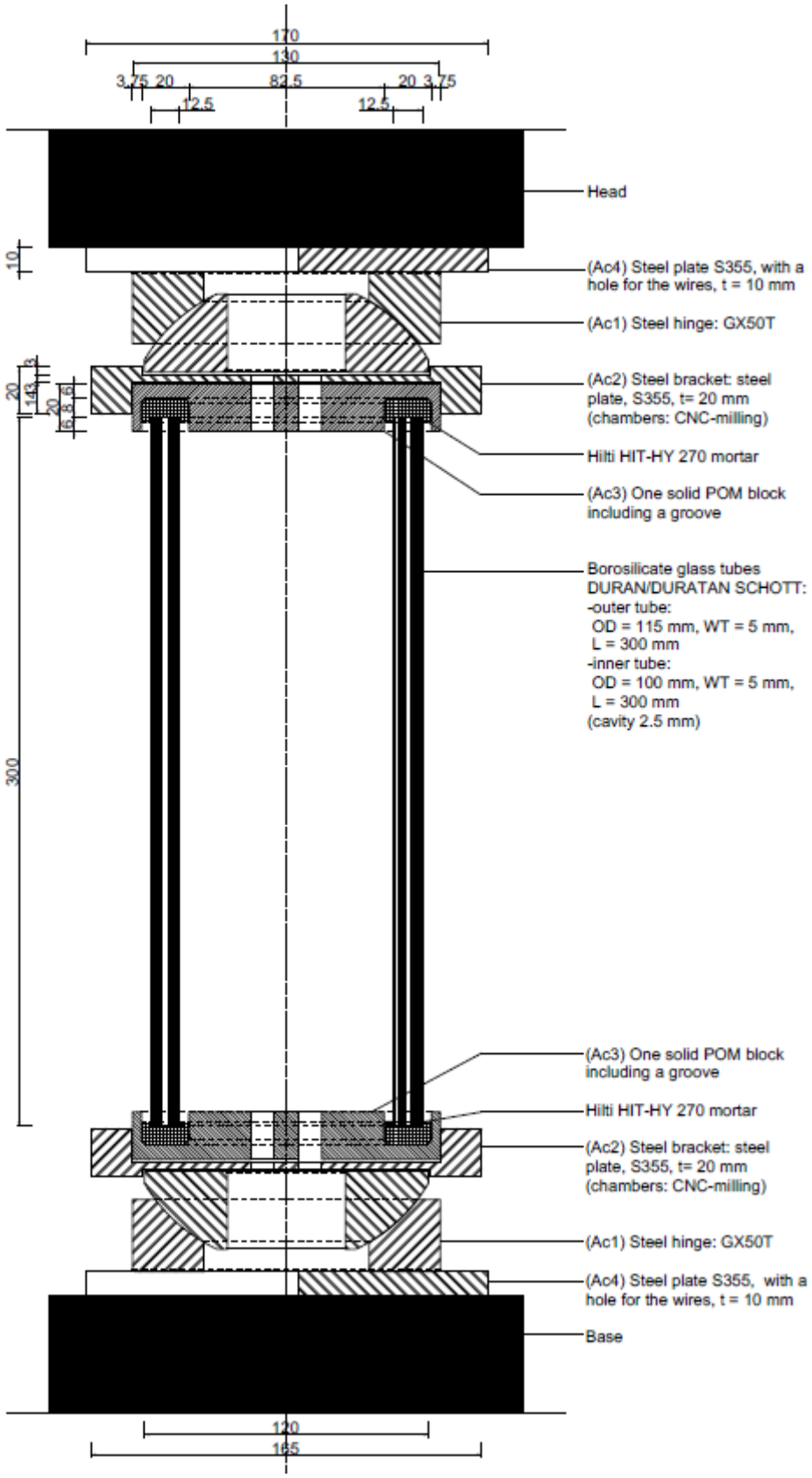

Figure 4 Samples 300 mm for testing

2.3. Test setup and the experiment

2.3.1. Small samples of 300 mm

The procedure to test one sample:

1. Place the sensors on the glass (inside and outside). Steps per sensor:

- Clean the glass
- Indicate the place for the sensor (perpendicular to the normal force)
- Stick the sensor with a small tape
- Hold it for a few minutes
- Remove the tape when the sensor sticks to the glass
- Solder one end of the wires onto the sensor

2. Inject the Hilti:

- A few timber blocks will be glued in the POM-block.
- The POM-block needs to be placed inside the steel bracket. The wires of the strain sensors placed on the inside of the glass, needs to be pulled through one of the holes in the POM-block and the steel.
- The threated rod needs to be fixed to one side (to the bottom connection steel/POM) with fixation (ring and nut) (as the bottom connection in figure 5).
- The Hilti-mortar will be injected in the grooves of the POM-block. Directly after that, the glass tubes will be placed on the POM. The timber blocks will keep the glass tubes at the right place until the Hilti mortar is hardened.
- The Hilti mortar will be hardened in 30 minutes.
- If one side is finished, the other side needs to be injected. The glass sample of 300 mm can be carried by hand, so for this, no extra equipment is necessary. The POM, Hilti and the glass tubes are not bonded together after injecting the Hilti is hardened. To be able to rotate the column, the steel, the POM, and the Hilti needs to be held together via a threaded rod ø=8 or 10 mm through the glass (see figure 5). This threaded rod will be delivered by Octatube. After rotating, the same procedure can be used to inject the mortar.

3. Now the samples are ready for testing and can be placed in the machine (figure 7):

- The sample needs to be placed in the machine, with the threated rod which hold everything together.
- The enclosure needs to be placed around the sample, to be sure no injuries are occurring during testing. *This enclosure needs to be made by the Technical University of Delft. (This one is already available in the basement).*
- After that the threated rod needs to be unscrewed a bit so that it will not contribute to the load-bearing behaviour. The other end of wires from the strain sensor needs to be plugged into the computer.
- Set the values to zero, for the strain sensors. (In figure 6, the principle is shown for the strain sensors in and outside and the inside of the column.)

4. The test:

- The sample in the machine will be loaded with compression load until failure (100-300 kN?).

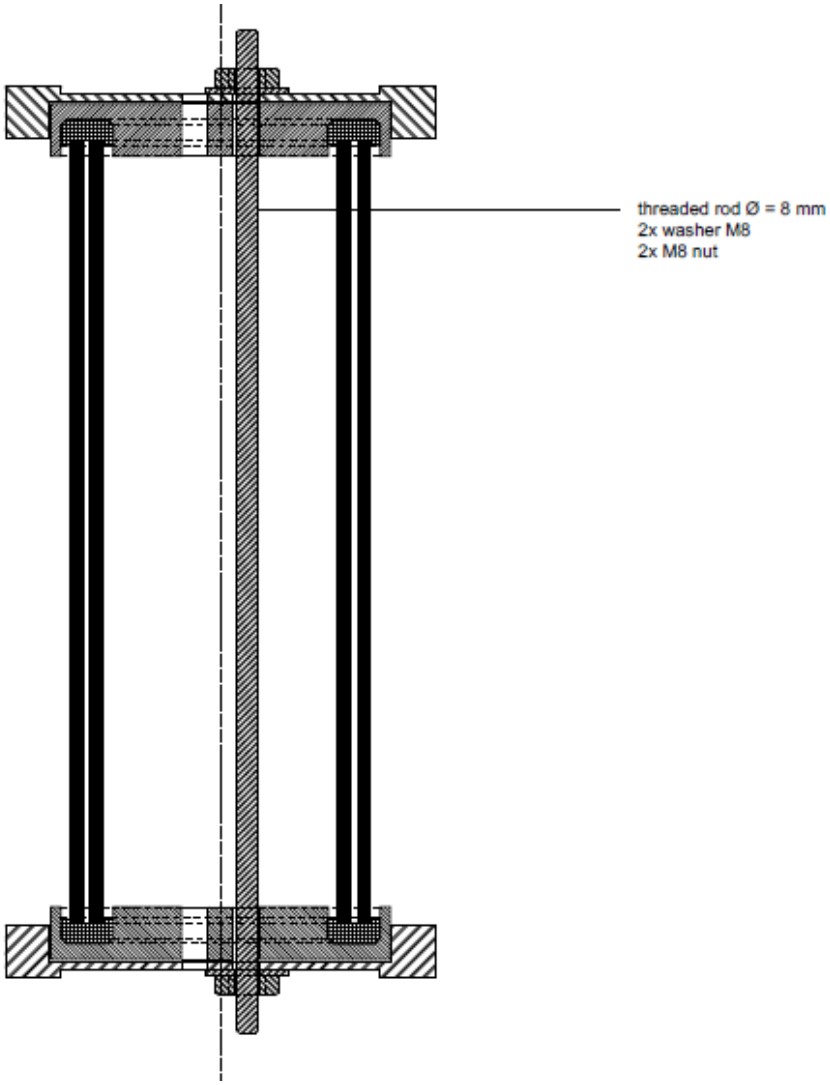

Figure 5 The 300 mm sample with threaded rod for production

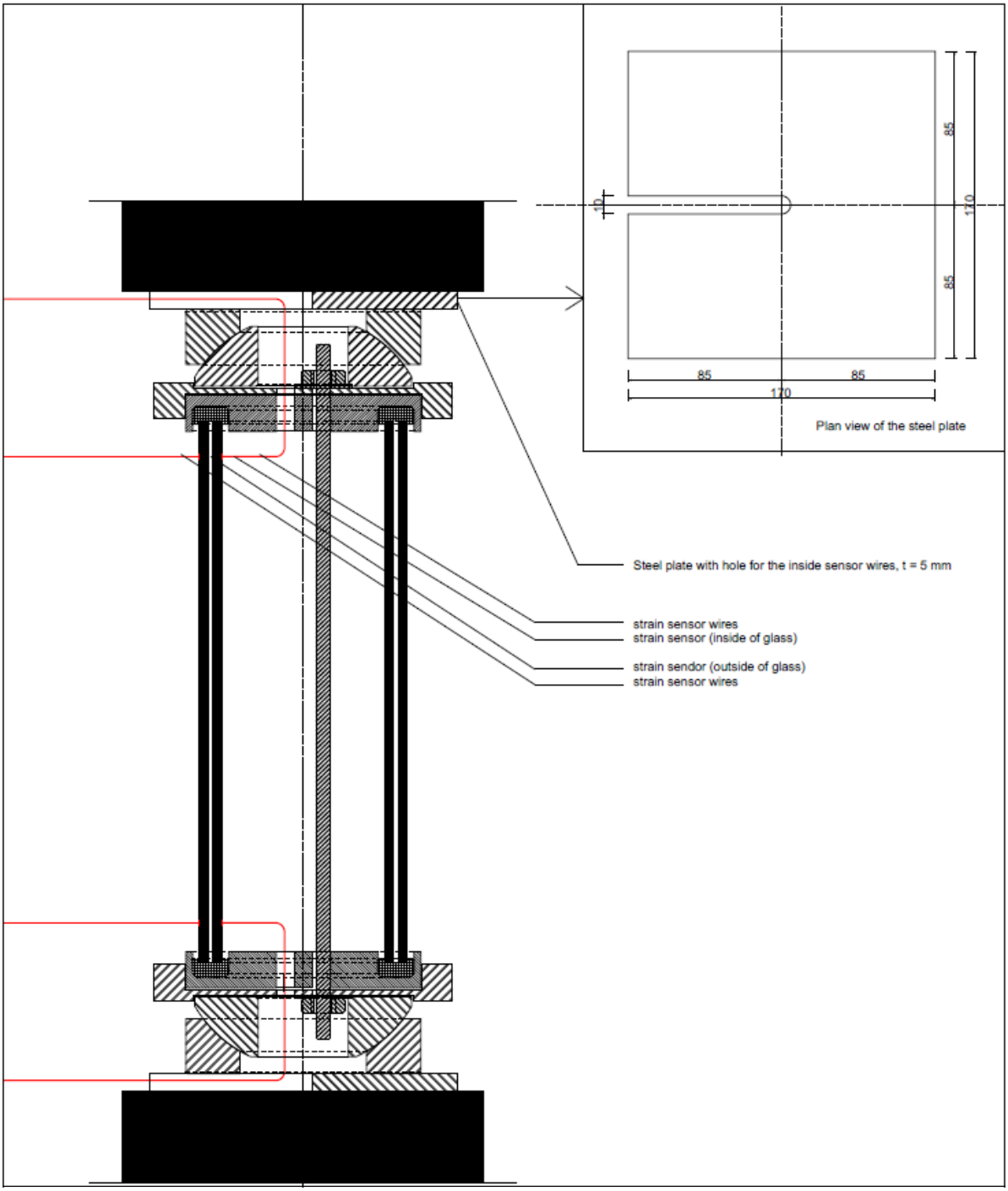

Figure 6 The principle of the test setup with strain sensors

2.3.1.1. Results and measurements

The compression test machine, which will be used during testing, is a displacement controlled hydraulic compression machine (see figures below). The samples will be clamped between two plates (head/base) and the base will be displaced at 1 mm per minute. The occurring reaction forces into the column are equal to the compression forces onto the column. The machine is adjustable for samples up to 5000 mm.

Figure 7 Compression machine at the TU Stevin lab II

The displacement (in z-direction) can be measured by sensors (see figure 8).

Figure 8 Sensor to control the displacement in z-direction during testing.

2.3.1.2. Takes/measurements

Below the measurements/tasks required from/during testing:

- During the mortar injection the following can be checked:
  - The mortar needs to be injected easily without problems.
  - The mortar needs to be well-distributed over the groove in the POM-block.
  - The glass needs to stay clean during/after injecting the mortar.
- To check if the forces are uniformly distributed from the connection into the glass:
  - Strain sensors (parallel to the glass) needs to be placed at both glass tubes, close to the connections, to check if the loads are uniformly distributed into the glass (available at the Technical University of Delft). In this way there can be checked if the forces will be uniformly distributed into the glass by the Hilti mortar. This is necessary to avoid local peak stresses.
    - *6 strain sensors on the outside per glass sample (3 close to the top connection and 3 close to the bottom connection).*
    - *And 6 strain sensors on the inside per glass sample (3 close to the top connection and 3 close to the bottom connection)*
    - *(So, in total 12 strain sensors per sample. There are 6 samples: 72 strain sensors in total.)*
- Compression forces/post-failure behaviour:
  - Look at the way the Hilti mortar breaks: does it crack/crush/splash/etc?
  - Is the Hilti mortar able to take up more stress than 53 N/mm^2 (see figure 9)? If so, then it is possible to overstress the mortar. The stress can be calculated when the force onto the samples is known. Via the following formula:

    $$\sigma = \frac{F}{A}$$

    The force will be required during the test.
  - What is the weakest point of the sample: the glass or the connection? So what breaks first?
  - What is the post-failure behaviour of the glass column?
    - How does the glass break?
    - How is the interlayer behaving if the glass is broken?
    - Does the laminated glass tube cracks differently than single tubes?
    - Are the samples robust? Do they show some structural integrity?
  - Are the strain values in the glass tubes from the sensors comparable with the strain values calculated by hand?
  - To verify the hand calculation of the displacement of the column. These values can be received from the load versus z-displacement curve from the test.

In the abovementioned questions, the differences between DURAN and DURATAN samples needs to be covered.

1.5 Hilti HIT-HY 70

"Gutachterliche Stellungnahme für die Verwendbarkeit von Hilti HIT-HY 70 im Glasbau", d.d. 25 oktober 2011.

Sterkte

$\sigma_{RK,5\%} = 58{,}7\ N/mm^2$

$A_1 = 1{,}70$ lange duur

$A_1 = 1{,}00$ korte duur

$A_2 = 1{,}00$ binnen situatie

$A_3 = 1{,}10$ temperatuur tot 60°C

$A_4 = 1{,}00$ algemene factor, maar niet van toepassing

$$\sigma_{RK,0,korte\ duur} = \frac{58{,}7}{1{,}00 * 1{,}00 * 1{,}10 * 1{,}00} = 53{,}36\ N/mm^2$$

$$\sigma_{RK,0,lange\ duur} = \frac{58{,}7}{1{,}70 * 1{,}00 * 1{,}10 * 1{,}00} = 31{,}39\ N/mm^2$$

$$\sigma_{d,toelaatbaar,korte\ duur} = \frac{\sigma_{RK,0,korte\ duur}}{\gamma_M} = \frac{53{,}36}{1{,}15} = 46{,}4\ N/mm^2$$

$$\sigma_{d,toelaatbaar,lange\ duur} = \frac{\sigma_{RK,0,lange\ duur}}{\gamma_M} = \frac{31{,}39}{1{,}15} = 27{,}3\ N/mm^2$$

Stijfheid

$E_{gemiddeld} = 1700\ N/mm^2$

$E_{min} = 1000\ N/mm^2$

$E_{max} = 2500\ N/mm^2$

Figure 9 Allowable stress Hilti mortar (Gutachterliche Stellungsname. 2011).

3. Experiments part 2 (yet unknown)

These experiments are no longer a part of the thesis. This will be planned after the thesis is finished.

After performing experiments part 1, the design team (SCHOTT, Kömmerling H.B.Fuller, TUD) will assess the 300 mm samples. After that, the experiments part 2 can continue.

References

Figure list

Figure 1 - Own picture. Delft. Retrieved on March, 3, 2021.

Figure 2 - Made by Octatube. Delft. Retrieved on May, 19, 2021.

Figures 3,4,5,6, - Own pictures. Delft. Retrieved on May, 31, 2021.

Figure 7,8 - Own pictures. Delft. Retrieved on April, 12, 2021.

Figure 9 - Gutachterliche Stellungsname from October, 25, 2011. Delft. Retrieved on May, 7, 2021.

Appendix 13 – Preparing the samples

This chapter shows how one sample is prepared for testing.

A.13.1. Strain sensors

In this chapter a step-by-step plan is given to glue the sensors to the glass tubes and to solder the wires. There are 12 sensors attached to one sample, 6 close to the top connection (3 on the inner tube and 3 on the outer tube) and 6 close to the bottom connection (3 on the inner tube and 3 on the outer tube). This means that there are 72 sensors glued to the glass.

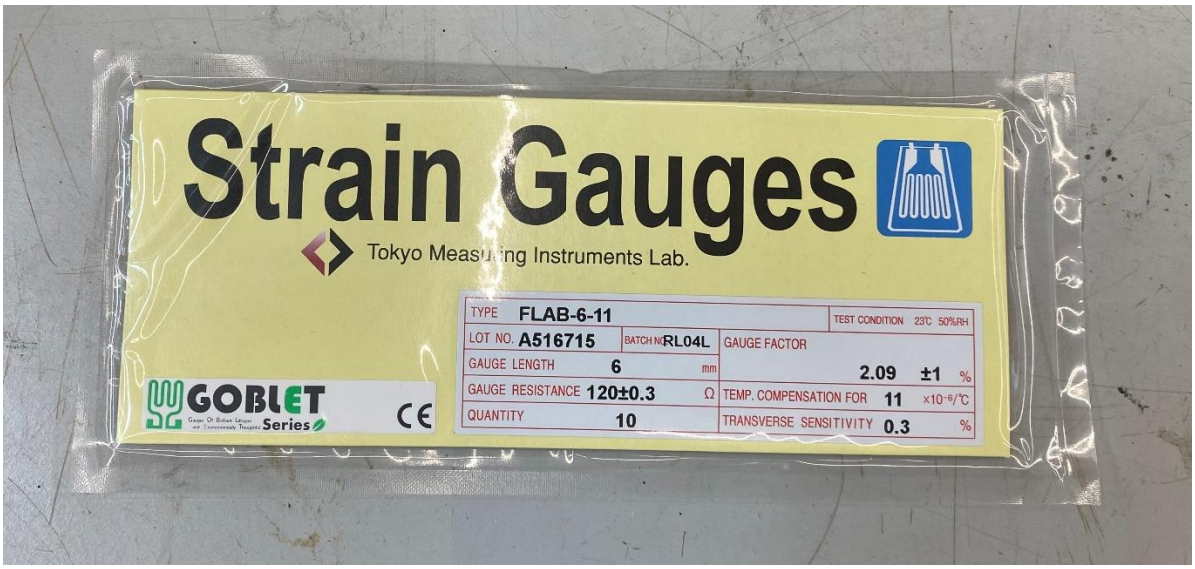

Figure 1 The strain sensors.

Step 1: sand the glass on the spot where the sensors will be placed.

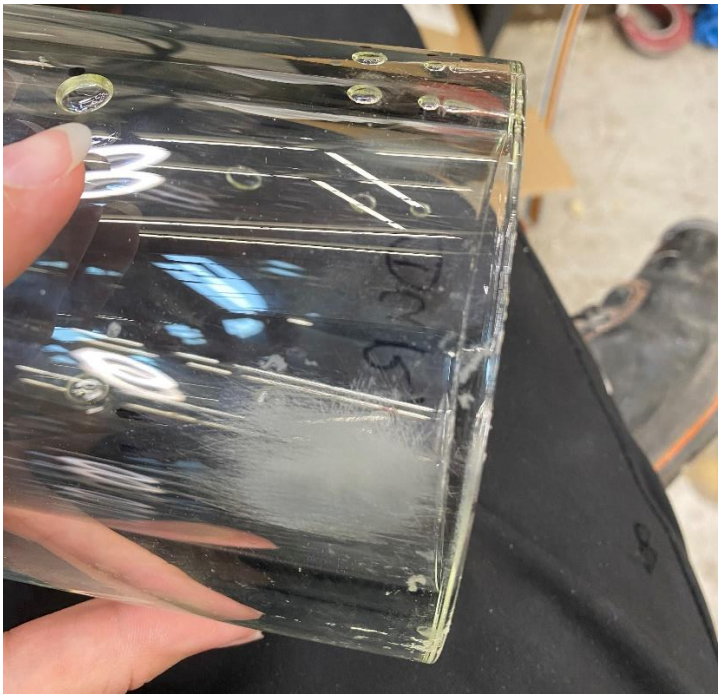

Figure 2 Sanding the glass.

Step 2: Grease the glass with Acetone.

Figure 3 Grease the glass.

Step 3: Determine and mark the location for the sensor.

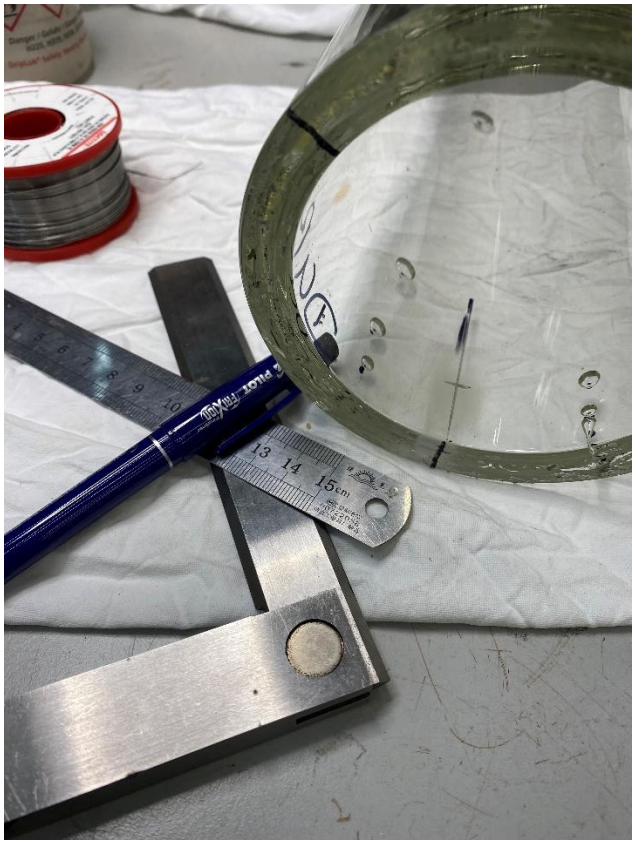

Figure 4 Determine and mark the location.

Step 4: Stick the sensor with a small tape and put glue on the other side of the sensor.

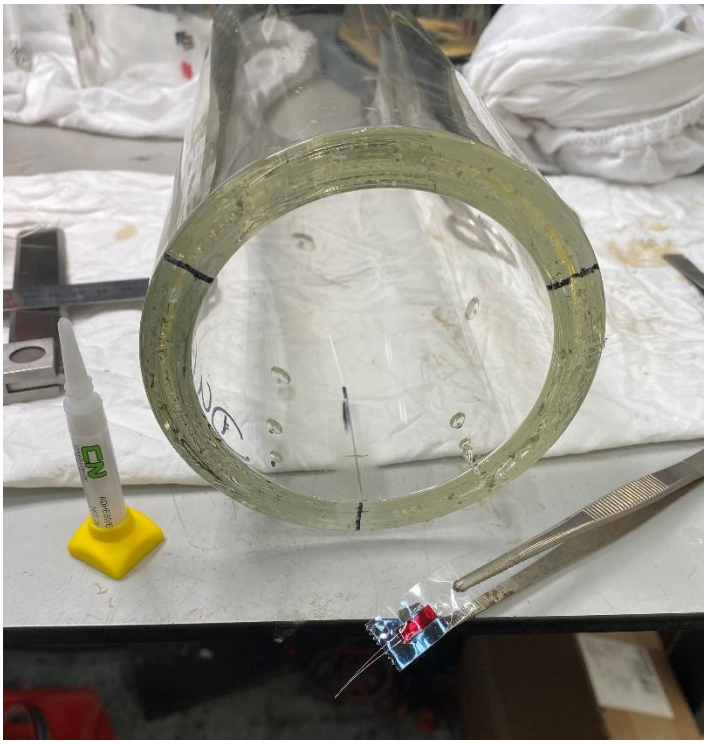

Figure 5 Stick and glue the sensor.

Step 5: Put the glued side of the sensor to the glass, and hold it for a few minutes.

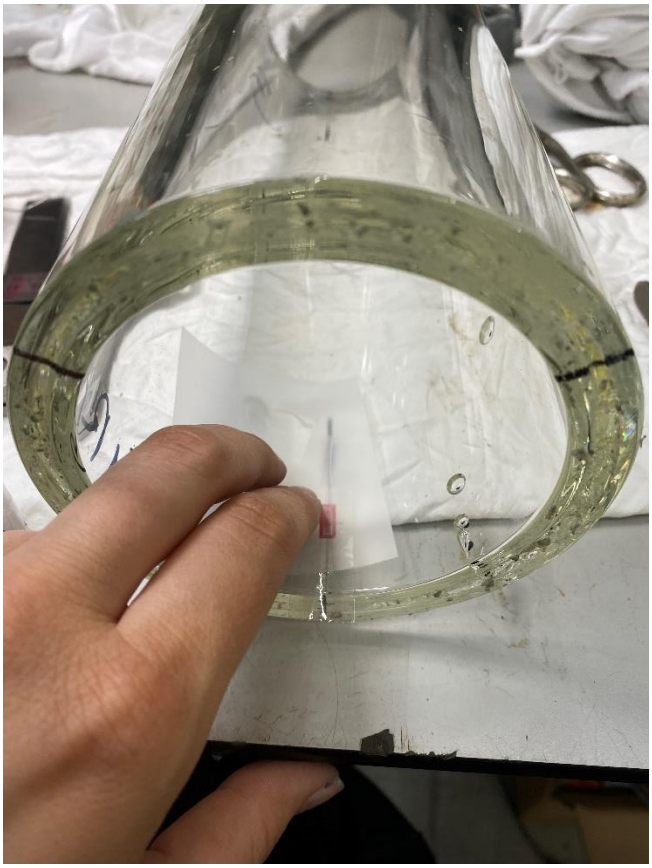

Figure 6 Glue the sensor and hold it.

Step 6: Remove the tape when the sensor is glued.

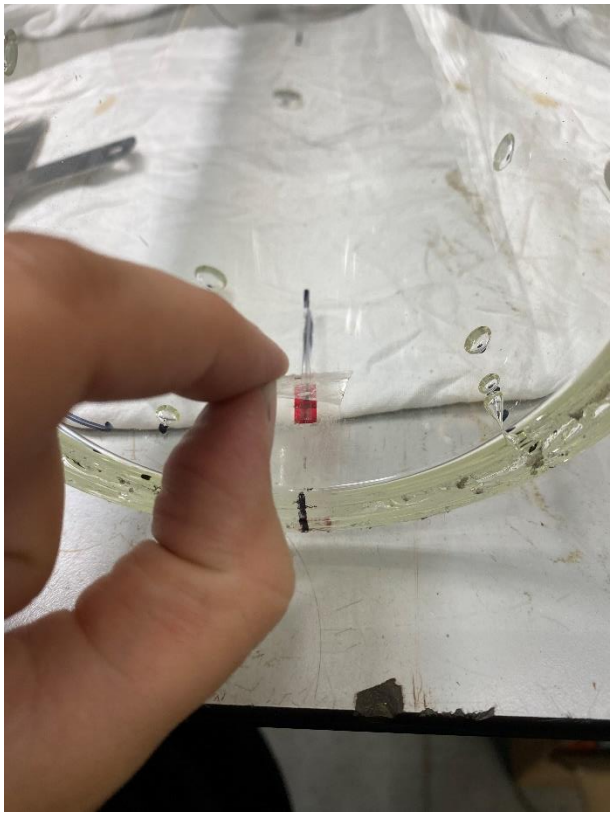

Figure 7 Remove the tape.

Step 7: Glue the connector to the glass.

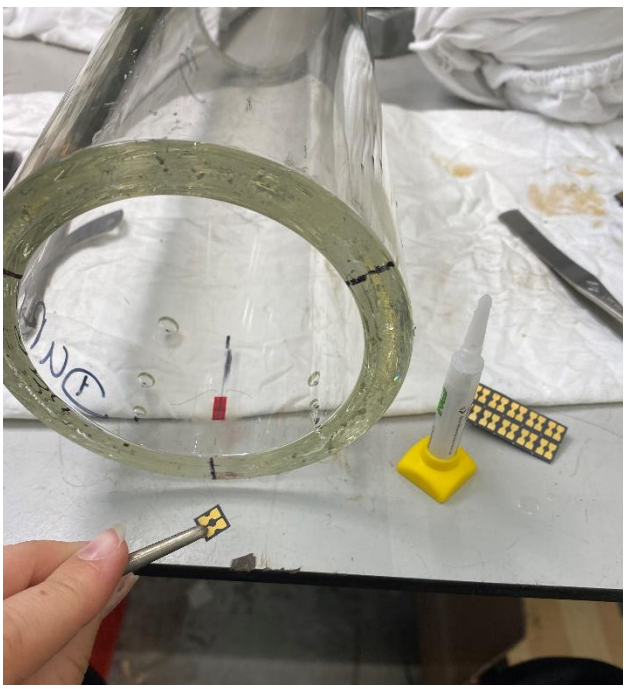

Figure 8 Glue the connector.

Step 8: Solder some tin to the connector.

Figure 9 Solder tin to the connector.

Step 9: Solder the wires from the sensor to the connector.

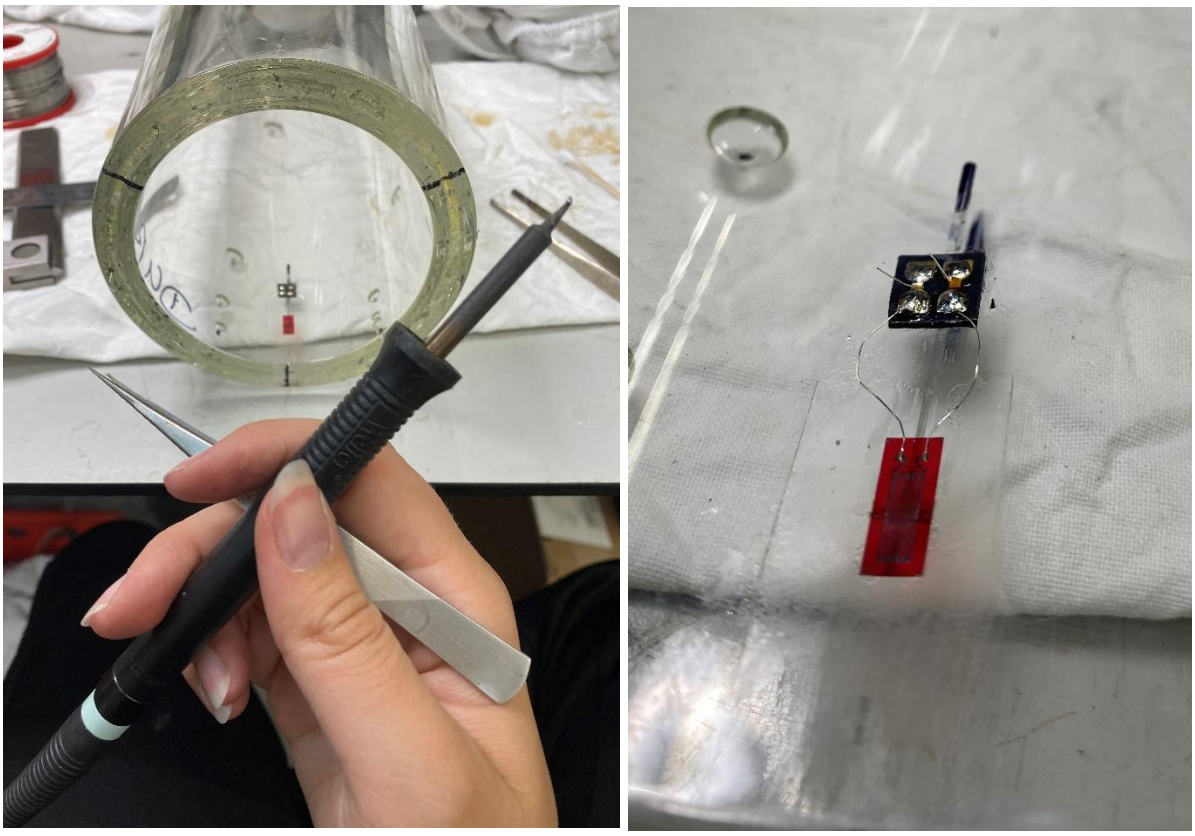

Figure 10 Solder the wires from the sensor to the connector.

Step 10: Cut off the remaining wire.

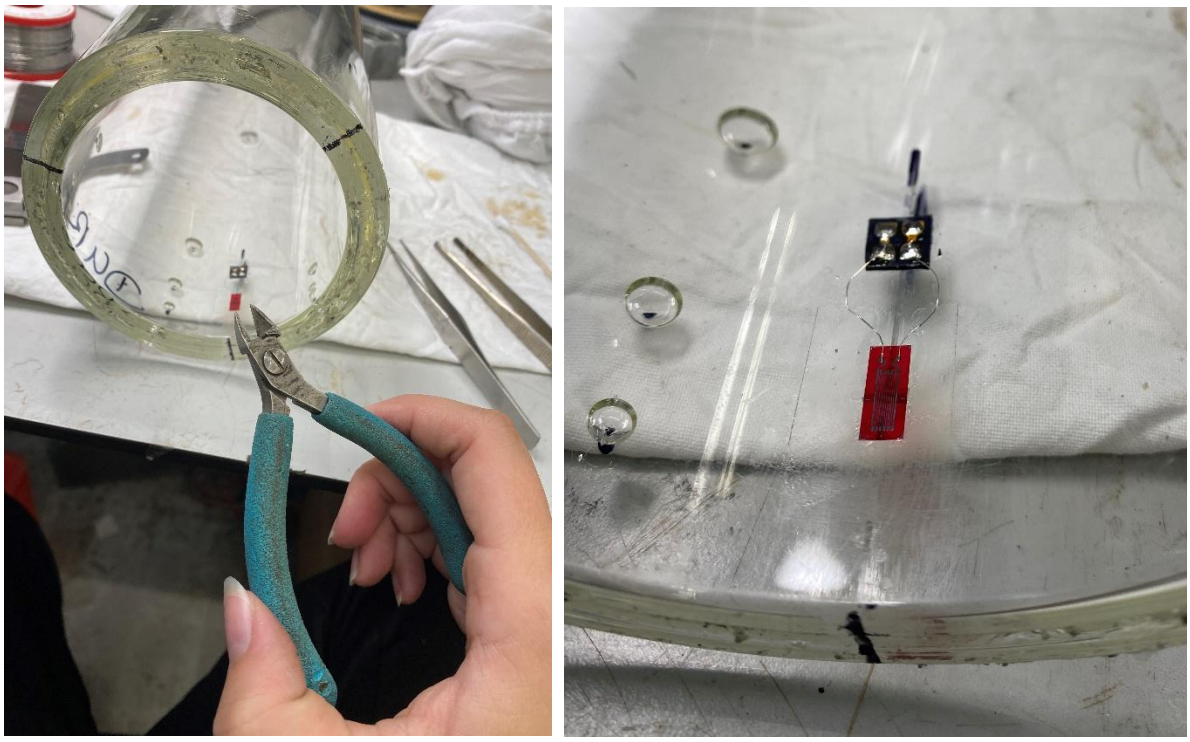

Figure 11 Cut off the remaining wire.

Step 11: measure the resistance to be sure that the plus and the min poles do not collide, otherwise a short circuit may occur.

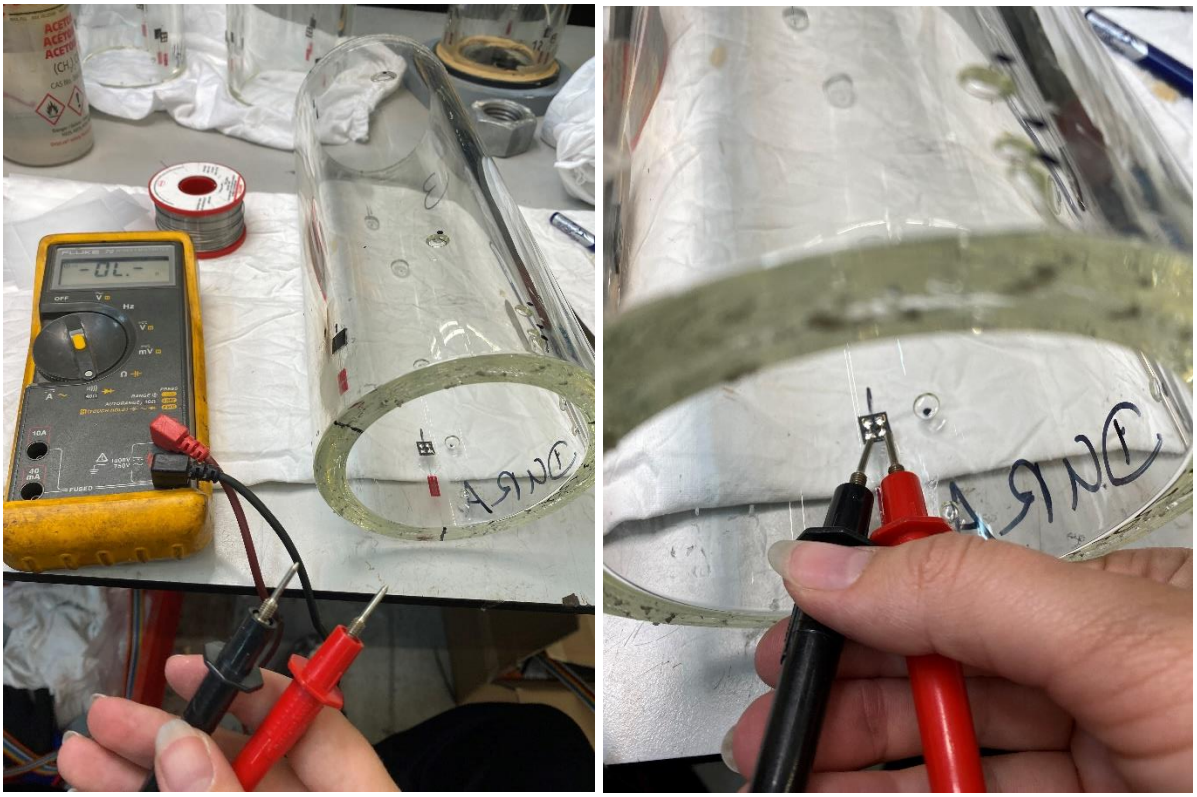

Figure 12 Check the plus and the minus do not collide.

Step 12: Solder wires to the inside sensors, and after this, the Hilti can be injected. The resistance in the wires also needs to be checked. In figure 15 is shown how the wires are look like after soldering it to the inside sensors.

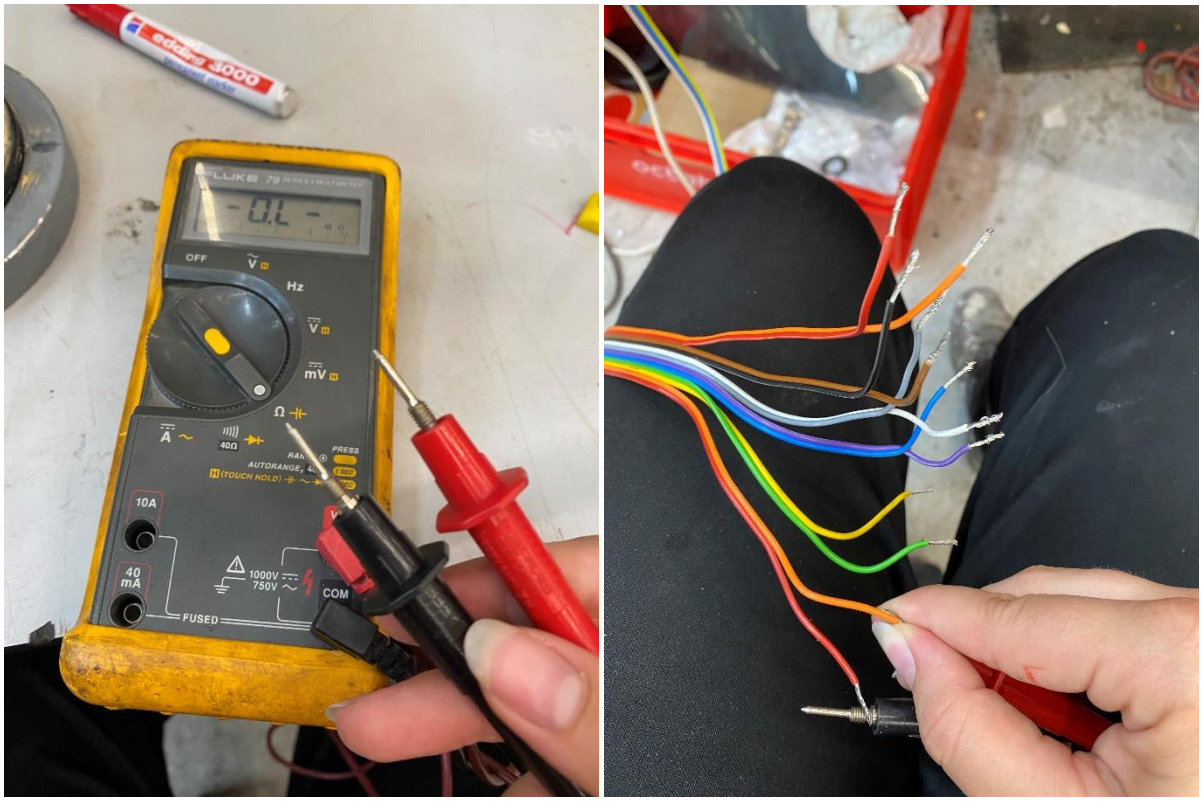

Figure 13 Measure the resistance in the wires.

A.13.2. Hilti mortar

In this chapter the way the Hilti mortar is injected into the POM-blocks is given. In figure 14 the POM-block is given, which is put in the steel connection plate. In figure 15 the steel and the POM-block are shown with the glued timber pieces. This timber pieces hold the glass at the right position until the Hilti mortar is hardened.

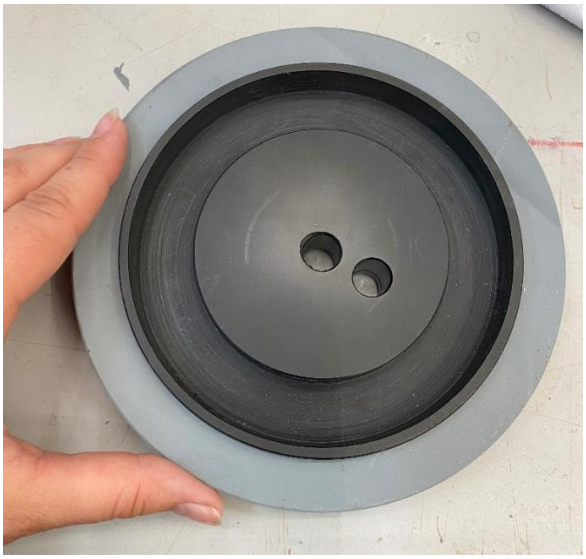

Figure 14 The POM-block in the steel connection plate.

Figure 15 The timber pieces glued into the POM-block.

The Hilti needs to be injected, then it needs to be smoothed out, and directly afterwards the glass needs to be put on top of it. This needs to be done within 5 minutes, because the Hilti start to harden quite fast. In figure 16, the POM-block in the steel is shown. First the wires attached to the inside sensors needs to be pulled through the POM and the steel connection plate. After that the Hilti mortar can be injected, see figures 16 and 17.

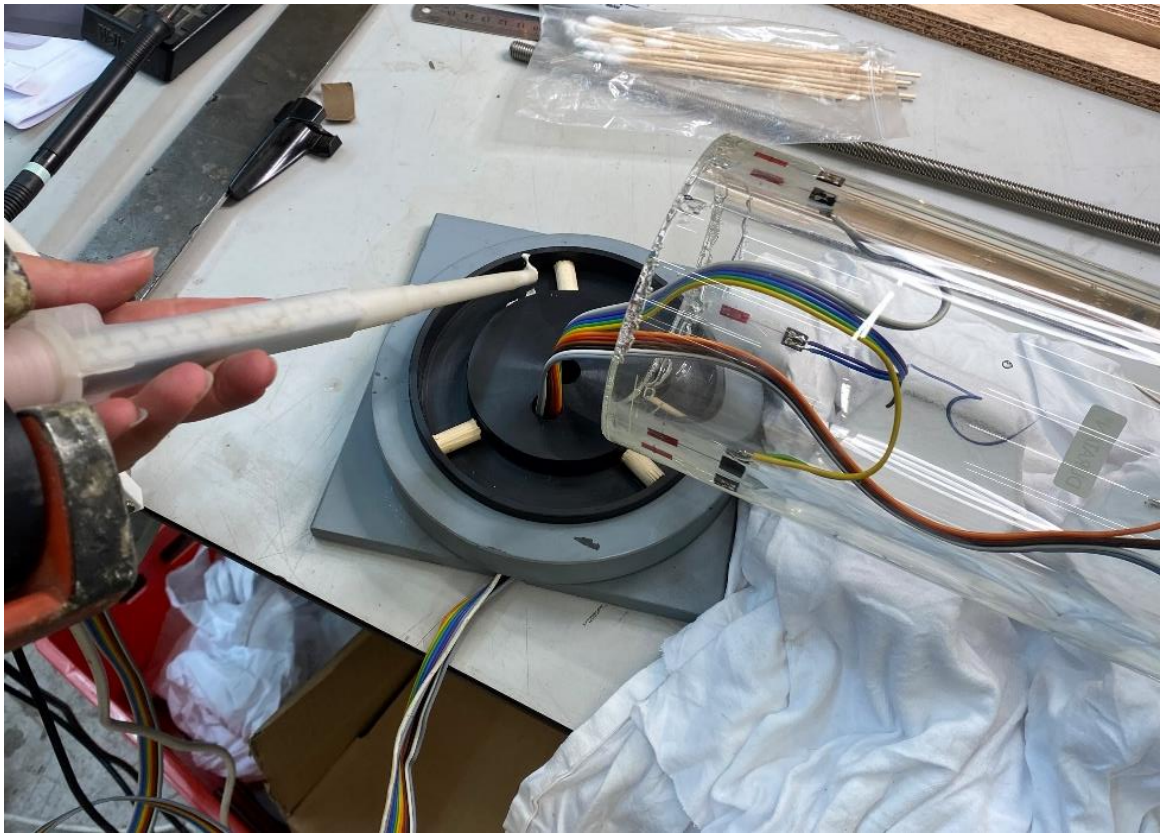

Figure 16 The wires are pulled through the POM and the steel and afterwards the Hilti mortar can be injected.

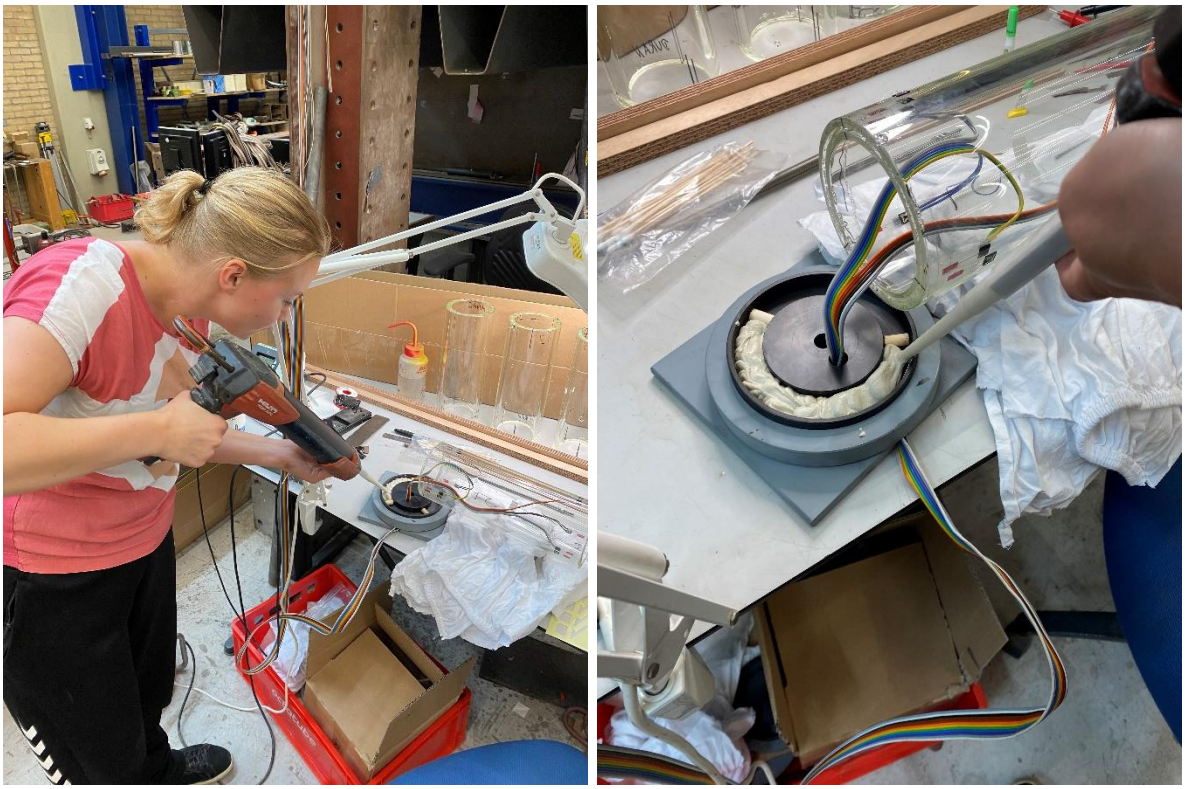

Figure 17 Injecting the Hilti mortar for one of the samples.

In the pictures in figure 18, a try-out is shown of injecting the Hilti mortar with the tool. The Hilti does not bond but it sticks to the glass and the POM. Afterwards the POM can be reused for the other samples. At 18.1 a POM-block and the Hilti tool is shown. At 18.2 is shown that the Hilti is injected and smoothed out. While the Hilti hardens, it gets warm and the colour changes a bit, which is shown in 18.3. At 18.4, the Hilti is hardened and cooled down. As shown, it is also lifted up a bit to take the Hilti out of the POM-block, so that the POM-block can be reused.

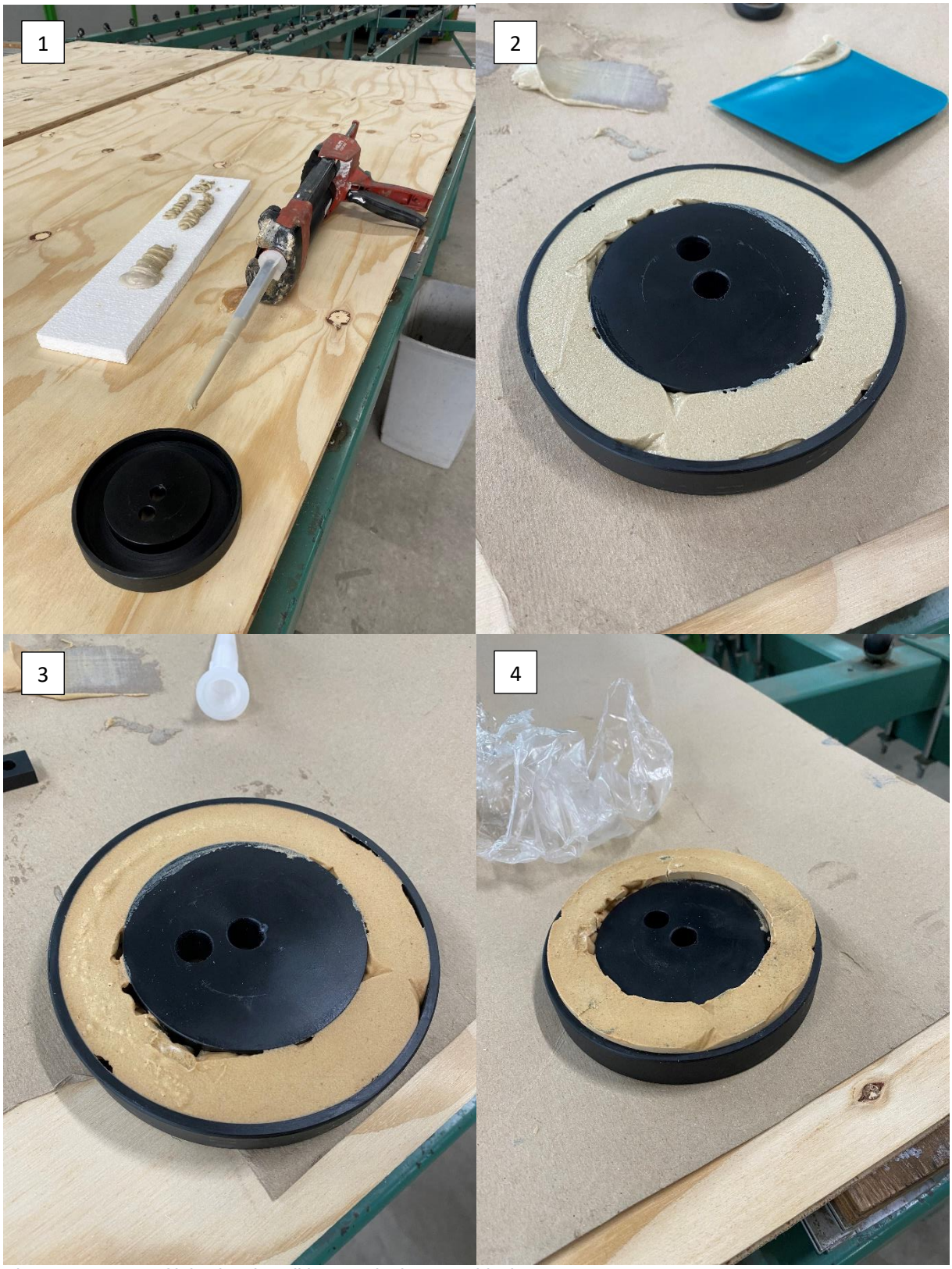

Figure 18 Try-out of injecting the Hilti mortar in the POM-block.

To be sure that enough Hilti was injected under the glass tubes, a bit too much Hilti used then necessary. In the figures 19 is shown, how to inject he Hilti so that it is net and that the glass remains clean.

Figure 19 The way to inject the Hilti so that it is net.

After injecting the Hilti mortar, the wires could be soldered for the outside sensors. Then it was ready to be placed into the machine.

A.13.3. The testing machine

Another compression machine was used then beforehand described in the experimental plan, due to the fact that only smaller samples are tested during this thesis project. Furthermore, it works the same as the one described in the experimental plan. It is a displacement controlled hydraulic compression machine (see figure 20). The samples will be clamped between two plates (head/base), whereby the base plate will come up slowly. The occurring reaction forces into the sample are equal to the compression forces onto the column.

In figure 21 the test set-up is shown. A camera is put in place, and two plexiglass panels are placed, one to sit behind while operating the computer and one in front to be able to see the sample crack during testing. The wires for the inside sensors can go through a hole in the top plate (figure 22).

The wires are put into an amplifier (figure 23 and 24), and after that the strain values of the sensors are set to zero. This amplifier will amplify the values of the strain sensors with 1000000.

In figure 25, the sample is shown ready for testing. The machine controlled. During testing, the load versus displacement and the strain values can be checked (figure 26).

A few more pictures during testing are shown in figures 27, 28, and 29. In figure 30, the hinge is shown for the connection, the standard product: GX50T from Techniparts.

Figure 20 The compression test machine.

Figure 21 The test set-up.

Figure 22 The wires from the inside sensors can go through a hole in the top plate to the computer.

Figure 23 The wires are put into an amplifier.

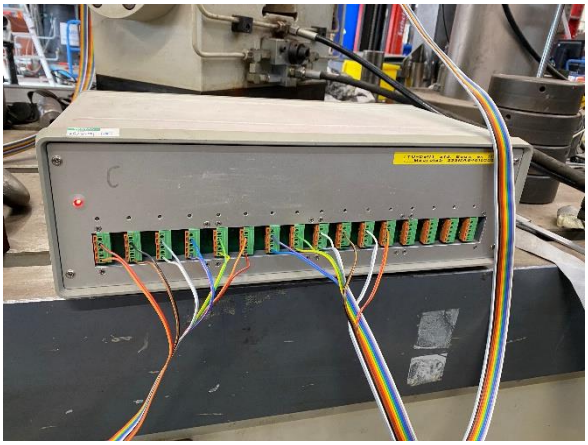

Figure 24 The amplifier with the wires attached.

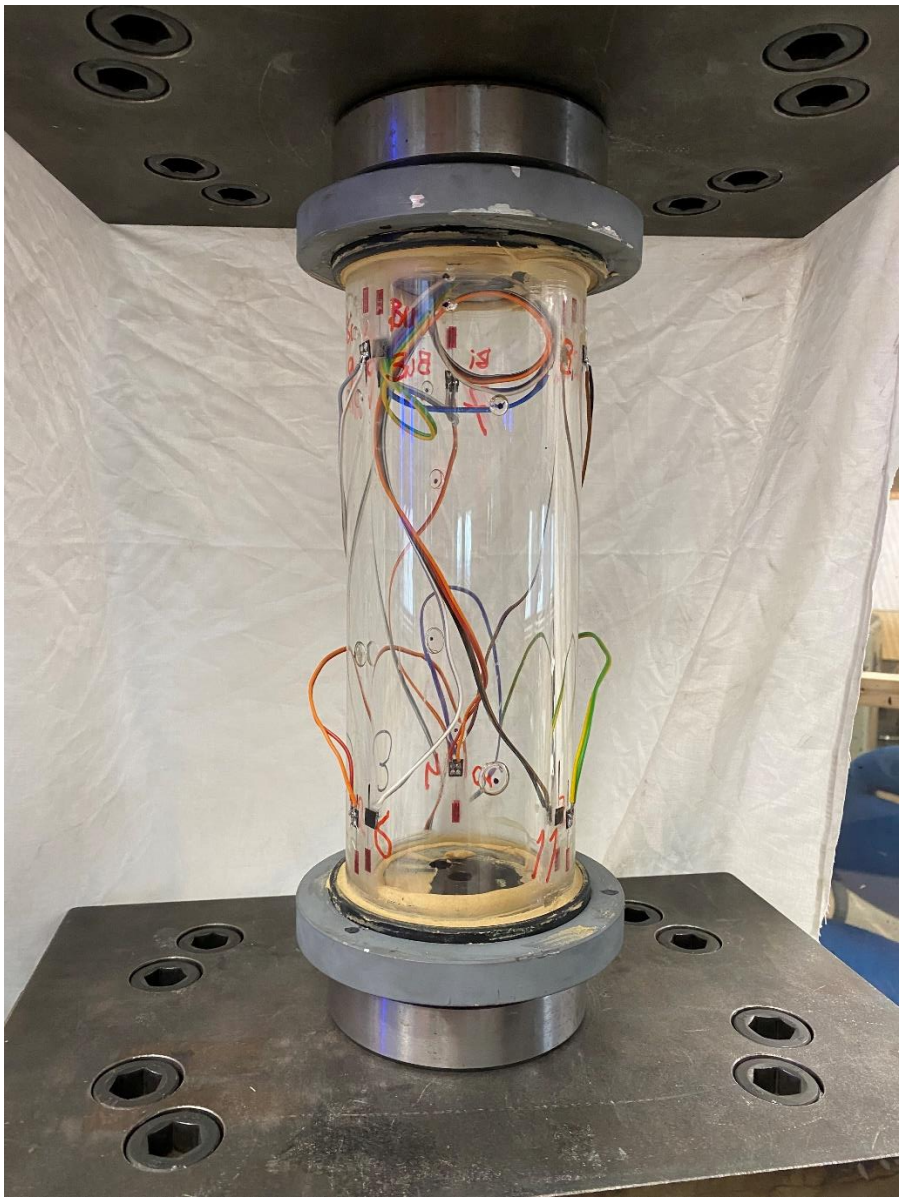

Figure 25 A sample in the machine.

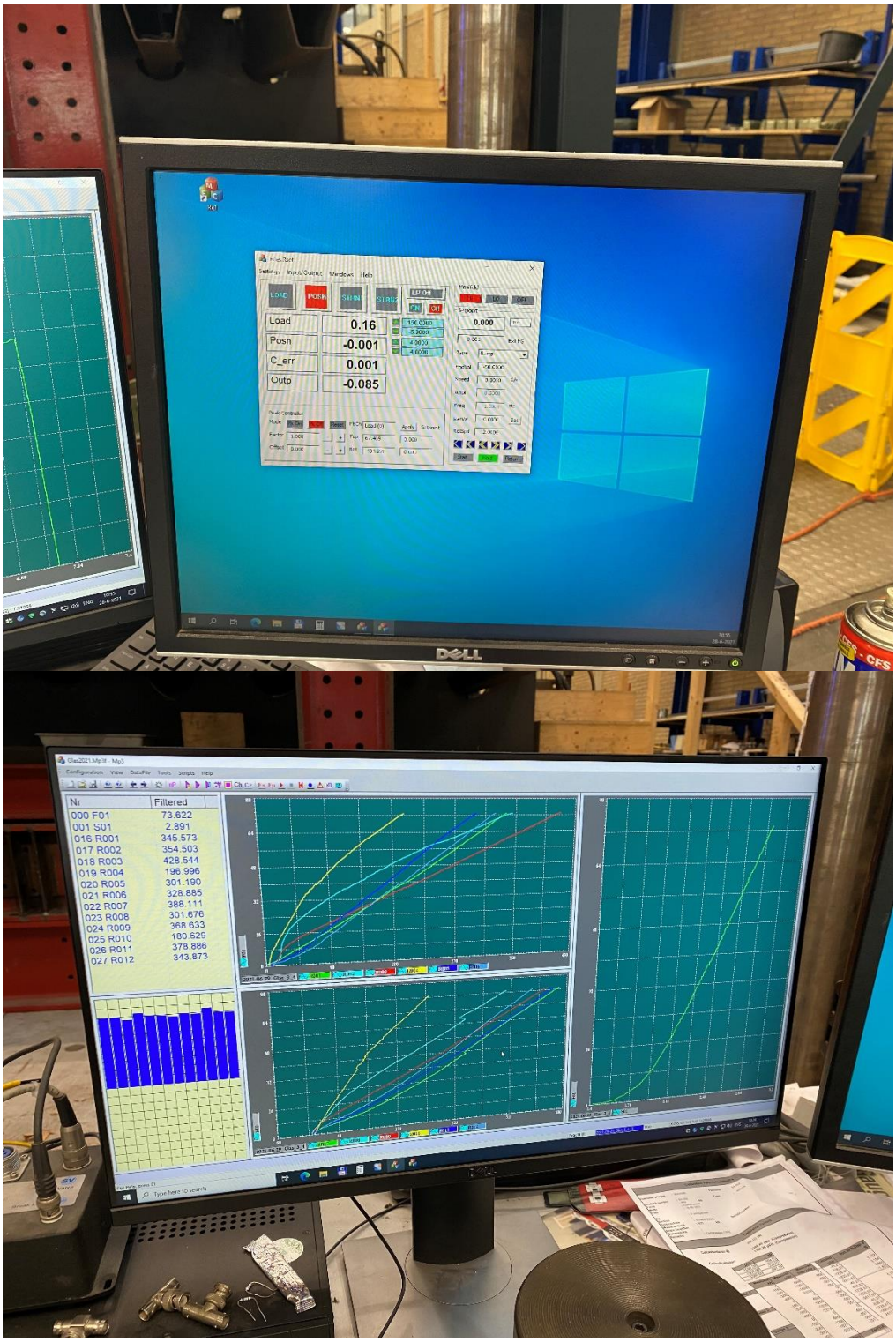

Figure 26 The computer where the load, the displacement and the strains could be checked during testing.

Figure 27 Preparing a sample in the machine.

Figure 28 Preparing the sample in the machine.

Figure 29 Controlling the cracks from the sample and making notes during testing.

Figure 30 The hinge, product GX50T from Techniparts.

References

Figure list

All figures - Own pictures. Delft. Retrieved on June, 24–30, 2021.

Appendix 14 – Test results

First of all, observations during and after testing will be given and results will be shown. After that, the tasks/measurements will be discussed which were set before testing. Strain sensors 1 till 6 were placed at the outer tube on the outside of the sample and sensors 7 till 12 were placed at the inner tube on the inside of the sample.

A.14.1. Observations and results during/after testing

A.14.1.1. Test 1 - sample 5

Sample 5 was made from DURATAN (heat-strengthened) glass tubes. Figure 1 (right) and 2 show the positioned sample in the machine before the test started. As can be seen in figure 1 (left) not many air bubbles are visible in the laminated tube.

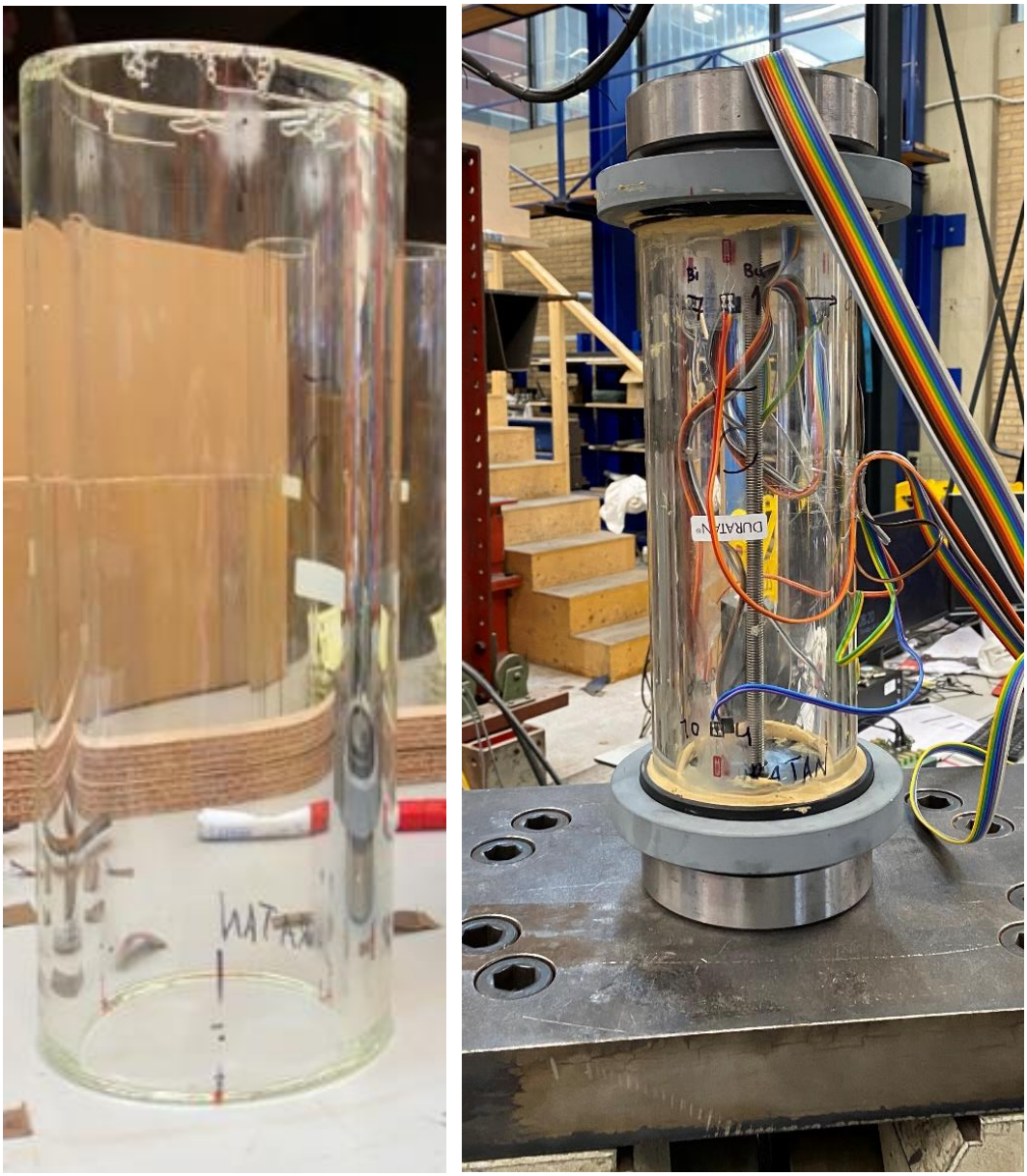

Figure 1 Sample 5 - Test 1.

Figure 2 In the first test, a plexiglass enclosure was used to ensure safety (later on plexiglass panels were used to stand behind. In this way the sample itself was more visible during testing).

After 160 kN nothing happened with the glass sample yet. After that, the machine could no longer cope, because low pressure was turned on instead of high pressure. When the switch was made to high pressure, the glass broke in one explosion (figure 4). It would have been better to turn off the machine and to start over. At the outer tube, cracks are visible which are parallel to the length of the tubes with approximately 4 mm between them. The inner tube broke into small pieces. The machine had gone to 600 kN, but it was not possible to conclude at which force the glass exploded. The glass broke without pieces shattering off and the connection remained intact. The Hilti was intact as well without crushing/cracking/etc. (figure 3). Figure 4 shows more pictures of the cracked end result.

Figure 3 The connection parts and the Hilti remained intact.

Figure 4 The broken glass.

To test if it was possible to inject Hilti properly, after the test, sample 5 is used (figure 5).

Figure 5 Neatly made sample 5 to show.

Below the load versus displacement curve is given from the test. As can be seen, there is a kink in the curve at 160 kN. After that the load goes to 600 kN at once. All strain sensors were still at its position, even after the sample exploded into small pieces. Below the load versus strain curve is given until 160 kN. After 160 kN, the curve was not reliable anymore. Moreover, until 50 kN, the strains were performing equal. After 50 kN, strain sensor 10 was deviating. Number 10 was placed at the inside close to the bottom connection. This sample did not have many air bubbles in the interlayer material.

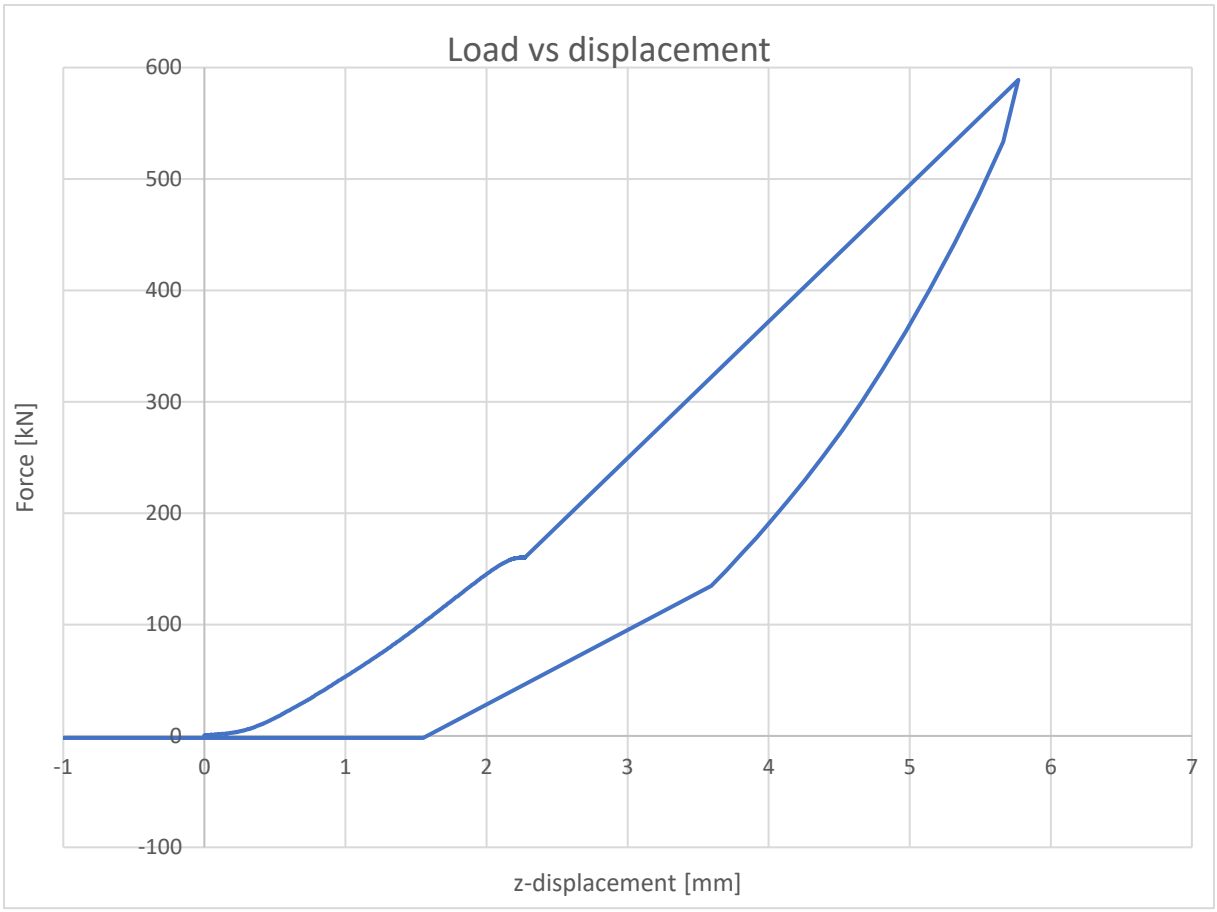

Graph 1 Load versus displacement curve - test 1 – sample 5.

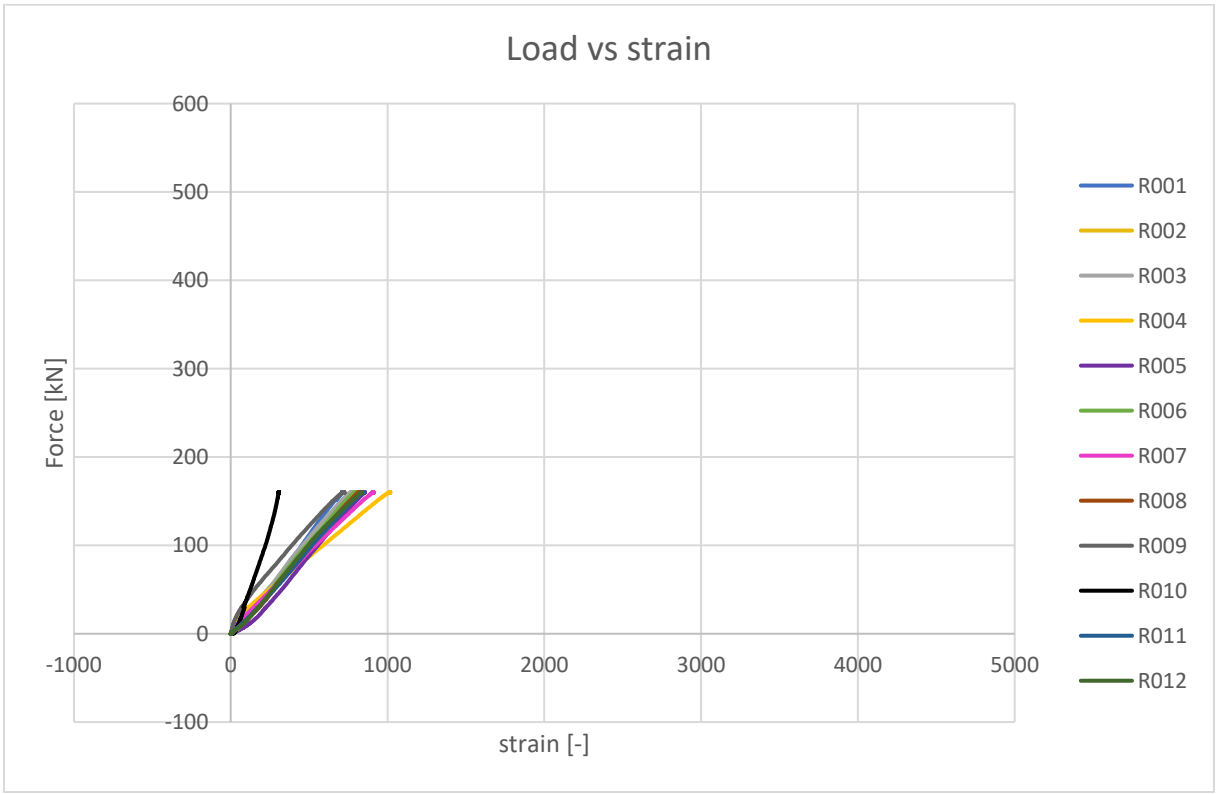

Graph 2 Load versus strain curve until the force was taken off - test 1 - sample 5.

A.14.1.2. Test 2 - sample 4

Sample 4 was made from DURATAN glass tubes. As can be seen in figure 6 (left), many air bubbles were present in the interlayer material. Figure 6 (right) shows the sample ready for testing. Graph 4 shows that strain sensor 12 was not working. To be sure, the resistance in the wire was measured. Sensor 12 could not be fixed anymore, because it was placed on the inside, where it was no longer possible to reach. Most of the bubbles were located where the sensors 7, 1, 4, and 10 were placed.

At 120 kN a lot of cracks appeared at the same time, where many air bubbles were present. The cracks were parallel to the length of the glass tube. It happened close to strain sensor numbers 7, 1, 4 and 10 (see figure 7). It cracked at once, so from one end to the other over the whole length of the glass sample. As can be seen in graph 4, not much happened with the strains. Strain 9 deviated a bit, but no visible cracks appeared around sensor 9. At 125 kN, sensor 7 deviated a bit, but started working again later on (graph 4).

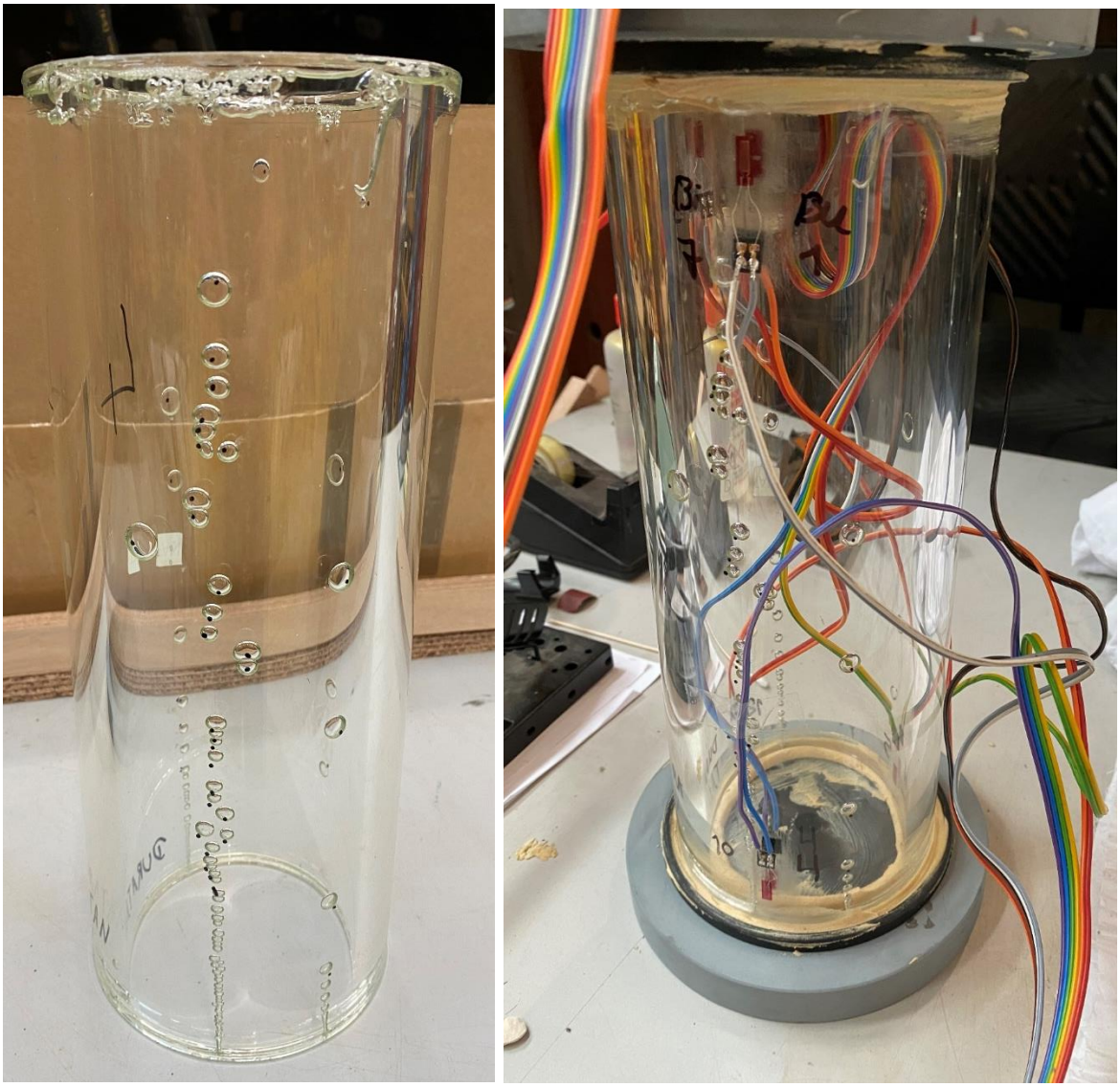

Figure 6 Sample 4 – test 2.

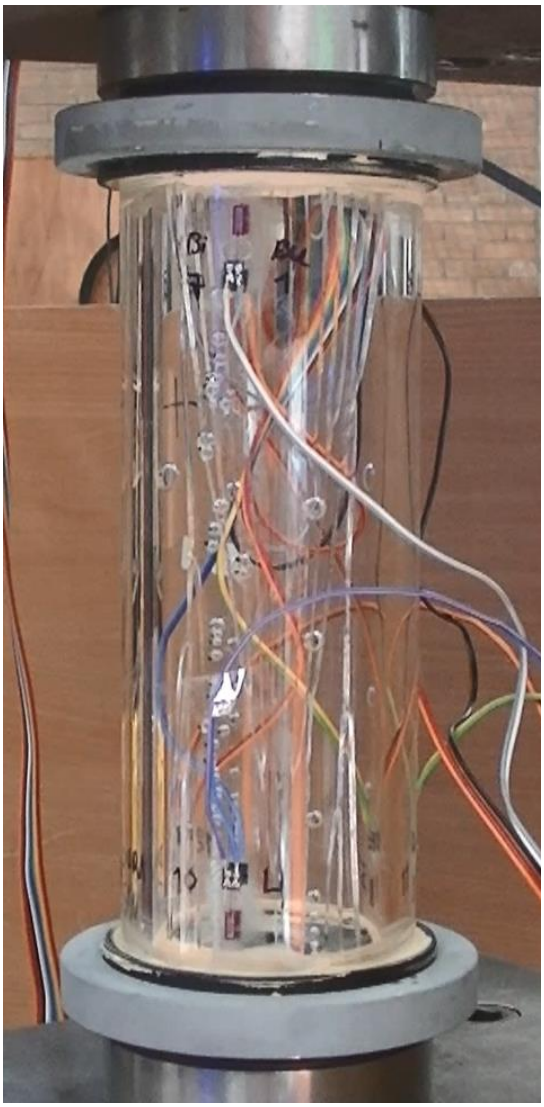

Figure 7 The first cracks appeared around 120 kN.

After that more straight cracks kept occurring, parallel to the length of the glass tubes, while the glass was under more and more compression loading. The cracks were cracking right away from one side to the other over the full length with a lot of speed (figure 8).

At around 200 kN, sensor 7 was deviating, and stopped working. At 225 kN sensor 9 was deviating, but came back on. After 275 kN, sensors 1, 4, 7 and 10 stopped working, when more and more cracks appeared close to these sensors (graph 4).

After that, at 350-370 kN, the glass started to shatter off (figure 9) in the middle of the tube. After 370 kN, glass shattered off at the top (figure 10), whereby the steel connection plate moved to a crooked position.

The sample was completely broken at 390 kN. This is visible in the load vs displacement curve as well. The curve became less steep and stopped (graph 3). When the base plate of the machine was lowered down, the force was taken off the sample. When the force was taken off, the tube exploded on the inside (figure 11). The outer tube was compressed, and the inner tube was exposed to tension. During testing, the compression was normative. When the force was taken off, the compression was overruled by tension, whereby the inner tube broke. The connections and the Hilti mortar remained intact (figure 12).

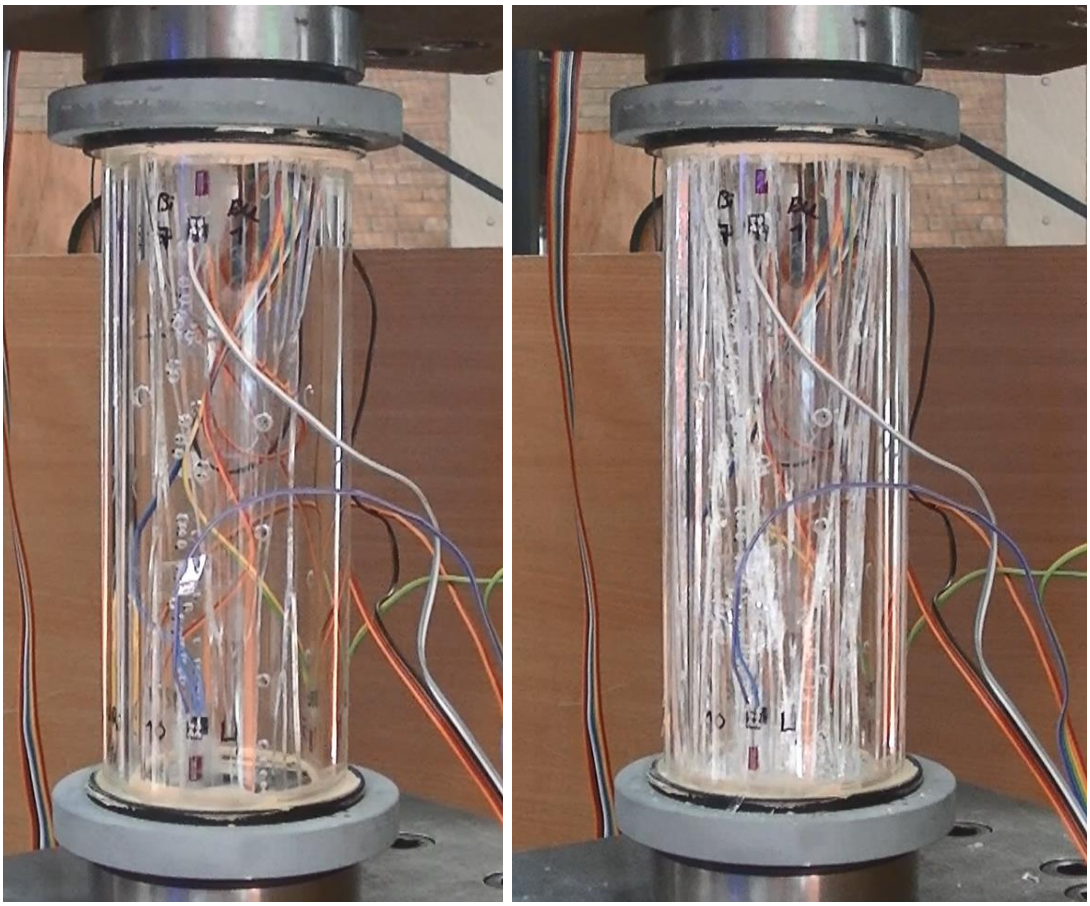

Figure 8 More straight cracks appeared (left: 210 kN and right: 300 kN).

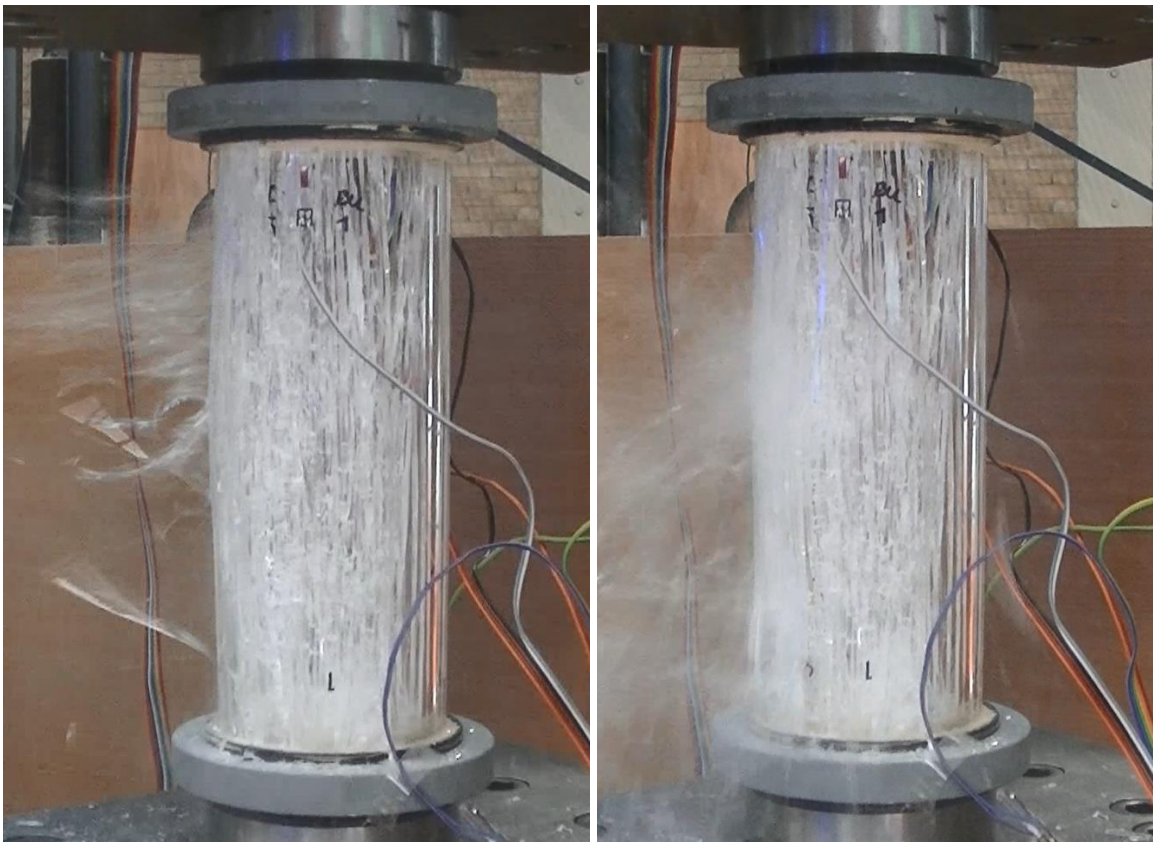

Figure 9 Glass shattering off (left: 350 kN, right: 370 kN).

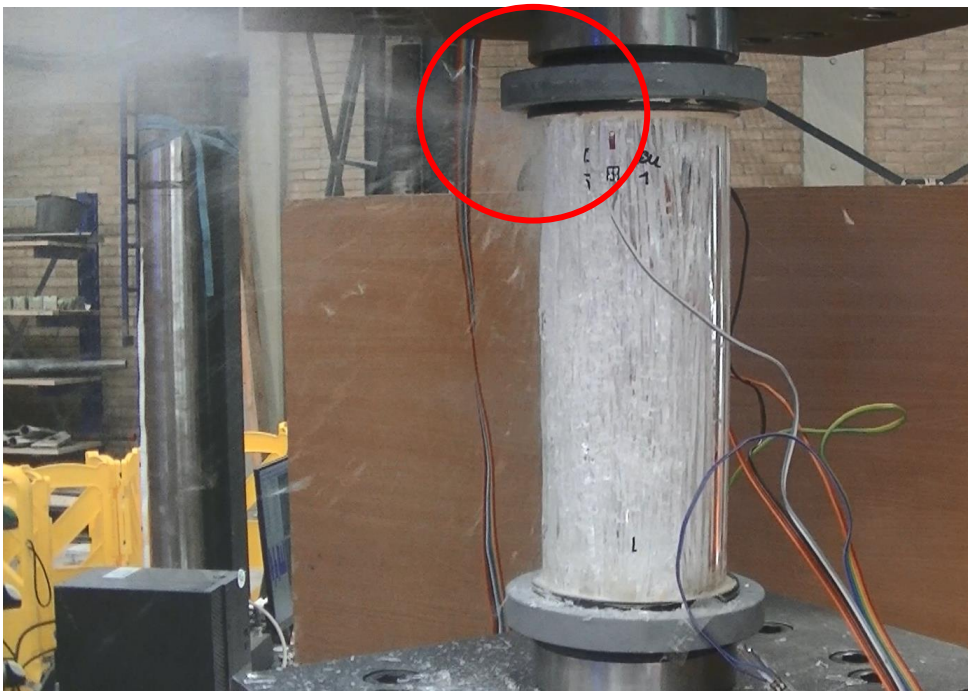

Figure 10 Glass shattering off at the top left, whereby the steel connection plate moved to a crooked position (370 kN).

When the force was decreasing after it was taken off, a few kinks occurred in the load versus displacement curve (graph 3, red circles). These are probably the points at which the inner tube cracked.

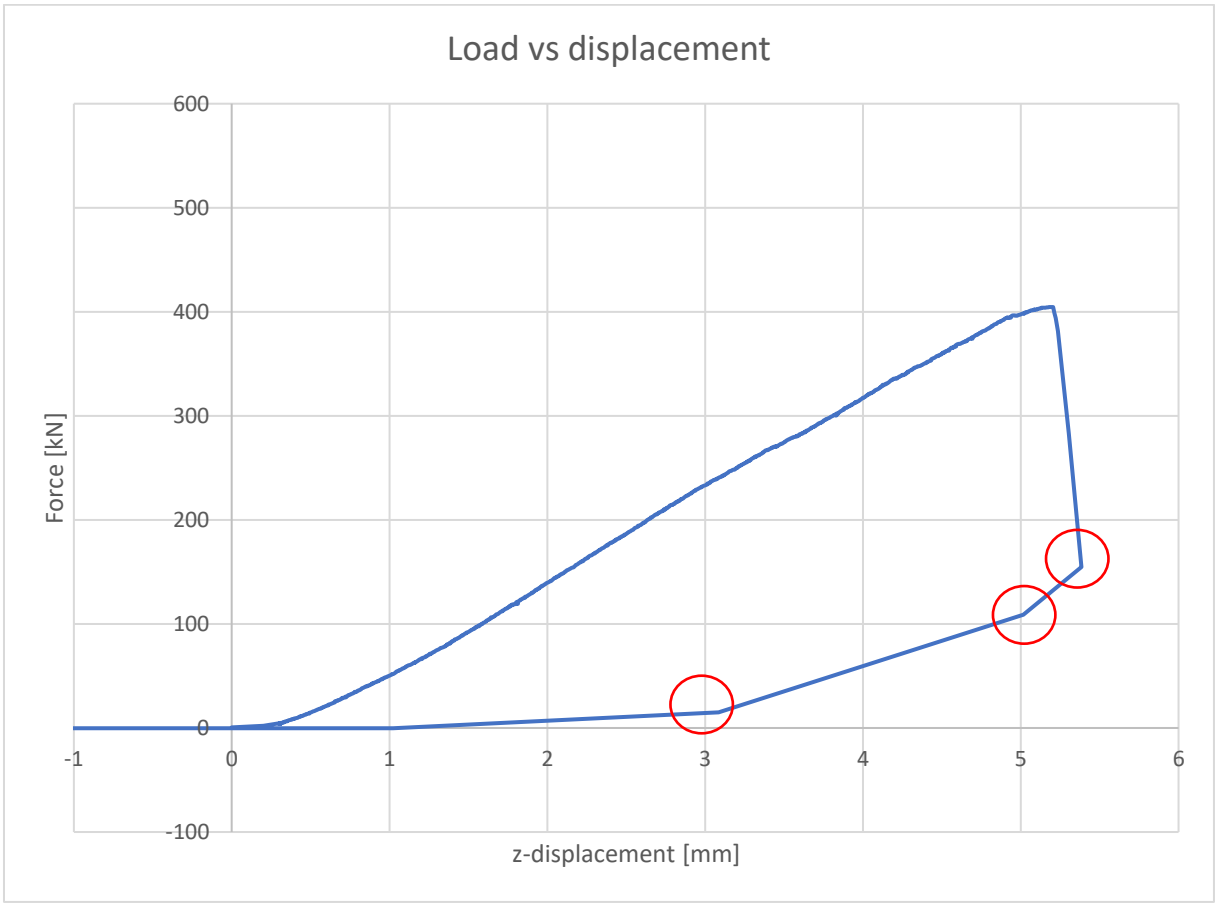

Graph 3 Load versus displacement curve - test 2 - sample 4.

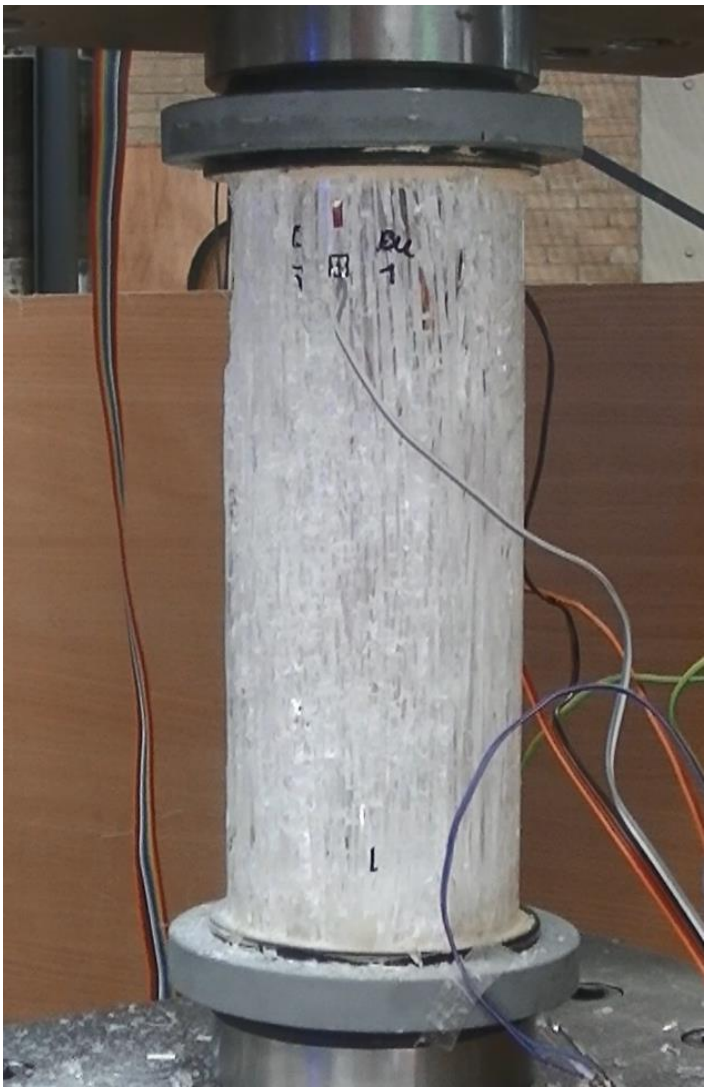

Figure 11 Exploded glass after the force was taken off the sample (390 kN).

Figure 12 The connection remained intact.

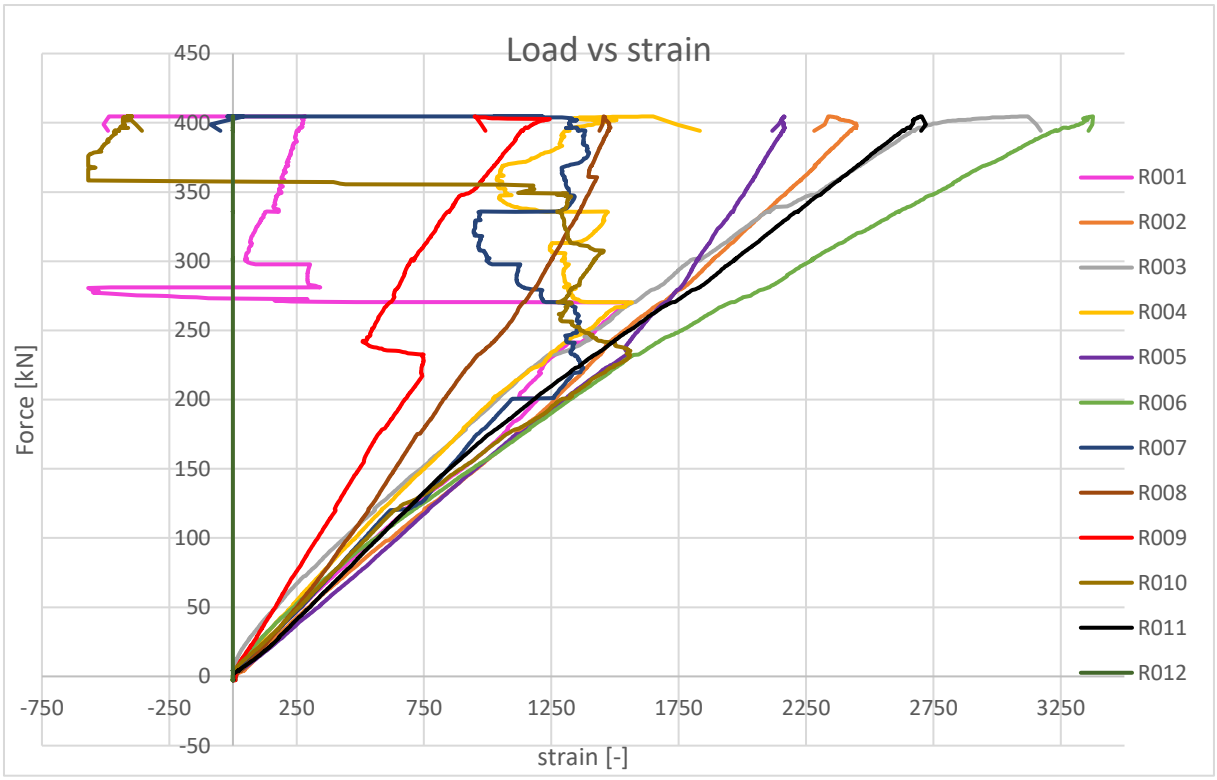

Graph 4 Load versus strain curve till force was taken off - test 2 - sample 4.

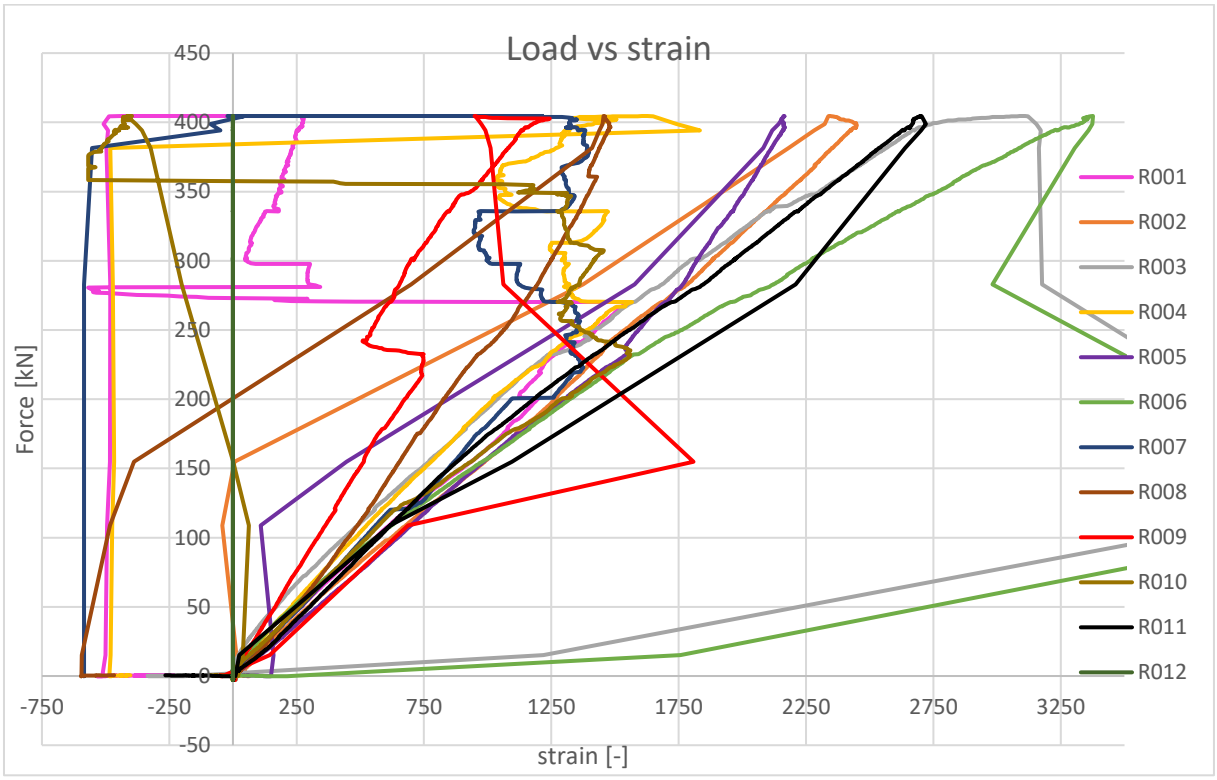

Graph 5 Load versus strain curve till force was till the end - test 2 - sample 4.

Figures 13 and 14 show more pictures of the cracked sample.

Figure 13 The cracked sample number 4.

Figure 14 Cracked sample number 4.

A.14.1.3. Test 3 - sample 1(a and b)

Sample 1 was made from DURAN (annealed) glass tubes. Figure 15 (right) shows the sample ready for testing. As can be seen in figure 15 (left), not many air bubbles were present.

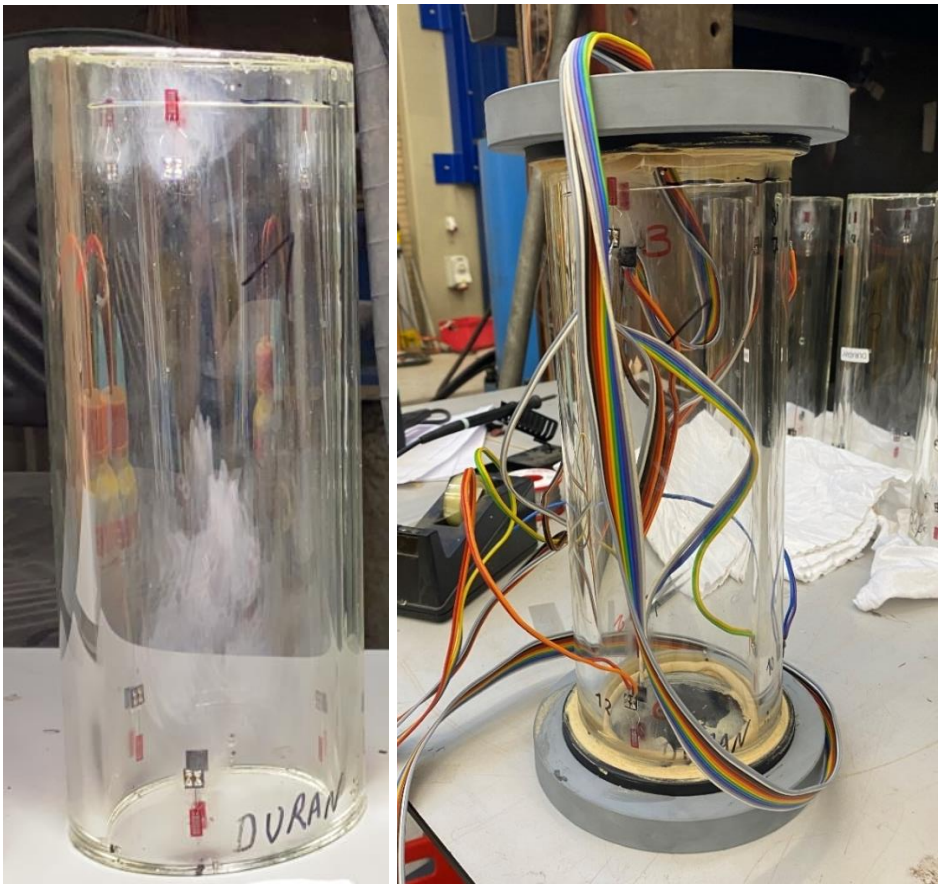

Figure 15 Sample 1 – test 3.

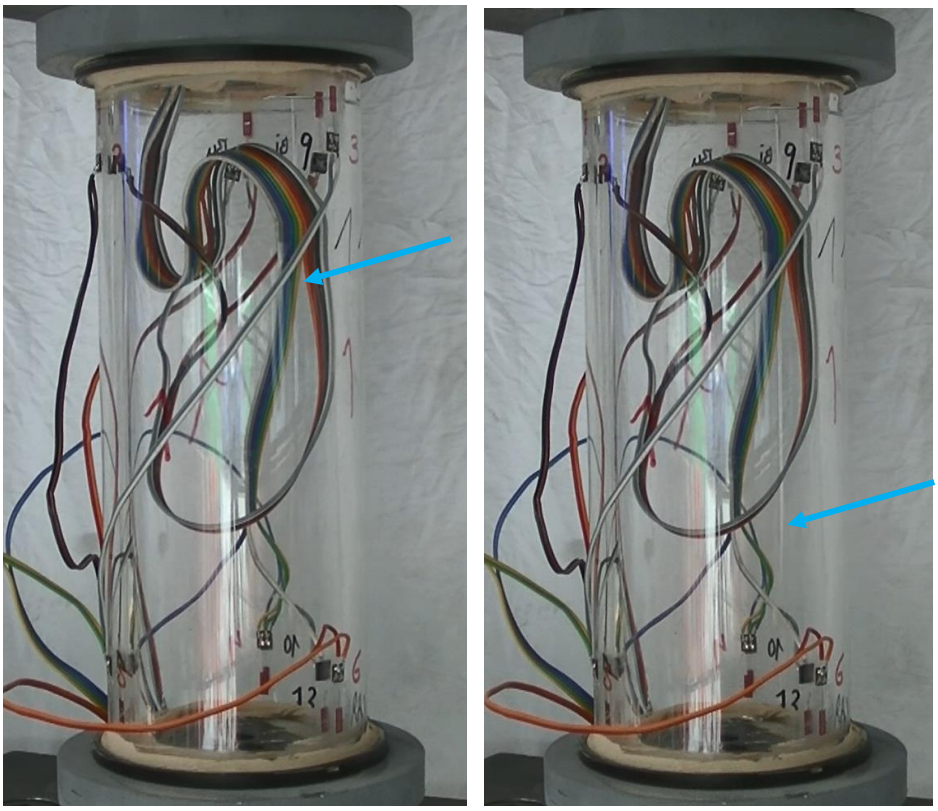

Figure 16 At 420 kN a slow growing crack appeared next to sensor 7 and at 580 kN the crack was moved towards the bottom.

At 160 kN the first crack appeared at the inner tube on the left next to strain sensor 1/7. The crack was parallel to the length of the tube. After that a few small cracks appeared somewhere at the top connection, but did not propagated over the full length. At 190 kN, strain sensor 8 (next to a crack) stopped working, and sensor 2, 9 and 12 were deviating.

At 420 kN, strain sensor 7 fell out, but came back on afterwards (graph 6). At that time, a crack was visible close to sensor 1/7 (figure 16, left, at the blue arrow). It slowly cracked further towards the bottom connection. At 580 kN the crack was moved towards the bottom connection (figure 16, right). Graph 6 shows that at 490 kN sensor 8 falls out.

At 590 kN, two cracks appeared close to sensors 6/12 (figure 17, left). The cracks slowly moved towards the middle of the tube (figure 17, middle). At 600 kN, another crack appeared close to sensors 3/9 (figure 17, middle). At 660 kN, the earlier formed cracks are continuing slightly and one small crack appeared at the bottom (figure 17, right).

Figure 18 shows that another crack appeared close to sensor 8, which continued cracking slowly towards the top. A few seconds later, at 680 kN, the crack moved towards the top (figure 18, right). Afterwards, at around 690 kN, one small piece of glass shattered off.

At 700 kN the machine had stopped, because it could no longer handle the forces (figure 19, left). After that, cracks appeared perpendicular to the length of the sample (red circle in figure 19, right). These perpendicular cracks probably appeared at where the load versus displacement curve showed a kink (graph 8, red circle).

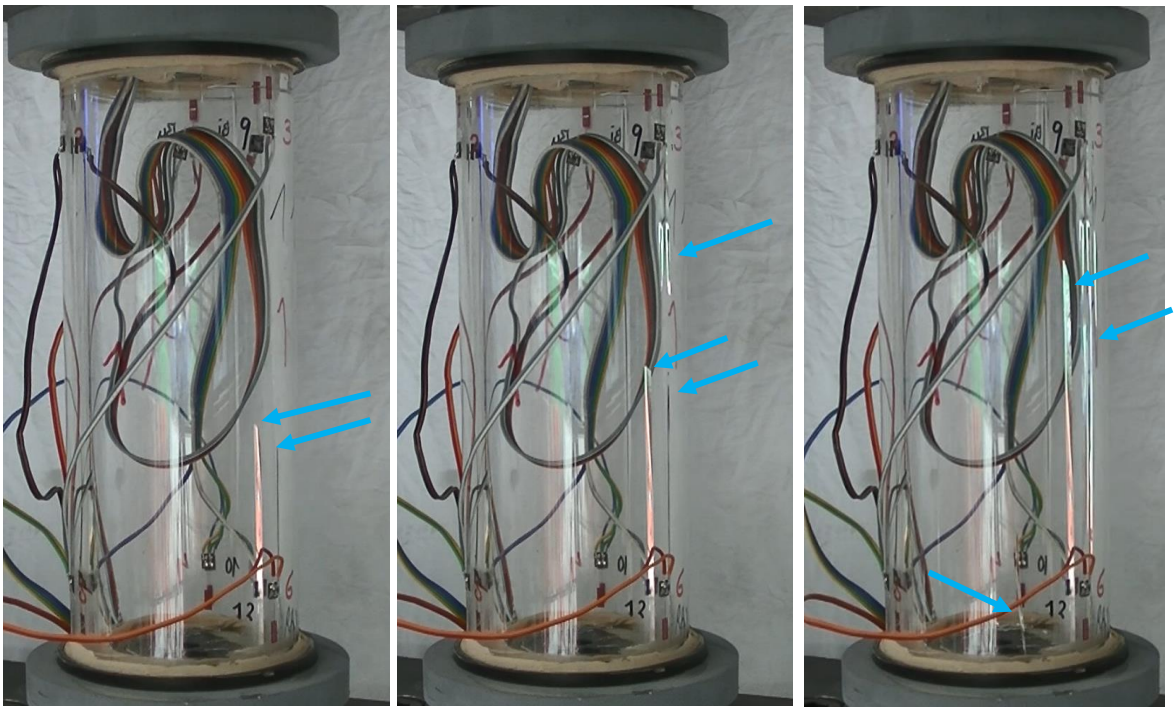

Figure 17 At 590 two cracks appeared close by sensors 6/12 (left). At 600 kN, it continued cracking to the middle of the tube, and another crack appeared close to sensors 3/9 (middle). At 660 kN, the earlier formed cracks are continuing and one small crack appeared at the bottom (right).

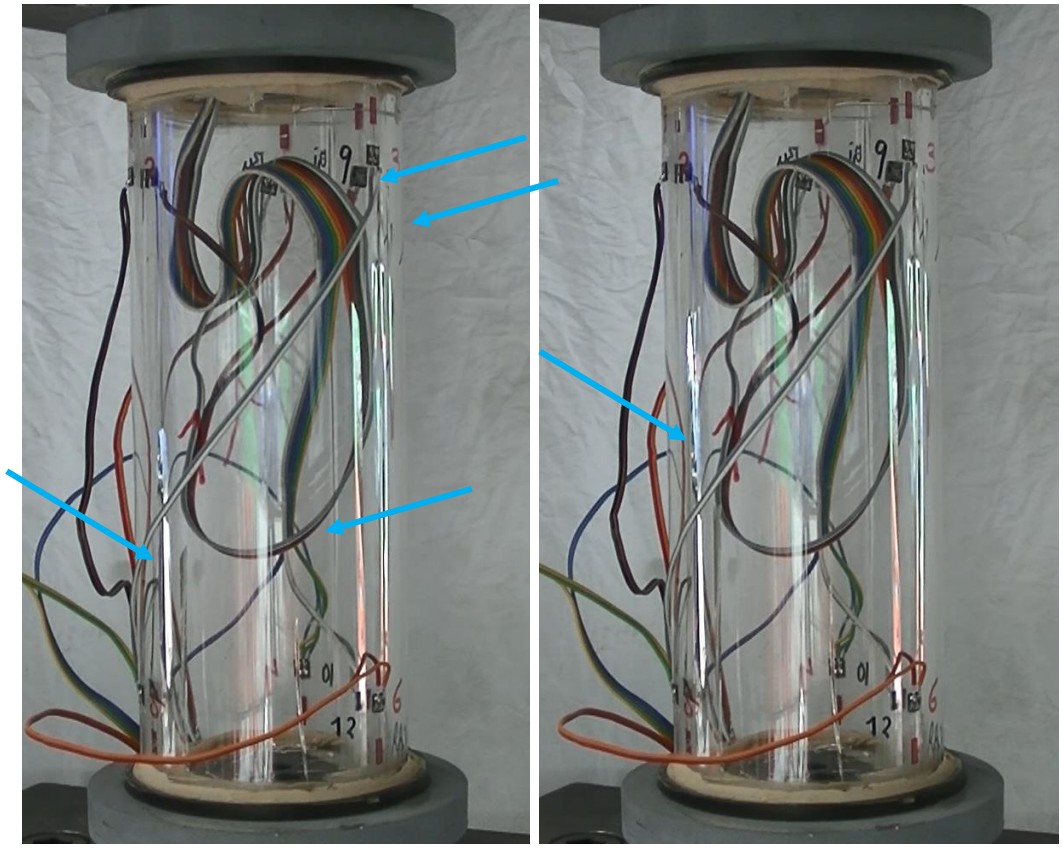

Figure 18 Another crack appeared close to sensor 8 (left). A few seconds later, at 680 kN, the same crack moved further towards the top (right).

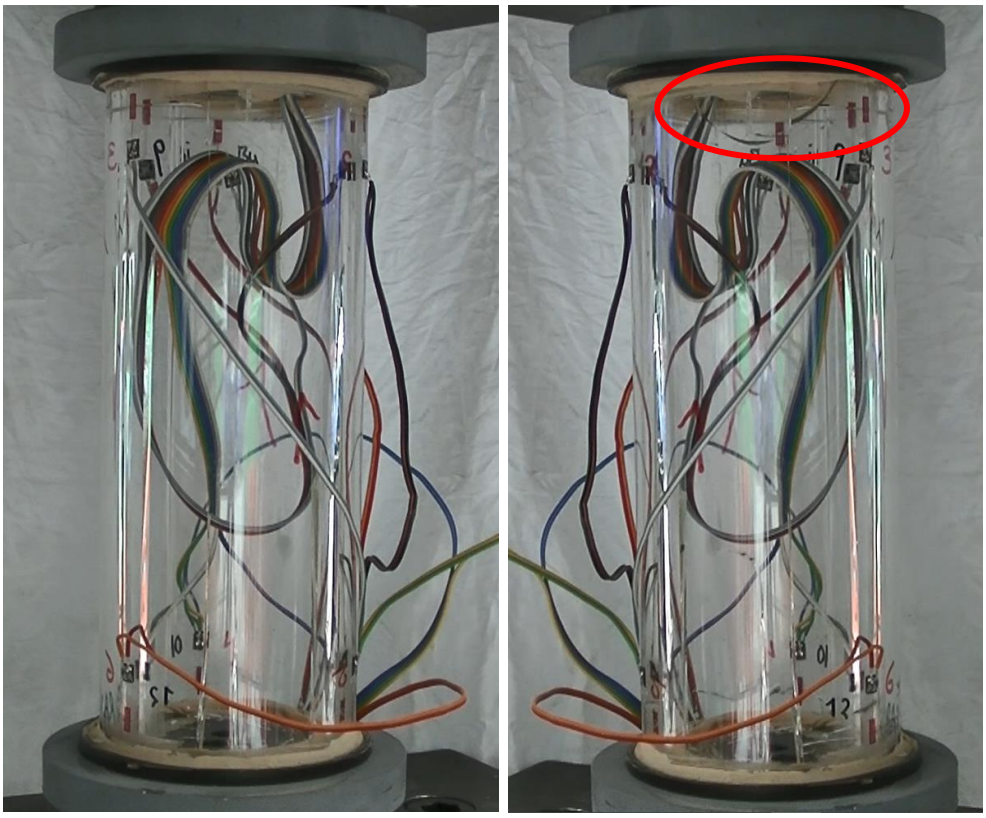

Figure 19 Sample 1 at 700 kN, before the force was taken off (left). Sample 1, after the force was taken off (right).

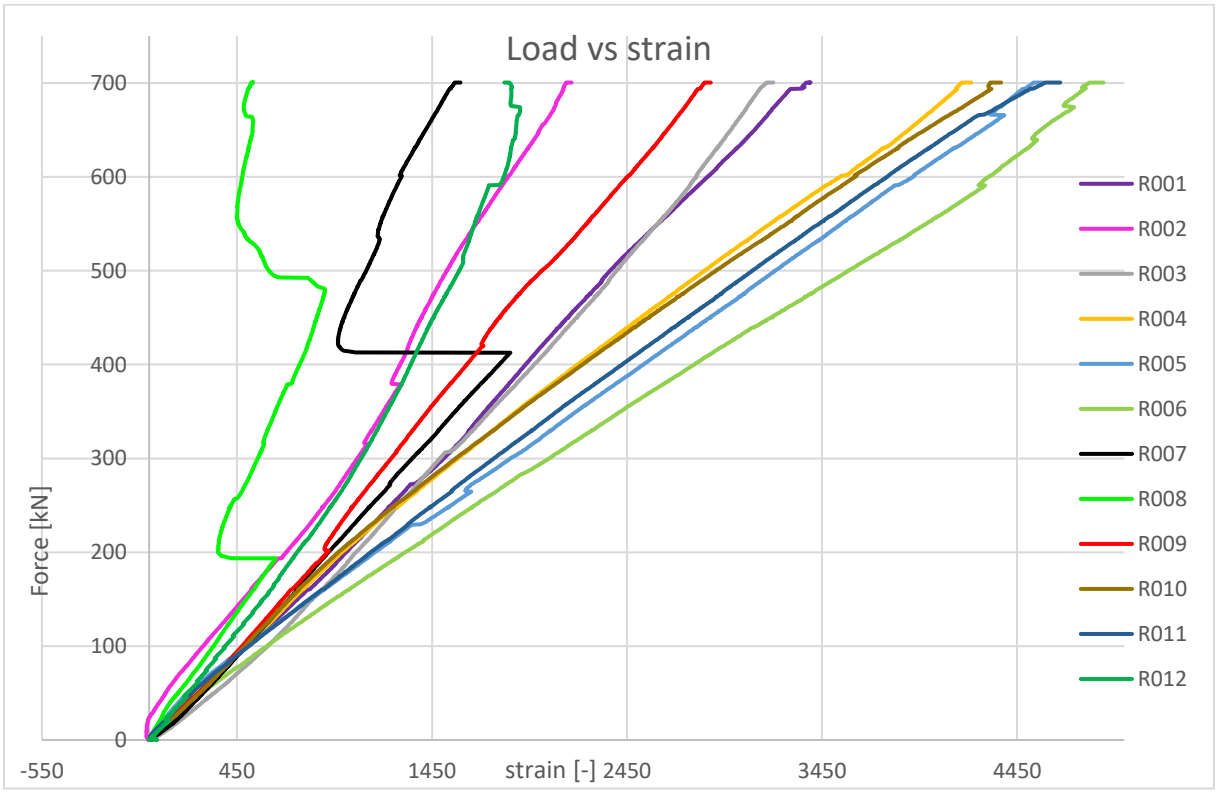

Graph 6 Load versus strain curve till force was taken off - test 3 - sample 1.

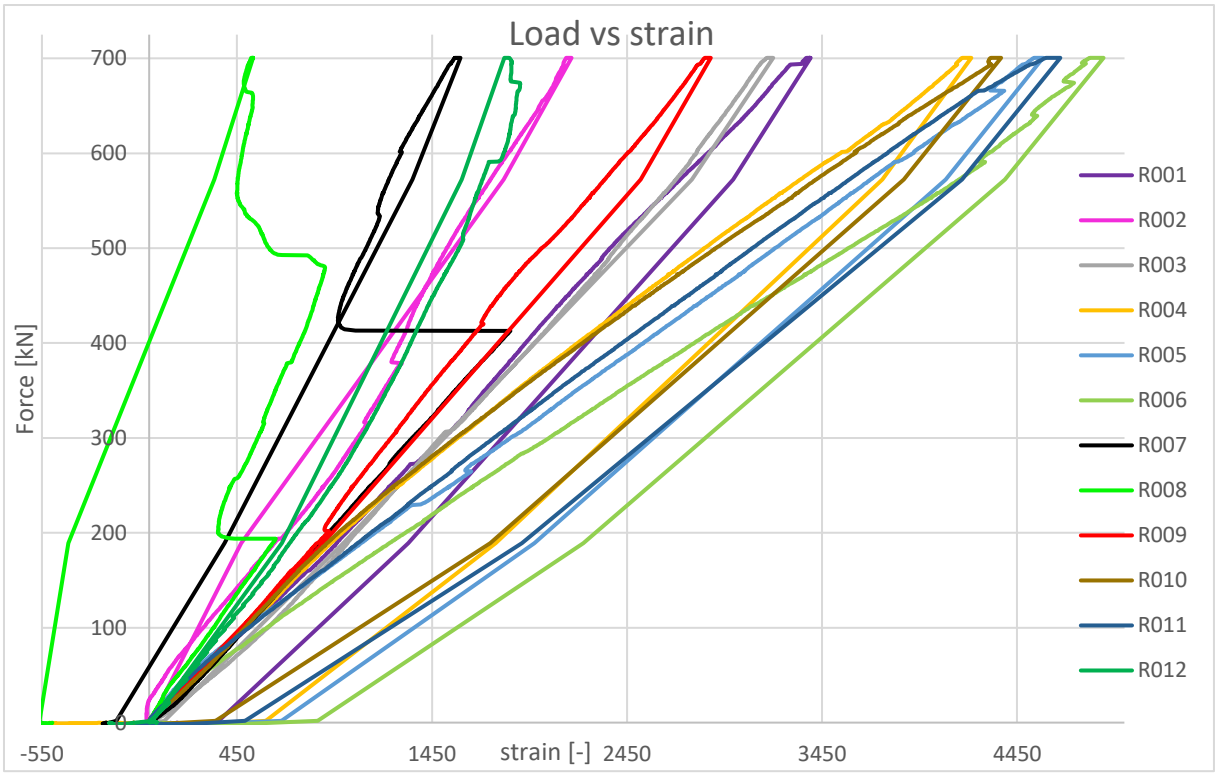

Graph 7 Load versus strain curve till the end - test 3 - sample 1.

Graph 8 Load versus displacement - test 3 - sample 1.

Since the tube could withstand more load, the machine was started for the second time. As can be seen in graph 9, a few sensors were already deviating at the beginning.

At 120 kN more cracks appeared, and at 140 kN the glass shattered. At 200 kN the glass shattered at the bottom. The glass continued cracking/shattering at 240 kN. At 290 kN the glass shattered at the bottom again (figure 20). At 325 kN the glass started to shatter in total, whereby the computer was stopped (graph 11). So, during the second test, fewer parallel cracks appeared. The glass shattered more than during the first test. The connections and Hilti remained intact.

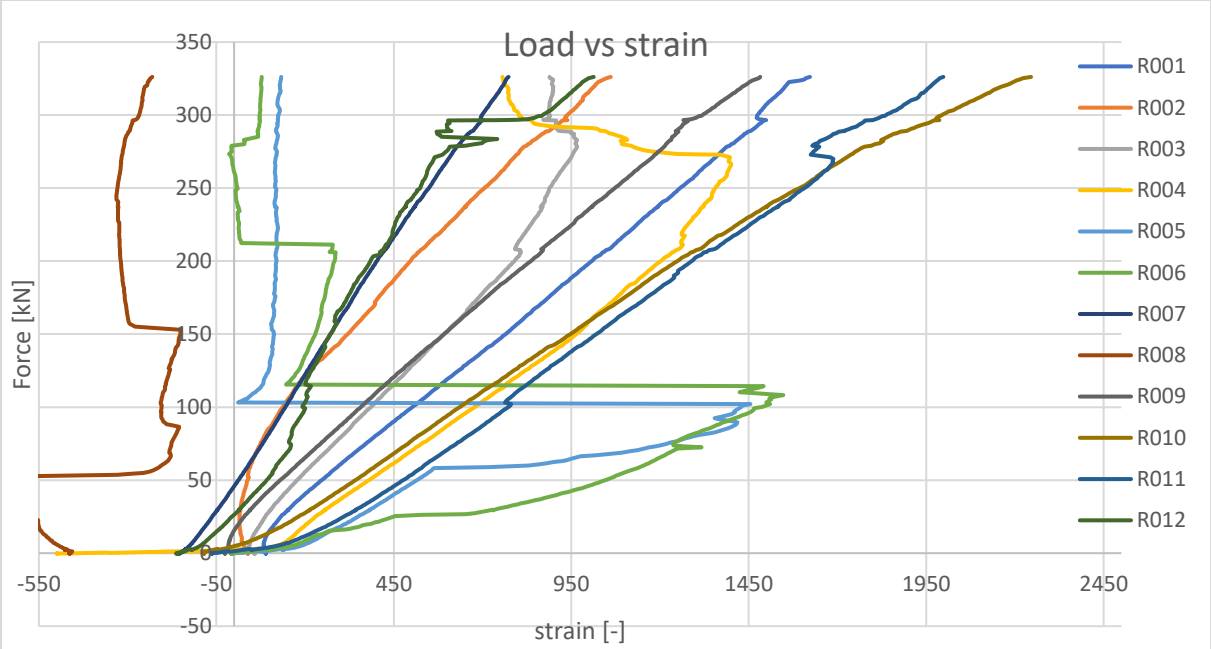

Graph 9 Load versus strain curve till force was taken off - test 3 - sample 1 (second time loading).

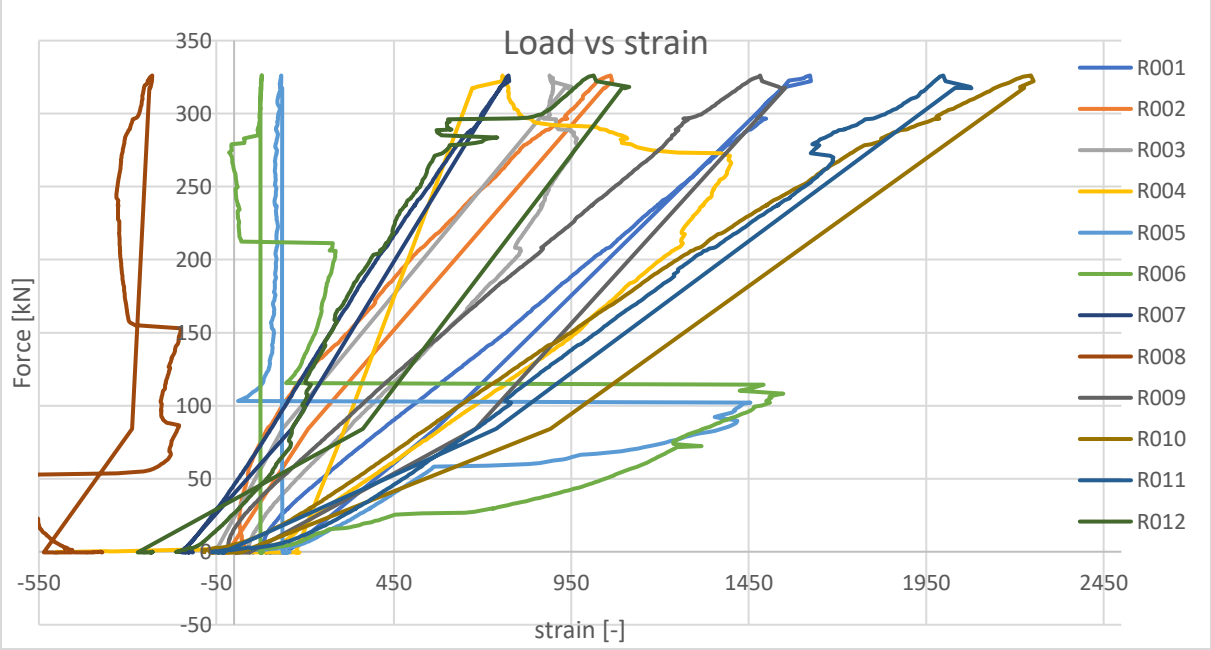

Graph 10 Load versus strain curve till the end - test 3 - sample 1 (second time loading).

Graph 11 Load versus displacement curve - test 3 - sample 1 (second time loading).

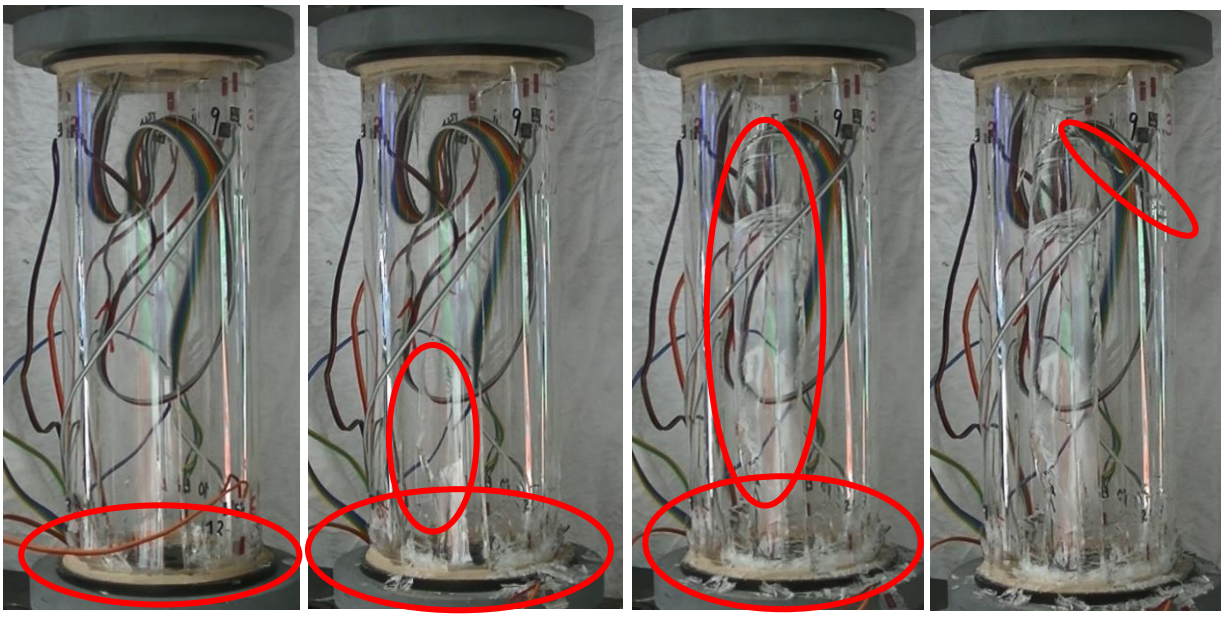

Figure 20 Small cracks appeared at the bottom (left). The glass shattered at the bottom and slightly in the middle of the sample (second). The glass shattered more and more in the middle of the sample (third). After the force was taken off, more diagonal cracks appeared (right).

Figure 21 shows more pictures of the cracked sample.

Figure 21 The cracked sample number 1.

A.14.1.4. Test 4 - sample 3

Sample 3 was made from DURAN glass tubes. Figure 22 (left) shows the sample positioned in the testing machine. As can be seen in figure 22 (right), a few air bubbles were present in the interlayer material.

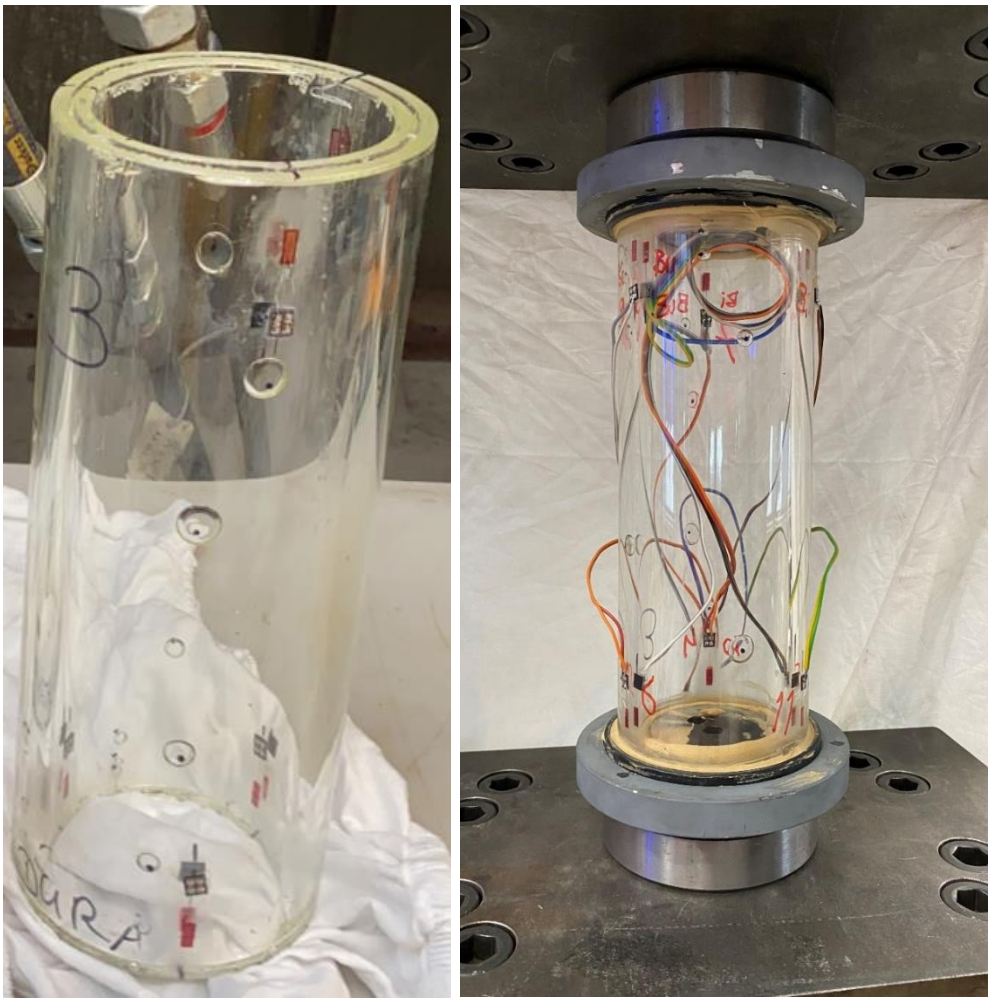

Figure 22 Sample 3 – test 4.

Sensors 4 and 10 deviated in the beginning, but came back on. At 95 kN the first parallel straight crack appeared close to sensors 6/12 (figure 23, left). Sensor 12 stopped, but came back on (graph 12). At around 110 kN, a new crack appeared close to the first crack, between sensors 6/12 and 4/10. At 125 kN sensor 9 was deviating and at 150 kN, sensor 10 was deviating (graph 12). At 175 kN another small crack appeared next to the first crack. Sensor 11 was deviating slightly around 210 kN, and directly after that, two more cracks appeared between sensors 6/12 and 5/11 (figure 23). The cracks slowly grew towards the top connection.

At 240 kN a few small cracks appeared at the top connection. At 250 kN the first crack cracked slightly further towards the top connection. At 350 kN, sensor 7 decreased. The cracks at the top slowly moved further towards the bottom connection. At 475 kN, sensor 8 stopped and sensors 2, 4, and 6 were deviating. At 495, 555, 580, 590, 635, 660 kN, the glass crackled, but no real cracks were visible. At 670, 695, 700 kN, the glass shattered at the location where the first three cracks appeared. At 730 kN, the glass crackled again. At 740 kN the glass shattered and cracked (figure 24, left). At 745 kN the force was taken off

and a few perpendicular cracks appeared (figure 24, right). The curve in graph 14 became less steep as well. The connections and Hilti remained intact.

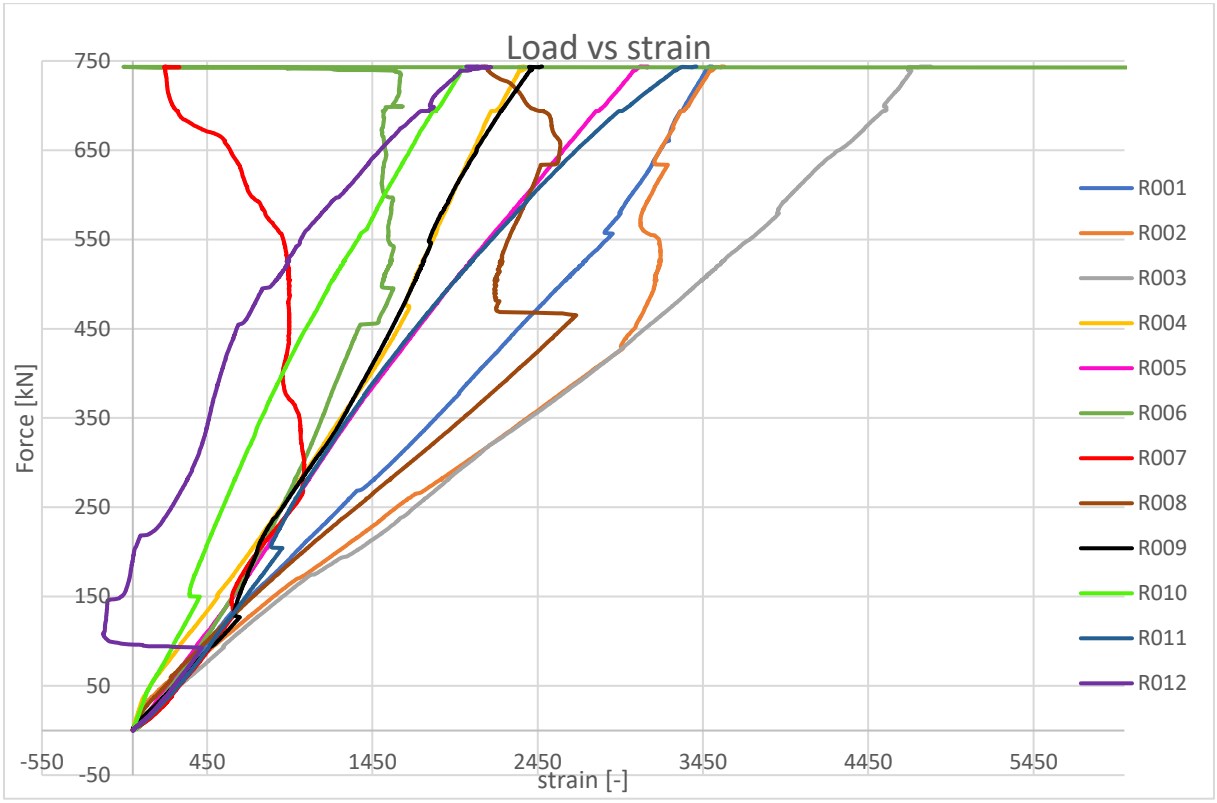

Graph 12 Load versus strain curve till force was taken off - test 4 - sample 3.

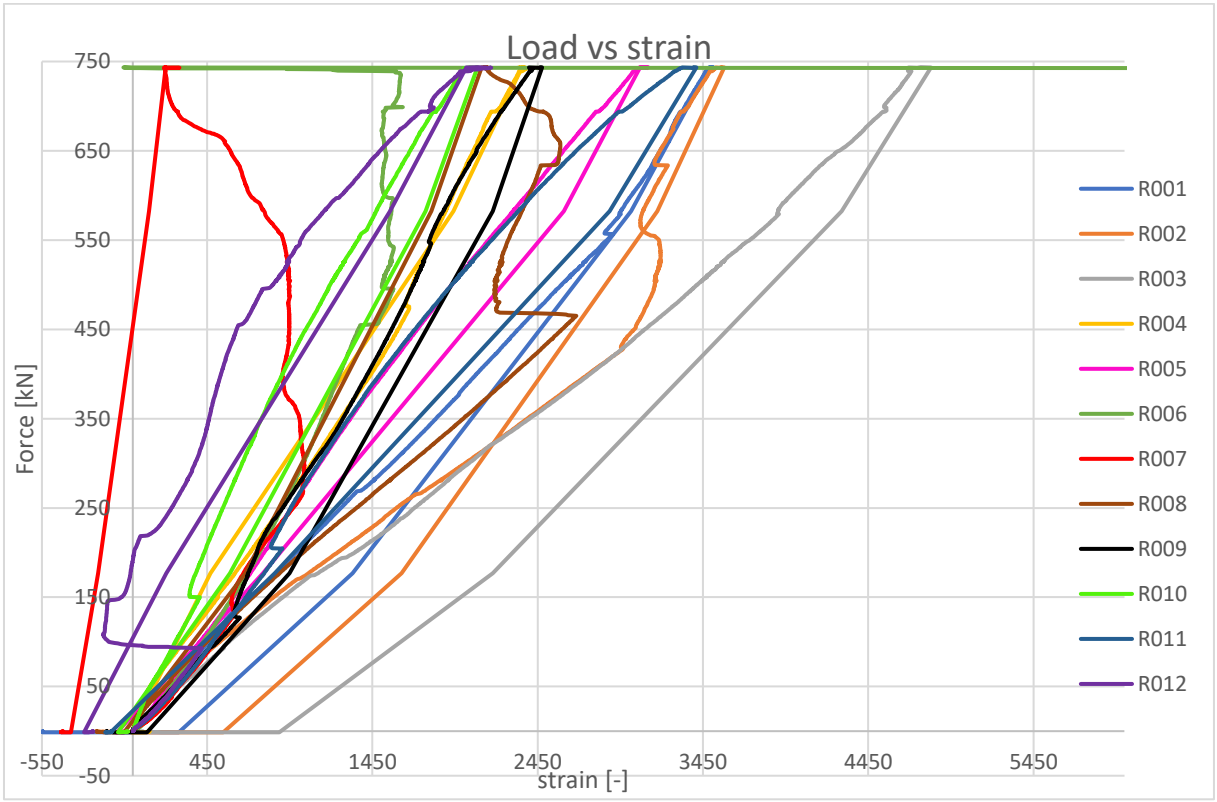

Graph 13 Load versus strain curve till the end - test 4 - sample 3.

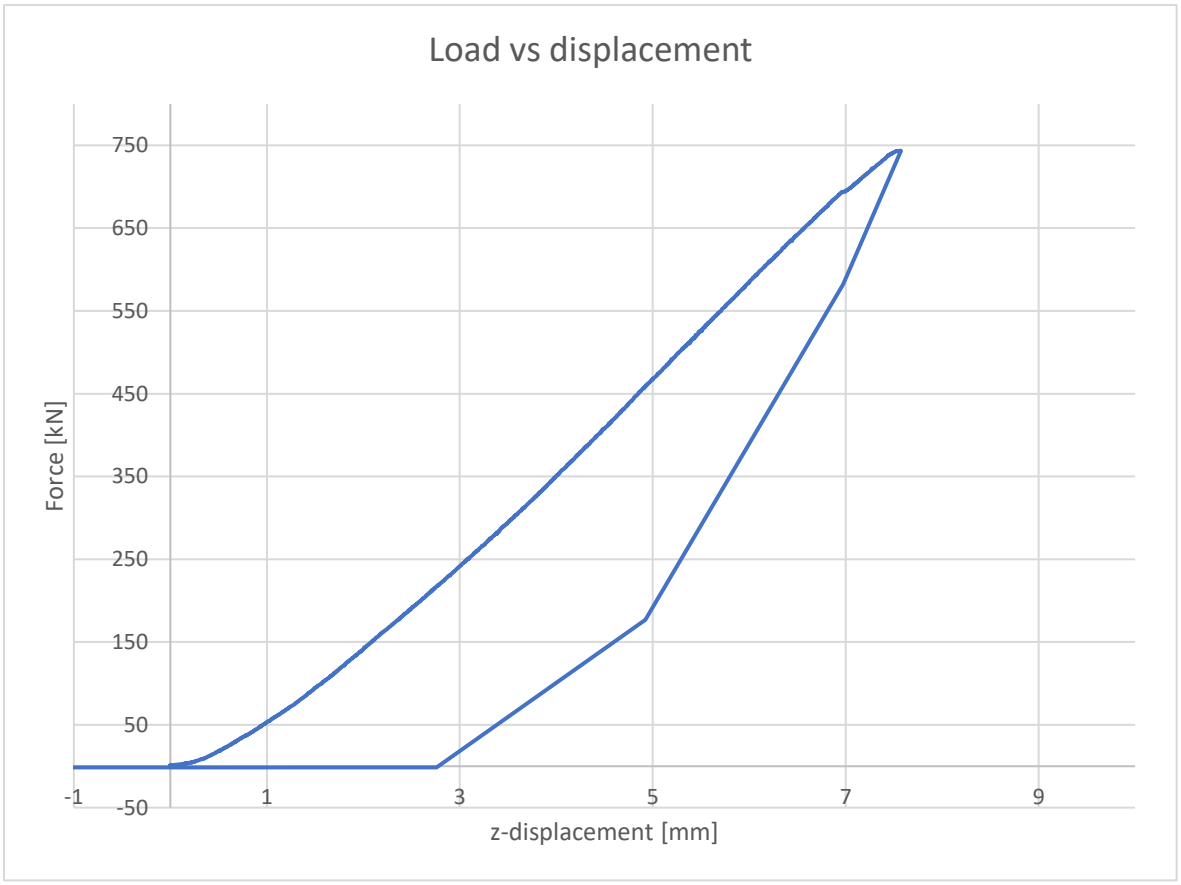

Graph 14 Load versus displacement curve - test 4 - sample 3.

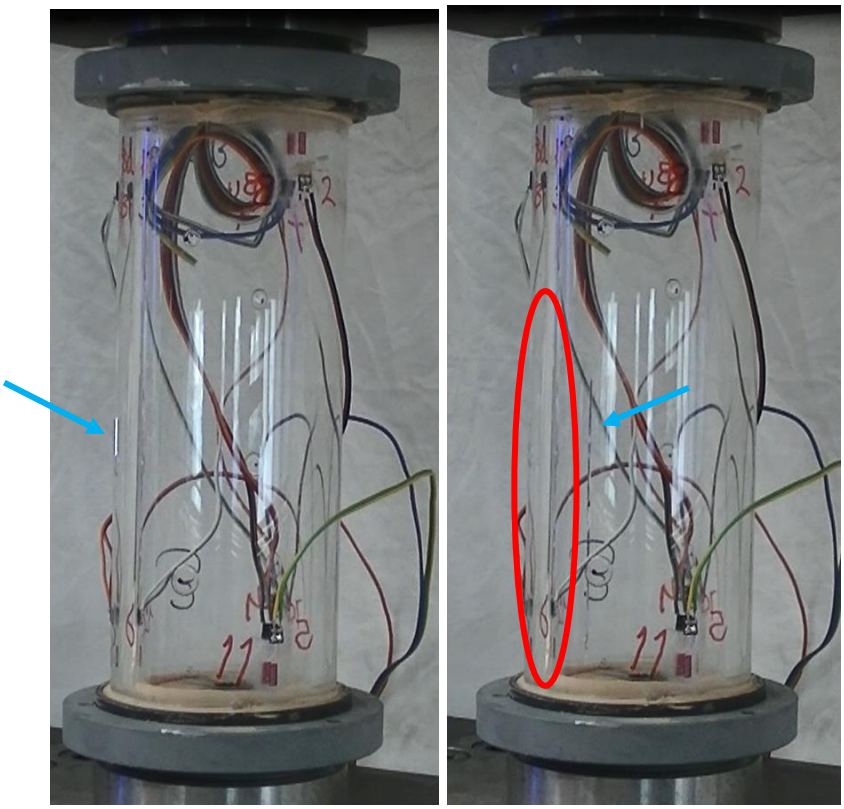

Figure 23 The first crack appeared at 95 kN close to sensors 6/12: blue arrow (left). After 210 kN the fourth crack appeared: blue arrow (right). The first three cracks are all close to each other: red circle (right).

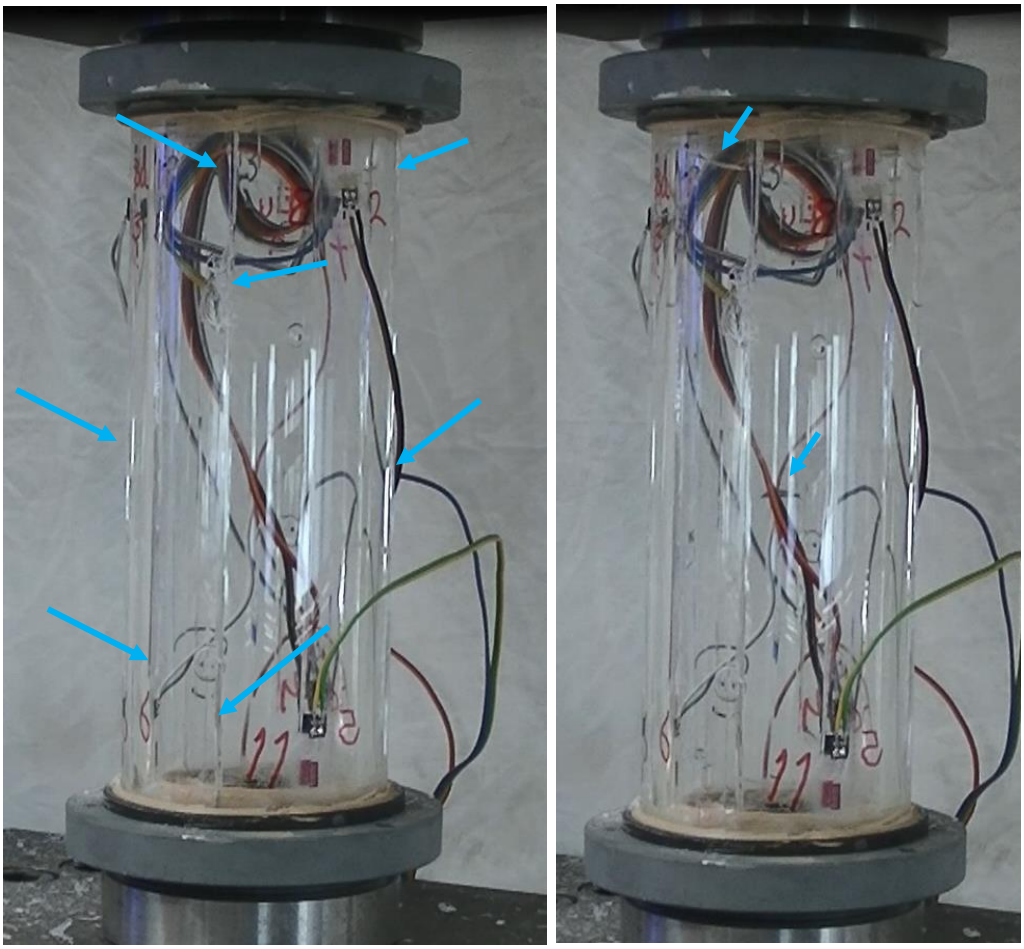

Figure 24 At 740 kN the glass shattered and crackled (left). At 745 kN the force was taken off and a few perpendicular cracks appeared: blue arrows (right).

Figures 25 and 26 show more pictures of the cracked sample.

Figure 25 The first few cracks are visible of the cracked sample (left). A few stopped cracks are visible: black arrows (right).

Figure 26 The cracked sample 3.

A.14.1.5. Test 5 - sample 6

Sample 5 was made from DURATAN glass tubes. Figure 27 (right) shows the sample ready for testing. As can be seen in figure 27 (left)not many air bubbles are present in the interlayer material.

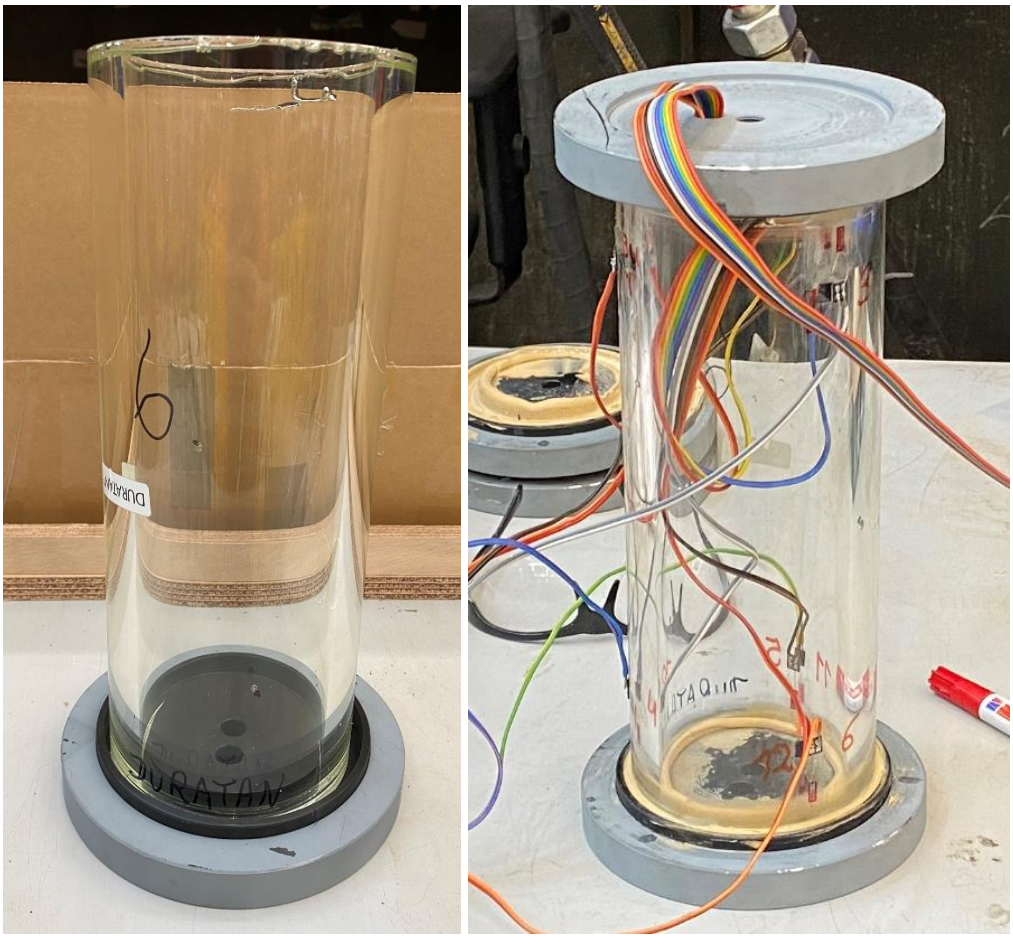

Figure 27 Sample 6 – test 5.

Until 200 kN, all sensors performed equally well (graph 15). At 120 kN the first crack appeared between sensor 3/9 and 2/8 (figure 28, left). At 190 kN, a crack appeared close to the first one, which slowly continued cracking and stopped in the middle. At around 200 kN another crack appeared close to sensors 1/7 at the top, which cracked directly towards the bottom (sensors 4/10) (figure 28, right).

Close to sensors 2/8 and 5/11, a straight parallel crack appeared at 220 kN, which cracked with a lot of speed. At that location, more cracks appeared directly afterwards until 280 kN (figure 29, left and middle). At 220 kN, sensors 2 and 8 deviated. Strain 8 stopped deviating after 225 kN (graph 15). At 280 kN close to sensors 2/9 a new crack appeared (figure 29, middle). Sensors 2, 8 and 11 stopped at 340 kN. At 350 kN a new crack appeared around sensor 3/9 (figure 29, right).

At 355, 395 and 440 kN, the glass shattered and cracked at where the first cracks appeared. At 365, 380, 390 and 420 kN the glass crackled. At 450 kN the glass shattered and continued doing so. At 460 a new crack appeared from the top to bottom over the length close to sensors 3/9 and 6/12, and directly afterwards two more cracks appeared at the right side of these sensors (figure 30, left). At 485 and at 490 kN the glass shattered and the force was taken off (figure 30, middle and right). At 490 kN sensors 2 and 5 stopped (graph 15).

After that, the inner tube exploded into small pieces. Graph 17 shows that the curve became less steep at 500 kN. The connection and the Hilti remained intact (figure 32).

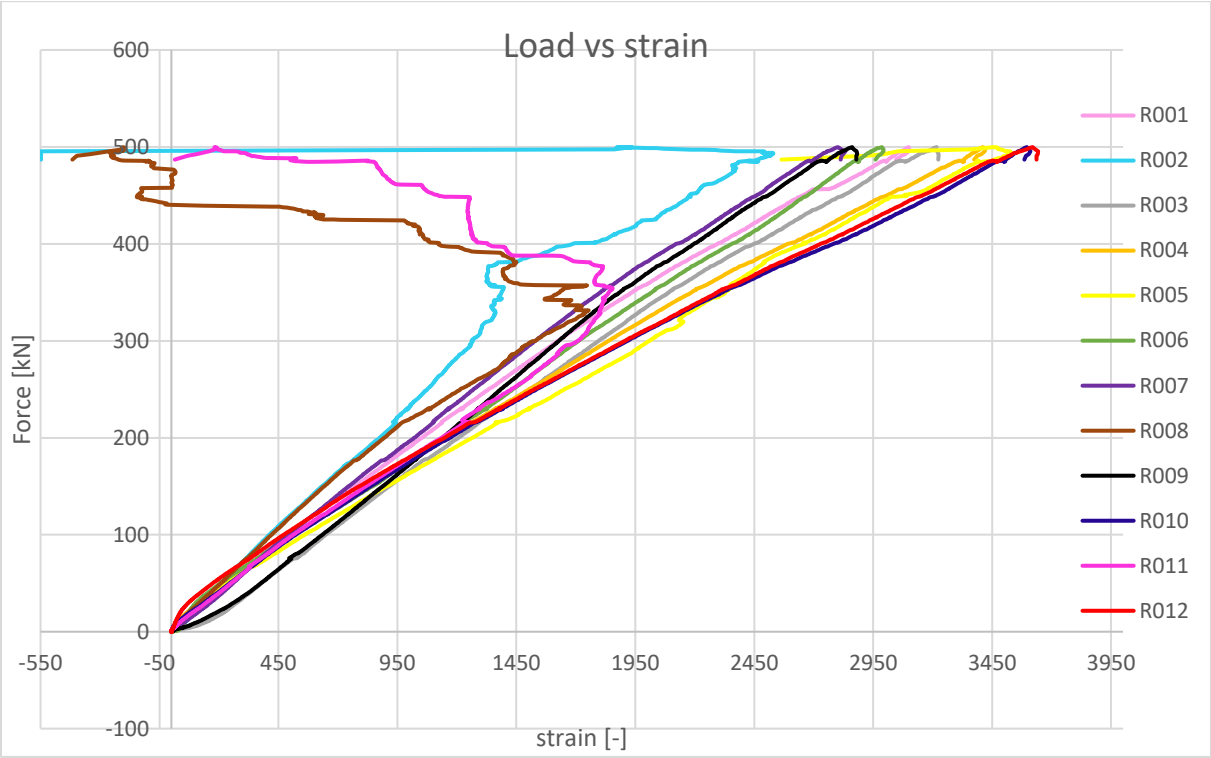

Graph 15 Load versus strain curve till force was taken off - test 5 - sample 6.

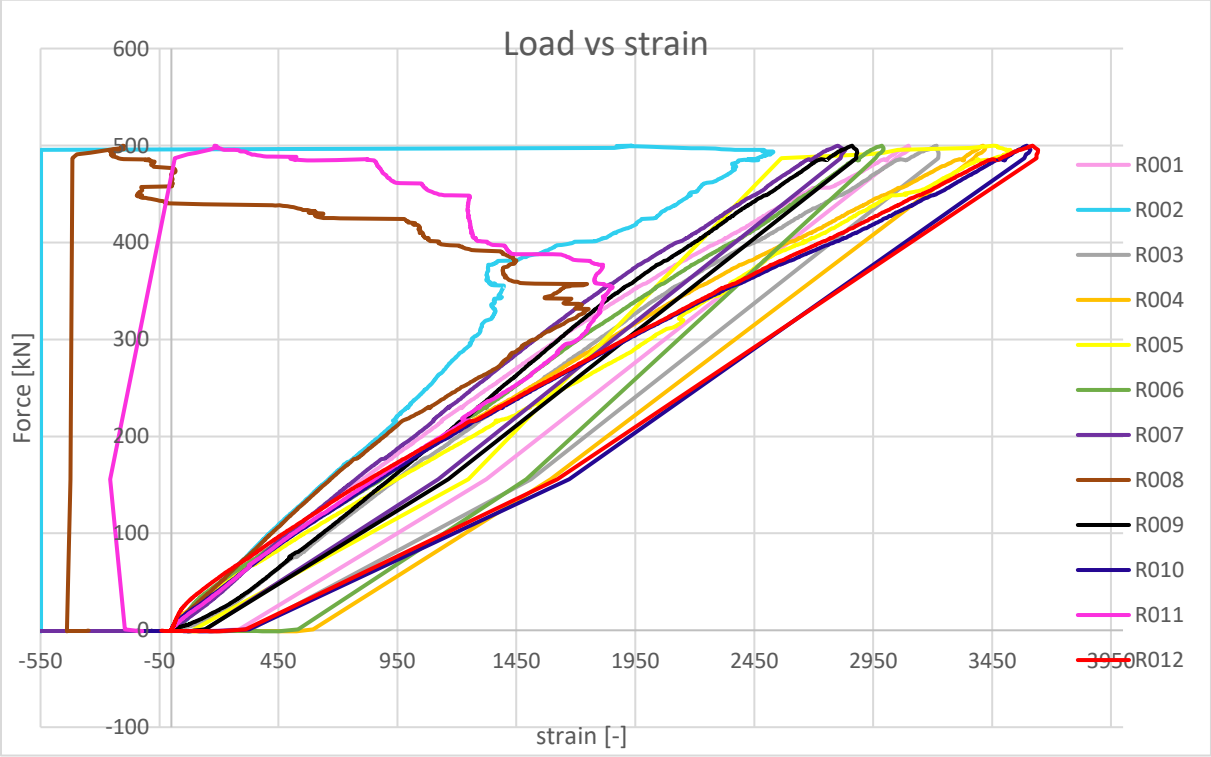

Graph 16 Load versus strain curve till the end- test 5 - sample 6.

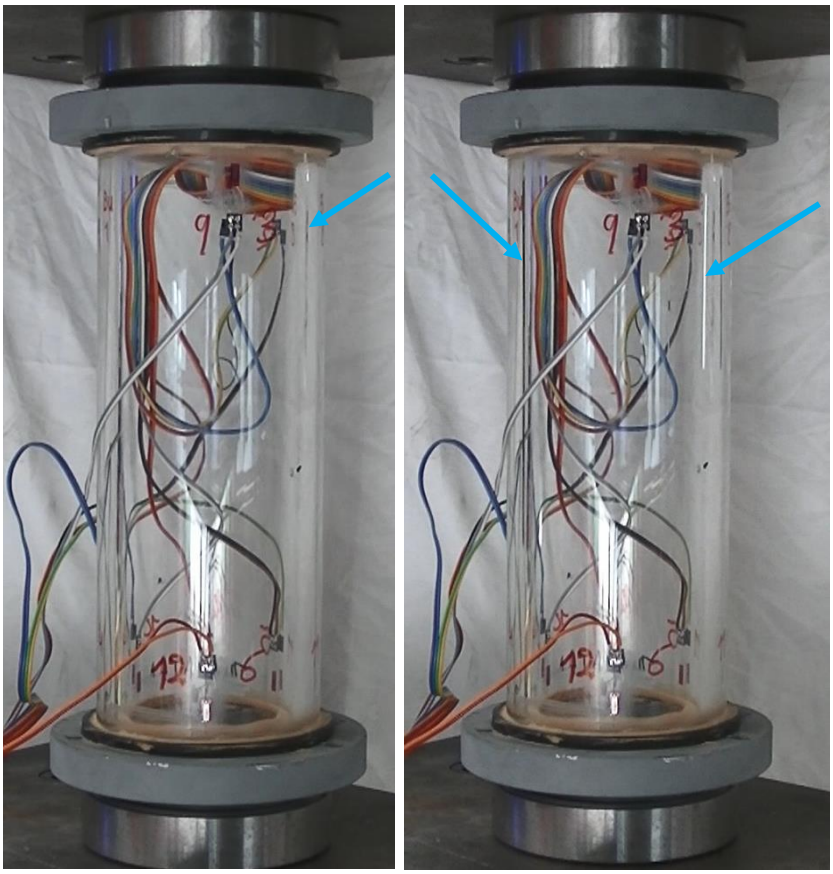

Figure 28 The first crack appeared at 120 kN (left). At 190 kN a new crack appeared close to the first crack and directly after that a third crack appeared (left arrow, right figure), which cracked in a few seconds directly to the bottom (right).

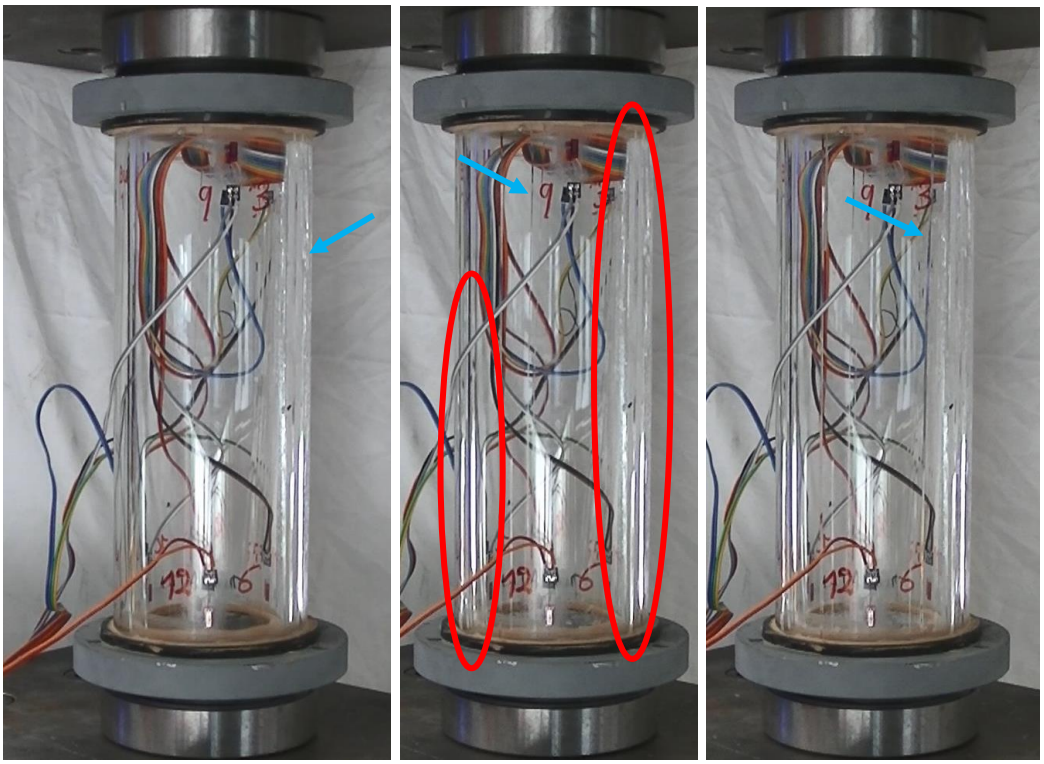

Figure 29 At 220 kN, with a lot of speed, more cracks appeared (left). At 280 kN the cracks continued cracking (red circles) and a new crack appeared: blue arrow (middle). At 350 kN a new crack appeared (right).

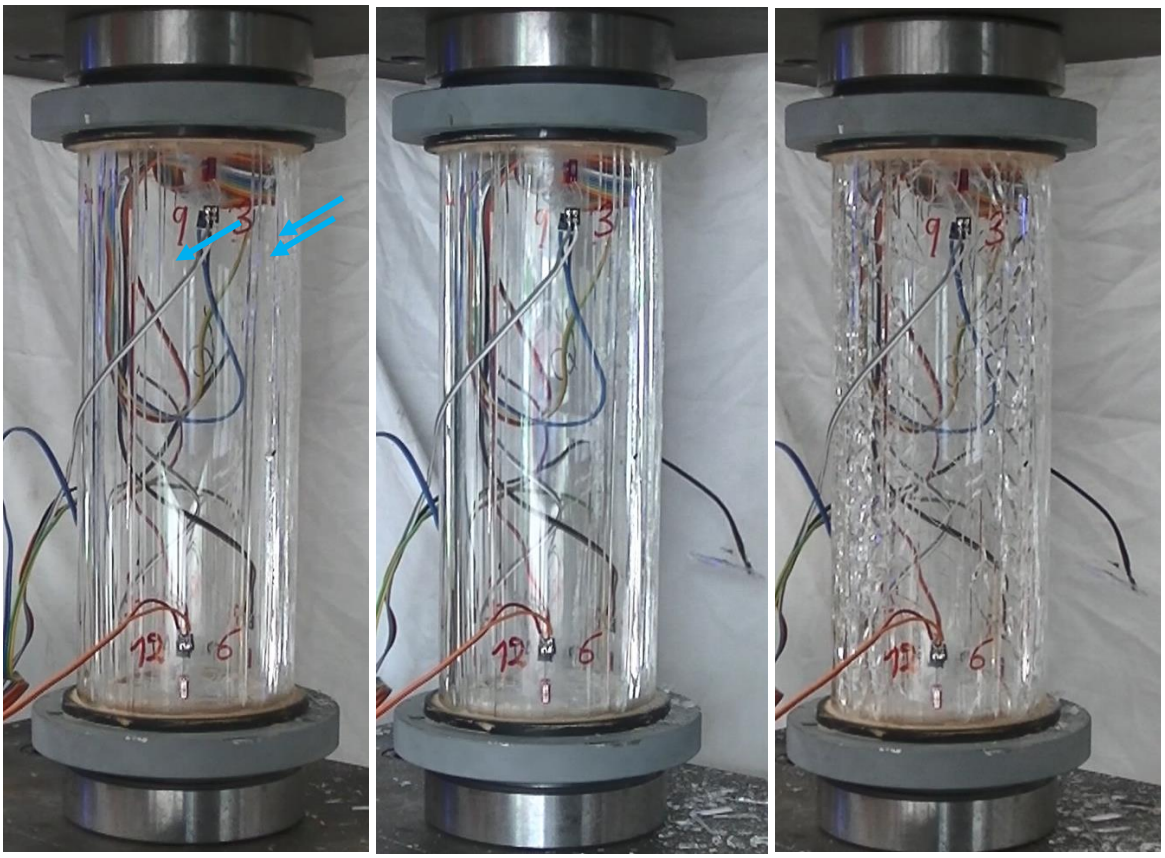

Figure 30 At 460 kN a few more cracks appeared left and right from sensors 3/9 and 6/12 (left). At 490 kN the force was taken off (middle). Right after the force was taken off, the inner tube exploded (right).

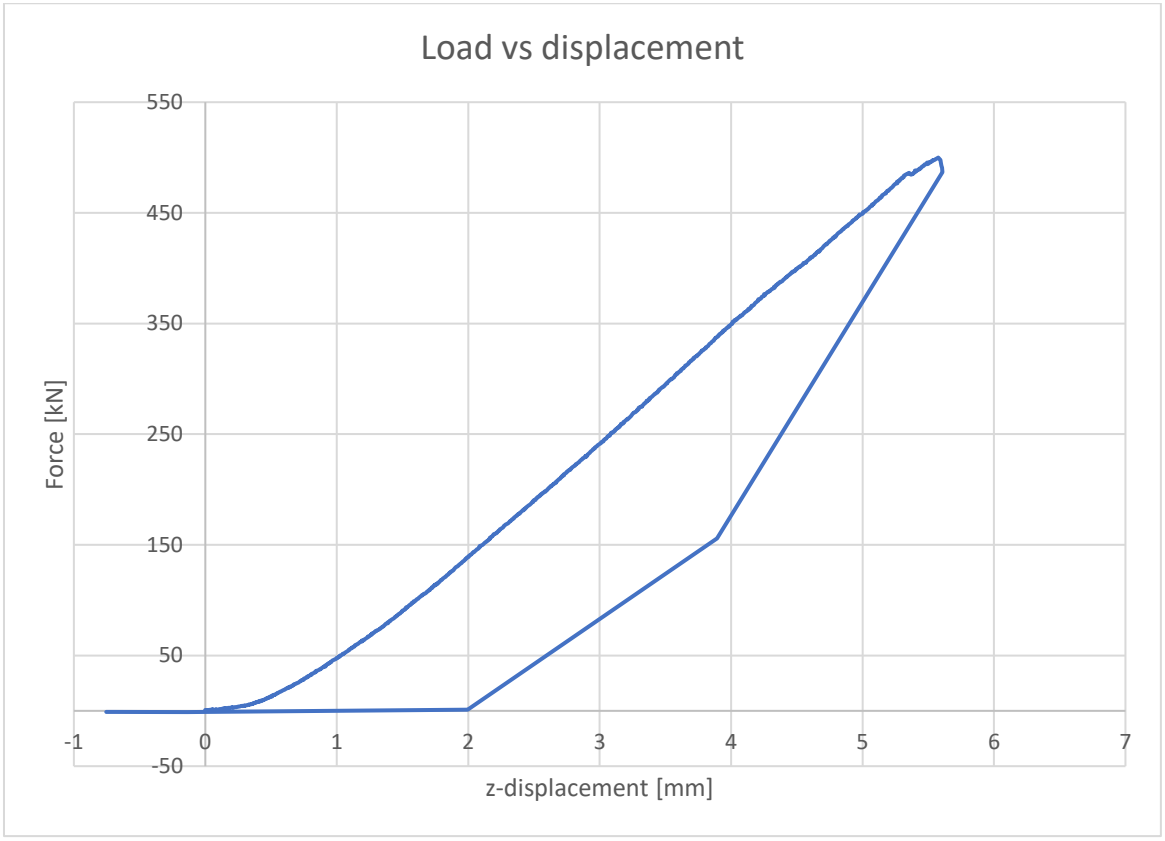

Graph 17 Load versus displacement curve - test 5 - sample 6.

Figures 31 and 32 show more pictures of the cracked result of sample 6.

Figure 31 The cracked sample 6.

Figure 32 The glass sample taken out of the connection after testing.

A.14.1.6. Test 6 – sample 2

Sample 2 was made of DURAN glass tubes. Figure 36 (right) shows sample 2 ready for testing. Unfortunately, one straight crack parallel to the length of the tubes had appeared out of a sudden in the inner tube. It happened over night between 24th of June and 25th of June (figure 33, 34 and 35). Furthermore, as can be seen in figure 35, sample 2 had a few small air bubbles.

Figure 33 Sample 2 – test 6.

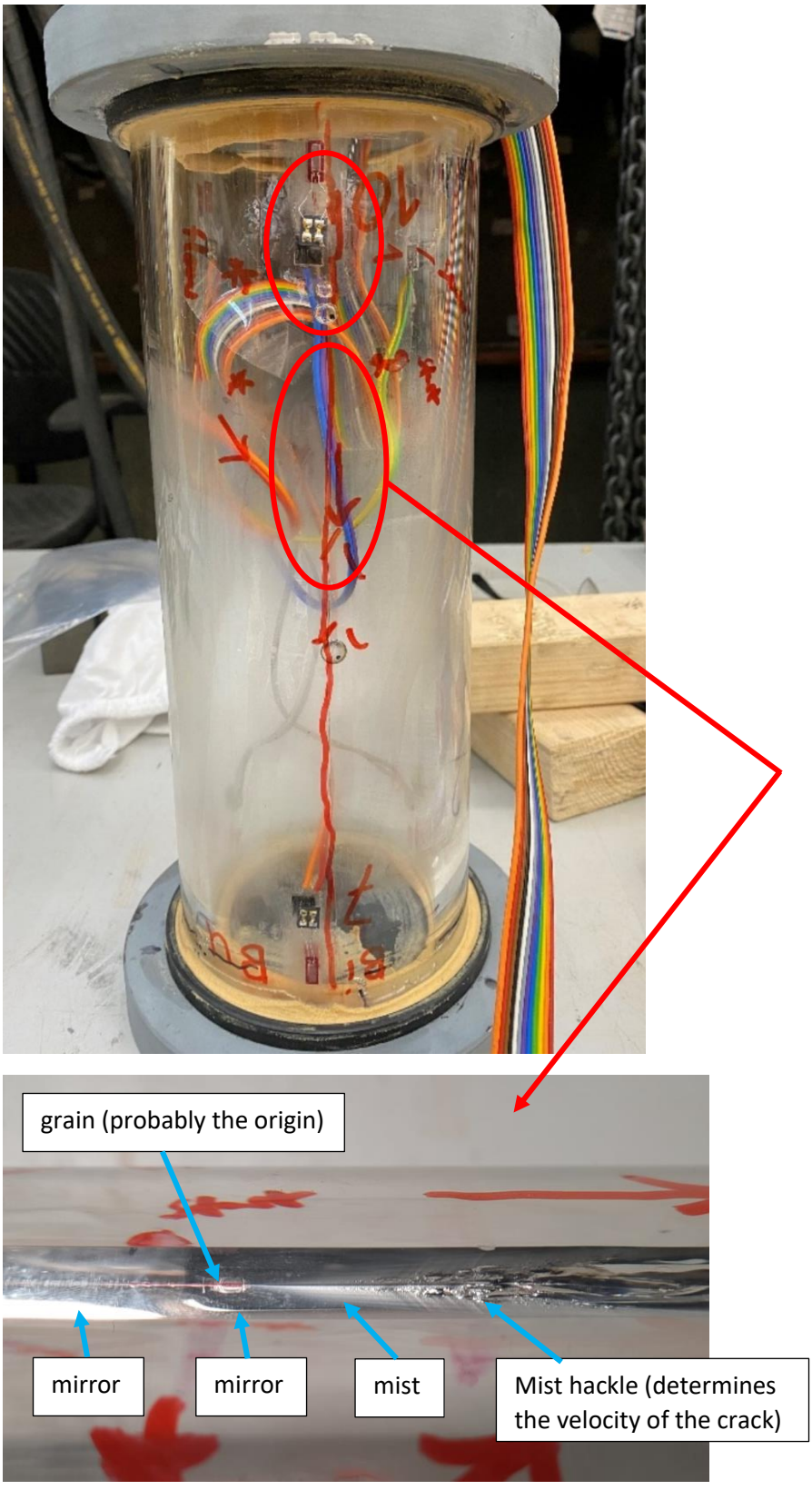

Figure 34 the crack which was already in the sample before testing.

The position of the grain is probably where the crack started (figure 34). Around that grain a mirror is visible which continues to the left. Furthermore, the mist and the mist/velocity hackle are giving direction and velocity to the propagation of the crack (Quinn, G., D. 2020). The crack appeared 2 months after the tubes were made and 4-5 days after the sample was

bonded together by the interlayer material. Figure 34 shows that the crack cracked to the bottom. This can be seen due to the direction of the branches. A high velocity is needed to get branches in the crack. Furthermore, in figure 34 (at the top red circle) it is visible that the crack went around the strain connector (the black part glued to the glass). Behind the sensor, many small air bubbles were present, where the crack went through to the top.

Figure 35 More pictures on the crack that appeared out of a sudden before testing.

Until 300 kN, all sensors performed equally well (graph 18). At 190 kN a small crack appeared at the bottom connection. At around 275 kN another small crack appeared at the top connection (figure 36, left). At 280 and 290 two small cracks appeared close to sensors 1/7 at the bottom.

At 300 kN, sensor 11 stopped, but came back on. At 350 kN sensor 1 deviated (graph 18). At 350 and 360 kN a few continued cracking. At 400 kN sensor 7 stopped and came back as well (graph 18). At 440 kN, close to sensors 4/10 a few more cracks appeared, and slowly continued cracking towards the middle of the tube towards the bottom. At 505 and 550 kN a few more cracks appeared (figure 36, middle). The crack that appeared before testing, opened up at 570 kN. At 640-675 kN the crack next to it continued cracking to the bottom connection (figure 36, right). At 650 kN, sensor 12 stopped, but came back on (graph 18).

At 700 kN the glass crackled, and continued doing so until 730 kN. A few cracks appeared at the bottom/top, but those did not continued cracking. A few cracks were visible between sensors 3/9 and 1/7 at the bottom. At 740-750 kN new cracks appeared between sensors 6/12 and 4/10 at the top, but stopped cracking in the middle (figure 37, left).

Sensors 10 stopped performing around 720 kN, and sensor 9 slightly deviated (graph 18). At 750 kN, the load vs displacement curve became less steep (graph 20), and the glass shattered at the bottom (figure 37, middle). After that the force was taken off and a few perpendicular cracks appeared at the top/bottom (figure 37, right).

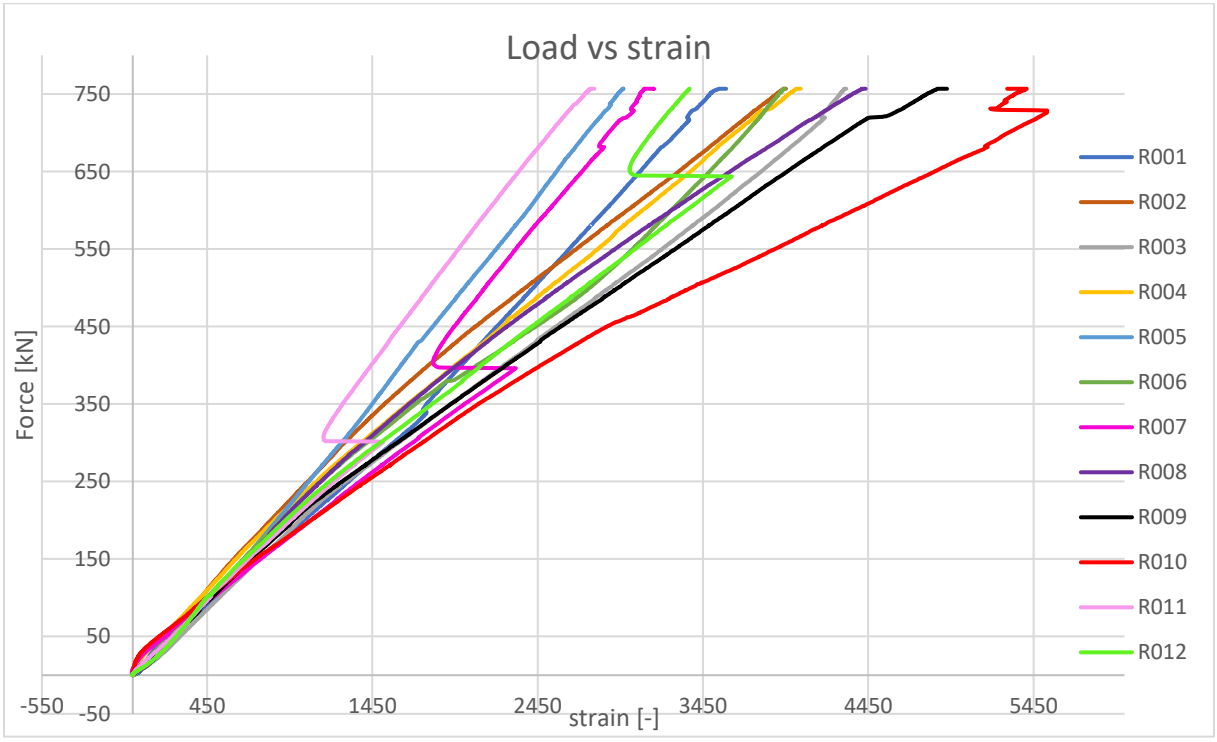

Graph 18 Load versus strain curve till force was taken off - test 6 - sample 2.

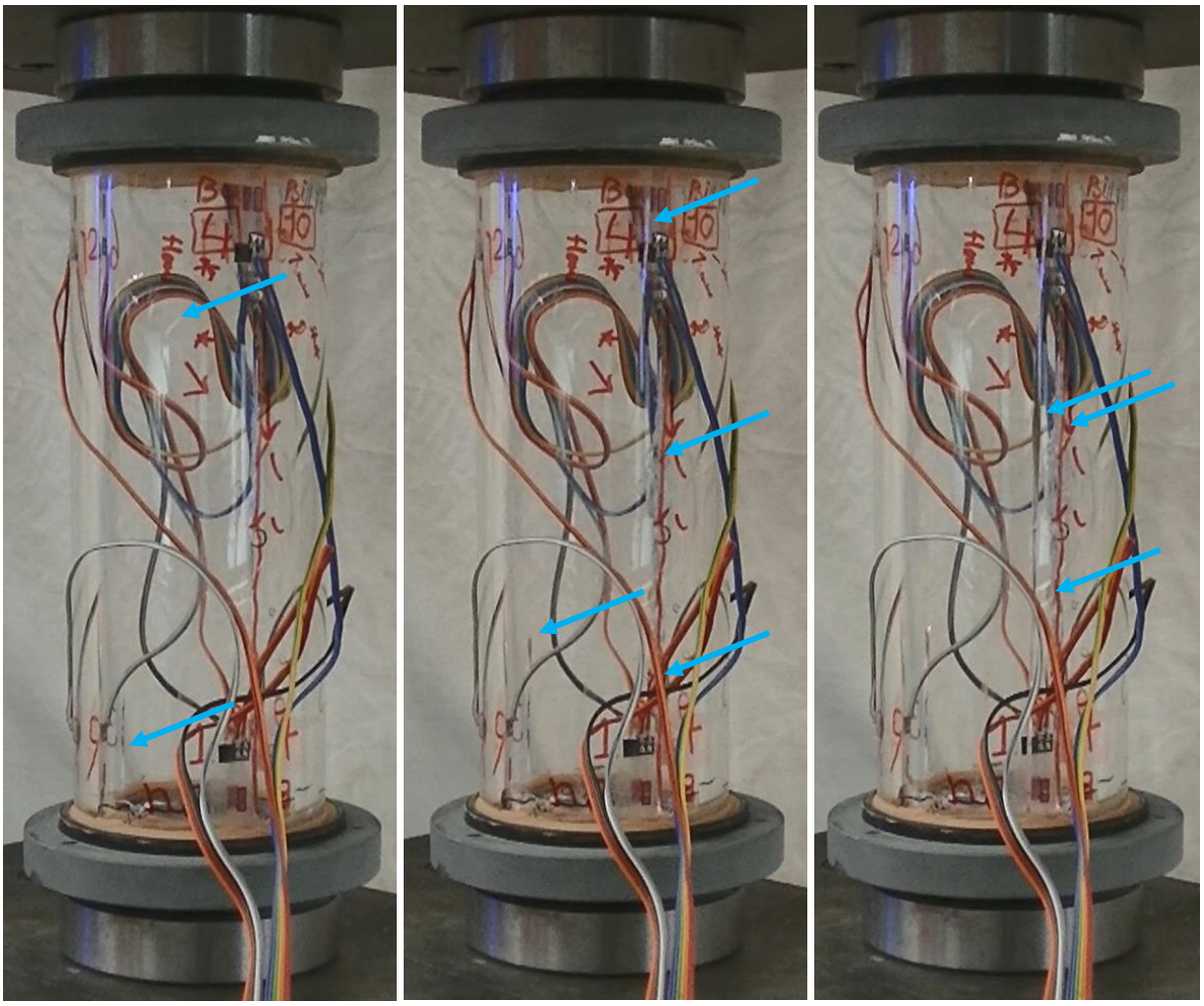

Figure 36 At the bottom and the top a crack appeared and slowly continued. This picture is taken at 280 kN (left). At 550 kN the crack which was already present continued cracking, and a few more cracks appeared (middle). The crack appeared before testing opened up and continued cracking. At 675 kN the crack next to it slowly cracked to the bottom (right).

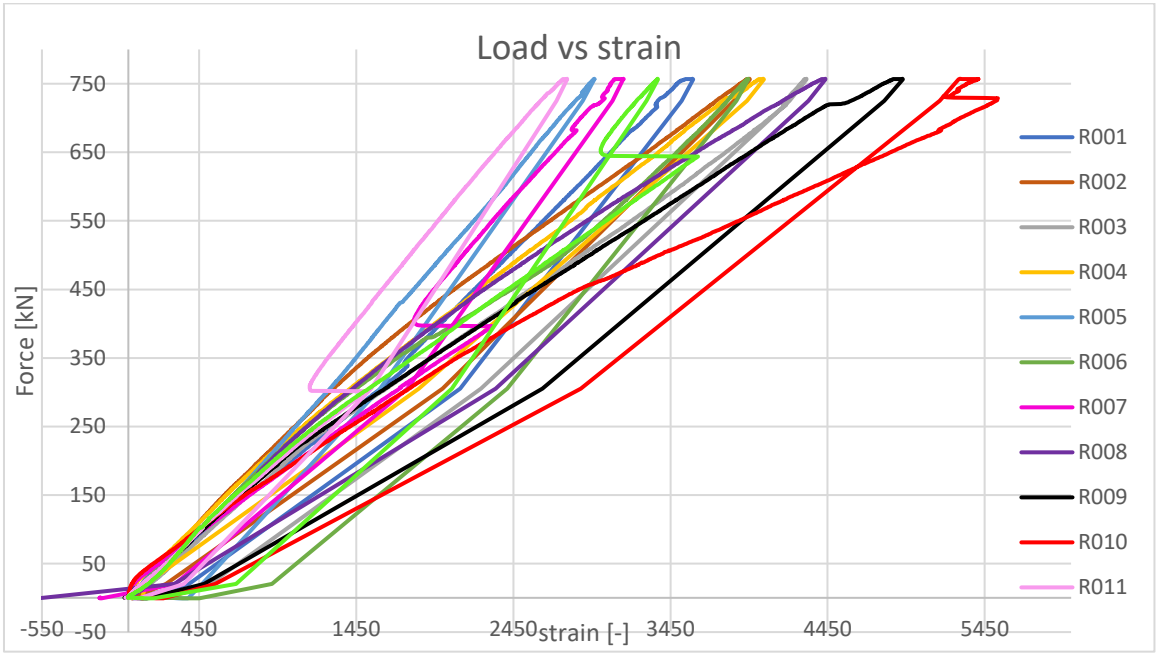

Graph 19 Load versus strain curve till the end - test 6 - sample 2.

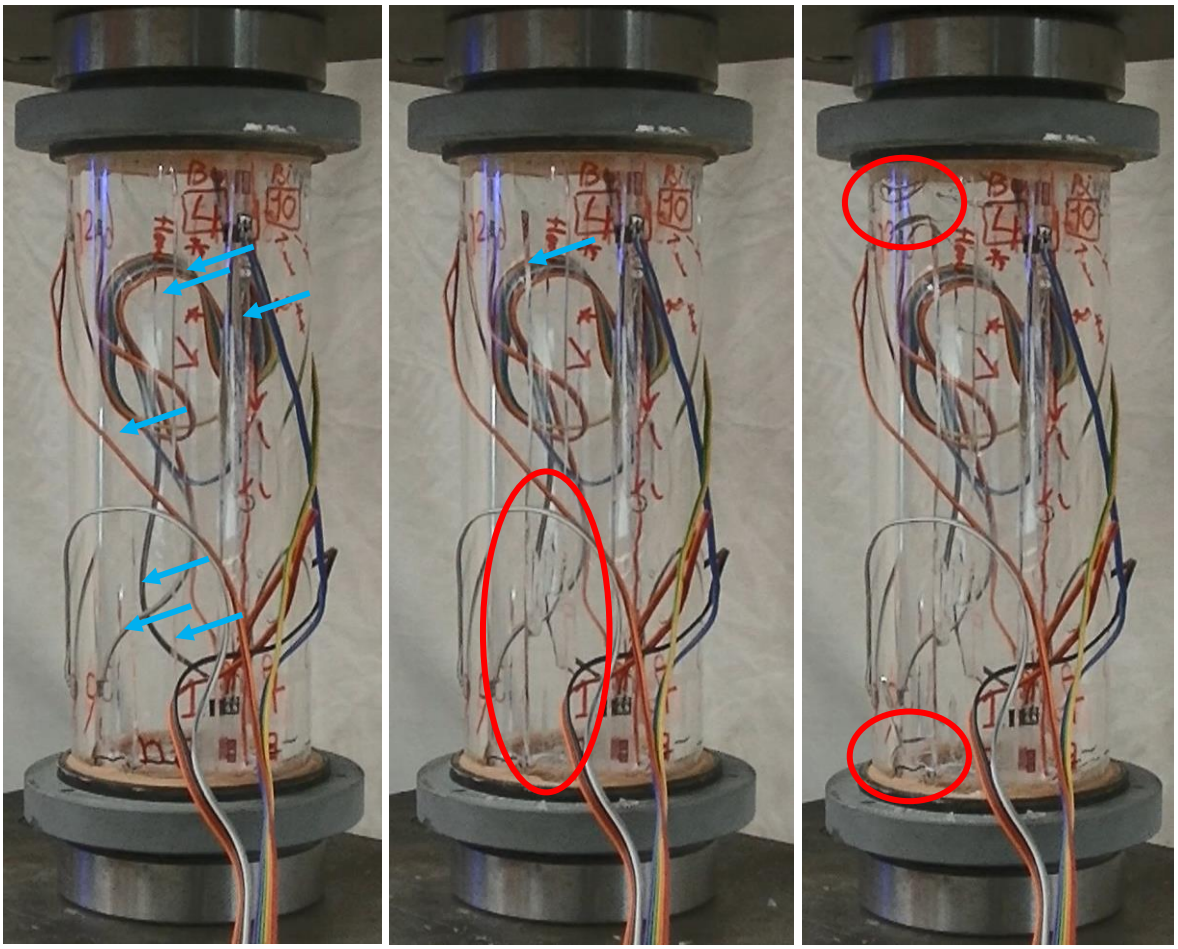

Figure 37 At 750 kN a few more cracks appeared at the top and the bottom but stopped cracking in the middle of the tube (left). The glass shattered at the bottom: red circle (middle). After the force was taken off a few perpendicular cracks appeared (right).

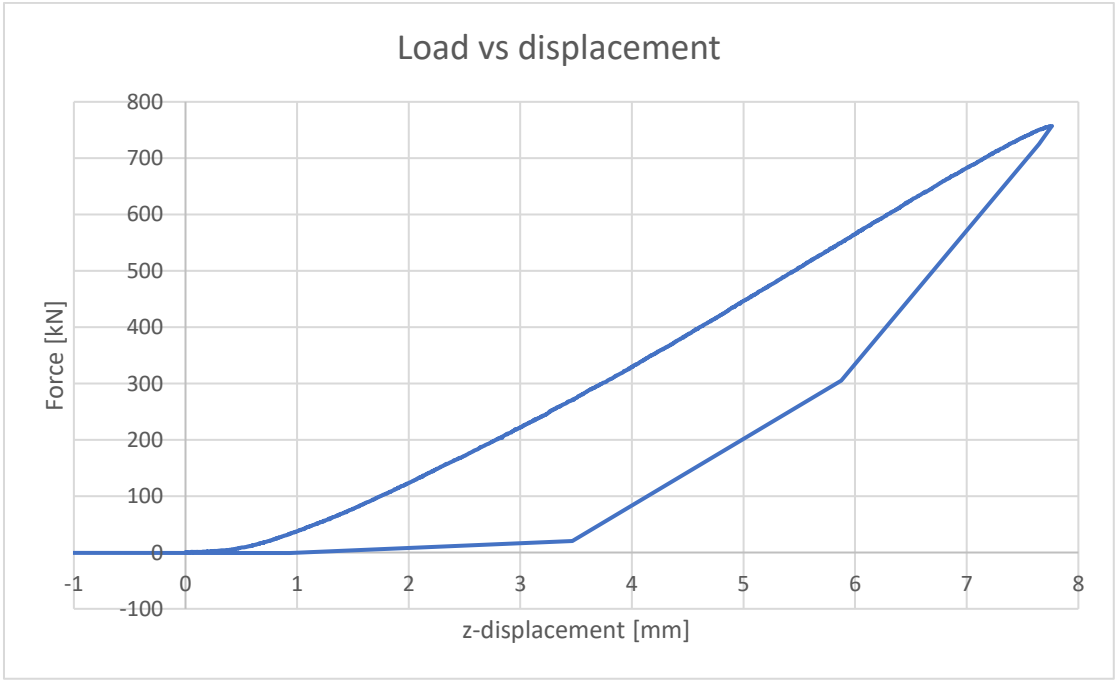

Graph 20 Load versus displacement curve - test 6 - sample 2.

Figure 38 shows more pictures of the cracked result of sample 2.

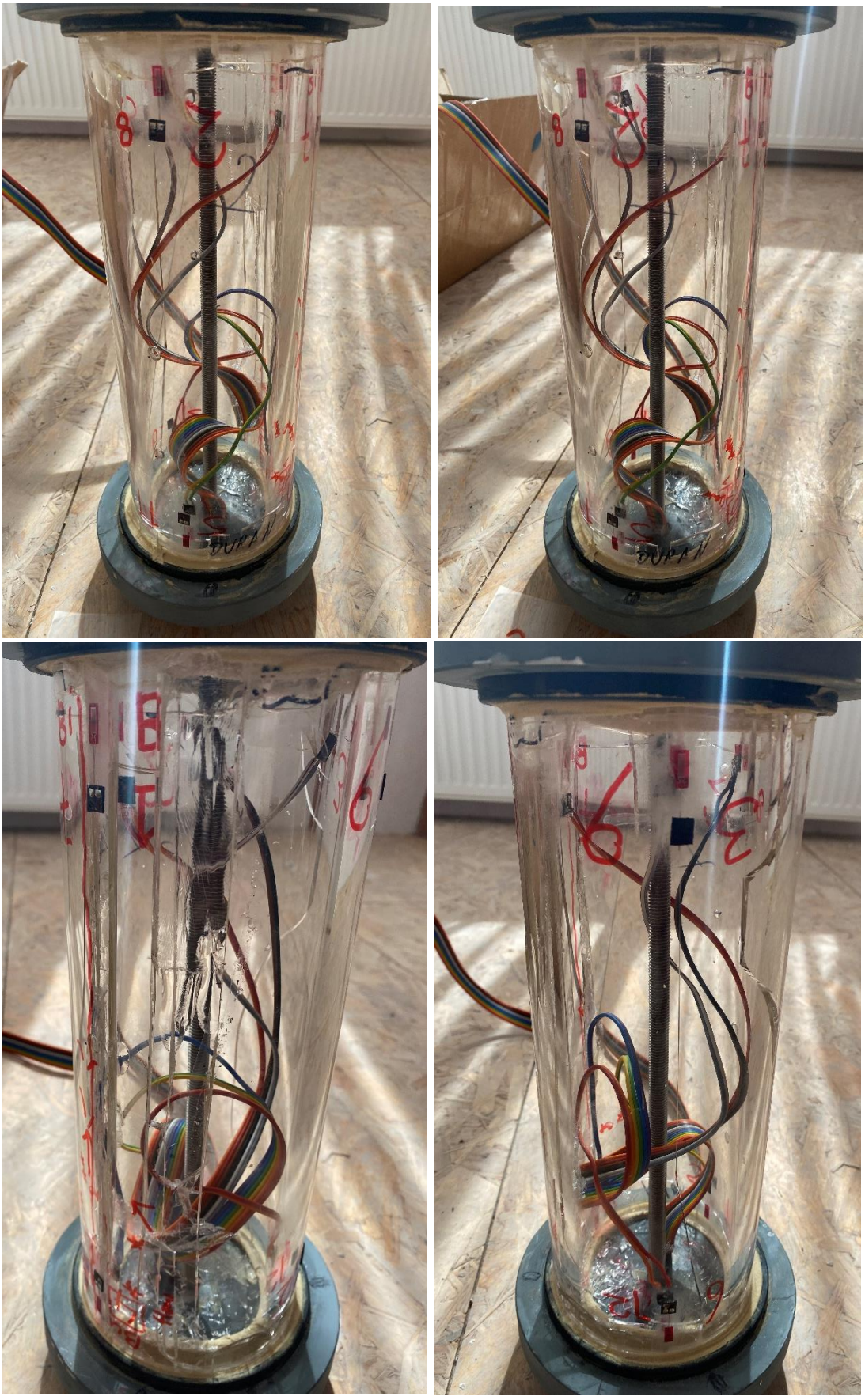

Figure 38 Cracked sample 2.

A.14.1.7. Graph of all samples together

Graph 23 shows the load versus displacement curves from samples 1,2,3,4 and 6. As can be seen the slopes are the same for all samples. Sample 5 (HS) is not included in the graphs below, because the curve is not reliable due to the fact that the machine failed performing after 160 kN. Sample 2 (AN) already had a crack before testing. As can be seen in graphs 21 and 22, the starting points are deviating from each other. This was caused by the difference between the moment the sample was settled in the machine, and when the machine was able to start.

The force was taken off when the load versus displacement curves became less steep. At that point the glass shattered. As can be seen, the heat-strengthened samples (DURATAN) failed earlier than the annealed glass (DURAN) tubes. Only a few cracks parallel to the length of the tube appeared in the AN samples. When the force was taken off, a few small perpendicular cracks occurred. More cracks appeared parallel to the length of the tube in the HS samples then in the AN samples. The inner tube of the HS samples cracked into small pieces after the force was taken off. The curve of sample 4 is different from the other curves. Probably because, in this tube the most air bubbles were present.

As can be seen from all the load versus strain graphs, some strains are deviating from others. This had probably to do with the fact that not all the strain sensors were exactly glued parallel to force onto the glass.

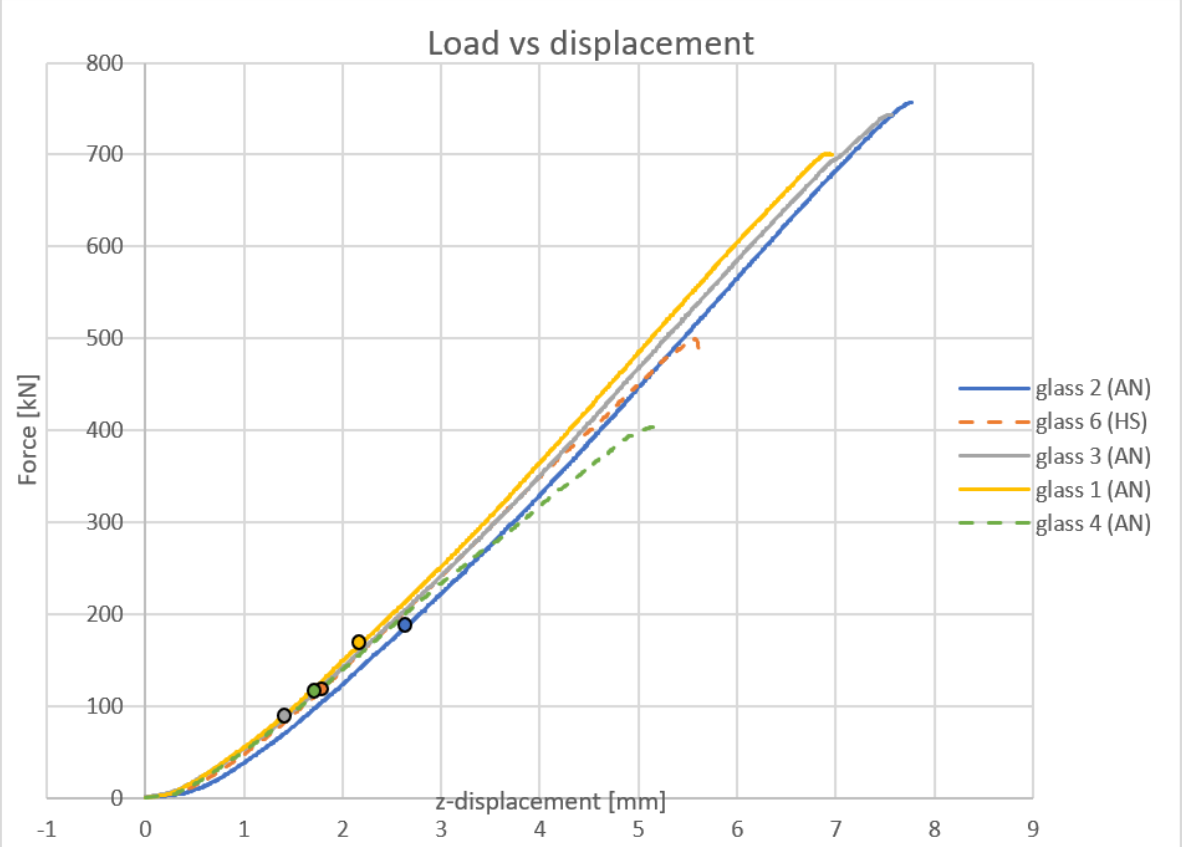

Graph 21 Load versus displacement curve until the force was taken off (without first deviations) – samples 1,2,3,4 and 6.

In all the load versus displacement curves (obtained during testing) the displacements from the components of the testing machine are included as well. As can be seen in all of the load versus displacement curves, the curves did not change after cracks appeared. This means

that the samples remained strong and stiff even after fracture. In table 1, all the samples are listed with the corresponding failure load and the load where the first crack was introduced into the sample.

test	sample	type	Failure load [kN]	failure stress (σ) [N/mm^2]	theoretical failure tensile stress [N/mm^2]	Maximum load [kN]	Maximum stress (σ) [N/mm^2]	theoretical maximum tensile stress [N/mm^2]	remarks
1	5	HS	>160	>50	>10	?	-	-	machine failed after 160 kN
2	4	HS	120	37	7	390	121	24	a lot of air bubbles
3	1	AN	160	50	10	700	217	43	-
4	3	AN	95	30	6	745	231	46	-
5	6	HS	120	37	7	490	152	30	-
6	2	AN	(second crack at 190)	-	-	750	233	47	Already had one crack before testing

Table 1 Failure load and load where the first crack was introduced - all samples.

A.14.1.8. Polarised light to check stresses in the sample – samples 3, 6, and 2

For the samples 3, 6 and 2 the stresses were checked inside the sample by the use of polarised light and filters. Due to differences in wave lengths, different colours occur. A different colour means that stresses are present. To create polarised light, a computer screen was used with a white background. Furthermore, the filter, shown in figure 39 (left), was used. With the filter in front of the screen, the white computer screen became black (see figure 40). In figure 39 (right) a sketch is given from the set-up, which is used to create these optical stresses.

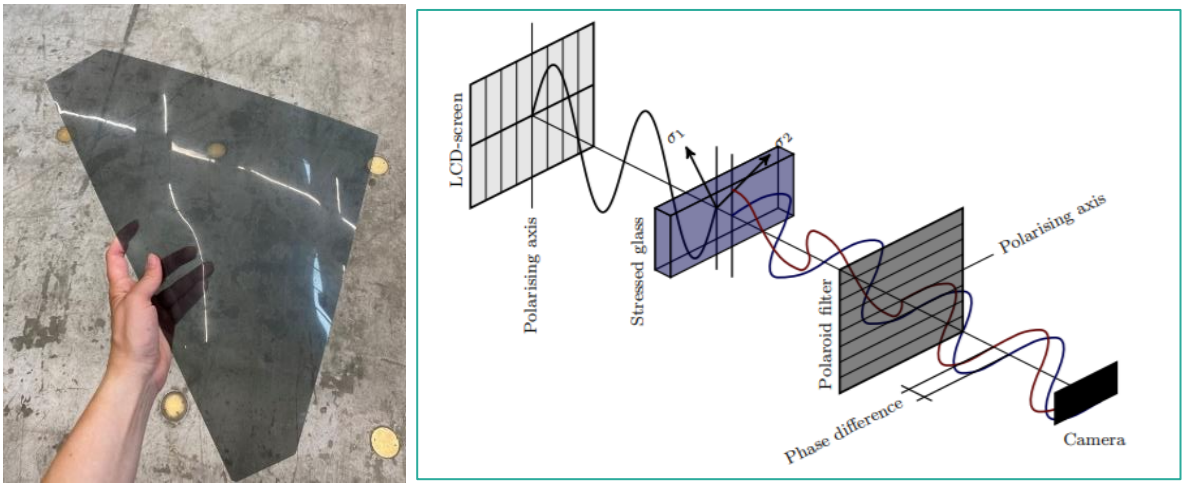

Figure 39 Polarised filter (left). Schematical set-up to create optical stresses (right) (Aurik, M. 2017).

Figure 40 shows sample 3 with AN glass tubes. The pictures show that no extra stresses were visible in the tube itself. This means that in the interlayer material not many stresses were present. However, around the air bubbles stresses were present.

Figure 41 (left) shows sample 6 with HS glass tubes. Again, around the air bubbles stresses were present. Furthermore, heat-strengthened glass is prestressed. The stresses due to the prestressing were visible in the tubes as well. In figure 41 (right) a single heat-strengthened glass tube is shown with the filtered light. The same ‘cross-linked’ pattern occurred in the single glass tube. For sample 6, the light was stronger, because two heat-strengthened tubes were shown.

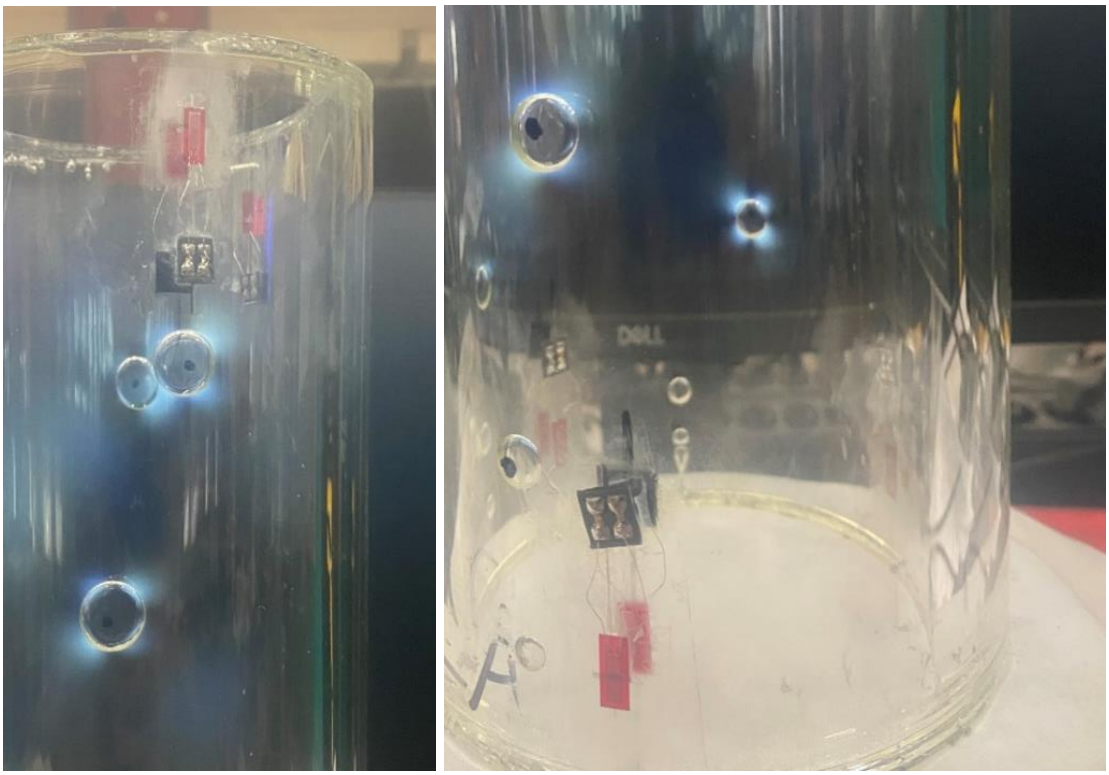

Figure 40 Sample 3: stresses around the air bubbles in the interlayer material.

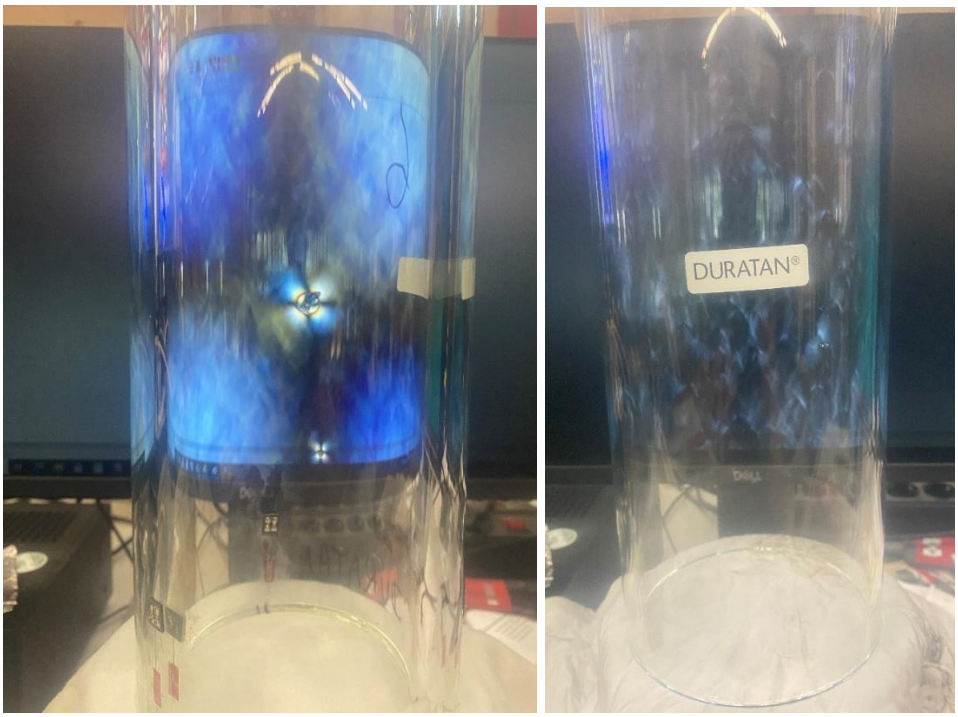

Figure 41 Sample 6 (left): stresses around the air bubbles and prestressed stresses. A single DURATAN tube (right): prestressed stresses.

Sample 2 (AN glass) was already cracked out of a sudden before testing. Figure 42 (left) shows an air bubble in sample 2. Some stress was present around this air bubble, but the colour was not as bright as in samples 3 and 6. In figure 42 (right) an air bubble is shown in sample 2 located at the crack. As can be seen, almost no stresses were present anymore.

No stresses were present anymore around these air bubbles where the crack was located. This means that the stress was released due to the crack in the inner tube.

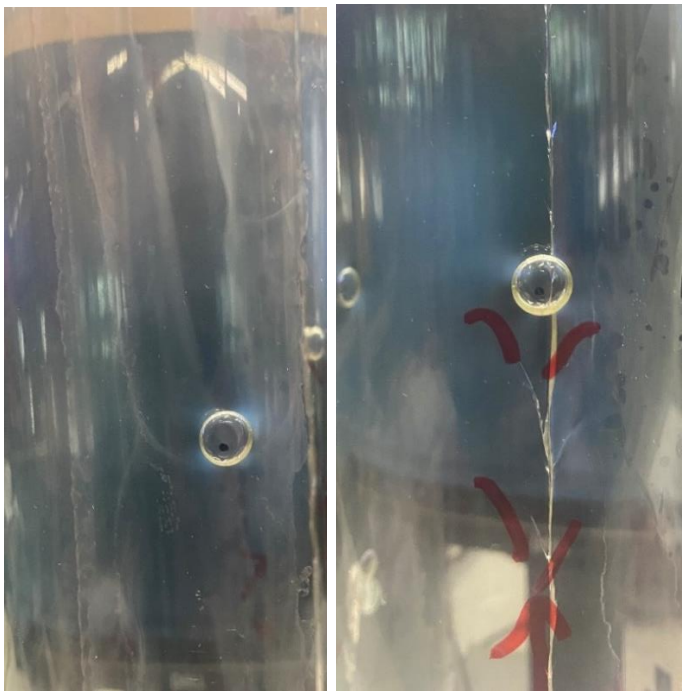

Figure 42 Sample 2: Some stresses were present around the air bubble (left). Sample 2 at the location of the crack: no stresses were present anymore around that air bubble (right).

A.14.1.9. Analysis of the cracks

After the experimental tests were performed, a few cracks were analysed with a microscope, the 'Keyence vhx7000' (figure 43). All of the cracks were discussed with Veer, F. and Bristogianni, T. Furthermore, the Fractography of Ceramics and Glasses, Practice Guide is used to determine the type of cracks (Quinn, G., D. 2020).

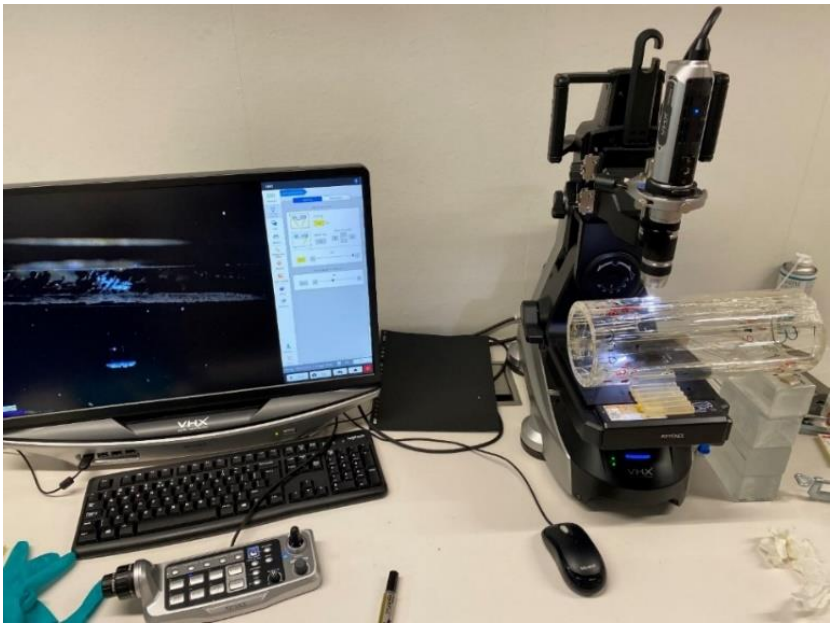

Figure 43 Further analysis of the cracks with the microscope 'Keyence vhx7000'.

In figure 44 and 45, annealed glass cracks are visible. At the red circle in figure 50, the perpendicular crack is shown, which occurred when the force was taken off. At the red

arrows (figures 50 and 51) the direction of the crack propagation is visible. These cracks were caused by the axial compression force. At the blue circle, twist hackles (blue arrows) are visible.

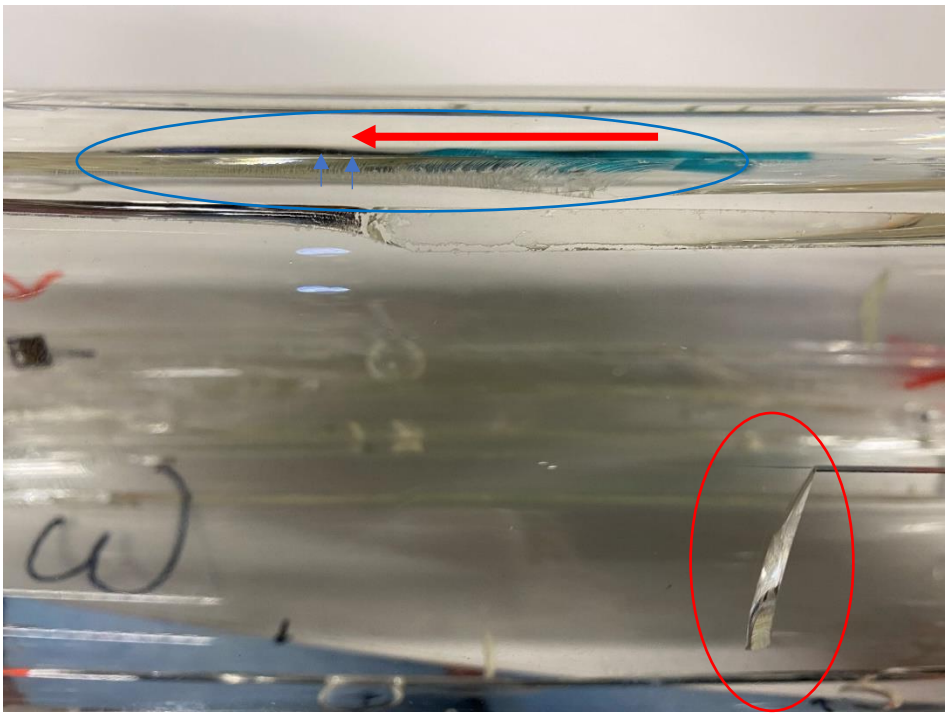

Figure 44 Patterns for annealed glass cracks – sample 3.

At figure 45 (red circle), mist and velocity hackles are visible, and Wallner lines are shown (red arrow) due to uniform tension. At the blue circle, the crack along the surface is shown.

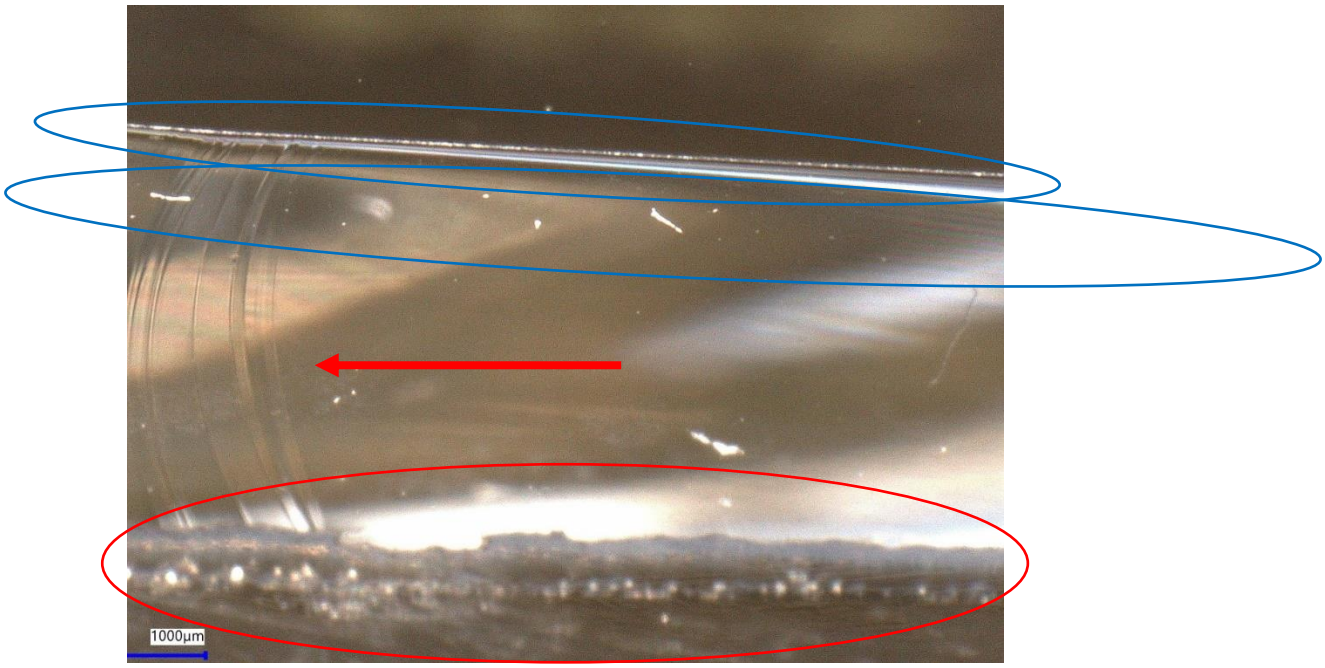

Figure 45 Crack in annealed glass sample - sample 3.

Figure 46 shows the earlier mentioned crack which stopped cracking in the middle of the AN tube (sample 3). This pattern looks like a deformation in the interlayer material whereby delamination occurs. The morphology seems too rough for a glass crack. This is a logical

continuation. If the glass cracks and the interlayer material did not crack, then delamination occurs.

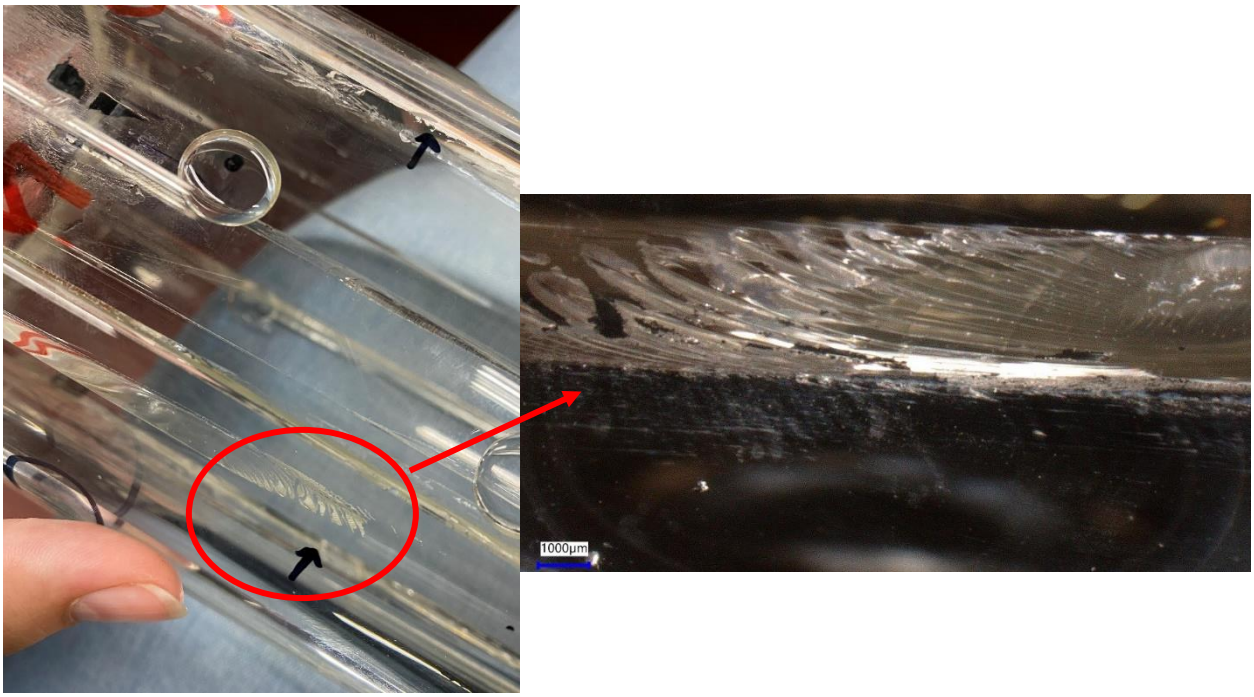

Figure 46 At both the black arrows, delamination occurs – sample 3.

In figure 47, some dendritic patterns are visible. This is also a result of delamination.

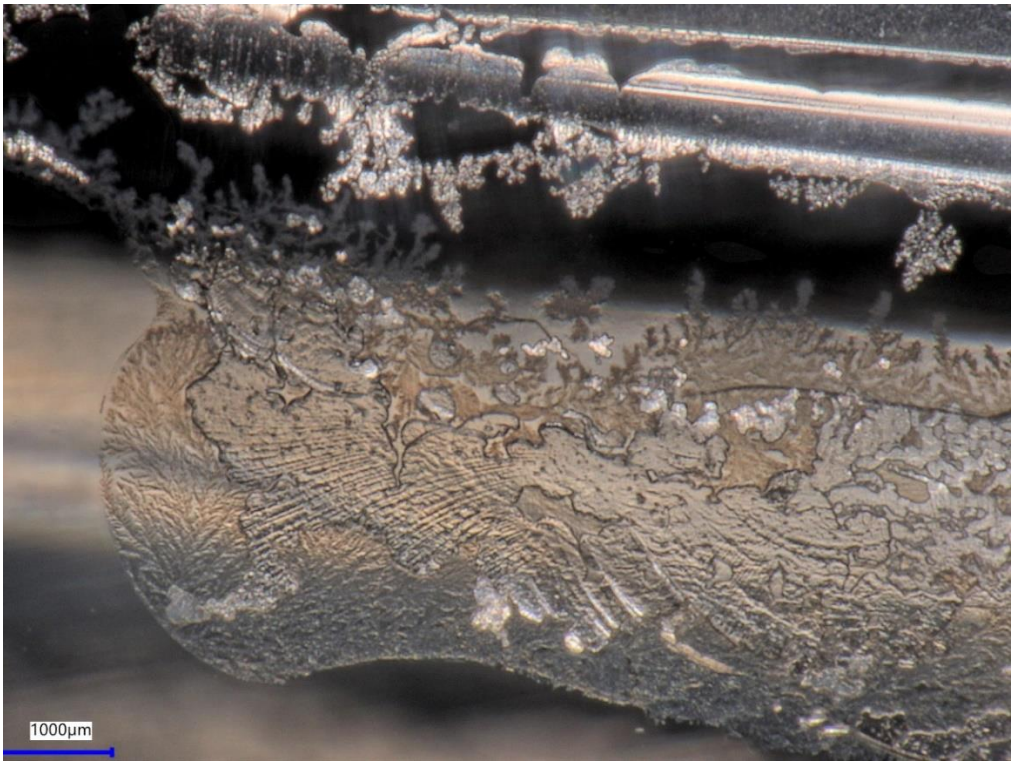

Figure 47 Dendritic patterns due to delamination - sample 3.

In the figures 48-54 a few cracks are shown which are typical for heat-strengthened glass. As can be seen, straight cracks appeared at the outer tube (figure 48 and 50) and the inner tube cracked into small pieces (figure 48, 49, 52 and 53).

Figure 48 At the outer tube straight cracks are visible and the inner tube cracked into smaller pieces – sample 6.

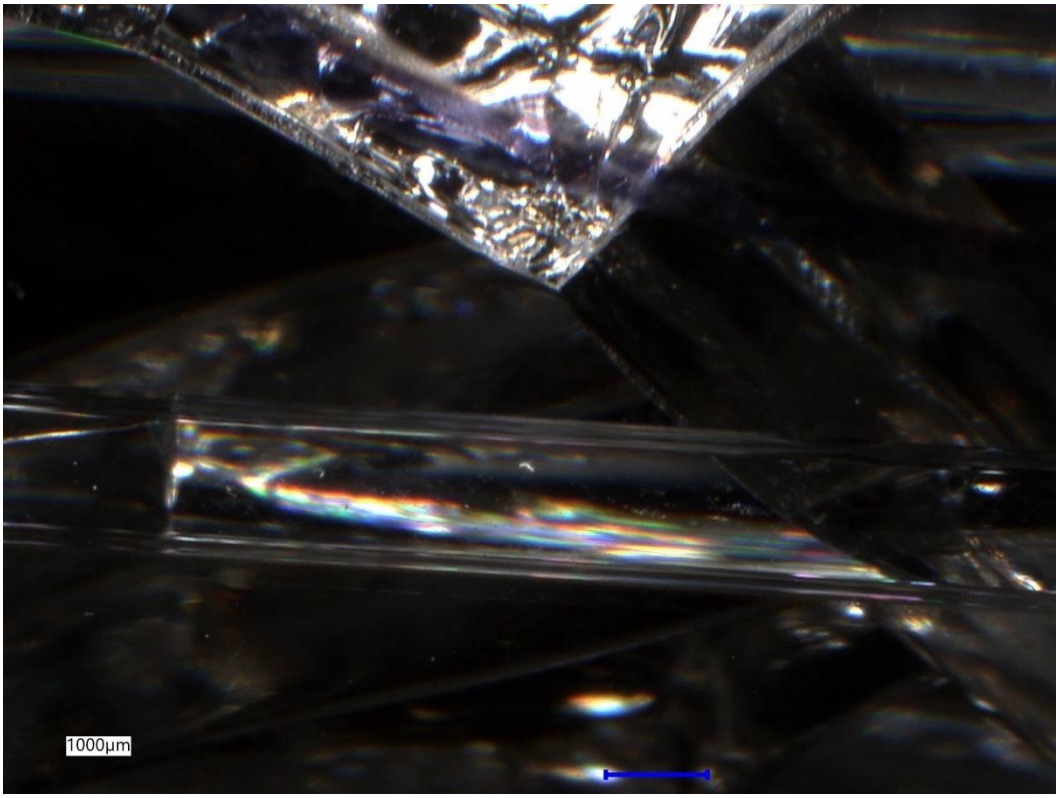

Figure 49 Multiple cracks in different directions on the inner tube - sample 6.

In figure 50, a straight crack is shown from the outer tube. At the bottom, mist and velocity hackles are shown. In the crack itself, Wallner lines are visible.

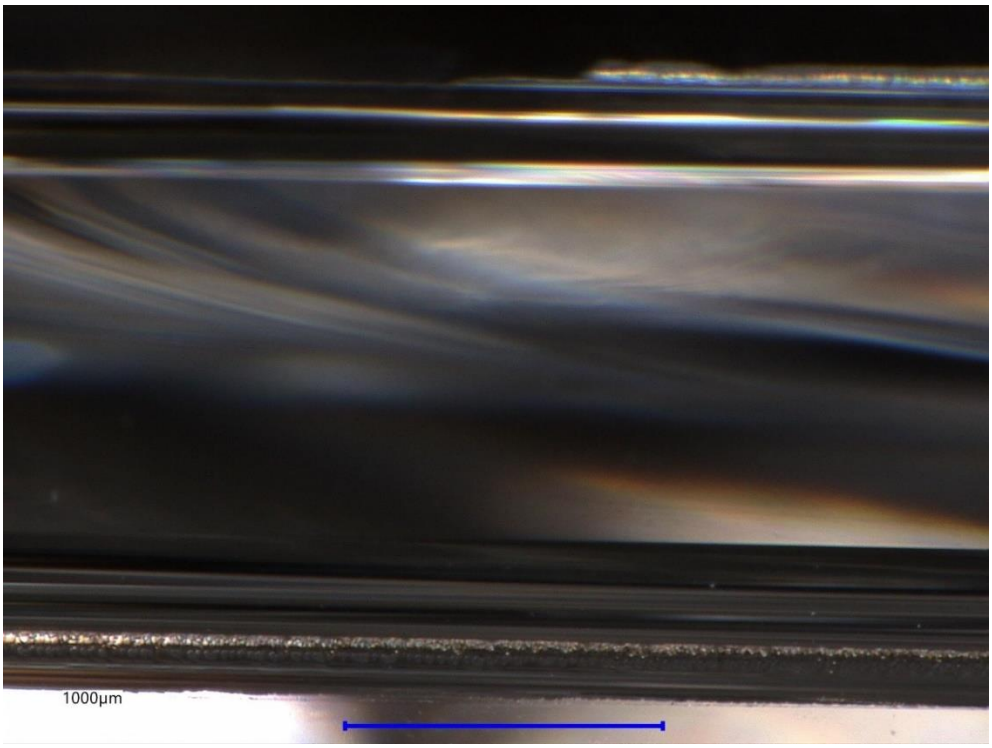

Figure 50 A straight crack on the outer tube - sample 6.

In figure 51, a crack is shown in the middle of the picture with Wallner lines. At the blue arrows a few twist hackles are shown. At the blue circle, delamination is visible. At figure 53, at the blue arrow, the direction of the crack propagation is shown. At the red arrows, twist hackles are shown.

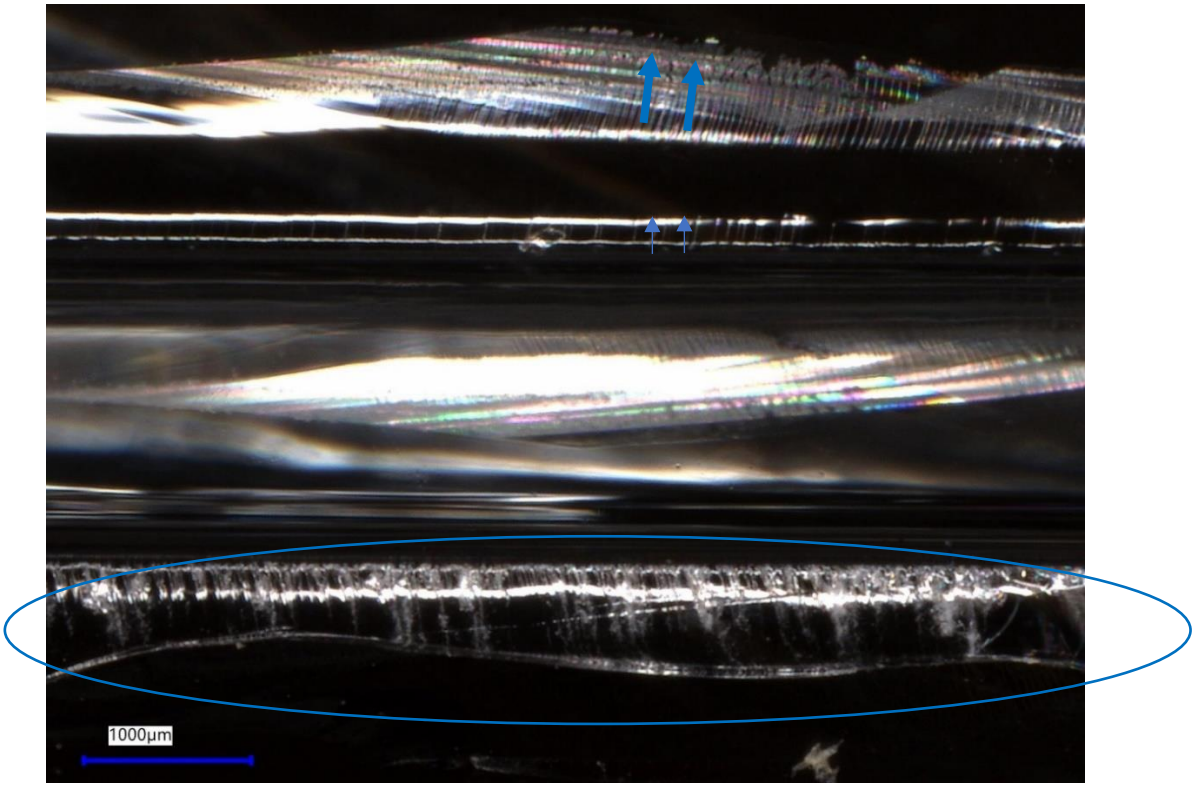

Figure 51 A glass crack is shown in the middle and delamination is visible on the bottom side - sample 6.

Figure 52 Straight cracks at the outer tube, and a few perpendicular cracks appeared when the force was taken off - sample 6.

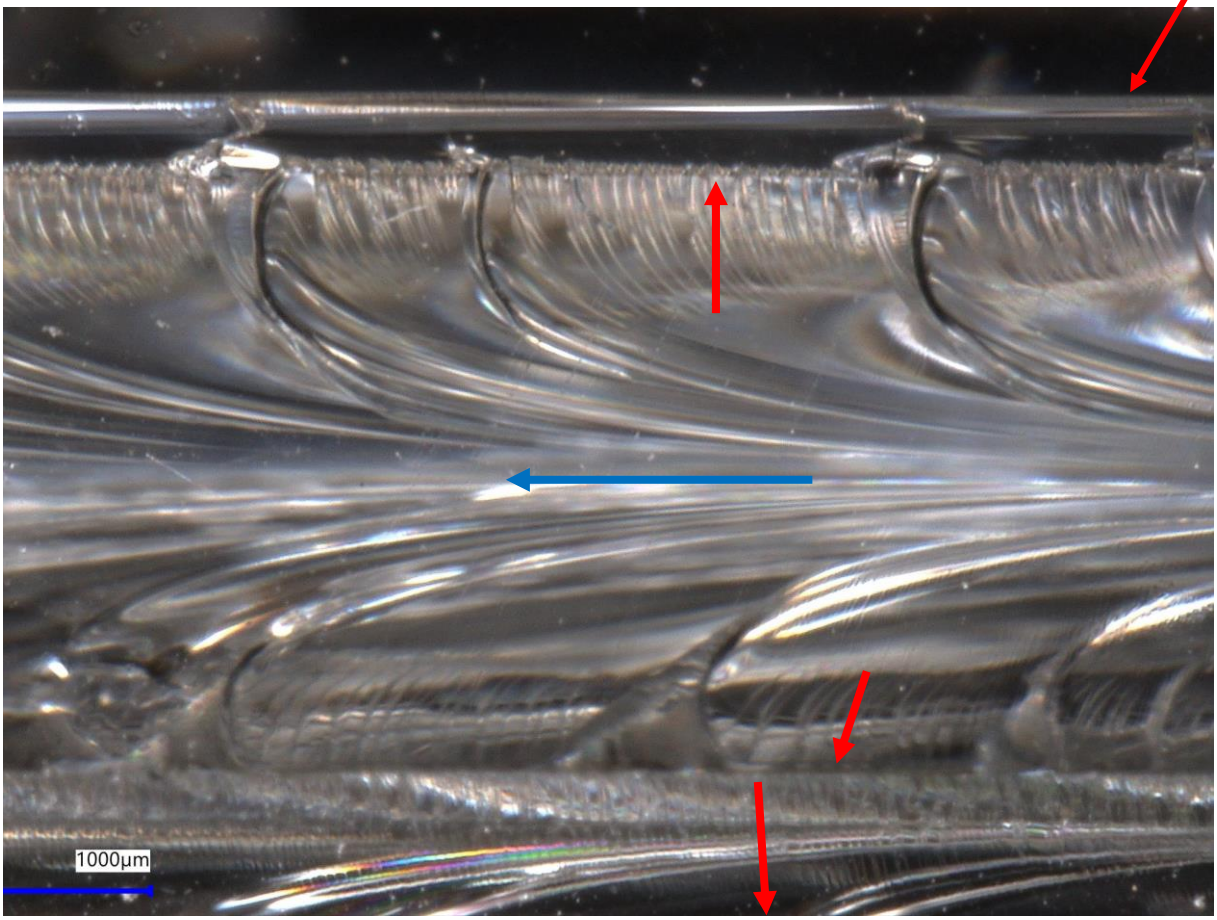

Figure 53 A close-up from figure 53 - sample 6.

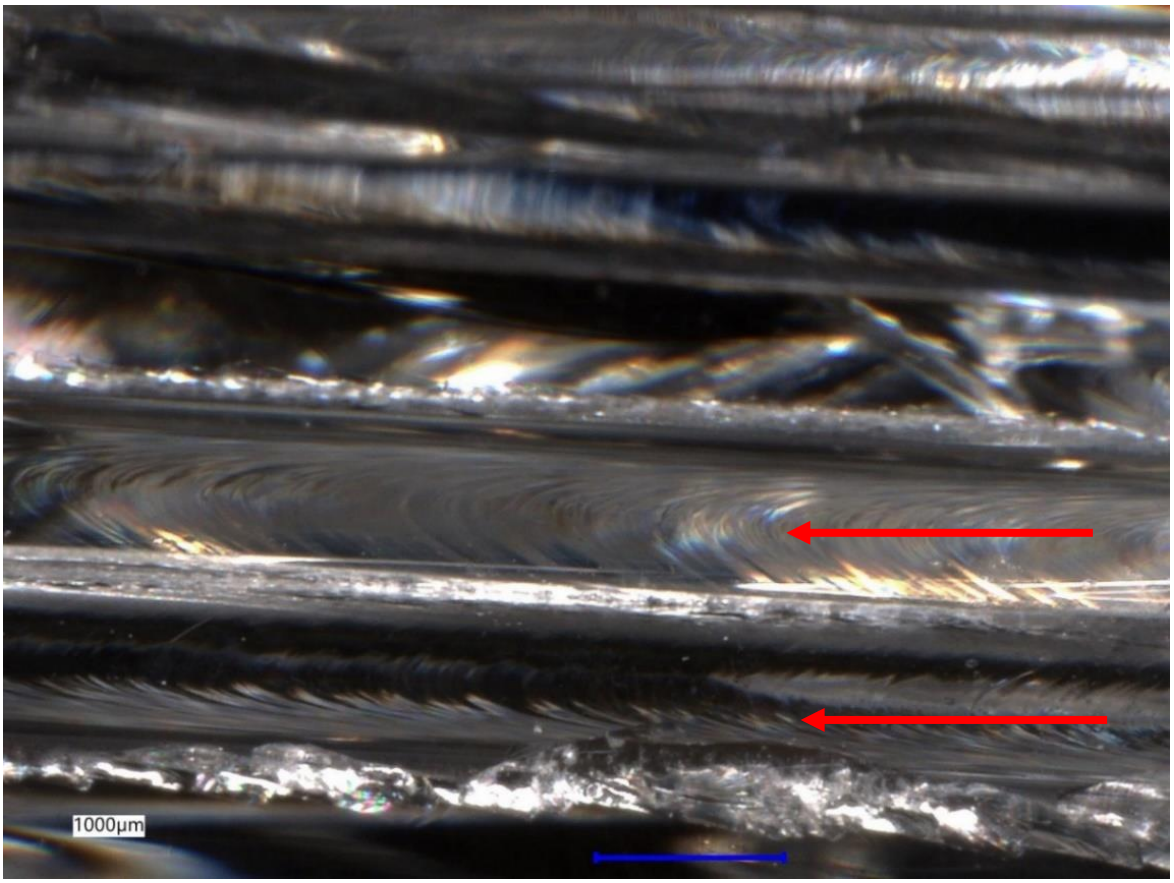

Figure 54 Glass cracks - sample 6.

At figure 54 the direction of the crack propagation is shown (red arrows). This is a typical tempered glass crack (Dugnani, R., et al. 2014). At the bottom of figure 54, mist and velocity hackles are shown.

A.14.2. Tasks/measurements experiments

In the experimental plan a few takes/measurements were defined before testing:

- During the mortar injection (chapter A.14.2.1.):
    1. The mortar needs to be injected easily without problems.
    2. The mortar needs to be well-distributed over the groove into the POM-block.
    3. The glass needs to stay clean during/after injection of the mortar.
- To check if the forces are uniformly distributed from the connection into the glass (chapter A.14.2.2.):
    4. Looking at the strain sensors, was the strain the same at every sensor and if so, was the force well-introduced into the glass?
- Post-failure behaviour (chapter A.14.2.3.):
    5. How does the Hilti mortar break: does it crack/crush/splash/etc?
    6. What is the weakest point of the sample: the glass or the connection? So, what breaks first?
    7. What is the post-failure behaviour of the glass sample?
        a. How does the glass break?
        b. How is the interlayer behaving if the glass is broken?
        c. Does the laminated glass tube crack differently than single tubes?

d. Are the samples robust? Do they show some structural integrity?

- Compression force (chapter A.14.2.4.):
  8. Is the Hilti mortar able to take up more stress than 53 N/mm^2?
  9. Are the strain values in the glass tubes from the sensors comparable with the strain values calculated by hand?
  10. Is the displacement in the glass tubes comparable with the displacement calculated by hand?

These abovementioned questions will be answered in the following chapters. In here the difference between DURAN and DURATAN samples will become clear as well.

A.14.2.1. Injection of Hilti mortar

1. The mortar needs to be injected easily without problems.

The Hilti mortar is easy to inject, but it already starts to harden quickly after approximately 5 minutes. Within these 5 minutes, the Hilti needs to be injected, smoothed out and the glass needs to be placed on top. It was possible within these 5 minutes, but it needed to be done quite fast. After these steps, the Hilti became warm, and afterwards it cooled down. These steps and the reaction took place in approximately 30 minutes, as was mentioned in the brochure from the Hilti mortar. In the tests enough/too much Hilti mortar was used to be sure that enough Hilti was placed under the glass tubes. In figure 5 and 55 a neat sample is shown. To smoothen out the Hilti mortar, a flexible scraper was used with a piece cut out (appendix 13, figure 19).

Figure 55 The Hilti mortar was properly injected – sample 5.

2. The mortar needs to be well-distributed over the groove into the POM-block.

First off, one sample has been tried out with the help of Octatube. Figure 56 (left) shows a POM-block where the Hilti mortar was injected in. At the right picture (figure 56), the Hilti was taken out of the POM-block (shown at the bottom side). As can be seen in figure 56 (right), the Hilti was not evenly well-distributed and messy.

Figure 56 The first try of injecting Hilti in a POM-block (left). The Hilti was taken out of the POM and is shown at the bottom side (right).

After that, the Hilti injection was tried out for a second time. The clue is to hold the spout against the bottom of the POM-block where it will be injected. In this way the Hilti was better distributed over the bottom of the POM-block. In figure 57 a part of the Hilti is shown from the second try-out, which was taken out of the POM afterwards. As can be seen, it was well-distributed into the POM-block.

Figure 57 The second time to try-out the way of injecting Hilti. It was possible to pull out the glass later on (left). In this figure the Hilti was pushed out of the POM and a part of the bottom is shown which was well-distributed in the POM-block (right).

3. The glass needs to stay clean during/after injecting the mortar.

Figures 5 and 55 show that when the Hilti was injected properly, the glass stayed clean as well. In the first 5 minutes, the remaining material could be cleaned/swiped off the glass, but this was not possible for the inside glass any more. So, it needs to be done carefully to keep the glass clean. Furthermore, not too much Hilti needs to be used, because when the glass

is placed on top of the Hilti (when it is not hardened yet), the Hilti will squeeze up, and it cannot be cleaned on the inside of the tube anymore. This phenomenon can be seen in figure 1. In the tests too much was used to make sure there was enough Hilti. When less Hilti was used (just enough) it could stay clean and neat (figure 5 and 55).

A.14.2.2. Introduction of forces from the connection into the glass

4. Looking at the strain sensors, was the strain the same at every sensor and if so, was the force well-introduced into the glass?

Looking at the load versus strain graphs (given in the previous chapters), in the beginning all sensors were approximate showing the same strain value. Mostly one or two strain sensors started deviating between 50-250 kN. Perhaps the deviations of the values of the strain sensors was caused by the strain sensors not being positioned quite vertically. Some strain sensors were able to come back on after a moment of deviating or stopping. So, it looks like the laminated glass tubes were able to re-distribute the forces (also after cracking).

However, it is difficult to conclude that the Hilti distributed the forces well, because there were more parameters influencing the result. Perhaps, the glass was not placed completely perpendicular to the connection. As can be seen in figure 58, when the connection is not placed perpendicular to the glass tubes, it may be possible that most of the load is coming in one part of glass. This can cause peak stresses and then the glass starts cracking and shattering at that location. Glass is re ally sensitive to peak stresses. Even sharp edges or a small piece under the glass can cause peak stresses in the glass. To make sure that the glass and the connection are placed correctly, a spirit level can be used.

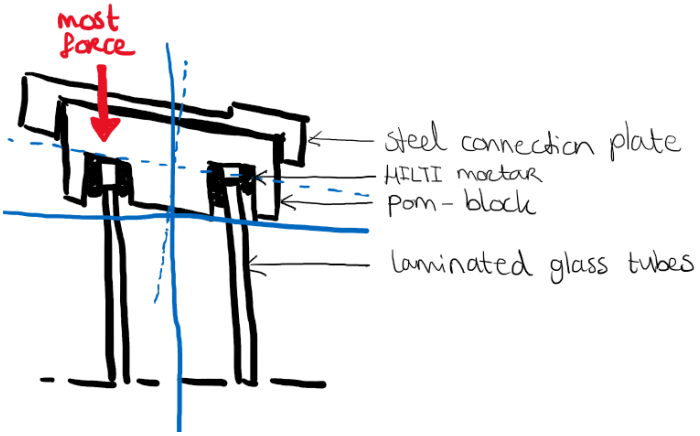

Figure 58 If the glass is not placed perpendicular to its support, an uneven load distribution occurs.

As described in appendix 13 (appendix 13, figures 14,15 and 16), a few timber pieces were placed in the POM-block to keep the glass in its place when the Hilti was not hardened yet. Also, these timber pieces could have contributed to an uneven introduction of forces into the glass. The timber pieces were placed perpendicular to the grain, so that it should have a lower Young's modulus. However, it probably still had some stiffness, which could influence the load introduction. In figure 59 two spots are marked (black dots), where a timber piece was placed, for sample 2 (AN). As can be seen, a small crack appeared, but did not propagated. Figure 60 shows one heat-strengthened sample (sample 6) where the timber piece was placed (black dot). In here, not much deviation is visible at that spot compared to the other cracks in the glass tube.

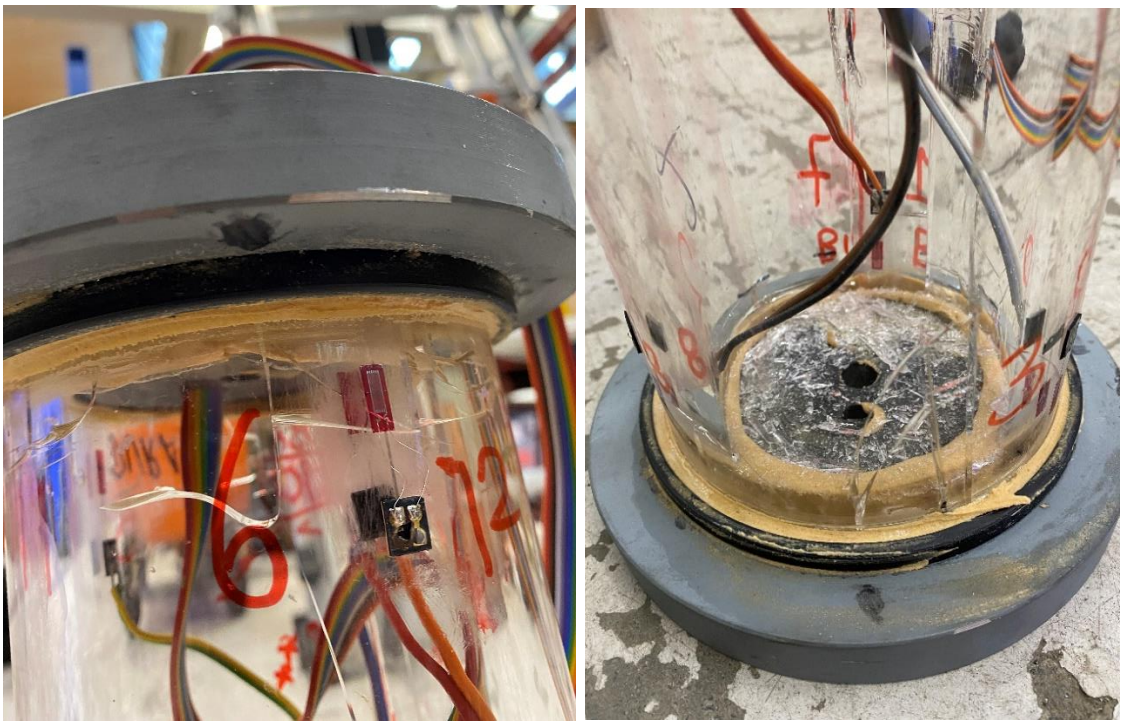

Figure 59 At the black dot (placed on the steel) a timber piece was placed inside the POM-block. A small crack is visible at that location, but the crack did not propagate any further (left and right).

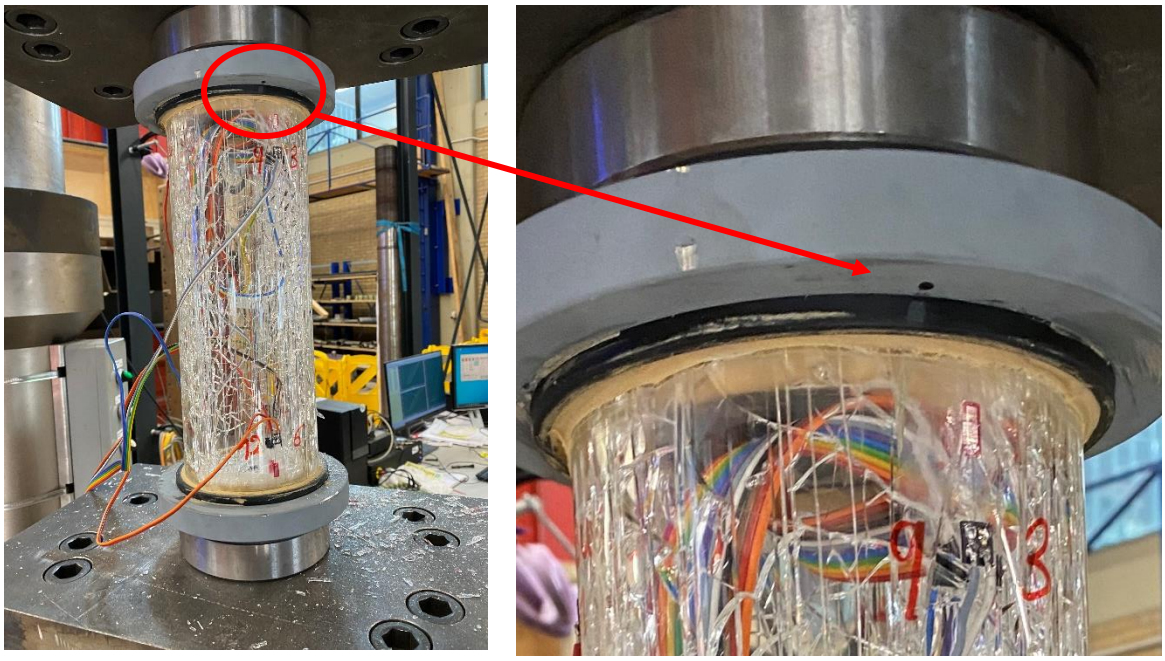

Figure 60 A spot at sample 6 where the timber piece was placed inside the POM-block. Not much deviation is visible compared to the other cracks in the tube.

In the design, the timber pieces were left out. The glass needs to be marked at the right height, and it needs to be held by a machine at the right height until the Hilti is hardened. That the connection is placed perpendicular to the glass tubes, need to be controlled with a spirit level.

A.14.2.3. Post-failure behaviour

5. How does the Hilti mortar break: does it crack/crush/splash/etc?

As mentioned in the previous chapters, the connections (steel/POM) remained intact during all the tests. The Hilti mortar remained intact as well, no cracks/crushes/etc were visible (figure 61).

Figure 61 The connection components remained intact (sample 6).

6. What is the weakest point of the sample: the glass or the connection? So, what breaks first?

The glass tubes broke and the connections remained intact for all samples.

According to the assumptions/calculations (equation A.10.7 and A.10.10), the glass should have handled a force of around 250 kN before cracking. Then the glass should have a tensile force of 15.6 N/mm^2 for annealed glass for short-term loading (equation A.10.10), which is possible according to the allowable practical tensile stress of 15.5 N/mm^2 (equation A.9.17). The corresponding compression stress for 250 kN is then 78 N/mm^2 (equation A.10.7). According to the literature study, glass can handle a compression force between 260-350 N/mm^2 (chapter 2.1.3. and A.9.3.). The first cracks into the samples occurred between 95-160 kN, which is earlier than expected (equation A.14.1-A.14.4).

$$\sigma_{comp} = \frac{F}{A} = \frac{95*10^3}{3220} = 29.5\ \frac{N}{mm^2} < 200\frac{N}{mm^2} \quad \text{(A.14.1)}$$

$$\sigma_{tens} = 29.5 * 0.2 = 5.9\frac{N}{mm^2} < 15.5\frac{N}{mm^2} \quad \text{(A.14.2)}$$

$$\sigma_{comp} = \frac{F}{A} = \frac{160*10^3}{3220} = 49.7\ \frac{N}{mm^2} < 200\ \frac{N}{mm^2} \quad \text{(A.14.3)}$$

$$\sigma_{tens} = 49.7 * 0.2 = 9.9\ \frac{N}{mm^2} < 15.5\frac{N}{mm^2} \quad \text{(A.14.4)}$$

In the calculations a perfectly hinged connection was taken into account. For the samples quite large hinges were used, and perhaps this affected the functioning of the hinge as a hinged connection. Besides, it could be that the glass had defects or that the tolerances in the glass affected the sample so that cracks appeared earlier than calculated. For example,

the tolerances in the glass can result in different thicknesses of the interlayer whereby extra stresses can occur.

Moreover, due to the shrinkage in the lamination and the air bubbles inside the cavity, more stresses occurred. For example, glass sample 4 had many air bubbles inside the cavity. As could be seen in figures 40 and 41, more uneven stresses were present around these air bubbles. It led to an earlier failure compared to the other samples while loaded under less load. So, a lot of these air bubbles contributed to an earlier breakage of the glass. Due to these stresses, the first crack appeared quicker than was calculated in the hand calculations.

However, all the load versus displacement curves continued even after cracks appeared. This means that the samples remained stiff or strong. Due to the crack the local stresses were relieved. This was visible in the polarised figure from sample 2 as well (figure 2). Around the air bubbles that were localised around the crack, no stresses were visible anymore.

7.a. How does the glass break?

The laminated annealed glass samples had a few cracks that started at the bottom or at the top connection. Some of them slowly propagated towards the other side parallel to the length of the tube, and some of them stopped cracking in the middle of the tube. The same cracks appeared on the inside as on the outside. When the force was taken off, a few perpendicular cracks occurred. When the load versus displacement curve became less steep, the glass started shattering and the force was taken off. Shattering of the glass mostly happened closely by the top or at the bottom connection.

The outer tube of the laminated heat-strengthened glass samples had a lot of cracks that started at the top or at the bottom connection. The crack moved directly with a lot of speed to the other side of the tube, parallel to the length. This is probably because there was more stress inside the glass due to the fact that it was prestressed, and so the crack propagated with more energy. The inside tube cracked after the force was taken off into a lot of small pieces. When the load versus displacement curve became less steep, the glass started shattering and the force was taken off. Shattering of the glass mostly happened closely to the top or at the bottom connection.

In figure 62 different crack results are shown for an annealed glass sample (left) and a heat-strengthened sample (right).

Due to the fact that the tubes were laminated together, no local bending could occur and the tubes remained strong. Furthermore, the cracks started at the top or the bottom of the glass. This can be a caused by tensile stresses occurred due to transversal elongation (chapter A.10.3.1 and equation A.10.9).

For the annealed samples both tubes cracked, so this means that there was a good cooperation between them. With the heat-strengthened samples the outer tube broke first, and afterwards when the force was taken off, the inner tube broke.

Figure 62 The cracked result from an annealed sample – sample 2 (left), and from a heat-strengthened sample – sample 5 (right).

7.b. How is the interlayer behaving if the glass is broken?

The glass tubes were kept bonded together during the tests, which means that there was a strong connection between the tubes due to the interlayer material. Both glass tubes were 5 mm thick each, and when the glass shattered off, the pieces were no thicker than 1 or 2 mm.

Furthermore, if a crack appeared, the tube wants to bend. Due to the fact that the tubes were bonded together, it was not possible for the tubes to bend, which means that it kept its load-bearing capacity.

By analysing the cracks with a microscope, a few patterns of delamination, as dendritic patterns, were visible. This can not be avoided into laminated glass elements.

7.c. Does the laminated glass tube crack differently than single tubes?

Steven Engels (Engels, S. 2020) sent a few pictures from the compression tests, performed during his thesis on single DURAN (figure 67, left) and DURATAN (figure 67, right) tubes. These tubes had almost the same dimensions as the tubes used in this project: diameter 120 mm, wall thickness 5 mm, and length 290 mm. A difference between his tests and this research was the implementation of the connection. He used clamped connections: the glass was directly placed on a 10 mm thick POM-plate. For safety, tape was attached on the outside of the glass tube and a plexiglass enclosure was placed around the glass tube (Engels, S. 2020). As can be seen in figure 63, the DURAN tubes cracked with a few cracks parallel to the force, and the DURATAN tubes cracked with a few cracks parallel to the length of the tube and into pieces.

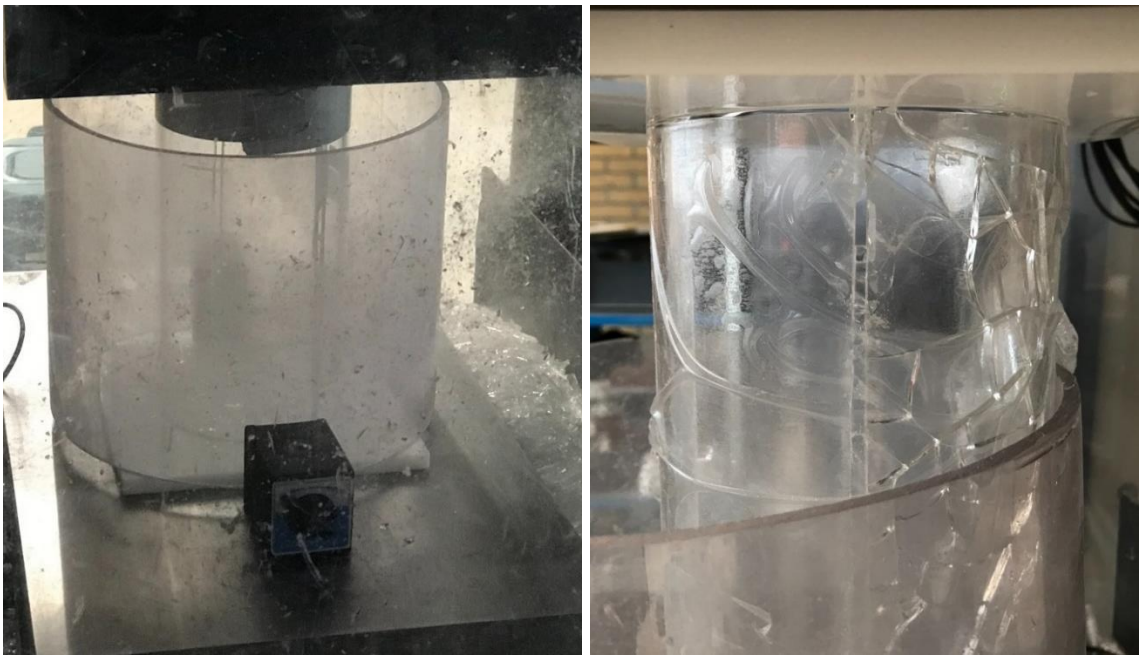

Figure 63 Test results from Steven Engels: DURAN (left) and DURATAN (right). (Engels, S. 2020)

So, the annealed (DURAN) laminated annealed glass tubes cracked in the same way as the single tubes did. The heat-strengthened (DURATAN) laminated tubes broke differently. In this project, the outer tube cracked only in straight cracks parallel to the length of the tube and the inner tube cracked into small pieces.

7.d. Are the samples robust? Do they show some structural integrity?

The samples are definitely robust, after the first crack appeared (around 95-160 kN), the annealed samples failed at 700-750 kN, and the heat-strengthened samples failed at 390-500 kN. After 700-750 and 390-500 kN, the glass started shattering, which could cause injuries. The samples were able to carry approximately 4 times the load after the first crack until the glass started to shatter. So, the glass samples do have a large load-bearing capacity, even after the first crack appeared. After the first crack appeared, the local stresses were relieved, whereby the load versus displacement curve continued without deviations. This means that the glass remained stiff even after the first crack, so the samples did have a good safety mechanism.

The heat-strengthened glass shattered into smaller pieces, but it shattered with more speed. So, looking into these aspects, annealed glass had a larger load-bearing capacity, and it shattered at a later moment and with less speed than the heat-strengthened glass samples did. This means that annealed glass samples are more robust than the heat-strengthened glass samples.

The samples are having a structural integrity, because they were able to withstand loading without directly failing after a fracture. In this way, the samples do give a warning (the first crack) before failing, so that people can bring themselves to safety. After the first crack the AN samples were able to withstand around 4 times more load, and the HS samples around 3 times.

The heat-strengthened glass samples are less reliable than the annealed glass samples, because the heat-strengthened glass samples cracked in many pieces out of a sudden, and it is unknown which tube had more prestressing. This makes the samples unpredictable. The cracks from the annealed glass samples propagated slowly, and less cracks appeared in the

annealed glass samples than in the heat-strengthened samples. Due to this, more glass remained intact, whereby was is able to carry more loads even after cracking.

A.14.2.4. Compression force/stress

8. Is the Hilti mortar able to take up more stress than 53 N/mm^2?

It was possible to overstress the Hilti mortar for short-term loading (long-term loading was not tested in this thesis project). As calculated in equation A.14.5, if the force onto the samples would be more than 171.8 kN, the Hilti would be overstressed. The allowable stress on Hilti is 53.36 N/mm^2 for short-term loading (figure 9 in appendix 12).

$$\sigma = \frac{F}{A} = \frac{171.8*10^3}{3220} = 53.4\ N/mm^2 \qquad \text{(A.14.5)}$$

$$\sigma = \frac{F}{A} = \frac{390*10^3}{3220} = 121.1\ N/mm^2 \qquad \text{(A.14.6)}$$

$$\sigma = \frac{F}{A} = \frac{750*10^3}{3220} = 232.9\ N/mm^2 \qquad \text{(A.14.7)}$$

The samples have been loaded up to 390-750, and the Hilti did not crush/splash/crack at all. So, it is possible to overstress it for the short-term loading. The Hilti was overstressed up to 121.1 and 232.9 N/mm^2 (equations A.14.6 and A.14.7).

121.1 and 232.9 N/mm^2 are also the compression stresses on the columns before failure.

9. Are the strain values in the glass tubes from the sensors comparable with the strain values calculated by hand?

In appendix 13, table 4, a strain value of the two glass tubes is given of 0.00148 for a compression force of 300 kN. In the experimental tests, these values were amplified with 100000. So, this means that according to the hand calculations a strain of around 1479 will be present in the two glass tubes. In table 3 from appendix 13, the strain was calculated for a force of 500 kN as well, then the strain values need to be around 2465. Not all samples were able to carry this force. Cracks were not taken into account in the hand calculations, so these values can vary from the experimental results.

Both tubes had sensors, so the force of 100, 300 or 500 kN is divided into the two tubes. In table 2, 3 and 4, the strain value is given per tube. The force is divided into two, which means that both tubes will carry the same amount of force. In reality, this division will not be exactly 50%-50%. The outer tube will probably carry a bit more, due to the fact that the area of the cross-section is bigger. Nevertheless, it will give a good estimate of the range of the strain values into the glass tubes. For a compression force of 100 kN, both glass tubes need to have a strain of around 459-532 (table 2), for a compression force of 300 kN, a strain of around 1378-1560 (table 3), and for a compression force of 500 kN, a strain of around 2297-2660 (table 4).

Components	Length or Thickness [mm]	A [mm2] =	A [mm^2]	E [N/mm^2]	F [kN]	σ [N/mm^2]	ε [-]	u or ΔL [mm]	k [N/mm]	ε*1000000 [-]
outer tube	300	PI*((115/2)^2-((105/2)^2))	1727,88	63000	50	28,94	0,000459	0,1378	362853,9515	459,3216251
inner tube	300	PI*((100/2)^2-((90/2)^2))	1492,26	63000	50	33,51	0,000532	0,1596	313373,8672	531,8460922
total:			3220,13		100					

Table 2 The strain value of the inner and the outer tube for a compression force of 100 kN.

Components	Length or Thickness [mm]	A [mm2] =	A [mm^2]	E [N/mm^2]	F [kN]	σ [N/mm^2]	ε [-]	u or ΔL [mm]	k [N/mm]	ε*1000000 [-]
outer tube	300	PI*((115/2)^2-((105/2)^2))	1727,88	63000	150	86,81	0,001378	0,4134	362853,9515	1377,964875
inner tube	300	PI*((100/2)^2-((90/2)^2))	1492,26	63000	150	100,52	0,001596	0,4787	313373,8672	1595,538277
total:			3220,13		300					

Table 3 The strain value of the inner and the outer tube for a compression force of 300 kN.

Components	Length or Thickness [mm]	A [mm2] =	A [mm^2]	E [N/mm^2]	F [kN]	σ [N/mm^2]	ε [-]	u or ΔL [mm]	k [N/mm]	ε*1000000 [-]
outer tube	300	PI*((115/2)^2-((105/2)^2))	1727,88	63000	250	144,69	0,002297	0,6890	362853,9515	2296,608125
inner tube	300	PI*((100/2)^2-((90/2)^2))	1492,26	63000	250	167,53	0,002659	0,7978	313373,8672	2659,230461
total:			3220,13		500					

Table 4 The strain value of the inner and the outer tube for a compression force of 500 kN.

The graphs of sample 5 are not reliable, because the machine stopped too early. In sample 4, strain 12 was not working. Below the failure forces are given from the samples:

- sample 4: 390 kN
- sample 1: 700 kN
- sample 3: 745 kN
- sample 6: 490 kN
- sample 2: 750 kN

sample	type of glass	force [kN]	strain 1	strain 2	strain 3	strain 4	strain 5	strain 6	strain 7	strain 8	strain 9	strain 10	strain 11	strain 12	average strain
4	HS	100	561	624	439	481	648	563	518	454	333	528	573	0	520
4	HS	300	54	1881	1794	1302	1822	2268	1002	1249	698	1419	1964	0	1405
1	AN	100	507	276	608	498	497	603	497	330	476	491	511	388	474
1	AN	300	1509	1067	1490	1581	1851	2049	1347	556	1240	1570	1766	1086	1426
1	AN	500	2360	1525	2394	2844	3206	3581	1111	616	2010	2902	3089	1588	2269
3	AN	100	457	525	580	304	406	426	494	447	512	257	481	-144	395
3	AN	300	1567	2010	2033	1081	1132	1031	1036	1679	1091	662	1125	376	1235
3	AN	500	2593	3159	3414	1692	1929	1510	947	2190	1697	1193	1929	846	1925
6	HS	100	485	411	648	512	559	509	491	421	635	523	513	472	515
6	HS	300	1624	1261	1795	1837	2008	1711	1529	1527	1628	1916	1707	1905	1704
2	AN	100	496	415	523	407	459	446	481	461	478	449	467	446	461
2	AN	300	1576	1280	1607	1381	1262	1416	1692	1398	1599	1751	1510	1495	1497
2	AN	500	2424	2376	2885	2519	2006	2765	2130	2586	2937	3379	1793	2728	2544

Table 5 The strain values (sensor 1-12) for the glass tubes at 100, 300 and 500 kN – samples 1,2,3,4, and 6.

The strains for all the samples are given in table 5 for 100 (orange), 300 (blue) and 500 kN (green). As said, some strain values were deviating, because of fracture in the glass. In the hand calculation cracks were not taken into account. In table 4 an average strain is given for the sample.

For 100 kN, the averages of the samples are in the same range as the value form the hand calculations, only the average value of sample 3 is lower, but this has to do with the fact that strain 12 was not working (graph 14). For 300 kN, most of the average strains are in the same range. Only sample 3 is not in range, due to the fact that strain 12, and the average strain of sample 6 is a bit higher than the average. Furthermore, only the annealed glass samples (1,2 and 3) were able to carry more force than 500 kN. Sample 1 and 2 are in range, and the average strain for sample 3 is again a bit lower due to sensor 12.

Overall, the strains from the test were in the same ranges as calculated by hand (in appendix 10) and according to tables 2, 3 and 4, the higher the force was, the more it deviated as more cracks occurred.

10. Is the displacement in the glass tubes comparable with the displacement calculated by hand?

From the average strain (table 4 and 5) the displacements were calculated from the glass tubes for 100, 300 and 500 kN (table 5). This was compared to the displacement calculated by hand (in appendix 10). The displacement was calculated via the following equation:

$$u = \varepsilon * L \qquad \text{(A.14.8)}$$

Looking into tables 3, 4 and 5 of appendix 13, for 100 kN, the glass should have a displacement of around 0.1479 mm, for 300 kN around 0.4436 mm, and for 500 kN around

0.7394 mm. Looking at table 6, all the displacements are approximately in the same range as calculated by hand.

sample	type of glass	force [kN]	average strain (*1000000)	average strain	Length or Thickness [mm]	u or ΔL [mm]
4	HS	100	520	0,00052	300	0,156052
4	HS	300	1405	0,00140	300	0,421479
1	AN	100	474	0,00047	300	0,14209
1	AN	300	1426	0,00143	300	0,427763
1	AN	500	2269	0,00227	300	0,680688
3	AN	100	395	0,00040	300	0,118626
3	AN	300	1235	0,00124	300	0,370551
3	AN	500	1925	0,00192	300	0,577495
6	HS	100	515	0,00051	300	0,154464
6	HS	300	1704	0,00170	300	0,511164
2	AN	100	461	0,00046	300	0,138185
2	AN	300	1497	0,00150	300	0,449196
2	AN	500	2544	0,00254	300	0,763234

Table 6 The displacement obtained from the average strain values from the tests at 100, 300 and 500 kN – samples 1,2,3,4, and 6.

References

Engels, S. (2020). Structures from Borosilicate glass tubes: From experimental data to structural design. MSc, Technical University of Delft.

Dugnani, R., Zednik, R., J., Verghese, P. (2014). Analytical Model of Dynamic Crack Evolution in Tempered and Strengthened Glass Plates. International Journal of Fracture. University of Michigan - Shanghai Jiao Tong University Joint Institute shanghai, CHINA. DOI: 10.1007/s10704-014-9975-z

Quinn, G., D. (2020). Fractography of Ceramics and Glasses. Practice Guide. Third edition. NIST National Institute of Standards and Technology. DOI: https://doi.org/10.6028/NIST.SP.960-16e3.

Figure, table and graph list

All figures except 63 and 39 (right) - Own pictures. Delft. Retrieved on July, 1-9, 2021.

Figure 39 (right) - Aurik, M. (2017). Structural Aspects of an Arched Glass Masonry Bridge, MSc, Technical University of Delft.

Figure 63 - Made by Engels, S. (2020). Delft. Retrieved on June, 30, 2021.

Table 1-7 - Own made tables. Delft. Retrieved on July, 1-10, 2021.

Graph 1-21 - Own made graphs. Delft. Retrieved on July, 1-8, 2021.